The 44 Annual NMR Meeting of the NMR Society of Japan

and

The 1st Asia-Pacific NMR Symposium

Abstracts

November 8th(Tue) – 11th(Thu), 2005

Osanbashi Hall, Yokohama, Japan

Supporting Organizers

Conference Sponsor

The NMR Society of Japan

Conference Co-sponsors

The Chemical Society of Japan
Japan Society of Magnetic Resonance in Medicine
The Japanese Biochemical Society
The Pharmaceutical Society of Japan
The Japanese Society of Polymer Science of Japan,
The Protein Science Society of Japan
The Biophysical Society of Japan
Japan Society for Bioscience, Biotechnology, and Agrochemistry
The Physical Society of Japan,
The Japan Society for Analytical Chemistry

Supporting Sponsor

Yokohama City

Conference Organization

Conference Chair **Hideo Akutsu**

Executive Committee

Chair	**Akira Naito**
Vice-Chairs	**Tetsuo Asakura**
	Masato Katahira
	Ichio Shimada

International Advisary Board

Chair	**Masatsune Kainosho (Japan)**
Committee Members	**Tai-huang Huang (Taiwan ROC)**
	Mitsu Ikura (Canada)
	Weontae Lee (Korea)
	Ray Norton (Australia)
	Mingji Zhang (PR China)

Welcome to Yokohama!

Hideo Akutsu, D.Sci.
Conference Chair of The 1st Asia-Pacific NMR Symposium

The history of International NMR Symposium in the Asia-Pacific area has just got started. Partly thank to the remarkable economic development, NMR research in this area is now on a rising tide. To cope with this new situation, this symposium will provide an opportunity for discussion among physicists, chemists, biologists and other scientists from the Asia-pacific countries as well as the rest of the world. The symposium will focus on the state-of-the-art methodological developments and on recent application of NMR spectroscopy in fields of organic and inorganic chemistry, structural biology, material science and polymer sciences, and NMR imaging. Especially, I encourage young NMR scientists to actively participate in this meeting through discussions on the new frontier of NMR science and getting acquainted with young researchers as well as the established people. Yokohama is an exciting city not only for meeting but also for culture. I am sure you enjoy your stay in Yokohama.

November, 2005

General Information

Speakers

Durations of oral presentations are 15 min for short presentations (L, ALS, BLS), 30 min for long presentations (ALL, BLL), and 45 min for keynote (KL) and plenary (PLL) lectures. Speakers should provide 3-5 min for discussion

Presenters should come to PC Registration desk 1 hour before your presentation starts and check your powerpoint.

Posters

Poster should be displayed by the noon time of November 8th for NP posters and by the noon time of November 10th for AP posters. Posters should be removed by 17:00 of November 11th.

Poster presenters are requested to explain your posters at their posters in the following duty time.

November 8(Tue)	17:00 – 18:30	NP(even number) + AP(even number)
November 9(Wed)	13:30 – 15:00	NP(odd number)+AP(odd number)
November 10(Thu)	13:30 – 15:00	AP(even number)+NP(even number)
November 11(Fri)	14:45 – 16:15	AP(odd number)+NP(odd number)

Special Events

November 9th 18:15 – 20;15 Welcome reception in Osanbashi Hall
(Sponsored by Bruker BioSpin Japan)

November 10th 19:40 – 21:30 Conference Banquet
(Royal Wing in Yokohama Bay)

Access to the Osanbashi Hall

http://www.osanbashi.com/

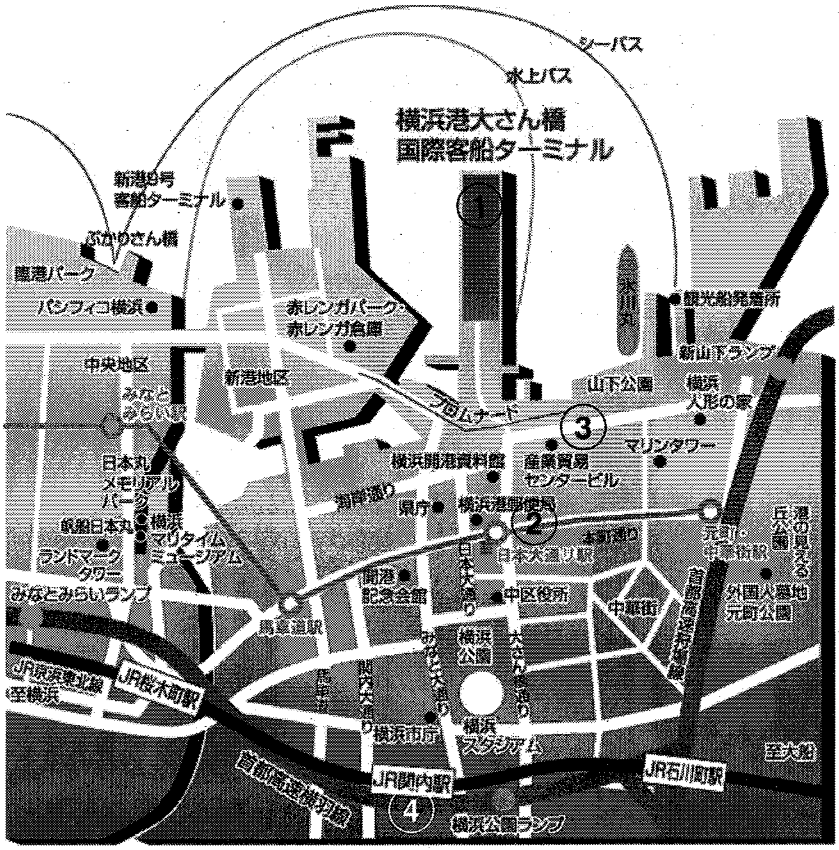

1. OSANBASHI HALL
2. Nihon-odori sta.
3. Industry & Trade Center
4. Kannai sta.

(a) Access to Yokohama City from Narita Airport

1) Narita Airport → (Limousine Bus: about 90 min.) → Yokohama Station
2) Narita Airport → (JR Narita Express: about 90 min.) → Yokohama Station

(b)Access to Osanbashi Hall from Yokohama Station

1) 7 min. walk from Nihonohdohri Station ② on the Minato Mirai Line from Yokohama Station.
2) 15 min. walk from Kannai Station ④ on the JR Negishi Line which is second stop from Yokohama Station.
3) 20 min. by taxi from Yokohama Station.

Osanbashi Hall

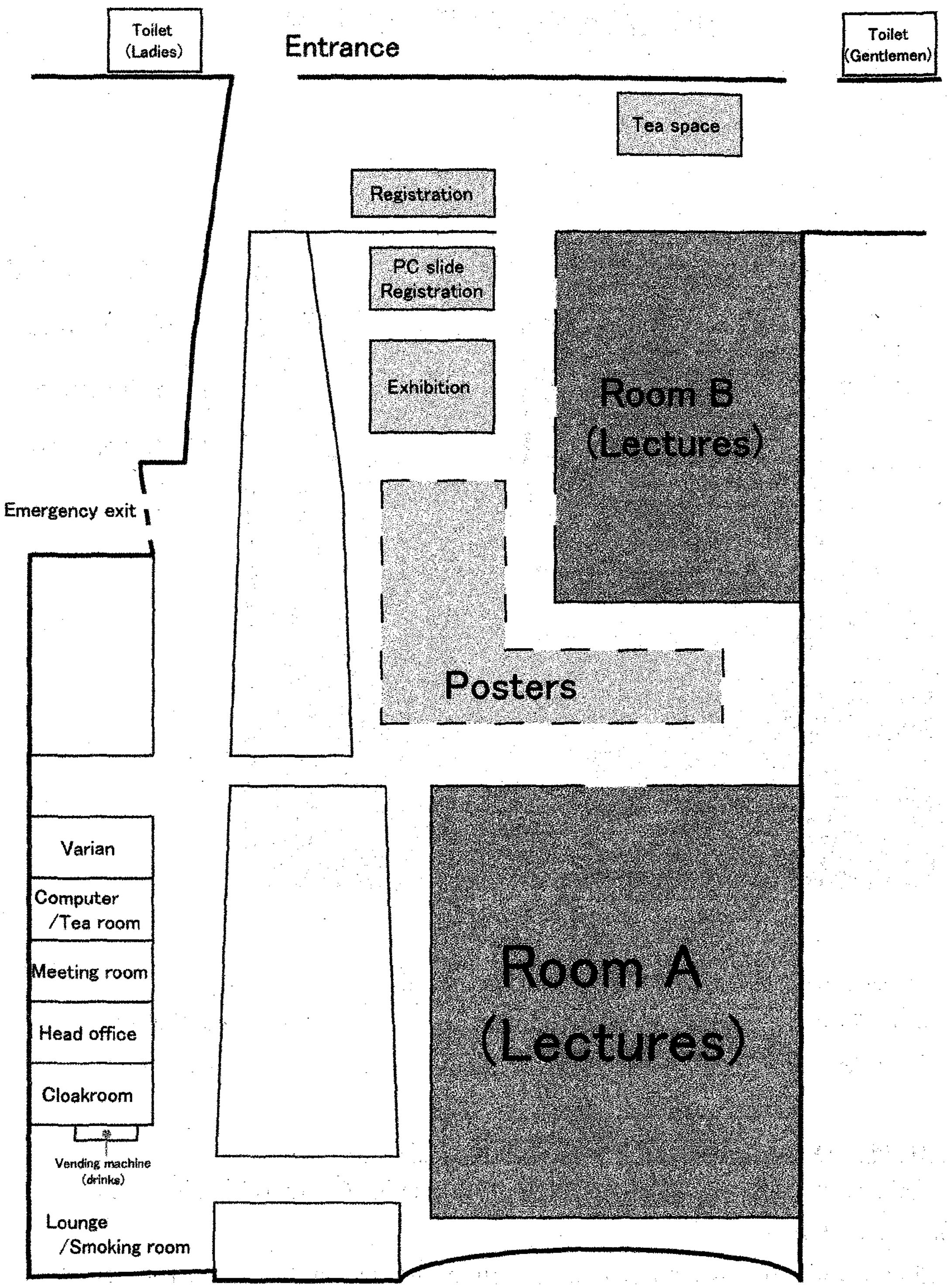

Program of The 44th NMR Meeting of the NMR Society of Japan
And
The 1st Asia-Pacific NMR Symposium

November 8th (The 44th Annual NMR Meeting of the NMR Society of Japan)

9:30-18:30 General Oral and Poster Presentations

November 9th (The 44th Annual NMR Meeting of the NMR Society of Japan)

9:00-16:15 General Oral and Poster Presentations

16:30 Opening of the 1st Asia-Pacific NMR Symposium

16:30-18:00 Keynote Lectures

Masatsune Kainosho (CREST/JST)

Jacob Schaefer (Washington University, USA)

18:15-20:15 Welcome Reception

November 10th (The 1st Asia-Pacific NMR Symposium)

8:30-10:00 Plenary Lectures

Alex Pines (University of Calfornia, Berkley, USA)

Anthony Watts (University of Oxford, UK)

10:15-19:00 Parallel Oral Presentations and Poster Presentations

19:40-21:30 Conference Banquet

November 11th (The 1st Asia-Pacific NMR Symposium)

8:30-16:15 Parallel Oral Presentations and Poster Presentations

16:15-18:45 Symposium on "Technical Developments of NMR"

Plenary Lecture

Lucio Frydman (Weizmann Institute of Science, Israel)

Invited Lecture

Ago Samoson (National Institute of Chemical Ohysics and Biophysics, Estonia)

18:45 Closing of the Conference

Schedule of the Conference

The 44th Annual NMR meeting of the NMR society of Japan				The 1st Asia-Pacific NMR symposium					
Nov. 8 (Tue)		Nov. 9 (Wed)		Nov. 10 (Thu)			Nov. 11 (Fri)		
8:30	Registration			8:30	Plenary Lectures		8:30	Solution NMR A4	Solution NMR B4
		9:00	Solution MMR 2						
9:30	Solid State NMR 1			10:00	Coffee Break		10:15	Coffee Break	
10:45	Coffee Break	10:30	Coffee Break	10:15	Solution NMR A1	Solid State NMR B1	10:30	Solution NMR A5	Solid State NMR B5
11:00	Solution NMR 1	10:45	Solution NMR 3						
12:00	Meeting	11:45	Lunch	12:00	Lunch		12:00	Lunch	
12:30	Lunch								
13:30	Instrumentation	13:30	Poster	13:30	Poster		13:15	Solution NMR A6	Solid State NMR B6
	Poster Award Presentation								
15:05	Coffee Break	15:00	Solution NMR methodology & Imaging	15:00	Solution NMR A2	Solid State NMR B2	14:45	Poster	
15:20	Poster Award Presentations	16:15	Coffee Break	16:45	Coffee Break		16:15	Symposium 1 Plenary Lecture	
17:00-18:30	Poster	16:30	Keynote Lectures	17:00	Solution NMR A3	Solution NMR B3 & Imaging	17:30	Coffee Break	
							17:45	Symposium 2	
		18:15-20:15	Welcome Reception	19:40-21;30	Banquet		18:45	Closing	

Speaker Presentations

The 44th Annual NMR Meeting of the NMR Society of Japan (1st day)
November 8 (Tue)

8:30-9:30 Registration

9:30-10:45 **Solid State NMR 1**
Chair: I. Ando

L1 Proton dynamics in inorganic solid acid $(NH_4)_3H(SO_4)_2$
Koh-ichi Suzuki, Shigenobu Hayashi
Research Institute of Instrumentation Frontier, National Institute of Advanced Industrial Science and Technology (AIST)

L2 Complete ^{13}C and ^{15}N signal assignments and structural analysis of the crystalline chitin binding domain of chitinase A1 by solid-state MAS NMR
Hiroki Tanaka[1], Izumi Yabuta[1], Yuko Nagasaki[2], Masashi Hara[2], Takahisa Ikegami[1], and Toshimichi Fujiwara[1], Takeshi Watanabe[2], and Hideo Akutsu[1]
[1]Institute for Protein Research, Osaka University, Osaka, Japan, [2]Faculty of Agriculture, Niigata University, Niigata, Japan

L3 Structural changes induced by ATP hydrolysis in microcrystalized protein-DNA filaments detected by Solid State NMR
Minoru Hatanaka[1], Masayoshi Honda[2,3], Satoko Ishibe[2], Tsutomu Mikawa[2,3,6] Yutaka Ito[3,4,5], Takehiko Shibata[2,3], and Toshio Yamazaki[1]
[1]Genomic Sciences Center, RIKEN, [2]Bio-supramol. Struct - Func. Group, RIKEN, [3]Grad. Sch. of Integrated Sci., Yocohama City Univ, [4]Grad. Sch. of Sci., Tokyo Metropolitan Univ., [5]CREST・JST, [6]Structurome Res. Group, RIKEN/Harima Institute

L4 Is it possible to directly detect the overtone NMR for half-integer quadrupolar nuclei?
Hajime Okamoto, Yuya Yamazaki, Hiroki Nose, and Daisuke Kuwahara
The University of Electro-Communications

L5 Dynamic aspect of supramolecular PEO-urea crystal revealed by solid-state ^{13}C MAS exchange NMR
Toshikazu Miyoshi and Wei Hu
Institute of Nanotechnology, National Institute for advanced Industrial Science and Technology

10:45-11:00 Coffee Break

11:00-12:00 **Solution NMR 1**
Chair: Y. Nishimura

L6 Structure and mode of interaction with RNA of mouse neural protein, Musashi1
Yohei Miyanoiri [1], Satoshi Saitoh [2], Hiroyuki Miyashita [2], Hisanori Kobayashi [2] Seiichi Uesugi [2], Takao Imai [3], Hideyuki Okano [3] and Masato Katahira [1,4]
[1] Department of Supramolecular Biology, International Graduate School of Arts and Sciences, Yokohama City University

L7 Characterisation of the nucleotide-binding domain of the human mitochondrial ABC transporter ABCB6 by heteronuclear multidimensional NMR and homology modelling
Kaori Kurashima-Ito[1,2,3], Teppei Ikeya[4], Hiroshi Senbongi[1], Tsutomu Mikawa[1,2,3], Takehiko Shibata[1,2] and Yutaka Ito[1,2,3]
[1]Cellular and Molecular Biology Laboratory, RIKEN,, [2]Molecular and Cellular Physiology Laboratory, Graduate School of Integrated Science, Yokohama City University, [3]CREST/Japan Science and Technology Agency (JST) and [4]National Institute of Advanced Industrial Science and Technology (AIST)

L8 Clarification of repair mechanism of (6-4) photolyase using NMR
Akira Kato[1], Takumi Ueda[1,2], Takeshi Todo[3], Hiroaki Terasawa[1], and Ichio Shimada[1,4]

[1]Graduate School of Pharmaceutical Sciences, the University of Tokyo, [2]Japan Biological Information Research Center (JBIRC), Japan Biological Informatics Consortium (JBIC), [3] Radiation Biology Center, Kyoto University, [4] Biological Information Research Center (BIRC), National Institute of Advanced Industrial Science and Technology (AIST)

L9 Rapid protein-ligand interaction analysis system using wheat germ cell-free protein synthesis
Keiko Matsubara[1], Yukinori Nara[1], Akiko Iihara[1], Michiko Kitano[2], and Toshiyuki Kohno[2]
[1]ZOEGENE Corporation and [2]Mitsubishi Kagaku Institute of Life Sciences (MITILS)

12:00-12:30 **Meeting of the NMR Society of Japan**

12:30-13:30 **Lunch**

13:30-14:15 **Instrumentation**
Chair: N. Asakawa

L10 Routine, automated solution state dynamic nuclear polarisation (DNP) NMR spectroscopy of small molecules
Andrew Sowerby[1], and Michio Shimizu[2]
[1]Oxford Instruments Plc., [2]Oxford Instruments KK

L11 Resolution improvement of the HTS bulk magnet at 3 Tesla
Takashi Nakamura[1], Yoshiaki Yoshikawa[2], Yoshitaka Ito[2] and Hiroyuki Koshino[1]
[1] RIKEN, [2] IMRA MATERIAL R&D Co. Ltd.

L12 Development of microMAS probehead for mass-limited solid state samples
Kazuo Yamauchi, Daisuke Hasegawa, and Tetsuo Asakura
Department of Biotechnology, Tokyo University of Agriculture and Technology

14:15-15:05 **Poster Award Presentations**
Chair: T. Hiraoki

PL1 Diffusional behavior of poly(β-benzyl L-aspartate) in the rod-like and random-coil forms as studied by high field-gradient NMR method
Sho Kanesaka, Shigeki Kuroki, and Isao Ando
Department of Chemistry and Materials Science, Tokyo Institute of Technology

PL2 Local environments of slags: the first application of ^{43}Ca MQMAS technique.
Keiji Shimoda[1], YasuhiroTobu[1], Koji Kanehashi[1], Takahiro Nemoto[2], Yuichi Shimoikeda[2], and Koji Saito[1]
[1]Advanced Technology Research Laboratories, Nippon Steel Corporation, [2]JEOL Ltd.

PL3 Novel solid-state NMR protein structural analysis by the simulated anneal spectral fitting under the constraints of conformation-dependent ^{13}C chemical shifts.
Yoh Matsuki[1,2], Hideo Akutsu[2], and Toshimichi Fujiwara[2]
[1]JST-BIRD, [2]Institute for Protein Research, Osaka University

PL4 Characteization of backbone conformations and interaction on retinal protein by solid state NMR
Izuru Kawamura[1], Naoki Kihara[1], Satoru Tuzi[2], Yoichi Ikeda[3], Katsuyuki Nishimura[1], Hazime Saitô[2,4], Naoki Kamo[3] and Akira Naito[1]
[1]Graduate School of Engineering, Yokohama National. University, [2]Graduate School of Life Science, University of Hyogo, [3]Graduate School of Pharmaceutical Sciences, Hokkaido University, [4]Center for Quantum Life Science, Hiroshima University

PL5 Structure analysis of chlorosomes by ^{13}C spin-diffusion solid-state NMR
Ayako Egawa[1], Kengo Akiba[1], Tadashi Mizoguchi[2], Yoshinori Kakitani[3], Yasushi Koyama[3], Toshimichi Fujiwara[1] and Hideo Akutsu[1]
[1]Institute for Protein Research, Osaka University, [2]College of Science and Engineering, Ritsumeikan University, [3]Faculty of Science and Technology, Kwansei Gakuin University

15:05-15:20 **Coffee Break**

15:20-17:00 **Poster Award Presentations**
Chair: H. Shindo

PL6 Structural analysis of alanine tripeptide with anti-parallel and parallel β-sheet structures using solid state NMR
Michi Okonogi[1], Kazuo Yamauchi[1], Hiromichi Kurosu[2], and Tetsuo Asakura[1]
[1]Tokyo University of Agriculture and Technology, [2]Nara Women's University

PL7 Solid state NMR analysis of amphotericin B-sterol covalent conjugates forming a molecular assemblage in membrane
Yusuke Kasai, Shigeru Matsuoka, Yuichi Umegawa, Hiroyuki Ueno, Nobuaki Matsumori, Tohru Oishi, and Michio Murata
Department of Chemistry, Graduate School of Science, Osaka University

PL8 Dynamic structure analysis of antibiotic peptide Alamethicin in lipid bilayers by solid-state NMR
Takashi Nagao, Daishuke Ishioka, Katsuyuki Nishimura, and Akira Naito
Graduate school of Engineering, Yokohama National University

PL9 ^{19}F NMR Study of myoglobin bearing a fluorinated Heme -dynamics and thermodynamics of the acid-alkaline transition
Satoshi Nagao[1], Yueki Hirai[1], Shigenori Nagatomo[1], Hajime Mita[1], Yasuhiko Yamamoto[1], and Akihiro Suzuki[2]
[1]Department of Chemistry, University of Tsukuba, [2]Department of Materials Engineering, Nagaoka College of Technology

PL10 NDSB improves protein solution NMR spectra by suppressing protein aggregation
Takeshi Ishii, Kazuo Hosoda, Yasuko Iizuka, Kaori Wakamatsu, Hiroyuki Kogure, and Kenji Kubota
Department of Biochemical and Chemical Engineering, Faculty of Engineering, Gunma University

Chair: C. Kojima

PL11 Variable pressure NMR reveals the entire energy landscape of a protein: A conserved exited state conformer between ubiquitin and ubiquitin-like protein NEDD8
Ryo Kitahara[1], Eri Sakata[2], Takeshi Kasuya[2], Yoshiki Yamaguchi[2], Koichi Kato[2,3], Keiji Tanaka[4], Shigeyuki Yokoyama[1,3,5], and Kazuyuki Akasaka[1,6]
[1]RIKEN Harima Institute, [2]Department of Structural Biology and Biomolecular Engineering, Graduate School of Pharmaceutical Sciences, Nagoya City University, [3]RIKEN Genomic Sciences Center, [4]Department of Molecular Oncology, Tokyo Metropolitan Institute of Medical Science, [5]Department of Biophysics and Biochemistry, Graduate School of Science, The University of Tokyo, [6]Department of Biotechnological Science School of Biology-Oriented Science and Technology, Kinki University

PL12 NMR structural analysis of the CGG / CGG containing DNA complexed with the recognition drugs
Makoto Nomura[1], Shinya Hagihara[2,3], Yuki Goto[2], Kazuhiko Nakatani[2,3,4] and Chojiro Kojima[1]
[1]Graduate School of Biological Science, Nara Institute of Science and Technology, [2]Department of Synthetic Chemistry and Biological Chemistry, Graduate School of Engineering, Kyoto University, [3]PRESTO, Japan Science and Technology Agency, [4]The Institute of Scientific and Industrial Research, Osaka University

PL13 Solution structure of the cytoplasmic region of Na^+ /H^+ exchanger-1 complexed with the essential cofactor, calcineruin B homologous protein-1
Masaki Mishima[1], Shigeo Wakabayashi[2] and Chojiro Kojima[1]
[1]Graduate School of Biological Sciences, Nara Institute of Science and Technology, [2]Department of Molecular Physiology National Cardiovascular Center Research Institute

PL14 Methodological advances in a hetero-nuclear NMR-based metabolomics by stable isotope labeling of *Arabidopsis thaliana*
Yasuyo Sekiyama[1], Takashi Hirayama[2,3,4], Kazuo Shinozaki[1,4,5], Kazuki Saito[1,3,6] and Jun Kikuchi[1,2,3]

[1]RIKEN Plant Science Center, [2]International Graduate School of Arts and Sciences, Yokohama City University, [3]CREST, JST, [4]RIKEN Genomic Sciences Center, [5]RIKEN Plant Molecular Biology Laboratory, [6]Graduate School of Pharmaceutical Sciences, Chiba University.

PL15 A novel method for measuring the fast H/D exchange by ^{13}C observed 2D NMR
Kaoru Fujimura, Takeshi Tenno, Hidehito Tochio and Hidekazu Hiroaki
International Graduate School of Arts and Sciences, Yokohama City University

17:00-18:30 **Poster Presentations**

The 44th Annual NMR Meeting of the NMR Society of Japan (2nd day)
November 9 (Wed)

9:00-10:30 **Solution NMR 2**
Chair: D. Kouda

L13 Detergent screening for NMR structural studies of membrane proteins
S. Otomo (Z.-Y. Wang), K. Sato, N. Akiyama, Y. Shimada, and H. Suzuki
Faculty of Science, Ibaraki University

L14 A novel strategy for protein structural study under intracellular environment by using Xenopus laevis oocyte
Tomomi Sakai[1], Hidehito Tochio[1], Fuminori Sugihara[1], Tetsuro Kokubo[1], Yutaka Ito[2], Hidekazu Hiroaki[1] and Masahiro Shirakawa[3]
[1]International Graduate School of Arts and Sciences, Yokohama City University, [2]Graduate Schools of Science, Tokyo Metropolitan University, [3]Graduate School of Engineering, Kyoto University

L15 Distributed computing and NMR constraint-based high-resolution protein structure determination: applied for endothelin-1
H. Takashima[1], N. Mimura[1], T. Yoshida[2], T. Ohkubo[2], Y. Nishi[3] and Y. Kobayashi[2,3]
[1]Novartis Institutes for BioMedical Research, [2]Graduate School of Pharmaceutical Sciences, Osaka University, [3]Osaka University of Pharmaceutical Sciences

Chair: K. Kawano

L16 MAGICAL: Method for AssiGnments with Intelligent Combinatorial Amino acid Labeling
Rikou Tanaka, Chieko Komatsu, Kuniko Kobayashi, Takeshi Tanaka, Toshiyuki Kohno
Mitsubishi Kagaku Institute of Life Sciences (MITILS)

L17 The hetero-nuclear NMR-based metabomics by uniform stable isotope labeling in plant and animal systems
Jun Kikuchi
[1]Plant Science Center, RIKEN, [2]Int. Grad. Sch. Art. Sci. Yokohama City Univ. [3]CREST, JST

L18 Concentration and temperature dependences of the chemical shifts determined on a unified scale to study C–H•••O interactions in some binary aqueous mixtures of organic compounds
Kazuko Mizuno, Yuka Tamiya, Takuya Yamamura, and Mamoru Mekata
Faculty of Engineering, University of Fukui

10:30-10:45 Coffee Break

10:45-11:45 **Solution NMR 3**
Chair: M. Katahira

L19 Development of an amino acid-selective cross-saturation method for modeling protein-protein complex
Shunsuke Igarashi[1], Masanori Osawa[1], Koh Takeuchi[1,2], and Ichio Shimada[1,3]
[1]Graduate School of Pharmaceutical Sciences, the University of Tokyo, [2]Japan Society for the

Promotionof Science, [3]Biological Information Research Center, National Institute of Advanced Industrial Science and Technology

L20 NMR structure of CAG trinucleotide repeart DNA complexed with a small-molecule ligand inducing nucleotide flipping

Kazuhiko Nakatani[1,2], Shinya Hagihara[1], Yuki Goto[1], Akio Kobori[1], Masaki Hagihara[1], Gosuke Hayashi[1], Motoki Kyo[3], Makoto Nomura[4], Masaki Mishima[4] and Chojiro Kojima[4]

[1]Kyoto University, [2]PRESTO, JST, [3]Toyobo Co. Ltd., and 4Nara Institute of Science and Technology

L21 Analysis of variance on metabolites in saliva from young healthy females

Seizo Takahashi[1], Rina Yatsu[1], Yuki Kamiyama[1], Yukiharu Yamaguchi[2], Takashi Ogino[3]

[1.]Department of Chemical and Biological Sciences, Japan Women's University, [2.] Division of Clinical Technology, Pfizer Global R & D, Pfizer Japan Inc. [3.] National Institute of Neuroscience, NCNP

L22 Applications of CAST/CNMR to structural revision of terpenoids

Hiroyuki Koshino[1], Shunya Takahashi[1], and Hiroko Satoh[2]

[1]RIKEN (The Institute of Physical and Chemical Research), [2]National Institute of Informatics

11:45-13:30 **Lunch**

13:30-15:00 **Poster Presentations**

15:00-16:15 **Solution NMR Methodology & Imaging**

Chair: Y. Seo

L23 Calculation of nuclear magnetic shieldings using an analytically differentiated relativistic shielding formula

Hiroyuki Fukui, Keiichi Kudou

Faculty of Engineering, Kitami Institute of Technology

L24 Integrated high-field NMR-spectroscopic and multivariate analysis for disease model rat urine

Tadashi Nemoto[1], Masako Fujiwara[2], Kazunori Arifuku[2], Itiro Ando[3], Taeko Kataoka[1], Kenji Kanazawa[1], Katsuo Asakura[4], and Hiroaki Utsumi[4]

[1]National institute of Advanced Industrial Science and Technology (AIST), [2]JEOL DATUM LTD, [3]Environmental Research Center LTD, [4]JEOL LTD.

L25 *NMR-based metabolomics :* Pattern recognition analysis of hypertensive model rats and diurnal variation using ^{1}H-NMR spectroscopy of urine

Masako Fujiwara[1], Itiro Ando[2], Kazunori Arifuku [1] Kenji Kanazawa[3], and Tadashi Nemoto[3]

[1]JEOL DATUM LTD, [2]Envioronmental Research Center LTD, [3]National Institute of Advanced Industrial Science and Technology (AIST)

L26 NMR imaging investigation of rice cooking

Midori Kasai[1,2], Andrew Lewis[2], Florea Marica[2], Sonoko Ayabe[1], Keiko Hatae[1], and Colin A. Fyfe[2]

[1]Department of Nutrition and Food Science, Ochanomizu University, [2] Department of Chemistry, The University of British Columbia

L27 Simultaneous detection of glutamate, GABA and glutamine in the human brain at 4.7 T using a localized 2D CT-COSY with an ISIS pulse

Hidehiro Watanabe, Nobuhiro Takaya, and Fumiyuki Mitsumori

National Institutes for Environmental Studies

16:15-16:30 **Coffee Break**

16:30-18:00 **Keynote Lectures**

Chair: H. Akutsu

KL1 Optimal Isotope Labeling for NMR Protein Structure Determination: Stereo-Array Isotope Labeling (SAIL) Approach
Masatsune Kainosho
CREST of JST and Graduatee School of Science, Tokyo Metropolitan University

Chair: A. Naito

KL2 Structure and Function in Bacteria and Plants by REDOR
Lynette Cegelski, Sung Joon Kim, and Jacob Schaefer
Department of Chemistry, Washington University

18:15-20:15 **Welcome Reception**

The 1st Asia-Pacific NMR Symposium (3rd day)
November 10 (Thu)

8:30-10:00 **Plenary Lectures**
Chair: T. Terao

PLL1 New Developments in NMR and MRI at Berkeley: Materials and Biomedicine from Nanometers to Meters
Alex Pines
Lawrence Berkeley National Laboratory and University of California Berkeley

Chair: F. Separovic

PLL2 Receptor dynamics and structure in membranes resolved using solid state NMR
Anthony Watts
Biomembrane Structure Unit,
Biochemistry Department, Oxford University

10:00-10:15 **Coffee Break**

10:15-12:00 **Parallel Sessions A & B**

Parallel Session A Solution NMR A1
Chair: R. Norton

ALL1 NMR investigation on protein-protein interactions in cell signaling network
Mitsu Ikura
Division of Signaling Biology, Ontario Cancer Institute and Department of Medical Biophysics, University of Toronto

ALL2 Structure, folding, and substrate channeling of the E2 component of human mitochondria branched chain α-ketoacid dehydrogenase complex
Chang, C.F.[2], Naik, M.[1], Chou, H.T.[1], Lin, Y.J.[1], Lee, S.J.[1] and Huang, T.-h.[1],
[1]Inst. Biomed. Sci. & [2]Genomic Research Center

Chair: Chinpan Chen

ALS1 How to assemble a fungal umbrella: step-by-step instructions
Kwan, AH, Winefield, RD, Sunde, M, Templeton, MD, Mackay, JP
School of Molecular and Microbial Biosciences, University of Sydney

ALS2 Study of the gradual protein unfolding by NMR spectroscopy
Jianxing Song, Zheng Wei, Miaoqing Fang, and Jiahai Shi
Departments of Biochemistry and Biological Sciences, National University of Songapore

ALS3 Structural characterization of preS1 surface antigen in Hepatitis B virus by NMR

Seung-Wook Chi, Do-Hyoung Kim, Min Jung Kim, Si-Hyung Lee, Jae-Sung Kim, and Kyou-Hoon Han
Protein Analysis and Design Laboratory, Division of Drug Discovery, Korea Research Institute of Bioscience and Biotechnology

10:15-12:00 **Parallel Session B Solid State NMR B1**
Chair: T. Asakura

BLL1 High-resolution solid-state NMR analysis of biological supramolecular systems
Hideo Akutsu
Institute for Protein Research, Osaka University

BLL2 Amyloidβ peptide disruption of lipid membranes and the effect of metal ions
Tong-Lay Lau, Ernesto E. Ambroggio, Deborah J. Tew, Roberto Cappai, Colin L. Masters, Gerardo D. Fidelio, Kevin J. Barnham and Frances Separovic
University of Melbourne

Chair: T. Fujiwara

BLS1 Conformational and dynamics alteration of membrane proteins induced by 2D crystallization
Kazutoshi Yamamoto[1], Satoru Tuzi[1], Hazime Saitô,[2] Izuru Kawamura[3], and Akira Naito[3]
[1]Department of Life Science, University of Hyogo, [2]Center for Quantum Life Sciences, Hiroshima University, and [3]Graduate School of Engineering, Yokohama National University

BLS2 Can database potentials improve the accuracy of protein structures?
Haydyn D. T. Mertens and Paul R. Gooley.
Department of Biochemistry and Molecular Biology, Bio21 Institute of Biotechnology and Molecular Science , University of Melbourne

BLS3 A Novel Frequency-Selective Lee-Goldburg Cross-Polarization Solid-State NMR Pulse Sequence for Discernment of Bronsted and Lewis Acid Sites in Solid Acid Catalysts
Shing-Jong Huang, Shou-Heng Liu, Wen-Hua Chen, Yao-Hung Tseng, Jerry C. C. Chan, Shang-Bin Liu
Institute of Atomic and Molecular Sciences Academia Sinica

12:00-13:30 **Lunch**

13:30-15:00 **Poster Presentations**

15:00-16:45 **Parallel Sessions A &B**

Parallel Session A Soluton NMR A2
Chair: Mingjie Zhang

ALL3 FINDING ORDER IN DISORDERED PROTEINS
RS Norton,[1] ZP Feng,[1] DW Keizer,[1] RA Stevenson,[1] S Yao,[1] VJ Murphy,[2] CG Adda[2], M Foley,[2], RF Anders[2]
[1]The Walter and Eliza Hall Institute of Medical Research, [2]Department of Biochemistry, La Trobe University

ALS4 Structure and mechanism of amyloid fibrils by the gastric cancer-related GISP-like proteins
Yuan-Chao Lou, Meng-Ru Ho, Wen-Chang Lin and Chinpan Chen
Institute of Biomedical Sciences, Academia Sinica

ALS5 Analysis of ligand-induced domain rearrangement of a large-size protein by oritentation dependent TROSY shift changes - application of DIORITE to mRNA capping enzyme
Hiroshi Moriuchi [1], Yukio Mizuta [2], and Shin-ichi Tate [1]
[1] Biomolecular Engineering Research Institute (BERI), [2] JEOL Ltd.

Chair: Yunyu Shi

ALS6 Observation of intermediate states of the human prion protein by high pressure NMR spectroscopy
Werner Kremer[1], Norman Kachel[1], Ralph Zahn[2], Hans Robert Kalbitzer[1]*
[1]Institut für Biophysik und Physikalische Biochemie, Universität Regensburg, Universitätsstr, and [2]Institute of Molecular Biology and Biophysics, ETH

ALS7 NMR Structure of Rabbit Prion Protein(91-228)
Jun Li[1], Fanghua Mei[2], Gengfu Xiao[2], Donghai Lin[1]
[1]NMR Laboratory, Shanghai Institute of Materia Medica, Shanghai Institutes for Biological Sciences, Chinese Academy of Sciences, [2]State Key Laboratory of Virology, College of Life Sciences, Wuhan University,

ALS8 Pressure-jump NMR Study of Dissociation and Association of Amyloid Protofibrils
Yuji O. Kamatari [1,2,3], Shigeyuki Yokoyama[2,3,4], Hideki Tachibana[5], Kazuyuki Akasaka[2,6]
[1]Gifu University, [2]RIKEN Harima Institute, [3]Riken Genome Science Center, [4]The University of Tokyo, [5]Kobe University, [6]Kinki University

Parallel Session B Solid State NMR B2
Chair: F. Horii

BLL3 Structure of Silks studied using Solid-state NMR
Tetsuo Asakura
Department of Biotechnology, Tokyo University of Agriculture and Technology

BLS4 ^{29}Si and ^{27}Al NMR characteristics of octahedral Si-Al disorder in high-pressure aluminosilicate minerals
Xianyu Xue[1], Masami Kanzaki[1], Hiroshi Fukui[1], Eiji Ito[1], and Takafumi Hashimoto[2]
[1]Inst. Study Earth's Interior, Okayama Univ., [2]Faculty Sci., Kumamoto Univ.

BLS5 One-dimensional dynamical conformon investigated by nuclear spin relaxation
Naoki Asakawa, and Yoshio Inoue
Department of Biomolecular Engineering, Tokyo Institute of Technology

Chair: S. Kuroki

BLS6 NMR of Aluminium Alloys
Kate Nairn, Tim Bastow, George Yiapanis, Anita Hill.
CSIRO Manufacturing and Infrastructure Technology

BLS7 Chemical shift and spin-lattice relaxation of helium-3 confined in micropores
Shigenobu Hayashi
Research Institute of Instrumentation Frontier, National Institute of Advanced Industrial Science and Technology (AIST)

BLS8 Surface acidity of BF_3/Al_2O_3 catalyst as studied by solid state NMR and theoretical calculation
Feng Deng, Jun Yang, Anming Zheng, Mingjin Zhang, Qing Luo, Chaohui Ye
State Key Laboratory of Magnetic Resonance and Atomic and Molecular Physics, Wuhan Institute of Physics and Mathematics, Chinese Academy of Sciences

16:45-17:00 **Coffee Break**

17:00-19:00 **Parallel Session A & B**

Parallel Session A Solution NMR A3
Chair: M. Ikura

ALL4 Auto-inhibition of X11s/Mints Scaffold Proteins Revealed by the Closed Conformation of the PDZ Tandem
Jia-Fu Long, Wei Feng, Rui Wang, Ling-Nga Chan, and Mingjie Zhang
Department of Biochemistry, Molecular Neuroscience Center, Hong Kong University of Science and Technology

ALL5 Molecular recognition between PDZ domain of AF-6 and Bcr
Yunyu Shi, Jihui Wu, Quan Chen, Xiaogang Niu
Hefei National Laboratory for Physical Sciences at Microscale and School of Life Science, University of Science and Technology of China

Chair: Tai-huang Huang

ALS9 Probing the inter-domain motion of N-terminal tandem PDZ domains of PSD-95 with residual dipolar couplings
Wenning Wang[1], Jiafu Long[2] and Mingjie Zhang[2]
[1]Department of Chemistry, Fudan University, [2]Department of Biochemistry, Hong Kong University of Science and Technology,

ALS10 Solution Structure of the kinase inhibitory region and extended SH2 domain of SOCS3
J.J. Babon, S. Yao, D. DeSouza, L. Fabri, M. Baca and R.S. Norton
The Walter and Eliza Hall Institute of Medical Research, 1G Royal Parade, Parkville

ALS11 NMR Solution Structure of hPrxVI, a 25 kDa 1-Cys Human Peroxiredoxin Enzyme
Eunmi Hong[1], Joon Shin[1], Sang Won Kang[2],and Weontae Lee[1]
[1] Department of Biochemistry, Yonsei University, [2]Center for Cell Signaling Research and Division of Molecular Life Sciences, Ewha Womans University

ALS12 Redox-dependent conformational rearrangement of protein disulfide isomerase
Yoshiki Yamaguchi[1], Aya Maeno[1,2], Michiko Nakano[2], Chiho Murakami[1], Hiroaki Sasakawa[2], Takushi Harada[1], Eiji, Kurimoto[1], Takeshi Iguchi[3], Kenji Inaba[4], Osamu Asami[5], Tsutomu Kajino[5], Jun Kikuchi[6], and Koichi Kato[1,2]
[1]Graduate School of Pharmaceutical Sciences, Nagoya City University, [2]Institute for Molecular Science, [3]Bioscience Research Laboratory, Fujiya Co., Ltd., [4] Institute for Virus Research, Kyoto University, [5]Toyota Central Research & Development Labs. Inc., and [6]Plant Sciences Center, RIKEN

Parallel Session B Solution NMR B3 & Imaging
Chair: F. Mitsumori

BLL4 NMR study on Antibiotics Targets
Bong-Jin Lee
College of Pharmacy, Seoul National University

BLS9 Analysis of intracellular drug uptake using PFG NMR
Kyuhong Lee, Gyo-Seon Yeom, Jee-Hyun Cho, Chulhyun Lee, Chaejoon Cheong, Kwan Soo Hong
Korea Basic Science Institute

BLS10 Metabolomics by NMR: Assessment of Lentil Metabolite Diversity
Simone Rochfort, Craige Trenerry, Nathan Neumann, Joe Panozzo
Environmental Health and Chemistry, PIRVic, Department of Primary Industries

Chair: H. Fujiwara

BLS11 Diffusion based NMR and application
Maili Liu, Guoyun Bai, Xu Zzhang, Chaohui Ye
Wuhan Institute of Physics and Mathematics

BLS12 Development of a fully-adiabatic spin echo imaging sequence and its application to T_2 mapping in

the human brain at 4.7T
Fumiyuki Mitsumori[1], Hidehiro Watanabe[1], Nobuhiro Takaya[1], and Michael Garwood[2]
[1]National Institute for Environmental Studies, [2]University of Minnesota

BLS13 An improved protocol for small animal dynamic contrast-enhanced MRI and its related misregistration artifact of enhancing imaging pixels
Hideto Kuribayashi, Daniel P Bradley, Philip L Worthington, David R Checkley, Jean J Tessier and John C Waterton
AstraZeneca

BLS14 Mouse MRI probe for stereotaxic analysis
H. Wakamatsu[1], M. Yokoi[1], Y. Imaizumi[1], F. Sugihara[2], T. Ogino[3], and Y. Seo[1]
[1]Department of Regulatory Physiology, Dokkyo University School of Medicine, [2]Graduate School of Integrated Science, Yokohama City University, [3]Department of Biochemistry and Cellular Biology, National Institute of Neuroscience, National Center of Neurology and Psychiatry

19:40-21:30 **Banquet**

The 1st Asia-Pacific NMR Symposium (4th day)
November 11 (Fri)

8:30-10:15 **Parallel Session A & B**

Parallel Session A Solution NMR A4
Chair: F. Inagaki

ALL6 When NMR Beats X-ray in Solving Protein Structures
Ming-Daw Tsai
Genomics Research Center, Academia Sinica

ALS13 Solution Structures and Backbone Dynamics an Arsenate Reductase from *Bacillus subtilis:* Changes of Motional Properties Associated with the Conformational Switch upon Arsenate Reduction
You Li, Kuan Peng, Xianrong Guo, Bin Xia and Changwen Jin
Beijing Nuclear Magnetic Resonance Center,

ALS14 NMR evidence of domain swapping as a mechanism for regulating carbohydrate binding
Shih-Che Sue, Wei-Tin Lee, Jiun-Guo Yu, Wen-Jin Wu and Tai-huang Huang
Institute of Biomedical Sciences, Academia Sinica,

Chair: Ming-Daw Tsai

ALS15 Studies of the structures and interactions of chitin binding domains of chitinases
Kenichi Akagi[1] , Tohru Yamaguchi[2], Takanori Matsuura[1], Eriko Chikaishi[1], Izumi Yabuta[1], Yuko Nagasaki[3], Masashi Hara[3], Takeshi Watanabe[3], Hideo Akutsu[1], Atsushi Nakagawa[1], and Takahisa Ikegami[1]
[1]Institute for Protein Research, Osaka University, [2]Discovery Research Laboratories, Shionogi & Co., Ltd. [3]Faculty of Agriculture, Niigata University

ALS16 Determination of Recognition Sequences of Integrins $\alpha IIb\beta 3$, $\alpha v\beta 3$, and $\alpha 5\beta$-Specific Disintegrins by Rhodostomin and its Mutants
Woei-Jer Chuang, Chiu-Yueh Chen, Yi-Chun Chen, Yao-Husn Hsieh, Jia-Hau Shiu, and Yu-Chen Liu
Department of Biochemistry, National Cheng Kung University College of Medicine

ALS17 Cell-free synthesis of selectively isotope-labeled proteins for NMR studies
Kiyoshi Ozawa, Peter S. C. Wu, Madeleine J. Headlam, Dharshana Padmakshan, Slobodan Jergic, Nicholas E. Dixon and Gottfried Otting
Australian National University

Parallel Session B Solution NMR B4
Chair: Weontae Lee

BLL5 NMR Study on Membrane proteins-ligands Interactions
Ichio Shimada[1,2]
[1] Graduate School of Pharmaceutical Sciences, the University of Tokyo, [2] Biological Information Research Center (BIRC), National Institute of Advanced Industrial Science and Technology (AIST),

BLS15 A photochromic GFP-like protein and molecular/structural basis of the photochromism
Hideaki Mizuno[1], Tapas Kumar Mal[2], Akihiko Kikuchi[3], Markus Wälchli[4], Takashi Fukano[1],Ryoko Ando[1], Junichiro Taka[3], Jeyaraman Jeyakanthan[3], Yoshitsugu Shiro[3], Mitsuhiko Ikura[2], and Atsushi Miyawaki[1]
[1]Cell Function and Dynamics, Brain Science Institute, RIKEN, [2]Division of Molecular and Structural Biology, Ontario Cancer Institute and Department of Medical Biophysics, University of Toronto, [3]RIKEN Harima Institute/SPring-8, [4]Bruker Biospin Co. Ltd.

BLS16 The Use of Paramagnetic Metal Ions in NMR Studies of Protein Structures in Solution
Malene Ringkjøbing Jensen, Jens J. Led
University of Copenhagen

Chair: Daiwen Yang

BLS17 Conformation Transition of Fe-Coordinated Methionine in Thermophile *Hydrogenobacter thermophilus* Cytochrome *c*552
Shin-ichi J. Takayama[1], Yo-ta Takahashi[1], Hulin Tai[1], Shin-ichi Mikami[1], Tsuyoshi Udagawa[1], Hiroaki Sasaki[1], Shigenori Nagatomo[1], Hajime Mita[1], Yasuhiko Yamamoto[1], Yoshihiro Sambongi[2], Jun Hasegawa[3], Hikaru Hemmi[4], Ryo Kitahara[5], Shigeyuki Yokoyama[5], and Kazuyuki Akasaka[5]
[1]University of Tsukuba, [2]Hiroshima University, [3]Daiichi Pharmaceutical Co., Ltd., [4]National Food Research Institute, [5]RIKEN Harima Institute at Spring-8

BLS18 Determination of the Electronic and the Geometric Structure of the Metal Site of Metallo-proteins by Paramagnetic NMR
Jens J. Led, D. Flemming Hansen
University of Copenhagen

BLS19 Structure Determination of Cyclic Peptides of the Nocardamine Class from a Marine-Derived Bacterium of the Genus Streptomyces
Tae-Sik Kim, Hoshik Won
Department of applied chemistry, Hanyang Univ.

10:15-10:30 **Coffee Break**

10:30-12:00 **Parallel Sessions A & B**

Parallel Session A Solution NMR A5
Chair: Byong-Seok Choi

ALL7 Clean SEA-HSQC: a method to map solvent exposed amides in large non-deuterated proteins with gradient-enhanced HSQC
Donghai Lin, Kong Hung Sze and Guang Zhu
Dept. of Biochemistry, The Hong Kong University of Science and Technology

ALL8 Structure biology of ubiquitination and SUMOylation
Masahiro Shirakawa[1,2,3], Kenichiro Fujiwara[4], Ayako Ohno[5], Takeshi Tenno[1], Daichi Baba[1,4], Nobuo Maita[6], JunGoo Jee[7], Hidehito Tochio[4], Hidekazu Hiroaki[4]
[1]Graduate School of Engineering, Kyoto University, [2]RIKEN Genomic Science Center, [3]CREST, Japan Science and Technology Corporation, [4] Yokohama City University, [5]RIKEN, [6]Graduate

School of Systems Life Sciences, Kyushu University, [7]Laboratory of Chemical Physics, National Institute of Diabetes and Digestive and Kidney Diseases, National Institutes of Health, USA

ALS18 Solution structure of the DNA binding domain of RPA from Saccharomyces cerevisiae and its interaction with single-stranded DNA and SV40 T antigen
Chin-Ju Park, Joon-Hwa Lee, Sung-Jae Cho & Byong-Seok Choi
Department of Chemistry and National Creative Research Initiative Center, Korea Advanced Institute of Science and Technology,

ALS19 Recognition mechanism of the target by RNA aptamer and Musashi protein, studied with the aid of residue specific labeling, ^{13}C-detection and RDCs
Akimasa Matsugami[1], Yohei Miyanoiri[1], Hidehito Tochio[1], Yusuke Tamura[2], Michiko Kudo[2], Seiichi Uesugi[2], Tomoko Misono[3], Penmetcha Kumar[3], Takao Imai[4], Hideyuki Okano[4], Masato Katahira[1,5]
[1]International Graduate School of Arts and Sciences, Yokohama City University, [2]Graduate School of Environment and Information Sciences, Yokohama National University, [3]NAIST, [4]Keio University, [5]Genomic Sciences Center, RIKEN

Parallel Session B Solid State NMR B5
Chair: K. Takegoshi

BLL6 Industrial applications of solid state NMR using high magnetic fields
Koji Saito
Nippon Steel Corporation Advanced Research Technology Lab.

BLS20 Properties of carbon supported Pt catalysts studied by ^{13}C NMR
Kee Sung Han, Oc Hee Han
Daegu Center, Korea Basic Science Institute

BLS21 Geopolymers: A multinuclear SS NMR investigation of structural ordering
Peter Duxson[1], John L. Provis[1], Grant C. Lukey[1], Frances Separovic[2] and Jannie S.J. van Deventer[1]
[1]Department of Chemical and Biomolecular Engineering, [2]School of Chemistry The University of Melbourne

BLS22 High sensitive resistively-detected NMR experiments using all-electrical semiconductor GaAs nano-scale device
T. Ota[1,2], G. Yusa[1,2], K. Muraki[1], N. Kumada[1], S. Miyashita[3], and Y. Hirayama[1,2]
[1]NTT Basic Research Laboratories, [2]SORST-JST, [3]NTT-AT

12:00-13:15 **Lunch**

13:15-14:45 **Parallel Sessions A & B**

Parallel Session A Solution NMR A6
Chair: I. Shimada

ALL9 Structure, Function and Dynamics of a Novel Helicobacter pylori Response Regulator Protein
Weontae Lee
Department of Biochemistry and Biomolecular NMR Labortory, Yonsei University

ALL10 A General Strategy for the Assignment of Aliphatic Side-chain Resonances of Uniformly ^{13}C,^{15}N-labeled Large Proteins
Yingqi Xu, Zhi Lin, Chien Ho, Daiwen Yang
Department of Biological Sciences, National University of Singapore,

ALS20 Solution Structure of the Plant Defensin VrD1 from Mung bean: A Possible Mechanism for Insecticidal Activity Against Bruchids
Yaw-Jen Liu and Ping-Chiang Lyu

[1]Department of Life Sciences, [2]Institute of Bioinformatics and Structural Biology, National Tsing Hua University

ALS21 Chelerythrine binds at the BH groove of Bcl_{XL}, inhibiting its prosurvival activity by more than one mechanism
Yong-Hong Zhang, Mei Chin Lee, Kah Fei Wan, Shing-Leng Chan, Yu Chen Yang, Anirban Bhunia, Victor C. Yu and Yu-Keung Mok
National University of Singapore, Institute of Molecular and Cell Biology and Bioinformatics Institute

Parallel Session B Solid State NMR B6
Chair: H. Kaji

BLL7 Structure and dynamics of biologically active peptides and proteins bound to magnetically oriented vesicle systems as studied by solid-state NMR
Akira Naito
Graduate School of Engineering, Yokohama National University

BLS23 Development of modulated rf sequences for decoupling and recoupling of nuclear spin interactions in sample-spinning solid-state NMR
Yusuke Nishiyama[1], Toshio Yamazaki[1], and Takehiko Terao[2]
[1]RIKEN Genomic Sciences Center,[2]Graduate School of Science, Kyoto University

BLS24 Efficient Spin-Spin Scalar Coupling Mediated ^{13}C-^{13}C Polarization Transfer in Solid-State NMR Spectroscopy
Yun Mou, John C. H. Chao and Jerry C. C. Chan
Department of Chemistry, National Taiwan University,

BLS25 Determination of a spin diffusion constant by triplet-DNP
Akinori Kagawa[1], and Kazuyuki Takeda[1]
[1]Graduate School of Engineering Science, Osaka University

BLS26 ESR Detected by Measuring Mechanical Forces of a Cantilever in Samples of Low Spin Concentration
Sang Gap Lee, Sun Ho Won, Seung-Bo Saun, Soonchil Lee and Ki-Woong Kim
Department of Physics, Korea Advanced Institute of Science and Technology,

14:45-16:15 **Poster Presentations**

16:15-17:30 **Symposium 1**
Chair: K. Saito

PLL3 Developments in Single-Scan Multidimensional NMR and MRI
Lucio Frydman
Department of Chemical Physics, Weizmann Institute of Science

Chair: T. Nakamura

ALL13 Experimental Frontiers of Solid State NMR
A. Samoson, R. Stern, I. Heinmaa, T. Tuherm
National Institute of Chemical Physics and Biophysics Akadeemia

17:30-17:45 **Coffee Break**

17:45-18:45 **Symposium 2**
Chair: M. Shirakawa

ALS22 AvanceII – A Versatile NMR Spectrometer

Markus Wälchli

Bruker–BioSpin Japan

ALS23 Processing Strategies in Radial NMR Spectroscopy

Eric Kupce

Varian Ltd.,

ALS24 3D ESR-MRI with Sub-Micrometer Resolution Using Magnetic Resonance Force Microscopy

Yohsuke Yoshinari[1,2] and Shigenori Tsuji[1,2]

[1]Advanced Technology Division, JEOL Ltd., [2] CREST, Japan Science and Technology Agency,

18:45 **Closing**

Poster Presentations

November 8(Tue)	17:00 – 18:30	NP(even number) + AP(even number)
November 9(Wed)	13:30 – 15:00	NP(odd number)+AP(odd number)
November 10(Thu)	13:30 – 15:00	AP(even number)+NP(even number)
November 11(Fri)	14:45 – 16:15	AP(odd number)+NP(odd number)

Poster presentation

(A) Solution NMR

A-1. Methodology

NP1 Separation of each component in which has very close molecular weight in the DOSY method
Satoshi Sakurai
JEOL Ltd.

NP2(PL10) NDSB improves protein solution NMR spectra by suppressing protein aggregation
Takeshi Ishii, Kazuo Hosoda, Yasuko Iizuka, Kaori Wakamatsu, Hiroyuki Kogure, and Kenji Kubota
Department of Biochemical and Chemical Engineering, Faculty of Engineering, Gunma University

NP3 ^{1}H, ^{2}H, ^{13}C, and ^{15}N Full automatic pulse width calibrations for cryogenically cold probes
Nobuaki Nemoto[1], Yoshiaki Yamakoshi[1], Yoshiki Kida[1], Kaoru Tashiro[1], Sarara Kannari[1], Taku Kawahara[2], Koji Tsubono[2], Tamio Kanai[2], Tomomitsu Kurimoto[1], Katsuo Asakura[1], and Masami Hosono[1]
[1] JEOL Ltd., [2]JEOL Datum Ltd.

AP4 Two-dimensional ^{129}Xe-^{1}H heteronuclear overhauser spectroscopy (HOESY) using laser-polarized ^{129}Xe
Junko Fukutomi, Yuko Adachi, Hirohiko Imai, Atsuomi Kimura, and Hideaki Fujiwara
Division of Health Sciences, Graduate School of Medicine, Osaka University

AP5 NMR studies of stereo-array isotope-labeled (SAILed) proteins
Mitsuhiro Takeda[1], Takuya Torizawa[1], Tsutomu Terauchi[1], Akira M. Ono[1], Seiji Tsuchiya[1], Peter Guntert[2] and Masatsune Kainosho[1, 3]
[1]CREST, JST, [2]RIKEN GSC, 3Graduate School of Science, Tokyo Metropolitan University

AP6 Rapid acquisition of high resolution triple-resonance spectra using nonlinear sampling and maximum entropy reconstruction
Yoshiki Shigemitsu[1], Takahiro Anzai[1], Markus Waelchli[2] and Yutaka Ito[1,3,4]
[1]Department of Chemistry, Tokyo Metropolitan University, [2]Bruker Biospin, [3]Research Group for Bio-supramolecular Structure-Function, RIKEN, [4]CREST, JST

AP7 The study of inclusion complex formation of 4-sulfothiacalix(4)arene sodium salt with Xe by means of hyperpolarized ^{129}Xe NMR under continuous flow of the Xe gas
Yuko Adachi, Akari Kaneko, Junko Fukutomi, Atsuomi Kimura, and Hideaki Fujiwara
Division of Health Sciences, Graduate School of Medicine, Osaka University

AP8(PL15) A novel method for measuring the fast H/D exchange by ^{13}C observed 2D NMR
Kaoru Fujimura, Takeshi Tenno, Hidehito Tochio and Hidekazu Hiroaki
International Graduate School of Arts and Sciences, Yokohama City University

AP9 Molecular identification of uniformly stable isotope labeled animal cellsfor a hetero-nuclear NMR-based metabonomics
Michitaka Suto[1], Takashi Nishihara[1] Yuuri Tsuboi[3], Takashi Hirayama[1,2,3,4], and Jun Kikuchi[1,2,3]
[1]Int. Grad. Sch. Arts Sci., Yokohama City Univ, [2]RIKEN Plant Science Center,[3]RIKEN Plant Mol. Biol. Lab., [4]CREST, JST

AP10 Noise Suppression of NMR Signal by Piecewise Polynomial Truncated Singular Value Decomposition
Hoshik Won
Department of applied chemistry, Hanyang Univ.

AP11 Studies of Chemical Shift Anisotropy Shielding Effect in Co(III)-N,N'-Disalicylidene-diaminotoluene Macrocyclic Complexes

Changjun Lee, and Hoshik Won
Department of applied chemistry, Hanyang Univ.

A-2. Application to proteins and peptides

NP12(PL9) ^{19}F NMR Study of myoglobin bearing a fluorinated Heme -dynamics and thermodynamics of the acid-alkaline transition
Satoshi Nagao[1], Yueki Hirai[1], Shigenori Nagatomo[1], Hajime Mita[1], Yasuhiko Yamamoto[1], and Akihiro Suzuki[2]
[1]Department of Chemistry, University of Tsukuba, [2]Department of Materials Engineering, Nagaoka College of Technology

NP13 TRE box Recognition by Streptomyces Transcriptional Repressor TraR
Takeshi Tanaka[1], Chieko Komatsu[1], Kuniko Kobayashi[1], Mariko Sugai[1], Masakazu Kataoka[2], and Toshiyuki Kohno[1]
[1]Mitsubishi Kagaku Institute of Life Sciences (MITILS), [2]Department of Environmental Science and Technology, Faculty of Engineering, Shinshu University

NP14 Effect of input data on protein structure calculation with automated NOE assignment
Aiko Sakurai and Koshi Matsubara
Mitsubishi Chemical Group Science And Technology Research Center, Inc., Analytical Services Division, Yokohama Laboratory

NP15 Solution structure and function of ASABFd18c, antibacterial peptide isolated from a nematode, ascaris suum
Manabu Nakano[1], Tomoyasu Aizawa[1], Kazunori Miura[2], Hirokazu Hoshino[1],Mitsuhiro Miyazawa[3], Yuusuke Kato[3], Yasuhiro Kumaki[1], Makoto Demura[1], Sakae Tsuda[2], Keiichi Kawano[1], and Katsutoshi Nitta
[1]Division of Biological Sciences, Graduate School of Science, Hokkaido Univ., [2]National Institute of Advanced Industrial Science and technology, [3]National Institute of Agrobiological Science

NP16 Specific Interaction of Human TRF2 with a G-quadruplex Structure
Yuuka Hirao[1], Tadateru Nishikawa[2], Shingo Hanaoka[2], Hideyasu Okamura[2], Noriyuki Iwasaki[1], Satoko Akashi[1], Mamoru Sato[1] and Yoshifumi Nishimura[1]
[1] Graduate School of Integrated Science, Yokohama City University, [2] Kihara Memorial Yokohama Foundation for the Advancement of Life Science

NP17 Solution structure of a DNA-binding unit of FMBP-1 from *Bombyx mori*
Shin Saito[1], Daisuke Matsumoto[1], Kyosuke Kawaguchi[1], Takeshi Yamaki[1], Tomoyasu Aizawa[1], Shigeharu Takiya[2], Yasuhiro Kumaki[1], Makoto Demura[1], Katsutoshi Nitta[1], and Keiichi Kawano[1]
[1]Graduate School of Science, [2]Center for Advanced Science and Technology, Hokkaido University

NP18 NMR studies of the chromo domain from a histone acetyltransferase, Esa1
Hideaki Shimojo[1], Yoshihito Moriwaki[1], Masahiko Okuda[1,2], Masami Horikoshi[3], and Yoshifumi Nishimura[1]
[1]Graduate School of Integrated Science, Yokohama City University, [2]Kihara Memorial Yokohama Foundation for the Advancement of Life Sciences, [3]Laboratory of Developmental Biology, Institute of Molecular and Cellular Biosciences, University of Tokyo

NP19 The effect on the structure and activity of growth-blocking peptide by C-terminal elongation with parasitism
Yoshitaka Umetsu[1], Tomoyasu Aizawa[1], Kaori Muto [2],Hiroko Yamamoto[1], Mineyuki Mizuguchi[2], Makoto Demura[1],Katsutoshi Nitta[1], Yoichi Hayakawa[3], and Keiichi Kawano[1]

NP20 NMR structural study of a transducer protein *p*HtrII
Kokoro Hayashi[1], Yuki Sudo[2], Masaki Mishima[1], Naoki Kamo[2] and Chojiro Kojima[1]
[1]Graduate School of Biological Science, Nara Institute of Science and Technology, [2]Graduate School of Pharmaceutical Sciences, Hokkaido University

NP21 Structure and dimerization of rice phytochrome B PAS1domain
Toshitatsu Kobayashi[1], Masaki Mishima[1], Ryo Tabata[1],Kayo Akagi[2], Nobuya Sakai[2], Etsuko Katoh[2], Makoto Takano[2], Toshimasa Yamazaki[2] and Chojiro Kojima[1]
[1]Graduate School of Biological Sciences, Nara Institute of Science and Technology, [2]National Institute of Agrobiological Sciences

NP22 Dyanamic structure of DNA-binding domain of E.coli PhoB
Hideyasu Okamaura[1,2], Kozo Makino[3], and Yoshihumi Nishimura[1]
[1] Graduate School of Integrated Science, Yokohama City University, [2] Kihara Memorial Yokohama Foundataion for the Advancement of Life Sciences, [3] Department of Applied Chemistry, National Defence Academy

NP23 HSQC signal assignment of JSP1 by the novel method using wheat germ cell-free protein synthesis system
Akiko Iihara[1], Michiko Kitano[2], Keiko Matsubara[1], and Toshiyuki Kohno[2]
[1]ZOEGENE Corporation and [2]MITSUBISHI KAGAKU INSTITUTE OF LIFE SCIENCE

NP24 NMR structure of the PX Domain of Bem1p
Atsuhiko Maeda, Kenji Ogura, Masataka Horiuchi, Hiroyuki Kumeta, Yuko Fujioka, Fuyuhiko Inagaki
Department of Structural Biology, Graduate School of Pharmaceutical Sciences, Hokkaido University

AP25 Three-dimensional solution structure of the C-terminal domain of a novel galactose-binding protein from the earthworm
Hikaru Hemmi[1], Atsushi Kuno[2], Shigeyasu Ito[3], Ryuichiro Suzuki[3], Tsunemi Hasegawa[3] and Jun Hirabayashi[2]
[1]National Food Research Institute, [2]Research Center for Glycoscience, National Institute of Advanced Industrial Science and Technology (AIST), 3Department of Material and Biological Chemistry, Yamagata University

AP26 The structural transition of the fifteen residue peptide on the ganglioside GM1 micelles.
Naoki Fujitani[1], Hiroki Shimizu[2], Teruhiko Matsubara[3], Takashi Ohta[2], Noriko Nagahori[1], Yayoi Yoshimura[1], Yuuki Komata[1], Toshinori Sato[3], and Shin-ichiro Nishimura[1,2]
Division of Biological Sciences, Graduate School of Science, Frontier Rsearch Center for Post-Genomic Science and Technology, Hokkaido University, [2]Rsearch Center for Glycoscience, National Institute of Advanced Industrial Science and Technology (AIST), [3]Department of Biosciences and Informatics, Keio University

AP27 Solution structure of the mouse TRP14 protein homologous to the human TRP14 protein
Naoya Tochio [1], Seizo Koshiba [1], Makoto Inoue [1], Yoshihide, Hayashizaki [1], Takanori Kigawa [1,2], and Shigeyuki Yokoyama [1,3,4]
[1]RIKEN GSC, [2]Tokyo Inst. of Tech., [3]RIKEN Harima, [4]Univ.of Tokyo

AP28 Examination of the solution structures between native and E. coli-expressed membrane proteins
H. suzuki, Y. Mochizuki, Y. Shimada, M. Kobayashi, T. Nozawa, and S. Otomo(Z.-Y. Wang)
Faculty of Science, Ibaraki University

AP29 Mouse structure proteomics: solution structure of the mouse enhancer of rudimentary protein reveals a novel fold
Hua Li[1], Makoto Inoue[1], Takashi Yabuki[1], Masaaki Aoki[1], Eiko Seki[1], Takayoshi Matsuda[1], Emi Nunokawa[1], Yoko Motoda[1], Atsuo Kobayashi[1],Takaho Terada[1,2], Mikako Shirouzu[1,2], Seizo Koshiba[1], Yi-Jan Lin1, Peter Guntert[1], Harukazu Suzuki[1], Yoshihide Hayashizaki[1], Takanori Kigawa[1], and Shigeyuki Yokoyama[1,2,3]
[1]RIKEN GSC, [2]RIKEN Harima Institute and [3]The University of Tokyo

AP30(PL11) Variable pressure NMR reveals the entire energy landscape of a protein: A conserved exited state conformer between ubiquitin and ubiquitin-like protein NEDD8

Ryo Kitahara[1], Eri Sakata[2], Takeshi Kasuya[2], Yoshiki Yamaguchi[2], Koichi Kato[2,3], Keiji Tanaka[4], Shigeyuki Yokoyama[1,3,5], and Kazuyuki Akasaka[1,6]
[1]RIKEN Harima Institute, [2]Department of Structural Biology and Biomolecular Engineering, Graduate School of Pharmaceutical Sciences, Nagoya City University, [3]RIKEN Genomic Sciences Center, [4]Department of Molecular Oncology, Tokyo Metropolitan Institute of Medical Science, [5]Department of Biophysics and Biochemistry, Graduate School of Science, The University of Tokyo, [6]Department of Biotechnological Science School of Biology-Oriented Science and Technology, Kinki University

AP31 NMR characterization of a refolding intermediate of β_2-microglobulin

Atsushi Kameda[1], Masaru Hoshino[1], Takashi Higurashi[1], Masato Shimizu[2], Eugene Hayato Morita[2], SatoshiTakahashi[1], Hironobu Naiki[3,4] and Yuji Goto[1,4]
[1]Inst. Protein Res., Osaka Univ., [2]INCS, Ehime Univ., [3]Fac. Med. Sci., Univ. of Fukui, [4]CREST/JST

AP32 Structure determination of the DNA binding domain in ERCC-1/ XPF heterodimer

Mika Masuyama [1,2] , Sonoko Ishino [1], Izuru Ohki [1], Tatsuya Nishino [1], Hiroshi Moriuchi [1], Hiroshi Ueno [2], Kousuke Morikawa [1], and Shin-ichi Tate [1],
[1] Biomolecular Engineering Research Institute (BERI), [2] Nara Women's University

AP33 Structure of carboxyl-terminal domain of transcription factor Hex in complex with transcription factor HNF1a POU_S domain

Shinichiro Asai[1], Yuki Horie[1], Ojeil F. Ezomo[1], Tamio Noguchi[2], and Shunsuke Meshitsuka[1]
[1] Institute of Regenerative Medicine and Biofunction,Tottori University Graduate School of Medical Science, [2]Nagoya University Graduate School of Bioagricultural Sciences

AP34 Solution structure of two human Myb-like DNA-binding domain repeats

Yukiko Doi-Katayama[1], Fumiaki Hayashi[1], Makoto Inoue[1], Takanori Kigawa[1], Shigeyuki Yokoyama[1,2,3], and Hiroshi Hirota[1,4]
[1]RIKEN Genomic Sciences Center, [2] RIKEN Harima Institute at SPring-8, [3] Graduate School of Science, The University of Tokyo, [4] Graduate School, Yokohama City University

AP35 Solution structure of the hydrophobic helix of NRSF/REST bound to the PAH1 domain of mSin3B

Mitsuru Nomura[1,2], Hiroko Uda-Tochio[3], Kiyohito Murai[4], Nozomu Mori[5], and Yoshifumi Nishimura[1]
[1]Graduate School of Supramolecular Biology, Yokohama City University, [2]Kihara Memorial Yokohama Foundation for the Advancement of Life Sciences, [3]RIKEN Genomic Sciences Center, [4]Division of Neuroscience, Beckman Research Institute, City of Hope, [5]Department of Anatomy and Neurobiology, Nagasaki University School of Medicine

AP36 Structural and functional analyses of the antifreeze-like domain of human sialic acid synthase

Yoko Ito[1], Toshiyuki Hamada [1,2], Takamasa Abe[2] , Fumiaki Hayashi[2] , Peter Guntert[2], Makoto Inoue[2] , Takanori Kigawa[2], Takaho Terada[2], Mikako Shirouzu[2], Mayumi Yoshida[2] , Akiko Tanaka[2], Sumio Sugano[3] , Shigeyuki Yokoyama[1,4,5], and Hiroshi Hirota[1,2].
[1] Graduate School of Yokohama City University, [2]RIKEN Genomic Sciences Center, [3]Graduate School of Frontier Sciences, TheUniversity of Tokyo, [4]RIKEN Harima Institute at SPring-8, [5] Graduate School of Science, The University of Tokyo

AP37 NMR study on the interaction of the transactivation domain of ATF-2 with MAP kinase p38 α

Michiko Ishizu , Noriyuki Iwasaki , Aritaka Nagadoi ,and Yoshifumi Nishimura
Graduate School of Supramolecular Biology, Yokohama City University

AP38 Aromatic-amide interactions in glycine- and tyrosine-rich, repetitive sequences as revealed by NMR

Yasuhiro Kumaki[1], Manabu Nakano[2], Masakatsu Kamiya[2], Tomoyasu Aizawa[2], Makoto Demura[2], Keiichi Kawano[1,2], and Norio Matsushima[3]
[1]High-Resolution NMR Laboratory, [2]Division of Biological Sciences, Graduate School of Science, Hokkaido University, [3]School of Health Sciences, Sapporo Medical University

AP39 Observation of protein binding to membrane with photo-CIDNP technique

Takahide Kouno[1], Meneyuki Mizuguchi[1], Yoshihiro Mori[1], Isei Tanida[2], Takashi Ueno[2], Eiki Kominami[2], and Keiichi Kawano[3]
[1]Faculty of Pharmaceutical Sciences, Toyama Medical and Pharmaceutical University, [2]Department of Biochemistry, Juntendo University of Medicine, [3]Division of Biological Sciences, Graduate School of Science, Hokkaido University

AP40(PL13) Solution structure of the cytoplasmic region of Na^+ /H^+ exchanger-1 complexed with the essential cofactor, calcineruin B homologous protein-1

Masaki Mishima[1], Shigeo Wakabayashi[2] and Chojiro Kojima[1]
[1]Graduate School of Biological Sciences, Nara Institute of Science and Technology, [2]Department of Molecular Physiology National Cardiovascular Center Research Institute

AP41 Solution structure and dynamics of Ufm1, a novel ubiquitin-like post-translational modifier

Hiroaki Sasakawa[1], Eri Sakata[2], Yoshiki Yamaguchi[2], Masaaki Komatsu[3], Keiji Tanaka[3], and Koichi Kato[1,2]
[1]Institute for Molecular Science, [2]Graduate School of Pharmaceutical Sciences, Nagoya City University,

AP42 NMR studies on the 57kDa Escherichia coli periplasmic oligopeptide binding protein OppA

Kayano Moromisato[1], Kaori Kurashima-Ito[2,3], Kaoru Nishimura[4], Jeremy Tame[4] and Yutaka Ito[1,3,5]
[1]Department of Chemistry, Tokyo Metropolitan University, [2]Molecular and Cellular Physiology Laboratory, Graduate School of Integrated Science, Yokohama City University, [3]Research Group for Bio-supramolecular Structure-Function, RIKEN, [4]Protein Design Laboratory, Graduate School of Integrated Science, Yokohama City University, [5]CREST, JST

AP43 Structural and Functional Characterization of WSSV Novel Protein VP230

Yang Liu, Jinlu Wu, Sivaraman Jayaraman, Choy Leong Hew
Department of Biological Sciences, National University of Singapore

AP44 Structural Basis of Syndecan-4 Function and Its Interaction with Syntenin1 PDZ2 domain complex

Bon-Kyung Koo[1], John R. Couchman[3], Eok-Soo Oh[2], and Weontae Lee[1]
Department of Biochemistry and Protein Network Research Center, College of Science, Yonsei University, Seoul Korea

AP45 Solution structure of SSD domain of Bacillus subtilis Lon protease

Iren Wang, Yuan-Chao Lou, Shih-Chi Lo, Alan Yueh-Luen Lee, Chinpan Chen and Shih-Hsiung Wu
Institute of Biological Chemistry and Institute of Biomedical Sciences, Academia Sinica, Institute of Biochemical Sciences, National Taiwan University

AP46 Structure of the C-terminal domain of insulin-like growth factor binding protein-2 (IGFBP-2) and interactions with IGFs: An NMR study

Zhihe Kuang[1,2], Shenggen Yao[1], David W. Keizer[1], Chunxiao C. Wang[1], Kerrie A. McNeil[2], Briony E. Forbes[2], Leon A Bach[3], John C. Wallace[2] and Raymond S. Norton[1]
[1] The Walter and Eliza Hall Institute of Medical Research, [2] School of Molecular and Biomedical Science, The University of Adelaide, [3] Department of Endocrinology and Diabetes and Monash University Department of Medicine,

AP47 Domain organization and dimer-interface structure of severe acute respiratory syndrome-associated coronavirus nucleocapsid protein

Chung-ke Chang, Shih-Che Sue, Cheng-Kun Tsai, Yen-Chieh Chiang, Wen-Jin Wu and Tai-huang Huang
Institute of Biomedical Sciences, Academia Sinica

AP48 Direct NMR Resonance Assignments of the Active Site Histidine Residue in Serine Protease: The Case of Escherichia coli thioesterase/protease I (TEP-I)

Wen-Jin Wu, S. I. Tyukhtenko and T-h Huang
Institute of Biomedical Sciences, Academia Sinica

AP49 Characterization and structural analyses of nsLTP1 from mung bean

Ku-Feng Lin[1], Yu-Nan Liu,[1] Shang-Te D. Hsu,[2] Chao-Sheng Cheng,[1] Dharmaraj Samuel,[1] Alexandre M. J. J. Bonvin,[2] and Ping-Chiang Lyu[1]
[1] Department of Life Sciences, National Tsing Hua University, [2] NMR Department, Bijvoet Center for Biomolecular Research, Utrecht University

AP50 THE HATH DOMAIN OF HUMAN HEPATOMA-DERIVED GROWTH FACTOR CAN FORM A DOMAIN-SWAPPED DIMER WITH MUCH HIGHER AFFINITY FOR HEPARIN AS CELL INTERNALIZATION

Wei-Tin Lee[1], Shih-Che Sue[1], Chia-hui Wang[2], Jiun-Guo Yu[1], Szi-chieh Yu[1], Shao-Chen Lee[2], Wen-Jin Wu[1], Wen-guey Wu[2]*, and Tai-huang Huang[1]*
[1]Institute of Biomedical Sciences, Academia Sinica., [2]Institute of Bioinformatics and Structural Biology, College of Life Sciences, National Tsing Hua University

AP51 Structural basis of the Sso7c4 protein with novel DNA-binding fold from Sulfolobus solfataricus

Chun-Hua Hsu and Andrew H.-J. Wang
Institute of Biological Chemistry, Academia Sinica

AP52 Insight into the inhibition of human lysozyme amyloidogenesis by camelid antiboty binding

S.-T.D. Hsu, P.-H. Chan, M. Dumoulin, J. Christodoulou, J.R. Kumita, E. Pardon, S. Muyldermans, L. Wyns, C.V. Robinson and C.M. Dobson
Department of Chemistry University of Cambridge

AP53 Solution Structure of UBL Domain in PAPase I, a Novel CTD Phosphatase

Sunggeon Ko, Junghye Huh, Jong-Bok Yoon and Weontae Lee
Department of Biochemistry, College of Science, and Protein Network Research Center, Yonsei University.

AP54 Structure and molecular dynamics simulation of antimicrobial peptides from frog

Won-Je Kim,Woo-sung Son,Yong-jin Kim,Min-duk Seo, and Bong-jin Lee
National Research Laboratory(MPS) College of Phamacy

AP55 Solution Structures and Anticancer Activities of 11-residue Peptide Analogues Derived from an Antimicrobial Peptide, Gaegurin 5

Hyun-Jung Kim, Min-Duk Seo, Hyung-Sik Won, and Bong-Jin Lee
National Research Laboratory (MPS)College of Pharmacy

AP56 Structural characterization of urease accessory proteins

Na Young Sohn, Ji-Hoon Kim, Hyung-Sik Won, and Bong-Jin Lee
National Research Laboratory, College of Pharmacy, Seoul National University

AP57 RNA binding modes of Escherichia coli RNase P protein.

Jae-Sun Shin, Jiyoung Park, Junsang Ko, Seong-Ok Kim, and Byong-Seok Choi
Korea Advanced Institute of Science and Technology

AP58 Structural characterization of the transcription factor BldD, from Streptomyces coelicolor A3(2): Domain composition, interdomain interaction, and DNA binding

Hyun-Suk Ko[1], Chang-Jin Lee[2], Sa-Ouk Kang[2], Bong-Jin Lee[3], and Hyung-Sik Won[1]
[1]Department of Biotechnology, Division of Life Sciences, College of Biomedical & Health Science, Konkuk University, [2]School of Biological Sciences, Seoul National University, [3]College of Pharmacy, Seoul National University

AP59 Studies of Protein Domains in the Transacylase Component of Human Mitochondrial Branched-Chain Ketoacid Dehydrogenase

Chi-Fon Chang[1], Yi-Jan Lin[2], Hui-Ting Chou[3], Max Wynn[4], David T. Chuang[4], Tai-Huang Huang[1]
[1]Gemomics Research Center, Academia Sinica, [2]RIKEN Genomic Sciences Center, [3]Institute of Biomedical Sciences Academia Sinica, [4]Dept of Biochemistry, U. of Texas Southwestern Medical Center

AP60 Solution Structure and Dynamics of YKR049C, a Putative Redox Protein from *Saccharomyces cerevisiae*

Jin-Won Jung [1,3] , Chul-Jin Lee [1,3] , Adelinda Yee [2,3] , Bin Wu [2,3] , Cheryl H. Arrowsmith [2,3] and Weontae Lee [1,3*]
[1] Department of Biochemistry and Protein Network Research Center, Yonsei University, [2] Ontario Cancer Institute and Department of Medical Biophysics, University of Toronto, [3] Northeast Structural Genomics Consortium

AP61 NMR and structural studies of a putative polyketide synthesis protein XC5357 from a plant pathogen Xanthomonas campestris

K.-H. Chin, C.-L. Zhu, S.-H. Chou
Institute of Biochemistry, National Chung-Hsing University

AP62 Solution Structure and Structural Characterization of Selective Melanocortin Receptor Antagonists

Chul-Jin Lee[1] , Song-Zhe Li[2], Sung-Kil Lim[2], Ja-Hyun Baik[3] and Weontae Lee [1]
[1] Department of Biochemistry and HTSD-NMR & Application National Research Laboratory, College of Science, Yonsei University, [2]Department of Internal Medicine, College of Medicine, Yonsei University, [3]School of Life Science and Biotechnology, Korea University

AP63 Structural and Functional Characterization of a Telomere Binding Protein, NgTRF1 Derived from *Nicotiana glutinosa*

Heeyong Park[1], Sunggeun Ko[1], Hansol Bae[2], Woo Taek Kim[2] and Weontae Lee[1]
[1]Department of Biochemistry and HTSD-NMR & Application National Research Laboratory, College of Science, Yonsei University, [2]Department of Biology, Yonsei University

AP64 NMR Studies on Integrase Interactor1/hSNF5

Hyun-Seob Jung, Jin-Won Jung, Joon Shin and Weontae Lee
Department of Biochemistry and HTSD-NMR & Application National Research Laboratory, Yonsei University

AP65 Solution Structure of Modified Human Parathyroid Hormones: Towards Minimal and Potent Ligand Design for Receptor Activation

Suhyun Ma[1], Ahrim Yoo[2], Sung-Kil Lim[3] and Weontae Lee[1]
[1]Department of Biochemistry and Protein Network Research Center, HTSD-NMR & Application National Research Laboratory, College of Science, Yonsei University, [2]Department of Chemical and Biological Engineering,[3]Department of Internal Medicine, School of Medicine

AP66 Solution Structure and Dynamics of the Domain III of the JEV and DENV Envelope Proteins

Jya-Wei Cheng, Chih-Wei Wu, Yi-Ting Lin, Ya-Ping Tsao,Kuo-Chun Huang, and Suh-Chin Wu
Institute of Biotechnology and Department of Life Science, National Tsing Hua University

AP67 Structure of Human Growth Inhibitory Factor-Metallothionein-3

Hui Wang [‡], Bin Cai [¶], Hongyan Li [‡], Zhong-Xian Huang [¶] and Hongzhe Sun [‡]
[‡] Department of Chemistry and Open Laboratory of Chemical Biology, The University of Hong Kong, [¶] Department of Chemistry, Fudan University

AP68 Solution Structures and Dynamics of the Sterile α Motif (SAM) Domain of the Deleted in Liver Cancer 2 (DLC2): a Monomeric Structure with Membrane-binding Properties

Hongzhe Sun, [†], Hongyan Li, [†] King-Leung Fung, [†] Dong-Yan Jin, [§] Stephen SM Chung, Yick-Pang Ching, [§] Irene Oi-lin Ng, [¶] Kong-Hung Sze, [‡] Ben CB Ko [†]
[†] Department of Chemistry and Open Laboratory of Chemical Biology, Department of [§] Biochemistry,[#] Physiology and [¶] Pathology, The University of Hong Kong,

A-3. Application to nucleic acids and their complexes, lipids, and polysaccharides

NP69 NMR study of the specific interaction of human TRF1 on DNA containing telomeric sequence

Shin Morita[1], Yuuka Hirao[1], Hideyasu Okamura[1,2], and Yoshifumi Nishimura[1]

[1] Yokohama City University, Graduate School of Integrated Science, [2]Kihara Memoriaru Yokohama Foundation for the Advancement of Life Science

AP70(PL12) NMR structural analysis of the CGG / CGG containing DNA complexed with the recognition drugs

Makoto Nomura[1], Shinya Hagihara[2,3], Yuki Goto[2], Kazuhiko Nakatani[2,3,4] and Chojiro Kojima[1]
[1]Graduate School of Biological Science, Nara Institute of Science and Technology, [2]Department of Synthetic Chemistry and Biological Chemistry, Graduate School of Engineering, Kyoto University, [3]PRESTO, Japan Science and Technology Agency, [4]The Institute of Scientific and Industrial Research, Osaka University

AP71 NMR spectral analyses of three structural isomers of disubstituted -β-cyclodextrins by glucose groups and their inclusion phenomena

Yu Tsutsumi[1,2], Yasuko Ishizuka[1], and Hiroshi Nakanishi[1,2]
[1] Biological Information Research Center and Research Center for Compact Chemical Process; National Institute of Advanced Industrial Science and Technology, Tsukuba Central, [2] Department of Biological Science and Technology, Tokyo University of Science

AP72 Application of ultra-high magnetic field to saccharide molecules: ^{1}H NMR spectra of glycosyl α-CD and glycosyl β-CD

Yasuko Ishizuka[1、2], Kenji Takasugi[3], Yu Tsutsumi[2,4], Kenji Kanazawa[2], Tadashi Nemoto[2], Tsukasa Kiyoshi[5], and Hiroshi Nakanishi[2,4,6*]
[1] Research Center for Glycoscience, National Institute of Advanced Industrial Science and Technology, Japan, [2] Biological Information Research Center, National Institute of Advanced Industrial Science and Technology, Japan, [3] JEOL Ltd., [4] Department of Biological Science and Technology, Tokyo University of Science, [5] Tsukuba Magnet Laboratory, National institute for Materials Science, [6] Research Center for Compact Chemical Process, National Institute of Advanced Industrial Science and Technology

A-4. Application to genomic science

NP73 Solution structure of the LIM domain of human CLP-36 protein

Xu-rong Qin[1], Fumiaki Hayashi[1], Mikako Shirouzu[1,2], Takaho Terada[1,2], Takanori Kigawa[1], Makoto Inoue[1], Takashi Yabuki[1], Masaaki Aoki[1], Eiko Seki[1], Takayoshi Matsuda[1], Hiroshi Hirota[1], Mayumi Yoshida[1], Akiko Tanaka[1], and Shigeyuki Yokoyama[123]
[1]RIKEN GSC、[2]RIKEN Harima Institute and [3]University of Tokyo

NP74 Human structure proteomics: solution structure of the RGS domain of regulator of G-protein signaling 5 (RGS 5)

Huiping Zhang[1], Fumiaki Hayashi[1], Mikako Shirouzu[1,2], Takaho Terada[1,2], Takanori Kigawa[1], Makoto Inoue[1], Takashi Yabuki[1], Masaaki Aoki[1], Takayoshi Matsuda[1], Eiko Seki[1], Hiroshi Hirota[1], Mayumi Yoshida[1], Akiko Tanaka[1], Sumio Sugano[3], and Shigeyuki Yokoyama[1,2,4]
[1]RIKEN GSC, [2]RIKEN Harima Institute, [3]The Institute of Medical Science, The University of Tokyo and [4]Graduate School of Science, The University of Tokyo

NP75 Solution structure of the two CUT domains of SATB2

Kyoko Inoue[1], Toshio Nagashima[1], Fumiaki Hayashi[1], Mikako Shirouzu[1,2], Takaho Terada[1,2], Takanori Kigawa[1], Makoto Inoue[1], Takashi Yabuki[1], Masaaki Aoki[1], Takayoshi Matsuda[1], Eiko Seki[1], Hiroshi Hirota[1], Mayumi Yoshida[1], Akiko Tanaka[1], Osamu Ohara[3,4], and Shigeyuki Yokoyama[1,2,5]
[1]RIKEN Genomic Sciences Center, [2]RIKEN Harima, [3]RIKEN RCAI, [4]Kazusa DNA Research Institute, [5]Graduate School of Science, University of Tokyo

NP76 Structural and functional analysis of MSP domains

Hiroshi Endo[1], Fumiaki Hayashi[1], Mayumi Yoshida[1], Mikako Shirouzu[1,2], Takaho Terada[1,2], Takanori Kigawa[1], Makoto Inoue[1], Takashi Yabuki[1], Masaaki Aoki[1], Takayoshi Matsuda[1], Eiko Seki[1], Hiroshi Hirota[1], Akiko Tanaka[1], Yoshihide Hayashizaki[1], and Shigeyuki Yokoyama[1,2,3]
[1]RIKEN GSC, [2]RIKEN Harima Institute, Graduate School of Science, [3]The University of Tokyo

NP77 Structural and Functional analysis of immunoglobulin like domains

Reiko Hatta[1], Fumiaki Hayashi[1], Kayoko Nagashima[1], Chisato Kurosaki[1], Xu-rong Qin[1], Mayumi Yoshida[1], Mikako Shirouzu[1,2], Takaho Terada[1,2], Takanori Kigawa[1], Makoto Inoue[1], Takashi Yabuki[1], Masaaki Aoki[1], Takayoshi Matsuda[1], Eiko Seki[1], Hiroshi Hirota[1], Akiko Tanaka[1], Osamu Ohara[3,4], and Shigeyuki Yokoyama[1,2,5]
RIKEN GSC[1], RIKEN Harima Institute[2], RIKEN RCAI[3], KAZUSA DNA Institute[4], Graduate School of Science, The University of Tokyo[5]

NP78 Solution structure of nuclear move domain of nuclear distribution gene C homolog

Toshio Nagashima[1], Fumiaki Hayashi[1], Mikako Shirouzu[1,2], Takaho Terada[1,2], Takanori Kigawa[1], Makoto Inoue[1], Takashi Yabuki[1], Masaaki Aoki[1], Takayoshi Matsuda[1], Eiko Seki[1], Hiroshi Hirota[1], Mayumi Yoshida[1], Akiko Tanaka[1], Yoshihide Hayashizaki[1], and Shigeyuki Yokoyama[1,2,3]
[1]RIKEN Genomic Sciences Center, [2]RIKEN Harima, and [3]Graduate School of Science, University of Tokyo

AP79 KUJIRA, a package of integrated modules for systematic and interactive analysis of NMR data: Application to quick and accurate structure analysis in combination with CYANA calculations

N. Kobayashi[1], S. Koshiba[1], P. Guntert[1], S. Sugano[4], T. Kigawa[1] and S. Yokoyama[1,2,3]
[1]RIKEN GSC, [2]RIKEN Harima Institute, [3]Graduate School of Science, The university of Tokyo, [4]Graduate School of Frontier Sciences, The university of Tokyo

A-5. Organic and natural products

AP80(PL14) Methodological advances in a hetero-nuclear NMR-based metabolomics by stable isotope labeling of *Arabidopsis thaliana*

Yasuyo Sekiyama[1], Takashi Hirayama[2,3,4], Kazuo Shinozaki[1,4,5], Kazuki Saito[1,3,6] and Jun Kikuchi[1,2,3]
[1]RIKEN Plant Science Center, [2]International Graduate School of Arts and Sciences, Yokohama City University, [3]CREST, JST, [4]RIKEN Genomic Sciences Center, [5]RIKEN Plant Molecular Biology Laboratory, [6]Graduate School of Pharmaceutical Sciences, Chiba University.

AP81 Selective Me-HMBC, A NEW TECHNIQUE USEFUL FOR IMPROVING SENSITIVITY OF HMBC CROSS PEAKS OF METHINE PROTON SIGNALS ATTACHED TO A METHYL GROUP

Kazuo Furihata[1], and Haruo Seto[2]
[1]Division of Agriculture and Agricultural Life Sciences, University of Tokyo. [2]Dept. of Applied Biology and Chemistry, Tokyo University of Agriculture

AP82 Complete Assignment and Conformation of Kadsuphilactone A, A Novel Triterpene Dilactone from *Kadsura philippinensis*

Ya-Ching Shen[1], Yu-Chi Lin[1], Chi-Fon Chang[2], Tai-huang Huang[2], and Yuan-Bin Cheng[1]
[1]Department of Marine Resources, National Sun Yat-Sen University, [2]Institute of Biomedical Science, Academia Sinica

AP83 Tasumatrols P-T, Five New Taxoids from *Taxus sumatrana*

Ya-Ching Shen, Yun-Sheng Lin, Shaw-Man Hsu, Shih-Sheng Wang, Ching-Te Chien, Yao-Haur Kuo, Chang-Hung Chou and Ashraf Taha Khalil
Institute of Marine Resources National Sun Yat-sen University

AP84 Structural Studies of the Stereochemical Cycloadducts of Bicyclolactone via Diels-Alder Reaction

Chanwoo Seo, Hoshik Won
Department of applied chemistry, and Hanyang Univ.

AP85 Solution State Structure of gallium-binding Bleomycin-A2 by NMR

Misun Lee, and Hoshik Won
Department of applied chemistry, Hanyang Univ.

AP86-1 ^{129}Xe NMR of hyperpolarized xenon adsorbed on calixarenes

Young Ju Lee(1)(2), Ki Deok Park(1), Kye Chun Nam(2), Kikuko Hayamizu(3), Mineyuki Hattori(3)
(1) Gwangju Center, Korea Basic Science Institute(KBSI), (2) Department of Chemistry, Chonnam National University, (3) National Institute of Advanced Science and Technology (AIST)

AP86-2 Slice selection applied to BPPLED and LED DOSY pulse sequences
Ki Deok Park, Young Ju Lee
Gwangju Center, Korea Basic Science Institute

A-6. Inorganic and analytical chemistry

AP87 NMR Studies of Oxo- and Peroxo-vanadium(V) Complexes of malate ligand
Sam-Soo Park, Jun-Kyu Lee, Man-Ho Lee, and Jong Rack Sohn
Department of Applied Chemistry, Kyungpook National University

(B) Solid state NMR

B-1. Methodology

NP88 ^{2}H natural-abundance MAS-NMR under high field of 21.9 T
Takashi Mizuno[1], Kiyonori Takegoshi[2], Masataka Tansho[3], and Tadashi Shimizu[3]
[1]JEOL ltd., [2]Faculty of Science, Kyoto University, [3]NIMS

NP89 MQMAS with strong RF pulses using a microcoil
Munehiro Inukai[1], Kazuyuki Takeda[1], and Masahiro Kitagawa[1]
[1]Graduate School of Engineering Science, Osaka University

NP90 The power of super high magnetic field (21.8 T) solid state NMR for practical inorganic materials
Yasuhiro Tobu[1], Keiji Shimoda[1], Koji Kanehashi[1], Moriaki Hatakeyama[1], Koji Saito[1], and Tadashi shimizu[2]
[1]Advanced Technology Research Laboratories, Nippon Steel Corporation, [2] Independent Administrative Institution National Institute for Materials Science

AP91 Remarkable reduction of RF power by duration & amplitude time averaged spin exchange at magic angle in solid-state NMR spectroscopy
Katsuyuki Nishimura, and Akira Naito
Graduate School of Engineering, Yokohama National University

AP92(PL3) Novel solid-state NMR approach for structural analysis of proteins and peptides utlizing ^{13}C chemical shift.
Yoh Matsuki[1,2], Hideo Akutsu[2], and Toshimichi Fujiwara[2]
[1]JST-BIRD, [2]Institute for Protein Research, Osaka University

AP93 Separation of chemical-shift anisotropy under magic-angle spinning using a new scheme of two-dimensional acquisition
Masashi Fukuchi, and Kiyonori Takegoshi
Department of Chemistry, Graduate School of Science, Kyoto University

AP94 One-dimensional solid-state NMR methods using selective soft pulses to detect the through-space ^{13}C-^{13}C correlation: Homonuclear cross polarization
Qing Luo, Hironori Kaji, and Fumitaka Horri
Institute for Chemical Research, Kyoto University

AP95 A new technique for cross polarization compatible with high spinning frequencies and high magnetic fields.
Weng Kung Peng, Kazuyuki Takeda, and Masahiro Kitagawa
Osaka University, Japan

B-2. Application to polymer science

NP96 Structural analysis of poly(γ -biphenylmethyl-L-glutamate) and poly(γ -biphenylethyl-L-glutamate) by solid state NMR
Ayaka Minemura[1], Yuko Oonishi[1], Hiromichi Kurosu[1] and Junzi Watanabe[2]
[1] School of Natural Science and Ecological Awareness, Graduate School of Humanities and Sciences, Nara Women's University, [2]Department of Organic and Polymeric Materials, Tokyo Institute of Technology

NP97 Higher-order structure of poly (ethylene-co-1,5-hexadien) as studied by solid state NMR and quantum chemistry
Yuuri Yamamoto[1], Aki Fujikawa[1], Masato Sone[2], Shigemitsu Murase[3], Naofumi Naga[4] and Hiromichi Kurosu[1]
[1]School of Natural Science and Ecological Awareness, Graduate School of Humanities and Sciences, Nara Women's University, [2]Department of Chemical Engineering, Tokyo University of Agriculture & Technology, [3]Department of Organic and Polymer Materials Chemistry, Tokyo University of Agriculture & Technology, [4]Department of Applied Chemistry, Shibaura Institute of Technology

NP98 Morphological deformation and enzymatic degradation of biodegradable polyester
T. Morimura,S. Maruno,K. Kasuya, T. Yamanobe and T. Komoto
Department of Chemistry, Gunma University

NP99 Crystallization behavior and morphology of poly(m-xylylene adipamide)
Hiroyuki Shida, Akira Igarashi, Hiroki Uehara, Takeshi Yamanobe and Tadashi Komoto
Department of Chemistry, Gunma University

NP100 Dependence on Mixing Ratio of Crystallinity and Miscibility:Solid-State ^{13}C NMR study of Semicrystalline Poly(vinyl isobutyl ether)/ Poly(ε-L-lysine) Blends
Yoshifumi Murata, Atsushi Asano, and Takuzo Kurotsu
Department of Applied Chemistry, National Defense Academy

NP101 Crystallization behavior of vinylidene chloride copolymers
M. Mochida[1], T. Yamanobe[1], T. Komoto[1], M. Honda[2] and N. Anazawa[2]
[1]Department of Chemistry, Gunma University, [2]Asahi Kasei Life&Living Corporation

NP102 Solid state NMR studies of poly (alkyl propiolate)s
Kouo Suzuki, Terumi Kohiyama, Yasuteru Mawatari, Masahiro tabata and Toshifumi Hiraoki
Graduate school of Engineering, Hokkaido University

NP103 Conformational transformation of poly(β -benzyl L-aspartate) as studied by solid-state ^{13}C NMR
S. Kasahara, K. Takegoshi, and A. Shoji*
Department of Chemistry, Graduate School of Science, Kyoto University, *Department of Biological Science, Faculty of Engineering, Gunma University

NP104 Transition between the glassy crystal and the plastic crystal in poly (3-alkylthiophene)
Koji Yazawa[1], Naoki Asakawa[1], Takakazu Yamamoto[2], and Yoshio Inoue[1]
[1]Department of Biomolecular Engineering, Tokyo Institute of Technology, [2]Chemical Resources Laboratory, Tokyo Institute of Technology

NP105 Study of structure of ionic aggregates in poly (ethylere-ran-methacrylic acid) ionomers by means of nuclear magnetic resonance spectrometer at high magnetic field 21.9T
Yusuke Yamamoto, Miwa Murakami, Masataka Tansho, and Tadashi Shimizu
High Magnetic Field Center, National Institute for Materials Science

NP106(PL1) Diffusional behavior of poly(β -benzyl L-aspartate) in the rod-like and random-coil forms as studied by high field-gradient NMR method
Sho Kanesaka, Shigeki Kuroki, and Isao Ando

Department of Chemistry and Materials Science, Tokyo Institute of Technology

AP107 Transformation of crystal structure of ultra high molecular weight polyethylene as studied by solid state NMR

T. Yamanobe, K. Hashizume, K. Kanou,H. Uehara and T. Komoto
Department of Chemistry, Gunma University

AP108 Solid-state ^{13}C NMR study on microbial poly(ε -L-Lysine) and its derivatives

Shiro Maeda[1], Junnosuke Muranaka[1], Chizuru Sasaki[2] and Ko-Ki Kunimoto[2]
[1]Department of Applied Chemistry and Biotechnology, Faculty of Engineering, University of Fukui, [2] Graduate school of Natural Science and Technology, Division of Material Engineering, Kanazawa University

AP109 Characterization of microbial poly(ε -L-lysine)/ poly(L-lactic acid) blend films by solid-state NMR

Shiro Maeda[1], Osamu Kinoshita[1], Yasuhiro Fujiwara[1], Kensuke Sakurai[2], Chizuru Sasaki[3], and Ko-Ki Kunimoto[3]
[1]Depertment of Applied Chemistry and Biotechnology, and [2]Department of Materials Science, Faculty of Engineering, University of Fukui, [3]Division of Material Engineering, Graduate School of Natural Science and Technology, Kanazawa University

B-3. Application to biological science

NP110(PL5) Structure analysis of chlorosomes by ^{13}C spin-diffusion solid-state NMR

Ayako Egawa[1], Kengo Akiba[1], Tadashi Mizoguchi[2], Yoshinori Kakitani[3], Yasushi Koyama[3], Toshimichi Fujiwara[1] and Hideo Akutsu[1]
[1]Institute for Protein Research, Osaka University, [2]College of Science and Engineering, Ritsumeikan University, [3]Faculty of Science and Technology, Kwansei Gakuin University

NP111 Effect of cholesterol on structure of PLC-delta1 PH domain at membrane surface studied by solid state NMR

Akiko Hatakeyama, Takio Sugita, Masashi Okada, Hitoshi Yagisawa, and Satoru Tuzi
Graduate School of Life Sciene, University of Hyogo

NP112(PL4) Characteization of backbone conformations and interaction on retinal protein by solid state NMR

Izuru Kawamura[1], Naoki Kihara[1], Satoru Tuzi[2], Yochi Ikeda[3], Katsuyuki Nishimura[1], Hazime Saitô[2,4], Naoki Kamo[3] and Akira Naito[1]
[1]Graduate School of Engineering, Yokohama National. University, [2]Graduate School of Life Science, University of Hyogo, [3]Graduate School of Pharmaceutical Sciences, Hokkaido University, [4]Center for Quantum Life Science, Hiroshima University

NP113 Solid state NMR study of interaction between PLC-delta1 EF-hand domain and lipid bilayer

Satoko Tanaka, Masashi Okada, Hitosi Yagisawa, and Satoru Tuzi
Department of Life Science, Graduate School of Life Science, University of Hyogo

NP114 The structural model for the amyloid fibril formed by β2-microglobulin fragment based on solid-state NMR

Kentaro Iwata, Toshimichi Fujiwara, Yoh Matsuki, Hideo Akutsu, Hironobu Naiki and Yuji Goto
Instute for Protein Reseach, Osaka University

NP115 DOQSY NMR determination of the repeated biomimetic polypeptides

Yasumoto Nakazawa[1], Jacco D. van Beek[2], Beat H. Meier[2], Kousuke Ohgo[1] and Tetsuo Asakura[1]
[1]Department of Biotechnology, Tokyo University of Agriculture & Technology, [2]Laboratory for Physical Chemistry, ETH Zurich

NP116(PL7) Solid state NMR analysis of amphotericin B-sterol covalent conjugates forming a molecular assemblage in membrane

Yusuke Kasai, Shigeru Matsuoka, Yuichi Umegawa, Hiroyuki Ueno, Nobuaki Matsumori, Tohru Oishi, and Michio Murata

Department of Chemistry, Graduate School of Science, Osaka University

NP117 Specific interaction of bovine lactoferricin with acidic phospholipid bilayers and elucidation of its antimicrobial activity
Masako Umeyama, Katsuyuki Nishimura, and Akira Naito
Graduate School of Engineering, Yokohama National University

NP118(PL8) Dynamic structure analysis of antibiotic peptide Alamethicin in lipid bilayers by solid-state NMR
Takashi Nagao, Daishuke Ishioka, Katsuyuki Nishimura, and Akira Naito
Graduate school of Engineering, Yokohama National University

NP119 Development of phase-modulated Lee-Goldburg sequence for X-^{1}H (X=^{15}N,^{13}C) dipolar recoupling under very fast MAS
Hiroki Ishii, Masashi Fukuchi, Kiyonori Takegoshi, and Akira Shoji
Department of chemistry, Graduate School of Science, Kyoto University

AP120(PL6) Structural analysis of alanine tripeptide with anti-parallel and parallel β-sheet structures using solid state NMR
Michi Okonogi[1], Kazuo Yamauchi[1], Hiromichi Kurosu[2], and Tetsuo Asakura[1]
[1]Tokyo University of Agriculture and Technology, [2]Nara Women's University

B-4. Application to materials science

NP121 ^{23}Na MQMAS at 21.9T (^{1}H 930 MHz)
Toshihito Nakai[1], Naoyuki Fujii[1], Kenji Takasugi[1], Hiroaki Utsumi[1], and Tadashi Shimizu[2]
[1]JEOL Ltd., [2]National Institute of Materials Science

NP122 Structure of duplex oxide layer in porous alumina studied by ^{27}Al MAS and MQMAS NMR
Takahiro Iijima[1†], Seiichi Kato[1], Ryuichi Ikeda[1], Shinobu Ohki[1], Giyuu Kido[1], Masataka Tansho[1], and Tadashi Shimizu[1]
[1]National Institute for Materials Science, Japan [†]Present address: Department of Chemistry, Graduate School of Science, Kyoto University

NP123 Research of the tautomerism for 9-hydroxyphenalenone derivatives by the solid-state exchange NMR
Hiroyuki Koyano[1], Taisuke Manaka[1], Daisuke Kuwahara[1], and Tomoyuki Mochida[2]
[1]Department of Physical Chemistry, University of Electro-Communications, [2] Department of Chemistry, Faculty of Science, Toho University

NP124 Dynamics Analysis of a Hole-Transport Material for Organic LEDs by Solid-State ^{13}C NMR
Junya Shimada[1], Naoki Tsukamoto[1], Hironori Kaji[1,2], and Fumitaka Horii[1]
[1]Institute for Chemical Research, Kyoto University, [2]PRESTO, JST

AP125 Molecular dynamics in paramagnetic materials as studied by static-powder and magic-angle spinning ^{2}H NMR
Motohiro Mizuno, You Suzuki, and Kazunaka Endo
Graduate School of Natural Science and Technology Kanazawa University

AP126 Conformational analysis of TPD by two-dimensional solid-state double-quantum NMR spectroscopy and quantum chemical calculations
Tomonori Yamada [1], Naoki Tsukamoto [1], Hironori Kaji [1,2], and Fumitaka Horii [1]
[1] Institute for Chemical Research, Kyoto University, [2] PRESTO, JST

AP127 Solid state ^{7}Li NMR study of anode hard-carbons for lithium-ion battery optimized to hybrid electric vehicle
Kazuma Gotoh[1], Hiroyuki Ishida[1], Mariko Maeda[2], Aisaku Nagai[2], Atsushi Goto[3], Shinobu Ohki[3] and Masataka Tansho[3]
[1] Dep. of Chemistry, Faculty of Science, Okayama University, [2] Nishiki Reseach Laboratry, Kureha

Chemical Industry, [3] Tsukuba Magnet Laboratry, National Institute for Materials Science

AP128 Effect of chemical exchange of Xenon in zeolite NaY on ^{129}Xe chemical shift measured by high-pressure in situ NMR probe
Takahiro Ueda[1,2], Hironori Omi[2], Kuniyoshi Maezawa[2], Noriko Kato[2], Keisuke Miyakubo[2], and Taro Eguchi[1,2]
[1]The Museum of Osaka University, [2]Department of Chemistry, Graduate School of Science, Osaka University,

AP129 Changes in sodium cation sites probed by ^{23}Na NMR and PFGNMR of adsorbed ammonia in calcined NaA
Makoto Yamaguchi
Institute of Research and Innovation

AP130(PL2) Local environments of slags: the first application of ^{43}Ca MQMAS technique.
Keiji Shimoda[1], YasuhiroTobu[1], Koji Kanehashi[1], Takahiro Nemoto[2], Yuichi Shimoikeda[2], and Koji Saito[1]
[1]Advanced Technology Research Laboratories, Nippon Steel Corporation, [2]JEOL Ltd.

AP131 Location, Acid Strength and Mobility of the acidic Protons in Keggin 12-H3PW12O40: A Combined Solid-State NMR Spectroscopy and DFT Quantum Chemical Calculation Study
Jun Yang, Michael J. Janik, Anmin Zheng, Mingjin Zhang, Matthew Neurock, Robert J. Davis, Chaohui Ye, and Feng Deng
Wuhan Institute of Physics and Mathematics, Chinese Academy of Sciences

B-5. Liquid crystals and membrane

NP132 Discrimination of enantiomers by means of NMR spectroscopy using chiral liquid crystalline solution VII - Relation with an anisotropic molecular motion -
Makiko Sugiura, Yoshinori Nakao, and Masayoshi Ito
Kobe Pharmaceutical University

AP133 Diffusion of Rodlike Poly (γ-benzyl L-glutamate) in Concentrated Solution As Studied by the Field-Gradient ^{1}H NMR Methods
Shigeki Kuroki, and Kazuhiro Kamiguchi
Department of Chemistry and Materials Science, Tokyo Institute of Technology

(C) NMR imaging

C-1. Methodology

AP134 Novel fluid dynamical behavior of laser-polarized ^{129}Xe in a laminar flow
Tatsuya Asanuma, Takashi Hiraga, and Mineyuki Hattori
Photonics Research Institute, National Institute of Advanced Industrial Science and Techonology (AIST)

AP135 TR-dependent Steady-State iDQC in vivo MRI of Mice Brains
Dennis W. Hwang, Chao-Hsiung Hsu, Chieh-Wei Chang,Wen-Yih I. Tseng, and Lian-Pin Hwang
Department of Chemistry, National Taiwan University

C-2. Medical and in vivo NMR imaging

NP136 Imaging of a recovery process in a rat spinal cord injury model using manganese enhanced MRI
Akihiko Fujikawa[1], Yuko Kawai[3], Ichio Aoki[4], Takayuki Yamaji[2], Hiroyuki Takamatsu[1], Sousuke Miyoshi[1], Shintaro Nishimura[1], Masahiro Umeda[4], Toshihiro Higuchi[3], and Chuzo Tanaka[3]

[1]Advanced Technology Platform Research Laboratory, [2]Applied Pharmacology II Research Laboratory, Astellas Pharma Inc.,[3]Department of Neurosurgery, 4Dwpartment of Medical Informatics, Meiji University of Oriental Medicine

AP137 Brain tissue segmentation on the 3D MDEFT Image obtained at 4.7T
Nobuhiro Takaya[1], Hidehiro Watanabe[1], Masayuki Yamaguchi[1,2], and Fumiyuki Mitsumori[1]
[1]National Institute for Environmental Studies, [2]University of Tsukuba

AP138 Anisotropic diffusion of water in plant stem
Nobuaki Ishida
National_Food Reserach Institute

AP139 Analysis of hyperpolarized ^{129}Xe washout curve by simultaneous measurement in mouse lungs and brain
Takashi Masutani, Michiko Narazaki, Akari Kaneko, Akiko Nakabou, Tsuyoshi Ueyama, Tetsuya Wakayama, Atsuomi Kimura and Hideaki Fujiwara
Graduate School of medicine, Osaka University

AP140 Compartment model analysis of the dynamics observed in hyperpolarized ^{129}Xe NMR spectroscopy in mouse
Akari Kaneko, Michiko Narazaki, Atsuomi Kimura and Hideaki Fujiwara
Graduate School of medicine, Osaka University

(D) Technical and theoretical developments of NMR.

D-1. Calculation, simulation, and data analysis

NP141 NMR-based metabolomics-newly developed software of integrated NMR-spectroscopic and multivariate analysis "Alice2 for metabolome"
Kazunori Arifuku[1], Itiro Ando[2], Masako Fujiwara [1], and Keiko Hirakawa[3]
[1] JEOL DATUM LTD, [2] Environmental Research Center LTD, [3]Nippon Medical School

NP142 Automatic RF power determination by MUSASHI
Katsuo Asakura, Tomomitsu Kurimoto, and Nobuaki Nemoto
JEOL LTD.

AP143 Non-equispaced fourier transforms for multidimensional filter diagonalization method evolution matrices
Kenji Takasugi[1] and Sseziwa Mukasa[2]
[1]JEOL Ltd., [2]JEOL USA, Inc.

AP144 NMR-based metabolomics : Chemometric method for mixture analysis using ^{1}H spectra; Classification of teas in the world
Masako Fujiwara[1], Itiro Ando[2] and Kazunori Arifuku[1]
[1]JEOL DATUM LTD, [2]Envioronmental Research Center LTD.

AP145 Orientational restraints in Cyana
Kimmo Paakkonen, and Peter Guentert
Riken Genomic Sciences Center

AP146 Homodimeric structure determination without manually assigned inter-monomer constraints in the CYANA program
Yi-Jan Lin, and Peter Guntert
Protein Structure Team, GSC, RIKEN

AP147 Metabolic characterization of small intestinal tissue in rats following hemorrhagic shock using multivariate statistical batch processing of ^{1}H NMR spectra of PCA extracts of the tissue
Keiko. Hirakawa[1], Kaoru Koike[2], Kazunori Arifuku[3], Kyoko Uekusa[1], Youkichi Ohno[1,4], Kengo

Onodera[5], Junichi Aiboshi[5], and Yasuhiro Yamamoto[6]
[1]NMR Laboratory and Department of Legal Medicine, Nippon Medical School, [2]Field of Surgery, Emergency and Critical Care Medicine, Tohoku University Graduate School of Medicine, [3]Joint Technology Division, JEOL DATUM LTD, [4]Field of Social Medicine, Legal Medicine, Nippon Medical School Graduate School of Medicine, [5]Department of Critical Care Medicine, Nippon Medical School, [6]Field of Sugery, Emergency and Critical Care Medicine, Nippon Medical School, Graduate School of Medicine

AP148 Towards structure determinations of complex and membrane proteins using the stereo-array isotope labeling (SAIL) method and the CYANA program
Teppei Ikeya[1,2], Tsutomu Terauchi[2,3], Peter Guntert[4] and Masatsune Kainosho[2,3]
[1]Japan Biological Information Consortium (JBiC), [2]Graduate School of Science, Tokyo Metropolitan University, [3]CREST, Japan Science and Technology Agency (JST), [4]RIKEN Genomic Sciences Center

AP149 Toward highly efficient molecular identification algorithm in a hetero-nuclear NMR-based metabomics
Eisuke Chikayama, Yasuyo Sekiyama, Takashi Hirayama, Kazuki Saito, Kazuo Shinozaki and Jun Kikuchi
Plant Science Center, RIKEN

AP150 New approach for assessment of protein structure from NMR spectra using reduced relaxation matrix
Masashi Yokochi, Yoshihiro Kobashigawa and Fuyuhiko Inagaki
Department of Structural Biology, Graduate School of Pharmaceutical Sciences, Hokkaido University

AP151 Combination of Isomer Generation and NMR Simulation for Structure Elucidation - Examples of Artemisinin and Uncarine E
Nguyen Tien Tai[1], Ho Tu Bao[2], Dam Hieu Chi[2]
[1]Institute of Chemistry, Vietnamese Academy of Science and Technology, [2]Japan Advanced Institute of Science and Technology (JAIST)

D-3. Instrumentation

NP152 Development of low temperature (<4K)NMR cryostat probe(cryo-probe)
Y. Mogami, A. Ikeda, T. Momose, and K. Takegoshi
Department of chemistry, Graduate School of Science, Kyoto University

AP153 A cooling system for long time solid-state MAS experiments with sensitivity enhancement at liquid nitrogen temperature
Hiroki Takahashi[1], Fumihiko Yonezawa[2], Hideo Akutsu[1] and Toshimichi Fujiwara[1]
[1]Institute for Protein Research, Osaka University, [2]AIRTECH CO., LTD.

AP154 System for storing hyperpolarized ^{129}Xe gas during production in a 4.7T magnetic field
Atsushi Wakai[1,2], Kazuhiro Nakamura[1,2], Jeff Kershaw[1,2], David Wright[1,2], and Iwao Kanno[1].
[1]Akita Research Institute of Brain and Blood Vessels, Akita, Japan., [2]Akita Industry Promotion Foundation, Akita

(E) Others

AP155 ^{75}As, ^{113,115}In and ^{123}Sb NMR studies of indirect nuclear spin-spin coupling in InX (X = As, Sb)
Takahiro Iijima[1†], Kenjiro Hashi[1], Atsushi Goto[1], Tadashi Shimizu[1], and Shinobu Ohki[2]
[1]National Institute for Materials Science, Tsukuba, Japan, [2]CREST, Japan Science and Technology Agency, Japan, [†]Present address: Department of Chemistry, Graduate School of Science, Kyoto University

AP156 Establishment of annotation processing system for BMRB database at PDBj

Eiichi Nakatani[1,2], Yoh Matsuki[1,2], Haruki Nakamura[2], and Hideo Akutsu[2]
[1]Japan Science and Technology Agency – BIRD, [2]Institute for Protein Research, Osaka University

Speaker Presentations

L1

Proton Dynamics in Inorganic Solid Acid $(NH_4)_3H(SO_4)_2$

Koh-ichi Suzuki and Shigenobu Hayashi

Research Institute of Instrumentation Frontier, Nat'l Inst. of Adv. Ind. Sci. and Tech. (AIST), Tsukuba Central 5, 1-1-1 Higashi, Tsukuba, Ibaraki 305-8565, Japan

1. Introduction

Inorganic solid acids such as $CsHSO_4$ are attractive for materials of electrolyte membranes in fuel cells because of the high proton conductivity in a high temperature phase without humid atmospheres. Previously, we reported the proton dynamics in $CsHSO_4$ and $Cs_2(HSO_4)(H_2PO_4)$ studied by ^1H solid-state NMR and concluded that the proton transport is limited by reorientation of the tetrahedral anion. In the present work, we have studied proton dynamics in $(NH_4)_3H(SO_4)_2$ by means of ^1H solid-state NMR.

2. Experimental

$(NH_4)_3H(SO_4)_2$ crystal was grown by slow evaporation of the aqueous solution containing stoichiometric amounts of $(NH_4)_2SO_4$ and H_2SO_4.

The measurements of ^1H solid-state NMR were performed with Bruker ASX200, ASX400, MSL400 and Minispec mq20 spectrometers at Larmor frequencies of 200.13, 400.13, 400.13 and 19.65 MHz, respectively.

3. Results and Discussion

The ^1H line assigned to the acidic proton can well be distinguished from that of ammonium protons in the ^1H MAS NMR spectrum at the spinning rate of 30 kHz. The chemical shifts of acidic and ammonium protons are 14.7 and 6.6 ppm, respectively. The former value indicates the presence of strong hydrogen bonds.

^1H static NMR spectra show motional narrowing with raising the temperature, as shown in Fig. 1. In the temperature range higher than about 350 K, the acidic proton shows the narrower peak with fine structures whereas ammonium protons have the broad one. In the high temperature phase (T > 408 K), the two components start to collapse into a single sharp line due to translational diffusion of both protons.

We will also present temperature and frequency dependences of ^1H spin-lattice relaxation times (T_1) and discuss on proton dynamics.

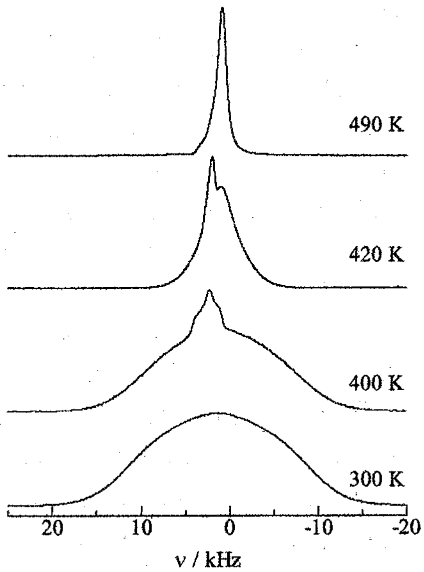

Fig. 1. ^1H static NMR spectra of $(NH_4)_3H(SO_4)_2$

L2

Complete ^{13}C and ^{15}N signal assignments and structural analysis of the crystalline chitin binding domain of chitinase A1 by solid-state MAS NMR

○Hiroki Tanaka[1], Izumi Yabuta[1], Yuko Nagasaki[2], Masashi Hara[2], Takahisa Ikegami[1], Toshimichi Fujiwara[1], Takeshi Watanabe[2], and Hideo Akutsu[1]
[1]*Institute for Protein Research, Osaka University, Osaka, Japan*
[2]*Faculty of Agriculture, Niigata University, Niigata, Japan*

Chitinase A1 from *Bacillus Circulans* WL-12 has a 45-residue domain that binds to polysaccharide chitin. Since this domain specifically binds to fibrous insoluble chitin, it is difficult to make crystalline or solution protein-chitin complex. Such a sample condition impedes the structural analysis of complex by X-ray and solution NMR. Thus, we apply solid-state NMR to study the binding mechanism of the chitinase. We have first made solid-state NMR experiments on a crystalline state of the unbound protein, since the crystalline proteins are known to give higher spectral resolution. The solid-state NMR study of the unbound state provides several structural parameters such as chemical shifts and dipolar couplings for distance restraints. Comparison of the unbound protein with chitin-protein complex would contribute to the understanding of the binding mechanism.

We prepared uniformly ^{13}C-, ^{15}N-labeled protein to correlate ^{13}C-^{13}C and ^{13}C-^{15}N for the structural analysis. Polyethylene glycol was added to the protein solution as the precipitant. To prepare a large amount of protein crystals, we accelerated the crystallization process by concentrating the solution with a rotary evaporator. We performed multidimensional solid-state NMR experiments at the ^{1}H resonance frequency of 700 MHz under 16 kHz magic angle spinning conditions: 2D RFDR, 2D DARR, 2D NCACB, 3D NCOCA, and 3D NCACO.

The typical ^{13}C linewidth was about 0.3 ppm in crystal state as shown in the figure. This should be compared with the linewidth of about 1 ppm in ordinal protein precipitants. The obtained multidimensional NMR spectra have sufficient spectral resolution to make complete backbone and C^{β} signal assignments.

The secondary structure was predicted from the chemical shifts by using the empirical chemical shift database software, such as TALOS. The predicted structure almost agreed with the solution structure previously reported. We are now making multidimensional ^{13}C-^{13}C spin diffusion experiments for collecting the distance restraints. The solid-state NMR strategy for the three-dimensional structure determination of the uniformly labeled protein will be discussed.

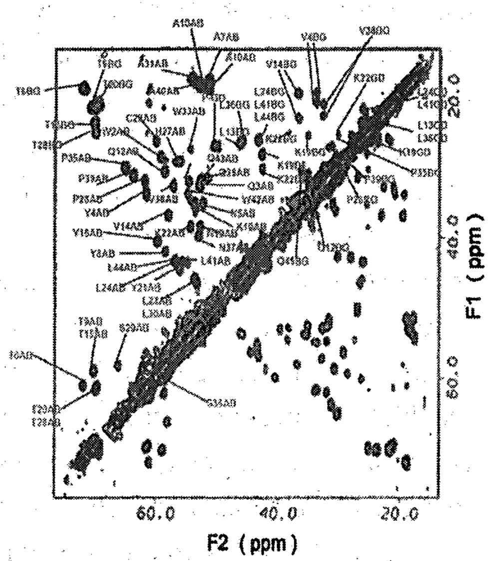

Fig. 2D RFDR spectrum and assignments of chitin binding domain

L3

Structural changes induced by ATP hydrolysis in microcrystalized protein-DNA filaments detected by Solid-State NMR

○Minoru Hatanaka[1], Masayoshi Honda[2,3], Satoko Ishibe[2], Tsutomu Mikawa[2,3,6],Yutaka Ito[3,4,5], Takehiko Shibata[2,3], Toshio Yamazaki[1]

[1]Genomic Sciences Center, RIKEN; [2]Bio-supramol. Struct - Func. Group, RIKEN; [3]Grad. Sch. of Integrated Sci., Yocohama City Univ.; [4]Grad. Sch. of Sci., Tokyo Metropolitan Univ.; [5]CREST・JST; [6]Structurome Res. Group, RIKEN/Harima Institute

Recent considerable progress in spin manipulating techniques and sample preparation methods has enabled solid-state NMR to determine the structure and analyze the dynamics of proteins. In particular microcrystalization of proteins extensively improved the spectra obtained in resolution and sensitivity. Since solid-state NMR is suitable for systems that are difficult to study by solution-state NMR or X-ray crystallography, such as membrane and fibrous proteins, its combination with microcrystalizatization is rapidly becoming an essential technique for the studies of biological systems. In our research we investigated structural changes of RecA-DNA complex accompanied with ATP hydrolysis introducing this combination as one of examples. RecA protein is necessary to homologous genetic recombination and DNA repair, and forms a filament on DNA or even by itself. The structure of the RecA-DNA complex has not been determined due to difficulty of preparing the sample for solution-sate NNR or X-ray crystallography in spite of its necessity for elucidation of their interaction at atomic resolution. We first prepared microcrystal of [u-^{15}N] RecA(WT)-dT14-ATPγS complex and performed ^{15}N- and ^{31}P-CPMAS experiments (figures blow). In these measurements we for the first time succeeded to observe ATP hydrolysis in microcrystal by solid-state NMR, and the spectra showed that the structural changes of the protein accompanied with the hydrolysis mainly occurred around backbone. Furthermore ^{15}N{^{31}P}- and ^{31}P{^{15}N}- HETCOR indicated that there were relatively strong interactions between ζ-nitrogens of Lysines in the protein and phosphorous of the DNA backbone at the RecA-dT14-ADP form.

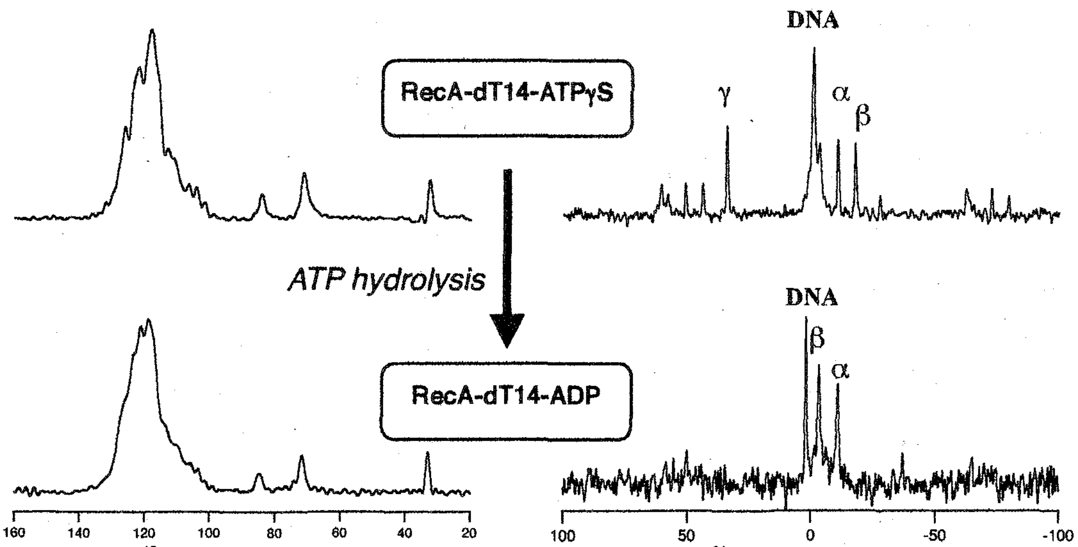

L4

Is it possible to directly detect the overtone NMR for half-integer quadrupolar nuclei?

Hajime Okamoto, Yuya Yamazaki, Hiroki Nose, Daisuke Kuwahara

The University of Electro-Communications, 1-5-1, Choufugaoka, Chofu-shi, Tokyo, 182-8585, Japan

Quadrupolar nuclei with half-integer spins are present in many important engineering materials such as ceramic materials, clay minerals, and functional zeolites. Most of these materials exhibit their useful functions in the solid state. Hence, it is useful to obtain solid-state high-resolution NMR spectra of half-integer quadrupolar nuclei for finding out the origin of the functionalities.

In this study, we derived a theoretical description for the overtone NMR of half-integer quadrupolar nuclei in solids. It was shown that the overtone NMR had the ability to produce high-resolution solid NMR spectra for the quadrupolar nuclei under magic angle spinning conditions. Furthermore, we performed computer simulations to depict the complete motions of the OT magnetizations. It was found that, in the static magnetic field of 7.05T, the OT NMR of solid $^{23}Na_2MoO_4$ could be directly measured after a single OT pulse. The sensitivity of the OT NMR was about 12% compared to that of the ^{13}C NMR. In addition, it became apparent that if using direct detection, we could not obtain such NMR spectra that have two or more resonance lines corresponding to nonequivalent sites in a crystallite.

Therefore, in order to obtain the usual NMR spectra that have separated resonance lines corresponding to chemically nonequivalent sites, we have to adopt indirect detection schemes. In the conference, we will present further details about the indirect detection and some experimental results.

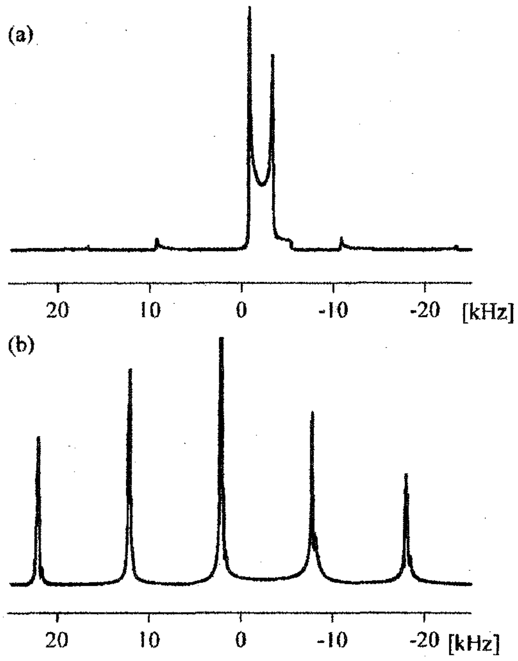

Figure. 1 MAS NMR spectra for a spin -3/2 nucleus in a polycrystalline solid. (a)MAS NMR spectrum for the CT. (b)OT MAS NMR spectrum observed after a single OT pulse.

L5

Dynamic Aspect of Supramolecular PEO-Urea Crystal Revealed by Solid-state ^{13}C MAS exchange NMR

Toshikazu Miyoshi and Wei Hu
Research Institute of Nanotechnology, National Institute for Advanced Industrial Science and Technology,
1-1-1 Higashi, Tsukuba, Ibaraki 305-8565, Japan

<Introduction> Secondary intermolecular interactions play important roles for the design of new materials which have unique self-assembled and supramolecular structures. Much attention has been paid to "static" structures and bulk properties of self-assemble systems. It is expected that secondary intermolecular interactions largely influence on dynamics of each molecule which is related to the properties of materials. Nevertheless, there was no convincing result about "dynamic" structures, since such an analysis requires a highly molecular resolution. One dimensional (1D)-MAS exchange NMR which can characterize geometry and time parameters for molecules on an atomic resolution is suitable for characterization of dynamics of complicated supramolecules. Poly(ethylene oxide) (PEO) and urea forms supramolecular crystal in methanol via hydrogen bonding network. WAXD revealed that 2/3 urea forms a nanochannel and 1/3 urea form a complex with PEO in the channels.

<Experiment> Poly(ethylene oxide) with a M_w of 20,000 was obtained from Polysciences Inc. Urea and Bis(acetylacetonato)Copper(II) (Cu(II)-AA) were received from Wako Chem. Com. The supramolecules were obtained by dissolving PEO with a weight of 1 g to 100 ml saturated methyl alcohol solution of urea while the solution was continuously stirred. The white precipitate appeared soon. After one day of stirring, Cu (II)-AA was added to the mixture and stirred together for 1.5h, in order to shorten the ^{1}H relaxation time in the system. The precipitate was filtered and dried under vacuum at 313K. DSC measurement was performed using a Seiko SSC/6000(DSC 6000) in an N_2 atmosphere with a heating rate of 10 K/min. The ^{13}C CPMAS NMR measurements were conducted on a BRUKER AVANCE 300 spectrometer, equipped with 7 and 4 mm VT CPMAS NMR probes. The ^{1}H and ^{13}C carrier frequencies are 300.1 and 75.5MHz, respectively.

<Result and Discussion> ^{13}C direct polarization spectrum shows the stoichiometry of four PEO repeat units per nine urea molecules, which is consistent with previously reported value. Furthermore, ^{1}H-^{13}C HETCORE shows an intimate mixing for different molecules. Figure 1 (a) and (b) shows ^{1}H-^{13}C HETCORE spectrum for Supramolecule PEO-UREA crystal with CP time of 1ms and (b) slice data with different CP times. Observation of polarization transfer from PEO protons to UREA carbon shows molecular level mixing. We apply 1D-MAS exchange NMR to the system. Surprisingly, PEO and UREA also show significant dynamics in the same dynamic window. We will report detailed dynamics for PEO and UREA in the crystal, and furthermore compare with those in bulk states. Here we will reveal how secondary interactions and nano-space alert the dynamics of PEO and UREA in supramolecules.

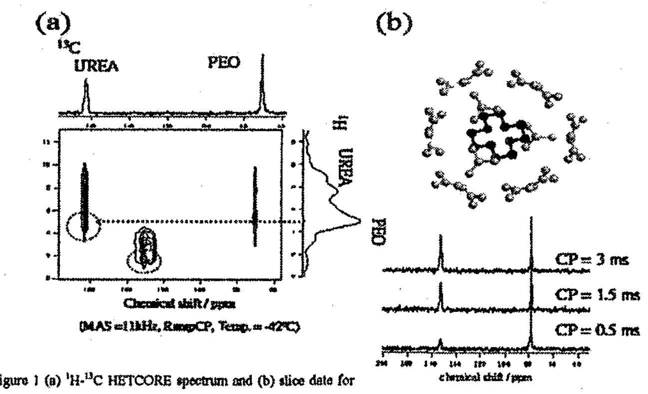

Figure 1 (a) ^{1}H-^{13}C HETCORE spectrum and (b) slice date for PEO-UREA supramolecules at 231K.

L6

Structure and mode of interaction with RNA of mouse neural protein, Musashi1

Yohei Miyanoiri [1], Satoshi Saitoh [2], Hiroyuki Miyashita [2], Hisanori Kobayashi [2] Seiichi Uesugi [2], Takao Imai [3], Hideyuki Okano [3] and Masato Katahira [1,4]

[1] Department of Supramolecular Biology, International Graduate School of Arts and Sciences, Yokohama City University, 1-7-29 Suehiro-cho, Tsurumi-ku, Yokohama 230-0045, Japan
[2] Department of Environment and Natural Sciences, Graduate School of Environment and Information Sciences, Yokohama National University, 79-7 Tokiwadai, Hodogaya-ku, Yokohama 240-8501, Japan
[3] Department of Physiology, Keio University School of Medicine, 35 Shinanomachi, Shinjyuku-ku, Tokyo 160-8582, Japan
[4] Genomic Sciences Center, RIKEN, 1-7-22 Suehiro-cho, Tsurumi-ku, Yokohama, 230-0045, Japan.

Musashi1 regulates asymmetric division of neural progenitor cells through the inhibition of the translation of a certain mRNA. Musashi1 has two RNA binding domains, RBD1 and RBD2, which specifically bind to RNA that contains (G/A)U_nAGU (n = 1 to 3) sequences. We have already elucidated the origin of higher affinity to target RNA of RBD1 than that of RBD2 on the basis of comparison of their structures, mode of interactions, surface electrostatic potentials and backbone dynamics (*J. Biol. Chem.*, **278**, 41309 – 41315, 2003).

We have also exhibited that RBD1-RBD2, produced by naturally occurring link of RBD1 and RBD2, binds RNA much stronger than RBD1. This phenomenon implies that strong affinity to RNA of RBD1-RBD2 originates from cooperative effect of both RBDs. To elucidate mode of interactions with RNA of RBD1-RBD2, we analyzed chemical shift perturbations of RBD1-RBD2 upon binding of RNA. The large perturbations were observed for the β-sheet and a domain linker region. In the course of the addition of RNA, interesting thing was found. At the initial stage of the addition of RNA, perturbation was mainly observed for residues of an RBD1 part of RBD1-RBD2. At the following stage of the addition, perturbation was observed for residues of an RBD2 part of RBD1-RBD2. This suggests that RBD1 and RBD2 of RBD1-RBD2 may play a different role in the target RNA recognition.

In order to determine the relative orientation of two RBDs in the complex with the target RNA, we have obtained residual dipolar couplings, RDCs, for RBD1-RBD2 with a gel method. RDCs were obtained for the complex with the RBD1-RBD2 : RNA ratio of 1:1 and 1:0.5. RDCs were obtained also for RBD1-RBD2 alone. On the basis of obtained RDCs, structural change of RBD1-RBD2 on binding to RNA will be discussed.

L7

Characterisation of the Nucleotide-Binding Domain of the Human Mitochondrial ABC Transporter ABCB6 by Heteronuclear Multidimensional NMR and Homology Modelling

Kaori Kurashima-Ito[1,2,3], Teppei Ikeya[4], Hiroshi Senbongi[1], Tsutomu Mikawa[1,2,3], Takehiko Shibata[1,2] and Yutaka Ito[1,2,3]

[1]Cellular and Molecular Biology Laboratory, RIKEN, 2-1 Hirosawa, Wako-shi, Saitama 351-0198, Japan, [2]Molecular and Cellular Physiology Laboratory, Graduate School of Integrated Science, Yokohama City University, 1-7-29 Suehiro-cho, Tsurumi-ku, Yokohama 230-0045, Japan, [3]CREST/Japan Science and Technology Agency (JST) and [4]National Institute of Advanced Industrial Science and Technology (AIST), Tokyo Waterfront Bio-IT Research Building 2-42 Aomi, Koto-ku, Tokyo, 135-0064, Japan

Human ATP-binding cassette, sub-family B, member 6 (ABCB6) is a mitochondrial half-type ATP-binding cassette (ABC) transporter. Though the function of ABCB6 has not been identified, this protein is proposed to be responsible for iron homeostasis in mitochondria, as is the case with its *Saccharomyces cerevisiae* homologue, Atm1p, which transports a precursor of the iron-sulphur cluster from the mitochondrial matrix to the cytosol.

In order to understand the structural basis for the conformational changes accompanying the substrate transportation cycle, which is controlled by ADP/ATP-binding and ATP hydrolysis, we have studied the C-terminal nucleotide-binding domain of ABCB6 spanning residues Phe558–Arg842 (ABCB6-C) in both the nucleotide-free and ADP-bound states by heteronuclear multidimensional NMR. We also performed homology modelling of ABCB6-C, which was used to interpret the obtained NMR data including the chemical shift perturbation upon ADP-binding.

Backbone resonance assignment on the nucleotide-free form of ABCB6-C showed that the resonances for approximately 30% of non-proline residues, which are mainly distributed around the nucleotide binding loops and in the Helical domain, were not observed. We concluded that this incompleteness in the assignments is due to the exchange regime between multiple conformations at an intermediate rate on the NMR time scale. These localised conformational dynamics remain in the ADP-bound state with the exception of the regions responsible for the recognition of the adenine base and α/β-phosphate groups. These results revealed that the dynamic cooperativity, which has already been discovered for a prokaryotic ATP-binding cassette, MJ1267, also exists in the NBD of a higher eukaryotic ABC transporter, and is presumably shared by all ABC transporters. Since the Helical domain is proposed to be responsible for the interaction with the transmembrane domain, this cooperativity may explain the mechanism of coupled functions between the nucleotide binding domain and the transmembrane domain in the substrate transportation cycle of ABC transporters.

L8

Clarification of repair mechanism of (6-4) photolyase using NMR

Akira Kato[1)], ○Takumi Ueda[1),2)], Takeshi Todo[3)], Hiroaki Terasawa[1)], Ichio Shimada[1),4)]
[1)] Graduate School of Pharmaceutical Sciences, the University of Tokyo, [2)] Japan Biological Information Research Center (JBIRC), Japan Biological Informatics Consortium (JBIC), [3)] Radiation Biology Center, Kyoto University, [4)] Biological Information Research Center (BIRC), National Institute of Advanced Industrial Science and Technology (AIST)

UV irradiation induces various DNA lesions, including (6-4) photoproducts. (6-4) photolyases, with a molecular mass of 60 kDa, use light to convert the (6-4) photoproducts to the original bases. The equilibrium between the (6-4) photoproduct and its oxetane intermediate in the (6-4) photolyase is essential for the reaction. Based on the site-directed mutagenesis analyses, Hitomi *et al.* found that the alanine mutantions of His-354 and His-358, which are thought to be located within the catalytic site of the enzyme, resulted in almost complete loss of the repair activity, and they proposed that His-354 and His-358 are responsible for the oxetane intermediate formation (*J. Biol. Chem.* (2001) **276,** 10103-9). In the present study, we aimed to observe the equilibrium state between the (6-4) photoproduct and the oxetane intermediate in the complex, and elucidate the role of the His-354 and His-358 in the oxetane intermediate formation.

Assignments of the resonances from Trp-291 and Trp-398, which are thought to be close to His-354 and His-358, respectively, were established by site-directed mutagenesis. Assignments of the resonances from the methyl groups of the (6-4) photoproduct bases in the complex were performed by observations of the exchange peaks between the resonances from the free and bound forms in the ^{13}C HSQC-NOESY spectra.

In order to observe the equilibrium between the (6-4) photoproduct and the oxetane intermediate, we performed TROSY-CPMG experiments of the complex by changing the spin-echo interval times. As a result, the signal reduction rate during the spin-echo duration for the resonance from Trp-291 was significantly decreased with increasing the spin-echo interval times, suggesting that Trp-291 is in equilibrium between several states with different chemical shifts in μs-ms timescale in the complex. No similar phenomenon for the resonance from Trp-291 was observed in a H354A mutant. Based on these results, we conclude that the observed phenomenon for the resonance from Trp-291 in the complex is caused by the equilibrium between the (6-4) photoproduct and the oxetane intermediate.

In order to determine the relative position between the enzyme and the (6-4) photoproduct bases, we performed steady-state NOE experiments. We saturated each one of the resonances from the methyl groups of the (6-4) photoproduct bases in the complex. As a result, NOEs between 5' side methyl and Trp-291 and between 3' side methyl and Trp-398 were observed. These results suggest that His-354 and His-358 are close to 5' and 3' side of the (6-4) photoproduct bases, respectively, and thus we propose an oxetane intermediate formation mechanism that His-354 accepts a hydrogen from 5' side of the (6-4) photoproduct bases, and His-358 donates a hydrogen to the 3' side of the bases.

L9

Rapid Protein-ligand interaction analysis system using Wheat Germ Cell-Free Protein Synthesis

Keiko Matsubara[1], Yukinori Nara[1], Akiko Iihara[1], Michiko Kitano[2], Toshiyuki Kohno[2]

[1]ZOEGENE Corporation and [2] Mitsubishi Kagaku Institute of Life Sciences (MITILS)

We developed a rapid protein-ligand interaction analysis system using our original high quality wheat germ extract (WGE) cell-free protein synthesis. Soluble and functional domains were firstly selected by high-throughput small-scale WGE cell-free synthesis. Then, the domains were efficiently selective-labeled by inhibiting trans-aminase activities in WGE. NMR spectrum of the labeled proteins were subjected to effective HSQC assignment method that can save time and protein amount. This system provides useful information to protein-ligand interaction analysis for drug design.

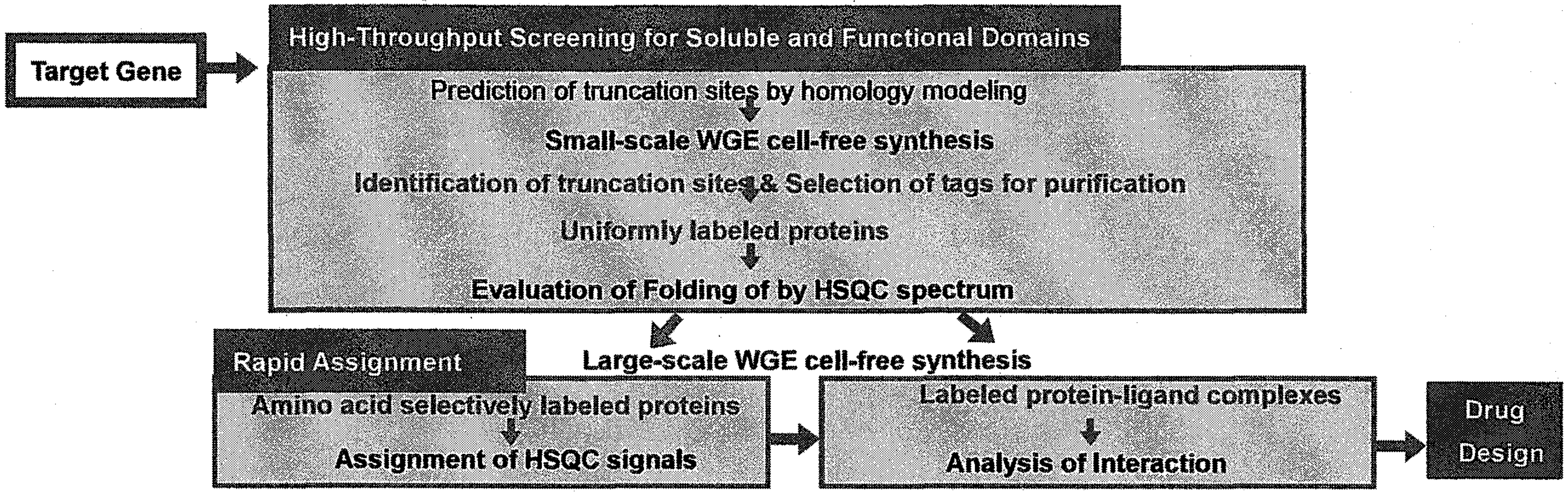

ZOEGENE Corporation 1000, Kamoshida-cho, Aobaku, Yokohama KANAGAWA 227-8502 (in Science & Technology Research Center of Mitsubishi Chemical Corporation) URL http://www.zoegene.co.jp E-mail: 6308790@cc.m-kagaku.co.jp

L10

Routine, automated solution state Dynamic Nuclear Polarisation (DNP) NMR spectroscopy of small molecules.

Andrew Sowerby[1] and Michio Shimizu[2]
[1]Oxford Instruments Plc., Abingdon, Oxfordshire, UK
[2]Oxford Instruments KK, 2-11-6, Tomioka, Koto-ku, Tokyo, 135-0047, Japan

Dynamic Nuclear Polarisation (DNP) NMR spectroscopy is one of a number of hyperpolarisation techniques that have been demonstrated to greatly enhance the sensitivity of NMR spectroscopy. Although the chemical applications of DNP NMR are potentially far wider than other polarisation techniques, DNP NMR, like other hyperpolarisation techniques, has to date suffered from practical limitations.

Amersham Health (now part of GE Healthcare) has recently developed technology with which the sample is hyperpolarised in a cryogenic insert inside a dedicated magnet and subsequently dissolved and transferred to a conventional NMR spectrometer in order to perform single-scan NMR spectroscopy.

Oxford Instruments has used this technology as a basis for the development of an automated DNP NMR Polariser that can be interfaced to a conventional NMR spectrometer. The DNP Polariser delivers a solution of hyperpolarised sample to a NMR tube located in a high-resolution NMR magnet, using a fully automated dissolution system.

Solution state DNP NMR spectroscopy will be most advantageous to applications benefiting from routine 13C and 15N NMR spectroscopy of small organic molecules with a lower limit of detection and/or condensed timescales with respect to conventional NMR.

DNP NMR spectra of a variety of small molecules are presented that demonstrate the reliability and repeatability of automated DNP NMR experiments. Specifications and capabilities of the first generation of a production DNP Polariser are discussed and preliminary data recorded using this apparatus are presented.

(The presentation will be given by Michio Shimizu in Japanese.)

L11

Resolution improvement of the HTS bulk magnet at 3 Tesla

Takashi Nakamura[a], Yoshiaki Yoshikawa[b], Yoshitaka Ito[b] and Hiroyuki Koshino[a]
[a]RIKEN 2-1 Hirosawa, Wako, Saitama 351-0198, Japan
[b]IMRA MATERIAL R&D Co. Ltd., 5-50 Hachiken-cho, Kariya, Aichi 448-0021, Japan

We developed the High *Tc* Superconducting (HTS) bulk magnet for NMR measurements several years. This year we will report about resolution improvement of the HTS bulk magnet. The HTS materials are typically RE-Ba-Cu-O (where RE is a rare-earth element; Y, Sm, Nd, etc.) and prepared in the melt-texturing process. The magnitude of the trapped field is proportional to the critical current density and the volume of the superconductor. Therefore, we have to develop the apparatus for generate low temperature and larger bulk. The cooling ability was improved to 38 K from 58 K on the pulse-tube refrigerator. Single domain large bulk was difficult to synthesis over 50 mm in diameter. We succeeded in making the HTS bulk about Sm-Ba-Cu-O of a diameter of 60 mm. Our HTS bulk magnet achieved progress of drastic enhancement of spectral resolution. Fig.1 shows the resolution of the magnet reached 600 Hz without shimming. We reported magnetic field stability of this magnet with 0.4 Hz/hour last year, and one step more approached to a magnet for high resolution NMR by resolution improvement of this year.

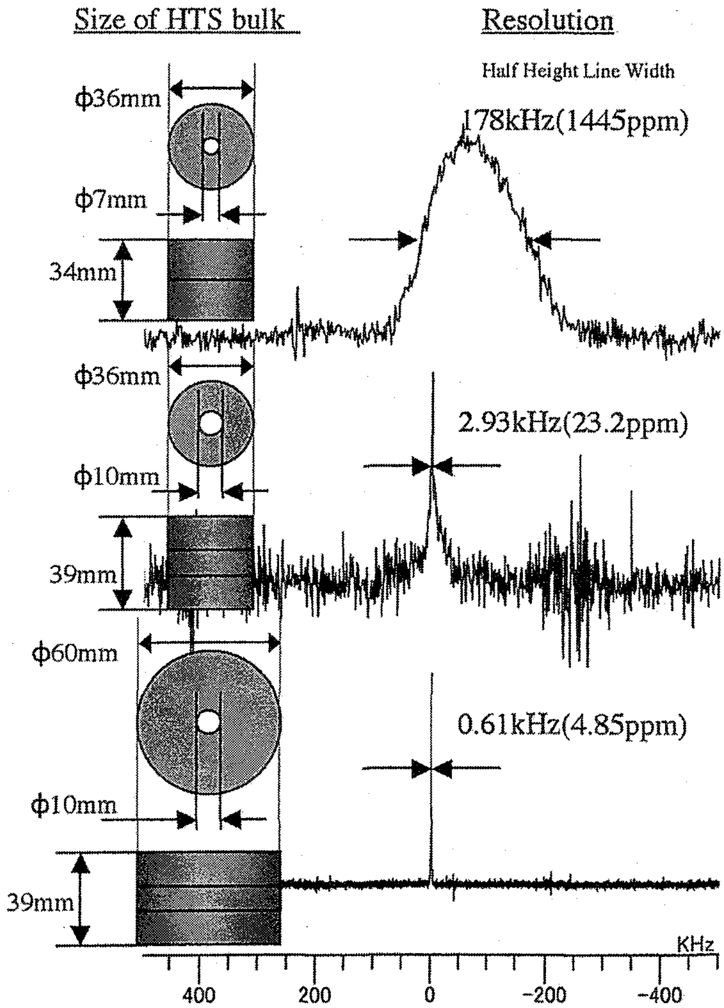

Fig.1. Spectral improvement of the HTS bulk magnet. Upper spectrum acquired by ^{1}H spin echo experiment, middle and lower spectra acquired by ^{1}H single pulse experiment. Sample was silicone rubber about 1.2 mm in diameter by 1mm length.

L12

Development of MicroMAS Probehead for Mass-limited Solid State Samples

Kazuo Yamauchi, Daisuke Hasegawa, and Tetsuo Asakura
kyamauch@cc.tuat.ac.jp
Department of Biotechnology, Tokyo University of Agriculture and Technology
Naka-cho 2-24-16, Koganei-shi, Tokyo 184-8588, Japan

A major disadvantage of NMR is its relative insensitivity, as a result only bulk properties of materials can be obtained. The microcoil NMR has advantageous in the sense of versatility, operationally and also cost. It is already applied in high resolution NMR, however, the microcoil for solid state NMR is still limited (ref. 1,2,3) because it was obtained only wide line spectra are observed in static sample. The microcoil probehead with magic angle spinning (MicroMAS) is necessary to obtain high resolution solid state NMR spectra and it will be a favorable tool for the investigation of mass limited solid state samples.

The RF circuit with microcoil (1.2mm Ø) is made by the modification from the MAS probehead. The sample rotor is designed conventional spinning module and rotor with modification for microcoil to perform microMAS. Figure 1 shows the detail of the rotor; the zirconia micro-rotor (1mm outer diameter and 500μm inner diameter) is plugged in the conventional rotor. The microMAS system is checked and it rotates up to 7kHz.

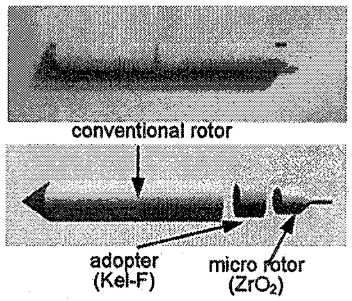

Figure 1: Photo and illustration of the rotor for MicroMAS probehead and the components.

^{13}C CP/MAS spectra are observed with reference samples and also biological samples e.g. 1μg (one thread) of *bombyx mori* silk fibroin fiber (~8% of [1-^{13}C]-Gly). Moreover, 2D RFDR spectra are also tested to demonstrate the determination of structures of solid state peptide samples. Figure 2 shows an example of the spectrum which has enough sensitivity to analyze the distances of carbons in [U-^{13}C] alanine.

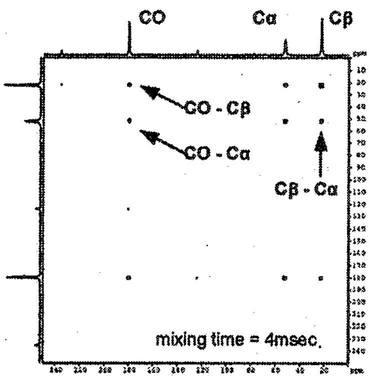

Figure 2: ^{13}C RFDR spectrum of [U-^{13}C] alanine using MicroMAS probehead. Cross peaks give the information on the distances between carbon atoms.

[Acknowledgement]
This development was supported by SENTAN, JST.

[References]
(1) K. Yamauchi, J.W.G. Janssen, A.P.M. Kentgens, *J. Magn. Reson.* 167 84 (2004).
(2) P.J.M. van Bentum, J.W.G. Janssen, A.P.M. Kentgens, *Analyst* 129 793 (2004).
(3) K. Yamauchi, T. Imada, T. Asakura, *J. Phys. Chem. B* (2005) in press.

L13

Detergent Screening for NMR Structural Studies of Membrane Proteins

S. Otomo(Z.-Y. Wang), K. Sato, N. Akiyama,
Y. Shimada, and H. Suzuki

Faculty of Science, Ibaraki University Mito 310-8512, Japan

Recently, we have determined the solution structures of core light-harvesting membrane proteins (LH1 α and β) from wild-type purple photosynthetic bacterium *Rhodospirillum rubrum* (1). Both the LH1 α and β proteins (ca. 6.1kDa) in organic solutions reveal a long α helical structure in the transmembrane regions, highly similar to those of the corresponding LH2 α and β proteins determined by X-ray crystallography. Here, we report preliminary results on the detergent screening for the two membrane proteins in order to obtain NMR spectra of good quality. The LH1 α and β can serve as good models for membrane proteins in terms of their relatively low molecular weights and availability from natural source. A comprehensive examination of detergent effects on the NMR spectral quality and structural stability of membrane proteins was reported by Krueger-Koplin et al. (2), in which lyso-phosphatidylglycerols were shown to be most effective for yielding homogeneous and stable samples that are suitable for the NMR structural determination.

Twenty detergents including four types (anionic, cationic, ampholytic and non-ionic) and two series of different lengths of hydrocarbon side groups were employed in this study. 2D ^{1}H-^{15}N HSQC spectra were used to evaluate the sample properties and spectral quality. Both the anionic and cationic detergents yielded poor spectra for the LH1 α and β proteins with the numbers of observed peaks much fewer than expected. *n*-Octyl-β-D-glucopyranoside (OG) was the best for LH1 α protein, resolving all amide signals at 45 °C. The solution sample was stable for one week. However, the spectrum of LH1 β protein was poorly resolved in OG, indicating aggregation as revealed by small-angle neutron scattering (3). The best result for the LH1 β protein was obtained with phosphocholines. Six phosphocholines with the hydrocarbon side chain ranging from n=8 to n=16 were tested, and decylphosphocholine (n=10) was shown to give the best spectrum in which all signals were resolved.

References: (1) Z.-Y. Wang, et al., *J. Mol. Biol.* **347**, 465-477(2005); (2) Krueger-Koplin et al., *J. Biomol. NMR*, **17**, 43-57(2004); (3) Z.-Y. Wang, et al., *Biochemistry* **42**, 11555-11560(2003).

L14

A Novel Strategy for Protein Structural Study under Intracellular Environment by using *Xenopus laevis* Oocyte

Tomomi Sakai[1], Hidehito Tochio[1], Fuminori Sugihara[1], Tetsuro Kokubo[1], Yutaka Ito[2], Hidekazu Hiroaki[1] and Masahiro Shirakawa[3]
International Graduate School of Arts and Sciences, Yokohama City University[1],
Graduate Schools of Science, Tokyo Metropolitan University[2],
Graduate School of Engineering, Kyoto University[3]

While heteronuclear multidimensional NMR is routinely used for protein structure determination, relatively less attention has been paid to its intrinsic non-invasiveness against living cells and organisms. Taking advantage of this non-invasiveness, we have developed a novel strategy to investigate protein structures under intracellular condition.

African clawed frog, *Xenopus laevis,* is a popular model animal in many of biological research areas. Especially, *Xenopus* oocytes provide an excellent gene expression system, where protein products are readily expressed by injecting mRNA into the oocyte. In this study, we inject *Xenopus* oocytes with isotope labeled proteins instead of mRNA, so that the injected protein can be investigated under intracellular environment by heteronuclear multidimensional NMR. Calmodulin was chosen for the test case and ^{15}N labeled protein was injected into healthy living *Xenopus* oocytes at the final concentration of 100-150 μM for each oocyte. About 250 of injected oocytes were then placed into NMR tube and ^{1}H-^{15}N HSQC spectra were taken at 18℃. The crosspeaks were broadened possibly due to higher viscosity and molecular crowding effect of the cytosol, resulted in poor signal to noise ratio compared to that of *in vitro* HSQC. Nevertheless, numbers of crosspeaks were recognized, and most importantly the spectra were similar to that of Ca^{2+} free calmodulin acquired in *in vitro* solution. Considering the fact that cytoplasmic Ca^{2+} level of the oocytes is only 0.1 μM while outside was adjusted to 5mM in our experiments, HSQC spectra obtained here are thought to arise from ^{15}N labeled calmodulin which is experiencing intracellular environment. Thus, we could successfully observed NMR signals from proteins inside living cells. The results of various proteins will be presented and general applicability of our new strategy will be discussed.

We are also exploiting a novel MRI gene reporter system by employing *Xenopus laevis* embryo system, aiming to realize *in vivo* monitoring of genes expression in higher eukaryotes. Recent progress will be presented and discussed.

L15

Distributed Computing and NMR Constraint-Based High-Resolution Protein Structure Determination: Applied for Endothelin-1

H. Takashima[1], N. Mimura[1], T. Yoshida[2], T. Ohkubo[2], Y. Nishi[3] and Y. Kobayashi[2,3]
[1] Novartis Institutes for BioMedical Research, Novartis Pharma, Ohkubo 8, Tsukuba, Ibaraki, 300-2611 Japan; [2] Graduate School of Pharmaceutical Sciences, Osaka University, 1-6 Yamadaoka, Suita, Osaka, 565-0871 Japan; [3] Osaka University of Pharmaceutical Sciences, Takatsuki, Osaka 569-1094, Japan.

Human endothelin-1 (ET-1) is a potent cardiovascular bioactive peptide. Its activity is based on the C-terminal residues, e.g., Trp 21 in particular. Despite of its pharmacological significances, the C-terminal strand of the peptide had had dispersed structure in previous studies of NMR (figure left). Here, we implemented a distributed computing to the solution structure determination of ET-1 to evaluate efficiency of the method for NMR constraint based structure calculations. With use of tens of thousands of random initial structures, to explore the conformational space comprehensively, we determined high-resolution structures with good convergences of C-terminal (figure middle) as well as previously defined N-terminal structures, which are strongly constricted by two disulfide bonds (the cystine-stabilized α-helix motif) [1]. The previous studies had likely missed the C-terminal convergence because of initial structure dependencies with insufficient number of calculations. The number of calculations we performed is 100 times larger than that used in ordinary structure determination.

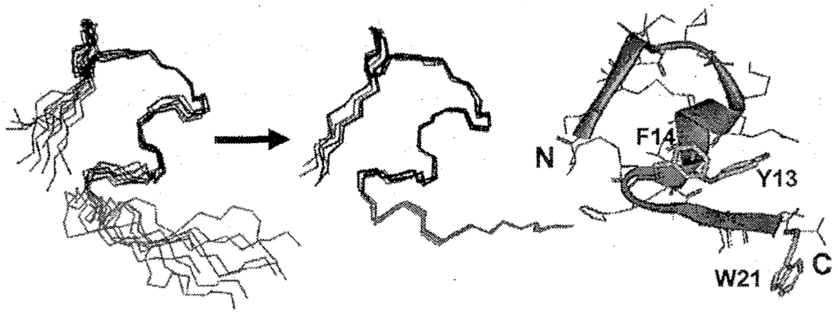

The C-terminal folding is hydrophobic core around Tyr 13 (figure right). This conformation does not agree with a previously reported X-ray crystal structure. To clarify the discrepancy, we performed photo-CIDNP NMR with combination of MALDI-TOF-MS. The photo-CIDNP results revealed that the Tyr 13 aromatic ring is concealed in a hydrophobic interaction. MALDI-TOF-MS experiments showed this is an intra-molecular interaction in monomeric form, which is also supported by sedimentation analysis and 2D-NMR cross peak line shapes. Thus, we confirmed the intra-molecular hydrophobic core around Tyr 13 in aqueous solution. The C-terminal conformational discrepancy between the solution and crystal was caused by the intermolecular hydrogen bond between Tyr 13 of one molecule and Asp 8 of the other in dimer like formation of crystalline ET-1.

1. Takashima, H., Mimura, N., Ohkubo, T., Yoshida, T., Tamaoki, H., and Kobayashi, Y. (2004) *J.Am.Chem.Soc.* **126,** 4504-4505.

2. Takashima, H., Tamaoki, H., Teno, N., Nishi, Y., Uchiyama, S., Fukui, K., and Kobayashi, Y. (2004) *Biochemistry*, **43**, 13932-13936.

L16

MAGICAL: Method for AssiGnments with Intelligent Combinatorial Amino acid Labeling

Rikou Tanaka, Chieko Komatsu, Kuniko Kobayashi, Takeshi Tanaka, and Toshiyuki Kohno
Mitsubishi Kagaku Institute of Life Sciences (MITILS)

NMR methods have been developed rapidly, and we can now automatically assign NMR signals for small and soluble proteins. However, it is still difficult to assign NMR signals of large, less soluble, and unstable proteins. To overcome these drawbacks, we have developed a novel assignment method using combinatorial amino acid labeling (MAGICAL: Method for AssiGnments with Intelligent Combinatorial Amino acid Labeling). With this method, we can now easily assign all the NMR signals of large proteins at lower (100 – 200 μM) concentration, only with 2D NMR measurements, even in the case of larger proteins such as 40 kDa. Furthermore, this method may be applied to proteins that are not stable to be analyzed by long 3D NMR measurements.

In the present study, we demonstrate the applications of this method to the NMR signal assignments of large proteins, such as maltose binding protein (MBP, 382AA) or other proteins, and to protein–protein or protein–ligand interactions analyses.

L17

The hetero-nuclear NMR-based metabomics by uniform stable isotope labeling in plant and animal systems

Jun Kikuchi[1,2,3]

[1]*RIKEN Plant Science Center;* [2]*Int. Grad. Sch. Arts Sci., Yokohama City Univ;* [3]*CREST, JST*

As any biological scientist does not doubt importance of metabomics in post-genomics-proteomics era, recent methodological advances of MS-based analysis lead in this field, whereas an NMR-based approaches are recognized as a minor one due to its low sensitivity. However, my laboratory is trying to initiate this field by developing new methods using a hetero-nuclear NMR-based approach. This has been achieved by the combination of the uniform stable-isotope labeling of higher plants and multi-dimensional NMR experiments [1,2] used in protein structure determination. The sample extraction methodologies were investigated for wide-range of organic solvents, allowing approximately 2-fold increase of the measurable metabolites in fluorinated solvents than widely used solvent systems such as Acetone/water or Chloroform/methanol [3]. Highly efficient algorithm for molecular identification observed in the mixture states is also developed by use of Java program searching our in-house metabolite standard chemical shift tables [4]. Using this novel approach, we can analyze the dynamic molecular networks inside cells, tissues and organisms. Furthermore, we have achieved uniform stable-isotope labeling of animals by feeding with uniformly labeled (such as ^{13}C, ^{15}N) plants [5]. Therefore, I propose these methodologies, the hetero-nuclear NMR experiments with the uniform stable-isotope labeling would be applicable for metabomics studies in nutrigenomics, drug discovery, toxicology and health-care assessment.

References

[1] Kikuchi, J., Shinozaki, K. and Hirayama, T. (2004) *Plant Cell Physiol.* 45, 1099-1104.

[2] Kikuchi, J. and Hirayama, T. (2005) *Biotech. Agri. Forestry* (invited paper).

[3] Sekiyama, Y., Chikayama, E., Hirayama, T., Shinozaki, K., Saito, K. and Kikuchi, J. (44th NMR conference).

[4] Chikayama, E., Sekiyama, Y., Hirayama, T., Saito, K., Shinozaki, K. and Kikuchi, J. (44th NMR conference).

[5] Suto, M., Nishihara, T., Tsuboi, Y., Hirayama, T. and Kikuchi, J. (44th NMR conference).

Key words : Stable isotope labeling, Metabomics, Nutrigenomics, Plant, Animal

L18

Concentration and Temperature Dependences of the Chemical Shifts Determined on a Unified Scale to Study C–H•••O Interactions in Some Binary Aqueous Mixtures of Organic Compounds

Kazuko Mizuno*, Yuka Tamiya, Takuya Yamamura, and Mamoru Mekata
Faculty of Engineering, University of Fukui, Fukui 910-8507, Japan

Introduction. An external reference method is essential to study the concentration dependence of chemical shifts for a series of sample solutions. It is also inevitable to correct the data in terms of the differences in the bulk volume magnetic susceptibilities between each sample and the external reference solutions.[1]

We have been studying concentration and temperature dependences of ^{1}H and ^{13}C chemical shifts for several series of binary aqueous mixtures of organic compounds with polar groups to identify the hydration mechanism of CH groups in the compounds. In the present work, we show the changes in the chemical shifts of water protons and the solutes together with those in the frequencies and absorption intensities for C–H stretching vibration bands with concentration to identify the properties of the chemical shifts on blue-shifting C–H•••O interaction. The temperature dependence of the chemical shifts is also discussed.

Method. ^{1}H- and ^{13}C-NMR spectra were measured with a JEOL EX-400 and AL-300 NMR spectrometers at 1.0, 25.0 and 50.0°C with an accuracy of ±0.1°C. The temperature was calibrated with a thermocouple inserted into the sample tube set in the probe of Superconducting Magnet prior to the measurements.

Chemical shifts were determined by the external double reference method[1] with bulbed capillary tubes manufactured by Shigemi Co. The capillary was 2 mm in diameter with a blown-out sphere of 3mm in diameter at the bottom. The bulbed capillary was filled with a reference substance liquid(TMS) up to 60 mm high and inserted into the center of the sample tube of 5 mm in diameter.

Observed chemical shifts for a series of sample solutions at a temperature were corrected following the equation

$$\delta = \delta_{obs} - (4\pi/3\kappa)\,\Delta\delta_{ref} \qquad (1),$$

where $\Delta\delta_{ref}$ is the difference in the chemical shifts between two reference peaks, and κ is the shape factor for the bulbed capillary tube, which was obtained experimentally.

Chemical shifts of a sample measured at a temperature T were corrected to be referred to the reference substance at a reference temperature T_r (25.0°C) following the equation

$$\delta^{Tr}(T) = \delta^{T}(T) - (4\pi/3)\{\chi_{ref}(T) - \chi_{ref}(T_r)\} \times 10^{6} + \delta_{cap}(T) - \delta_{cap}(T_r) \qquad (2),$$

where $\chi_{ref}(T)$ and $\chi_{ref}(T_r)$ are the volume magnetic susceptibilities of the reference substance at T and Tr, respectively.

Results. We discuss the specific properties of C–H•••O interaction from the concentration and temperature dependences of ^{1}H- and ^{13}C chemical shifts for the CH groups obtained.

Reference. 1) K. MIZUNO, Y. TAMIYA, AND M.MEKATA, *Pure Appl. Chem.* 76, 105-114, 2004.

L19

Development of an amino acid-selective cross-saturation method for modeling protein-protein complex

Shunsuke Igarashi[1], Masanori Osawa[1], Koh Takeuchi[1,2], Ichio Shimada[1,3]
[1]Graduate School of Pharmaceutical Sciences, the University of Tokyo, Tokyo 113-0033, Japan, [2]Japan Society for the Promotion of Science, Tokyo 102-8471, Japan, [3]Biological Information Research Center, National Institute of Advanced Industrial Science and Technology, Tokyo 135-0064, Japan

We have recently developed cross-saturation (CS) and transferred cross-saturation (TCS) methods to identify the interface of protein-protein complex [1, 2]. Irradiation of the unlabelled "saturation-donor" protein and subsequent cross-saturation to the uniformly ^{2}H, ^{15}N-labeled "acceptor" protein decreases the intensity of the acceptor's NMR signals. Mapping of those affected residues indicates the binding interface on the acceptor structure. We report here an amino acid-selective CS method for modeling donor-acceptor complex. This method uses a highly deuterated donor protein except for the selected amino acid, which are expressed in *E. coli* cultured in the fully deuterated M9 mediums including the target amino acid with protons. These selectively ^{1}H-labeled residues are utilized as "saturation-donors", causing cross-saturation at the specific site of the acceptor. Combination of pairwize information of the donor amino acid type and correspondingly cross-saturated residues on the acceptor could specify the residue number(s) of the donor. This pairwize information enables us to determine the relative orientation of two proteins in the complex.

First, we have investigated the amino acid-selective ^{1}H-labeling efficiency and selectivity of protein by NMR techniques, showing that Ala, Arg, Leu, Met, Phe, and Tyr are suitable for the selective labeling. However, Asp and Gln are not applicable, due to their metabolism to other amino acids. Then, this selective CS method has been applied to a structure-known complex (PDB ID: 1CMX) of yeast ubiquitin hydrolase (YUH, M.W. 26kDa) as a donor and yeast ubiquitin (M.W. 8.4kDa) as an acceptor. We prepared Ala, Arg or Tyr-selective ^{1}H-labeled YUH, since YUH interface with ubiquitin includes Ala and Tyr residues, not any Arg residue. Either Ala or Tyr-selective CS was observed at ubiquitin interface residues Leu 71 and Leu 73 for Ala and Gly 75 for Tyr, while no cross-saturation was observed by Arg-selective CS experiment. Currently, a few more amino acids are under investigation. Specification of the donor residues on YUH and modeling of the complex will be discussed.

[1] Takahashi H et al., *Nat Struct Biol.*, 7, 220-3 (2000).
[2] Nakanishi T et al., *J Mol Biol.*, 318, 245-9 (2002).

L20

NMR structure of CAG trinucleotide repeart DNA complexed with a small-molecule ligand inducing nucleotide flipping

Kazuhiko Nakatani,[1,2] Shinya Hagihara,[1] Yuki Goto,[1] Akio Kobori,[1] Masaki Hagihara,[1] Gosuke Hayashi,[1] Motoki Kyo,[3] Makoto Nomura,[4] Masaki Mishima[4] and Chojiro Kojima[4]

[1]Kyoto University, Kyoto, Japan, [2]PRESTO, JST, [3]Toyobo Co. Ltd., Tsuruga, Japan, and [4]Nara Institute of Science and Technology, Ikoma, Japan

Trinucleotide repeat expansions in genomic DNA are the molecular basis of a growing number of hereditary diseases. The characteristic feature of these diseases is a phenomenon termed as anticipation. A longer repeat length would lead to the increasing disease severity and decreasing age at onset in succeeding generations. The mechanism of $(CAG)_n$, $(CTG)_n$, and $(CGG)_n$ repeats expansion is considered to correlate to the increased stability of the metastable hairpin form consisting of CXG/CXG triads involving X-X mismatches. Ligands binding to $(CXG)_n$ repeats would be important molecular probes for determining the repeat length and the repeat expansion mechanism. Here we show the solution structure of the first identified ligand, naphthyridine–azaquinolone (NA), complexed with the CAG/CAG triad.

Complex formation between NA and an 11-mer DNA duplex containing CAG/CAG was monitored by ^{1}H one-dimensional imino proton spectra while NA was titrated. Signals from free DNA and the NA-DNA complex were observed separately on a slow-exchange timescale. The stoichiometry was easily and unambiguously determined to be 2:1 (NA:DNA), and no intermediate was observed. NMR spectra of the NA-DNA complex were recorded using $^{13}C^{15}N$-labelled DNA. The determined solution structure of the complex revealed the invasive ligands binding to the A-A mismatch and flanking G-C base pairs, causing the widowed cytosines to flip out from π-stack. Hydrogen-bond pairs between NA and DNA, naphthyridine-guanine and azaquinolone-adenine, are well stacked in the right-handed DNA helix, showing structural mimicry of Watson–Crick base pairing. This is the first observation that the small molecular ligand induced the base flipping of the nucleotide base in the Watson-Crick base pair.

Reference

Kazuhiko Nakatani, Shinya Hagihara, Yuki Goto, Akio Kobori, Masaki Hagihara, Gosuke Hayashi, Motoki Kyo, Makoto Nomura, Masaki Mishima, and Chojiro Kojima. Small molecule ligand induces nucleotide flipping in $(CAG)_n$ trinucleotide repeats. *Nature Chemical Biology*, 2005 Jun; 1(1): 39-43.

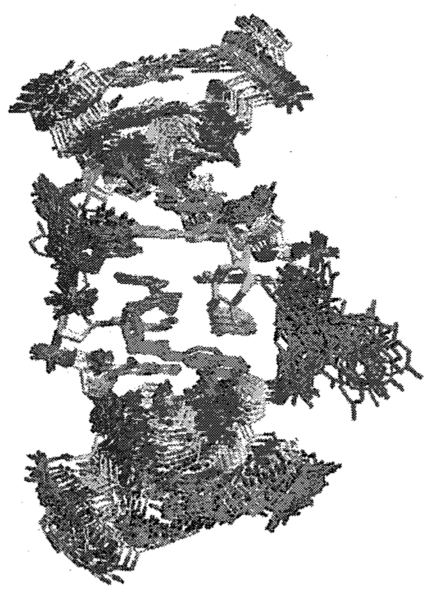

(right) Figure 1. NMR structures of **NA–CAG–CAG** complex. DNA is colored white and blue except for the phosphate group, which is colored orange and red. Two **NA** molecules are colored yellow and orange. 30 complex structures are superimposed focusing on A6, G7, A17, G18, NA1, and NA2 residues.

L21

Analysis of Variance on Metabolites in Saliva from Young Healthy Females.

Seizo Takahashi[1], Rina Yatsu[1], Yuki Kamiyama[1], Yukiharu Yamaguchi[2], Takashi Ogino[3]

[1]Department of Chemical and Biological Sciences, Japan Women's University,

[2]Division of Clinical Technology, Pfizer Global R & D, Pfizer Japan Inc.

[3]National Institute of Neuroscience, NCNP

Introduction Metabolites in saliva fluctuates their concentration under various physiological control. The aim of present study was to get insights into the intra- and inter-subject variability of drug response using an internal hormonal control of young healthy females. Last year, the factors to cause fluctuations of Acetate and Lactate concentration were reported. Presently most resonances observed in saliva were analyzed.

Materials & Methods Fresh saliva over 300 samples were collected into Sallivet™ (ca. 2 mL), and 0.48mL was transferred to a standard 5mm NMR tube with 0.02mL deuterium oxide. ^{1}H-NMR spectra of 400MHz were acquired on a Bruker AMX-400WB spectrometer at 290K. Spectral peaks were resolved by matNMR in the frequency domain using the Voigt line-shape function. JMP™ was used for statistical analyses. Daily fluctuations were analyzed using PLS_toolbox™ under MATLAB™.

Results (1) Spectral intensities of Acetate and Lactate made log-normal distributions. Normal distribution was observed, however, the observed distributions were mostly between normal and log-normal. (2) The standard deviations were proportional to the means of intensities. The result suggests that the physiological alteration should be analyzed from the relative change of metabolite concentration. (3) The intensity correlations between methyl and methylene of same molecular species were poorer than expected, suggesting that the presence of intermolecular interactions in specimen perturbs the intensities. (4) The correlations of intensity among molecules were found difficult to evaluate by numeric, since multi-phase structures were hidden. (5) Factor analysis of pyruvate revealed that it was contributed from ethanol, lactate and acetate successively, and another series was β-hydroxybutylate, acetate, iso-butylate, and n-butylate. The result looks compatible to the biochemical metabolic scheme. (6) Most daily fluctuation was explained by 2 principal components. They were irrelevant to the physiology of hormonal control. The result was consistent to the previous finding that metabolites in saliva make fluctuation by a number of factors other than internal one. (7) Overall distribution of time-average of single person was similar to the sample-average of specified days. The result indicates that variations of intra-subjects are larger than the inter-subjects.

Discussions Biological system comprises a network of enzymatic reactions; parallel or one step enzymatic reaction would make a normal distribution, while infinite successive reaction would make a log-normal distribution. The present study uncovered that metabolites mostly comprise a chain of finite successive reactions. According to a network theory, the substance of normal distribution is vital to life but scarcely observable, which was unfounded by the present study. Further analysis of distribution would reveal the apparent number of steps in enzymatic reactions. It is possible that the variance of subjects reside in the change of distribution rather than average concentrations.

L22

Applications of CAST/CNMR to Structural Revision of Terpenoids

Hiroyuki Koshino[1], Shunya Takahashi[1], and Hiroko Satoh[2]

[1]RIKEN (The Institute of Physical and Chemical Research), 2-1 Hirosawa, Wako, Saitama 351-0198, Japan.

[2]National Institute of Informatics, 2-1-2 Hitotsubashi, Chiyoda-ku, Tokyo 101-8430, Japan.

CAST/CNMR is a computer system that ensures highly accurate prediction of ^{13}C NMR chemical shift values, which are calculated by using NMR data of carbons in the same structural enviroments[1]. A stereochemical coding method CAST (CAnonical-representation of STereochmistry)[2-4] made it possible to treat information on stereochemistry in the system. We developed a function that effectively took into account ring structural environments by adopting a CAST notation on ring structures with a new ring-perception algorithm[5]. In the 43rd annual NMR meeting, we reported structural revisions of recently reported terpenoids, amentotaxin BB, peribysins C and D, and daurichromene D. In the studies of the applications of CAST/CNMR, many misassignments of terpenoid structures have been found and their correct structures were confirmed by the reconsideration of the reported spectral data and by taking into account the results of the ^{13}C NMR prediction with CAST/CNMR. In the case of (*23Z*)-cycloart-23-en-3β,25-diol (**1**) and related triterpenoids, we synthesized authentic samples of *E* and *Z* isomers for the confirmation. The applications of CAST/CNMR to the structural revisions of some natural terpenoids will be described together with the detailed methodologies in the CAST/CNMR system.

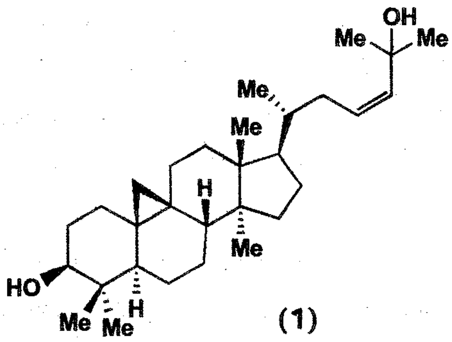

(**1**)

References.

1) H. Satoh, H. Koshino, J. Uzawa, and T. Nakata, *Tetrahedron*, **59**, 4539-4547 (2003).
2)H. Satoh, H. Koshino, K. Funatsu, and T. Nakata, *J. Chem. Inf. Comput. Sci.*, **40**, 622-630 (2000).
3)H. Satoh, H. Koshino, K. Funatsu, and T. Nakata, *J. Chem. Inf. Comput. Sci.*, **41**, 1106-1112 (2001).
4) H. Satoh, H. Koshino, and T. Nakata, *J. Comput. Aid. Chem.*, **3**, 48-55 (2002).
5) H. Satoh, H. Koshino, T. Uno, S. Koichi, S. Iwata, and T. Nakata, *Tetrahedron*, **61**, 7431-7437 (2005).

L23

Calculation of nuclear magnetic shieldings using an analytically differentiated relativistic shielding formula

H. Fukui and K. Kudo
Kitami Institute of Technology

<Abstract>

Two expressions for nuclear magnetic shielding tensor components based on analytically differentiating the electronic energy of a system are presented. The first is based on a second-order Douglas-Kroll-Hess (DKH2) approach, in which the electronic states of the transformed Dirac Hamiltonian are correct to second order with respect to both the nuclear potential V and magnetic vector potential $\overrightarrow{A}$. The second expression is based on the method of Barysz-Sadlej-Snijders (BSS), in which the electronic states are completely correct with respect to V and correct to second order with respect to $\overrightarrow{A}$. The two approaches are applied to the calculation of nuclear magnetic shieldings of hydrogen halides with common gauge origins. Both methods yield similar results except for the paramagnetic shielding of the nucleus I.

<Result and Conclusion>

Two analytical differentiation expressions for calculating nuclear magnetic shielding tensor components were derived at the coupled Hartree-Fock (CHF) level. The first approach is based on the second-order Douglas-Kroll-Hess (DKH2) method, and the second approach is based on the method of Barysz-Sadlej-Snijders (BSS). The second method is more exact than the first method. The two approaches were applied to the calculation of nuclear magnetic shieldings of hydrogen halides with common gauge origins. Each shielding of halogen and hydrogen atoms was computed using the two common gauge origins placed at the positions of halogen and hydrogen nuclei. The dependence of the computed shieldings on the gauge origin was small enough except for σ^{iso} of the proton in HI. Comparison of the results of present two approaches for hydrogen halide shieldings showed that the relativistic corrections of higher than second order are negligibly small except for the paramagnetic shielding of the I nucleus. The present results were found to be consistent with previously reported values for hydrogen halide shieldings, except for large disorepancies for the anisotropy of proton shielding of HI compared to previous reports. The large anisotropy values for proton shieldings of HI shown in the present calculations are not thought to be due to error because the present values are similar for the two different approaches with the two different common geuge origins. Unfortunately, no experimental values for the anisotropy of proton shielding in HI are available for verification. It is concluded that the present two expressions for calculating nuclear magnetic shielding yield self-consistent and reliable results.

L24

NMR-based Metabolomics

Integrated High-Field NMR-Spectroscopic and Multivariate Analysis for Disease Model Rat Urine

Tadashi Nemoto[1], Masako Fujiwara[2], Kazunori Arifuku[2], Itiro Ando[3], Taeko Kataoka[1], Kenji Kanazawa[1], Katsuo Asakura[4], and Hiroaki Utsumi[4]
[1]National Institute of Advanced Industrial Science and Technology (AIST)
[2]JEOL DATUM LTD, [3]Envioronmental Research Center LTD, [4]JEOL LTD.

Among so-called 'omics' research fields, metabolomics study has been becoming another attractive field as a last piece of system biology in post genome-sequencing era. Metabolomic research by high field NMR spectroscopy offers highly sensitive detection of gross metabolite profile with better resolution. The application of ^{1}H-NMR to metabolomic research is basically simple and straightforward. For fundamental experimental studies, urine samples from disease model rats at different age and sex with various sampling periods of the day were collected. Consequently, samples were measured as water-suppressed 1D ^{1}H NMR spectrum by using a JEOL ECA-800 spectrometer. FIDs were processed by absolute value differentiation method after FFT to skip phase and/or baseline correction. Without any spectral assignment, spectrum were converted into numeric value datasets by bucket integration and then subjected to multivariate method of Principal Component Analysis (PCA). Using this collective analysis, we can clarify and evaluate physiological or pre-symptomatic status of each individual rat in various conditions. The accumulation of basic knowledge and know-how's has been undergoing. We (AIST, JEOL and JEOL DATUM) have been launched 50/50 matching fund joint research for 2 yeares since FY2005 for this aim.

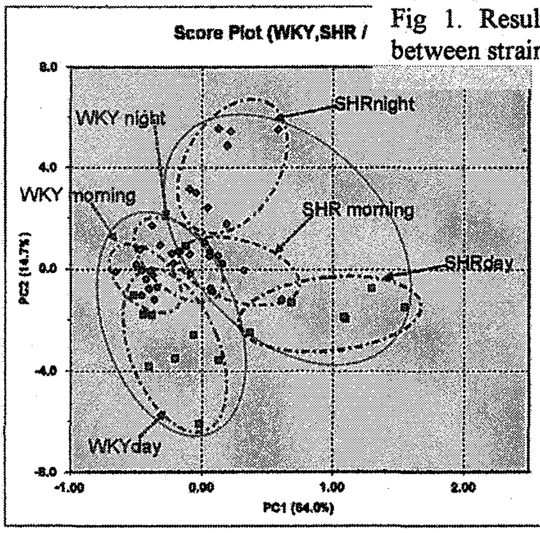

Fig 1. Result of PCA showed clear classification between strains (WKY &SHR) and times of the day.

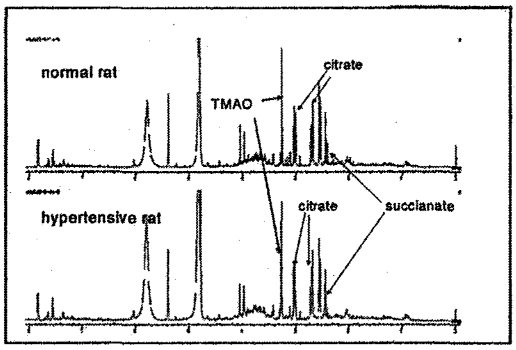

Fig 2. Example spectra of normal and hypertensive model rat urines together with marker candidate peaks concluded by this analysis.

L25

NMR-based Metabolomics

Pattern Recognition Analysis of Hypertensive Model Rat and Diurnal Variation using ^{1}H-NMR Spectroscopy of Urine

Masako Fujiwara[1], Itiro Ando[2], Kazunori Arifuku [1]
Kenji Kanazawa[3], and Tadashi Nemoto[3]
[1]JEOL DATUM LTD, [2]Envioronmental Research Center LTD, ,
[3]National Institute of Advanced Industrial Science and Technology (AIST),

NMR-based Metabolomic analysis has mainly been used for toxicology or drug discovery. Recently, various life-style related diseases, such as hypertension, diabetes, and hyperlipidemia, have become serious topics of concern. To acquire potential information on disease status, including pre-symptomatic data, detection of profile difference from the normal in natural conditions is essential. We performed an experiment with rats: 10 rats of spontaneously hypertensive (SHR/Izm) and 10 rats of normal (Wistar Kyoto, WKY) under conditions of minimized intentional stress. The urine samples were collected during the daytime and nighttime and the ^{1}H-NMR spectra were measured by using JEOL ECA-500. All the spectra were analyzed by the pattern recognition method and classified by their pattern differences by using the software Alice2 for Metabolome (JEOL). Separation of urinary data due to diurnal variation and also to the difference between the two strains of rat was achieved in the PCA score plot (Fig.1). Differences of the urinary profiles in the respective separation were effectively extracted as marker variables (Fig.2) by the SIMCA method

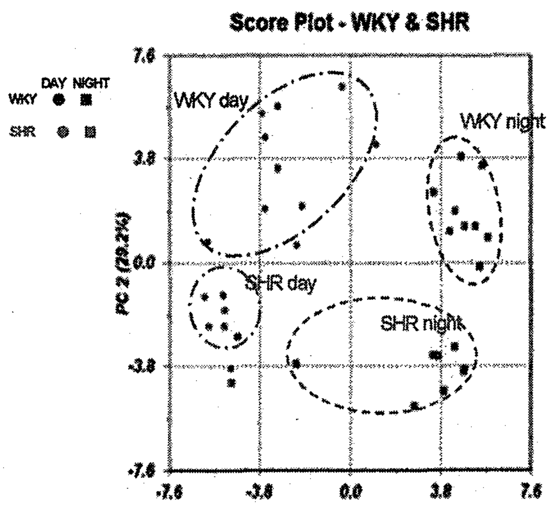

Fig1 PCA (Principal Component Analysis) score plot (PC1-PC2)

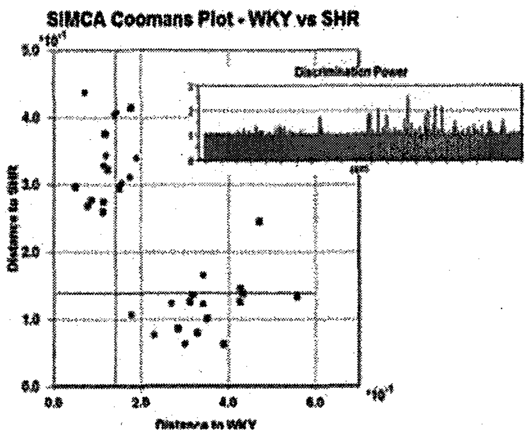

Fig.2 SIMCA (Soft Independent Modelling of Class Analogy) method generates discrimination power via variables between two strains.

L26

NMR imaging investigation of rice cooking

Midori Kasai[1,2], Andrew Lewis[2], Florea Marica[2], Sonoko Ayabe[1], Keiko Hatae[1], Colin A. Fyfe[2]

[1]Department of Nutrition and Food Science, Ochanomizu University, 2-1-1 Otsuka, Bunkyo-ku, Tokyo 112-8610, Japan

[2]Department of Chemistry, The University of British Columbia, 2036 Main Mall, Vancouver, BC, Canada V6T 1Z1

1. Introduction

To predict the optimum cooking conditions of rice, one needs quantitative information regarding the cooking process, particularly the water content within the grains and its distribution. In this study, we have established a method for the visualization and quantification of the cooking of rice using NMR imaging.

2. Materials and Methods

Japonica rice (Oryza sativa L. Japonica cv. Nipponbare) grown in Japan was used as sample and milled up to 90%. The water of ratio to rice was 1.4 (w/w). The sample was cooked in the vial (ϕ15mm, H45mm) and was taken out after each cooking time and cooled in water. A Bruker Avance DRX 360 NMR spectrometer operating at 360 MHz (8.4T) for ^1H with microscopic imaging capabilities was used for the experiments. Calibration of water T_2 values in water/rice starch mixtures were made using the exactly the same multi slice multi echo (MSME) pulse sequence used for the imaging studies.T2 images of the samples was calculated to water contents using calibration curve by software.

3. Results and discussions

The cooking process of rice could clearly be followed by NMR imaging using the first echo images. Each pixel in the T_2 images was calculated from a series of echoes of the water ^1H signal. The distributions of the T_2 values in the rice grains changing with increasing cooking time was elucidated and was transformed into that of water content. The differences in water content and distribution in the rice grains at each cooking time was visualized and quantified successfully.

3. Conclusions

The experimental protocol developed here will be useful to detect and quantify differences in the cooking behavior of various types of rice.

L27

Simultaneous Detection of Glutamate, GABA and Glutamine in the Human Brain at 4.7 T using a Localized 2D CT-COSY with an ISIS Pulse

H. Watanabe, N. Takaya, F. Mitsumori
National Institute for Environmental Studies
Onogawa 16-2, Tsukuba, Ibaraki, 305-8506, Japan

Glutamate (Glu) and γ-amino butyric acid (GABA) are major neurotransmitters (excitatory and inhibitory, respectively) in the human brain. Glutamine is a precursor and a storage form of glutamate. Thus, *in vivo* detection of Glu, GABA and Gln will give us the useful information for glutamatergic and GABAergic neurons, and astrocytes. We have demonstrated *in vivo* detection of these metabolites in the human brain using a localized 2D CT-COSY at 4.7 T. This sequence uses 90 degree, 180 degree and 90 degree pulses as slice selective pulses. Compared to 90 degree pulses, the band width for 180 degree pulses is narrower because of RF power limitation. This causes slice displacement errors due to chemical shift dispersion and it is a critical problem especially at high field. The slice profile of 180 degree pulse is also worse than that of 90 degree pulse. In this work, we propose a localized 2D CT-COSY with an ISIS pulse for one direction to overcome that.

First, we demonstrated the improvement of slice displacement and profile in phantom experiments using water ^1H signal. Figure 1 shows the slice profiles with the proposed method and the original method. Slice profile of the proposed method is better than that of the original method. The slice displacement error of the proposed method is about two times smaller than that of the original method. Next, we did human volunteer studies. Figure 2 shows a CT-COSY spectrum of the human brain and a diagonal spectrum obtained by a proposed method. Diagonal peaks of glutamate C4H, glutamine C4H and GABA C2H are resolved. A cross peak between glutamate C4H and glutamate C3H is also detected.

Therefore, we conclude that a localized 2D CT-COSY with an ISIS pulse can detect glutamate, GABA and glutamine in the human brain with the features of minimization of the slice displacement error and a better slice profile.

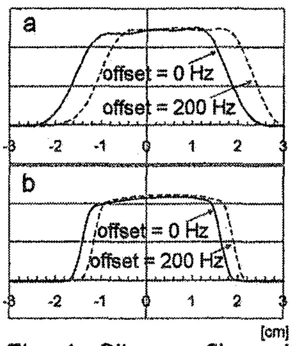

Fig. 1. Slice profiles with the original method (a) and with the proposed method (b).

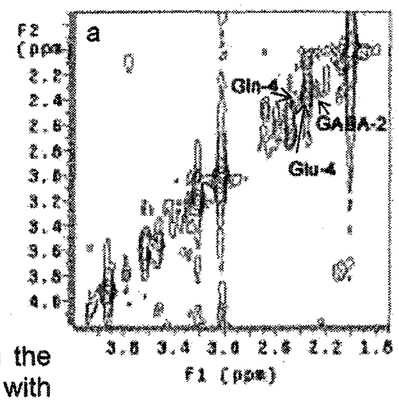

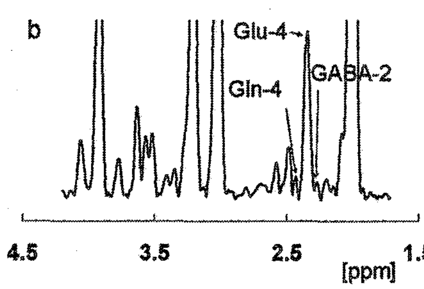

Fig. 2. Human brain 2D spectrum obtained by a localized 2D CT-COSY with an ISIS pulse (a) and a diagonal spectrum (b).

KL1

Optimal Isotope Labeling for NMR Protein Structure Determination: Stereo-Array Isotope Labeling (SAIL) Approach

Masatsune Kainosho

CREST of JST and Graduate School of Science, Tokyo Metropolitan University

Protein structural determinations by NMR spectroscopy have been virtually limited to those smaller than 25 kDa, although so much effort has been exerted to extend the limit. Methods such as random fractional deuteration, or selective protonation, are compromises at the expense of signal sensitivity and the accuracy of the resultant structure. More robust and uncompromised techniques should therefore be exploited, if NMR spectroscopy is to remain to be a competitive method for structural determinations of larger proteins and protein complexes.

During the 40 year history of biological NMR spectroscopy, it has been clear that concomitant advances in spectroscopic methods and in preparative methods of isotopically labeled proteins are essential to overcome the numerous difficulties. The SAIL (Stereo-Array Isotope Labeling) technology for protein NMR spectroscopy exclusively utilizes chemically or enzymatically synthesized amino acids, designed to have an optimal stereo- and regiospecific pattern of stable isotopes, from which proteins are obtained by cell-free synthesis. As demonstrated for a few proteins, SAIL offers sharpened lines, spectral simplification without loss of information, and the ability to rapidly collect the structural restraints required to solve a high-quality solution structure. SAIL is expected to largely eliminate the key limiting factors for detailed solution structure determinations of larger proteins. In this lecture, I would like to present some of the recent results obtained using this strategy.

KL2

Structure and Function in Bacteria and Plants by REDOR

Lynette Cegelski, Sung Joon Kim, and Jacob Schaefer

Department of Chemistry, Washington University, St. Louis MO 63130

Most of the recent applications of solid-state NMR to biological science have focused on the determination of the total structure of a peptide or protein in a micro-crystal, or a reconstituted model membrane, or a precipitated amyloid fibril or plaque. These applications have successfully adapted many of the popular multi-dimensional solution-state NMR experiments to the special demands of the solid state for samples that are either mechanically spun or aligned. For the last 25 years, our laboratory has been engaged in an effort to use solid-state NMR to detect (with a minimum of perturbation) stable isotope labels that have been introduced *in vivo* in bacteria, plants, insects, and shellfish. The goal is obviously not to determine a total structure but rather to connect partial local structure with biological function. We illustrate this strategy with two examples: (i) a correlation between structure and antimicrobial activity of vancomycin and oritavancin analogues in cell-wall complexes of whole cells of *Staphylococcus aureus* and (ii) a correlation between photorespiration and glycine metabolism in intact leaves of *Glycine max* (soybeans). In both examples, the principal NMR tool is rotational-echo double resonance (REDOR), whose use is illustrated in the figure below.

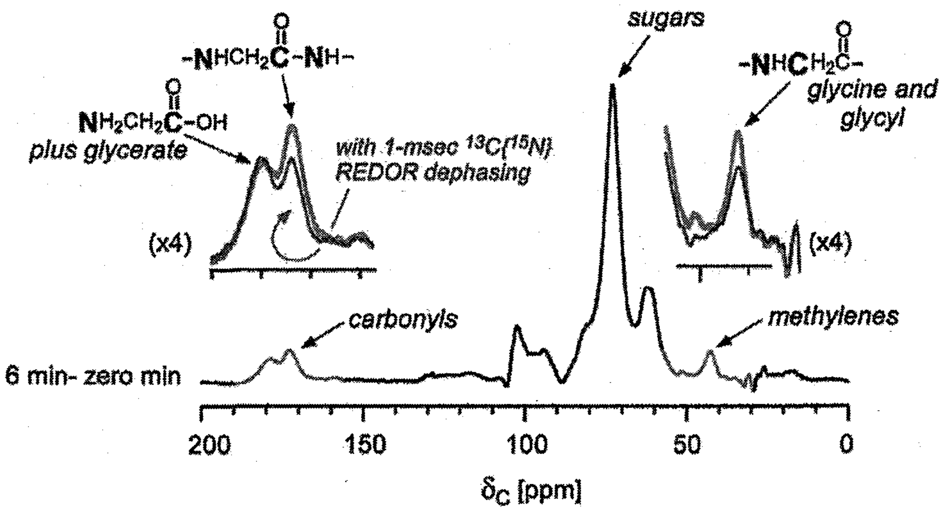

Cross-polarization magic-angle spinning ^{13}C NMR spectrum of an intact lyophilized soybean leaf (uniformly ^{15}N-labeled by $^{15}NH_4{}^{15}NO_3$) exposed for 6 minutes to $^{13}CO_2$ at 300 ppm (by volume). This is a difference spectrum resulting from the subtraction of the spectrum of an unexposed leaf. Each of the spectra in the difference resulted from the accumulation of 110,000 scans. The relative scaling of the two spectra was chosen to minimize the natural-abundance difference peaks between 10 and 30 ppm. Only peaks arising from the ^{13}C label remain, and their integration gives an accounting of total ^{13}C assimilation in the leaf during the labeling period. Two carbonyl-carbon difference peaks (in blue) are observed: one at 179 ppm (near the chemical shift of the carboxyl carbon of free glycine) and the other at 171 ppm (the characteristic chemical shift of the peptide carbonyl carbon of glycyl residues in α-helical local conformations). The 171-ppm peak and a 43-ppm methylene-carbon peak (both in red) decrease in intensity following a $^{13}C\{^{15}N\}$ dipolar evolution period for 1 msec (insets), indicating directly bonded ^{13}C-^{15}N pairs.

PLL1

New Developments in NMR and MRI at Berkeley: Materials and Biomedicine from Nanometers to Meters

A. Pines
Senior Scientist, Lawrence Berkeley National Laboratory and Glenn T Seaborg Professor of Chemistry, University of California Berkeley, Berkeley, CA 94720, USA

ABSTRACT

Novel methodologies of NMR and MRI from molecular to macroscopic scales will be described. Microtesla magnetic resonance with SQUID detectors has extended from *in vitro* solution spectroscopy to *in vivo* human imaging. We have further extended the observation of high-resolution NMR and MRI in inhomogeneous fields using "shim pulses" in inhomogeneous fields and nonlinear gradients. First results have been obtained using one sided systems, thereby enhancing the promise of an approach to scanning *ex-situ* detection of magnetic resonance which would make it possible to obtain high-resolution information about objects or subjects that are immobile or otherwise inaccessible to traditional methods of NMR and MRI. The combination of optical and magnetic resonance using laser-polarized atoms and enhanced *remote* detection using SQUIDs and lasers for reconstruction of images and spectra allows the exploration of species identification, distribution and flow, in solution, in porous materials and in microfluidic channels. Furthermore, *functionalized* molecular biosensors using hyperpolarized agents with continuous bubbling/dissolution and flow have been used to detect target molecules and protein conformational changes upon substrate binding. The NMR biosensor methodology is being combined with *remote* detection for enhanced sensitivity in the examination of ultralow concentration species in solution. Such approaches also open the possibility of magnetic resonance for multiplexed molecular assaying, with applications in physics, chemistry, materials science, and biomedicine.

Collaborating with Jean-Pierre Dutasta and Thierry Brotin in Lyon, Yiqiao Song, Pabitra Sen et al at Schlumberger-Doll Research, and the groups of Bernhard Bluemich in Aachen, and John Clarke, Dmitry Budker, Jeffrey Reimer and David Wemmer at Berkeley

PLL2

Receptor dynamics and structure in membranes resolved using solid state NMR

Anthony Watts, Biomembrane Structure Unit,
Biochemistry Department, Oxford University, Oxford, OX1 3QU, UK.

It is now possible to resolve local dynamics within a membrane bound protein at near physiological conditions in natural membrane fragments or in reconstituted complexes, using solid state NMR approaches [1, 2]. This information is obtained by isotopically (^{2}H, ^{13}C, ^{19}F, ^{15}N, ^{17}O) labeling selective parts of either a ligand, or the protein understudy, and observing the nucleus in non-crystalline, macromolecular complexes [3,4].

Ligands with complex structure have differential mobility at their binding sites. Substituted imidazole pyridines, for example, which inhibit the H^+/K^+-ATPase and have therapeutic use, are constrained in the imidazole moiety, but shows significant flexibility at the pyridine group [5] (see figure). It is this group which has a direct interaction with an aromatic (phe198) residue, with the potential for π-electron sharing [6]. Similarly, the steroid moiety of ouabain undergoes motions which are similar to those of the protein, but the rhamnose undergoes a high degree of flexibility at fast rates of motions whilst interacting with Tyr198 [7]. The quaternary ammonium group of acetyl choline, undergoes both kinds of interaction which are driven by thermal fluctuations and may be functionally significant [8].

Membrane protein 2°-structural elements are often considered as relatively well defined, with connections of (relatively unstructured or mobile) loops, which are not necessarily easily defined structurally. However, these loops may be the most important domains for ligand binding, leading to subsequent activation. In addition, these loops are the regions where protein-protein interactions occur, thereby transferring a signal between an activated receptor and protein transduction in the signal cascade. It has been possible to show that solid state NMR detection (from the ^{15}N spectral anisotropy of selectively labeled peptides) of loop regions of a receptor embedded in its natural membrane, permits the identification of the available crystal structure which is closest to the structure for the membrane-embedded, physiologically relevant structure [9].

[1]. Watts, A. (2005) Solid state NMR in drug design and discovery, *Nature Drug Discovery,* 4, 555-568
[2]. Watts, A., Straus, S.K., Grage, S., Kamihira, M., Lam, Y.-H. and Xhao, Z. (2003) Membrane protein structure determination using solid state NMR. In: *Methods in Molecular Biology – Techniques in Protein NMR Vol. 278* (ed. K. Downing), Humana Press, New Jersey, pp. 403-474.
[3]. Watts, A. (1999) NMR of drugs and ligands bound to membrane receptors. *Curr Op in Biotechn,* 10, 48-53.
[4]. Watts, A. (2002) Direct studies of ligand-receptor interactions and ion channel blocking. *Mol Memb Biol,* 19, 267-275
[5]. Watts, J.A., Watts, A. & Middleton, D.A. (2001) A model of reversible inhibitors in the gastric H+/K+-ATPase binding site determined by REDOR NMR. *J. Biol. Chem.* 276, 43197-43204.
[6]. Kim, C.G., Watts, J.A. & Watts, A. (2005) Ligand docking in the gastric H+/K+-ATPase - homology modelling of reversible inhibitor binding sites. *J. Med Chem.* (in press).
[7]. Middleton, D.A., Rankin, S., Esmann, M. and Watts, A. (2000) New structural insights into the binding of cardiac glycosides to the digitalis receptor revealed by solid-state NMR. *PNAS,* 97, 13602-13607
[8]. Williamson, P.T.F., Watts, J.A., Addona, G.H. Miller, K.W. and Watts, A. (2001) Dynamics and orientation of $N^+(CD_3)_3$-bromoacetylcholine bound to its binding site on the nicotinic acetylcholine receptor. *PNAS,* 98, 2346-2351.
[9]. Kamihira, M., Vosegaard, T., Mason, A.J., Straus, S.K., Nielsen, N.C. & Watts, A. (2005) Structural and orientational constraints of bacteriorhodopsin in purple membranes determined by oriented-sample solid-state NMR spectroscopy. *J. Struct. Biol.* 149, 7-16.

See also: www.bioch.ox.ac.uk/~awatts/

ALL1

NMR investigation on protein-protein interactions in cell signaling network

Mitsu Ikura

Division of Signaling Biology, Ontario Cancer Institute and Department of Medical Biophysics, University of Toronto, 610 University Ave., Toronto, Ontario, M5G 2M9, Canada

Structural elucidation of protein-protein interactions is crucial to understand the complicated signaling network in cells. Continued technical advances in NMR spectroscopy greatly improved our ability to analyze structures and dynamics of large protein complexes in solution and thus made significant contributions to structural elucidation of signaling molecules. In the past decade, my laboratory has been focusing on applications of various NMR methodologies to investigate protein-protein complexes involved in gene transcription and intracellular signaling. We have used NMR to investigate the intracellular Ca^{2+} sensor protein calmodulin and its interactions with various target proteins. This led to our hypothesis that protein conformational plasticity is key to multifunctionality of calmodulin. Our previous NMR and biochemical studies on transcriptional regulation by TATA binding protein (TBP) and a TBP-associated factor (TAF) revealed the interplay between TAF and an activator such as VP16 at the same binding site on TBP, underscoring the significance of time-dependent molecular interaction processes in switching gene transcription on and off. More recently, we I have been investigating protein complexes involving an activator/repressor interaction (E-protein/AML1-ETO). In this study, a combined NMR/molecular biology approach has helped us to map the exact binding region within a large protein. I will discuss various experimental aspects of these NMR studies currently ongoing in my laboratory.

ALL2

Structure, folding, and substrate channeling of the E2 component of human mitochondria branched chain α-ketoacid dehydrogenase complex

Chang, C.F.[2], Naik, M.[1], Chou, H.T.[1], Lin, Y.J.[1], Lee, S.J.[1] and Huang, T.-h.[1], [1]Inst. Biomed. Sci. & [2]Genomic Research Center, Academia Sinica, Nankang, Taipei, Taiwan, R.O.C.

The mammalian branched chain α-ketoacid dehydrogenase (BCKD) complex is a member of the highly conserved α-ketoacid dehydrogenase complexes comprising pyruvate dehydrogenase complex (PDC), α-ketoglutarate dehydrogenase complex (KGDC) and the BCKD complex with similar structure and function. The BCKD complex catalyzes the oxidative decarboxylation of branched-chain α-ketoacids derived from leucine, isoleucine and valine to give rise to branched-chain acyl-CoAs. The reaction products are indirectly channeled into the Krebs cycle or linked to lipid and cholesterol biosynthesis. In patients with inherited maple syrup urine disease (MSUD), the activity of the BCKD complex is deficient, which results in the accumulation of branched-chain α-ketoacids. This metabolic block has severe clinical consequences including often-fatal ketoacidosis, neurological derangement and mental retardation in survivors. There are three catalytic components in human BCKD: a heterotetrameric ($\alpha_2\beta_2$) branched-chain α-ketoacid decarboxylase or E1, a homo-24 meric dihydrolipoyl transacylase or E2 and a homodimeric dihydrolipoamide dehydrogenase or E3. The BCKD complex is organized around the cubic E2 core, to which 12 copies of E1, and unspecified copies of E3, the BCKD kinase and the BCKD phosphatase are attached through ionic interactions. The molecular mass of the BCKD multienzyme complex is estimated to be 4×10^6 daltons. The *E2* subunit of the branched-chain α-ketoacid dehydrogenase (BCKD) employs three components, the lipoyl-bearing domain (LBD), the subunit-binding domain (SBD) and the core domain to fulfill its function in substrate channeling and substrate recognition. We have employed multidimensional heteronuclear NMR, CD, fluorescence and Langevin dynamics molecular modeling methods to determine the structure, dynamics and folding of several truncated fragments of the human BCKD complex (hbLBD), including LDB (a.a. 1-84), SBD (a.a. 104-152) and a di-domain comprising residues 1 – 168 of the E2 component (DD). The results of which will be reported in this talk.

References:

1. Chang, C.F., Chou, H.T., Chuang, J., Chuang, D. and Huang, T.-h. J. Biol. Chem. (2002) 277, 15865-15873.
2. Naik, M., Chang, Y.C. and Huang, T.-h. FEBS Lett. (2002) **530**, 133-138.
3. Naik, M. and Huang, T.-h. (2004) Protein Sci. **13**, 2483-2492
4. Kouza, M., Chang, C.-F., Hayryan, S., Yu, T.H., Li, M.S., **Huang, T.-h.** and Hu, C.K. (2005) Biophys. J. (in press).

ALS1

How to assemble a fungal umbrella: step-by-step instructions

Kwan, AH, Winefield, RD, Sunde, M, Templeton, MD, Mackay, JP
School of Molecular and Microbial Biosciences, University of Sydney, NSW 2006 Australia
HortResearch, Auckland, NZ

Class I hydrophobins are a remarkable class of fungal proteins that form polymeric, water repellent monolayers on the surface of structures such as spores and fruiting bodies. Similar monolayers are being discovered on an increasing range of biological structures, including filamentous bacteria and frog egg foam. Hydrophobin monolayers are amphipathic and particularly robust, and are able to reverse the polarity of the surface on which they are formed. There are also significant similarities between these polymers and amyloid fibrils. However, structural information on these proteins and the rodlets they form has been elusive. Here we describe the three-dimensional structure of the monomeric form of the hydrophobin EAS. EAS forms a beta-barrel structure punctuated by several disordered regions and displays a complete segregation of charged and hydrophobic residues on its surface, consistent with its ability to form an amphipathic polymer. Using the structure, together with a wide range of available biophysical data, we have been able to propose a convincing model for the polymeric rodlet structure adopted by these proteins. X-ray fibre diffraction data on partially aligned EAS rodlets are consistent with our model. Our data provide the first molecular insight into the nature of hydrophobin rodlet films and have significant implications for our understanding of the increasingly common amyloid state.

ALS2

Study of the gradual protein unfolding by NMR spectroscopy

Jianxing Song, Zheng Wei, Miaoqing Fang & Jiahai Shi

Departments of Biochemistry and Biological Sciences
National University of Singapore, 10 Kent Ridge Crescent, Singapore 119260

Protein folding problem is a great challenge in molecular biology and many issues associated with the folding mechanism still remain unsolved and controversial. It has been extensively thought that small single-domain proteins fold and unfold via a two-state mechanism. However, our characterization of the pH-induced unfolding of a 37-residue CHABII first indicated that a continuum of equilibrium intermediates existed even between the native and molten-globule states of the protein (1-3). Therefore, NMR spectroscopy was used to gain atomic-resolution details as well as the molecular mechanism of the gradual unfolding of CHABII. The results led to the following findings:

1) In contrast to the common belief, at least for CHABII the disruption of the tight side-chain packing could be a gradual process.
2) At pH 4.0, CHABII formed the smallest molten globule identified so far, with a highly native-like secondary structure and tertiary topology, but a severely-disrupted side-chain packing.
3) The gradual unfolding of CHABII was triggered by the progressive protonation of His21 but its mechanism is different from that previously uncovered for apomyoglobin.
4) Replacement of His21 by Phe significantly enhanced the tertiary packing as evident from a significant increase in NOE number. This enhancement of the packing resulted in an increase of the thermal stability by 17 °C.

Currently, we are investigating the relationship between the gradual unfolding and NMR dynamics on the different time scales.

References:

1. **Song J**, Gilquin B, Jamin N, Drakopoulou E, Guenneugues M, Dauplais M, Vita C, Menez A. (1997) NMR solution structure of a two-disulfide derivative of charybdotoxin: ***Biochemistry***. 36, 3760-6

2. **Song J,** Jamin N, Gilquin B, Vita C, Menez A. (1996) A gradual disruption of tight side-chain packing: 2D ^{1}H-NMR characterization of acid-induced unfolding of CHABII ***Nat Struct Biol.*** 6, 129-34.

3. Wei Z & **Song J**. (2005) Molecular mechanism underlying the thermal stability and pH-induced unfolding of CHABII ***J Mol Biol.*** 348, 205-18.

ALS3

Structural characterization of preS1 surface antigen in Hepatitis B virus by NMR

Seung-Wook Chi, Do-Hyoung Kim, Min Jung Kim, Si-Hyung Lee, Jae-Sung Kim, and Kyou-Hoon Han

Protein Analysis and Design Laboratory, Division of Drug Discovery, Korea Research Institute of Bioscience and Biotechnology, Yusong P. O. Box 115, Daejon, Korea

Human hepatitis B virus (HBV) is a small enveloped DNA virus, which causes acute and chronic hepatitis in humans. HBV envelope consists of three surface glycoproteins called the large (L), middle (M), and small (S) proteins. All these proteins are translated from a single open reading frame that is divided into preS1, preS2, and S domains. L protein is mainly distributed on infectious viral particles and its preS1 domain was suggested to contain a specific binding site for human hepatocyte receptors and can induce virus neutralizing antibodies. In this study we characterized the structure and dynamics of the full-length preS1 domain (1-119) by using NMR spectroscopy. The full-length preS1 domain turns out to be intrinsically unstructured but contain local structural elements in aqueous solution. In particular, the free structure of preS1 (21-47) epitope region was compared with the structures bound to monoclonal antibodies.

BLL1

High-Resolution Solid-State NMR Analysis of Biological Supramolecular Systems

Hideo AKUTSU
Institute for Protein Research, Osaka University, Yamadaoka, Suita, Japan

To understand the organization of biological activities, investigations on biological supramolecular systems such as membrane proteins in membranes, translational machineries and energy conversion systems are important. However, the methodology for structural analysis of supramolecular system is still poor. Although X-ray crystallography is a powerful method, crystallization of membrane system, for example, is very difficult. While electron microscopy can handle membrane system directly, it also needs two-dimensional crystals for high-resolution analysis. Thus, high-resolution solid-state NMR is becoming an important method for the investigations on biological supramolecular systems. Solid-state NMR has been developed very rapidly in the last decade to cope with this new field.

We have developed a series of methodologies of high-resolution solid sate NMR under magic angle spinning (MAS), which include pulse sequences for magnetization transfer, sequential assignment of polypeptide signals, and obtaining structural parameters. By using these methods, we have determined the high-resolution structure of membrane bound Mastoparan X, which is the activator of G-protein. By using magnetization transfer between the membrane and peptides, the mode of interaction of Mastoparan X and the phospholipid membrane was also determined. We are now also working on H^+-ATPsynthase subunits using solution- and solid-state NMR. Although the F_1 complex is water-soluble, the F_o complex is embedded in the membrane. F_o subunit c is a good target for solid-state NMR. An approach to this kind of large membrane protein will be presented.

BLL2

Amyloid-β peptide disruption of lipid membranes and the effect of metal ions

Tong-Lay Lau[1,2], Ernesto E. Ambroggio[3], Deborah J. Tew[2], Roberto Cappai[2], Colin L. Masters[2], Gerardo D. Fidelio[3], Kevin J. Barnham[2] and Frances Separovic[1]

[1] School of Chemistry, The University of Melbourne, VIC 3010, Australia
[2] Department of Pathology, The University of Melbourne and the Mental Health Research Institute of Victoria, VIC 3010 Australia
[3] CIQUIBIC – CONICET – Departamento de Química Biológica, Facultad de Ciencias Químicas, Haya de la Torre y Medina Allende, Ciudad Universitaria, Córdoba, Argentina

Address correspondence to: Frances Separovic, School of Chemistry, University of Melbourne, VIC 3010, Australia, Tel: +61 3 8344 6464; Fax: +61 3 9347 5180; E-mail: fs@unimelb.edu.au

β-Amyloid peptide (Aβ) found deposited in the brain of patients suffering from Alzheimer's Disease (AD) is linked with neurotoxicity and cell death. Since Aβ is cleaved from a larger trans-membrane protein, the amyloid precursor protein, studies of the interaction of Aβ with membrane bilayers may be relevant to biological activity. Metal ions have been shown to bind to the histidine residues of Aβ and have been implicated in AD. We report the results of studies of Aβ(1-42) carried out in model membranes and the effect of metal ions (Cu^{2+} and Zn^{2+}). The effect of the phospholipids and the metals on peptide structure was observed by circular dichroism spectroscopy; while the integrity of the membrane was observed using ^{31}P and ^{2}H nuclear magnetic resonance, fluorescence and Langmuir Blodgett monolayer methods. The peptide and metal ions interact with the phospholipid headgroups although the effect on the bilayer and the peptide structure was different for membrane-incorporated or associated peptides. Incorporated peptides appear to disrupt the membrane more severely than associated peptides, which may have implications in disease states. Changes in the peptide structure promoted by the metal ions appear to modify the effect of Aβ on model lipid membranes. The interaction of the metal ions and the Aβ peptide on membrane bilayers suggests the possibility of biological consequences resulting from the loss of membrane integrity, which could lead to cell dysfunction associated with AD.

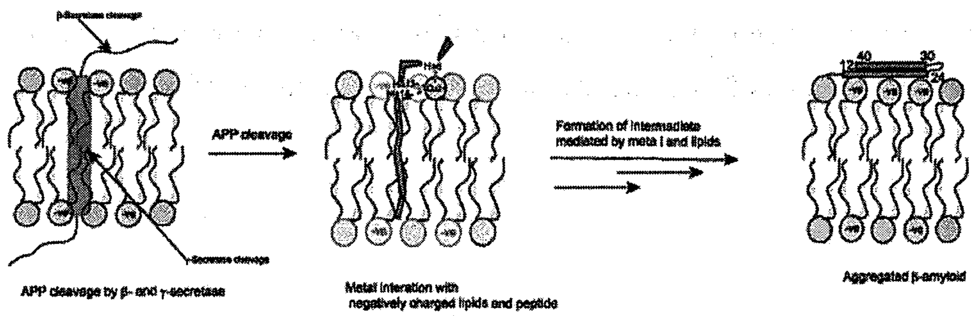

BLS1

Conformational and dynamics alteration of membrane proteins induced by 2D crystallization

Kazutoshi Yamamoto,[1] Satoru Tuzi,[1] Hazime Saitô,[2] Izuru Kawamura,[3] and Akira Naito[3]
[1]Department of Life Science, University of Hyogo, [2]Center for Quantum Life Sciences, Hiroshima University, and [3]Graduate School of Engineering, Yokohama National University

Membrane proteins such as bacteriorhodopsin (bR) are far from rigid body at *ambient temperature*, in spite of current 3D structural model revealed by cryo-electron microscope or X-ray diffraction. Indeed, they are flexible at fully hydrated state of biological relevance as viewed from site-directed solid-state ^{13}C NMR: they undergo various kinds of molecular motions with correlation times in the order of 10^{-2} – 10^{-8} s, depending upon portions under consideration.[1-3] Accordingly, it should be anticipated that ^{13}C NMR signals are substantially broadened as far as they are either uniformly or densely ^{13}C-labeled. Naturally, site-directed NMR approach using selectively ^{13}C-labeled amino-acid residues such as [3-^{13}C]Ala or [1-^{13}C]Val residues are alternative approach to circumvent this problem, although ^{13}C NMR signals are not always fully visible when other types of amino-acid residues were utilized for ^{13}C enrichment.

Still, it is anticipated that ^{13}C NMR spectral features arising from 3D structure/dynamics of such membrane proteins could be modified when specific helix-helix contact is removed in disrupted (monomeric sample) or distorted 2D crystals (D85N mutant). To clarify this problem, we compared ^{13}C NMR spectra of [3-^{13}C]Ala-/[1-^{13}C]Val-labeled bR, D85N mutant reconstituted in egg PC bilayer at pH 7 and 10 (M-like state) and naturally occurring respective 2D crystalline preparation. Surprisingly, the former three preparations yielded almost the same spectral features, even though these spectra are quite different when their 2D crystalline preparations were compared. This means that resulting spectral changes occurring in the loops and some transmembrane helices are not sensitive to such a conformational change as far as most of the signals are significantly suppressed in the monomeric preparations. It is noted, however, that such conformational changes in the loop region (and transmembrane helices) are well visualized at lower temperature by increased helix-helix contact as viewed from [1-^{13}C]Val-labeled peaks. Indeed, the loop structures turned out to be portions which could be very easily modified by such interactions.

1 H. Saitô, S. Tuzi, S. Yamaguchi, M. Tanio, and A. Naito, 2000, *Biochim. Biophys. Acta,* 1460, 39-48

2 H. Saitô, S. Tuzi, M. Tanio and A. Naito, 2002, *Annu. Rep. NMR Spectrosc.*, 47, 39-108

3 H. Saitô, 2004, *Chem. Phys. Lipids,* 132, 101-112

BLS2

Can database potentials improve the accuracy of protein structures?

Haydyn D. T. Mertens and Paul R. Gooley.
Department of Biochemistry and Molecular Biology, Bio21 Institute of Biotechnology and Molecular Science , University of Melbourne, Parkville, Victoria, Australia, 3010.

The refinement of protein structures determined by nuclear magnetic resonance (NMR) against database potentials of mean force allows for the exclusion of unfavourable conformations of the protein backbone during a structure calculation, resulting in protein structures with a marked improvement in Ramachandran statistics[1]. In this presentation we challenge the popular belief that the inclusion of such empirically derived potentials in protein structure determination provides only a cosmetic improvement in the quality of NMR structures. Using multiple sets of residual dipolar couplings as quality assessment criteria for several proteins we show that a significant improvement in the accuracy of structures is achieved upon refinement against the commonly used Ramachandran database potential of mean force. Comparison is also made between this method of database refinement and present water refinement protocols[2,3].

References

[1] Kuszewski, J. and Clore, G.M. (2000) Sources of and solutions to problems in the refinement of protein NMR structures against torsion angle potentials of mean force. Journal of Magnetic Resonance 146, 249-254.

[2] Spronk, C.A., Linge, J.P., Hilbers, C.W. and Vuister, G.W. (2002) Improving the quality of protein structures derived by NMR spectroscopy. J Biomol NMR 22, 281-9.

[3] Linge, J.P., Williams, M.A., Spronk, C.A., Bonvin, A.M. and Nilges, M. (2003) Refinement of protein structures in explicit solvent. Proteins 50, 496-506.

BLS3

A Novel Frequency-Selective Lee-Goldburg Cross-Polarization Solid-State NMR Pulse Sequence for Discernment of Brønsted and Lewis Acid Sites in Solid Acid Catalysts

Shing-Jong Huang,[a] Shou-Heng Liu,[a] Wen-Hua Chen,[a] Yao-Hung Tseng,[b] Jerry C. C. Chan,[b] Shang-Bin Liu,[a,*]

[a] Institute of Atomic and Molecular Sciences, Academia Sinica, P.O. Box 23-166, Taipei, Taiwan 106, R.O.C.
[b] Department of Chemistry, National Taiwan University, Taipei, Taiwan 106, R.O.C.

Solid-state ^{31}P NMR spectroscopy, using the adsorbed trialkylphosphine oxides as the probe molecule,[1-2] has been shown to be a useful technique for characterizing the detailed acid features, namely type, location, strength, and concentration of acid sites in solid acid catalysts. In general, the acidic strengths can be directly inferred from the observed ^{31}P NMR chemical shifts[1], whereas determinations of their locations and concentrations are accomplished by choosing probe molecules with proper molecular sizes and by incorporating data obtained from elemental analyses, respectively.[2] However, discernment of Brønsted and Lewis acidities mostly rely on additional information obtained from partially hydrated samples, and hence is somewhat questionable and ambiguous. Recently, this problem has been tackled by using solid-state 2D ^{1}H↔^{31}P HETCOR NMR of adsorbed trimethylphosphine oxide (TMPO)[3] and by ^{1}H/^{31}P/^{27}Al CP, TRAPDOR and REDOR NMR using TMPO-d_9 as the probe.[4] Nonetheless, the former technique is rather time-consuming and the latter two limited by their cumbersomeness and related costs in synthesizing the deuterated adsorbates. Herein, we present a novel and simple solid-state NMR strategy (Fig. 1) by incorporating a frequency-selective Gaussian excitation pulse into Lee-Goldburg cross-polarization[5] (LG-CP) so that only ^{31}P signals exclusively arising from ^{31}P nuclei connected to protons (i.e., Brønsted acid sites) were detected. Consequently, this represents a novel method for unambiguous discernment of Brønsted vs. Lewis acidities, as will be demonstrated using a variety of different solid acid catalysts, such as microporous zeolites, Al-modified mesoporous molecular sieves and metal oxides.

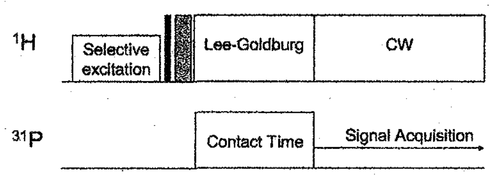

Fig. 1 Schematics of the Modified frequency-selective LG-CP pulse sequence. The darken pulse in the proton channel denotes a $\pi/2$ pulse, and the purpose of the subsequent shaded pulse is to align the excited magnetization with the effective field of the LG irradiation.

REFERENCES

1. (a) Rakiewicz, E. F.; Peters, A. W.; Wormsbecher, R. F.; Sutovich, K. J.; Mueller, K. T., *J. Phys. Chem. B* **102**, 2890 (1998). (b) Osegovic, J. P. and Drago, R. S., *J. Phys. Chem. B* **104**, 147 (2000).
2. Zhao, Q.; Chen, W. H.; Huang, S. J.; Wu, Y. C.; Lee, H. K.; Liu, S. B., *J. Phys. Chem. B* **106**, 4462 (2002).
3. Alonso, B.; Kur, I.; Massiot, D., *Chem. Commun.* 804 (2002).
4. Karra, M. D.; Sutovich, K. J.; Mueller, K. T., *J. Am. Chem. Soc.* **124**, 902 (2002).
5. (a) van Rossum, B. J.; de Groot, C. P.; Ladizhansky, V.; Vega, S.; de Groot, H. J. M., *J Am. Chem. Soc.* **122**, 3465 (2000). (b) Ladizhansky, V.; Vega, S., *J. Chem. Phys.* **112**, 7158 (2000).

ALL3

FINDING ORDER IN DISORDERED PROTEINS

RS Norton,[1] ZP Feng,[1] DW Keizer,[1] RA Stevenson,[1] S Yao,[1] VJ Murphy,[2] CG Adda[2], M Foley,[2], RF Anders[2]

[1]*The Walter and Eliza Hall Institute of Medical Research, Parkville 3050, Australia*
[2]*Department of Biochemistry, La Trobe University, Bundoora 3083, Australia*

Apical membrane antigen 1 (AMA1), a merozoite surface protein found in all species of *Plasmodium*, is a strong candidate for inclusion in a malarial vaccine. The 62-kDa ectodomain of AMA1 consists of three disulfide-stabilised domains, and this disulfide-bond stabilised conformation is essential for protection, as the antigen is not an effective vaccine after reduction and alkylation.

The solution structure of domain III (14 kDa), determined from NMR data acquired on $^{13}C/^{15}N$-labelled protein [1], consists of a disulfide-stabilised core interrupted by a disordered loop, as well as unstructured N- and C-terminal regions. Naturally-occurring mutations across > 120 different *P. falciparum* strains in domain III that are located far apart in the primary sequence cluster in the region of the disulfide core. Nearly all the polymorphic sites have high solvent accessibility, consistent with their location in epitopes recognised by protective antibodies.

We have also determined the structure of domain II (16 kDa). While CD and hydrodynamic data were consistent with a folded structure for domain II, its NMR spectra showed broad lines and significant peak overlap, more typical of a molten globule. Consistent with this, domain II bound the fluorescent dye ANS. We have nonetheless determined a structure, which defines the secondary structure elements and global fold. The two disulfide bonds link the N- and C-terminal regions of the molecule, which come together to form a four-stranded β-sheet linked to a short helix. A long loop linking the N- and C-terminal regions contains four other α-helices, the locations of which are not fixed relative to the β-sheet core, even though they are well-defined locally [2]. This region of domain II contains the epitope recognised by the invasion-inhibitory antibody 4G2 [3], even though it does not contain any of the polymorphisms that are regarded as having arisen in response to the pressure of immune recognition.

While AMA1 contains disordered regions interspersed with ordered structure, another merozoite surface protein, MSP2, is predominantly disordered and forms amyloid-like fibrils upon storage. Nonetheless, we have found that an 8-residue peptide corresponding to residues 8-15 adopts a well-defined β-hairpin structure in solution and forms fibrils similar to those formed by full-length MSP2. Thus, in contrast to the more common pathway of amyloid formation by structured proteins, which proceeds via partially unfolded intermediates that then undergo β-aggregation, MSP2 is an example of a largely unstructured protein with a small structured core that plays a key role in amyloid formation.

1. Nair M et al. (2002) *J Mol Biol* 322, 741-753.
2. Feng ZP et al. (2005) *J Mol Biol* 350, 641-656.
3. Pizarro JC et al. (2005) *Science* 308, 408-11.
4. Keizer DW et al. (2005) submitted.

ALS4

Structure and mechanism of amyloid fibrils by the gastric cancer-related GISP-like proteins

Yuan-Chao Lou[a], Meng-Ru Ho[a,b], Wen-Chang Lin[a] & Chinpan Chen[a]
[a]Institute of Biomedical Sciences, Academia Sinica, Taipei 115, Taiwan, ROC; [b]Institute of Bioinformatic and Structural Biology, National Tsing Hua University, Hsinchu 300, Taiwan, ROC.

Gastric cancer (GC) is the most prevalent malignant neoplasm and the leading cause of cancer death in many countries. However, the prognosis of GC patients is dismal, emphasizing the necessity for prevention, early detection, and better treatment for GC patients. A novel gene of GISP (GastroIntertinal Secretory Protein) was identified and suggested to have important clinical significance and applications for gastric cancer by our collaborator. Three genes related to GISP that include LITs (lithostathines), PAPs (pancreatitis-associated proteins), and PBCGF (pancreatic beta cell growth factor) were further found based on sequence comparison. These GISP-like proteins all share a common C-type animal lectin motif. Also, both human LIT and PAP proteins are found to be overexpressed during the very early stages of Alzheimer's disease (AD), indicating that they may play a role in the etiology of AD. To gain insight into structure-function relationships, we have applied a variety of biophysical experiments for structural studies on GISP-like proteins. Both human LIT and PAP were found to form amyloid fibrils at neutral pH. By contrast, amyloid fibrils could not be seen on GISP. In this presentation, NMR solution structure of human PAP and its conformational changes associated with globular to amyloid fibril transformation will be discussed and so do the preliminary studies of other GISP-like proteins. These biophysical studies on GISP-like proteins may provide valuable information for designing and searching the lead compounds for gastric cancer therapeutics as well as for the disease related to the amyloid fibrils.

ALS5

Analysis of ligand-induced domain rearrangement of a large-size protein by orientation dependent TROSY shift changes – application of DIORITE to mRNA capping enzyme

Hiroshi Moriuchi[1], **Yukio Mizuta**[2], **and <u>Shin-ichi Tate</u>**[1]
[1] Biomolecular Engineering Research Institute (BERI)
6-2-3, Furuedai, Suita, Osaka 565-0874, Japan
[2] JEOL Ltd. 3-1-2 Musashino, Akishima, Tokyo 196-8558, Japan

Establishing the methods to achieve weakly-aligned state of a protein in solution has paved a way to expand the NMR application. Residual dipolar coupling (RDC) observed from a weakly-aligned protein have been used in several aspects of protein structure research, which include structure refinement, 3D homology search, analysis of structure dynamics in the time range where spin relaxation parameter are not sensitive to motion. Due to their long-range nature, RDCs are in particular useful to elucidate the relative orientation of domains or the spatial arrangement of subunits in a protein. In spite of their distinctive feature for obtaining global structure of a protein, there is unavoidable molecular weight limitation in measuring the RDCs. This comes from the rapid transverse relaxation of so-called anti-Trosy component of a doublet for ^{1}H-^{15}N spin pair in a ^{1}H-coupled HSQC spectrum, which is due to the interference between dipolar and CSA relaxation processes. To overcome this intrinsic problem in RDC measurement, we devised an alternative approach that is far from the present molecular weight limitation. This approach uses the orientation induced TROSY shift changes to determine a molecular alignment tensor; DIORITE (Determination of Induced ORIentation by Trosy Experiment).

In this presentation, we are going to present our recent application of DIORITE to the analysis of domain rearrangement of mRNA capping enzyme (CE; 38kDa) from chlorella virus PBCV-1. The DIORITE analysis in combination with double-quantum pulse EPR experiments for the bi-radical labeled CEs have revealed that the GMP-bound form of CE in solution, which structure is different from the corresponding X-ray structure. Based on the present structure and extensive analysis of its enzymatic reactions, a new reaction mechanism of CE will be discussed.

ALS6

Observation of intermediate states of the human prion protein by high pressure NMR spectroscopy

Werner Kremer[1], Norman Kachel[1], Ralph Zahn[2], Hans Robert Kalbitzer[1*]

[1]Institut für Biophysik und Physikalische Biochemie, Universität Regensburg, Universitätsstr. 31, 93040 Regensburg, Germany, and [2]Institute of Molecular Biology and Biophysics, ETH Hönggerberg,, CH-8093 Zürich, Switzerland (Present address: Alicon AG, Wagistrasse 23, 8952 Zürich-Schlieren, Switzerland)

Abstract

Conformational intermediates of the human prion protein *hu*PrP^C were characterized by a combination of hydrostatic pressure (up to 200 MPa) with two-dimensional NMR spectroscopy. All pressure effects showed to be reversible and there is virtually no difference in the pressure response between N-terminal truncated *hu*PrP^C(121-230) and the full length *hu*PrP^C(23-230). High-pressure resonance indicates that the folded core of the human prion protein occurs in two structural states N_1 and N_2 in solution associated with rather small differences in free enthalpies (3.2 kJ/mol). At atmospheric pressure approximately 22% of the protein are already in the pressure favored conformation N_2. There is a second process representing a possible folding intermediate I with average free enthalpies of 14.2 kJ/mol which could represent a preaggregation state of the protein. The most pressure-sensitive region is the loop between β-strand 1 and α-helix 1, indicating that this region might be the first entry point for the infectious conformer to convert the cellular protein. Importantly residues Ile139, His140, and Phe141 exhibit a cluster of very low ΔG_0 values and seem to be the most unstable part of the protein.

ALS7

NMR Structure of Rabbit Prion Protein(91-228)

Jun LI[1], Fanghua MEI[2], Gengfu XIAO[2], Donghai LIN[1,*]

[1] NMR Laboratory, Shanghai Institute of Materia Medica, Shanghai Institutes for Biological Sciences, Chinese Academy of Sciences, Shanghai 201203, China;
[2] State Key Laboratory of Virology, College of Life Sciences, Wuhan University, Wuhan, Hubei 430072, China.

The prion protein (PrP) has attracted a lot of interest due to its relation to transmissible spongiform encephalopathies (TSEs), which are a group of invariably fatal neurological diseases characterized by loss of motor control, dementia, and paralysis wasting. Species barriers to the TSE agent are strongly influenced by the PrP amino acid sequence of both the donor and recipient animals. It was reported that rabbit is one of the few animal species that appear to be resistant to infection by the TSE agent. In this present work, the solution structure of rabbit prion protein (91-228), refolded to resemble the normal cellular isoform PrP^C spectroscopically and immunologically, has been studied using multi-dimensional heteronuclear NMR techniques. Fig. 1 shows a 2D ^{15}N-^{1}H HSQC spectrum recorded on a 1 mM ^{15}N-labeled rabbit PrP^C(91-228) sample using Varian Unity Inova 600 spectrometer at 25 ℃. A suite of 3D heteronuclear NMR experiments were performed for resonance assignments. Almost complete backbone resonance assignments were obtained with an exception of Q91. More than 90% side chain resonances were assigned. Secondary structures of rabbit PrP^C(91-228) was identified by the Chemical Shift Index (CSI) approach based on chemical shifts of H_α, $^{13}C_\alpha$, $^{13}C_\beta$, $^{13}C'$, indicating that this protein domain contains three α-helices (residues 143-153, 171-186, and 199-227) and two short antiparallel β-strands (residues 128-133 and 159-165). The N-terminus (residues 91-120) is largely unstructured. Distance restraints were derived from 3D ^{15}N- and ^{13}C-edited NOESY-HSQC spectra. The ARIA/CNS interactive procedure is being used to calculate the structure of rabbit PrP^C(91-228). A total of 1400 NOE cross-peaks have been assigned unambiguously at the current stage of structure calculation.

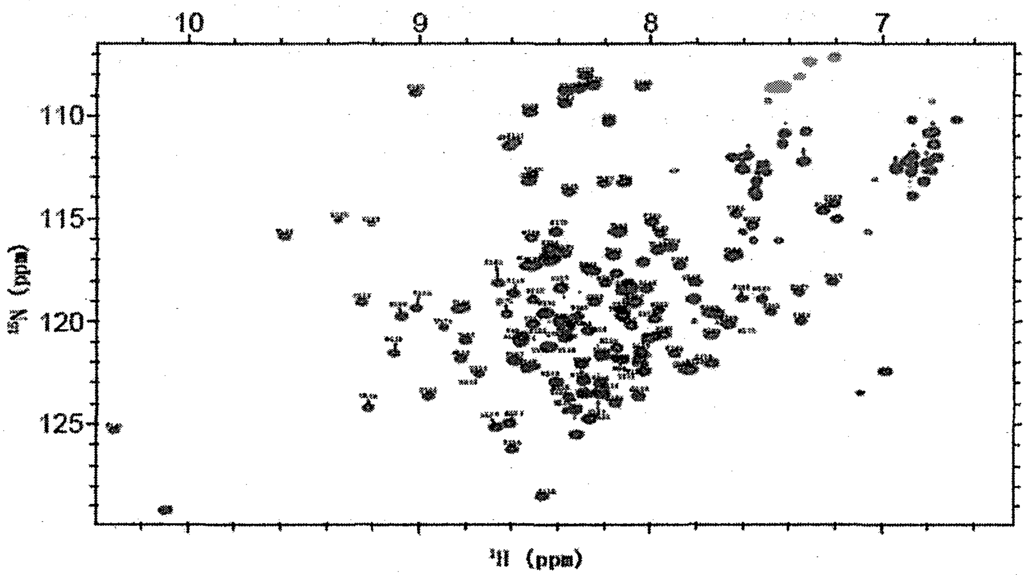

Fig. 1 2D ^{15}N-^{1}H HSQC spectrum of rabbit PrP^C(91-228)

ALS8

Pressure-jump NMR Study of Dissociation and Association of Amyloid Protofibrils

Yuji O. Kamatari [1,2,3], Shigeyuki Yokoyama[2,3,4], Hideki Tachibana[5], Kazuyuki Akasaka[2,6]
[1]Gifu University, [2]RIKEN Harima Institute, [3]Riken Genome Science Center, [4]The University of Tokyo, [5]Kobe University, [6]Kinki University

A number of diseases such as Alzheimer's disease, Parkinson's disease, prion disease, and autosomal dominant hereditary amyloidosis from lysozyme variants, are associated with the formation of amyloid fibrils. Understanding of mechanism of amyloid formation and controlling it is a central issue in amyloidosis. We present an application of a high pressure NMR system for controlling of amyloid protofibrils formation. In this study, the dissociation and reassociation processes of amyloid protofibrils initiated by pressure-jump have been monitored with real-time ^{1}H NMR spectroscopy using intrinsically denatured disulfide-deficient variant of hen lysozyme. Upon pressure-jump up to 2 kbar, the matured protofibrils grown in several months become fully dissociated into monomers within a few days. Upon pressure-jump down to 30 bar, the dissociated monomers immediately start reassociating. The association and dissociation cycle can be repeated reproducibly by alternating pressure, establishing a notion that the protofibril formation is simply a slow kinetic process toward thermodynamic equilibrium. The outstanding simplicity and effectiveness of pressure in controlling the protofibril formation opens a new route for investigating mechanisms of aggregation and amyloid fibril formation as well as for production of proteins in industrial applications.

Reference

Kamatari YO, Yokoyama S, Tachibana H, Akasaka K. 2005, Pressure-jump NMR Study of Dissociation and Association of Amyloid Protofibrils. J Mol Biol. 349, 916-921.

BLL3

Structure of Silks studied using Solid-state NMR

Tetsuo ASAKURA
Department of Biotechnology, Tokyo University of Agriculture and Technology,
2-24-16 Naka-cho, Koganei, Tokyo 184-8588, Japan, *e-mail:asakura@cc.tuat.ac.jp*

Nature can provide us with many lessons about environmentally friendly technologies and futuristic materials with improved properties. There are many kinds of silks from silkworms and spiders with different structure and property. Thus, silks are suitable to study the structure-property relationship for molecular design of fibers with high strength and high elasticity. NMR offers a wealth of methods to study, on a molecular as well as on a macroscopic level, the structure and function of silks.

In this talk, structural analysis of silk fibroin from the domesticated silkworm, *Bombyx mori* (*B. mori*) will be described. The backbone and side-chain torsion angles were determined from the angle-dependent ^{13}C, ^{15}N and ^{2}H solid state NMR spectra of blocks of the oriented and stable-isotope labeled silk fibers. The dynamics of the ^{2}H labeled *B. mori* silk fiber was also clarified.[1)]

On the other hand, the primary structure of the silk is heterogeneous although there are many repeated sequences in the chain. Therefore detailed structural characterization with several solid-state NMR techniques coupled with synthesis of selectively isotope-labeled model peptides seems to be very effective. We used combination of several solid-state NMR techniques such as use of conformation-dependent ^{13}C chemical shifts on the basis of ^{13}C chemical shift contour plots as a function of torsion angle, 2D spin-diffusion NMR and REDOR (rotational echo double resonance) methods. The secondary structure of the appropriate model peptide, $(AG)_{15}$, as a model for the crystalline domain of *B. mori* silk fibroin before spinning (Silk I) was clarified to be repeated β-turn type II structure by combination of several solid-state NMR studies mentioned above.[2)] The appearance of lamella structure after Silk II treatment of $(AG)_{15}$ was shown from detailed NMR analysis of each Ala $^{13}C\beta$ peak of fifteen $(AG)_{15}$ peptides with selectively different ^{13}C Ala $C\beta$ labelings.[3)]

1) C. Zhao and T. Asakura , *Prog. NMR Spec.*, **39**, 301-352 (2001) and references therein.
2) T. Asakura, et al., *Macromolecules* (2005) in press.
3) T. Asakura, et al., *Protein Sci.* (2005) in press.

BLS4

^{29}Si and ^{27}Al NMR characteristics of octahedral Si-Al disorder in high-pressure aluminosilicate minerals

Xianyu Xue[1], Masami Kanzaki[1], Hiroshi Fukui[1], Eiji Ito[1], Takafumi Hashimoto[2]
[1] Inst. Study Earth's Interior, Okayama Univ., Misasa, Tottori, 682-0193 Japan
(xianyu@misasa.okayama-u.ac.jp)
[2] Faculty Sci., Kumamoto Univ., Kurokami 2-36-1, Kumamoto 860-8555 Japan

Introduction

Characterizing Si-Al order/disorder is an important task of materials sciences and mineralogy. In the case of tetrahedral coordinated Si and Al, numerous studies have revealed that NMR is a particularly powerful tool: the ^{29}Si chemical shift changes systematically to less negative value with increasing Al/Si ratio in the next nearest neighbor (NNN) environment. Down into the earth's interior, density increase is accompanied by an increase in cation coordination, such that at the deeper part of the Earth's mantle (>660 km), all minerals contain Si and Al solely in octahedral coordination. Here we report the first ^{29}Si and ^{27}Al NMR results on high-pressure aluminosilicate minerals containing interconnected octahedral Si and Al. This study is not only important for understanding the thermodynamic and physical properties of the Earth's interior, but also of theoretical interest because the range of chemical shift due to octahedral Si-Al disorder has been unknown thus far.

Experimental Methods

High-pressure samples have been synthesized using a Kawai-type double-stage uniaxial split-sphere multi-anvil apparatus. ^{29}Si and ^{27}Al MAS NMR spectra were obtained at a resonance frequency of 79.5 and 104.3 MHz, respectively, using a Varian Unity-Inova 400 MHz spectrometer and a Jakobsen-type 5 mm or Doty 4 mm CP-MAS probe. Chemical shifts are referenced externally to tetramethylsilane (TMS) for ^{29}Si, and 1 *M* aqueous solution of $Al(NO_3)_3$ for ^{27}Al.

Results and Discussions

The first mineral studied is phase egg ($AlSiO_3OH$) synthesized at about 17 GPa and 1000°C. The structure of this phase has been refined from powder X-ray diffraction to a rutile-like structure with an ordered arrangement of Si and Al octahedra, although the significance of partial Al-Si disorder was not evaluated (Schmidt et al., 1998, Am. Mineral., 83, 881). There is one unique Si and one Al site in the unit cell: each Si has 3Si and 6Al NNN and each Al has 6Si and 3Al NNN, with 1/3 NNN of each linked through edge-sharing and 2/3 corner-sharing. However, our ^{1}H-^{29}Si cross-polarization (CP)-MAS NMR results revealed three peaks near −183.4 ppm, −173.9 ppm and −159.4 ppm, suggesting the presence of Si-Al disorder. The relative intensities are 21.6%, 70.7% and 7.7%, which do not vary with contact times between 0.01 and 20 ms and thus must reflect the true abundance ratio. These peaks roughly fall within the range reported for octahedral Si, and are less negative than that of the structurally similar SiO_2 stishovite (-191.3 ppm), in which each Si has all Si NNN. Thus, the trend in ^{29}Si chemical shift with Si-Al NNN replacement for octahedral Si is similar to that of tetrahedral Si. We have estimated the abundance distribution of different species using a random mixing model. We found that the observed intensities can be accounted for with 10% Si-Al disorder, if disorder at the three edge-sharing NNN sites have a predominant influence over that of corner-sharing NNN on the ^{29}Si chemical shift. The ^{27}Al MAS NMR spectra also show features indicative of the presence of a range of quadrupolar parameters, consistent with structural disorder. Parallel investigation on other high-pressure aluminosilicate minerals that similarly contain interconnected octahedral Si and Al is also in progress. The latest results will be presented at the symposium.

BLS5

One-dimensional dynamical conformons investigated by nuclear spin relaxation

Naoki Asakawa* and Yoshio Inoue

Department of Biomolecular Engineering, Tokyo Institute of Technology. 4259 B-55 Nagatsuta-cho, Midori-ku, Yokohama, Kanagawa 226-8501, Japan, email:nasakawa@bio.titech.ac.jp

Introduction Nuclear magnetic resonance(NMR) spectroscopy under inhomogeneous magnetic field is one of promising nondestructive methods for investigating transport phenomena. Several attempts have recently been reported to make NMR measurements of ultra slow diffusion in solids. Among these, the pulse field gradient(PFG) technique with strong magnetic field gradient(MFG) has been given much attention for detection of such diffusions. However, the PFG technique involves some problems if the target system has large internal MFG compared to external PFG and/or large heterogeneous MFG. In solids the diffusion coefficient can often be small and a local internal MFG, which in some cases heterogeneous and/or anisotropic, can be remained, resulting in the crucial limiting factor of the method. Here we describe a novel method for investigating the conformon dynamics and internal magnetic field gradient in low-dimensional solids by nuclear magnetic relaxation measurements.

Methods Our method constitutes of the three procedure: i) estimation of the diffusion coefficient, D, from the slop of the R_1 *vs.* ω plot and the second moment of spectrum if the longitudinal relaxation rate show the $\omega^{-0.5}$ dependence, ii) the transverse relaxation measurements with the CPMG spin echo as a function of echo time, and the best fit simulation by 1D Bloch-Torrey simulation[1], offering the values of D/L_s and L_sG, and iii) the determination of a set of parameters:D, L_s, and G from i) and ii).

Results and Discussion The longitudinal relaxation of poly(4-methylthiazole-2,5-diyl) with a regioregularity of the head-to-head type[HH-P4MeTz] shows the $\omega^{-0.5}$ dependence at 295K.[2] The dependence can be described by the calculation of dynamical susceptibility based on a one-dimensional random walk model. The following equation is obtained as a conclusion;

$$T_1^{-1} = M_2 f(\omega) = \frac{M_2}{\sqrt{2}}\tau_c^{1/2}\omega^{-1/2} \quad (\text{if } \omega < \tau_c^{-1}), \quad (1)$$

where $f(\omega)$ is the correlation function, τ_c is the correlation time identical to the inverse of the jumping rate, and M_2 is the second moment of the interaction that affects the relaxation. For the one-dimensional random walk model, $\Delta x^2/\tau_c = 2D$, where Δx is the jump distance of one random step during time τ_c; for the conformon of HH-P4MeTz, τ_c is determined as 0.33ns and Δx is estimated as the length of the monomer(0.4nm). Therefore, $D = 2.4 \times 10^{-10}\text{m}^2\cdot\text{s}^{-1}$.

In many glassy or disordered solids, distribution in the correlation time was realized and accounded by modifying the correlation function with the extended exponential function(Kohlrausch-Williams-Watts function) or by using modifying the spectral density function with Cole-Cole, Cole-Davidson, Havriliak-Negami types, and so on. The critical slowing down can often be observed at temperatures closed to the second-order phase transition or glass transition; for NMR longitudinal relaxation experiments, the accelaration of the spin relaxation can be observed and also detected a teperature independent plateau due to reaching the slow motion regime($\omega_L \gg \tau_c^{-1}$). This indicates that the structural relaxation rate (τ_c^{-1}) is smaller than the resonance frequency. The existence of the slower structural relaxation rate than the resonance frequency must induce a singularity at the angular frequency of $\omega = \tau_c^{-1}$ in the spectral density function, which should lead to the change in the power law. For HH-P4MeTz such a singularity was not detected near the order-disorder transition temperature;namely, the $\omega^{-1/2}$ dependence was preserved. We describe the alternative explanation for the preservation of the power law in the following.

Assuming the one-dimensional fluctuation instead of the isotropic one (Debye model) and distribution of the correlation time, the spectral density function with a correlation time distribution becomes to be the following form:[3]

$$f(\omega) = \frac{\omega^{-1/2}}{\sqrt{2}}\int_0^\infty p(\tau_c)\tau_c^{1/2}d\tau_c, \quad (2)$$

where $p(\tau_c)$ is a probability of which structural relaxation time is τ_c. From Eq.2, the $\omega^{-1/2}$ law is preserved irrespective of the structural heterogeneity and the ^{1}H-^{1}H spin diffusion, by virtue of separation of variables, ω and τ_c. This situation is realistic when the one-dimensional modulation waves of backbone twist has a dispersion. From the above mentioned procedure for fitting, we were able to uniquely determine the three parameters for HH-P4MeTz: D, L_s, and G by using the value of D determined above($L_s = 22\mu$m and $G = 356\text{T}\cdot\text{m}^{-1}$).

The method developed here will be useful to investigate transport phenomena in low dimensional solids, such as transport of elementary excitations such as lattice defects, excitons, and charge carriers, and so on. Further, recent developments on magnetic resonance force microscopy(MRFM) show that one can perform *in situ* imaging with a scale of several tens of nanometers, where ultra high magnetic field gradients of over $10^3 \sim 10^4$ T/m are generally used. Up to now, there are no publications available to obtain spin-echo measurements under a condition of such a huge MFG, which can be comparable to local magnetic field gradient with atomic scale. The method presented here will be useful for analyses of such experiments as well.

[1] N.Asakawa, K.Matsubara, and Y.Inoue, Chem.Phys.Lett., **406**, 215(2005).

[2] S.Mori, Y.Inoue, T.Yamamoto, and N.Asakawa, Phys.Rev, B71, 054205(2005).

[3] N.Asakawa, M.Ohira, K.Yazawa, T.Yamamoto, and Y.Inoue, eprint:arXiv:cond-mat/0507515.

BLS6

NMR of Aluminium Alloys

Kate Nairn, Tim Bastow, George Yiapanis, Anita Hill.

CSIRO Manufacturing and Infrastructure Technology, Private Bag 33, Clayton South, Vic, 3169, Australia.
Email: kate.nairn@csiro.au

Small precipitate particles provide aluminium alloys with their strength. The particles also affect ductility, creep resistance and corrosion properties. Identification of the relative amounts of the various precipitate phases is vitally important in designing better alloys and in designing better heat-treatments for the current alloys. Measurement of the fraction of alloying element still in solid solution is crucial to identify the driving force for further precipitation.

Fortunately, several important alloying elements are NMR-active. ^{45}Sc spectra can be used to trace the growth of precipitate particles in Al-Sc welding alloys [Celotto 2000]; ^{7}Li spectra of Al-Li alloys reveal the two different precipitates that can form in these materials; and ^{63}Cu NMR gives a wealth of information on the complicated precipitation properties in a range of Al-Cu containing alloys [Bastow 2003].

This paper presents a brief review of precipitation processes as studied by NMR, and compares the results obtained from the NMR spectra with those obtained using other metallurgical techniques (such as hardness and transmission electron microscopy). Particular emphasis is given to characterising the effect of small additions of Cd upon the precipitation process in Al-4 wt.% Cu via ^{63}Cu NMR.

A typical ^{63}Cu NMR spectrum of an Al-4wt.% Cu alloy is shown in the figure. These measurements are performed on metal powders, without spinning the sample. Although the lines are broad, well resolved peaks are observed. These peaks correspond to particular phases within the alloy system.

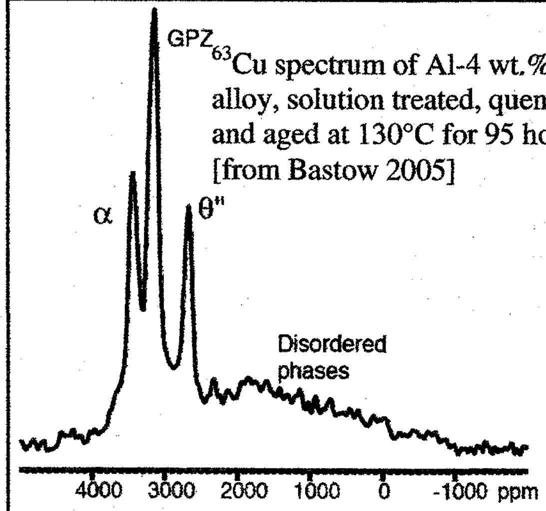

^{63}Cu spectrum of Al-4 wt.% Cu alloy, solution treated, quenched, and aged at 130°C for 95 hours. [from Bastow 2005]

S. Celotto and T.J.Bastow, Philosophical Magazine A, **80**, 1111-1125, 2000.
T.J. Bastow and S. Celotto, Acta mater. **51**, 4621-4630, 2003.
T.J. Bastow and K. Nairn, Magnetic resonance to study nanoprecipitation in light metal alloys, Chapter in "Nanostructure Control", eds. A.J. Hill and R.L. Hannink, to be published by Woodhead Publishing.

BLS7

Chemical shift and spin-lattice relaxation of helium-3 confined in micropores

Shigenobu Hayashi

Research Institute of Instrumentation Frontier, National Institute of Advanced Industrial Science and Technology (AIST), Tsukuba Central 5, 1-1-1 Higashi, Tsukuba, Ibaraki 305-8565.

^{129}Xe NMR is widely used to explore the pore using xenon as a probe. The diameter of a xenon atom is about 0.44 nm, and thus pores smaller than 0.44 nm are difficult to be characterized. The diameter of He (about 0.28 nm) is smaller than that of ^{129}Xe, and ^{3}He is much more NMR-sensitive than ^{129}Xe . Consequently, ^{3}He NMR is expected to be useful to characterize the smaller pores within the shorter time. In the present work, the smaller micropore has been explored by ^{3}He NMR.

^{3}He NMR spectra were obtained at room temperature and at Larmor frequency of 152.45 MHz. Fig. 1 shows the ^{3}He NMR spectrum for KA zeolite (molecular sieve 3A) at the ^{3}He gas pressure of 100 kPa. The spectrum consists of two peaks. The peak marked by * is ascribed to ^{3}He in the gas phase, because this peak is observed even when the sample tube was empty. The gas peak at 100 kPa is set at 0 ppm in this work. Another peak is ascribed to ^{3}He in the micropore, whose position depends on the material. The chemical shifts are 1.72, 0.28 and –0.58 ppm for KA zeolite, NaA zeolite (molecular sieve 4A) and high-silica ZSM-5, respectively.

The effective channel dimensions are about 0.3, 0.4 and 0.54 nm (actually 0.51×0.55 nm and 0.53×0.56 nm) for KA zeolite, NaA zeolite and high-silica ZSM-5, respectively. The chemical shift increases with decrease in the pore size. Thus, the signal of ^{3}He confined in the micropore is shifted by interaction with the pore wall. This correlation is similar to that for the ^{129}Xe chemical shift.

In conclusion, ^{3}He NMR is useful to probe sub-nanometer pores, which is complimentary to ^{129}Xe NMR and the gas absorption method. A calibration curve should be built up by measuring a number of model substances whose pore sizes are clearly defined. Once the calibration curve is obtained, the pore size and its distribution can be derived for unknown samples.

Spin-lattice relaxation times of ^{3}He in the micropores will also be presented and the relaxation mechanism will be discussed.

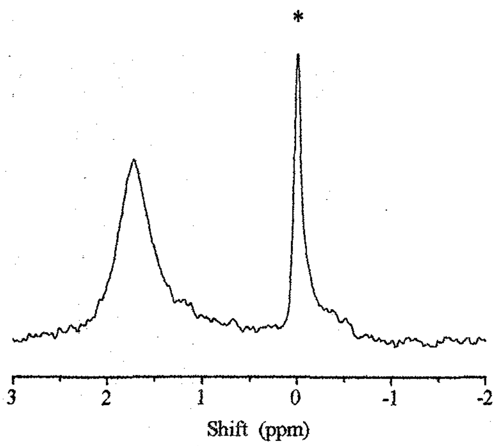

Fig. 1. ^{3}He NMR spectra for KA zeolite. The pressure of the gas phase was 100 kPa. The * marks indicate the signal of the gas phase.

BLS8

Surface acidity of BF_3/Al_2O_3 catalyst as studied by solid state NMR and theoretical calculation

Feng Deng, Jun Yang, Anming Zheng, Mingjin Zhang, Qing Luo, Chaohui Ye

State Key Laboratory of Magnetic Resonance and Atomic and Molecular Physics, Wuhan Institute of Physics and Mathematics, Chinese Academy of Sciences, Wuhan 430071, China

Alkylation of isobutane with butene produces the important component of high-octane and clean-burning gasoline. Industrial alkylation processes are using either sulfuric acid or hydrofluoric acid as acid catalysts. The liquid acid alkylation catalysts are highly toxic, corrosive and dangerous to life or health during the use and the transportation. Many different types of solid acid have been studied both in industry and academic institutions as the alkylation catalysts. $BF_3/\gamma\text{-}Al_2O_3$ is one of the most promising alkylation catalysts for either HF or H_2SO_4 replacement. However, the structure and nature of acid sites on the $BF_3/\gamma\text{-}Al_2O_3$ solid acid catalyst are still unclear though there are many patents concerning with preparation and catalytic performance of the catalyst. In this work, multinuclear solid-state NMR techniques and DFT quantum chemical calculations were employed to investigate the detailed structure of acid sites on $BF_3/\gamma\text{-}Al_2O_3$ alkylation catalyst. The NMR experiment results indicate that gaseous BF_3 is able to react with the hydroxyl groups present on the surface of $\gamma\text{-}Al_2O_3$, leading to the formation of new Brönsted and Lewis acid sites. The $^{1}H/^{11}B$ and $^{1}H/^{27}Al$ TRAPDOR experiments suggest that the 3.7 ppm signal in ^{1}H NMR spectra of the $BF_3/\gamma\text{-}Al_2O_3$ catalyst is due to a bridging B-OH-Al group that acts as Brönsted acid site of the catalyst. On the other hand, Lewis acid site on the surface of the catalysts, as revealed by ^{31}P MAS and $^{31}P/^{27}Al$ TRAPDOR NMR of adsorbed trimethylphosphine, is associated with 3-coordinate $-OBF_2$ species. ^{13}C NMR of adsorbed 2-^{13}C-acetone indicates that Brönsted acid strength of the catalyst is slightly stronger than that of zeolite HZSM-5, but still weaker than that of 100% H_2SO_4, which is in well agreement with theoretical prediction. In addition, DFT calculations also reveal the detailed structure of various acid sites formed on the $BF_3/\gamma\text{-}Al_2O_3$ catalyst and the interaction of probe molecules with these sites.

ALL4

Auto-inhibition of X11s/Mints Scaffold Proteins Revealed by the Closed Conformation of the PDZ Tandem

Jia-Fu Long, Wei Feng, Rui Wang, Ling-Nga Chan, and Mingjie Zhang

Department of Biochemistry, Molecular Neuroscience Center, Hong Kong University of Science and Technology, Clear Water Bay, Kowloon, Hong Kong, P. R. China

X11s/Mints are a family of multi-domain adaptor proteins composed of divergent N-termini, a conserved PTB domain, and a pair of PDZ domains at the C-termini. Many proteins can interact with the PDZ tandem of X11s, although mechanism of such interaction is unclear. We discover that the highly conserved carboxyl tail of X11α folds back and inserts into the target-binding groove of the first PDZ domain (PDZ1). The binding of the carboxyl tail to PDZ1 occludes other target peptides from binding. This auto-inhibited conformation of X11 requires the two PDZ domains and the entire carboxyl tail to be covalently connected to form an integral structural unit. The auto-inhibited conformation of the X11 PDZ tandem not only provides mechanistic explanations to the unique target binding properties of the protein, but also hints at potential regulatory mechanisms for the X11–target interactions.

ALL5

Molecular recognition between PDZ domain of AF-6 and Bcr

Yunyu Shi, Jihui Wu, Quan Chen, Xiaogang Niu
Hefei National Laboratory for Physical Sciences at Microscale and School of Life Science, University of Science and Technology of China, Hefei, 230026, China

Protein-protein interaction plays an important role in various cellular processes. Understanding how individual protein-protein interaction function in time and space require detailed genetic, biochemical, and structural characterization. NMR spectroscopy is highly suited to investigate molecular interactions between proteins or proteins and peptides at close to physiological conditions. It is possible to obtain a high resolution structure of a complex and also feasible to map the interaction interface.
The human AF-6 gene has been identified as a fusion partner of ALL-1 in human acute myeloid leukemia. Now, it is known that AF-6 is a component of tight junctions and adhesion junctions. It may functions as a molecular scaffold integrating the signals related to cell adhesion and cytoskeletal reorganization. We determine the three dimensional complex structure of the AF-6 PDZ domain with C-terminal peptide of protein kinase Bcr. We found that the binding mode of AF-6-PDZ/Bcr is significantly different from that of the canonical class Ⅰ or class Ⅱ PDZ domain. In addition, our results revealed that AF-6 PDZ domain/Bcr complex undergoing fast chemical exchange between binding state and free state. Implications of this phenomena for AF-6 function is also discussed

ALS9

Probing the inter-domain motion of N-terminal tandem PDZ domains of PSD-95 with residual dipolar couplings

Wenning Wang[a], Jiafu Long[b] and Mingjie Zhang[b]
(a. Department of Chemistry, Fudan University, Shanghai 200433, China; b. Department of Biochemistry, Hong Kong University of Science and Technology, Clear Water Bay, Kowloon, Hong Kong, China)

PDZ domain-containing proteins play central roles in binding, clustering, and sub-celluar targeting of membrane receptors. In multi-PDZ proteins, the tandem arrangement of PDZs was shown to be functionally significant [1]. In this study, the solution structure of the first two PDZ domains of PSD-95 complexed with Cypin peptide is solved with multi-dimensional NMR spectroscopy. Residual dipolar couplings of backbone NH were used to identify the mobility of the structure. Analysis of the alignment tensors and the data pattern of dipolar couplings [2] implies that the two peptide-binding PDZ domains move independently in solution without any static inter-domain orientation. This contrasts with the case of ligand-free form of PDZ1-2 [1], which has a relatively fixed domain orientation. The change of inter-domain mobility upon peptide binding accounts for the entropy gain during the target binding of PSD-95 scaffold protein.

References:

1. Long, J., Tochio, H., Wang, P., Fan, J.-S, Sala, C., Niethammer, M., Sheng, M. and Zhang, M. (2003) *J. Mol. Biol.* **327**, 203-214.
2. Braddock, D. T., Cai, M., Baber, J. L., Huang, Y., Clore, G. M. (2001) *J. Am. Chem. Soc.* 123, 8634-8635

ALS10

Solution Structure of the kinase inhibitory region and extended SH2 domain of SOCS3.

J.J. Babon, S. Yao, D. DeSouza, L. Fabri, M. Baca and R.S. Norton
The Walter and Eliza Hall Institute of Medical Research, 1G Royal Parade, Parkville

SOCS3 is a member of the SOCS family of proteins (CIS, SOCS1-7), that inhibit cytokine signalling by binding to tyrosine phosphorylated signalling intermediates such as receptor sub-units and Janus kinases (JAKs). The SOCS family is characterised by an N-terminal domain of varying length, a src-homology 2 (SH2) domain and a C-terminal SOCS box. SOCS3 shows a strong interaction with phosphotyrosines on a number of cytokine receptors, including the gp-130 receptor, via its SH2 domain and can then inhibit receptor bound JAK tyrosine kinase activity through the action of the kinase inhibitory region (KIR) (1), a stretch of twelve amino acids immediately C-terminal to the SH2 domain. The SOCS box itself interacts directly with the elongin B/C complex and may regulate the stability of both SOCS3 and SOCS3-associated signalling proteins (2).

As full length SOCS3 displays very poor solubility we determined the solution structure of a 164 amino acid region of SOCS3 by nuclear magnetic resonance (NMR). This construct encompasses the kinase inhibitory region (KIR), extended SH2 subdomain (ESS) and SH2 domain. The structure was determined in complex with a tyrosine phosphorylated peptide from the gp-130 receptor. SOCS3 was well structured over the majority of its length except for the presence a 40 residue stretch that we determined as being completely flexible and unstructured on the basis of NOEs and relaxation data. This region has functional significance. The structure of SOCS3 generates a number of insights into functional aspects of the protein.

(1) Nicholson SE, Willson TA, Farley A, Starr R, Zhang JG, Baca M, Alexander WS, Metcalf D, Hilton DJ, Nicola NA. (1999) *EMBO J.* **18:** 375-385.

(2) Zhang JG, Farley A, Nicholson SE, Willson TA, Zugaro LM, Simpson RJ, Moritz RL, Cary D, Richardson R, Hausmann G, Kile BJ, Kent SB, Alexander WS, Metcalf D, Hilton DJ, Nicola NA and Baca M. (1999) *Proc Natl Acad Sci.* **96**: 2071-2076

ALS11

NMR Solution Structure of hPrxVI, a 25 kDa 1-Cys Human Peroxiredoxin Enzyme

Eunmi Hong[a], Joon Shin[a], Sang Won Kang[b] ,and Weontae Lee[a]*

[a]*Department of Biochemistry, Yonsei University, Seoul 120-749, Korea;* [b]*Center for Cell Signaling Research and Division of Molecular Life Sciences, Ewha Womans University, Seoul 120-749, Korea*

Peroxiredoxins (Prxs) are the family of thiol-specific antioxidant proteins and they are also known as thioredoxin peroxidases (TPx) or alkyl-hydroperoxide reductases. Human PrxVI (hPrxVI) belongs to the distinct class of 1-Cys Prx, which contains only one N-terminal conserved cysteine residue, and cannot use thioredoxin. Even though a physiological reducer for hPrxVI is still unknown, it has been shown that hPrxVI mediates the reduction of hydrogen peroxide with the use of electrons from a nonphysiological electron donor, dithiothreitol (DTT). The solution structure of the hPrxvi was determined using heteronuclear multidimensional NMR spectroscopy. NMR data shows that the secondary structure of hPrxVI in the reduced state consists of ten β-strands and six α-helices. The secondary structure of the wild-type monomeric hPrxVI in solution is slightly different from that of the dimeric mutant form determined by X-ray crystallography. The topology of hPrxvi could be divided into two globular domains, which include a large N-terminal domain with thioredoxin fold and a small C-terminal domain. The N-terminal domain is comprised of seven β-sheets and five α-helices, whereas the C-terminal domain is four β-sheets and one α-helix. Two domains are connected by a long flexible loop. This study will serves as a structural framework in understanding various biological functions of peroxiredoxins.

ALS12

Redox-dependent conformational rearrangement of protein disulfide isomerase

Yoshiki Yamaguchi[1], Aya Maeno[1, 2], Michiko Nakano[2], Chiho Murakami[1], Hiroaki Sasakawa[2], Takushi Harada[1], Eiji Kurimoto[1], Takeshi Iguchi[3], Kenji Inaba[4], Osamu Asami[5], Tsutomu Kajino[5], Jun Kikuchi[6], and Koichi Kato[1, 2]
[1]Graduate School of Pharmaceutical Sciences, Nagoya City University, Nagoya, Japan, [2]Institute for Molecular Science, Okazaki, Japan, [3]Bioscience Research Laboratory, Fujiya Co., Ltd., Hadano, Japan, [4] Institute for Virus Research, Kyoto University, Kyoto, Japan, [5]Toyota Central Research & Development Labs. Inc., Nagakute, Japan, and [6]Plant Sciences Center, RIKEN, Yokohama, Japan

Protein disulfide isomerase (PDI) is a folding assistant operating in the endoplasmic reticulum, and catalyzes the formation, breakage and rearrangement of disulfide bonds of its substrate proteins. PDI has a modular structure with four globular domains, *a*, *b*, *b'* and *a'* plus a C-terminal acidic extension. The homologous *a* and *a'* domains contain a cysteine pair in a WCGHCK active site sequence motif directly involved in thiol-disulfide exchange reactions. So far the solution structures of the *a* and *b* domains have been reported to be thioredoxin folds. We have shown that substrate binding site of PDI is primarily composed of the *b'* and *a'* domains.

Here we report NMR structural analyses of three-dimensional structures, substrate recognition, and domain-domain interactions of the *b'* and *a'* domains of thermophilic fungal PDI. Isotopically labeled *b'* and *a'* domains as well as the fragments composed of these two domains were expressed in *E.coli*. Inspection of NOE, chemical shift, and residual dipolar coupling data revealed that 1) the *b'* and *a'* domain assumes typical thiredoxin folds, 2) substrate analogs, e.g. somatostatin and mastoparan, bind a hydrophobic area spanning the *b'* and *a'* domains in their oxidized form, and 3) reduction of the active site of the *a'* domain results in its increased contact with the *b'* domain, rendering the hydrophobic area less accessible. On the basis of these data, we suggest that this conformational rearrangement causes redox-dependent interaction of PDI with its substrates. By use of intact PDI labeled with ^{13}C at cysteinyl carbonyl carbon, we have also demonstrated that redox behavior of the active sites are significantly different between the *a* and *a'* domains. Thus, substrate binding and catalytic activity of PDI are regulated by the versatile domain-domain interactions of this modular enzyme.

BLL4

NMR study on Antibiotics Targets

Bong-Jin Lee

College of Pharmacy, Seoul National University, San 56-1, Sillim-Dong, Kwanak-Gu, Seoul 151-742, Korea

abstract

Today scientific strategy in drug discovery and development is changing rapidly. After determining the three-dimensional structure of bioactive macromolecules, which are the main targets of novel drugs, small molecules can be designed and synthesized to fit into the binding pockets. Many druggable protein targets are being discovered with completion of the analysis of human and many bacterial genomes. Researchers in several large pharmaceutical firms are already making their efforts to discover drugs targeting these proteins. In our lab, we have studied the structure of antibiotics target proteins from pathogenic bacteria by using NMR. The structure-function relationship of several proteins from Bacillus pasteurii and Helicobacter pyroli proteins will be discussed in this talk.

BLS9

Analysis of intracellular drug uptake using PFG NMR

Kyuhong Lee, Gyo-Seon Yeom, Jee-Hyun Cho, Chulhyun Lee, Chaejoon Cheong, Kwan Soo Hong
KOREA BASIC SCIENCE INSTITUTE

Intracellular molecular drug uptake of nicotineamide into cells has been observed using a PFG NMR(pulse field gradient) technique at Bruker 600 MHz (14.1 T) NMR spectrometer. PFG NMR is one of methods for measuring molecular diffusion. The apparent two components of diffusion of drug molecules were measured from media with in-vivo cells. From the experimental data, we are able to analyze the apparently different two diffusion coefficients which are from intra- and extra-cellular drug molecules and how many drug molecules go into the cells as a function of time. The PFG NMR can be a useful tool to realize if a drug molecule entered the cells or not. It can be used for a drug/molecule screening in micro-sized compartment.

Acknowledgments
This work was supported by the Basic Science Research Program from the Ministry of Science and Technology, the Republic of Korea, by the 21st Century Frontier R&D Program from the Ce nter for Biological Modulators.

BLS10

Metabolomics by NMR: Assessment of Lentil Metabolite Diversity

Simone Rochfort[1], Craige Trenerry[1], Nathan Neumann[2], Joe Panozzo[2]

Environmental Health and Chemistry, Primary Industries Research Victoria
Department of Primary Industries
[1]Werribee Centre, 621 Sneydes Road, Werribee Victoria 3030 Australia
[2]Horsham Centre, 110 Natimuk Road, Horsham Victoria 3400 Australia

Metabolomics is the study, quantification and qualification of the metabolites a system (cell, tissue, or organism) produces. The characterisation of system's metabolites utilises cutting edge technology in analytical science, in particular, Nuclear Magnetic Resonance spectroscopy (NMR). NMR can be employed with computational algorithms for analysis and integration of information and be used in the analysis of secondary metabolites.

There are thousands of cultivars of lentils but relatively few are produced commercially. At the Department of Primary Industries the aim is to produce varieties of plants that may provide health advantages beyond basic nutrition (ie. functional food). The disease target is type II diabetes – a disease that is of increasing prevalence. There is epidemical evidence that lentils, chickpeas in particular, reduce the severity of this disease. Our aim is to investigate and enhance this effect by selecting for commercial production, varieties of plants that contain greater quantities of beneficial bioactives. The initial work is an assessment of biochemical diversity of the available chickpea strains. This assessment is carried out employing NMR metabolomic techniques.

This paper will discuss the data acquisition parameters and data handling issues that must be considered and present our initial results demonstrating the power of NMR techniques for metabolome assessment.

BLS11

Diffusion Based NMR and Application

Maili LIU Guoyun BAI, Xu ZHANG and Chaohui YE

Wuhan Center for Magnetic Resonance, State Key Laboratory of Magnetic Resonance and Molecular and Atomic Physics, Wuhan Institute of Physics and Mathematics, Chinese Academy of Sciences, Wuhan 430071, PR China

Diffusion based NMR spectroscopy, also known as diffusion-ordered spectroscopy (DOSY), has become a powerful tool in studying intermolecular interaction and characterizing biological molecules in body fluids. There are a number of factors that may affect the accuracy of diffusion coefficient measurement, such as thermal convection, chemical exchange and internuclear Overhauser effect (iNOE). Effect of thermal convection has been known for many years and can be compensated by using double gradient spin-echo. The effect of chemical exchange and iNOE on diffusion coefficient can be used as new parameters to study the molecular interaction. The dependence of diffusion coefficient on the molecular size provide a now dimension for separation of complex mixture, as well as the study of binding capacity and dynamics of ligands on proteins. In this presentation, the recent works from our laboratory in reducing artifacts in NMR diffusion measurement and application of the approach is introduced.

Key references

1. Yang, YH; Bai, GY; Zhang, X; Ye, CH; Liu, ML. 2004. H-1 NMR spectroscopic evidence of interaction between ibuprofen and lipoproteins in human blood plasma. ANALYTICAL BIOCHEMISTRY 324 (2): 292-297, 2004.
2. Maili Liu, Huiru Tang, Jeremy K. Nicholson and John C. Lindon. Use of ^{1}H NMR determined diffusion coefficients to characterize lipoprotein fractions in human blood plasma. *Magn. Reson. Chem.* **40,** S83-S88, 2002. (invited submission)
3. Xu Zhang, Cong-Gang Li, Chao-Hui Ye, and Mai-Li Liu, Determination of Diffusion Coefficient Using Multiple Spin-Echo NMR Spectroscopy with Free of Convection and Background Gradient Artefacts. *Anal Chem*,.73(15) 3528-3534 2001
4. Maili Liu; J.K. Nicholson; J.A. Parkinson and J.C. Lindon; Measurement of biomolecular diffusion coefficients in blood plasma using 2-dimensional ^{1}H-^{1}H diffusion-edited total correlation NMR spectroscopy (DETOCSY). *Anal. Chem.* **69,** 1504-1509(1997).
5. Maili Liu; J.K. Nicholson and J.C. Lindon. High resolution diffusion and relaxation edited one- and two-dimensional ^{1}H NMR spectroscopy of biological fluids. *Anal. Chem.*, **68,** 3370-3376(1996).

BLS12

Development of a fully-adiabatic spin echo imaging sequence and its application to T_2 mapping in the human brain at 4.7T

F. Mitsumori[1], H. Watanabe[1], N. Takaya[1], M. Garwood[2]
[1]Natl Inst. for Environmental Studies, [2]University of Minnesota

T_2 is an important parameter which produces contrasts in the *in vivo* MRI. However, T_2 measurement at high field is problematic. A spin echo sequence using an ordinary sinc pulse as the slice selective refocusing pulse cannot refocus all the coherence due to the incomplete slice selection. When multiple-echoes are collected by the method, the loss of coherence is cumulative in each 180-degree pulse, leading to erroneous T_2 measurements. The occurrence of stimulated echoes after second 180-degree pulse makes the situation more complicated. At high field this problem becomes worse due to the increase in the B_1 inhomogeneity. It has been known that the use of a pair of adiabatic pulses for the refocusing gives very precise slice selection, being used for localized spectroscopy (LASER) (1), and for a single echo spin echo sequence (2). We implemented multiple pairs of the hyperbolic secant pulses for the refocusing to the spin echo sequence to obtain accurate T_2 decay in the multi-echo measurements.

T_2 values in various gel phantoms obtained by this sequence were compared with those obtained by a non-selective CPMG sequence, and proved to be well coincided. Then, the method was applied to the human brain. Twelve (six male and six female) adult volunteers were examined. Six echoes were collected with TR/TE of 4000/26, 52, 78, 104, 130, and 156 ms with an echo spacing of 13 ms. Data matrix of 256 x 128 was collected in the FOV of 25.6 x 25.6 cm with a slice thickness of 2.5mm, giving a spatial resolution of 1 x 2 x 2.5 mm. Slice plane was set across the basal ganglia region in the transaxial orientation.

A typical T_2 map is shown in Figure 1 along with a T_1 map obtained in the same slice. T_2 values in the grey matters (GM) in caudate, putamen, and thalamus were 54±2, 50±2, 55±3 ms, respectively, while those in white matters (WM) in genu and splenium in corpus callosum were 52±3, and 65±4 ms, respectively. The T_2 value in globus pallidus was as short as 34±1 ms, and that of CSF was as long as 840±150 ms. In general, T_2 values in the brain parenchyma were 30 ~ 40 % decreased compared with those values obtained at 1.5T. One notable thing is that WM in optical radiation and posterior part of corpus callosum (splenium) showed long T_2 over 60 ms, even longer than those in the neighboring GM, while deep WM in the frontal cortex along with anterior part of corpus callosum (genu) had shorter T_2 than those in neighboring cortical GM. The inverse T_2 contrast between GM and WM in the human brain was also reported in the occipital lobe at 1.5T (3), 4T and 7T (4). These findings mean that the T_2 values are not any more used to simply distinguish GM and WM.

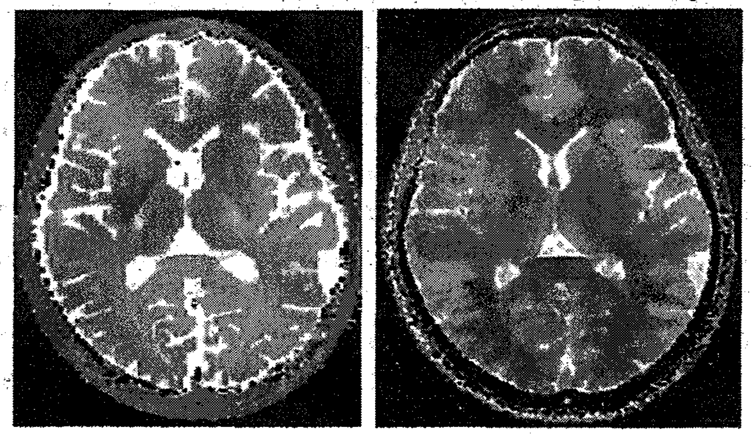

Figure1. T_2 map (left), and T_1 map (right) in the human brain.

References
1. M.Garwood, L.DelaBarre, J.Magn.Reson., 153, 155-177 (2001).
2. D.G.Shupp et al., Magn. Reson. Med., 30, 18-27 (1993).
3. J.Zhou et al., ibid, 46, 401-406 (2001)
4. R.Bartha et al., ibid, 47, 742-750 (2002).

BLS13

An improved protocol for small animal dynamic contrast-enhanced MRI and its related misregistration artifact of enhancing imaging pixels

Hideto Kuribayashi, Daniel P Bradley, Philip L Worthington, David R Checkley, Jean J Tessier and John C Waterton
AstraZeneca, Macclesfield Cheshire SK10 4TG UK

Contrast agents, such as Gd-DTPA, are widely used in MRI to enhance abnormal tissues. Conventional gadolinium contrast agents distribute widely in blood plasma and extracellular-extravascular space after intravenous injection. Dynamic contrast-enhanced (DCE) MRI, which measures contrast agent kinetics, is a powerful tool for the evaluation of tissue perfusion and vascular permeability. DCE-MRI measurements are ideally obtained with the simultaneous acquisition of an arterial input function (AIF) to permit accurate compartmental modeling. Working with small animals, such as rodents, requires a very high time resolution to obtain a useful AIF. Keyhole imaging can improve the temporal resolution of DCE-MRI. Here the only central region of *k*-space is acquired during the dynamic part of the acquisition. However, the limited *k*-space sampling can cause distortion of the images. In this study, we used peripheral line updating, referred to as "semikeyhole", and applied this to a saturation recovery spoiled gradient recalled-echo T_1-weighted imaging sequence. With this technique an AIF in the rat abdominal aorta was acquired robustly with a time resolution of 0.5 seconds (1)

In the same experiment, however, misregistration of enhancing AIF pixels was observed along the phase-encoding direction around injection time. Comparing a variety of possible sliding-window reconstruction techniques illustrated that the shift was observed in the images whose corresponding *k*-spaces contained lines acquired during the rise-time of the gadolinium first-pass. Both the direction and the period of the shift observed suggested that the phase shift induced by a given phase-encoding gradient was perturbed by contrast agent phase shift ($\Phi_{Gd}(t)$) which could be expressed as (2): $\Phi_{Gd}(t) = P \cdot TE \cdot C_p(t)$, where $C_p(t)$ is the paramagnetic concentration, P is a function of the Larmor frequency, the molar magnetic susceptibility, and the paramagnetic compartment geometry, and TE is the echo-time of the pulse sequence used. The maximum plasma concentration of Gd-DTPA could be estimated from the number of pixels shifted by a linear $\Phi_{Gd}(t)$ and this agreed with that calculated from the dosage divided by the estimated plasma volume of a rat. In conclusion, we have shown that a large increase in gadolinium concentration during *k*-space sampling can cause a phase shift that manifests, after Fourier transformation, in the misregistration of the enhancing pixels in the phase encoding direction. If uncorrected, this misregistration artifact can be severe enough to compromise the measurement of small vessel AIF by MRI.

References: 1. Kuribayashi H et al. Magn Reson Med Sci 2004;3:207-210.
2. Conturo TE et al. Magn Reson Med 1992;27:375-390.

BLS14

Mouse MRI Probe for Stereotaxic Analysis

H. Wakamatsu[1], M. Yokoi[1], Y. Imaizumi[1], F. Sugihara[2], T. Ogino[3], [O]Y. Seo[1]

[1]Department of Regulatory Physiology, Dokkyo University of Medicine, Mibu,
[2]Graduate School of Integrated Science, Yokohama City University, Yokohama,
[3]Department of Biochemistry and Cellular Biology, National Institute of Neuroscience, National Center of Neurology and Psychiatry, Kodaira, Japan

Introduction Our new project is to detect minimal brain injury in the shaken-baby syndrome. We will take a rat model that was established by Ueda et al (Neuroscience Letters, **385**,82-86 2005). A high-spatial resolution image and a diffusion analysis can be useful to detect and follow pathological changes in the brain. In order to analyze rat brain stereotaxically, we have developed the stereotaxic coordinates in the magnetic devices. We have already established it for the rat brain with much bigger magnet using Biospec 4.7/40. It is reasonable to take a higher field to get a better image from small brains of neonatal, infantile, and juvenile rats which are similar size to mouse. In order to establish basic system, we had made a probe with the stereotaxic coordinates for mice inside Micro2.5 gradient system (Bruker Biospin) that allows us only 39 mm in diameter for animal and RF coils.
Methods A set of the conventional fixation devices (a bite bar and a pair of ear bars) was installed in an acrylic tube (5 mm thickness). The position of the bite bar can be adjusted either the level position (the stereotaxic coordinates) or -2 mm down position (best position for the RF-coil) (Fig. 1).
Results Using this probe, we can get reasonable quality of images as shown in Fig. 2 (An GE image (TR/TE = 400/4.4 ms) with a slice thickness of 0.5 mm was obtained by AMX-300wb (7.05 T) with a 16-mm (o.d.) surface coil (Doty)).
Our plan We are now trying to install gas anesthesia system to keep a stable vital condition of mouse, and heat insulation system to keep body temperature of mouse.

Figure 1: Assembly of probe

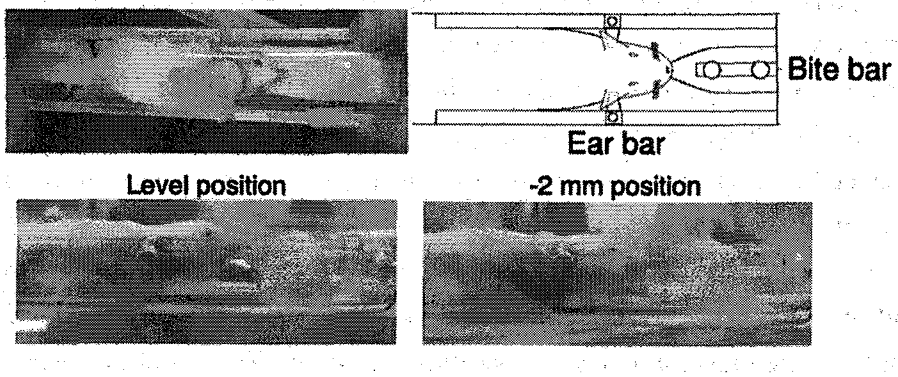

Figure 2: Transverse gradient-echo image of mouse brain

ALL6

When NMR Beats X-ray in Solving Protein Structures

Ming-Daw Tsai

Genomics Research Center, Academia Sinica, Taiwan, and Ohio State University, USA

Structures of proteins, protein-protein complexes, and protein-complexes have been solved by NMR for the following systems: human tumor suppressor p16, human Ki67 protein FHA complexed with a phosphoprotein fragment from human NIFK protein, and DNA polymerase X free and bound to DNA and MgdNTP. None of these systems has been solved by X-ray crystallography. The advantages of NMR in dealing with these systems include the flexibility of some of the proteins, the problem associated with phosphorylation and with protein-protein complexes. Biological significance and implications will also be discussed.

ALS13

Solution Structures and Backbone Dynamics an Arsenate Reductase from *Bacillus subtilis:* Changes of Motional Properties Associated with the Conformational Switch upon Arsenate Reduction

You Li, Kuan Peng, Xianrong Guo, Bin Xia and **Changwen Jin**

Beijing Nuclear Magnetic Resonance Center, Peking University, Beijing 100871, China. Telephone: +86-10-6275-6004; Fax: +86-10-6275-3790; Email: changwen@pku.edu.cn

Abstract

Arsenate reductase (ArsC) from *Bacillus subtilis* plays an important role in catalyzing the reduction of arsenate to arsenite, which is then extruded from cells through an efficient and specific transport system. We have determined the solution structures of the reduced and oxidized forms of *B. subtilis* ArsC. In addition, the kinetic experiments show that the reduced *B. subtilis* ArsC shows activities of both arsenate reductase and phosphatase. Remarkably, the oxidized *B. subtilis* ArsC remains the phosphatase activity, although it is much lower than that of the reduced form. The structural and kinetic studies demonstrate a different mechanism of *B. subtilis* ArsC from that in other organism. Furthermore, we performed the backbone dynamics studies of *B. subtilis* ArsC in the reduced and oxidized forms. The results indicate that several features of the dynamics are notably different, especially the redox functional regions of P-loop and the fragment of Cys82-Cys89. The conformational rigidity of ArsC upon the reduction of arsenate to arsenite provides further insights in understanding the mechanism of the catalytic reaction.

ALS14

NMR EVIDENCE OF DOMAIN SWAPPING AS A MECHANISM FOR REGULATING CARBOHYDRATE BINDING

Shih-Che Sue, Wei-Tin Lee, Jiun-Guo Yu, Wen-Jin Wu and Tai-huang Huang

Institute of Biomedical Sciences, Academia Sinica, Taipei, Taiwan, R.O.C.

Hepatoma-derived growth factor (HDGF) is a heparin/heparin sulfate binding protein. The exogenously treated HDGF is transported to cytosol through the binding between N-terminal HATH domain (Met1 ~ Tyr100) and the high capacity heparan sulfate on cell surface. Here we demonstrate that the HATH domain can adopt a domain-swapping dimer under physiological conditions to enhance the heparin-binding that with two orders of magnitude higher than that of the monomer. For understanding the structural basis of the enhanced binding effect, NMR technique is used here. Combining the result of intermolecular NOEs and chemical shift comparison, the structural elements of β-sheet 5, helix A and helix B are involved in domain swapping and loop 4 plays the role as a hinge loop. Another flexible loop 2 region undergoes the most significant structural perturbation upon forming dimer, implying a region of dimeric interface. A structural model is further proposed based on the NMR evidence. Two HATH monomers align side by side and two heparin binding sties conjugate into a serial manner. The two-order magnitude binding enhancement can be accounted by the well-known multivalency effect. The discovery of domain swapping in HATH-dimer as a mechanism for enhancing heparin binding and for regulating the function of growth factor provide new leads for understanding the molecular mechanism of protein-carbohydrate interaction on cell surface.

ALS15

Studies of the structures and interactions of chitin binding domains of chitinases

Kenichi Akagi[1], Tohru Yamaguchi[2], Takanori Matsuura[1], Eriko Chikaishi[1], Izumi Yabuta[1], Yuko Nagasaki[3], Masashi Hara[3], Takeshi Watanabe[3], Hideo Akutsu[1], Atsushi Nakagawa[1], and Takahisa Ikegami[1]

[1]Institute for Protein Research, Osaka University, Japan. [2]Discovery Research Laboratories, Shionogi & Co., Ltd. [3]Faculty of Agriculture, Niigata University, Japan.

Chitinase A1(ChiA1) is a glycosidase that hydrolyzes chitin, and its chitin-binding domain (ChBD), ranging from Ala^{655} to Gln^{699} located at the C-terminal part, binds specifically to insoluble chitin, which is the major constituent of the shells of crustaceans, the exoskeletons of insects, and the cell walls of many fungi. We have determined the structure of $ChBD_{ChiA1}$ from *Bacillus circulans* WL-12 by X-ray crystallography with the phase determined by the molecular replacement method using the structure previously determined by NMR as the model. To evaluate the accuracy of the crystal structure, the residual dipolar coupling (RDC) constants were measured for the nuclear pairs of ^{15}N-$^{1}H_N$, $^{13}C\alpha$-$^{1}H\alpha$, $^{13}C\alpha$-^{13}Co, ^{13}Co-^{15}N, and methyl ^{1}H-^{13}C. They fitted well to the RDC values back-calculated from the coordinates of the crystal structure, indicating the high accuracy of the structure. Furthermore, we measured the $^{3}J_{NC\gamma}$ and $^{3}J_{CoC\gamma}$ coupling constants to verify the χ_1 angles of the aromatic residues, and the cross-correlated relaxation (CCR) between the $^{1}H_N$-^{15}N vector of a residue *i* and the $^{1}H\alpha$-$^{13}C\alpha$ vector of the previous residue *i*-1 to check the ψ angles of $ChBD_{ChiA1}$ in solution. Since these results demonstrated that the crystal structure was the same as the structure in solution, we next investigated the dynamics by measuring the relaxation rates of the amide ^{15}N nuclei. The order parameters, S^2, were almost constant and high through the sequence, and no significant exchange rate, R_{ex}, was detected in an additional CPMG R_2 experiment. Therefore, we have concluded that $ChBD_{ChiA1}$ is structurally very rigid and undergoes no significant conformational change when it binds to solid chitin. Since the interaction between $ChBD_{ChiA1}$ and solid chitin can be assumed as a rigid body docking, our accurate structure would be useful for the future cyber simulation.

We also investigated Chitinase C (ChiC) from *Streptomyces griseus* HUT6037, discovered as the first family 19 chitinase in a bacterium other than higher plants. Since its chitin-binding domain ($ChBD_{ChiC}$) is able to interact also with a soluble form of chitin, such as oligosaccharide, the study on the interaction between $ChBD_{ChiC}$ and the substrate under the equilibrium condition was possible using a soluble form of chitin unlike $ChBD_{ChiA1}$. At first, the solution structure of $ChBD_{ChiC}$ was determined by using ^{13}C, ^{15}N, and ^{1}H resonance NMR, which showed a very different conformational feature in the putative chitin-interaction region from that of $ChBD_{ChiA1}$. Then, the interaction between ^{15}N- or ^{13}C-labeled $ChBD_{ChiC}$ and hexa-*N*-acetyl-chitohexaose (Hex) was monitored through chemical shift perturbations in the amide and aromatic nuclei and saturation transfer experiments. The comparison among the conformations of $ChBD_{ChiA1}$, $ChBD_{ChiC}$, and other typical chitin- and cellulose-binding domains, which have three solvent-exposed aromatic residues responsible for binding to polysaccharides, has suggested that they have, respectively, adopted different binding sites in the evolutionary process keeping almost the same backbone conformations.

ALS16

Determination of Recognition Sequences of Integrins αIIbβ3, αvβ3, and α5β1-Specific Disintegrins by Rhodostomin and its Mutants

Woei-Jer Chuang, Chiu-Yueh Chen, Yi-Chun Chen, Yao-Husn Hsieh, Jia-Hau Shiu, and Yu-Chen Liu

Department of Biochemistry, National Cheng Kung University College of Medicine, Tainan 701, Taiwan

Rhodostomin (Rho) is obtained from *Calloselasma rhodostoma* venom and belongs to the family of disintegrins. Rho consists of 68 amino acids including six disulfide bonds and a **PRGD**MP sequence at the positions of 48-53. Our previous report showed that Rho expressed in *P. pastoris* possesses the same function and structure as native protein. In order to identify the amino acid residues required for selective recognition of integrins αIIbβ3, αvβ3, and α5β1, we mutated the residues in the RGD loop or C-terminal region of Rho, expressed the proteins in *P. pastoris,* and used the platelet aggregation and cell adhesion assays to identify the mutant proteins that can selectively inhibit integrins αIIbβ3, αvβ3, and α5β1. We found that the mutant proteins containing the sequences AKGDWN (P48A/R49K/M52W/P53N) and ARGDDL (P48A /M52D/P53L) in the RGD loop can selectively inhibit Integrins αIIbβ3 and αvβ3, respectively. The mutant proteins containing the sequences ARGDXP in the RGD loop exhibited better activity in inhibiting integrin α5β1. In order to understand structural and dynamic requirements for integrins αIIbβ3, αvβ3, and α5β1 recognition, we determined 3D structures and backbone dynamics of wild-type (PRGDMP) and mutant proteins (ARGDWN, AKGDWN, ARGDDL, ARGDMP, and ARGDNP) of Rho using NMR spectroscopy. Structural analyses of Rho and its mutants showed that they have the same tertiary fold with three two-stranded antiparallel β-sheets. The RGD motif, the binding site for integrin, lies in a nine-residue loop joining two strands of β-sheet. Compared to 3D structure of Rho, the D residue of ARGDDL mutant has different orientation and the W52 residue of AKGDWN and ARGDWN interacted with A48, as well as Y67 and H68 at the C-terminus. In dynamic study the R_2 values of R49 and D51 of Rho were 8.32 and 10 s^{-1}, respectively. In contrast, the R_2 values of R49 and D51 of P48A mutant were 5.98 and 6.5 s^{-1}, resulting in the absence of Rex in these residues. These results demonstrate that the residues adjacent to the RGD motif of RGD-containing disintegrins affect their function, structure, and dynamics in recognizing integrins.

ALS17

Cell-free synthesis of selectively isotope-labeled proteins for NMR studies

Kiyoshi Ozawa, Peter S. C. Wu, Madeleine J. Headlam, Dharshana Padmakshan, Slobodan Jergic, Nicholas E. Dixon and Gottfried Otting

Research School of Chemistry, Australian National University, Canberra ACT 0200, Australia

Modern cell-free *in vitro* protein synthesis presents a powerful tool for the synthesis of isotope-labeled proteins in high yields. The production of selectively ^{15}N-labeled proteins from ^{15}N-labeled amino acids is particularly economic. Yields are often sufficient to analyze the proteins by two-dimensional NMR spectra recorded of the crude reaction mixture without concentration or chromatographic purification of the protein. Here we show several different applications. (i) Cell-free protein synthesis yields proteins in a nascent state that enables formation of soluble, native protein-protein complexes even if one of the protein components is prone to self aggregation and precipitation. We demonstrate labeling of one protein with ^{15}N in the presence of another. Protein-protein interactions can rapidly be analyzed by ^{15}N-HSQC spectra(1). (ii) Proteins with ^{19}F-labelled or other non-natural amino acids can be made with little background from natural amino acids(2). (iii) Biotinylated proteins are readily accessible. Our experience with *E. coli* S30 extracts will be discussed(3). A strategy for the assignment of ^{15}N-HSQC spectra of proteins from a limited number of selectively labelled samples will be presented.

(1) Ozawa, K. et al. (2005) Cell-free *in vitro* protein synthesis in an autoinduction system for NMR studies of protein-protein interactions. *J. Biomol. NMR* in press

(2) Ozawa, K. et al. (2005) Translational incorporation of L-3,4-dihydroxyphenylalanine (DOPA) into proteins. *FEBS J.* **272**, 3162-3171.

(3) Ozawa, K. et al. (2005) Cell-free synthesis of ^{15}N-labeled proteins for NMR studies. *IUBMB Life* in press

BLL5

NMR Study on Membrane proteins-ligands Interactions

Ichio Shimada[1,2]

1. Graduate School of Pharmaceutical Sciences, the University of Tokyo, Hongo, Bunkyo-ku, Tokyo 113-0033, Japan
2. Biological Information Research Center (BIRC), National Institute of Advanced Industrial Science and Technology (AIST), Aomi, Koto-ku, Tokyo 135-0064, Japan
Tel, Fax number: +81-3-3815-6540
e-mail: shimada@iw-nmr.f.u-tokyo.ac.jp

Protein-protein interactions are essential in many biological processes, such as signal transduction, immune response, and cellular recognition. In particular, membrane proteins, which represent 20-30 % of the total proteins encoded by the human genome, play important roles through interactions with intra- and extra-cellular ligands and the transmission of information across membranes. Structural information about the interactions between membrane proteins and their ligands provides insights into the membrane protein functions and is also useful for drug development.

Even with the recent expansion of structural genomics and the general appreciation of their biological significance, little is known about the structures and functions of membrane proteins. This is mainly due to practical problems in handling the membrane proteins. One common problem is the low stability of membrane proteins, under conventional experimental conditions. Although surfactant-solubilized membrane proteins have generally been used in structural analyses, the solubilization of membrane proteins frequently causes conformational instability, followed by aggregation or denaturation.

In this paper, we report our recent data regarding the interaction between membrane proteins and ligands.

BLS15

A photochromic GFP-like protein and molecular/structural basis of the photochromism

Hideaki Mizuno[1], Tapas Kumar Mal[2], Akihiko Kikuchi[3], Markus Wälchli[4], Takashi Fukano[1], Ryoko Ando[1], Junichiro Taka[3], Jeyaraman Jeyakanthan[3], Yoshitsugu Shiro[3], Mitsuhiko Ikura[2], and Atsushi Miyawaki[1]

[1]Cell Function and Dynamics, Brain Science Institute, RIKEN, 2-1 Hirosawa, Wako-city Saitama 351-0198, Japan; [2]Division of Molecular and Structural Biology, Ontario Cancer Institute and Department of Medical Biophysics, University of Toronto, Toronto, Ontario M5G 2M9, Canada; [3]RIKEN Harima Institute/SPring-8, 1-1-1 Kouto, Mikazuki-cho Sayo Hyogo 679-5148, Japan; [4]Bruker Biospin Co. Ltd., 3-21-5 Ninomiya, Tsukuba-city Ibaraki 305-0051, Japan

Green fluorescent protein (GFP) has become a useful tool to label protein in living cells. GFP forms a chromophore auto-catalytically from its own amino acid residues without any cofactor. A variety of GFP mutants and GFP-like proteins with different colors and properties are now available, enabling a multi-color labeling of different proteins. We have recently developed a photochromic fluorescent protein, Dronpa, which can be turned on and off upon light illumination (1,2). Dronpa originally has a green fluorescence (bright state), loses the fluorescence by strong 488-nm illumination (dark state), and regain the fluorescence by 405-nm illumination (the bright state again). This photochromic reaction is completely reversible. Dronpa has been used to analyze dynamic aspects of intracellular events, including nucleocytoplasmic shuttling of MAP kinase. Dronpa can also be applied to be the media material of a memory device which can be read, written, and erased repeatedly by light. We have addressed the structural basis for the phorochromism. An X-ray crystallographic analysis revealed that the overall structure of Dronpa is a β-barrel consisting of 11 β-strands and the chromophore is placed at the central part of the barrel. NMR data showed that a chromophore structure, 4-(*p*-hydroxybenzyliden)-5-imidazolinone, is formed from the residues Cys^{62}-Tyr^{63}-Gly^{64}. We'll discuss details about the light-dependent behavior of the chromophore by comparing NMR spectra of Dronpa in the bright and dark state.

1) Ando et al., Science 306, p1370 (2004)

2) Habuchi et al., Proc. Natl. Acad. Sci. USA 102, p9511 (2005)

BLS16

The Use of Paramagnetic Metal Ions in NMR Studies of Protein Structures in Solution

Malene Ringkjøbing Jensen and Jens J. Led

The Biophysical NMR Group, Department of Chemistry, University of Copenhagen, Universitetsparken 5, DK-2100 Copenhagen Denmark

Paramagnetic metal ions are potential sources of information about the structures of proteins. The dipolar interactions between the unpaired electrons of a paramagnetic metal ion and the protein nuclei contain valuable long-range structure information. Moreover, they can easily be detected by nuclear magnetic resonance (NMR) spectroscopy through enhanced nuclear relaxation rates and changes in chemical shifts. These interactions are therefore often used to refine and improve the structures of native metallo-proteins such as iron-sulfur proteins, blue copper proteins and calcium binding proteins. More recently, the approach has been extended to non-metallo proteins by incorporating a paramagnetic metal ion in the protein, using a metal binding tags artificially attached to the protein.

Here, we demonstrate that the approach can be extended to non-metallo proteins even without the use of metal-binding tags. This requires that the protein has a potential metal binding site that can bind a paramagnetic metal ion temporarily.[1] Therefore, we have identified a series of potential metal binding sites on the surface of the *native* form of the protein *E. coli* thioredoxin.

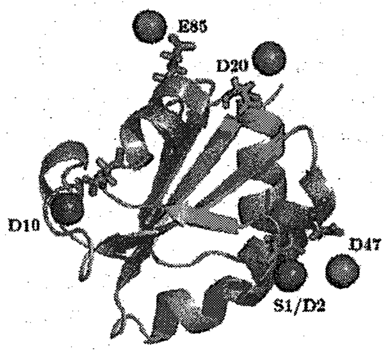

FIGURE 1. The structure of Trx showing the five different Ni^{2+} binding sites. The carboxylate side chains are shown in green while the Ni^{2+} ions are shown in gray.

Furthermore, we have shown that detailed information about the structure of the protein can be obtained from paramagnetic constraints derived from a metal ion bound temporarily to one of these sites in the protein. No metal binding tags or chelating agents were applied to bind the paramagnetic metal ion. The approach is expected to be valuable in other proteins that crystallize with metal ions, use metal ions as cofactors or bind metal ions for temporary stabilization or storage.

1. Malene R. Jensen, Gitte Petersen Conni Lauritzen, John Pedersen and Jens J. Led: Metal Binding Sites in Proteins:Identification and Characterization by Paramagnetic NMR Relaxation. *Biochemistry* 44, In Press.

BLS17

Conformation Transition of Fe-Coordinated Methionine in Thermophile *Hydrogenobacter thermophilus* Cytochrome c_{552}

Shin-ichi J. Takayama[1], Yo-ta Takahashi[1], Hulin Tai[1], Shin-ichi Mikami[1], Tsuyoshi Udagawa[1], Hiroaki Sasaki[1], Shigenori Nagatomo[1], Hajime Mita[1], Yasuhiko Yamamoto[1], Yoshihiro Sambongi[2], Jun Hasegawa[3], Hikaru Hemmi[4], Ryo Kitahara[5], and Kazuyuki Akasaka[5]
[1]*Department of Chemistry, University of Tsukuba, Tsukuba 305-8571,* [2]*Graduate School of Biosphere Science, Hiroshima University, Higashi-Hiroshima 739-8528,* [3]*Daiichi Pharmaceutical Co., Ltd., Edogawa-ku, Tokyo 134-8630,* [4]*National Food Research Institute, Tsukuba 305-8642,* [5]*Structural and Molecular Biology Laboratory, RIKEN Harima Institute at Spring-8, 1-1-1 Kouto, Mikazuki-cho, Sayo, Hyogo 679-5148*

A monoheme cytochrome c_{552} (HT) from a thermophile *Hydrogenobacter thermophilus* is a small electron transfer protein composed of 80 amino acid residues. One of characteristics of HT is high thermostability. Circular dichroic spectrometry using a pressure-proof cell revealed that the oxidized and reduced forms of HT exhibit the denaturation temperatures of 109.8 °C and 129.7 °C, respectively. In a ^{1}H NMR spectrum of the oxidized form of HT, paramagnetically shifted signals arising from heme peripheral methyl and Fe-coordinated methionine (Met61) protons were resolved in downfield and upfield shifted regions, respectively. As expected from its high thermostability, the resolved signals were observed well up to 96 °C, demonstrating that the structural features of the heme active site in HT were intact at this temperature. On the other hand, the signals exhibit considerable line-broadening at low temperatures. Interestingly, the line-broadening occurs only on the heme peripheral and Met61 proton signals, of which T_1 values are essentially independent of temperature. These results indicated that the line-broadening is due to an exchange process which is possibly associated with a change in the heme Fe coordination structure.

In order to elucidate structure factors responsible for the line-broadening, we have carried out high pressure NMR study of the oxidized form of HT. The downfield-shifted heme methyl proton signals at 200 MPa once disappeared completely at 0 °C and reappeared, with altered shifts, at -20 °C. Additionally, the Met61 methyl proton signal split into two peaks at -20 °C, demonstrating that Met61 methyl group exists in two distinctly different environments. Therefore Met61 is likely to undergo a transition between two conformation states. Such conformation transition of Met61 modulates the heme electronic structure, through the Fe-Met coordination bond, which is sensitively reflected in the heme methyl proton shift pattern. Preliminary results indicated that ^{1}H-^{15}N HSQC connectivities observed for the residues in a long loop region bearing Met61 are largely influenced by the pressure, suggesting a possible correlation between the conformation transition of Met61 and structure dynamics of the loop region.

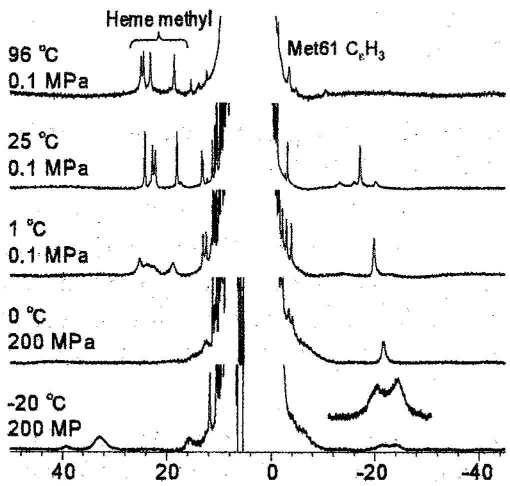

References
S. J. Takayama *et al., Biochemistry*, **44**, 5488-5494 (2005).
S. Uchiyama *et al., J. Am. Chem. Soc.*, **126**, 14684-14685 (2004).
N. Tachiiri *et al., J. Biol. Inorg. Chem.*, **9**, 733-742 (2004).
N. Terui *et al., J. Am. Chem. Soc.*, **125**, 13650-13651 (2003).
Y. Yamamoto *et al., J. Am. Chem. Soc.*, **124**, 11574-11575 (2002).

BLS18

Determination of the electronic and geometric structure of the metal site in metallo-proteins by paramagnetic NMR.

Jens J. Led, D. Flemming Hansen

The Biophysical NMR Group, Department of Chemistry, University of Copenhagen, Universitetsparken 5, DK-2100 Copenhagen, Denmark

The biological function of metalloproteins stems from the geometric and electronic structures of their metal sites. Thus, in blue copper proteins such as plastocyanins, an unusual electronic structure of the metal site is believed to contribute to the rapid, long-range electron transfer reactivity that characterizes these proteins. Detailed knowledge of the geometric and electronic metal site structures of the blue copper proteins is, therefore, imperative for understanding the function of the proteins at the molecular level

So far, the geometric structure of the metal site in blue copper proteins has been determined primarily by X-ray crystallography and extended X-ray absorption fine structure (EXAFS), while the electronic structure of the blue copper site has been determined theoretically from quantum chemical calculations and experimentally by X-ray absorption spectroscopy (XAS). However, all of these structures refer to the solid state. Yet, the function of metalloproteins takes place in solution. It is, therefore, of interest to study the structural characteristics of the metal site in solution.

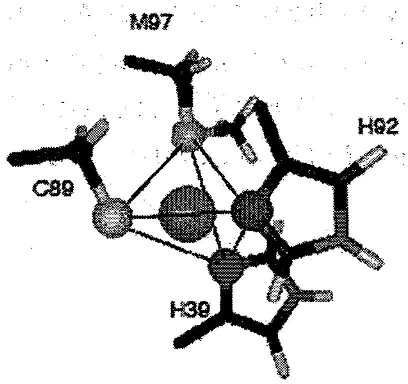

Figure 1. The coordination sphere of the catalytic site in plastocyanin. The site has a distorted tetrahedral geometry with the copper ion strongly bound to the S atom of the cysteine C89, and to the N atoms of the two histidines H39 and H92, while weakly bound to the axial S atom of M97.

Here it will be shown how the geometric and electronic structure of the metal site of paramagnetic metalloproteins (Figure 1) in solution can be determined precisely from experimental NMR data and quantum chemical calculations.[1-3] The blue copper protein, plastocyanin from *Anabaena variabilis* (*A.v.*) was used as an example.

1. D. Flemming Hansen and Jens J. Led. "Mapping the Electronic Structure of the Blue Copper Site in Plastocyanin by NMR Relaxation." *J. Am. Chem. Soc.* 126, 1247-1252 (2004).

2. D. Flemming Hansen, Serge I. Gorelsky, Hans E. M. Christensen, Edward I. Solomon and Jens J. Led. "Improvement of the method for mapping the electronic structure of blue copper proteins by NMR relaxation." Submitted.

3. D. Flemming Hansen and Jens J. Led. "Determination of the geometric structure of the metal site in a blue copper protein by paramagnetic NMR." Submitted.

BLS19

Structure Determination of Cyclic Peptides of the Nocardamine Class from a Marine-Derived Bacterium of the Genus Streptomyces

Tae-Sik Kim, Hoshik Won, * Hejae Shin

Department of Applied Chemistry, Hanyang University

** Marine Natural Products Laboratory, Korea Ocean Research & Development Institute*

Actinomycetes have been the most significant source for compounds with biological activity and clinical usefulness. In an effort to search for novel marine natural products, we have collected more than 3,000 strains of actinomycetes from marine invertebrates, plants, and sediments. Herein we report the results of our chemical investigation on the biologically active metabolites from marine actinomycetes and structure determination based on comprehensive spectroscopic analysis. Bioactive cyclic peptides of the nocardamine class were isolated from strains of actinomycetes and highly purified for NMR studies. Complete ^{1}H, ^{13}C-NMR signal assignments were made by using various homonuclear and hetereonuclear 2D-NMR techniques. The structure of compounds 1-3 were also determined by utilizing NOE observation and molecular dynamic computations.

ALL7

Clean SEA-HSQC: a method to map solvent exposed amides in large non-deuterated proteins with gradient-enhanced HSQC

Donghai LIN, Kong Hung SZE and Guang ZHU*
Dept. of Biochemistry, The Hong Kong University of Science and Technology, Clear Water Bay, Kowloon, Hong Kong, SAR, P. R. of China

Abstract
The SEA-HSQC method selectively observes solvent exposed amide protons with a SEA element. This experiment can effectively eliminate both NOE contributions from aliphatic protons and exchange-relayed NOE contributions from fast exchanging hydroxyl or amine protons, and suppress artifacts due to longitudinal relaxation contributions during the mixing period. The SEA-HSQC experiment can be used to map the solvent exposed residues in proteins to resolve the problem of resonance overlap, facilitate ligand binding studies, and measure exchange rates, kex. We have successfully applied this method to map a binding site on a protein-ligand complex and study the protein folding processes.

ALL8

Structure biology of ubiquitination and SUMOylation

Masahiro Shirakawa[1,2,3], Kenichiro Fujiwara[4], Ayako Ohno[5], Takeshi Tenno[1], Daichi Baba[1,4], Nobuo Maita[6], JunGoo Jee[7], Hidehito Tochio[4], Hidekazu Hiroaki[4]

[1]Graduate School of Engineering, Kyoto University, Japan, [2]RIKEN Genomic Science Center, Yokohama, Japan, [3]CREST, Japan Science and Technology Corporation, Japan, [4] Yokohama City University, Kanagawa, Japan, [5]RIKEN, Wako, Japan, [6]Graduate School of Systems Life Sciences, Kyushu University, Fukuoka, Japan, [7]Laboratory of Chemical Physics, National Institute of Diabetes and Digestive and Kidney Diseases, National Institutes of Health, Bethesda, USA

Ubiquitination and SUMOylation, modifications in which single or multiple ubiquitin or SUMO (Small Ubiquitin-like modifier) molecules are conjugated to a protein, serve signaling functions that control various cellular processes.

The ubiquitin tag is recognized by downstream effectors, most of which carry one or more of various ubiquitin recognition motifs. Of the motifs, UBA (ubiquitin-associated) domain and UIM (ubiquitin-interacting motif) are most frequently found, and occur in proteins that have been implicated in the ubiquitin-proteasome system and endocytotic pathways. To obtain the structural basis for recognition by these ubiquitin recognition motifs, we solved the structures of a UIM of human proteasome subunit S5a in complex with the ubiquitin-like domain (UbL) of human HR23B and the UBA of yeast Dsk2p in complex with yeast ubiquitin, by multi-dimensional NMR spectroscopy.

An interesting feature of ubiquitin tags is their linkage specificity. Functions of two different forms of polyubiquitin chain have been characterized, in which the isopeptide bond linkages involve Lys48 or Lys63. The former is mostly used to target proteins for proteasomal degradation, whereas the latter has been linked to a variety of cellular events, none of which relies on degradative signaling via the proteasome or lysosomes. We have performed NMR experiments to analyze the subunit interafaces and conformational properties of Lys48 and Lys63-liked di- and tetraubiquitin chains.

Finally, the structures of SUMO-modified thymine DNA glycosylase (TDG) will be also discussed.

ALS18

Solution structure of the DNA binding domain of RPA from *Saccharomyces cerevisiae* and its interaction with single-stranded DNA and SV40 T antigen

Chin-Ju Park, Joon-Hwa Lee, Sung-Jae Cho & Byong-Seok Choi

Department of Chemistry and National Creative Research Initiative Center, Korea Advanced Institute of Science and Technology, 373-1, Guseong-dong, Yuseong-gu, Daejon 305-701, Korea

Replication Protein A (RPA) is a three-subunit complex with multiple roles in DNA metabolism. DNA binding domain A in the large subunit of human RPA (hRPA70A) binds to single-stranded DNA (ssDNA) and is responsible for the species-specific RPA--T antigen (T-ag) interaction required for Simian Virus 40 replication. Although *Saccharomyces cerevisiae* RPA70A (scRPA70A) shares high sequence homology with hRPA70A, the two are not functionally equivalent. To elucidate the similarities and differences between these two homologous proteins, we determined the solution structure of scRPA70A, which closely resembled the structure of hRPA70A. The structure of ssDNA-bound scRPA70A, as simulated by Residual Dipolar Coupling-based homology modeling, suggested that the positioning of the ssDNA is the same for scRPA70A and hRPA70A, although the conformational changes that occur in the two proteins upon ssDNA binding are not identical. NMR titrations of hRPA70A with T-ag showed that the T-ag—binding surface is separate from the ssDNA binding region and is more neutral than the corresponding part of scRPA70A. These differences might account for the species-specific nature of the hRPA70A--T-ag interaction. Our results provide insight into how these two homologous RPA proteins can exhibit functional differences, but still both retain their ability to bind ssDNA.

ALS19

Recognition mechanism of the target by RNA aptamer and Musashi protein, studied with the aid of residue specific labeling, ^{13}C-detection and RDCs

Matsugami, A.[1], Miyanoiri, Y.[1], Tochio, H.[1], Tamura, Y.[2], Kudo, M.[2], Uesugi, S.[2], Misono, T.[3], Kumar, P.[3], Imai, T.[4], Okano, H.[4] and Katahira, M.[1,5]

[1]Department of Supramolecular Biology, International Graduate School of Arts and Sciences, Yokohama City University, 1-7-29 Suehiro-cho, Tsurumi-ku, Yokohama 230-0045, Japan, [2]Yokohama National University, [3]AIST, [4]Keio Univ., [5]Genomic Science Center, RIKEN.

RNA aptamer Tat protein of HIV stimulates transcription of the viral genome through binding to the trans-activating region (TAR) located at the 5' end of all pre-messenger RNA transcripts. We have obtained an RNA aptamer that binds Tat 100-times more strongly than the authentic TAR by means of the in vitro selection method. The sequence of the aptamer contains of two nearly symmetrical Tat binding sites.

In order to elucidate the structural basis of the extremely high affinity of the aptamer to Tat, the structure of the aptamer complexed with argininamide, the simplest analogue of Tat, was determined by NMR. Unique structural features which could be responsible for the high affinity were found. Then we tried to determine the structure of the aptamer complexed with an RNA-binding peptide of Tat, which is a more realistic analogue of Tat. However, spectral overlapping hindered the analysis of the complex.

Here, we have prepared three peptides in which a single arginine residue of GRKKRRQ, an RNA-binding peptide of Tat, was specifically ^{13}C, ^{15}N-labeled. Non-labeled aptamer complexed with each of the three peptides were utilized for structural analysis. ^{13}C, ^{15}N-labeled aptamer was prepared, and its complex with a non-labeled peptide was also utilized for the analysis. Simplification of spectra by specific labeling enhances the identification of intermolecular contacts of each arginine residue, which plays a major role in recognition with the aptamer.

In order to obtain the information on the hydrogen bonds involving Arg residues of the peptide, ^{13}C-detection of C^{ζ}-N^{ε} and C^{ζ}-N^{η} correlation peaks for Arg residues has been carried out. ^{13}C-detection may also be applicable for a resonance assignment procedure for RNA.

The structure of the complex was analyzed on the basis of unambiguous intermolecular NOEs derived from specific labeling of peptides. Two adjacent U:A:U base triples are formed at the center of the aptamer, as observed in the case of the complex with argininamide. A detailed view on the recognition of Tat by RNA aptamer was obtained from the analysis.

Musashi protein Musashi plays a dominant role in regulation of asymmetric division of neural stem cells through the inhibition of the translation of a certain mRNA. It contains two RNA-binding domains, RBD1 and RBD2. We have already elucidated the origin of higher affinity to RNA of RBD1 than that of RBD2, on the basis of comparison of their structures, mode of interactions, surface electrostatic potentials and backbone dynamics.

We have also exhibited that RBD1-RBD2, produced by naturally occurring link of RBD1 and RBD2, binds RNA much stronger than RBD1. Interestingly, at the initial stage of the addition of RNA, perturbation was mainly observed for residues of an RBD1 part of RBD1-RBD2, while at the following stage, perturbation was also observed for residues of an RBD2 part. This suggests that RBD1 and RBD2 may play a different role in RNA binding. Residual dipolar couplings, RDCs, for RBD1-RBD2 in a free state and a complex state with the target RNA have been obtained with a gel method. On the basis of RDCs, the structural change of RBD1-RBD2 on complex formation will be discussed in terms of the recognition of the target.

BLL6

Industrial Applications of Solid State NMR using High Magnetic Fields

Koji Saito
Nippon Steel Corporation, Advanced Research Technology Lab. 20-1 Shintomi Futtsu City, Japan

A new approach to structural analysis of inorganic polymer, we called slag which is by products of steel making, has been proposed using multi-nuclear solid state NMR at high magnetic field that is capable of obtaining the structural information of each element composing the slag such as F, Si, Al, Mg and O, and effective to both crystalline and non-crystalline solid materials. In this study, we applied mainly ^{27} Al (I=5/2) and ^{25} Mg(I=3/2) and ^{17}O(I=3/2) solid state NMR two types of steel -making slags. In ^{27}Al NMR measurements, two dimensional ^{27}Al multiple-quantum magic angle spinning (MQMAS) NMR was applied which can average the second-order quadrupolar interaction. Drastic improvement of spectral resolution at high magnetic field (16.4T) 5QMAS experiment clarified the existence of at least 11 chemical sites of Al in slag. And, we successfully obtained ^{25}Mg 3QMAS spectra in slag, when special probe has been developed to overcome low sensitivity. Additionally, solid state ^{17}O NMR is very useful and powerful tools for the structural analysis of oxygen in various inorganic materials. However, quite low sensitivity on NMR is main difficulty point. And then, we tried to synthesize each ^{17}O-labeled stating materials such as $Ca(*OH)_2$, Al_2*O_3 and $Si*O_2$ in order to overcome low sensitivity. Using these materials, the formation of slag network was investigated at 1273 to 1673K by ^{17}O MQMAS. The process of network formation of oxygen in slag could be observed by means of ^{17}O full labeled materials at each temperature. Moreover, ^{17}O selective labeled ($Si*O_2$ or Al_2*O_3)) materials became possible to assign each peak in spectra of full-labeled materials. ^{27}Al-^{17}O CP/MAS methods were applied in order to make connectivity clear. Finally, the inter-nuclear correlation spectra in solid state NMR provide detailed information on chemical bonding and chemical three dimensional structures of solid state materials. We applied both techniques of through-bond and through-space to analysis of connectivity between a quadrupolar nucleus (^{27}Al) and a spin-1/2 nucleus (^{31}P) via bridging oxygen in slag, and compared two methods. From above mentioned results, multi-nuclear solid state NMR is proved to be a very effective method in characterization of the slag.

Recent new development of super conducting magnet can make new application field for solid state NMR. Especially, NIMS in Tsukuba succeed in the development of 930 MHz (21.8T) solid state NMR system. In this paper, we would like to show two topics which have new finds in industrial application when this developed high field solid state NMR system is applied. Optimization of the drying process conditions for a steel-making converter in a steel works is very important since the process is off-line and time-consuming. However, it is very difficult to optimize drying process conditions (temperature, surface active agents, etc.), because the refractory mortar of steel converter is made of very complicated and mixture materials. To help understanding, we have analyzed the refractory mortar using solid state NMR at 16.4T because the refractory mortar is an amorphous materials, it means X-ray method can't give useful information. And then, we got new chemical structural information of the refractory mortar using ^{27}Al MQMAS at 16.4T. And also, we have first demonstrated the structural analysis of these complex materials using very high field 930MHz (21.8T) solid state NMR. This paper shows the effect of magnetic field strength in these materials on ^{27}Al MAS and MQMAS spectra. In particular, we find several new chemical sites using 21.8T with compared to the result of ^{27} Al MQMAS at 16.4T. At the same time, some relaxation information (T_1) of the refractory mortar will be discussed because of high resolution MAS spectra at 21.8T. It is clear that solid state NMR at high field give useful information to analyze complicated materials. Using this data, we can adjust and design the drying process and time in steel works.

Another topics is the application of ^{17}O to amorphous-ALPO. New results for amorphous-ALPO using 930 MHz solid state NMR system will be discussed.

BLS20

Properties of Carbon Supported Pt Catalysts Studied by ^{13}C NMR

Kee Sung Han and Oc Hee Han*
Daegu Center, Korea Basic Science Institute
1370 Sankyuckdong, Bukgu, Daegu 702-701, Republic of Korea

Carbon supported platinum (Pt/C) has been used for catalysts in fuel cell due to its higher catalytic activity than Pt black. However, its catalytic activity also strongly depends on the Pt particle size and the surface morphology which are sensitive to the sample preparation methods and pretreatment. Thus CO poisoning occurring during methanol oxidation and its removal procedure also can influence the particle size and surface morphology.

In this work, metal cleaning and methanol oxidation effect on Pt/C was investigated as a function of Pt content in a sample which is closely correlated with Pt particle sizes. Both results of metal cleaning and methanol oxidation indicate the line width (*Figure 1*) and ^{13}C chemical shift of CO adsorbed on Pt have non-linear behavior. Their steeper change for the size smaller than 5nm could be interpreted by different relative populations of various surface adsorption sites of Pt particles versus the particle size (*Figure 2*). The transmission electron microscopy (TEM) data indicates that the Pt particle size in all the samples increased by cleaning and after prolonged methanol oxidation the Pt particle size increased in 20% Pt/C, decreased in 60% Pt/C, and did not change in 40% Pt/C samples, respectively. The Pt size variation difference between this work and the previous reports of the particle growths by fuel cell operation is explained by the experimental temperature difference.

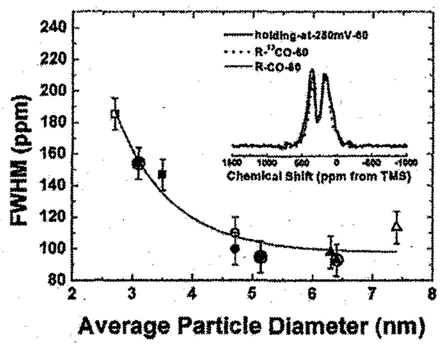

Figure 1. Line width (FWHM) of ^{13}C NMR spectra after prolonged methanol oxidation with respect to the average Pt particle size determined by TEM. The inset is the ^{13}C NMR spectra of 60% Pt/C samples.

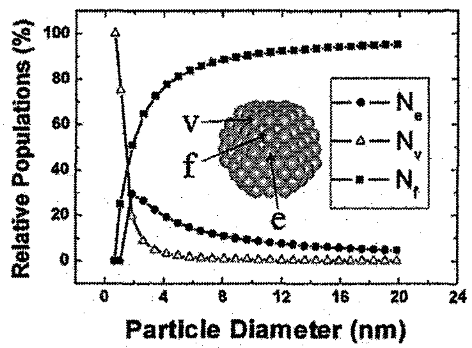

Figure 2. The relative population of edge (N_e), vertex (N_v) and face (N_f) sites on a cubooctahedral Pt in various size. The inset is the structure of Pt cubooctalhedron.

Acknowledgements

One of the authors (O. C. Han) gratefully acknowledges financial support from the Korea Science and Engineering Foundation through an International Cooperation Project.

BLS21

Geopolymers: A multinuclear SS NMR investigation of structural ordering

Peter Duxson*[1], John L. Provis[1], Grant C. Lukey[1], Frances Separovic[2] and Jannie S.J. van Deventer[1]

[1]Department of Chemical and Biomolecular Engineering
[2]School of Chemistry
The University of Melbourne, Victoria 3010, AUSTRALIA.
Telephone: +61-3-8344-6619 Fax: +61-3-8344-4153.
e-mail: jannie@unimelb.edu.au

Geopolymers are chemically hardened monolithic aluminosilicate gels formed by partial dissolution and polycondensation of aluminosilicate materials, such as fly-ash and calcined clays, in alkaline environments. Geopolymers have been proposed as an alternative to traditional Ordinary Portland Cement (OPC) for use in construction applications, due to their excellent mechanical properties, infinite scalability, low temperature requirement for synthesis and their intrinsic fire resistance. Like zeolites and some aluminosilicate gels, geopolymers are synthesized in aqueous media, albeit with much lower water weight fractions, typically less than 35%. Since geopolymer technology emerged from alkali-activated cements, their characterization has often been based on cement and concrete science. Use of ^{29}Si, ^{27}Al and ^{17}O MAS NMR spectroscopy is able to elucidate the structural Q^4(mAl) building blocks of geopolymer gels and the effect of alkali on the incorporation of aluminum into the matrix.

^{29}Si MAS-NMR spectra of geopolymers with $1.15 \leq$ Si:Al ≤ 2.15 show a typically broad resonance, similar to aluminosilicate gels. These spectra may be deconvoluted into components representing $Q^4(m\text{Al})$ (where $1 \leq m \leq 4$) silicon centres, as shown in Figure 1. The effect of different Si/Al ratios and alkali cations was elucidated, implying that geopolymers of low Si/Al ratio may contain Al-O-Al linkages, which is thought strictly forbidden in geopolymeric gels.

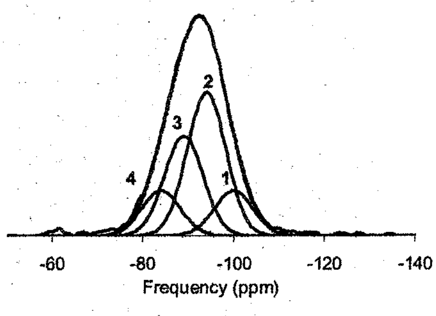

Figure 1: Deconvolution of ^{29}Si MAS NMR spectrum of geopolymer. The numbers on the figure represent the number of aluminum cations in each Q^4(mAl) structural unit.

^{27}Al MAS-NMR data have identified differences in the incorporation of aluminium and reactivity of raw materials based on differences in the alkali cation (sodium and potassium). Information from both ^{27}Al and ^{29}Si NMR has been combined to produce a statistical thermodynamic model, which is able to predict the structural ordering observed in NMR spectroscopy. Furthermore, ^{17}O 3Q MAS-NMR will be presented to corroborate the prediction of Al-O-Al linkages by the ^{29}Si NMR and thermodynamic model.

BLS22

High sensitive resistively-detected NMR experiments using all-electrical semiconductor GaAs nano-scale device

T. Ota[A,B], G. Yusa[A,B], K. Muraki[A], N. Kumada[A], S. Miyashita[C], and Y. Hirayama[A,B]

[A]NTT Basic Research Laboratories, 3-1, Monrinosato Wakamiya, Atsugi, 243-0198, Japan
[B]SORST-JST, 4-1-8 Honmachi, Kawaguchi, Saitama 331-0012, Japan
[C]NTT-AT, 3-1, Monrinosato Wakamiya, Atsugi, 243-0198, Japan

Nuclear spins are one of the most promising candidates for quantum bits because of their long coherence time. Exploration of control and detection of the nuclear spins in solid-state devices is highly requested for possible implementation of realistic scalable devices. In semiconductors, contact hyperfine interaction with conduction electrons enables us to access to the nuclear spins. Recently, we have succeeded in detecting and controlling, all-electrically, quite a small number($\sim 10^8$) of the nuclear spins using GaAs nano-scale device [1]. In this paper, we study electron-nuclear spin interaction, probed by resistively-detected NMR spectra, and find that NMR spectra measured in a nano-scale region sensitively depend on the nuclear spin polarization conditions.

Our device has metal split gates deposited on the surface of Hall device to squeeze conducting channel, and, then, we can induce current-driven nuclear spin polarization only in the nano-scale region between the split gates. In our device, although the electron-nuclear spin interaction is based on the degeneracy of different electron spin states, it is observed in a relatively wide magnetic field range, in which electron spin state is changed from unpolarized to polarized through the just degenerate point as the magnetic field increases [2]. This allows us to study under the different nuclear spin polarization conditions. RF pulses applied through a metal antenna gate deposited just above the split gates enable us to perform coherent control of the nuclear spin states, which are detected by change of resistance of the Hall device.

Figure 1 shows pulsed NMR spectra of ^{69}Ga nuclei taken at 5.2 T and 7 T in a dilution refrigerator. We applied π pulses with $\sim$100 µsec duration during the measurements. Three well-resolved peaks due to quadrupolar interaction of Ga nuclei with nuclear spin 3/2 are observed. The peak intensity comes from population difference of the nuclear spins between neighboring two levels. Asymmetric peak intensities indicate that nuclear spin distribution is far apart from thermal equilibrium. Note the electron spins are unpolarized (polarized) at 5.2 T (7 T). By comparing the NMR spectra at 5.2 T and 7 T, we find that relative peak height is opposite. This result indicates that population of the nuclear spins in the nano-scale region is sensitively affected by the nuclear spin polarization conditions.

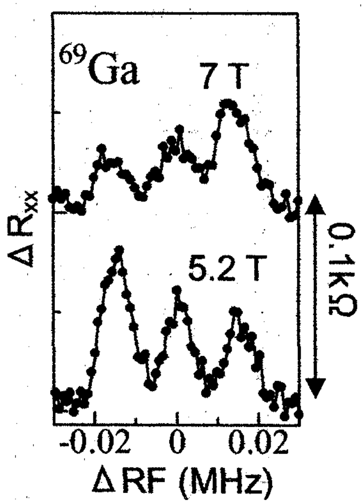

Figure 1
Resistively-detected pulsed NMR spectra of ^{69}Ga at B=5.2 T and 7 T.

[1] G. Yusa et al., Nature **434**, 1001 (2005), [2] K. Hashimoto et al., Phys. Rev. B **69**, 153306 (2004)

ALL9

Structure, Function and Dynamics of a Novel *Helicobacter pylori* Response Regulator Protein

Weontae Lee

Department of Biochemistry and Biomolecular NMR Labortory, Yonsei University, Seoul 120-749, Korea

Helicobacter pylori, one of the most common gram-negative bacterial pathogens in humans, encodes three two-component systems and two orphan response regulators that are involved in transcriptional regulation. Two-component signal transduction systems are modular phosphorelay regulatory pathways common in prokaryotes. RRs are modular proteins, usually composed of a conserved regulatory domain, which act as phosphorylation-activated switches and it is attached DNA binding domain. Response regulator HP1043 in *H. pylori* is proved to be essential for cell growth. HP1043 protein, a member of the OmpR subfamily of RRs, contains a DNA-binding domain, which is called as an effector domain. It was reported that HP1043 binds specifically to its own promoter (P_{1043}), suggesting it involved in auto-regulatory function. Recent reports suggested that *H. pylori* 1043 forms a dimer *in vivo* through N-terminal regulatory domain. We determined HP1043 as a symmetric dimer with two functional domains, an N-terminal regulatory and C-terminal DNA-binding/trans-activation domain. The structure determined by both NMR and X-ray crystallography shows a novel structural feature, differing from those of reported response regulator proteins. Three-dimensional structures showed that the both regulatory and effector domains do not have many inter-domain interaction, suggesting that both domains are relatively independent. The regulatory domain is comprised of α/β sandwich with a central β-sheet and five-parallel strands are wrapped by five α-helices on both sides. DNA-binding domain is composed of three α-helices flanked by anti-parallel β-sheets. Especially, backbone dynamics data indicate that flexibility of DNA binding domain is essential in interacting to DNA. The trans-activation loops known as the DNA binding motif showed very low S^2 and high R_{ex} values. The structural/dynamics information from RDC and backbone dynamics would supply us an insight for molecular/cellular function of a novel response regulator, HP1043.

ALL10

A General Strategy for the Assignment of Aliphatic Side-chain Resonances of Uniformly $^{13}C,^{15}N$-labeled Large Proteins

Yingqi Xu[1], Zhi Lin[1], Chien Ho[2], Daiwen Yang[1]
[1]Department of Biological Sciences, National University of Singapore, 14 Science Drive 4, Singapore 117543
[2]Department of Biological Sciences, Carnegie Mellon University, Pittsburgh, PA 15213

For proteins smaller than 25 kDa, backbone and side chain assignments can be obtained using uniformly $^{13}C,^{15}N$-labeled proteins with triple resonance experiments. Thus structure determination by NMR is very suitable for this type of small proteins. The same methods may fail, however, when applied to proteins larger than 30 kDa due to increased transverse relaxation rates. A combination of deuteration, specific labeling and TROSY techniques provide a solution to structure determination of large proteins. However, preparation of specially labeled samples is always costly and time-consuming, and may not be suitable for every protein. In order to obtain 3D protein structures with a reasonable resolution, it is necessary to constrain side-chains of all or most residues using NOEs among protons located at side-chains. This implies that complete or partial protonation at most side-chains is inevitable.

Here, we present a general strategy to assign side-chain resonances of all residues in uniformly $^{13}C,^{15}N$-labeled large proteins, which makes use of 4D-$^{13}C,^{15}N$-edited NOESY and prior assignment of backbone. Although most triple resonance experiments involving both ^{13}C and ^{15}N spins have very poor sensitivity for protonated large proteins, NOESY experiments are still sensitive enough to provide through-space correlations. H^{α} and H^{β} can be assigned from intra-residue or sequential HC-NH NOEs, provided that these NOEs are possibly differentiated from other inter-residue NOEs on the basis of prior assignment of H^N, N, C^{α}, and C^{β} spins. Otherwise, ambiguities in assignment can be resolved using both intra-residue and sequential NH-CH NOE correlations. If the ambiguity in assignment cannot be resolved due to a lack of sequential or intra-residue NOEs, an MQ-(H)CCH-TOCSY (1) experiment can be applied to confirm the assignment. Assignments of protons at γ, δ, and ε positions are much more challenging using the 4D $^{13}C,^{15}N$-edited NOESY since the chemical shifts of carbon spins at these positions are not available. Many H^{γ}s and some H^{δ}s give rise to both intra-residue and sequential NH-CH NOEs and thus can be assigned from the NOESY spectrum. The remaining unassigned spins can be assigned using the MQ-(H)CCH-TOCSY and 4D NOESY experiments. The strategy has been tested on a 214 residue protein (DdCAD-1) and applied to a maltose binding protein (MBP, 42 kDa) and a chain-selectively $^{13}C,^{15}N$-labeled hemoglobin (65 kDa). About 96%, 85% and 80% aliphatic side-chain spins in DdCAD-1, MBP and hemoglobin have been assigned, respectively. The strategy proposed here will be very useful for the structure determination and dynamics characterization of large proteins by NMR.

1. D. W. Yang, Y. Zheng, D. Liu & D. F. Wyss, *J. Am. Chem. Soc.* 126, 3710 (2004).

ALS20

Solution Structure of the Plant Defensin VrD1 from Mung bean: A Possible Mechanism for Insecticidal Activity Against Bruchids

Yaw-Jen Liu[1] and Ping-Chiang Lyu[1, 2]*

[1]*Department of Life Sciences,* [2]*Institute of Bioinformatics and Structural Biology, National Tsing Hua University, Hsinchu, Taiwan*

Vigna radiate plant defensin 1 (VrD1) is the first reported plant defensin exhibiting *in vitro* insecticidal activity against bruchids. We report here the NMR solution structure of VrD1 and the implication on its insecticidal activity. The root-mean-square deviation values are 0.51 ± 0.35 Å and 1.23 ± 0.29 Å for backbone and all heavy atoms, respectively. The VrD1 structure comprises a 3_{10} helix, an α-helix, and a triple-stranded anti-parallel β-sheet stabilized by four disulfide bonds, forming a typical cysteine-stabilized αβ motif. Among plant defensins of known structure, VrD1 is the first to contain a 3_{10} helix. Glutamate^{26} is highly conserved among defensins; VrD1 contains an arginine at this position, which may induce a shift in the orientation of Trp^{10}, thereby promoting the formation of this 3_{10} helix. Moreover, VrD1 inhibits *Tenebrio molitor* α-amylase. α-amylase plays an essential role in the digestion of plant starch in the insect gut, and expression of the common bean α-amylase inhibitor 1 in transgenic pea imparts complete resistance against bruchids. These results imply that VrD1 insecticidal activity has its basis in the inhibition of a polysaccharide hydrolase. Sequence and structural comparisons between two groups of plant defensins having different specificity toward insect α-amylase reveal that the loop between β2 and β3 is the probable binding site for the α-amylase. Computational docking experiments were used to study VrD1- α-amylase interactions, and these results provide information that may be used to improve the insecticidal activity of VrD1.

ALS21

Chelerythrine binds at the BH groove of Bcl_{XL}, inhibiting its pro-survival activity by more than one mechanism

Yong-Hong Zhang[1], Mei Chin Lee[2], Kah Fei Wan[2], Shing-Leng Chan[2], Yu Chen Yang[3], Anirban Bhunia[1], Victor C. Yu[2] and Yu-Keung Mok[1]

[1]Department of Biological Sciences, National University of Singapore, Singapore 117543
[2]Institute of Molecular and Cell Biology, 61 Biopolis Drive (Proteos), Singapore 138673
[3]Bioinformatics Institute, 30 Biopolis Street, #07-01 Matrix, Singapore 138671

Chelerythrine inhibits the Bcl_{XL}-Bak Bcl-2 homology 3 (BH3) peptide binding and displaces Bax, a BH3-containing protein, from Bcl_{XL}. Bcl_{XL} over-expressing cells that are completely resistant to apoptotic stimuli remain sensitive to chelerythrine. Using NMR, computer docking and site-directed mutagenesis, we show here that chelerythrine binds at the BH groove of Bcl_{XL}, adjacent to BH3 binding cleft which most other Bcl_{XL} inhibitors target. Mutations at the BH groove but not the BH3 binding cleft significantly reduced chelerythrine binding on Bcl_{XL} based on chemical shift perturbation by NMR titration. The abilities of chelerythrine to displace bound BH3 peptide from Bcl_{XL} is also affected by mutations at the BH groove. Other than residues on the BH groove and BH3 binding cleft, surprisingly, we also noticed that certain residues on the long flexible loop between helices α1 and α2 of Bcl_{XL} also have their chemical shifts perturbed by chelerythrine binding. The ability of chelerythrine to induce apoptosis in SH-SY5Y cells expressing Bcl_{XL} with truncated flexible loop is seriously hampered compared to wild type Bcl_{XL}. This could yet represent another inhibitory mechanism of chelerythrine on Bcl_{XL} as this flexible loop is a potential regulatory site for the pro-survival activity of Bcl_{XL}.

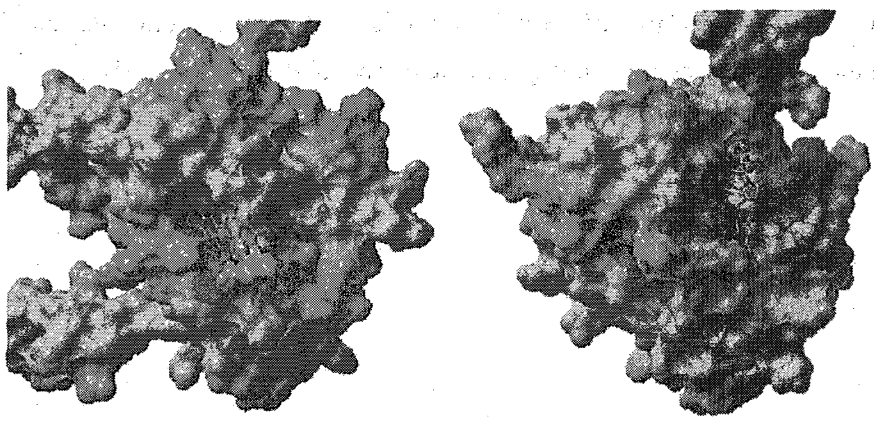

Molecular surface of Bcl_{XL} showing the binding sites of (a) chelerythrine on BH groove and (b) BH3I-1 on BH3 binding cleft. The residues that are essential for binding of chelerythrine on Bcl_{XL} are colored red (Y173) and blue (V135), while the ones for BH3I-1 are colored yellow (R100), green (R139) and purple (L130).

BLL7

Structure and dynamics of biologically active peptides and proteins bound to magnetically oriented vesicle systems as studied by solid-state NMR

Akira Naito
Graduate School of Engineering, Yokohama National University
79-5 Tokiwadai, Hodogaya-ku, Yokohama 240-8501, Japan

Spontaneously oriented bilayer system such as magnetically oriented vesicle system (MOVS) is shown to be an excellent media to study structure and orientation of membrane associated peptides and proteins.

Morphological changes of lecithin bilayers containing melittin around the gel-to-liquid crystalline phase transition temperature (tc) were examined by a solid-state NMR. Magnetic alignments were observed by solid-state ^{31}P NMR spectra for the melittin-lecithin vesicles at a temperature above the Tc by forming elongated vesicles (1). Using the magnetically oriented vesicle systems (MOVS), dynamic structures of melittin bound to the membranes were investigated by analyzing the ^{13}C anisotropic and isotropic chemical shifts of selectively ^{13}C-labeled carbonyl carbons of melittin at the static and magic-angle spinning conditions (2). These results indicate that melittin molecules adopt an α–helical structure and laterally diffuse to rotate rapidly around the membrane normal with tilt angles of the N-terminal helices being –34° and that of the C-terminal helices being 23°. The rotational-echo double-resonance method was used to measure the interatomic distance between [1-^{13}C]Val^{8} and [^{15}N]Leu^{13} to further identify the bending α-helical angles of 122° in the membrane. These structures further lead that the α–helices of melittin molecule penetrate the hydrophobic cores of the bilayers incompletely as a pseudo-trans-membrane structure and induce fusion and disruption of vesicles.

MOVS induced by dynorphin was successfully used to investigate the orientation of dynorphin bound to the lipid bilayers(3). It was found that dynorphin adopts an α–helical structure in the N-terminus from Gly^{2} to Leu^{5} by analyses of the isotropic chemical shifts obtained from the MAS experiments. In contrast, it adopts disordered conformations from the center to the C-terminus and is located on the membrane surface. It was further revealed that the N-terminal α–helix is inserted into the membrane with the tilt angle of 21° to the bilayer normal.

[References]

(1) A. Naito, T. Nagao, K. Nihimura, T. Mizuno, S. Tuzi, H. Saito, Biophys. J. 78, 2405 (2000).
(2) S. Toraya, K. Nishimura, and A. Naito, Biophys. J. 87, 3323 (2004).
(3) T. Uezono, S. Toraya, M. Obata, K. Nishimura, S. Tuzi, H. Saito, A. Naito, J. Mol. Struct. 749, 13 (2005).

BLS23

Development of modulated rf sequences for decoupling and recoupling of nuclear spin interactions in sample-spinning solid-state NMR

Yusuke Nishiyama[1], Toshio Yamazaki[1], and Takehiko Terao[2]

[1]RIKEN Genomic Sciences Center, Tsurumi, Yokohama, Kanagawa, 230-0045 Japan

[2]Department of Chemistry, Graduate School of Science, Kyoto University, Kyoto, 606-8502 Japan

An approach to design modulated rf sequences under sample spinning which decouple/recouple a specific nuclear spin interaction in solid state NMR is presented. The Euler angles of the spin rotation caused by a general rf field are forced to fulfill the symmetry principle theory for selecting an interaction of interest. The allowed Euler angles are expressed by using Fourier expansion. Then, modulated rf sequences are directly obtained from the Euler angles with a large degree of freedom of the Fourier coefficients. Rf sequences with high performance can be selected among them by numerically optimizing the Fourier coefficients. We develop amplitude- and phase-modulated rf sequences according to the present approach, chemical shift anisotropy recoupling sequence (Fig. 1a), double quantum homonuclear dipolar recoupling sequence (Fig. 1b), zero field NMR in high field (Fig. 1c) etc. The details will be given in the presentation.

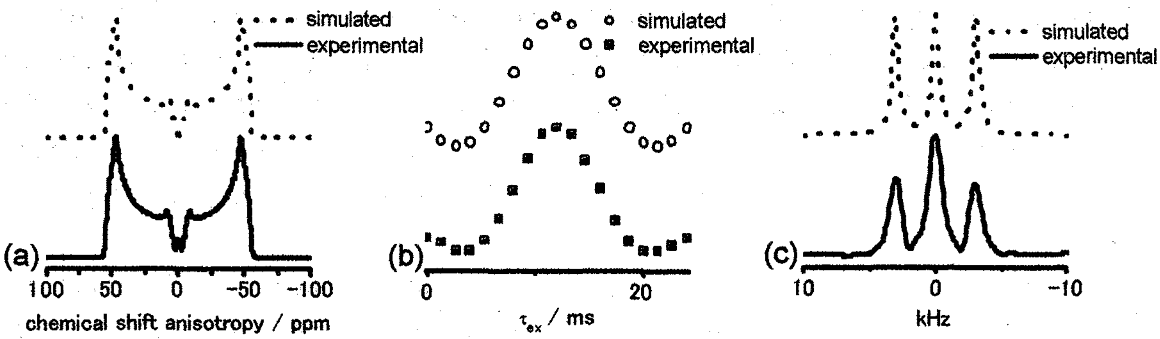

Fig.1 ^{15}N chemical shift anisotropy recoupled spectra of [^{15}N]-*N*-acetyl-D,L-alanine (simulated: (63.5, 85.5, 227.2) ppm) (a), ^{13}C double-quantum constant time build up curves of 10% α,α'-$^{13}C_2$ ammonium phthalate (simulated: 3.00Å) (b), and 13C zero-field NMR in high field spectra of 5% 2,3-$^{13}C_2$ ammonium succinate (simulated: 1.55Å) (c).

BLS24

Efficient Spin-Spin Scalar Coupling Mediated ^{13}C-^{13}C Polarization Transfer in Solid-State NMR Spectroscopy

Yun Mou, John C. H. Chao and Jerry C. C. Chan

Department of Chemistry, National Taiwan University,
No. 1, Section 4, Roosevelt Road, Taipei, Taiwan.

We demonstrate a solid-state NMR technique, with the acronym R-TOBSY, can be used to realize an efficient C' ↔ C_α transfer based on J-coupling under fast magic-angle spinning condition. No ^1H decoupling is required during the polarization transfer period. Experimental results are presented for model crystalline compounds as well as a non-crystalline 17-residue polypeptide MB(*i*+4)EK. Measurements on MB(*i*+4)EK demonstrate that 53 % of the initial C' polarization was transferred to the cross peaks at 7.05 T under 25 kHz MAS spinning.

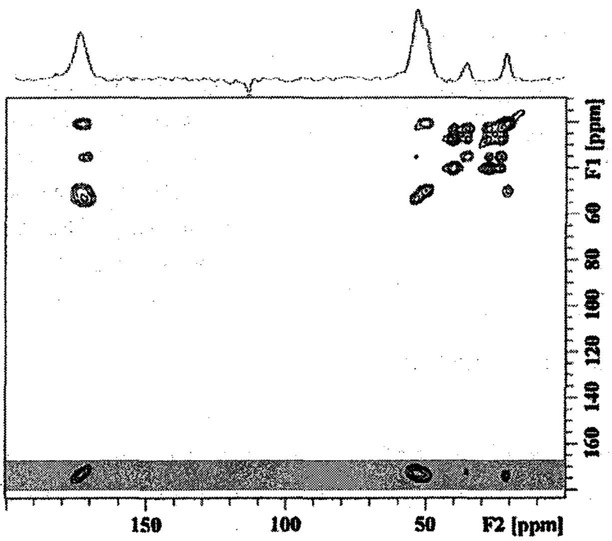

BLS25

Determination of a spin diffusion constant by triplet-DNP

Akinori Kagawa[1] and ○Kazuyuki Takeda[1]
[1]*Graduate School of Engineering Science, Osaka University, Japan*

A new approach is presented to determine a spin diffusion constant by means of triplet-DNP, i.e., dynamic nuclear polarization (DNP) using electron spins in the photo-excited triplet state[1, 2]. In molecular crystal doped with a small amount of guest molecules photo-excitable to the triplet state, large polarization of the electron spins in the photo-excited triplet state, created by pulsed laser irradiation, is transferred to the surrounding protons by applying microwave irradiation at the electron spin. Since the electron polarization can directly be transferred to only those protons which happen to be adjacent to the triplet electrons, the limited regions surrounding the guest molecules serve as sources of polarization, and it is in turn transported away by spin diffusion. And since the triplet-DNP sequence is repeatable with arbitral rates as long as the repetition-time interval is longer than the lifetime of the triplet state, the amount of polarization created at the sources is experimentally controllable.

For the low repetition rates, spin diffusion has a sufficiently long repetition-time interval to flatten the inhomogeneous profile of polarization. Thus, the buildup rate of overall proton magnetization is proportional to the DNP repetition rate. As increasing the repetition rate, on the other hand, the buildup rate begins to saturate as the polarization being created by DNP at the sources outweighs the transport capacity of spin diffusion, and eventually cease to increase with the repetition rate above a certain threshold determined by the spin diffusion constant. Hence, one can extract the spin diffusion constant from measurement of the buildup rate for various repetition rates of the triplet-DNP sequence. We demonstrate determination of a proton spin diffusion constant of an exceedingly diluted proton system in a single crystal sample of pentancene-doped 99.2%-deuterated naphthalene. This work provides another one of very few examples of experimental determination of a spin diffusion constant.

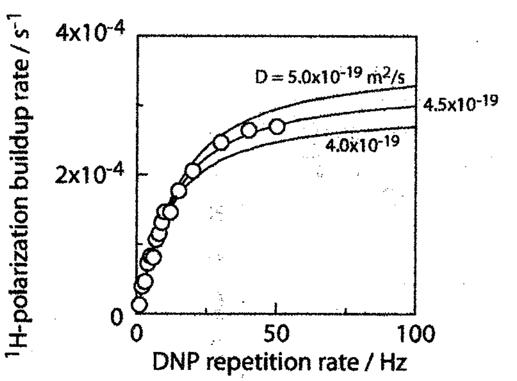

Fig.1. Circles: experimental DNP-repetition rate dependence of the buildup rate of proton polarization in a single crystal sample of pentacene-doped 99.2%-deuterated naphthalene. Solid lines: calculated profiles of the repetition rate dependence for spin diffusion constants of 5.0×10^{-19}, 4.5×10^{-19}, and 4.0×10^{-19} m^2/s, respectively.

Acknowledgment
The experiments were carried out at Molecular Chemical Physics Laboratory at Kyoto University, and we thank Prof. T. Terao and Prof. K. Takegoshi for their support.

[1] K. Takeda, K. Takegoshi, T. Terao, J. Phys. Soc. Japan 73 (2004) 2313.
[2] K. Takeda, K. Takegoshi, T. Terao, J. Phys. Soc. Japan 73 (2004) 2319.

BLS26

ESR Detected by Measuring Mechanical Forces of a Cantilever in Samples of Low Spin Concentration

SangGap Lee[a], Sun Ho Won, Seung-Bo Saun, Soonchil Lee and Ki-Woong Kim[b]

Department of Physics, Korea Advanced Institute of Science and Technology, 373-1 Guseong-dong, Yuseong-gu, Daejeon 305-701, Korea

Measuring mechanical forces of very soft cantilevers coupled to magnetic resonance, so called magnetic resonance force microscopy (MRFM), is a novel technique recommended for imaging a single molecule by magnetic resonance and for reading spin states in solid-state quantum computing. Moreover, MRFM is quite adequate for studying materials of a limited number of spins because signal-to-noise ratio (SNR) of MRFM is determined not by the number of spins but by a spin concentration. Our group reported on a room temperature force-detected ESR signal from a DPPH sample, the SNR of which was 10 or so [1]. Recently, we built a low temperature (~ 4 K) MRFM setup for magnetic resonance study of thin films. To date we have been improving force sensitivity of our low temperature MRFM apparatus and applying it to low spin concentration samples such as P-doped Si or high-k gate dielectric materials. We will report our progress in our MRFM instrumentation and discuss the preliminary data acquired from the low spin concentration samples. [1] Ki-Woong Kim *et al.*, *Sae Mulli* (The Korean Physical Society) 43, 114 (2001, in Korean)

---

[a]Electronic mail: leesg@kaist.ac.kr

[b]Present address: Korea Research Institute of Standards and Science, Daejeon 305-340, Korea

PLL3

Developments in Single-Scan Multidimensional NMR and MRI

Lucio Frydman

Department of Chemical Physics, Weizmann Institute of Science, 76100 Rehovot, Israel

We have recently introduced a scheme enabling the acquisition complete of multidimensional NMR data within a single continuous acquisition. Provided that an analyte's signal is sufficiently strong, the acquisition time of multidimensional NMR experiments can thus be shortened by several orders of magnitude. The new methodology is compatible with existing multidimensional pulse sequences (COSY, TOCSY, HSQC, imaging) and can be implemented using conventional hardware. The manner by which the spatial encoding of the NMR interactions –which is the new principle underlying ultrafast NMR protocols– proceeds in these experiments, will be discussed. Practical implementation of the protocol and its performance will also be exemplified with a variety of homonuclear and heteronuclear nD NMR and MRI acquisitions on chemical, biochemical and biological systems, carried out within a 0.1-1 s time scale.

ALL11

Experimental Frontiers of Solid State NMR

A. Samoson, R. Stern, I. Heinmaa, T. Tuherm
National Institute of Chemical Physics and Biophysics
Akadeemia Tee 23,
Tallinn 12618
ESTONIA

High performance technical ceramic materials sustain tensile stregth that allows about 90 Hzm for product of rotation frequency and rotor diameter. Reduction of the rotor size enables thus higher rotation frequencies and opens a perspective for investigation of new NMR phenomena.
We present some examples of relaxation, decoupling and recoupling at spinning speeds up to 70 kHz.
A possibility of efficient cooling is another advantage of rotor scaling. The cryoMAS(TM NICPB) opens new venues for solving solid state physics problems, e.g. refine J couplings in spin gap materials.

ALS22

Avance^{II} - A Versatile NMR Spectrometer

Markus Wälchli
Bruker – BioSpin Japan

Over more than a decade Bruker has been pioneering the digitalization of NMR systems. Starting with the digital lock in 1992, continuing with digital filters, digital quadrature detection and digital single chip pulse generation. With the Avance^{II} a second generation digital receiver system has been introduced, combining low noise and broadbandedness in one unit. A higher intermediary frequency ensures interference-free data acquisition.

On the probehead side the development of a variety of CryoProbes^{TM} has been most important in the field of biological applications. Improved high field solids probes also have an impact in this field.

Simple, automated and demanding experiments can easily be performed.

ALS23

Processing Strategies in Radial NMR Spectroscopy

Ēriks Kupče

Varian Ltd., 28 Manor Rd., Walton-on-Thames, UK

A three-dimensional NMR spectrum is mainly space, dotted with discrete bright responses, rather like the sky at night. By viewing plane projections at a few well-chosen orientations, we can reconstruct the entire spectrum. New reconstruction algorithms are examined and the projection-reconstruction technique is compared with alternative fast multidimensional methods.

References.

[1] Kupče, Ē. and Freeman, R., *J. Biomol. NMR*, **27,** 101–113, (2003).
[2] Kupče, Ē. and Freeman, R., *J. Amer. Chem. Soc.*, **126,** 6429–6440, (2004).

ALS24

3D ESR-MRI with Sub-Micrometer Resolution Using Magnetic Resonance Force Microscopy

Yohsuke YOSHINARI[1,2] and Shigenori TSUJI[1,2]
1. Advanced Technology Division, JEOL Ltd., 3-1-2 Musashino, Akishima, Tokyo 196-8558, Japan.
2. CREST, Japan Science and Technology Agency, Kawaguchi, Saitama 332-0012, Japan.

Magnetic resonance imaging (MRI) is very useful spectroscopy to visualize 3D real structures inside samples non-invasively. Low sensitivity of the conventional inductive detection of magnetic resonance phenomena however limits the spatial resolution by a few tens to hundreds micrometers in the typical setup. Magnetic resonance force microscopy (MRFM) [1], a promising MRI spectrometer combined with an atomic force microscopy technology, employs a mechanical detection of magnetic resonance, which is expected to improve the sensitivity dramatically over the inductive method. Indeed, Rugar and co-workers recently demonstrated the capability of detecting a single spin in the irradiated vitreous silica containing a low density of unpaired electron spins [2]. We have been making an effort to improve imaging technique of MRFM with the aim of visualizing nanoscopic structures and investigating functions of local systems inside a biological cell.

In this talk, we will report an application of ESR-MRFM to two practical samples: ~10 μm DPPH particles and ~20 μm liposome labeled by a nitroxide imaging agent; whose sizes are nearly the same size as that of human cell. The sample was fixed on a mechanical detector, so called cantilever typically used for atomic force microscopes, and loaded into our MRFM probe situated in vacuum of ~10^{-3} Pa at room temperature. A small and sharp tip made of a rare-earth permanent magnet placed in the vicinity of the sample was used to generate not only a static magnetic field but also a strong magnetic field gradient (8000 T/m) inside the sample. This field gradient plays an important role to define a very thin sensitive slice only in which the magnetic resonance condition is satisfied at the fixed resonant frequency. The cyclically saturated magnetization of spins in the slice by the magnetic resonance technique causes an oscillating force given by a product of the field gradient and the magnetization, which then vibrates the cantilever. The 3D image and the 2D cross section of the spin density maps in sub-micrometer resolution were reconstructed from the force distribution obtained by scanning the tip position relative to the sample [3,4].

[1] J.A.Sidles, Appl. Phys. Lett. **58** (1991) 2854-2856
[2] D.Rugar, R.Budakianm, H.J.Mamin and B.W.Chui, Nature **430** (2004) 329-332
[3] S.Tsuji, T.Masumizu and Y.Yoshinari, J.Magn.Reson. **167** (2004) 211-220
[4] S.Tsuji, Y.Yoshinari, H.S.Park and D.Shindo, submitted to J.Magn.Reson.

Poster Presentations

November 8(Tue)	17:00 – 18:30	NP(even number) + AP(even number)
November 9(Wed)	13:30 – 15:00	NP(odd number)+AP(odd number)
November 10(Thu)	13:30 – 15:00	AP(even number)+NP(even number)
November 11(Fri)	14:45 – 16:15	AP(odd number)+NP(odd number)

NP1

Separation of each component in which has very close molecular weight in the DOSY method

Satoshi Sakurai
JEOL Ltd., 3-1-2 Musashino, Akishima, Tokyo

The DOSY (Diffusion-ordered NMR spectroscopy) method has received much attention as a technique for separating NMR spectra in a mixed sample using the difference of the self-diffusion coefficient. Generally, it is thought that a diffusion coefficient and a molecular weight have close correlation. For this reason, we have not applied the DOSY method to the separation of a mixed sample in which each component has very close molecular weight. However, we confirmed the DOSY method is actually effective in such a mixed sample as shown below.

(Experiments)

We used the mixed sample of estrone and β-estradiol solved in DMSO-d_6. We performed the measurement by JNM-ECX400 and the DOSY processing by Delta software.

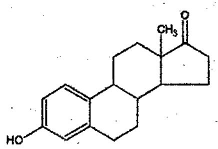

estrone
(M.W. = 270.37)

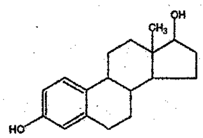

β-estradiol
(M.W. = 272.38)

(Results)

Since β-estradiol has two hydroxyl groups, so it has stronger hydrogen bonds with the solvent DMSO than estrone. It is the reason why they have a difference of diffusion coefficients. So we could separate the spectra from mixed sample in which each component has very close molecular weight by new DOSY processing function of Delta software.

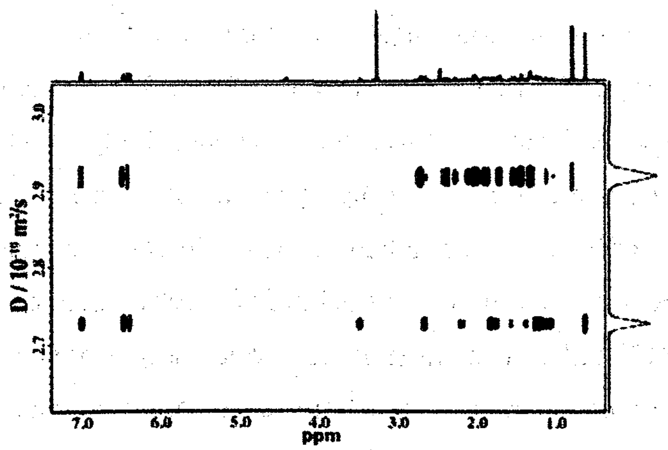

^{1}H DOSY-spectrum of estrone and β-estradiol

NP2 (PL10)

NDSB improves protein solution NMR spectra by suppressing protein aggregation

Takeshi Ishii, Takuya Miyakawa, Kazuo Hosoda, Yasuko Iizuka, Kaori Wakamatsu, Hiroyuki Kogure, Kenji Kubota

Department of Biochemical and Chemical Engineering, Faculty of Engineering, Gunma University, Kiryu, Gunma 376-8515, Japan

In solution NMR, aggregation of proteins (and other macromolecules) increases apparent molecular mass of the solutes, and leads to faster transverse relaxation rates (broader line widths) and lower signal intensities, which make spectrum analysis difficult. The aggregation of proteins is often accompanied by precipitation and denaturation of proteins, which decreases sample concentration and lowers the physiological significance of the NMR data, respectively. Thus the monodispersive nature of protein molecules in solution is quite important in protein NMR measurements, especially in multidimensional ones which require long measuring time. The monodispersive, non-aggregating conditions are usually set up by the screening of buffer conditions (the kind of buffers, pH, salt concentration, and temperature), e.g., by button tests. Despite such extensive screening, it is not rare to fail to find appropriate conditions under which protein molecules are monodispersive for a long time.

Non-detergent sulphobetaines (NDSBs) are a group of small zwitterionic molecules having a hydrophilic sulphobetaine group and a short hydrophobic group. Because of the small size of their hydrophobic groups, they do not form micelles even at a concentration as high as 1 M. NDSBs are known to increase the solubility and stability of proteins and to prevent protein aggregations. Such effects of NDSBs are beneficial in solution NMR measurements, and we previously found that the addition of NDSB-195, the smallest molecule among NDSBs, increases sensitivity of ubiquitin spectra. We also found, by dynamic light scattering measurements, that NDSB-195 decreases the aggregation rates of bovine serum albumin and ovalbumin, that the extent of such anti-aggregating effect varies depending on the kind of NDSBs used, and that a too high concentration of NDSBs rather leads to enhanced protein aggregations. Here we will report the enhancement of qualities of NMR spectra of other proteins by the addition of NDSBs, and the mechanisms whereby NDSBs prevent protein aggregations.

NP3

^{1}H, ^{2}H, ^{13}C, and ^{15}N Full Automatic Pulse Width Calibrations for Cryogenically Cold Probes

Nobuaki Nemoto,[1] Yoshiaki Yamakoshi,[1] Yoshiki Kida,[1] Kaoru Tashiro,[1] Sarara Kannari,[1] Taku Kawahara,[2] Koji Tsubono,[2] Tamio Kanai,[2] Tomomitsu Kurimoto,[1] Katsuo Asakura,[1] and Masami Hosono[1]

[1]JEOL Ltd., 3-1-2 Musashino, Akishima, Tokyo 196-8558
[2]JEOL Datum Ltd., 1156 Nakagami-cho, Akishima, Tokyo 196-0022

We report here ^{1}H, ^{2}H, ^{13}C and ^{15}N full automatic pulse width calibrations prior to multiple nuclear experiments of isotope labeled proteins using cryogenically cold probes. Generally speaking, compared with a probe operating at room temperature, a cryogenically cold probe enhances the sensitivity by a factor of three to four times. Therefore, such cold probes are widely used for structure determination of proteins in solution, because the solubility of proteins is not so high. On the other hand, because larger numbers of pulses are used in multiple nuclear experiments, the accumulation of the inaccuracy of pulse lengths finally causes large amount of signal loss, even if the degree of the inaccuracy of each pulse length would be small. Therefore, it is of utmost importance for optimum results to determine accurate 90° pulse lengths and to use them in actual measurements, even if a very sensitive cryogenically cold probe is used. We developed a tool to help RF setting of multiple nuclear experiments for labeled proteins in solution.[1,2] Since these were originally designed for $^{13}C/^{15}N$ doubly labeled proteins, we expand applications for ^{2}H, ^{13}C and ^{15}N triple labeled proteins using a cryogenically cold probe. 90° pulse lengths of ^{1}H, ^{2}H, ^{13}C and ^{15}N of triply labeled protein solution were successfully obtained with the expanded protocol. This full automatic RF pulse width calibration enables a very simple experimental setting of multiple nuclear experiments including ^{2}H decoupling on a NMR spectrometer with multi DDS/multi sequencer system.[3] We show data acquired using a cryogenically cold probe.

[1]T. Kurimoto et al., *Chem. Lett.*, **34**, 540-541 (2005).
[2]K. Asakura et al., *Chem. Lett.*, **34**, 670-671 (2005).
[3]N. Nemoto et al., *Concepts Magn. Reson. Part-B*, **25B**, 18-26 (2005)

AP4

Two-Dimensional ^{129}Xe- ^{1}H Heteronuclear Overhauser Spectroscopy (HOESY) Using Laser-Polarized ^{129}Xe

Junko Fukutomi,* Yuko Adachi, Hirohiko Imai, Atsuomi Kimura, and Hideaki Fujiwara
Division of Health Sciences, Graduate School of Medicine, Osaka University

Xenon has characteristic profile of hydrophobicity probably coming from many (54) electrons outside the nucleus. Its interaction with organic substances, therefore, is much interested from the standpoint of biochemistry as well as pure chemistry. The intermolecular interactions between ^{129}Xe and ^{1}H could be studied by means of heteronuclear Overhauser effct spectroscopy, but the 2D version (HOESY) of this spectroscopy would be enormously time-consuming because of low xenon sensitivity/concentration and weak ^{129}Xe-^{1}H coupling. In the present work, ^{129}Xe-^{1}H HOESY has been examined by adopting modified HOESY sequence and a hyperpolarizing setup capable of producing a continuous supply of polarized Xe gas for long period of time. To our knowledge, this is the first report of the Xe-^{1}H HOESY experiment, which has been realized by the laser-polarization technique.

Material and Methods: 100% diethyl phthalate ($C_{12}H_{14}O_4$) was used for the test solution. Data were acquired on Varian INOVA 400WB spectrometer (9.4T) while blowing polarized Xe gas intermittently into a sample solution in a 10mm size of probe. The polarization of ^{129}Xe is approximately 8% as checked by comparing the NMR S/N ratio enhancement. Mixing time of 100 msec and number of transients per increment of 32 were used. The temperature was set at 28℃. A pulse sequence is modified so that blowing of the polarized gas is synchronized with the RF pulse irradiation.

Result and Discussion: A 2D ^{129}Xe-^{1}H HOESY spectrum is shown in the figure below. Projected peaks at 1.3, 4.4, and 7.5ppm correspond to ^{1}H in CH_3, CH_2, and phenyl ring, respectively. ^{129}Xe peak at 190.5ppm corresponds to ^{129}Xe in diethyl phthalate. The cross peaks in the HOESY spectrum indicate effective cross relaxation between ^{129}Xe and ^{1}H. By analyzing the time dependence of peak intensities, quantitative extractions of σ and γ can be established between the two nuclei. This technique will offer a characteristic biosensor in analyzing biological materials.

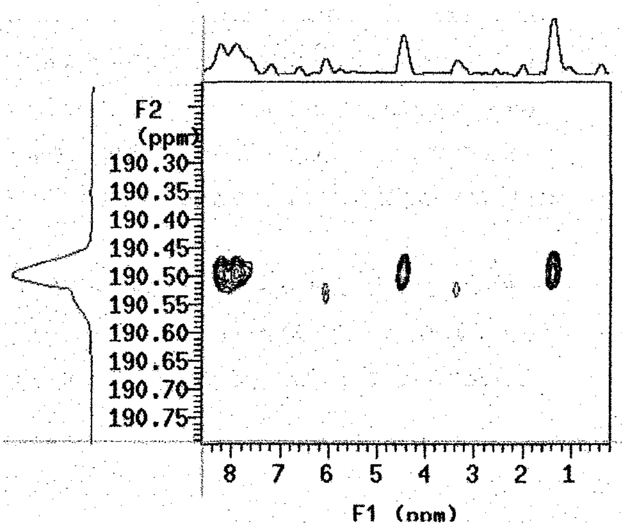

AP5

NMR Studies of Stereo-Array Isotope-Labeled (SAILed) Proteins:
Towards the high-throughput, high-precision structural determinations of larger proteins

Mitsuhiro Takeda[1], Takuya Torizawa[1], Tsutomu Terauchi[1], Akira M. Ono[1], Seiji Tsuchiya[1], Peter Güntert[2] and Masatsune Kainosho[1, 3]
[1]CREST, JST, [2]RIKEN GSC, [3]Graduate School of Science, Tokyo Metropolitan University

We have recently developed the SAIL (Stereo-Array Isotope-Labeling) method for proteins, which allows us to extend the accessible molecular weight limit for structural determinations by NMR. For efficient incorporation of SAILed amino acids, a cell-free synthesis system is essential. We previously found that the N-terminus of target protein synthesized by *E. Coli* cell-free system is non-uniform due to a decreased peptide deformylase (PDF) activity for N-formylmethionine (f-Met). This heterogeneity leads to an observation of two sets of signals in an NMR spectrum, which hampers NMR analysis of the target protein. Therefore, it is essential to establish generally applicable methods to prepare samples with uniform N-terminus.

PDF is a metalloenzyme and its activity is controlled by bound metal ions. We overexpressed recombinant PDF and purified it in buffers containing nickel salt, which is reported to increase the activity of PDF. Characterization of the prepared PDF showed that it has a catalytic activity for the formylated peptide. We applied the PDF to calmodulin (CaM) with non-uniform N-termini. Comparisons of ^{1}H-^{15}N HSQC of the CaM between before and after the PDF-addition showed that signals corresponding to formylated CaM were not detectable after the treatment (See figure). This result showed that the f-Met of CaM was deformylated by the added PDF.

Treatments of other target proteins with the prepared PDF are now in progress. We will provide NMR data acquired from PDF-treated, SAILed proteins.

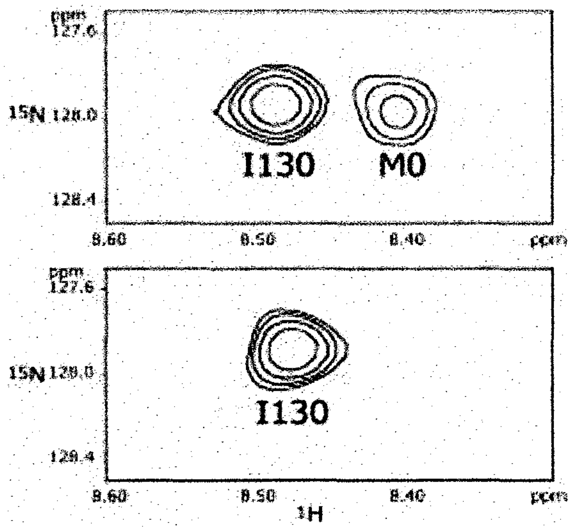

Expanded region of ^{1}H-^{15}N HSQC spectra of CaM before (upper) and after (lower) PDF-treatement.

M0 corresponds to f-Met.

AP6

Rapid acquisition of high resolution triple-resonance spectra using nonlinear sampling and maximum entropy reconstruction

Yoshiki Shigemitsu[1], Takahiro Anzai[1], Markus Wälchli[2] and Yutaka Ito[1,3,4]

[1]Department of Chemistry, Tokyo Metropolitan University, 1-1 Minami-Ohsawa, Hachioji, Tokyo 192-0397, Japan; [2]Bruker Biospin, 3-21-5 Ninomiya, Tsukuba, Ibaraki 305-0051, Japan; [3]Research Group for Bio-supramolecular Structure-Function, RIKEN, 1-7-29 Suehiro-cho, Tsurumi-ku, Yokohama 230-0045, Japan; [4]CREST, JST

NMR spectroscopy is an inherently insensitive technique, and many challenging applications such as protein studies are performed at the very limits of sensitivity and resolution. In addition to the improvements in hardware and pulse sequence technologies, new acquisition schemes for speeding up multidimensional NMR experiments are therefore demanded for dramatic improvements in both sensitivity and resolution.

Nonlinear sampling for indirectly acquired dimensions in combination with maximum entropy reconstruction has been shown to provide significant time savings in the measurement of multidimensional NMR experiments. We have been demonstrating this procedure for obtaining backbone resonance assignments of proteins with low solubility or proteins in living *E. coli* cells. In this presentation, we discuss the efficiency and accuracy of the nonlinear sampling scheme by comparing the spectra with those obtained by using the conventional linear sampling scheme as well as the recently developed projection reconstruction method, which also enables rapid collection of multi-dimensional NMR data.

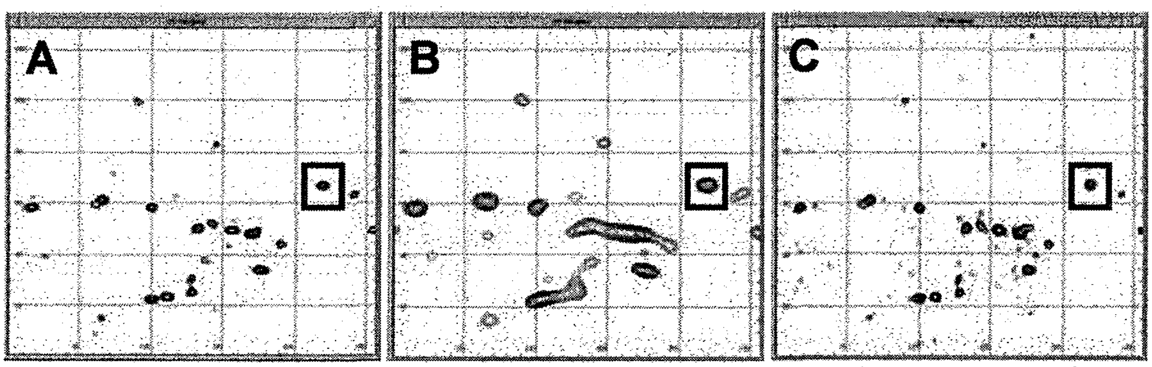

Figure:
2D ($^{13}C'$-$^{1}H^{N}$) slices extracted from 3D HNCO spectra of $^{13}C/^{15}N$-labelled *Thermus thermophilus* RecO (229 a.a., 24.7kDa). (A) 40* (^{13}C, t_1) x 24* (^{15}N, t_2) linear, (B) 10* (^{13}C, t_1) x 12* (^{15}N, t_2) linear and (C) 10* (^{13}C, t_1) x 12* (^{15}N, t_2) nonlinear complex points were collected. The 2D maximum entropy method was used for processing of both t_1 and t_2 dimensions.

AP7

The Study of Inclusion Complex Formation of 4-Sulfothiacalix(4)arene Sodium Salt with Xe by Means of Hyperpolarized ^{129}Xe NMR under Continuous Flow of the Xe Gas

Yuko Adachi*, Akari Kaneko, Junko Fukutomi, Atsuomi Kimura, and Hideaki Fujiwara*
Division of Health Sciences, Graduate School of Medicine, Osaka University

Introduction: Combining with the supply of Xe gas under continuous-flow mode, the hyperpolarized ^{129}Xe NMR can be used to investigate different kind of intermolecular interactions in solution in an extraordinarily high sensitivity with high precision. The inclusion complex formation of 4-Sulfothiacalix(4)arene Sodium salt (STCAS) with Xe has been investigated in the present study using hyperpolarized ^{129}Xe NMR as a diagnostic tool. STCAS is interested among different types of calixarenes because it is water-soluble besides it includes sulfur atoms as the bridging unit.

Materials and Methods: The hyperpolarized ^{129}Xe gas was produced by the continuous-flow type home-build apparatus and was bubbled into the D_2O solution containing STCAS with varying concentrations. ^{129}Xe NMR spectra were recorded on a Varian NMR spectrometer INOVA400WB at 9.4T and at various temperatures. The ^{129}Xe resonance frequency was 110.540 MHz. The method reported last year has been extended to include least squares fit on computer in the analysis of concentration dependence of the ^{129}Xe chemical shift.

Results and Discussion: When inclusion complex is formed according to eq.1 in solution,

$$\mathrm{Xe} + \mathrm{STCAS} \rightleftarrows \mathrm{Xe\text{-}STCAS}, \qquad \text{association constant} = K \qquad [1]$$

concentration dependent ^{129}Xe chemical shift (δ_{calcd}) is calculated as in eq.2,

$$\delta_{calcd} = \frac{\delta_{Xe} + \{K[STCAS]_0/(1+K[Xe])\}\delta_{Xe-STCAS}}{1 + K[STCAS]_0/(1+K[Xe])} \qquad [2]$$

where δ_{Xe} and $\delta_{Xe\text{-}STCAS}$ are the chemical shifts of Xe in the free dissolved state and in the Xe-STCAS complex in water, respectively, and [Xe], [STCAS] and [Xe-STCAS] represent concentrations of Xe, STCAS and Xe-STCAS complex in solution, respectively. Therefore, the association constant K and $\delta_{Xe\text{-}STCAS}$ can be determined by the least squares method so that the calculated concentration dependent ^{129}Xe chemical shift fits well with the observed ones. This was accomplished by using a commercial software ORIGIN from LightStone Co. Also temperature dependent study has given the thermodynamic parameters of the inclusion complex formation thorough the use of the temperature dependent association constants. The observed values of K, ΔH and ΔS are compared with other reported data in Table1.

Table 1 K(at 25 ℃), ΔH and ΔS values for Xe-substance interaction.

substance	K[M^{-1}]	ΔH[kJ/mol]	ΔS[J/K/mol]	solvent
STCAS	14	-12.0	-16.3	water
Metmyoglobin	146	-30.2	-58.7	water
Myoglobin	94	-21.4	-39.2	water
Cyanomyogobin	145	-37.7	-83.8	water
Cryptophane A	3000~(5℃)			$CHCl_2CHCl_2$
α-Cyclodextrin	2.28 (25℃)			DMSO
α-Cyclodextrin	22.9 (25℃)			water

AP8 (PL15)

A novel method for measuring the fast H/D exchange by ^{13}C observed 2D NMR

Kaoru Fujimura[1], Takeshi Tenno[2], Hidehito Tochio[1] and Hidekazu Hiroaki[1]
International Graduate School of Arts and Sciences, Yokohama City University[1]
Graduate School of Engineering, Kyoto University[2]

The H/D exchange experiment of amide protons of proteins provides information on the residues exposed to the solvent. We have developed a novel technique for measuring the exchange rate in a faster time scale that is difficult to determine by the conventional method. We employed a ^{13}C-detected ^{13}CO-^{15}N 2D HMQC to obtain the H/D exchange rates. Chemical shift values of both ^{15}N and ^{13}CO in a peptide bond are affected by the isotope type of its amide hydrogen (^{15}NH or ^{15}ND). When $^{13}C/^{15}N$-doubly labeled proteins are dissolved in 50% D_2O/H_2O buffer and if the amide hydrogen exchange rate with the solvent is slow enough, two cross-peaks representing ^{15}NH or ^{15}ND form would appear for each ^{13}CO-^{15}N pair in the 2D spectrum (Figure 1). The amide hydrogen exchange rates are directly related to the rate of $^{15}NH/^{15}ND$ exchange, and readily obtained by the line shape analysis based on the chemical exchange theory. The concept of this experiment was originally proposed by Kainosho et al., where only 1D NMR was utilized.[1,2) We expand this idea to 2D NMR which enable us to apply to uniformly labeled proteins. The analysis of ubiquitin at various different conditions (pH, temperature) will be presented.

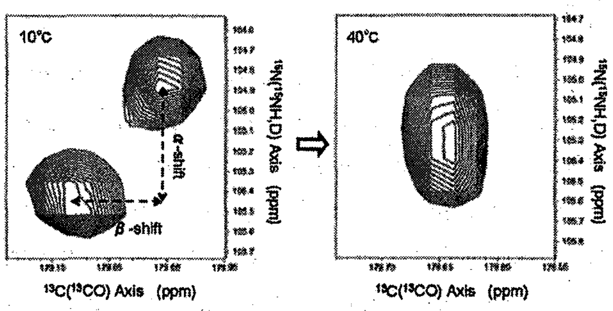

Figure 1. Selected regions of the ^{13}C-detected ^{13}C-^{15}N HMQC spectra of $^{13}C/^{15}N$-doubly labeled ubiquitin in 50% D_2O at 10℃ and 40℃. The increase in the exchange rate brings two cross-peaks closer.

Key Words
H/D amide hydrogen exchange, ^{13}C-detected ^{13}C-^{15}N HMQC, DEALS method

References

1) Kainosho M and Markley J, (1993). *NMR of Macromolecules.* (Edited by D. Rickwood and B. D. Hames), Oxford: IRL Press. Pp.140-152
2) Kainosho M and Nagao H. Biochemistry 26, 1068-1075 (1987)

AP9

Molecular identification of uniformly stable isotope labeled animal cells for a hetero-nuclear NMR-based metabonomics

Michitaka Suto[1], Takashi Nishihara[1] Yuuri Tsuboi[3], Takashi Hirayama[1,2,3,,4] & Jun Kikuchi[1,2,3]

[1]Int. Grad. Sch. Arts Sci., Yokohama City Univ; [2]RIKEN Plant Science Center, [3]RIKEN Plant Mol. Biol. Lab. & [4]CREST, JST

A metabonomics is the study of the quantitative measurement of inter/extrecelluler metabolites for animal cells system. 1D-^{1}H-NMR based approach followed by multivariate analysis to identify differences between clustered data sets in this field. That is to say, this approach can not identify each metabolites because of low signal separation in the 1D-^{1}H-NMR spectra. So, methodological advances for molecular identification are important issue in the metabonomics studies. We achieve better molecular identification using the hetero-nuclear NMR spectra. The key technology for this methodology is uniform stable isotope labeling of animal cells. First, we labeled food (plant) or culture fluid for animal cells with $^{13}CO_2$ or $^{13}C_6$-Glucose. Next, we uniformly labeled animal cells with the food or culture fluid. And we collected the biofluid, celluler extract for the hetero-nuclear NMR studies. While we constructed metabolite standard chemical shift database observed at the same condition as sample measurement. With this database, we assigned the multi-dimensional NMR signals (fig.1). Those are sugars, amino acids and TCA cycle organic acids. Further improvements for uniform stable labeling ratio in animal cells will be discussed in the conference.

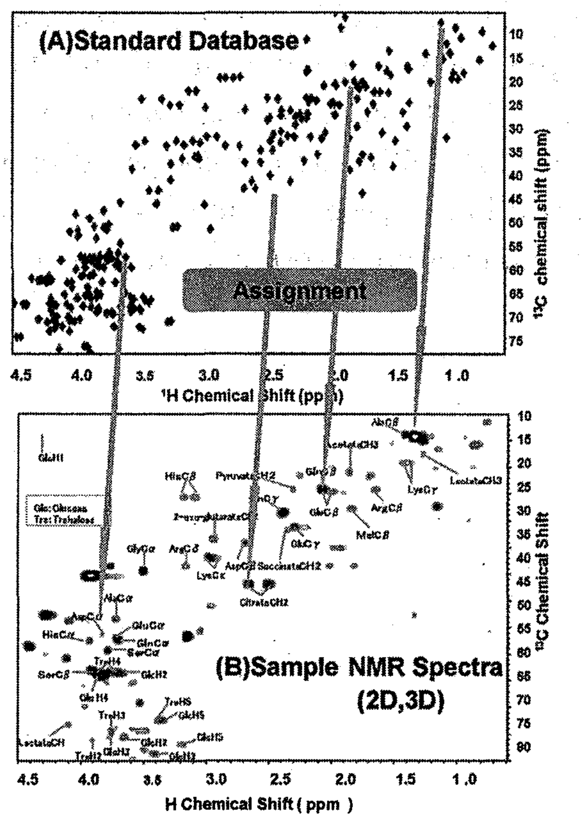

Fig.1 Assignment strategy for a hetero-nuclear NMR-based metabonomics(A) plot of metabolite standard chemical shift assigned in 100 mM-KPi, 10%-D_2O, pH=7, 298 K (B) 2D NMR spectra of biofluid sample

AP10

Noise Suppression of NMR Signal by Piecewise Polynomial Truncated Singular Value Decomposition

Hoshik Won

Department of Applied Chemistry, Hanyang University, Ansan 425-791, Korea

Singular value decomposition (SVD) has been used during past few decades in the advanced NMR data processing and in many applicable areas. A new modified SVD, piecewise polynomial truncated SVD (PPTSVD) was developed for the large solvent peak suppression and noise elimination in NMR signal processing. PPTSVD consists of two algorithms of truncated SVD (TSVD) and L_1 problems. In TSVD, some unwanted large solvent peaks and noises are suppressed with a certain soft threshold value while signal and noise in raw data are resolved and eliminated out in L_1 problem routine. The advantage of the current PPTSVD method compared to many SVD methods is to give the better S/N ratio in spectrum, and less time consuming job that can be applicable to multidimensional NMR data processing.

AP11

Studies of Chemical Shift Anisotropy Shielding Effect in Co(III)-N,N'-Disalicylidene-diaminotoluene Macrocyclic Complexes

Changjun Lee, Hoshik Won

Department of Applied Chemistry, Hanyang University, Ansan 425-791, Korea

In order to study the effect of cobalt atom to the NMR chemical shifts of the ligands in metal complex, six salen-type macrocyclic ligand with three different axial ligands, 2-picoline, 3-picoline, and 4-picoline were used to synthesize octahedral Co(III) complexes. All the synthesized ligands were identified by ^{1}H, ^{13}C-NMR and synthesized Co(III) complexes were then studied with NMR, UV-Vis, X-ray, CV and mass spectrometer for its structure and physicochemical properties. Co(III) ion has strong electrophilicity compensated from axial ligand and strong bonding with equatorial and affecting shifting of NMR chemical shifts. This can be lead to study furthermore to prove how cobalt anisotropic shielding effect can be a factor for NMR chemical shifts. From the calculation using McConnell's equation, methyl groups of 2-picoline and 3-picoline seemed to be shifted downfield whereas .'-, .'- carbons shifted to upfield. Also, .-carbon of all three picolines and carbon of methyl group in 4-picoline shifted downfield.

NP12 (PL9)

^{19}F NMR Study of Myoglobin Bearing a Fluorinated Heme -Dynamics and Thermodynamics of the acid-alkaline transition-

Satoshi Nagao,[1] Yueki Hirai,[1] Shigenori Nagatomo,[1] Hajime Mita,[1] Yasuhiko Yamamoto,[1] and Akihiro Suzuki[2]

[1]*Department of Chemistry, University of Tsukuba, Tsukuba 305-8571*

[2]*Department of Materials Engineering, Nagaoka College of Technology, Nagaoka 940-8532*

Taking advantages of ^{19}F NMR, we have shown that the introduction of ring-fluorinated hemes into hemoproteins provides spectroscopic probes highly sensitive to heme electronic nature which is relevant to functional properties of the proteins.[1,2] In the present study, our technique was applies to characterize dynamics and thermodynamics of a characteristic pH-dependent structure change known as "the acid-alkaline transition" in metmyoglobin (metMb) (Scheme 1).[3]

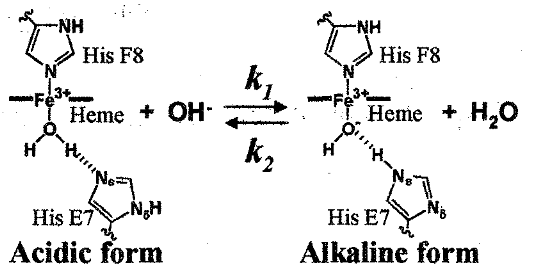

Scheme 1 The acid-alkaline transition in metMb.

In the spectra of metMb reconstituted with 7-PF (Mb(7-PF), Fig. 1), two signals were observed under low and high pH conditions (Fig. 2). Mb(7-PF) exists as a mixture of isomers possessing two heme orientations differing by a 180° rotation about the 5,15-*meso* axis (Fig. 1). Quantitative fitting of their pH-dependent shifts of ^{19}F NMR signals to the Henderson-Hasselbach equation yielded the p*K*a values, which are related to the equilibrium constants, of 8.32 ± 0.03 and 8.62 ± 0.03 for the *N* and *R* forms, respectively. Remarkable pH-dependent line broadening of the introduced CF_3 ^{19}F signal attributable to a fast exchange between the acidic and alkaline forms was observed. From the analysis based on the equation for the fast exchange limit, the reaction rate of $(1.1 \pm 0.2) \times 10^5$ s^{-1} was obtained for the k_2 value of the *R* form, and combined with the p*K*a value, the value of $(2.6 \pm 0.5) \times 10^{10}$ M^{-1} s^{-1} was determined for the k_1 value. The obtained k_2 value was comparable to the exchange rate of histidyl imidazole NH protons fully exposed to the solvent, indicating that the protonation of His E7 $N_\delta H$ associated with the transition is essentially a diffusion-controlled process. Therefore, the k_2 values of the *N* and *R* forms should be similar to each other. Consequently, the difference in the p*K*a value between the two forms is attributed to the k_1 value. This result indicates that the thermodynamic stability of the acidic form is crucial for the dynamics of the transition.

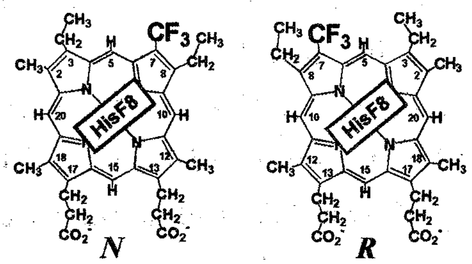

Fig. 1 Structure of 7-PF and two possible orientations of heme relative to His F8 in reconstituted Mb. *N* and *R* represent normal and reversed forms, respectively.

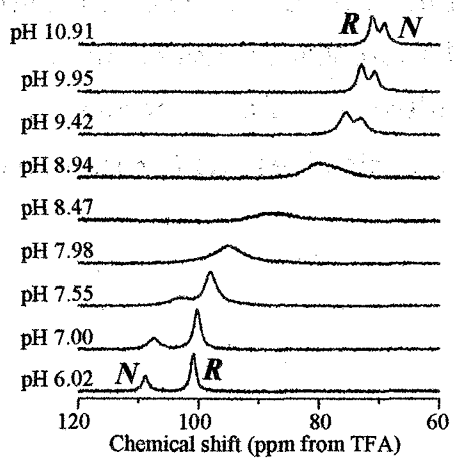

Fig. 2 ^{19}F NMR spectra of metMb(7-PF) at 25°C and the indicated pH values.

References

(1) Yamamoto, Y.; Nagao, S.; Hirai, Y.; Inose, T.; Terui, N.; Mita, H.; Suzuki, A., *J. Biol. Inorg. Chem.* **2004**, 9, 152-160.

(2) Hirai, Y.; Nagao, S.; Mita, H.; Suzuki, A.; Yamamoto, Y., *Bull. Chem. Soc. Jpn.* **2004**, 77, 1485-1486.

(3) Nagao, S.; Hirai, Y.; Suzuki, A.; Yamamoto, Y., *J. Am. Chem. Soc.* **2005**, 127, 4146-4147.

NP13

TRE box Recognition by *Streptomyces* Transcriptional Repressor TraR

Takeshi Tanaka[1], Chieko Komatsu[1], Kuniko Kobayashi[1], Mariko Sugai[1], Masakazu Kataoka[2] and Toshiyuki Kohno[1]

[1]*Mitsubishi Kagaku Institute of Life Sciences (MITILS),* [2]*Department of Environmental Science and Technology, Faculty of Engineering, Shinshu University*

The *traR* gene product, TraR, that regulates the pSN22 conjugation system in *Streptomyces*, is a 27 kDa protein that functions as a transcriptional repressor for the *tra* operon (*traA-traB-spdBs*) and *traR* itself. TraR binds to the dsDNAs including 12 bp consensus sequences, TRE box. The TRE boxes are located within the divergent promoter region for the *tra* operon and *traR*, and regulate their expression negatively. Although all of these regulators (TraR, TraA, TraB and SpdBs) have HTH motifs, their primary structures exhibit little similarity. Thus, it is significant work to determine structure-function relationships of such regulators. Previously, we reported the solution structure of TraR DNA binding domain (TraR100) consisted of winged-HTH motif. By NMR chemical shift perturbation experiment upon DNA complex formation, significant chemical shift changes were observed for residues in the wing region in addition to HTH.

In the present study, we report NMR titration studies of TraR100 with five TRE box sequences of pSN22 plasmid. TraR100 interacts with these TRE box sequences in distinct binding manner, resulted in variety of binding affinity determined by surface plasmon resonance. TraR100 most tightly binds to the promoter region of *tra* operon. These results suggest that preferential repression of *tra* operon is caused by high affinity binding manner of TraR.

NP14

Effect of Input Data on Protein Structure Calculation with Automated NOE Assignment

Aiko Sakurai and Koshi Matsubara
Mitsubishi Chemical Group Science And Technology Research Center, Inc.
Analytical Services Division, Yokohama Laboratory

We examined the effect of the input data, incomplete chemical shift assignments or reduced number of unassigned NOESY peaks, on automated NOE assignment and protein structure calculation with the computer program CYANA. The automated NOE assignment and structure calculation can significantly reduce the time necessary for the manual assignment of NOE spectra in structure determination process. Although the automated NOE assignment module requires almost complete chemical shift assignment, the completeness of the chemical shift assigned experimentally becomes degraded and the signal overlap in NOE spectra becomes severe with the increase in protein molecular weight. We, therefore, have interest in how far the quality of the calculated structure degrades when incomplete chemical shift list or reduced number of NOE peaks are used as input for CYANA. The chemical shift list and NOESY time domain data for the test protein of 132 amino acid residues were downloaded from BMRB, and NOESY spectra were processed with the program NMRPipe and peak-picked with the program NMRView. Structures were calculated with random omission of either proton chemical shifts up to 25% or NOESY peaks up to 50% and compared with the reference structure calculated with the complete chemical shift, NOE peak lists, and backbone torsion angle restraints predicted from chemical shifts with the program TALOS. CYANA yielded structures with root-mean-square deviation (RMSD) of backbone heavy atoms less than 2 Å to the reference structure with the omission of chemical shifts up to 15%. In the case of NOESY peaks, structures with RMSD less than 2 Å to the reference structure were obtained for omission up to 40%.

NP15

Solution Structure and Function of ASABFd18c, Antibacterial Peptide Isolated from a Nematode, *Ascaris suum*

Manabu Nakano[1], Tomoyasu Aizawa[1], Kazunori Miura[2], Hirokazu Hoshino[1], Mitsuhiro Miyazawa[3], Yuusuke Kato[3], Yasuhiro Kumaki[1], Makoto Demura[1], Sakae Tsuda[2], Keiichi Kawano[1], Katsutoshi Nitta[1]
[1]Division of Biological Sciences, Graduate School of Science, Hokkaido Univ.,
[2]National Institute of Advanced Industrial Science and technology,
[3]National Institute of Agrobiological Science

ASABF is antimicrobial peptide consisting of 71 residues and contains 4 intramolecular disulfide bridges derived from the body fluid of the nematode *Ascaris suum*. Our NMR studies have revealed that the secondary structure of ASABF consists of one α-helix, two β-strands with an antiparallel β-sheet and random coil regions. Based on this solution structure, ASABF is likely to be categorized into insect defensin family with Cysteine-Stabilized αβ(CSαβ) motif. C-terminal region of ASABF has flexible region, which complicates the 2D ^{1}H and ^{15}N NMR spectra. This C-terminal region of ASABF is remarkable because the flexible region has not been seen in the other CSαβ type antimicrobial peptide. Therefore we constructed recombinant ASABFd18c (ASABF 1-53) in order to clarify the role of this remarkable region.

In the case of ASABFd18c, the NMR spectra were improved by the dissolution of the congestion of signals from C-terminal residues and the structural convergence. We have determined the solution structure of ASABFd18c and have compared with ASABF. Although ASABFd18c maintains core structure similar to ASABF, ASABFd18c exhibits lower antimicrobial activity as against ASABF.

In the presentation, we will show the residual mobility by NMR relaxation analysis of ^{15}N-labeled peptide and discuss the relationship between function and structure of ASABF.

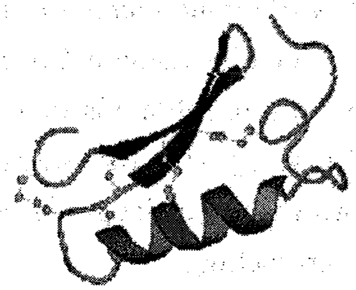

Fig. Solution structure of ASABFd18c
(A ribbon diagram of the structure of the lowest energy.)

NP16

Specific Interaction of Human TRF2 with a G-quadruplex Structure

Yuuka Hirao[1], Tadateru Nishikawa[2], Shingo Hanaoka[2], Hideyasu Okamura[2], Noriyuki Iwasaki[1], Satoko Akashi[1], Mamoru Sato[1] and Yoshifumi Nishimura[1]

[1] Graduate School of Integrated Science, Yokohama City University, 1-7-29, Suehiro-cho, Tsurumi-ku, Yokohama, 230-0045, Japan

[2]Kihara Memorial Yokohama Foundation for the Advancement of Life Sciences, 1-7-29, Suehiro-cho, Tsurumi-ku, Yokohama, 230-0045, Japan

Telomeres are the ends of eukaryotic linear chromosomes. Human telomeres consist of long tandem arrays of a double stranded TTAGGG/CCCTAA sequence followed by a single stranded DNA with a TTAGGG sequence repeatedly at their 3' ends. The double stranded DNA regions of human telomeres are specifically recognized by two proteins, hTRF1 and hTRF2, both of which play an important role in the negative regulation of the elongation of telomeres. It is well known that single stranded DNA containing telomeric sequence could form a four-stranded structure, G-quadruplex. Recently, it has been reported the crystal structures of parallel G-quadruplexes from human telomeric sequences consisting of two TTAGGG repeats in the presence of K^+ ions.

Here, we have found that hTRF2 could bind to a parallel G-quadruplex structure with TTAGGGTTAGGG sequence as well as to the double stranded telomeric DNA. We have measured ^{1}H-^{15}N HSQC spectra of the DNA-binding domain of hTRF2 or hTRF1 by changing the concentrations of the G-quadruplex structure by using NMR spectroscopy. In addition, we have constructed some mutants of hTRF2 and measured ^{1}H-^{15}N HSQC spectra of these mutants with the G-quadruplex structure to confirm specific interaction sites of hTRF2. These results suggested that the DNA-binding domain of hTRF2 interacts with the parallel G-quadruplex structure specifically. The DNA-binding domain of hTRF2 consists of a three helical bundle structure similar to the Myb domain. The second and third helices form a helix-turn-helix variation motif which binds to a double stranded telomeric DNA, while our results suggest that a part of the second helix of the DNA-binding domain of hTRF2 interacts with the G-quadruplex structure and A472 of hTRF2 is particularly involved in this interaction.

NP17

Solution structure of a DNA-binding unit of FMBP-1 from *Bombyx mori*

Shin Saito[1], Daisuke Matsumoto[1], Kyosuke Kawaguchi[1], Takeshi Yamaki[1], Tomoyasu Aizawa[1], Shigeharu Takiya[2], Yasuhiro Kumaki[1], Makoto Demura[1], Katsutoshi Nitta[1] and Keiichi Kawano[1]

[1]*Graduate School of Science,* [2]*Center for Advanced Science and Technology, Hokkaido University, Sapporo 060-0810, Japan*

Fibroin-modulator-binding protein (FMBP)-1 was first detected as a factor bound to intronic and upstream elements of the fibroin heavy chain gene. The DNA-binding region of FMBP-1 consists of four almost homologous tandem repeats (R1, R2, R3 and R4) composed of 23 amino acids, which are named the score and three amino acid peptide repeats (STPR). Interestingly, gene encoding homologous repeats, such as the STPR of FMBP-1, has been found in human, mouse, *Drosophila* and *Caenorhabditis elegans*. However, no three-dimensional structures of the protein domain containing several homologous tandem repeats of 23 amino acids have been established. In this study, the structure of each repeat of DNA-binding domain (STPR) has been determined by NMR and circular dichroism (CD) measurements. It included well-defined helices in N-terminal half (residues 3-10) maintained by a salt bridge that includes the conserved two residues, Glu-1 and Arg-9. In addition, the structure of α helices was stabilized by a hydrogen bond formed between a side chain of the N_{cap} residue, Ser/ Thr 2 and the backbone amide of Gln/ Glu 5.

The CD spectrum of the whole DNA-binding domain was almost identical to sum of the individual spectra. These results suggest that the individual repeats in the whole DNA-binding domain behave independently in terms of conformation and stability. The addition of DNA to the whole DNA-binding domain drastically changed the profile, that is, helices were induced by specific-DNA binding. However, individual spectrum curve in the presence of DNA fragment was not significantly different from that for each peptide alone, suggesting that the transition of the whole DNA-binding domain is cooperatively induced among the individual repeats.

Furthermore, in order to analyze conformational characteristics of the homologous repeats, we prepared a homologous repeat of human, and have carried the CD and NMR experiments. We will discuss the implications of these results.

R1	99	ETSEERAARLAKMSAYAAQRLAN	121
R2	122	ESPEQRATRLKRMSEYAAKRLSS	144
R3	145	ETREQRAIRLARMSAYAARRLAN	167
R4	168	ETPAQRQARLLRMSAYAAKRQAS	190

Sequences of FMBP-1 DNA-binding domain

NP18

NMR studies of the chromo domain from a histone acetyltransferase, Esa1

Hideaki Shimojo[1], Yoshihito Moriwaki[1], Masahiko Okuda[1,2], Masami Horikoshi[3], and Yoshifumi Nishimura[1]
[1]Graduate School of Integrated Science, Yokohama City University, 1-7-29 Suehiro-cho, Tsurumi-ku, Yokohama, 230-0045, Japan
[2]Kihara Memorial Yokohama Foundation for the Advancement of Life Sciences 1-7-29 Suehiro-cho, Tsurumi-ku, Yokohama, 230-0045, Japan
[3]Laboratory of Developmental Biology, Institute of Molecular and Cellular Biosciences, University of Tokyo, 1-1-1 Yayoi, Bunkyo-ku, Tokyo, 113-0032, Japan

In eukaryotic cells DNA is packaged into chromatin, whose structural unit is a nucleosome core that consists of the dimer of four histones, H2A, H2B, H3 and H4. During gene expressions in the eukaryotic cells the structure of chromatin should be remodeled to promote transcription. For example, the acetylations of histones promote the relaxation of chromatin structure and the transcription is promoted by recruiting RNA polymerase II. Although several distinct nuclear histone acethyltransferase, HAT complexes have been isolated from the yeast *Saccharomyces cerevisiae*, only the nucleosome acetylating H4, NuA4 complex is essential for cell growth. The NuA4 complex contains 12 polypeptides including the essential Sas2-related acetyltransferase 1, Esa1 subunit. Esa1 is required for G2/M cell cycle progression. Its targeted recruitment to ribosomal protein promoters is associated with the regulation of ribosomal protein genes in response to growth stimuli. The Esa1 protein is the catalytic subunit of the NuA4 complex and a member of the MYST family of HAT proteins. Esa1 contains an N-terminal chromo domain (41-78 amino acid) that was defined as a region of homology between heterochromatin protein 1, HP1 and Polycomb, Pc, and a C-terminal HAT domain (160-435 amino acid) that retains HAT activity. The chromo domain is a conserved protein fold consisting of about 50 amino acids found in a variety of chromosomal proteins, which are responsible for the transcriptional repression and/or activation. The Esa1 chromo domain plays a major role in Piccolo's ability to distinguish between histones and nucleosomes.

Here, we have determined the solution structure of the Esa1 chromo domain by using NMR. The recombinant Esa1 chromo domain was expressed in E. coli by using a pET-15b system and purified by an affinity chromatography method. For resonance assignment various 3D NMR spectra were obtained. The structure reveals that Esa1 chromo domain forms a strongly bent anti-parallel β-sheet.

NP19

The Effect on the Structure and Activity of Growth-blocking Peptide by C-terminal Elongation with Parasitism

Yoshitaka Umetsu[1], Tomoyasu Aizawa[1], Kaori Muto[2], Hiroko Yamamoto[1], Mineyuki Mizuguchi[2], Makoto Demura[1], Katsutoshi Nitta[1], Yoichi Hayakawa[3], and Keiichi Kawano[1]
[1]Graduate School of Science, Hokkaido University, Sapporo 060-0810, Japan
[2]Faculty of Pharmaceutical Sciences, Toyama Medical and Pharmaceutical University, Toyama 930-0194, Japan
[3]Faculty of Agriculture, Saga University, Honjo-1, Saga 840-8502, Japan

Growth-blocking peptide (GBP) is a 25-amino acid peptide isolated from the lepidopteran insect *Pseudaletia separata* whose development was halted in the last larval instar stage by parasitization with the parasitoid wasp *Cotesia kariyai*. Unexpectedly, it has been reported that GBP is not derived from parasitoid wasp, but rather from the hormone-like peptide of the host armyworm. Subsequent studies have shown that GBP has multiple functions, including stimulation of specific insect immune cells (plasmatocytes), proliferation of various types of cultured cells, and paralysis of larvae. Furthermore cDNA analysis suggested that 23-amino acid GBP (1-23GBP) would be expressed in non-parasitized larvae though 28-amino acid GBP (1-28GBP) would be expressed in parasitized larvae due to translation continue to next stop codon located at nucleotide sequence for 29th amino acid.

In this study, we characterized the GBP analogs, which have various C-terminal lengths by comparison of their bioactivity and stability with three-dimensional structure. The result indicated that 1-28GBP exhibits the strongest activity to suppress the growth of larvae. NMR analysis showed that these peptides had the same tertiary structure in core region. Therefore, the difference in activity is attributed to disordered region located in the C-terminal. We then investigated their interaction with a putative receptor. The results suggested the possibility that the structural change of C-terminal affects their activity.

Fig. The ensemble of the NMR solution Structure of GBP
(The tertiary structure of GBP consists of a well structured core and flexible N and C termini.)

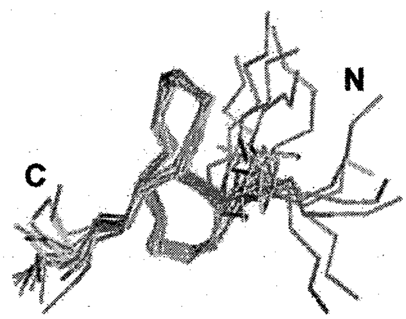

NP20

NMR structural study of a tranasducer protein *p*HtrII

Kokoro Hayashi[1], Yuki Sudo[2], Masaki Mishima[1], Naoki Kamo[2] and Chojiro Kojima[1]
[1]*Laboratory of Biophysics, Graduate School of Biological Science, Nara Institute of Science and Technology, 8916-5 Takayama, Ikoma, Nara 630-0192, Japan and* [2]*Laboratory of Biophysical Chemistry, Graduate School of Pharmaceutical Sciences, Hokkaido University, Sapporo 060-0812, Japan*

*p*HtrII is a two-transmembrane protein from extreme halophile and alkalophilic bacteria, *Natronomonas pharaonis*. It is called transducer protein, and composed of transmembrane region, linker region (that is called HAMP domain), methylation region and signaling region. *p*HtrII interacts with *pharaonis* phoborhodopsin (*p*pR, also called *pharaonis* sensory rhodopsin II, NpsRII). Light signals are transmitted to *p*HtrII through *p*pR, and phosphorylation cascades that modulate flagella motors are activated. The previous studies indicate that linker region of *p*HtrII has an important role in the signal transduction between *p*pR and *p*HtrII. However, this signaling mechanism and the structure of any HAMP domain have not been clear. In this study, we focused on the structure of *p*HtrII linker region to elucidate the signaling mechanism between *p*HtrII and *p*pR.

*p*HtrII(1-159) containing linker region was expressed in *E. coli*, and two trypsin resistant fragments were identified within the linker region of *p*HtrII(1-159) by MALDI-TOF MS and N-terminal sequencing. One of these fragments was *p*HtrII(100-159), and the other was *p*HtrII(100-149). Circular dichroism (CD) spectra showed that they formed α-helix structure. For *p*HtrII(100-149), most of $^{1}H/^{15}N/^{13}C$ backbone signals are assigned. Secondary structure estimated by chemical shifts is consistent with the results of CD spectra. The expression systems of *p*HtrII(100-159) and *p*HtrII(100-149) were prepared, but their structures were different from those of trypsin digested fragments. The α-helix content of *p*HtrII(100-159) was lower, and *p*HtrII(100-149) was random structure. We will discuss about the structural changes of *p*HtrII linker region, on the basis of NMR structural studies of *p*HtrII(100-159) and *p*HtrII(100-149).

NP21

Solution structure and dimerization of rice phytochromeB PAS1 domain

Toshitatsu Kobayashi[1], Masaki Mishima[1], Ryo Tabata[1], Kayo Akagi[2], Nobuya Sakai[2], Etsuko Katoh[2], Makoto Takano[2], Toshimasa Yamazaki[2] and Chojiro Kojima[1]

[1]Graduate School of Biological Sciences, Nara Institute of Science and Technology, 8916-5 Takayama, Ikoma, Nara 630-0101, Japan
[2]National Institute of Agrobiological Sciences, 2-1-2 Kan-non-dai, Tsukuba 305-8602, Japan

The phytochrome photoreceptor family regulates many cellular and developmental responses to light in higher plants. The C-terminal domain of phytochromes, consisting of two PAS domains (PAS1 and PAS2) and one histidine kinase-like domain, plays a crucial role in phytochrome dimerization, translocation from the cytoplasm to the nucleus, and downstream signaling. This C-terminal domain is connected to the photoactive N-terminal domain through a hinge region. Here we present the first atomic-resolution structure of a fragment of phytochrome, PAS1 domain of *Oryza sativa* (rice) phytochrome B, determined by solution NMR. This domain shared structural similarity to the other PAS domains, although one missing β-strand (Bβ) and two extra helices (the N-terminal Helix I and inserted Helix II) were found. The PAS1 domain with the hinge region formed stable homodimer, and the core region of loss-of-function missense mutation (Quail-box) was located on the β-sheet which is the dimer interface. NMR spectra of loss-of-function missense mutants suggest that the structural change of the β-sheet of the PAS1 domain induces hypocotyls elongation under continuous red-light and also inhibits the nuclear translocation. Thus the stable dimer formation or the relative orientation of the β-sheets may be an important factor to maintain the phytochrome function.

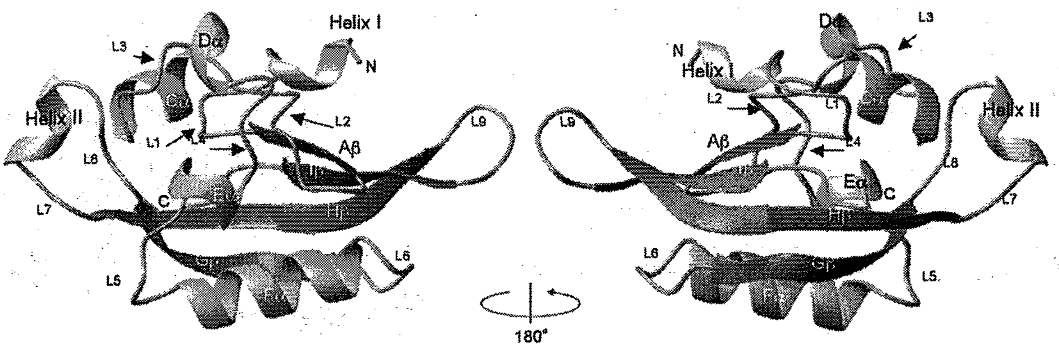

NP22

Dynamic Structure of DNA-binding domain of *E.coli* PhoB

Hideyasu Okamura[1,2], Kozo Makino[3], Yoshihumi Nishimura[1]
[1]Graduate School of Integrated Science, Yokohama City University
[2]Kihara Memorial Yokohama Foundation for the Advancement of Life Sciences
[3]Department of Applied Chemistry, National Defense Academy, Japan

PhoB is a transcriptional factor in the bacterial two-component signal transduction system and is activated under phosphate starvation. PhoB consists of 229 amino acids and contains two functional domains; an N-terminal half is a phosphorylation (receiver) domain and a C-terminal half is a DNA-binding (effector) domain (DBD). PhoB-like transcriptional factors compose a large familiy in bacterial species. Structures of the PhoB DBD in both a DNA-free form and a DNA-complex form already have been determined by NMR and X-ray diffraction. The structure of the PhoB DBD consists of an N-terminal four-stranded b-sheet, a central three-helical bundle and a C-terminal b-hairpin, showing a structural similarity to the winged helix family protein. The second and third helices in the three-helical bundle form a helix-turn-helix variant containing a loop, which is longer than the turn of the classical HTH motif and a putative interaction site for RNA polymerase. The PhoB DBD interacts with a DNA major groove by the third helix and interacts with a DNA minor groove by the C-terminal b-hairpin. However, we have recognized that the solution structure of the PhoB DBD in the free form has variable conformations in its internal hydrophobic core. So far, it has been recognized that much of protein function is strongly correlated with dynamics. Here, we have determined motional parameters for the backbone amide ^{15}N and the sidechain metyl ^{2}H of the PhoB DBD by model-free analysis. The motional parameters of the PhoB DBD show an irregular distribution in the interior of the molecule and it is related to function of the PhoB DBD.

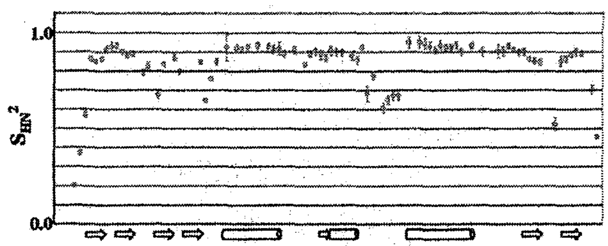

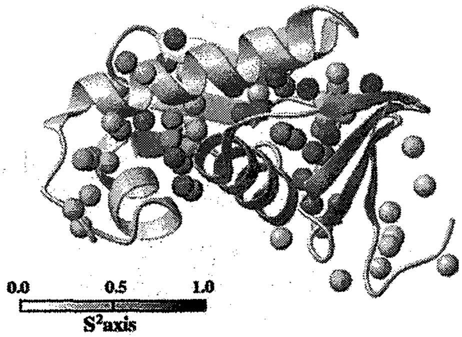

The motional parameters of the PhoB DNA-binding domain

NP23

HSQC Signal Assignment of JSP1 by an effective Method Using Wheat Germ Cell-Free Protein Synthesis System

Akiko Iihara[1], Michiko Kitano[2], Keiko Matsubara[1], Toshiyuki Kohno[2]
[1]ZOEGENE Corporation and [2] Mitsubishi Kagaku Institute of Life Sciences (MITILS)

We have produced an efficiently isotope-labeled JSP1 by inhibiting trans-aminase activities in our wheat germ cell-free protein synthesis system. Using highly effective amino acid selective $^{15}N/^{13}C$ labeled JSP1, we have rapidly assigned HSQC signals of JSP1 to analyze protein-ligand interactions. This assignment technology is very useful for the screening of drug-protein interactions by NMR measurement with a low concentration of protein samples.

Advantages of an Assignment

pink: new method
black: conventional

Sample

Unnecessary highly purified 0.1 – 0.2 mM

Highly purified 1 mM

Measurement

20 different labeled samples 4 kind of two dimensional NMR

4 – 6 kind of three dimensional NMR

Analysis

Simple and easy (1-3 hours without expertise)

Complicated and difficult (2-4 weeks for expert)

Analysis of Interaction

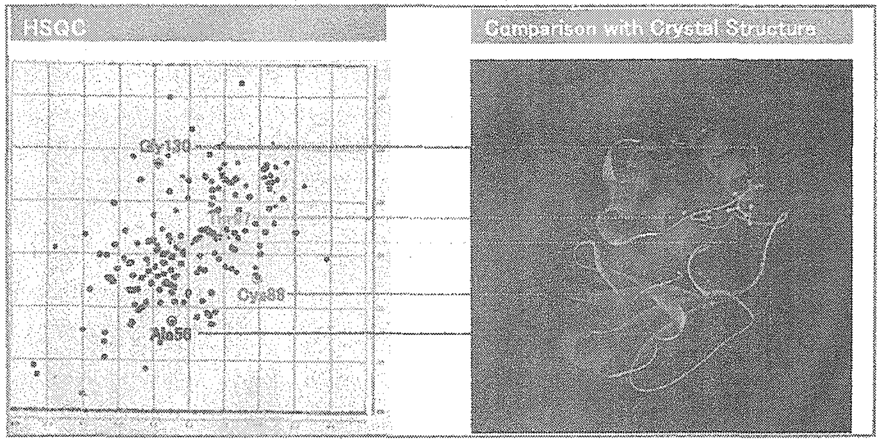

ZOEGENE Corporation 1000, Kamoshida-cho, Aobaku, Yokohama KANAGAWA 227-8502 (in Science & Technology Research Center of Mitsubishi Chemical Corporation) URL http://www.zoegene.co.jp E-mail 6308790@cc.m-kagaku.co.jp

NP24

NMR structure of the PX domain of Bem1p

Atsuhiko Maeda, Kenji Ogura, Masataka Horiuchi, Hiroyuki Kumeta, Yuko Fujioka, Fuyuhiko Inagaki

Department of Structural Biology, Graduate School of Pharmaceutical Sciences, Hokkaido University, Kita 12 Nishi 6, Kita-ku, Sapporo 060-0812, Japan

1. Introduction

The phox homology (PX) domain was identified in a number of different proteins including mammalian p47^{phox}, p40^{phox}, *Saccharomyces cerevisiae* Bem1p, and a variety of proteins involved in membrane trafficking. PX domains are known to recognize specific phosphoinositides. Such interaction plays a crucial role in recruiting proteins to appropriate sites in cell membranes. The yeast protein Bem1p, important for bud emergence, consists of tandem SH3 domains, PX domain and PB1 domain from N-terminus. Bem1p can bind to many signaling proteins such as Cdc24p, Cdc42p, Ste20p, and Cla4p through domain-domain interaction. Thus, Bem1p functions as a scaffold protein to assemble proteins. The function of PX domain in Bem1p is still elusive. Here, we determined the three-dimensional structure of the PX domain of Bem1p to reveal inter- or intra-molecular interactions which regulate the cell polarization in budding yeast.

2. Experimental

The NMR Samples of ca. 0.4 mM uniformly ^{15}N or $^{13}C/^{15}N$ labeled protein were prepared in 20 mM MES buffer (pH 7.0) containing 200 mM NaCl, 1 mM DTT, and 10% D_2O. All NMR data were acquired at 25 °C on Varian Unity INOVA 800 and 600 MHz spectrometers. The assignments of 99% backbone and 98% side chain resonances were obtained based on the series of standard NMR experiments. All data were processed by nmrPipe and data analysis was assisted by Sparky and PACES. Interproton restraints for the structure calculations were obtained from ^{15}N-edited NOESY and ^{13}C-edited NOESY. The three-dimensional structure of the Bem1p PX domain was determined using the CYANA 2.0 program.

3. Results

A total of 2239 NOE restraints and 167 dihedral restraints (83 ϕ, 84 φ) were used for structural calculation. RMSD of the 20 structures for the back bone atoms excluding the non structured region is 0.48 Å, and the RMSD for all heavy atoms is 1.01 Å. Bem1p PX is composed of an antiparallel β-sheet formed by three strands, four α-helices, and a flexible loop containing a PXXP (where X is any amino acid) motif. Electrostatic surface potential reveals that this domain also has a negatively charged pocket which is expected to interact with phosphoinositides (e.g. PtdIns(3)P).

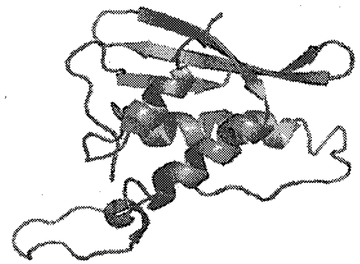

Figure. Ribbon diagram depicting lowest energy NMR structure of Bem1p PX domain.

NP25

Three-dimensional solution structure of the C-terminal domain of a novel galactose-binding protein from the earthworm

Hikaru Hemmi[1], Atsushi Kuno[2], Shigeyasu Ito[3], Ryuichiro Suzuki[3], Tsunemi Hasegawa[3] and Jun Hirabayashi[2]

[1] National Food Research Institute, Tsukuba, Ibaraki 305-8642, Japan; [2] Research Center for Glycoscience, National Institute of Advanced Industrial Science and Technology (AIST), Tsukuba, Ibaraki 305-8566, Japan; [3] Department of Material and Biological Chemistry, Yamagata University, Yamagata, Yamagata 990-8560, Japan

A novel 29-kDa lectin (EW29) has been isolated from the earthworm *Lumbricus terrestris* by affinity chromatography on asialofetuin-agarose in the screening of galectin-like proteins [1]. This lectin consists of two homologous domains (14,500 Da) showing 27% identity with each other and it has multiple short conserved motifs, "Gly-X-X-X-Gln-X-Trp," in the sequence. This short motif has been found in many carbohydrate-recognition proteins from various organisms such as plant lectin ricin B-chain and *Streptomyces lividans* xylanase A. Carbohydrate-recognition proteins having the short conserved motif form the R-type lectin family. Although EW29 was prepared essentially by the same strategy as that used for galectin, this lectin appears to be a member of the R-type lectin family. EW29 has hemagglutinating activity differing from other tandem repeat-type proteins in the R-type lectin family such as ricin, abrin, and *Sambucus sieboldina* agglutinin, however. Based on structural features, this type of lectin generally contains one sugar-binding site per domain, suggesting that the truncated mutant comprising a single domain may have no hemagglutinating activity. The C-terminal domain of EW29 binds to asialofetuin-agarose as strongly as the whole protein and retains its hemagglutinating activity 10-fold lower than the whole protein, whereas the N-terminal domain completely reduces its hemagglutinating activity. These results indicate that the C-terminal domain of EW29 has more than one sugar-binding site, but sugar-binding sites in the C-terminal domain have not been identified yet. R-type lectins are reported to have physiological functions such as enzyme targeting and glycoprotein hormone turnover. The physiological function of EW29, however, remains unknown.

Here we report the 3D structure of the C-terminal domain of EW29 from the earthworm *Lumbricus terrestris* using NMR spectroscopy. The solution structure of the C-terminal domain of EW29 represents β-trefoil fold of typical R-type lectin family. We will discuss the physiological function based on a comparison to the tertiary structures of other proteins in the R-type lectin family.

[1] Hirabayashi, J., Dutta, S. K. and Kasai, K. (1998) *J. Biol. Chem.* 273, 14450-14460.

AP26

The Structural Transition of the Fifteen Residue Peptide on the Ganglioside GM1 Micelles

Naoki Fujitani[1], Hiroki Shimizu[2], Teruhiko Matsubara[3], Takashi Ohta[2], Noriko Nagahori[1], Yayoi Yoshimura[1], Yuuki Komata[1], Toshinori Sato[3], and Shin-ichiro Nishimura[1,2]

[1]Division of Biological Sciences, Graduate School of Science, Frontier Research Center for Post-Genomic Science and Technology, Hokkaido University, Sapporo 001-0021, Japan
[2]Research Center for Glycoscience, National Institute of Advanced Industrial Science and Technology (AIST), Sapporo 062-8517, Japan
[3]Department of Biosciences and Informatics, Keio University, Yokohama 223-8522, Japan

The ganglioside GM1-binding peptide with a sequence of VWRLLAPPFSNRLLP derived from phage display methods showed a clear structural alteration in the presence and absence of GM1 micelles. The three-dimensional structures of the peptide in the free and the GM1 bound states were analyzed using two-dimensional NMR experiments with distance-restrained simulated annealing calculations. The NMR experiments for the peptide absent from GM1 micelles indicated that the peptide has two conformers derived from the exchange between *cis* and *trans* forms in the portion of Pro^7-Pro^8. Further NMR studies with the complex of the peptide and the GM1 micelles elucidated the *trans* form of the peptide bound to GM1. In the absence of absent from GM1 micelles, the peptide has a bent conformation without the regular secondary structures, supporting the theoretical model (Figure 1A). On the other hand, when bound to GM1 micelles, the peptide showed a structure highly stabilized by the hydrophobic interactions including β- and helical turns (Figure 1B). Based on these structural investigations, tryptophan, a core residue of the hydrophobic cluster, might be an essential residue for the recognition of the GM1 saccharides. The dynamic transition of the ligand peptide might play an important role in the function of GM1 as a multiple receptor as in the traditional pathway of cholera toxin infection.

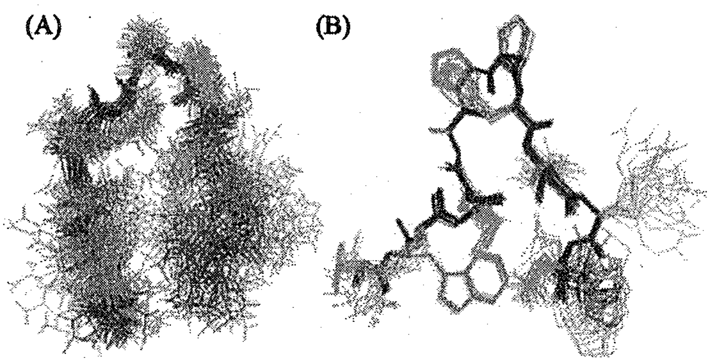

Figure 1. The 20 structures of GM1-binding peptide when absent from (A) and bound to (B) GM1 micelles.

AP27

Solution structure of the mouse TRP14 protein homologous to the human TRP14 protein

Tochio, N[1], Koshiba, S[1], Inoue, M[1], Hayashizaki, Y[1], Kigawa, T[1,2], and Yokoyama, S[1,3,4]

[1]RIKEN GSC, [2]Tokyo Inst. of Tech., [3]RIKEN Harima, [4]Univ. of Tokyo

The human thioredoxin-related protein 14 (TRP14) is involved in regulating tumor necrosis factor-alpha (TNF-alpha) -induced signaling pathways, and has 20% sequence identity with the human thioredoxin (Trx1). Like Trx1, TRP14 exhibits disulfide reductase activity and transfers electrons from cytosolic thioredoxin reductase. However, TRP14 does not donate electrons to ribonucleotide reductase, methionine sulfoxide reductase, and peroxiredoxins, which are well known substrates of Trx1.

In this study, we determined the solution structure of the mouse TRP14 (42-9-9) protein, which has 80% sequence identity with the human TRP14 protein. The structure reveals a typical thioredeoxin fold, which consists of five-stranded beta-sheet surrounded by four alpha-helices. However, mouse TRP14 protein has distinct structural features from Trx1, which are the two separated helices (alpha3a and alpha3b) and the extended loop between beta2 and alpha2. Corresponding regions are conserved in human TRP14. These results suggest that TRP14 family protein could recognize the specific target proteins, which are different from substrates of Trx1.

AP28

Examination of the Solution Structures between Native and *E. coli*-Expressed Membrane Proteins

H. Suzuki[1], Y. Mochizuki[2], Y. Shimada[2], M. Kobayashi[3], T. Nozawa[4] and S. Otomo(Z.-Y. Wang)[1,2],

[1]*Faculty of Science, Ibaraki University Mito 310-8512, Japan* [2]*Department of Biomolecular Engineering, Tohoku University, Sendai 980-8579, Japan,* [3]*Ariake National College of Technology, Omuta, Fukuoka 836-8585, Japan, and* [4]*National Institution for Academic Degree and University Evaluation, 1-29-1 Gakuen-nishimachi Kodaira-shi, Tokyo 187-8587 Japan*

Recently, we have shown that the solution structures of native light-harvesting membrane proteins (LH1 α and β, ca. 6.1kDa) from photosynthetic bacterium *Rhodospirillum rubrum* reveal a long a helical structure in the transmembrane regions(1). The LH1 membrane proteins have also been successfully expressed in *E. coli* cells and cell-free synthesis system(2). Here, we present results on the comparison of the solution structures between the native and *E. coli*-expressed LH1 β proteins.

E. coli expression system was constructed by introducing the LH1 β structural gene into expression vector pET20b with a His-tag at the C-terminus as described elsewhere(2). Purified LH1 β protein was labeled by ^{15}N using a novel method developed in this laboratory(3), and multidimensional NMR spectra were measured in $CDCl_3/CD_3OH$(1:1). 2D ^1H-^{15}N HSQC spectrum of the LH1 β expressed at 30 °C closely resembled that of its native counterpart, suggesting a high degree of structural similarity. Several signals of amide groups close to the C-terminal His-tag disappeared when expressed at 37 °C, implying that expression at higher temperature result in somewhat unstructured terminal region. Further assignment and structural analysis revealed that the solution structure of the LH1 β expressed at 30 °C was highly similar to that of the native protein. This is in good agreement with those of circular dichroism measurement and reconstitution experiment with native LH1 α protein and pigment molecule, bacteriochlorophyll *a*. The result of this study may provide useful insight into the mechanism of membrane protein insertion and structure formation in the most efficient and widely used *E. coli* expression system.

References: (1) Z.-Y. Wang, et al., *J. Mol. Biol.* **347**, 465-477(2005); (2) Y. Shimada, et al. *Biosci. Biotechnol. Biochem.* **68**, 1942-1948(2004); (3) H. Suzuki, et al., *Anal. Biochem.* (2005, in press).

AP29

Mouse Structure Proteomics: Solution Structure of the Mouse Enhancer of Rudimentary Protein Reveals a Novel Fold

○ Hua Li[1], Makoto Inoue[1], Takashi Yabuki[1], Masaaki Aoki[1], Eiko Seki[1], Takayoshi Matsuda[1], Emi Nunokawa[1], Yoko Motoda[1], Atsuo Kobayashi[1], Takaho Terada[1,2], Mikako Shirouzu[1,2], Seizo Koshiba[1], Yi-Jan Lin[1], Peter Güntert[1], Harukazu Suzuki[1], Yoshihide Hayashizaki[1], Takanori Kigawa[1], and Shigeyuki Yokoyama[1,2,3]

([1]RIKEN GSC, [2]RIKEN Harima Institute and [3]The University of Tokyo)

In most eukaryotes, the first three enzymatic activities of the pyrimidine biosynthesis pathway are contained within a single polypeptide of 200-240 kDa. In *Drosophila melanogaster*, this polypeptide is encoded by the *rudimentary* gene, *r*. The *enhancer of rudimentary* gene was originally identified as interacting with the *r* gene by a genetic screen. It encodes a small protein, Enhancer of Rudimentary (ER), which is evolutionarily highly conserved in organisms as diverse as vertebrates, invertebrates, and plants. The regulatory or enzymatic activity of ER has been implicated in pyrimidine biosynthesis and the cell cycle, but its molecular function remains unknown. In this study, we describe the solution structure of the mouse ER protein. ER was found to behave as a dimer in solution, and the solution structure of the ER monomer was determined by heteronuclear NMR spectroscopy. The ER monomer consists of a four-stranded antiparallel β-sheet, with a strand order of β2β1β3β4, and three α-helices (α1, α2 and α3) packed against one side of the sheet, with an overall topology of β1β2α1α2β3β4α3. A structural homology search revealed that ER forms a novel fold. These structural features of ER will shed light on its functional mechanism at the molecular level.

Key words: enhancer of rudimentary, NMR structure, pyrimidine biosynthesis

AP30 (PL11)

Variable pressure NMR reveals the entire energy landscape of a protein: A conserved exited state conformer between ubiquitin and ubiquitin-like protein NEDD8

○Ryo Kitahara[1], Eri Sakata[2], Takeshi Kasuya[2], Yoshiki Yamaguchi[2], Koichi Kato[2,3], Keiji Tanaka[4], Shigeyuki Yokoyama[1,3,5], Kazuyuki Akasaka[1,6]
[1]RIKEN Harima Institute, [2]Department of Structural Biology and Biomolecular Engineering, Graduate School of Pharmaceutical Sciences, Nagoya City University, [3]RIKEN Genomic Sciences Center, [4]Department of Molecular Oncology, Tokyo Metropolitan Institute of Medical Science, [5]Department of Biophysics and Biochemistry, Graduate School of Science, The University of Tokyo, [6]Department of Biotechnological Science School of Biology-Oriented Science and Technology, Kinki University

Variable pressure NMR enables one a direct access to excited state conformers of a protein with an atomic resolution under physiological condition. This allows an understanding of the entire energy landscape of a protein. The method utilizes the generally applicable theorem that the partial molar volume of a globular protein decreases in parallel with the loss of its conformational order (volume theorem). Residue-specific chemical shift and cross peak volume changes in $^{15}N/^{1}H$ HSQC spectra as well as spin relaxation analysis showed a conserved conformational fluctuation between the homologous proteins, human ubiquitin and ubiquitin-like protein NEDD8, in a larger conformational space than hitherto discussed based on X-ray structures.

Ubiquitin and NEDD8 share about 60 % identical amino acid sequence, and their basic folds are consistent with RMSD 0.6 Å for the main chain atoms. Although the two proteins have much similar chemistry for their post-translational modifications, the functional roles of the proteins are quite different. Similar large amplitude fluctuation, estimated in the time range of micro to milli seconds, is found by the NMR spin relaxation analysis for both folded conformers. Furthermore, a peculiar intermediary folded conformer is found in both the proteins in addition to the fully unfolded conformers, which undergoes local unfolding in the entire segment of residues 33-41 and in the parts of C-terminal segment of residues 68-76. Interestingly, the local unfolding takes place preferentially in regions where the amino acid sequence is conserved between the proteins. However, their thermodynamic stabilities are quite different, i.e., ΔG_{NI} =8.4±1.1 kJ/mol and ΔG_{NU} = 13.4±3.2 kJ/mol (at 30 °C) for NEDD8 and ΔG_{NI} = 15.2±1.0 kJ/mol and ΔG_{NU} = 31.3 ± 4.7 (at 0 °C) for ubiquitin, giving much larger equilibrium populations of I and U for NEDD8 than for ubiquitin. In conclusion, these similarities and differences in the conformational fluctuation between ubiquitin and NEDD8 show a different design of the entire energy landscape for their delicately designed functions. Thus, knowing a protein's energy landscape can give vital information to a protein's function.

AP31

NMR Characterization of a Refolding Intermediate of β_2-Microglobulin

○Atsushi Kameda[1], Masaru Hoshino[1], Takashi Higurashi[1], Masato Shimizu[2], Eugene Hayato Morita[2], Satoshi Takahashi[1], Hironobu Naiki[3,4] and Yuji Goto[1,4]
([1]Inst. Protein Res., Osaka Univ. [2]INCS, Ehime Univ. [3]Fac. Med. Sci., Univ. of Fukui [4]CREST/JST)

Dialysis-related amyloidosis (DRA) is a common and serious complication in patients receiving long-term hemodialysis. In this disease, β_2-microglobulin (β2m) is a major structural component of amyloid fibrils. Although native β2m cannot form the amyloid fibril *in vitro*, it was recently reported that the folding intermediate of β2m can form amyloid fibrils. As a precursor of amyloid fibril and a potential target for the prevention of DRA, it is important to understand the detailed structure of the folding intermediate. In this work, we characterized the structure of this folding intermediate at residue level.

The refolding of β2m from the acid denatured state took about 15 hrs at 2.8°C. During the refolding reaction, a series of HSQC spectra was recorded. These time-resolved spectra showed many peaks which had the identical chemical shifts to the native peaks and whose intensities increased monophasically with refolding time. There were also several peaks which were observed neither in the spectrum of the unfolded nor that of the native state. They are therefore considered to be the peaks of the folding intermediate (Fig. 1). Such peaks attenuated their intensities with time. Although the rate constants of increasing native peaks with time do not vary significantly among the residues, the intensities of native peaks immediately after the initiation of refolding, named burst-phase amplitudes, are different depending on the residues. The residues around *cis*-Pro32 and at the β-sheet core have relatively small amplitudes. Considering that this slow folding was driven by the *trans* to *cis* isomerization of Pro32, it is possible that the burst-phase amplitudes imply a degree of the structural similarity between the intermediate and the native state. This suggests that the intermediate has a similar fold to the native state, but contains a non-native *trans*-Pro32 and a disordered structure around Pro32, affecting the β-sheet region. This might play an important role in the amyloid fibril formation. To obtain a further structural insight into this intermediate, we now progress the direct analysis using the amino acid selective labeling techniques.

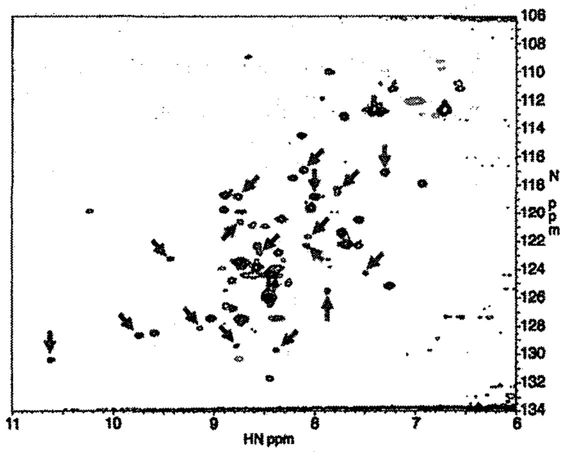

Fig. 1 HSQC spectrum 6 min after initiation of refolding. Arrows represents the unique signals assignable to the intermediate.

AP32

Structure determination of the DNA binding domain in ERCC-1/XPF heterodimer

<u>Mika Masuyama</u>[a,b], Sonoko Ishino[a], Izuro Ohki[a], Tatsuya Nishino[a], Hiroshi Moriuchi[a], Hiroshi Ueno[b], Kousuke Morikawa[a] and Shin-ichi Tate[a]
[a] Department of Structural Biology
Biomolecular Engineering Research Institute (BERI)
6-2-3 Furuedai, Suita, Osaka 565-0874, Japan
[b] Laboratory of Applied Microbiology and Biochemistry
Nara Women's University, Nara 630-8506, Japan

Nucleotide excision repair (NER) is a sophisticated DNA repair mechanism that eliminates a wide variety of DNA lesions. The endonuclease ERCC-1/XPF (Excision Repair Cross Complementation group 1 / Xeroderma Pigmentosum group F) complex is the structure-specific endonuclease that participates in the repair of DNA damage by making the 5'-incision. In the ERCC-1/XPF heterodimer, N-terminal part of the XPF subunit has the nuclease active site. C-terminal domains of both subunits contain two tandemly repeated helix-hairpin-helix (HhH) DNA binding motifs. Two proteins are thought to associate with each other at both N-terminal and C-terminal domains. The heterodimeric DNA binding domain in the ERCC-1/XPF complex plays a crucial role in positioning it at the appropriate location containing irregular DNA structures. Here, we report the solution structure of DNA binding domain in human ERCC-1/XPF heterodimer. Based on the DNA titration experiments, we will also discuss its DNA binding mode to irregularly structured DNAs and its significance for the ERCC-1/XPF functions.

AP33

Structure of carboxyl-terminal domain of transcription factor Hex in complex with transcription factor HNF1α POUs domain

Asai S.[1], Horie Y.[1], Ezomo O.F.[1], Noguchi T.[2], Meshitsuka S.[1]
[1] Institute of Regenerative Medicine and Biofunction,
Tottori University Graduate School of Medical Science,
86 Nishimachi Yonago Tottori 683-8503 Japan,
[2]Nagoya University Graduate School of Bioagricultural Sciences,
Chikusaku Nagoya Aichi 464-8604 Japan

Transcription factor Hex (haematopoietically expressed homeobox) is a homeobox protein that regulates differentiation and development of liver and monocyte. Hex has three functional domains, N-terminal domain, homeo domain and C-terminal domain, of which functions are repression, DNA binding and activation, respectively. We reported NMR spectra of Hex C-terminal domain (Hex-C) with GST tag and assigned the backbone and side-chain signals. Recently it has been found that Hex interacts with HNF (hepatocyte nuclear factor) 1α, which is important for liver differentiation. HNF1α has POU specific domain (POU_S) and homeo domain (POU_{HD}) as DNA binding domains. To explain the function of Hex-C in relation to HNF1α, the structural studies have been carried out by NNR.

Isotopically labeled Hex-C and non-labeled POU_S were expressed with GST tag by E.coli BL21(DL3) using pGEX vectors and purified by affinity chromatography of Glutathion Sepharose 4B. POU_S was obtained by hydrolysis by thrombin for 16h at 22℃. Hex-C and POU_S were purified by gel chromatography (HiLoad 16/60 Superdex 75pg, ÄKTA prime, Amersham). Protein solutions were concentrated by ultra-filtration (AMICON) or lyophilization. NMR spectra were measured in 50mM phosphate buffer with 10mM DTT by Varian Inova 500 spectrometer with a triple resonance probe.

We have obtained sufficiently resolved NMR spectra of Hex-C with GST (GST-Hex-C). But Hex-C did not provide good NMR spectra for analysis when GST tag is removed by hydrolysis. GST tag is beneficial not only for expression and purification but also for the NMR measurement and analyses of a small domain of proteins. The signals from S224 to C237 of GST-Hex-C in ^{1}H-^{15}N HSQC spectrum were shifted in complex with POU_S. To the contrary signals of N-terminus from D207 to T214 and C-terminus from D260 to G271 remained unchanged or were slightly shifted. It is thought that the specific binding of Hex-C with POU_S causes the chemical shift changes in the HSQC spectrum. Hex-C was supposed to have helices of an extended structure in a free state. But in the presence of POU_S, an activating domain of Hex-C may form a folded structure. The structure of negatively charged domains of transcription factors is thought to be an unfolded structure, but the conformation may be changed to a folded structure when in complex with the target protein. It has been reported that Hex influences various gene expressions either as an activator or a repressor. Hex may regulate the transcription of a certain gene by its binding with other transcription factors by an induced fit mechanism.

AP34

Solution structure of two human Myb-like DNA-binding domain repeats

Yukiko Doi-Katayama[1], Fumiaki Hayashi[1], Makoto Inoue[1], Takanori Kigawa[1], Shigeyuki Yokoyama[1,2,3], Hiroshi Hirota[1,4]
1: RIKEN Genomic Sciences Center, Tsurumi-ku, Yokohama 230-0045
2: RIKEN Harima Institute at SPring-8, Mikazuki-cho, Hyogo 679-5148
3: Graduate School of Science, The University of Tokyo, Tokyo 113-0033
4: Graduate School, Yokohama City University, Tsurumi-ku, Yokohama 230-0045

The murine tumor cell DnaJ-like protein 1 or MTJ1/ERdj1 is a membrane J-domain protein enriched in microsomal and nuclear fractions. Its human homologue HTJ1 also contains a large carboxyl-terminal cytosolic extension composed of two tryptophan-mediated repeats or Myb-like DNA-binding domain repeats. It is reported the C-terminus side Myb-like DNA-binding domain interacts with 1-antichymotrypsin, a member of the serine proteinase inhibitor (serpin) family *in vitro*. Here, we report the solution structure of two Myb-like DNA-binding domains in the human homologue HTJ1 by NMR spectroscopy. Both Myb-like DNA-binding domains have the similar fold, which consists of three helices maintained by a hydrophobic core. However, the electrostatic potential surface of these molecules shows distinct differences. The N-terminus Myb-like DNA-binding domain exhibits a positively charged broad surface, while the C-terminus domain shows characteristic negative patch with positively charged surface. These differences may be sufficient to control the specificity of each domain.

(a) (b)

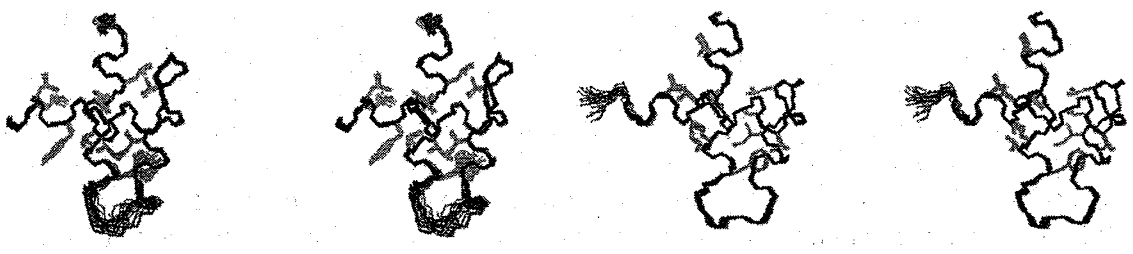

Stereoviews of 20 superimposed structures that form a hydrophobic core of Myb-like DNA-binding domains in HTJ1. (a) N-terminus Myb-like DNA-binding domain. (b) C-terminus Myb-like DNA-binding domain.

AP35

Solution structure of the hydrophobic helix of NRSF/REST bound to the PAH1 domain of mSin3B

○Mitsuru Nomura[1,2], Hiroko Uda-Tochio[3], Kiyohito Murai[4], Nozomu Mori[5] and Yoshifumi Nishimura[1]

[1]Graduate School of Supramolecular Biology, Yokohama City University, [2]Kihara Memorial Yokohama Foundation for the Advancement of Life Sciences, [3]RIKEN Genomic Sciences Center, [4]Division of Neuroscience, Beckman Research Institute, City of Hope, [5]Department of Anatomy and Neurobiology, Nagasaki University School of Medicine

In non-neuronal cells and neuronal progenitors many neuron-specific genes are repressed by neural restrictive silencer factor, NRSF (also known as REST) which is an essential transcriptional repressor recruiting the Sin3-HDAC complex. Here, we have revealed that the first paired amphipathic helix domain (PAH1) of mSin3B is an interacting domain with the N-terminal repressor domain of NRSF/REST. Then, we have determined the solution structure of mSin3B PAH1 associated with the minimal repressor domain of NRSF/REST. In the complex PAH1 holds a compact left-handed four-helix bundle structure followed by an ordered C-terminal tail. The fundamental architecture of the four helices of PAH1 is similar to the corresponding architectures of the PAH2 domains so far determined, however the lengths of the four helices of PAH1 are almost shorter than the corresponding helices in the PAH2 domains. In contrast to the amphipathic α-helix of Mad1 or HBP1 bound to PAH2, the short hydrophobic α-helix of NRSF/REST is captured in the hydrophobic cleft of PAH1. Each of four PAH domains of Sin3 seems to interact with a characteristic helix of a specific repressor; PAH1 needs a mostly hydrophobic helix and PAH2 needs an amphipathic helix in each target repressor.

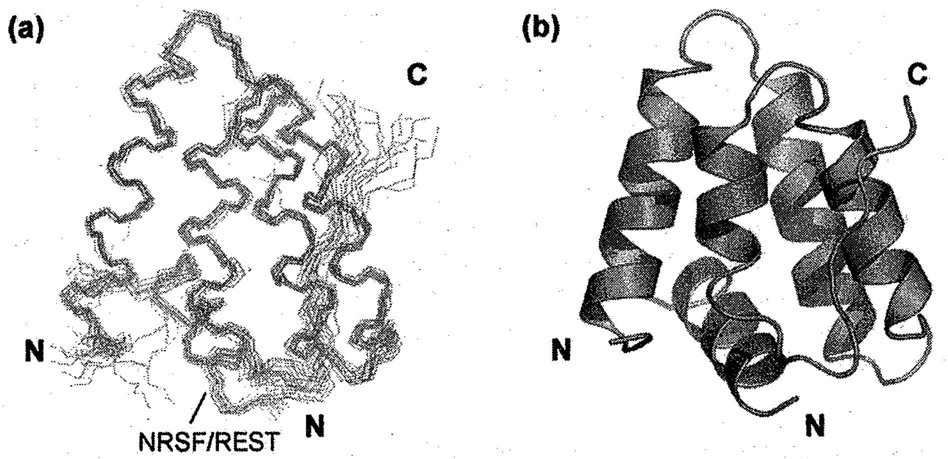

Figure 1. The three-dimensional structure of the NRSF/REST-mSin3B PAH1 complex. (a) Superposition of 20 lowest-energy structures. (b) Ribbon diagram.

AP36

Structural and functional analyses of the antifreeze-like domain of human sialic acid synthase

Yoko Ito[a], Toshiyuki Hamada[a,b], Takamasa Abe[b], Fumiaki Hayashi[b], Peter Guntert[b], Makoto Inoue[b], Takanori Kigawa[b], Takaho Terada[b], Mikako Shirouzu[b], Mayumi Yoshida[b], Akiko Tanaka[b], Sumio Sugano[c], Shigeyuki Yokoyama[b,d,e], and Hiroshi Hirota[a,b]

[a] *Graduate School of Yokohama City University, Tsurumi-ku, Yokohama 230-0045*
[b]*RIKEN Genomic Sciences Center, Tsurumi-ku, Yokohama 230-0045*
[c]*Graduate School of Frontier Sciences, The University of Tokyo, Tokyo 108-8639*
[d]*RIKEN Harima Institute at SPring-8, Mikazuki-cho, Sayo, Hyogo 679-5148,*
[e] *Graduate School of Science, The University of Tokyo, Tokyo 113-0033*

Sialic acids (acylated neuraminic acids: α-keto acids with a nine-carbon sugars) participate in many important biological recognition events. The biological significance of sialic acids underscores the necessity of characterizing their biosynthetic pathways.

Sialic acid synthase (SAS) catalyzes the condensation of phosphoenolpyruvate with either *N*-acetylmannosamine (ManNAc) (bacteria) or ManNAc 6-phosphate (vertebrates) to yield *N*-acetylneuraminic acid (NeuNAc) or NeuNAc 9-phosphate, respectively [1]. These enzymes are composed of two distinct domains that are joined by an extended linker region. The *N*-terminal domain (NeuB domain) has considered to bind the sugar substrates [2], while it has been proposed that the *C*-terminal domain [antifreeze-like (AFL) domain] is also involved in sugar binding, but the details of its function have remained elusive.

To obtain further understanding of the structural and mechanistic properties of the AFL domain in SAS, we determined the structure of the *C*-terminal AFL domain of human SAS by NMR spectroscopy using $^{13}C/^{15}N$ doubly labeled protein obtained through the cell-free protein expression system. The structure comprises one α- and two single 3_{10}-helices and a two-stranded antiparallel β-sheet (Fig. 1), which is included in the β-clip fold. Although it is similar to those of the fish type Ⅲ antifreeze proteins (AFPs), its peptide bond between Glu32 and Pro33 forms the *trans*-configuration, in contrast to the *cis*-configuration of the same peptide bond formation in all of the type Ⅲ AFPs. The substrate-binding arginine residue in bacterial AFL domain (e.g. Arg314 in *N. meningitides*) was replaced to glycine in human AFL domain, and thus, the human SAS probably does not have the same functions mechanism as the bacterial enzyme. Moreover, we have classified the type Ⅲ AFP family into several subfamilies, and have compared each of them through tertiary structure-based sequence analyses, using the evolutionary trace (ET) method [3]. The ET results highlight three crucial findings: 1) the procaryotic SAS shares the Arg314 residue, which plays an important role in substrate binding, 2) the class-specific residues of the human AFL domain are localized on one side, which might interact with substrates, 3) the residues for the ice-binding of the fish AFP were conserved specifically in the subfamily.

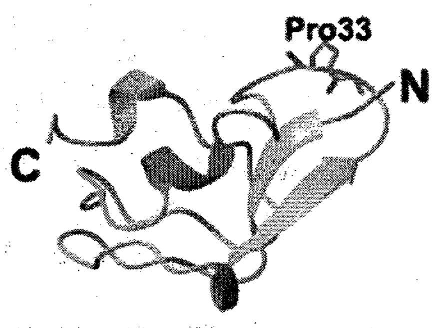

Fig. 1 The structure of human AFL domain

Reference
[1] S. M. Lawrence et al. (2000) *J. Biol. Chem.* **275**: 17869-17877.
[2] J. Gunawan et al. (2005) *J. Biol. Chem.* **280**: 3555–3563.
[3] O. Lichtarge et al. (1996) *J. Mol. Biol.* **257**: 342–358.

AP37

NMR study on the interaction of the transactivation domain of ATF-2 with MAP kinase p38 α

Michiko Ishizu, Noriyuki Iwasaki, Aritaka Nagadoi, and Yoshifumi Nishimura
Graduate School of Supramolecular Biology, Yokohama City University, 1-7-29,Suehiro-cho,Tsurumi-ku,Yokohama 230-0045

Abstract
Here, we have studied the interaction of the transactivation domain of activating transcription factor 2, ATF-2 with MAP kinase p38 α by using heteronuclear two-dimensional NMR techniques.

1 Introduction

The p38 MAP kinase is involved in the signal transduction pathway of the cellular stress and cytokine stimuli to nucleus. ATF-2 is a transcription factor that is phosphorylated by the p38 stress-activated kinase, containing an N-terminal transctivation domain (TAD) and a C-terminal DNA-binding domain. ATF-2 forms a homodimer with itself or a heterodimer with c-Jun and binds to cyclic AMP-response element (CRE), stimulating CRE-dependant transcription of genes.

2 Materials and Methods

The murine p38 α gene carried in pCold IV vector was transformed into BL21(DE3)-star. Cells were cultured and the supernatant of cell cultures was purified by column chromatography. The ^{15}N-labelled TAD of ATF-2 containing residues 20 - 106 of human ATF-2 was also expressed in *Escherichia coli* and purified by column chromatography.

The ^{15}N-^{1}H HSQC spectrum of ATF-2 TAD and the spectrum of the mixture of ATF-2 TAD and p38 α at the molar ratio of 1:1.1 were measured in solutions containing 20mM KPB pH7.0 ,5mM DTT, 30 μM $ZnCl_2$, 10 % D_2O at 300K.

3 Results and Discussion

The spectra of the ^{15}N-labelled TAD of ATF-2 without and with p38 α were compared. Significant chemical shift changes were observed in the α helix region (39E-50E) of ATF-2 TAD and small chemical shift changes were observed in the β strand region (34Q-36F). The NMR signals of 31G, 50E, 51M, 53L, 54K and 55F of ATF-2 TAD were disappeared in the presence of p38 α.

This suggests that ATF-2 TAD interacts with p38 α by using the so-called docking site of p38 α (Yang et al.,1998 ; C.I.Chang et al.,2002).

AP38

Aromatic-amide Interactions in Glycine- and Tyrosine-rich, Repetitive Sequences as Revealed by NMR

Yasuhiro Kumaki[1], Manabu Nakano[2], Masakatsu Kamiya[2], Tomoyasu Aizawa[2], Makoto Demura[2], Keiichi Kawano[1,2], and Norio Matsushima[3]

[1]High-Resolution NMR Laboratory and [2]Division of Biological Sciences, Graduate School of Science, Hokkaido University, [3]School of Health Sciences, Sapporo Medical University,

Ice nucleation protein (INP), heterogeneous nuclear ribonucleoprotein (hnRNP), prion protein, plant glycine-rich RNA-binding protein (GRRBP), ozone-inducible proteins and *Cicer arietinum* glycine-rich proteins (GRPs) contain repetitive glycine-rich sequences intercepted with aromatic residues such as tryptophan or tyrosine. INPs contain fifty eight tandem repeats of AGYGSTxTAGxxSxLx at the central region. Mammalian prion proteins contain four tandem repeats of PHGGGWGQ at the N-terminal region. The glycine-rich domains in GRRBP are regarded as multiple repeats of $Y(x)_hR_k(x)_l$, where x is mainly Gly, "k" is 1 or 2, and "h" and "l" range from 0 to 10. Also hnRNP have repetitive sequence similar to GRRBP. Ozone-inducible proteins from *Atriplex canescens* contain eight to ten tandem repeats of YGHGGG, respectively, while *Cicer arietinum* GRPs contain 8 tandem repeats of GGGNYG(H/N). The glycine- and tyrosine-rich regions are highly flexible because of the numerous glycines. The high flexibility and repetitiveness in the glycine-rich regions appear to make greatly difficult the determination of the three-dimensional structure by conventional NMR and X-ray analyses. NMR measurements were performed for synthetic peptides corresponding to sections of the sequences of these proteins in order to elucidate the structures.

As a result of NMR assignments, we found that the third residue in the sequence (Y/F/W)G(G/Q/H/N/S) showed significant upfield chemical shifts of amide protons. Such upfield shifts are ascribed to weakly polar interactions between aromatic rings of amino acids at position *i* and hydrogens of backbone amides at position *i*+2 (Ar(*i*)-HN(*i*+2)). The amide protons which are associated with Ar(*i*)-HN(*i*+2) interactions are located with above or below aromatic rings, therefore, show upfield ring current shifts. Our study indicates that not only Gly but also other residues can be *i*+2 donors in Ar(*i*)-HN(*i*+2) interactions in case the residue at position *i*+1 is Gly. This conclusion is not consistent with statistical survey based on crystal structures, where no Ar(*i*)–HN(*i*+2) interactions were found in case Gly at position *i*+1 and any residues other than Gly at position *i*+2. To understand the origin of this discrepancy, we investigate the relationship between amino acid sequence and chemical shift deviation of amide protons by use of BMRB database.

AP39

Observation of protein binding to membrane with photo-CIDNP technique

Takahide Kouno[1], Meneyuki Mizuguchi[1], Yoshihiro Mori[1], Isei Tanida[2], Takashi Ueno[2], Eiki Kominami[2], and Keiichi Kawano[3]

[1]Faculty of Pharmaceutical Sciences, Toyama Medical and Pharmaceutical University, Toyama 930-0194, Japan, [2]Department of Biochemistry, Juntendo University of Medicine, Tokyo 113-8421, Japan, [3]Division of Biological Sciences, Graduate School of Science, Hokkaido University, Sapporo 060-0810, Japan

The photo-CIDNP approach provides explicit information on the accessibility of amino acid residue in a protein to solvent. This technique is based on the cyclic photochemical reactions between a photoexcited dye and an amino acid residue located on the surface of a protein, and thereby selectively detects some aromatic amino acids histidine, tryptophan, and tyrosine when these side chains are accessible to the dye.

Previously, we studied on the solution structure of microtubule-associated protein light chain-3 (MAP-LC3) which is a human homologue of Atg8 included in yeast Atg (autophagy) family. Atg family is involved in autophagy induced under nutrient-starvation condition and Atg8 plays a key role in the formation of autophagosome that is vesicle for the transport of cytoplasm and organelles to the lysosome or vacuole. As a result of the structure calculation of MAP-LC3, this protein is composed of two distinct regions, the N-terminal and the C-terminal subdomains. In addition, we carried out a photo-CIDNP approach to obtain information about the N-terminal conformation of MAP-LC3. A tyrosine residue on the surface of the C-terminal subdomain did not indicate a CIDNP effect due to the presence of the N-terminal subdomain. Therefore, we concluded that two subdomains of MAP-LC3 make a contact each other, and MAP-LC3 adopts a single compact conformation in solution.

Moreover, we analyzed the functions of two subdomains included in MAP-LC3, and revealed that the N-terminal and the C-terminal subdomain are involved in the binding to microtubules and membrane components, respectively. However, we obtained no definite data about the latter interaction, such as the NOE between MAP-LC3 and membrane molecule. To resolve this issue, we performed the photo-CIDNP technique and tried to identify the surface of MAP-LC3 essential for the interaction with autophagosome membrane. The application of the photo-CIDNP will be useful to investigate the weak interaction between a protein and membrane.

AP40 (PL13)

Solution structure of the cytoplasmic region of Na^+/H^+ exchanger-1 complexed with the essential cofactor, calcineruin B homologous protein-1

○Masaki Mishima, Shigeo Wakabayashi and Chojiro Kojima
Graduate School of Biological Sciences, Nara Institute of Science and Technology, 8916-5 Takayama, Ikoma 630-0192, Japan, and Department of Molecular Physiology National Cardiovascular Center Research Institute, 5-7-1 Fujishiro-dai, Suita, Osaka 565-8565 Japan.

Na^+-H^+ exchanger-1 (NHE1) consists of 12-N terminal membrane-spanning helices and large C-terminal cytoplasmic region. NHE1 functions primarily in intracellular pH homeostasis and cell volume regulation. Recently, it was reported that calcineurin B homologous protein 1 (CHP1) serves as an essential cofactor to express high physiological levels of exchange activity. CHP1 deprivation resulted in drastic reductions (>90%) of the NHE1 activity. It was shown that CHP1 directly bound that juxtamembrane region of the cytoplasmic domain.

Here, we describe the solution structure of the cytoplasmic region of NHE1 (503-545) complexed with the essential cofactor, CHP1 (195 aa). We pursued NMR structural analysis of co-expressed and co-purified samples for the following reasons; CHP1-free NHE1 was readily degraded among the expression and purification schemes, and NHE1-free CHP1 aggregated during NMR measurements. However, co-expression and co-purification of NHE1 and CHP1 enabled us to obtain a stable complex for structural studies, which showed no significant degradation and aggregation for several weeks. Since our structural analyses targeted about 27 kDa complex, which was relatively large molecular weight for conventional NMR studies, utilization of triple labeling (60%-^{2}H/u-^{13}C/u-^{15}N) and recently developed computational methodology, CANDID, were clues for structure determination.

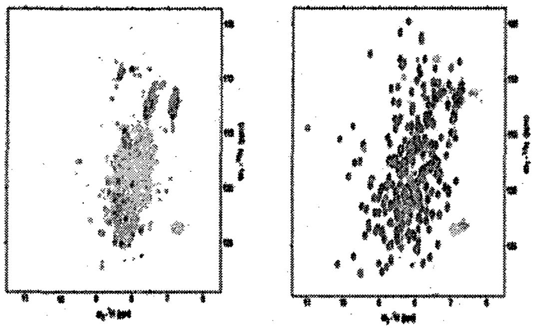

Fig.1
HSQC spectra of ^{15}N labeled CHP1. NHE1 free (left) and NHE1 bound (right).

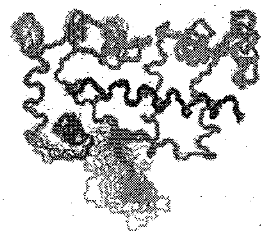

Fig.2
20 ensemble structures of the NHE1-CHP1 complex

As a result, NHE1 adopts 5-turn amphipathic helix composed of the residue 518 to 537. The protein–protein interface consists of the extensively hydrophobic concave undersurface of CHP1 and an apolar side of NHE1 helix. The interface ranges over both N-terminal domain and C-terminal domain of CHP1, of which total surface area buried is 1828 Å^2, accounts for the high affinity of the complex. We also discuss detail of the interaction based on the structure and the results of *in vitro* binding assay.

AP41

Solution structure and dynamics of Ufm1, a novel ubiquitin-like post-translational modifier

Hiroaki Sasakawa[1], Eri Sakata[2], Yoshiki Yamaguchi[2], Masaaki Komatsu[3], Keiji Tanaka[3], Koichi Kato[1, 2]

[1]Institute for Molecular Science, Okazaki, Japan, [2]Graduate School of Pharmaceutical Sciences, Nagoya City University, Nagoya, Japan, [3]Tokyo Metropolitan Institute of Medical Science, Tokyo, Japan

Ufm1, a novel post-translational modifier sharing ~20% sequence identity with ubquitin, is first cleaved at the C-terminus to expose its conserved Gly residue, which is essential for its subsequent conjugating reactions. The C-terminally processed Ufm1 is activated by E1-like enzyme, Uba5, by forming a high-energy thioester bond and is then transferred to its cognate E2-like enzyme, Ufc1, in a similar thioester linkage (1). To understand the biological functions of Ufm1, we have analyzed solution structure and dynamics of this protein.

NMR experiments were performed at 303 K using a Bruker Avance 600, DRX-500 with a cryogenic probe and JEOL JNM-ECA920. Spectral assignments were achieved using a standard set of double- and triple-resonance experiments and hydrogen bonds restraints were obtained by a hydrogen-deuterium experiment. Relaxation data were obtained from ^{15}N T_1 and ^{15}N T_2 and ^{1}H-^{15}N NOE measurements. NOE assignments and structure calculation were performed by use of CYANA 2.0 using total of 723 distance restraints, 38 hydrogen bonds information and 100 backbone dihedral angle restraints. The resulting r.m.s.d from the mean structure for backbone atoms was 0.571 Å, which was sufficient to determine the overall structure of Ufm1. Ufm1 assumes a typical ubiquitin fold but does not possess a negatively charged surface area characteristic for ubiquitin and other ubiquitin-like proteins, e.g. NEDD8 and parkin-Ubl. Model-free analysis revealed that the N-terminal β1-strand the α1-helix-β3-strand loop and the C-terminal β4-strand undergo chemical exchange processes. These regions correspond to the E1-interaction site of NEDD8, suggesting that the Uba5-binding site of Ufm1 also exhibits conformational fluctuation.

(Reference)

Komatsu, M., Chiba, T., Tatsumi, K., Iemura, S., Tanida, I., Okazaki, N., Ueno, T., Kominami, E., Natsume, T., Tanaka, K. 2004. A novel protein-conjugating system for Ufm1, a ubiquitin-fold modifier. *EMBO J.* 23: 1977-1986.

AP42

NMR studies on the 57kDa *Escherichia coli* periplasmic oligopeptide binding protein OppA

Kayano Moromisato[1], Kaori Kurashima-Ito[2,3], Kaoru Nishimura[4], Jeremy Tame[4] and Yutaka Ito[1,3,5]

[1]Department of Chemistry, Tokyo Metropolitan University, 1-1 Minami-Ohsawa, Hachioji, Tokyo 192-0397; [2]Molecular and Cellular Physiology Laboratory, [4]Protein Design Laboratory, Graduate School of Integrated Science, Yokohama City University, Japan; [3]Research Group for Bio-supramolecular Structure-Function, RIKEN, 1-7-29 Suehiro-cho, Tsurumi-ku, Yokohama 230-0045, Japan; [5]CREST, JST

Recent developments on protein stable isotope labelling and TROSY-based NMR measurements were applied to a 57kDa (517 amino acid residues) *Escherichia coli* periplasmic oligopeptide binding protein OppA. OppA has a remarkably broad substrate specificity, binding peptides of two or five amino-acid residues with high affinity, but little regard to sequence. It is therefore an ideal system for studying how different chemical groups can be accommodated in a protein interior.

For backbone resonance assignment, we performed three pairs of TROSY-based triple-resonance experiments, HNCA/HN(CO)CA, HN(CA)CB/HN(COCA)CB and HN(CA)CO/HNCO on uniformly $^{2}H/^{13}C/^{15}N$-labelled ligand free OppA sample (~1 mM). A nonlinear sampling scheme was utilised for indirectly acquired ^{13}C and ^{15}N dimensions, in order to increase sensitivity with greater number of scans while maintaining high resolution. Owing to the large size of the protein and limitations of conventional NMR experiments, full advantage was taken of TROSY based experiments for the backbone analyses.

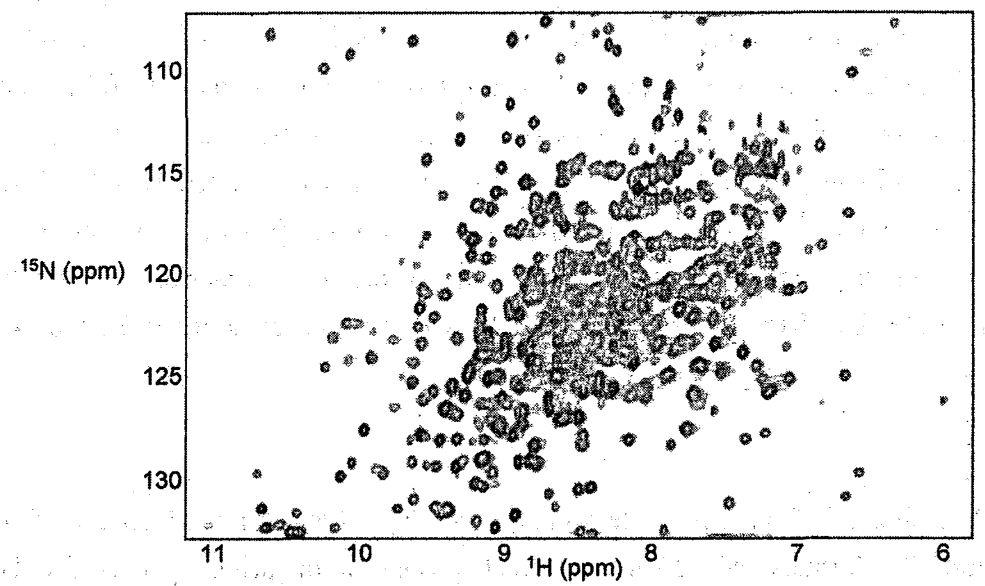

Figure:
2D ^{1}H-^{15}N TROSY-HSQC spectrum of $^{2}H/^{13}C/^{15}N$-labelled OppA

AP43

Structural and Functional Characterization of WSSV Novel Protein VP230

Yang Liu, Jinlu Wu, Sivaraman Jayaraman, Choy Leong Hew

Dept. of Biological Sciences, National University of Singapore, Singapore, 119260

Shrimp white spot syndrome virus (WSSV) has been the most serious pathogen infecting a broad host range including shrimps and crayfish, causing mass mortalities worldwide. There is presently no effective treatment for this disease. WSSV contains a 305kb double stranded circular DNA with approximately 180 open reading frames (ORFs). VP230 is a novel protein, which is highly abundant at both mRNA and protein level. It is hypothesized to be one of the important proteins required for the infection of this virus. The EST profiling has shown very high expression level for this gene. Pull down assay and co-immunoprecipitation has shown that VP230 is able to interact directly or indirectly with shrimp plasma proteins and ribosomal protein respectively. Therefore, we speculated that VP230 could play an important role in the transcription and/or translation of the virus. Structure approach was carried out to further understand the biological function of VP230.

In order to determine the solution structure of VP230, heteronuclear NMR experiments were performed on an 800 MHz Bruder Avance spectrometer equipped with pulse field gradient units or on a 500 MHz Bruker Avance spectrometer equipped with both an actively shielded cryoprobe and pulse field gradient units. The NMR spectra acquired for both backbone and side-chain assignments consisted of 15N-edited HSQC-TOCSY, HSQC-NOESY, and triple resonance experiments including HNCACB, CBCA(CO)NH, HNCO, HCCH-TOCSY and 13C-edited HSQC-NOESY. NOE restraints were derived from 15N and 13C-NOESY spectra acquired on 800 MHz spectrometers. NMR data were processed with Sparky program and analyzed with NMRView5. Hydrogen bond restraints were derived from examination of the HSQC-base hydrogen-deuterium exchange experiment. A set of manually assigned unambiguous NOE restraints together with dihedral angle restraints predicted by TALOS program using five chemical shift values (15N, Cα, Cβ, CO and Hα) was applied to calculate initial structure by CYANA program. With the initial structure more NOE cross-peaks in the two NOESY spectra were automatically assigned by CYANA program followed by manual check.

Concurrently, the crystal of this protein was obtained and data was collected at BNL, New York. The crystal structure was solved by Single wavelength Anomalous Diffraction (SAD) method. Two cadmium binding sites were also identified, though there is no conserved metal binding motif such as CXXC in the primary protein sequence. In order to check the specificity of heavy atoms binding, NMR titration was applied. Another metal ion, zinc, was also found to bind to VP230 in the similar binding fashion as cadmium. The structure and function relationship of this protein will be the focus for future studies.

AP44

Structural Basis of Syndecan-4 Function and Its Interaction with Syntenin1 PDZ2 domain complex

Bon-Kyung Koo[1], John R. Couchman[3], Eok-Soo Oh[2], and Weontae Lee[1*]

[1]Department of Biochemistry and Protein Network Research Center, College of Science, Yonsei University, Seoul 120-749 Korea [2]Department of Life Sciences, Division of Molecular Life Sciences and Center for Cell Signaling Research, Ewha Womans University, Seoul 120-750 Korea [3]Division of Biomedical Sciences, Faculty of Medicine, Imperial College of Science, Technology and Medicine, London, SW7 2AZ, United Kingdom

The transmembrane proteoglycans syndecans, which involved in the organization of cytoskeleton and/or actin microfilaments, have important roles as cell surface receptors during cell-cell and/or cell-matrix interaction. NMR and biochemical results indicate that syndecan-4 cytoplasmic domain(4L) becomes oligomeric and can activate protein kinase Cα (PKCα) only in the presence of phosphatidylinositol 4,5-bisphosphate(PIP_2) playing a critical role of multimerization status of 4L to regulate PKC activity. The complexation of 4L and PIP_2 was studied by heteronuclear-multidimensional NMR spectroscopy. Heteronuclear-edited and –filtered NOESY experiments were performed to collect NOE information for structure calculation. Oligomerization of the cytoplasmic domain of syndecan-4 is regulated either positively by PIP_2, or negatively through phosphorylation of serine 183 (Ser^{183}). Phosphorylation results in reduced PKCα activity by preventing PIP_2-dependent oligomerization of the syndecan-4 cytoplasmic domain. A marked effect of phosphorylation is a dramatic conformational change in the C2 region, which ablates an interaction site with the PDZ domain of syntenin1.

AP45

Solution structure of SSD domain of *Bacillus subtilis* Lon protease

Iren Wang[1,3], Yuan-Chao Lou[2], Shih-Chi Lo[2], Alan Yueh-Luen Lee[1], Chinpan Chen[2] and Shih-Hsiung Wu[1,3]

[1]Institute of Biological Chemistry, Academia Sinica, Taipei 115, Taiwan;
[2]Institute of Biomedical Sciences, Academia Sinica, Taipei 115, Taiwan;
[3]Institute of Biochemical Sciences, National Taiwan University, Taipei 106, Taiwan

Lon protease (an ATP-dependent protease) belongs to the ATPase associated with diverse cellular activities (AAA^+) superfamily and is mainly responsible for eliminating misfolded or damaged proteins as well as for controlling the cellular activities of the short-lived regulatory proteins. It consists of three distinct functional domains, and the sensor- and substrate-discrimination (SSD) domain, a subdomain of the central ATPase domain, is suggested as substrates-recognition and DNA binding sites. Therefore, knowing the tertiary structures of SSD domains is particularly intriguing for discerning their substrates-discriminating mechanism and the DNA binding mechanisms on Lon proteases. CD experiments showed that there is a conformational change for *Bacillus subtilis* Lon SSD domain (Bs-LonSSD) at extreme acidic and basic pH values. Since Bs-LonSSD contains a number of charged residues, it is probable that deprotonation or protonation of these charged residues causes the conformational change. Using multidimensional NMR techniques, 3D NMR solution structure of Bs-LonSSD at pH 5.8 was determined to comprise of four α-helices and a two-stranded parallel β-sheet, similar to that of *E. coli* Lon SSD domain. The ensemble of 15 NMR structures was well defined, with average root-mean-square deviations of 0.64 ± 0.05 Å for the backbone atoms and 1.58 ± 0.09 Å for heavy-atoms in secondary structure regions. Structural comparison among Lon SSD domains indicates that the positively charged cluster mainly formed by the residues of α3 may be responsible for DNA binding. It is hoped that these studies may shed light on the protein substrates-discriminating and the DNA binding mechanisms of Lon proteases.

AP46

Structure of the C-terminal domain of insulin-like growth factor binding protein-2 (IGFBP-2) and interactions with IGFs: An NMR study

Zhihe Kuang[1,2], Shenggen Yao[1], David W. Keizer[1], Chunxiao C. Wang[1], Kerrie A. McNeil[2], Briony E. Forbes[2], Leon A. Bach[3], John C. Wallace[2] and Raymond S. Norton[1]

[1] The Walter and Eliza Hall Institute of Medical Research, Parkville, Australia
[2] School of Molecular and Biomedical Science, The University of Adelaide, Australia
[3] Department of Endocrinology and Diabetes and Monash University Department of Medicine, Alfred Hospital, Melbourne, Australia

Insulin-like growth factor binding protein-2 (IGFBP-2) is the largest member of a family of six proteins (IGFBP-1 to 6) that bind insulin-like growth factors-I and -II (IGF-I/II) with high affinities. IGFBP molecules contain three domains of approximately equal length: the conserved Cys-rich amino- and carboxyl-terminal domains joined by a variable linker domain. The N- and C-domains bind IGFs simultaneously, resulting in high affinity (1). The C-domains are not only essential for high IGF binding affinity, but also appear to confer binding specificities. For example, C-BP-6, the C-domain of IGFBP-6, is the major determinant of the IGF-II preference of IGFBP-6 (2). In addition, different IGFBPs have distinct IGF-independent functions, which seem to be governed largely by their C-domains (2). The solution structure of C-BP-6 has been solved and the IGF-II binding site was mapped previously (3, 4).

Here we report the solution structure of C-BP-2, the C-domain of IGFBP-2, and compare it with that of C-BP-6. Like C-BP-6, C-BP-2 has a thyroglobulin type I fold containing an α-helix and a three-stranded β-sheet. C-BP-2 contains a longer unstructured loop I and longer extension at the C-terminus, which is unstructured and very mobile. These structural features are also reflected by the ^{15}N NMR relaxation data. The backbone dynamics of C-BP-2 were further investigated in different magnetic fields and the results are discussed with respect to functional implications and compared to those of C-BP-6 (4).

We have also conducted NMR titration experiments to study the interactions between N- and C-domains of IGFBP-2 and IGFs and to map the binding residues. For the first time, we show that the binding affinity of C-domain to IGF-I is significantly increased in the presence of N-BP-2, switching from the intermediate to slow exchange regime. Two possible mechanisms for this cooperativity between the N- and C-domains in IGF binding were further investigated in detail for the first time using NMR: the interaction between N- and C-domains and/or a conformational change of IGF-I. The findings will be presented and discussed.

(1) Denley et al., Cytokine Growth Factor Rev. 2005; in press. (2) Bach et al., Trends Endocrinol Metab. 2005; 16: 228-34. (3) Headey et al., Mol Endocrinol. 2004; 18: 2740-50. (4) Yao et al., Biochemistry. 2004; 43: 11187-95.

AP47

Domain Organization and Dimer-Interface Structure of Severe Acute Respiratory Syndrome-Associated Coronavirus Nucleocapsid Protein

Chung-ke Chang[1], Shih-Che Sue[1], Cheng-Kun Tsai[2], Yen-Chieh Chiang[3], Wen-Jin Wu[4] and Tai-huang Huang[1]

[1]Institute of Biomedical Sciences, Academia Sinica, Nankang, Taipei, Taiwan
[2]Department of Physics, National Taiwan Normal University, Taipei, Taiwan
[3]Department of Agronomy, National Taiwan University, Taipei, Taiwan

Severe acute respiratory syndrome (SARS) is a novel human disease caused by a new coronavirus (SARS-CoV). We investigated the domain organization of the nucleocapsid protein of SARS-CoV in solution and found that it contains two structural domains sandwiched between three disordered regions. The second structural domain is responsible for dimerization of the protein. The interface region of this structural domain is stabilized by multiple intermolecular hydrogen bonds and hydrophobic contacts. The conformation is reminiscent of the nucleocapsid protein of the porcine respiratory and reproductive syndrome virus. Bioinformatics analyses indicate that the overall domain organization and interface structure are probably common to most coronavirus nucleocapsid proteins.

AP48

Direct NMR Resonance Assignments of the Active Site Histidine Residue in Serine Protease: The Case of *Escherichia coli* thioesterase/protease I (TEP-I)

Wen-Jin Wu, Sergiy I. Tyukhtenko and Tai-Huang Huang

Institute of Biomedical Sciences, Academia Sinica, Nankang, Taipei, Taiwan 11529, Republic of China

Abstract:

Serine proteases possess the Asp-His-Ser catalytic triad commonly located near the surface of the enzymes. Due to the hydrogen bond interaction and rapid exchange rate with the bulk water, the $N^{\delta1}$ proton of the catalytic Histidine is rather short lived (fast transverse relaxation). Based on its catalytic importance, it is desirable to assign this proton resonance. In this paper, we report the first direct NMR correlation between the short-lived $N^{\delta1}$ proton and its covalently attached $N^{\delta1}$ nitrogen of the catalytic His157 residue in the enzyme Escherichia coli thioesterase/protease I.

AP49

Characterization and structural analyses of nsLTP1 from mung bean

Ku-Feng Lin,[§□] Yu-Nan Liu,[§□] Shang-Te D. Hsu,[‡] Chao-Sheng Cheng,[§] Dharmaraj Samuel,[§] Alexandre M. J. J. Bonvin,[‡] and Ping-Chiang Lyu[§,]

Department of Life Sciences, National Tsing Hua University[§], Hsinchu, Taiwan and NMR Department, Bijvoet Center for Biomolecular Research, Utrecht University[‡], 3584CH, Utrecht, The Netherlands

Abstract

Plant non-specific lipid transfer proteins (nsLTPs) are thermal stable proteins that are capable of transferring lipid molecules between bilayers *in vitro*. This family of proteins, abundant in plants, is proposed to be involved in defense, pollination and germination; the *in vivo* biological function remains, however, elusive. Here we report the purification and sequencing of an nsLTP1 from mung bean sprouts. We have also determined the solution structure of this nsLTP1, which represents the first 3D structure of the dicotyledonous nsLTP1 family. The global fold of mung bean nsLTP1 is similar to those of the monocotyledonous nsLTP1 structures and consists of four α-helices stabilized by four disulfide bonds. There are however some notable differences in the C-terminal tails and internal hydrophobic cavities. Circular dichroism and fluorescence spectroscopy were used to compare the thermodynamics and lipid transfer properties of mung bean nsLTP1 with that of rice nsLTP1. Docking of a lipid molecule into the solution structure of mung bean nsLTP1 reveals similar binding cavities and hydrophobic interactions as in rice nsLTP1 consistent with their comparable lipid transfer properties measured experimentally.

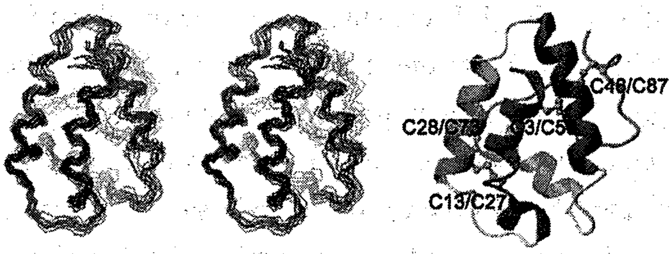

AP50

THE HATH DOMAIN OF HUMAN HEPATOMA-DERIVED GROWTH FACTOR CAN FORM A DOMAIN-SWAPPED DIMER WITH MUCH HIGHER AFFINITY FOR HEPARIN AS CELL INTERNALIZATION

Shih-Che Sue[1], Wei-Tin Lee[1], Jiun-Guo Yu[1], Wen-Jin Wu[1], Szi-chieh Yu[1],Ka-Lou Yu[1], Yu-Chieh Lin[1] , Shao-Chen Lee[2] ,Chia-hui Wang[2], Che-Jen Hsiao[2], Wen-guey Wu[*,2] and Tai-huang Huang[*,1]

[1]Institute of Biomedical Sciences, Academia Sinica, Taipei, Taiwan, R.O.C.;
[2]Institute of Bioinformatics and Structural Biology, College of Life Sciences, National Tsing Hua University, Hsinchu, Taiwan, R.O.C.;

Human hepatoma-derived growth factor (hHDGF) stimulates cell proliferation and is mitogenic for several cell lines. It consists of a well-structured N-terminal HATH domain harboring the heparin-binding site, and a disordered C-terminal domain capable of stimulating DNA synthesis. We investigate the cell internalization mechanism elicited from the N-terminal HATH domain and heparin sulfate on cell surface. We found that the exogenously treated red fluorescence-tagged HATH domain, i.e., HATH-DsRed, was internalized into the cytoplasm of CHO-K1 cell, indicating HATH domain with a cellular function of protein entry. However the entry was abolished when HATH-DsRed was treated to GAG-defective CHO-K1 cells, pgsA-745 cells. The results highlight the importance of the interactions among HTAH domain and heparan sulfate in the internalization process. Furthermore, we identify that the N-terminal HATH domain is capable to form dimeric formation under physiologic conditions to enhance the heparin-binding affinity. The binding of dimer is with two orders of magnitude higher affinity than that of monomer. Biochemical studies are performed to characterize the sequence specificity and optimal binding length of heparin for dimeric HATH domain. NMR chemical shift perturbation and intermolecular NOEs indicate the structural basis of dimer. That HATH-dimer is formed through a domain-swapping mechanism and a proposed structural model is builted to elucidate the heparin-binding enhancement. In final, the detection of HATH-dimer and the discovery of domain-swapping as a mechanism for enhancing heparin binding and for regulating the function of internalization provide new leads for understanding the molecular mechanism of the function of hHDGF.

AP51

Structural basis of the Sso7c4 protein with novel DNA-binding fold from *Sulfolobus solfataricus*

Chun-Hua Hsu and Andrew H.-J. Wang
Institute of Biological Chemistry, Academia Sinica

Sso7c4, a protein of the hyperthermophilic organism *Sulfolobus solfataricus*, has been proposed to play a regulatory role in gene transcription in Archaea. However, very little is known regarding the transcription process in Archaea. And Sso7c4, along with other proteins isolated so far, appears to be the first repressor-like proteins described in this kingdom. The protein is extremely stable to heat, acid and chemical agents. Here we report the structure of Sso7c4 with a novel homodimeric topological DNA-binding fold and show that it forms a swapped-hairpin barrel. Several amide resonances in HSQC spectra of Sso7c4 are shifted and broadened upon addition of small amounts of duplex DNA oligomers. The locations of the corresponding amides in the Sso7c4 structure define the surface that interacts with DNA. 1D NMR spectra of DNA titrated with protein indicated that Sso7c4 interacts with the DNA major groove. In addition, Sso7c4 was successfully crystallized and diffracted by x-ray radiation to high resolution (1.73 Å). Other biophysical methods (CD, SPR, etc.) have been carried out to characterize its DNA binding properties. A model for the Sso7c4-DNA complex consistent with the available structural, biophysical data is presented.

AP52

Insight into the inhibition of human lysozyme amyloidogenesis by camelid antibody binding

Shang-Te D. Hsu[1], Pak-Ho Chan[1], Mireille Dumoulin[1], John Christodoulou[1], Janet R. Kumita[1], Els Pardon[2], Serge Muyldermans[2], Lode Wyns[2], Carol V. Robinson[1], Christopher M. Dobson[1]

[1] Department of Chemistry, University of Cambridge, Lensfield Road, Cambridge CB2 1EW, United Kingdom
[2] Laboratorium voor Ultrastructuur, Department of Molecular and Cellular Interactions, Vlaams Interuniversitair Instituut voor Biotechnologie, Vrije Universiteit Brussel, Pleinlaan 2, 1050 Brussel, Belgium

Many human diseases such as Alzheimer's disease and type II diabetes are attributed to amyloidogenesis of proteins, misfolding of which can lead to deposits of fibril or plaque in various organs and tissues. One example is the non-neuropathic systemic amyloidosis caused by variants of human lysozyme with single point mutations (I56T, F57I, W64R and D67H). It was shown that the I56Tvariant is dynamically and structurally similar to the wild-type human lysozyme. Nonetheless, under physiollogically relevant conditions, I56T exhibits local cooperative and transient unfolding in the beta-domain and C-helix, a feature that is thought to be important for lysozyme amylodosis. A single-domain camelid antibody fragment (cAb-HuL5) raised against wild-type human lysozyme binds the alpha-domain of lysozyme, as identified by chemical shift perturbation mapping and H/D exchange by NMR, and inhibits the in vitro aggregation of the amyloidogenic variants. Using pulse-chase H/D exchange experiment by mass spectrometry, it was found that this particular antibody fragment did not reduce the cooperative unfolding process of I56T protein but instead accelerated it. This antibody fragment does not therefore act as an inihibitor by restoring the global cooperativity that is characteristic of the wild type lysozyme. We therefore aim to characterise changes of lysozyme backbone dynamics upon anitbody binding using NMR spectroscopy in order to elucidate the mechanism by which the antibody is inhibiting the formation of fibrils.

AP53

Solution Structure of UBL Domain in PAPase I, a Novel CTD Phosphatase

Sunggeon Ko, Junghye Huh, Jong-Bok Yoon and Weontae Lee

Department of Biochemistry, College of Science, and Protein Network Research Center, Yonsei University, Seoul 120-749.

Ubiqutin-proteasome pathway is one of the most important cellular processes which participate in cell cycle progression, signal transduction and abnormal protein exclusion. Recently a novel protein, PAPase I (proteasome associated phosphatase I), was discovered from a one-step affinity method to Rpn1 of 19S proteasome in HeLa cell. PAPase I can bind to Rpn 1 in 19S proteasome using Ubiqutin like domain (UBL) located on N-terminal region. C-terminal domain of PAPase I has a phosphatase activity assayed using p-nitrophenyl phosphate which means that Papase I is novel CTD-phosphatase. UBL has a high sequence homology to other ubiqutin proteins and it is related to PAPase I-19S proteasome complex as a bridge which leads to a new proteasome's world. CTD-phosphatase has a transcriptional activity and gene regulation. To identify solution structure and binding mechanism of UBL in Papase I, 13C/15N labeled UBL is overexpressed and purified in recombinant E.coli, BL21 pLys S and executed heteronuclear NMR experiments. There are two helixes and three β-strand structures which are similar to other ubiqutin like proteins. Ubiqutin has a binding activity to proteosome so that make a effect to proteosome's functions. To search what residues of UBL participate in UBL-proteosome complex, we make some mutants of binding partner, Rpn1. There are Rpn 1 mutant containing LRR-like domain which is a binding site to Rad23 is used for chemical shift perturbation assay and ITC experiment. These results show that PAPase I makes recognition for Rpn 1 using UBL domain and 19S proteasome may take a part in CTD phosphatase related proteasome activity regulation.

AP54

Structure and molecular dynamics simulation of antimicrobial peptides from frog

Won-Je Kim[1], Woo-Sung Son[1], Yong-Jin Kim[1], Min-duk Seo[1], Bong-Jin Lee[1]

[1]National Research Laboratory for Membrane Protein Structure, College of Pharmacy, Seoul National University, San 56-1, Shillim-dong, Gwanak-gu, Seoul, Republic of Korea.

we solved the three dimensional structures of several antimicrobial peptides from frog skin using NMR. These peptides consist of 20-46 residues in length and one or two amphipathic α -helical structures. The linear antimicrobial peptides adopt mainly an alpha -helical conformation in trifluoroethanol (TFE) / water solution, dodecylphosphocholine (DPC) and in sodiumdodecylphosphate (SDS) micelles, but adopts flexible random structure in aqueous solution. In molecular dynamics studies the motion of a molecule is simulated as a function of time using AMBER. Important factors on the antimicrobial and hemolytic activity could be obtained from the studies of structure-activity relationship of several antimicrobial peptides. Further structural investigation on these proteins and peptides are able to improve understanding structure-function relationships, which presents important information in the development of new drugs.

AP55

Solution Structures and Anticancer Activities of 11-residue Peptide Analogues Derived from an Antimicrobial Peptide, Gaegurin 5

Hyun-Jung Kim, Min-Duk Seo, Hyung-Sik Won, and Bong-Jin Lee

National Research Laboratory (MPS), College of Pharmacy, Seoul National University, Seoul 151-742, Korea

Abstract

Recently we have developed two antimicrobial peptide analogues with half size in length of the parent molecule, gaegurin 5 [Won, H.-S. et al. (2004) J. Biol. Chem. 279, 14784-14791]. All of the three peptides including gaegurin 5 possess broad spectra of bactericidal activities with no significant toxicity against normal animal cells. In the present work, their anticancer activities and three-dimensional structures were examined. Gaegurin 5 and its 11-residue analogues, named A4W-GGN5^{N11} and V8W-GGN5^{N11}, exhibited reasonable anticancer activities against various cancer cell lines. Solution structures of the A4W-GGN5^{N11} and V8W-GGN5^{N11} peptides in sodium dodecyl sulfate micelles suggested that the peptides would function by selective permeation of bacterial and tumor cell membranes. In particular, the unusual amphipathic axis and the critical tryptophan position could be regarded as important structural factors for their membrane interaction. Altogether, A4W-GGN5^{N11} and V8W-GGN5^{N11}, together with gaegurin 5, are suggested as potential therapeutic agents applicable to pharmaceutical development of new antibiotic and anticancer medicines.

AP56

Structural characterization of urease accessory proteins.

Na Young Sohn, Ji-Hoon Kim, Hyung-Sik Won, Bong-Jin Lee

National Research Laboratory (MPS), College of Pharmacy, Seoul National University, Seoul 151-742, Korea

abstract

Urease activation is critical to the virulence of many human and animal pathogens. Urease possesses multiple, nickel-containing active sites, and UreE, the only nickel-binding protein among the urease accessory proteins activates urease by transporting nickel ions. We performed NMR experiments to investigate the solution structure and the nickel-binding properties of *Bacillus pasterii*(Bp) UreE. The secondary structures and global folds of BpUreE were determined for its metal-free and nickel-bound forms. The results indicated that no major structural change of BpUreE arises from the nickel binding. The C-terminal tail region (Lys141-His147) was confirmed for the first time to be involved in the nickel binding. The conserved sequence in the C-terminal (144GHQH147) was confirmed to have an inherent nickel-binding ability. Altogether, we will discuss the first detailed structural data concerning the nickel-binding properties of intact, wild-type BpUreE in solution. We also performed NMR experiments on the structure of another urease accessory protein, UreG, and the interaction of UreG with UreE. The results showed that there was no particular interaction between the two accessory proteins, neither in the presence of nickel.

AP57

RNA binding modes of *Escherichia coli* RNase P protein

Jae-Sun Shin, Jiyoung Park, Junsang Ko, Seong-Ok Kim, and Byong-Seok Choi

Department of Chemistry, KAIST
373-1 Guseong-dong, Yuseong-Gu, Daejeon 305-701, Republic of Korea

Ribonuclease P (RNaseP) from *Escherichia coli* which consists of RNA (M1) and protein (C5) components removes 5'-leader sequences of tRNA precursors (pre-tRNA). C5 protein directly interacts with 5'-leader sequence of pre-tRNA and is involved in pre-tRNA recognition and catalysis. Besides its role in pre-tRNA processing, C5 protein might participate in other cellular metabolism in that other RNA (w2 RNA) rather than M1 RNA was shown to bind C5 protein with comparable affinity to M1 RNA by *in vitro* selection. In this study, we assigned backbone 1H/13C/15N resonances of C5 protein and examined protein-RNA interactions between C5 protein and pre-tRNA and between C5 protein and w2 RNA by using nuclear magnetic resonance (NMR) spectroscopy in solution. RNA binding modes of two different RNA substrates for C5 protein and their implications will be discussed.

AP58

Structural characterization of the transcription factor BldD, from *Streptomyces coelicolor* A3(2): Domain composition, interdomain interaction, and DNA binding

Hyun-Suk Ko[1], Chang-Jin Lee[2], Sa-Ouk Kang[2], Bong-Jin Lee[3], and Hyung-Sik Won[1]

[1] Department of Biotechnology, Division of Life Sciences, College of Biomedical & Health Science, Konkuk University, Chungju, Chungbuk 380-701, Korea; [2] Laboratory of Biophysics, School of Biological Sciences, Seoul National University, Seoul 151-742, Korea; [3] Research Institute of Pharmaceutical Sciences, College of Pharmacy, Seoul National University, Seoul 151-742, South Korea.

Abstract

BldD is a transcriptional regulator of a Gram-positive soil bacterium *Streptomyces coelicolor*. Although bldD mutant exhibits severe defects in both antibiotic production and morphological differentiation, it is still not clear whether BldD acts as a transcriptional activator or as a repressor. Furthermore, no detailed structural information has been available for BldD, although its C-terminus has been suggested as a putative DNA-binding site. In the present work, we clearly identified the molecular organization and the domain composition of BldD, and the domains were structurally characterized by CD and NMR spectroscopy. The results certified that the protein monomer consists of two structural domains and each domain could be regarded as a single folding unit possessing an independent thermodynamic cooperativity. Strikingly, only the N-terminal domain was responsible for both the dimerization and DNA binding of BldD, while the molecular function of the C-terminal domain remains to be identified. Finally, no or little interaction between the two domains was evidenced both in the DNA-free and DNA-bound states. Altogether, the present results establish the first detailed structural data of BldD and provide fundamental information for its unique and complicated action mechanism in *Streptomyces coelicolor*.

AP59

Studies of Protein Domains in the Transacylase Component of Human Mitochondrial Branched-Chain Ketoacid Dehydrogenase

Chi-Fon Chang[1], Yi-Jan Lin[2], Hui-Ting Chou[3], Max Wynn[4], David T. Chuang[4], Tai-Huang Huang[1,3]

[1]*Gemomics Research Center, Academia Sinica, Taipei 11529, Taiwan*
[2]*RIKEN Genomic Sciences Center, Yokohama 230-0045, Japan*
[3]*Institute of Biomedical Sciences Academia Sinica, Taipei 11529, Taiwan*
[4]*Dept of Biochemistry, U. of Texas Southwestern Medical Center, Dallas, Texas, U.S.A.*

The transacylase (E2) subunit of the branched-chain α-ketoacid dehydrogenase (BCKD) complex carries three independently folded domains which are linked together by flexible loops: The amino-terminal lipoyl-bearing domain (hbLBD, 1-84), the interim E1/E3-binding domain (hbSBD,104-152), and the carboxy-terminal inner-core domain. The hbLBD and hbSBD play central role in substrate channeling and substrate recognition. We have employed multidimensional heteronuclear NMR techniques to determine the structure and dynamics of three truncated fragments of the human BCKD complex: the hbLDB (a.a. 1-84), hbSBD (a.a. 104-152) and a di-domain (hbDD) comprising residues 1 – 168 of the E2 component. Solution structures of hbLBD and hbSBD have been determined. NMR results showed that solution structures of hbLBD and hbSBD determined in separate fragments are indistinguishable from that in hbDD. Analysis of backbone ^{15}N-T_1, ^{15}N-T_2 and ^{1}H-^{15}N-NOE relaxation data of hbDD showed the linker region is highly flexible. Together with the isothermal calorimetric titrations data, interactions between hbDD and branched-chain α-ketoacid decarboxylase (E1) or dihydrolipoamide dehydrogenase (E3) will be discussed.

AP60

Solution Structure and Dynamics of YKR049C, a Putative Redox Protein from *Saccharomyces cerevisiae*

Jin-Won Jung [1,3], Chul-Jin Lee[1,3], Adelinda Yee [2,3], Bin Wu[2,3], Cheryl H. Arrowsmith [2,3] and Weontae Lee [1,3*]

[1]Department of Biochemistry and Protein Network Research Center, Yonsei University, 134 Shinchon-Dong Seodaemoon-Gu, Seoul, Korea 120-749
[2]Ontario Cancer Institute and Department of Medical Biophysics, University of Toronto, 610 University Avenue, Toronto, ON, Canada, M5G 2M9
[3]Northeast Structural Genomics Consortium

YKR049C is a mitochondrial protein from *Saccharomyces cerevisiae* and conserved among yeast species including *Candida albicans*. However, no biological function for YKR049C has been ascribed based on its primary sequence information. In the present study, NMR spectroscopy and protein dynamics studies were used to determine the putative biological function of YKR049C based on its solution structure. YKR049C shows a well-defined thioredoxin fold with a unique insertion of helices between two β–strands. The central β–sheet divides the protein into two parts; a unique face and a conserved face. The 'unique face' is located between β2 and β3. Interestingly, the sequences most conserved among YKR049C families are found on this 'unique face', which incorporated L109 to E114. The side chains of these conserved residues interact with residues on the helical region with a stretch of hydrophobic surface. A putative active site composed by two short helices and a single Cys97 was also well observed. Our findings suggest that YKR049C is a redox protein with a thioredoxin fold containing a single active cysteine.

AP61

NMR and structural studies of a putative polyketide synthesis protein XC5357 from a plant pathogen Xanthomonas campestris

K.-H. Chin, C.-L. Zhu, S.-H. Chou

Institute of Biochemistry, National Chung-Hsing University, Taichung, 40227, Taiwan

Abstract

Microorganisms and plants synthesize a large variety of polyketide metabolites, many of which are medically important antibiotics or exhibit other pharmacological, such as antibacterial, antivirals, or antitumor activities. Tetracenomycin (TCM) C is a cytotoxic antibiotic produced by *Streptomyces glaucescens* and is notable for its broad activity against actinomycetes. Its synthesis is currently one of the models for the antibiotic production in *Streptomyces* species, and a model for the Tcm PKS catalyzed synthesis of the TCM C has also been set up. Reconstitution experiment of the PKS for TCM F2, a precursor of TCM C, suggests that the active PKS complex consists of at least four major proteins, including the Tcm*K*. –*L*, -*M*, and –*N* gene products. Tcm*J* is also one of the components of the PKS complex, but its function is currently unknown, although its addition to the Tcm*KLMN* complex can greatly increase the production of TCM F2 by nearly fourfold.

XC5357 from a local plant pathogen *Xanthomonas campestris* pv. *campestris* str. 17 is annotated as a polyketide synthesis protein from a bioinformatics approach. It consists of 113 amino acids, and shares a 32 % identity (55% similarity) with the Tcm*J* protein in the *Streptomyces glaucescens*. Until now, no tertiary structure for the Tcm*J*-like proteins has been reported. In the present manuscript, we report the nearly complete ^{1}H, ^{15}N assignment and ^{13}C assignment of XC5357 based on a suite of 2D and 3D-heteronuclear NMR spectra. The preliminary XC5357 structure has also been refined using the CYANA program against a bundle of 3D ^{15}N- and ^{13}C-edited NOESY spectra.

AP62

Solution Structure and Structural Characterization of Selective Melanocortin Receptor Antagonists

Chul-Jin Lee[1] , Song-Zhe Li[2], Sung-Kil Lim[2], Ja-Hyun Baik[3] and Weontae Lee [1]
[1] Department of Biochemistry and HTSD-NMR & Application National Research Laboratory, College of Science, Yonsei University, Seoul 120-740 Korea, [2] Department of Internal Medicine, College of Medicine, Yonsei University, Seoul, 120-749, Korea, [3]School of Life Science and Biotechnology, Korea University, Seoul, 136-701, Korea

The melanocortin receptors are involved in many physiological functions, including pigmentation, sexual function, feeding behavior, and energy homeostasis, making them potential targets for drugs to treat obesity, sexual dysfunction, etc. The melanocortin subtype-4 receptor (MC4R) is expressed in various regions of the brain, and the MC4R is involved in the modulation of food intake Thus, the MC4R has been recognized as a drug target controlling the food intake. Cyclic peptides SHU9119 (Ac-Nle-*c*[Asp-His-D-Nal(2')-Arg-Trp-Lys]-NH2) and JKC363(*c*[Mpr-Glu-His-D-Nal(2')-Arg-Trp-Gly-Cys]-Pro-Pro-Lys-Asp-NH_2) are known as potent antagonists of the melanocortin receptors. SHU9119 is non-selective antagonist, while JKC363 is selective antagonist of MC4R. Using nuclear magnetic resonance (NMR) spectroscopy, we have determined the solution structures for these potent agonists for the human melanocortin-4 receptor. Computational automated docking and molecular dynamics simulations of these cyclic peptides based on homology molecular model of the hMC4R, were performed. A complex structure of hMC4R-JKC363 was compared with that of a hMC4R-SHU9119 in attempts to identify a selective conformation of cyclic peptide. The His3 residue of JKC363 has a unique orientation compared with that of SHU9119, suggesting that the mechanism of JKC363 selective antagonism at the MC4R may be attributed to the difference of the His3 at the binding mode between JKC33 and SHU9119.

AP63

Structural and Functional Characterization of a Telomere Binding Protein, NgTRF1 Derived from *Nicotiana glutinosa*

Heeyong Park[1], Sunggeun Ko[1], Hansol Bae[2], Woo Taek Kim[2] and Weontae Lee[1]

[1]Department of Biochemistry and HTSD-NMR & Application National Research Laboratory, College of Science, Yonsei University, Seoul, Korea, [2]Department of Biology, Yonsei University, Seoul, Korea

Telomeres are vital for preserving chromosome integrity during cell division. Several genes encoding potential telomere-binding proteins have recently been identified in plants. NgTRF1 have been assumed to be double-stranded telomeric repeat binding factor of *Nicotiana glutinosa*, a diploid tobacco plant. However, its function and regulation mechanism is not much known. We designed two constructs that contain Myb-like domain and these proteins were identified as a symmetric dimer based on data from FPLC, cross-linking and NMR. The NMR structure provides us an effective function and binding mechanism to consensus double stranded telomere DNA. To determine the solution structures of NgTRF1, we use multidimensional heteronuclear NMR techniques and structure calculation by Cyana 2.1. The residues involved in DNA binding have been identified from HSQC peak perturbation, and confirmed by EMSA assay. Our data suggests that DNA binding mechanism and binding specificity of plant telomere binding proteins are quite different from those of human telomere binding proteins.

AP64

NMR Studies on Integrase Interactor1/hSNF5

Hyun-Seob Jung, Jin-Won Jung, Joon Shin and Weontae Lee

Department of Biochemistry and HTSD-NMR & Application National Research Laboratory, Yonsei University, Seoul, Korea

Retroviral integrase (IN) catalyzes the integration of retroviral cDNA into host chromosome. Ini1(integrase interactor 1) is a host protein that specifically binds and stimulates *in vitro* joining activity of IN. Ini1 has sequence homology with yeast transcription factor SNF5 and it is a component of the analogous mammalian SWI/SNF complex which could be involved in chromatin remodeling. IN protein also binds to only one of two repeat motifs in the conversed region of INi1. We determined that the specific repeat1 domain (RPT1) of INi1 interacts the swirm domain of a core subunit SWI/SNF complex called SRG3 and confirmed by mass spectrometry. We have initiated the structural study of RPT1 and the binding mechanism with swirm domain by NMR spectroscopy. NMR datas were acquired HNCACB, CBCA(CO)NH and HNCA for backbone resonance assignment and HNCO, (H)CCCO(NH) and H(CC)(CO)NH for side chains. NMR data was used to identify the interface and binding residues of the rpt1 with the swirm domain. The structure, function and interaction mode of RPT1 in the presence of swirm domain will also be discussed.

AP65

Solution Structure of Modified Human Parathyroid Hormones: Towards Minimal and Potent Ligand Design for Receptor Activation

Suhyun Ma[1], Ahrim Yoo[2], Sung-Kil Lim[3] and Weontae Lee[1]

[1]Department of Biochemistry and Protein Network Research Center, HTSD-NMR & Application National Research Laboratory, College of Science, Yonsei University, Seoul, Korea, [2]Department of Chemical and Biological Engineering, Korea University, Seoul, Korea, [3]Department of Internal Medicine, School of Medicine, Yonsei University, Seoul, Korea

Parathyroid hormone (PTH) which increases bone formation and the number of osteoblasts plays physiologically important roles in calcium homeostasis and bone remodeling by activating PTH receptor 1(PTHR1). To determine potent and minimal structural domain, we modified several residues which is considered as important to receptor activation. Based on previous studies, we substituted several amino acids to unnatural amino acids with long sidechain. In vitro cAMP signaling activities for analogue peptides were measured. Solution structure of analogue peptides in 30% TFE solution was determined using NMR spectroscopy. CD and NMR spectrum of these peptides show a typical helical conformation in 30% TFE solution. The substitution of Arg^{11} by homoarginine increases the cAMP formation and the substitution of same position by homophenylalanine shows more positive effects. These findings suggest that PTH peptide with N-terminal long sidechain, especially with benzene ring, binds stronger with receptor. To verify the pattern of optimal binding mode, we generated complex structures of peptide and receptor using molecular dynamics simulation. Our data will provide the minimal structural domain of PTH and give insights on osteoporosis drug design.

AP66

Solution Structure and Dynamics of the Domain III of the JEV and DENV Envelope Proteins

Jya-Wei Cheng, Chih-Wei Wu, Yi-Ting Lin, Ya-Ping Tsao, Kuo-Chun Huang, and Suh-Chin Wu

Institute of Biotechnology and Department of Life Science, National Tsing Hua University, Hsinchu, 300, Taiwan.

The flavivirus envelope protein is the dominant antigen in eliciting neutralizing antibodies and plays an important role in inducing immunologic responses in the infected host. We have determined the solution structure and dynamics of the major antigenic domain (domain III) of the Japanese Encephalitis Virus (JEV) and Dengue Virus (DENV) envelope proteins. The JEV and DENV domain III forms a β-barrel type structure composed of six antiparallel β-strands resembling the immunoglobulin constant domain. We have also identified epitopes of the domain III to its neutralizing antibody by chemical shift perturbation measurements. Site-directed mutagenesis experiments are performed to confirm the NMR results. Our study provides a structural basis for understanding the mechanism of immunologic protection and for rational design of vaccines effective against flaviviruses. (NSC93-2113-M-007-002, NSC93-3112-B-007-012, and 89-B-FA04-1-4)

AP67

Structure of Human Growth Inhibitory Factor-Metallothionein-3

Hui Wang[‡], Bin Cai[¶], Hongyan Li[‡], Zhong-Xian Huang[¶*] and Hongzhe Sun[‡*]
[‡]*Department of Chemistry and Open Laboratory of Chemical Biology, The University of Hong Kong, Pokfulam, Hong Kong; and* [¶]*Department of Chemistry, Fudan University, Shanghai, P. R. China*

Alzheimer's disease (AD) is characterized by progressive loss of neuron accompanied by the formation of intraneural neurofibrillary tangles and extracellar amyloid plaques.[1] Human neuronal growth inhibitory factor (GIF), classified as metallothionein-3 (MT-3), was found to promote cortical neuron survival and dendrite outgrowth in the cell culture studies.[2] Different from its two isoforms of MT-1/MT-2, MT-3 is likely to serve as intracellular distributors and mediators for zinc in the central nervous system.[3,4] We have examined the uptake and release of Zn^{2+} (and Cd^{2+}) from the protein and found to be different from that of MT-1 and MT-2.[5] However, the structure of the human MT-3 still remains unknown.

We expressed and purified ^{15}N-labeled human MT-3., the solution structure of α-domain of human MT-3 (residue 32-68) was determined by NMR spectroscopy with simulated annealing calculations. Similar to mouse MT-3, the human protein also shows two metal-clusters with the β-domain exhibiting more rapid internal dynamics compared to MT-1 and MT-2. Out data revealed that a longer loop in the acidic hexapeptide insertion presents although the overall folding of the human MT-3 in the α-domain being similar to mouse MT-3.[6] The dynamics of the protein was also investigated by NMR. Surprisingly, the ^{15}N relaxation analysis with the selected residues in the β-domain showed that the dynamics of in the β-domain is similar to that of α-domain.

We thank the NSFC/RGC, Area of Excellence of UGC and the University of Hong Kong for support!

References:

1. Selkoe DJ (1991) *Neuron* **6**, 487-498.
2. (a) Erickson JC, Sewell AK, Jensen LT, Winge DR, Palmiter RD (1994) *Brain Res.* **649**, 297-304;
(b) Palmiter RD, Findley SD, Whitmore TE, Durnam DM (1992) *Proc. Natl. Acad. Sci. U.S.A.* **89**, 6333-6337
3. Vasak M, Hasler DW (2000) *Curr. Opin. Chem. Biol.* **4**, 177-183.
4. Masters BA, Quaife CJ, Palmiter RD et al (1994) *J. Neurosci.* **14**, 5844-5857.
5. Zheng Q, Yang WM, Yu WH, Cai B, Teng XC, Xie Y, Sun H, Zhang MJ, Huang ZX (2003) *Protein Engn.* **16**, 865-870.
6. Öz G, Zangger K, Amitage IM (2001) *Biochemistry* **40**, 11433-11441.

AP68

Solution Structures and Dynamics of the Sterile α Motif (SAM) Domain of the Deleted in Liver Cancer 2 (DLC2): a Monomeric Structure with Membrane-binding Properties

Hongzhe Sun,[†,*] Hongyan Li,[†] King-Leung Fung,[†] Dong-Yan Jin,[§] Stephen SM Chung,[#] Yick-Pang Ching,[§] Irene Oi-lin Ng,[¶] Kong-Hung Sze,[‡] Ben CB Ko[†,*]

[†]Department of Chemistry and Open Laboratory of Chemical Biology, Department of [§]Biochemistry, [#]Physiology and [¶]Pathology, The University of Hong Kong, Pokfulam, Hong Kong, P. R. China.

The Deleted in Liver Cancer 2 (DLC2) gene encodes a Rho GTPase-activating protein (GAP) with growth suppressor function. In addition to the RhoGAP domain, this molecule also contains a sterile α motif (SAM) and a lipid-binding StAR-related lipid-transfer (START) domain. To gain insight on the function of DLC2, we have expressed and purified a recombinant $^{13}C/^{15}N$ doubly-labeled DLC2 SAM domain. The three-dimensional solution structure and dynamics of the SAM domain of DLC2, DLC2-SAM, was investigated by NMR spectroscopy together with molecular dynamic simulated annealing. We showed that DLC2-SAM is distinct from all other known SAM domains by the presence of a four-helix bundle. The spatial arrangement of this bundle composed of four α-helices is also unique. Although it has been shown that some members of the SAM domain family can form dimers and oligomers, both NMR and biochemical analyses indicated that DLC2-SAM exists as a monomer in solution. We also examined the interaction of DLC2-SAM domain with sodium dodecyl sulfate (SDS) micelles by NMR and CD spectroscopic techniques. 2D [^{1}H,^{15}N] HSQC spectra of DLC2-SAM in the presence of SDS displayed shifts of most residues although still well dispersed, in agreement with slightly decreased α-helical content based on CD spectra of DLC2-SAM in the absence and presence of SDS, suggesting that DLC2-SAM may interact with membrane lipids *in vivo* with secondary structure changes of the protein. Finally, we demonstrated that DLC2-SAM is dispensable for the self association of full-length DLC2 *in vivo*.

This project was supported by the Area of Excellence of UGC and the University of Hong Kong.

NP69

NMR study of the specific interaction of human TRF1 with telomeric DNA

Shin Morita[1], Yuuka Hirao[1], Hideyasu Okamura[1,2], and Yoshifumi Nishimura[1]
[1]Yokohama City University, Graduate School of Supramolecular Biology, 1-7-29,Suehiro-cho, Tsurumi-ku, Yokohama, 230-0045, Japan, [2]Kihara Memoriaru Yokohama Foundation for the Advancement of Life Science, 1-7-29, Suehiro-cho, Tsurumi-ku, Yokohama, 230-0045, Japan,

Telomeres are the ends of eukaryotic linear chromosomes that protect from end-to-end fusion and nuclease degradation. In human, the telomeric DNA is typically composed of 5-15 kb of double-stranded DNA with tandem repeats of the guanine-rich sequence TTAGGG and single-stranded DNA with a 3'-end overhang necessary to ensure complete chromosomal DNA replication. The telomeric DNA is packaged by two DNA binding proteins, hTRF1 and hTRF2, both of which play an important role in the negative regulation of the elongation of telomeres. It is well known that the single-stranded G-rich telomeric repeats are able to assemble into four-stranded quadruplex structures (Fig. 1). The activity of the telomerase was inhibited by quadruplex structures which stabilised by monovalent cation. Recently, we have found that hTRF2 DNA binding domain, hTRF2-DBD can bind to a parallel quadruplex structures of human telomeric DNA formed by K^+ ion in vitro. However, the biological significance was not possible to judge from this result.

In this study, we have examined the structure of the human antiparallel quadruplex of the telemoeric DNA bound to hTRF1-DBD by NMR and CD and compared with the results that previously reported[(1)]. Telomeric oligonucleotide, tr22 (d(AGGG(TTAGGG)$_3$)) was dissolved in 50mM buffered solution containing 100mM sodium chloride (pH 6.8), and annealed in a water bath. To investigate the structure of the annealed tr22, CD spectra was observed. The spectra showed the strong positive peak at about 295nm, followed by negative peak at about 260nm. From the result, it is proven that tr22 formed the antiparallel structures.

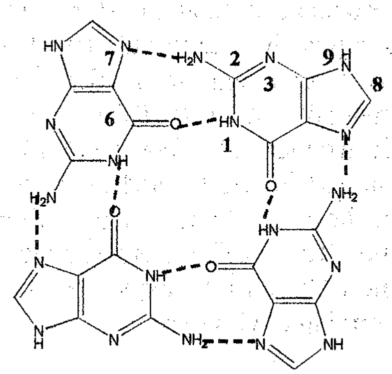

Fig.1 structure of quadruplex core

In the NMR experiments, signals of quadruplex were assigned by the ^1H-^{15}N HSQC,NOESY,^1H-^{13}C ct-HSQC,HCCH-COSY,HCCCH-COSY,HCCCCH-COSY,HCCCCCH-COSY,HCN,HCNCH experiments using Bruker AVANCE-600MHz spectrometer with a cryo probe. The interaction of TRF1-DBD and the quadruplex structure will be investigated using various NMR measurements. Then, the result will be compared with hTRF2-DBD result.

(1) Yuuka Hirao, et al., 43th NMR symposium (Tokyo, Japan)

AP70 (PL12)

NMR structural analysis of the CGG / CGG containing DNA complexed with the recognition drugs

Makoto Nomura[1], Shinya Hagihara[2,4], Yuki Goto[2], Kazuhiko Nakatani[2,3,4] and Chojiro Kojima[1]

[1]Graduate School of Biological Science, Nara Institute of Science and Technology, Nara 630-0101, Japan and [2]Department of Synthetic Chemistry and Biological Chemistry, Graduate School of Engineering, Kyoto University, Kyoto 618-8510, Japan and [3]PRESTO, Japan Science and Technology Agency and [4]The Institute of Scientific and Industrial Research, Osaka University, Osaka 567-0047, Japan

Fragile X syndrome is caused by fragile X mental retardation (FMR1) gene. Its mechanism of onset is the gene silencing of CGG trinucleotide repeats in the 5' untranslated region of exon 1. In the case of the expansion exceeds 200 threshold, the CpG is methylated and the gene expression is suppressed. The absence of the FMR1 gene product leads to the syndrome. Thus, in the viewpoint of diagnosis of fragile X syndrome, the quick detection technology of the frequency of CGG repeats is required. The naphthyridine dimer (**ND**) has been developed as the CGG / CGG recognition drug. However, the detail of the recognition mechanism is not known.

Our study aims to understand the recognition mechanism by the determination of the 3D structures of CGG/CGG containing DNA complexed with the recognition drugs. The **ND** titration experiment to 2.5 mM d(CTAACGGAATG) / d(CATTCGGTTAG) duplex was carried out monitoring the imino-proton region. The peak shifts were saturated at the **ND** concentration 5.0mM. These results showed the 1:2 complex was formed. The ^{1}H-^{1}H NOESY spectra of the 1:2 complex were recorded with 30, 200 and 300msec mixing times. TOCSY, DQF-COSY and natural abundance ^{1}H-^{13}C spectra were also recorded to complete the resonance assignment. Proton resonances were completely assigned including H5' and H5". The distance restraints were obtained from the complete relaxation matrix method, MARDIGRAS, and the 3D structure was determined. The four naphtyridine rings of two **NDs** were stacked in and formed hydrogen bonding to four G bases in the CGG / CGG region. Surprisingly, two C bases in the CGG / CGG were flipped out. Thus **ND** recognized the CGG / CGG sequence by the stacking and hydrogen bonding to G bases.

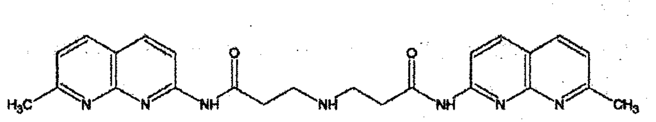

naphthyridine dimer (**ND**)

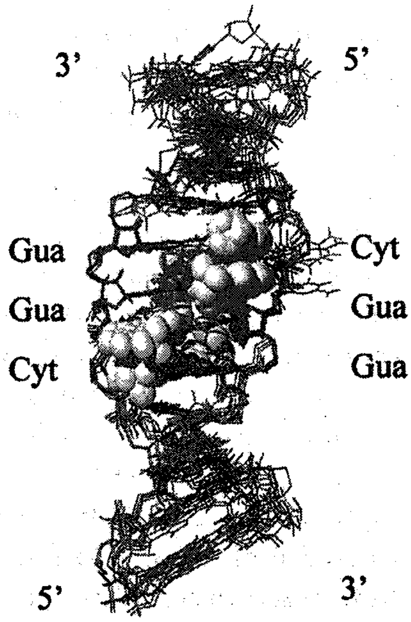

Figure 1. The chemical structure of **ND** (left) and the NMR structure of CGG/CGG containing DNA d(CTAACGGAATG) / d(CATTCGGTTAG) complexed with the two **NDs** (right).

AP71

NMR spectral analyses of three structural isomers of disubstituted – β -cyclodextrins by glucose groups and their inclusion phenomena

Yu Tsutsumi[1,2], Yasuko Ishizuka,[1] and Hiroshi Nakanishi [1,2] *

1) Biological Information Research Center and Research Center for Compact Chemical Process*; National Institute of Advanced Industrial Science and Technology, Tsukuba Central 5, 1-1-1, Higashi, Tsukuba, Ibaraki, 305-8565, Japan

2) Department of Biological Science and Technology, Tokyo University of Science, 2641 Yamazaki, Noda, Chiba 278-0022 Japan

It was very difficult to analyse ^{1}H NMR spectra of saccharide substituted cyclodextrins because of their heavily overlapped signals. We tried these analyses by using higher field magnet of 800 MHz NMR spectrometer. Various kinds of one and two dimensional NMR spectra of three β -cyclodextrins substituted by two glucose groups at 1,2-, 1,3-, and 1,4-positions in the CD ring were measured. It was found that several proton signals of nine glucose residues in these cyclodextrin compounds are split with each others among the three positional isomers and it was expected to lead to the complete proton signal assignments. The heavily overlapped proton NMR signals were analyzed in details and almost complete assignments of the signals of nine glucose groups were made. The results of the ^{1}H NMR analyses indicate that the structures of the CD rings of the three positional isomers are delicately different from each other and there is an inter-residual interaction between two branch glucose residues in 1,2-diglucose substituted β-cyclodextrin.

The analyses of inclusion phenomena between these cyclodextrins and phloridzin were performed by using these assigned proton signals of three structural isomers. Importent knowledges were obtained about the specific mechanism of inclusion phenomena between the CD isomers and phloridzin.

AP72

Application of ultra-high magnetic field to saccharide molecules: ^{1}H NMR spectra of glycosyl α-CD and glycosyl β-CD

Yasuko Ishizuka [1, 2] Kenji Takasugi [3] 、Yu Tsutsumi [2, 4], Kenji Kanazawa [2], Tadashi Nemoto [2]、Tsukasa Kiyoshi [5], and Hiroshi Nakanishi [2,4,6] *

1) Research Center for Glycoscience, National Institute of Advanced Industrial Science and Technology (AIST), Tsukuba Central 6, 1-1, Higashi, Tsukuba, Ibaraki 305-8566 Japan: 2) Biological Information Research Center, AIST, Tsukuba Central 6, 1-1, Higashi, Tsukuba, Ibaraki 305-8566 Japan: 3) JEOL Ltd. 1-2 Musashino 3-Chome, Akishima, Tokyo 196-8558, Japan: 4) Department of Biological Science and Technology, Tokyo University of Science, 2641 Yamazaki, Noda, Chiba 278-0022 Japan: 5) Tsukuba Magnet Laboratory, National Institute for Materials Science, 3-13 Sakura, Tsukuba, Ibaraki 305-0003, Japan: *6) Research Center for Compact Chemical Process, AIST, Tsukuba Central 5, 1-1-1, Higashi, Tsukuba, Ibaraki 305-8565 Japan

To analyze of ^{1}H NMR spectra of saccharide molecules are often very difficult work, because they show heavily overlapped spectral patterns. To conquer this NMR problem, we performed to analyze complex ^{1}H NMR spectra by using ultra-high magnet (920 MHz) spectrometer.

^{1}H NMR spectra of glycosyl α-CD and glycosyl β-CD, whose CD ring is constituted by six and seven only glucose residues, respectively were recorded on a spectrometer equipped with a 21.8 T magnet. An ultra-high magnetic field was effective for detecting the ^{1}H NMR signals with small differences in chemical shifts. It was found that the introduction of a glucose group to the CD ring as a branch residue caused deformation of the CD ring and gave some separate signals of equilibrated glucose residues.

Y. Ishizuka, K. Takasugi, Y.Tsutsumi, K. Kanazawa, T. Nemoto, T. Kiyoshi, H. Nakanishi, Carbohydr, Res., 340, 1343-1350 (2005).

NP73

Solution structure of the LIM domain of human CLP-36 protein

○Xu-rong Qin[1], Fumiaki Hayashi[1], Mikako Shirouzu[1,2], Takaho Terada[1,2], Takanori Kigawa[1], Makoto Inoue[1], Takashi Yabuki[1], Masaaki Aoki[1], Eiko Seki[1], Takayoshi Matsuda[1], Hiroshi Hirota[1], Mayumi Yoshida[1], Akiko Tanaka[1], Shigeyuki Yokoyama[123]
(RIKEN GSC[1]、RIKEN Harima Institute[2] and University of Tokyo[3])

Human CLP36, a cytoskeleton-associated protein, binds to alpha-actinin-1 and associates with actin filaments and stress fibers in activated platelets and endothelial cells. Through the binding, CLP36 could modulate the function of alpha-actinin-1, such as increasing its actin crosslinking and bundling activities.

CLP36 contains a N-terminal PDZ domain, a large intervening sequence, and a C-terminal LIM domain. We have determinded the structure of the LIM domain of CLP36 protein with NMR.

The folding topology retains both independent zinc binding modules (CCHC and CCCH). Each module consists of two antiparallel beta-sheets, and the CCCH module is terminated by an alpha-helix (Figure a and b). The two zinc fingers pack together via a hydrophobic interface formed by conservatively substituted residues.

By comparing with several other LIM domains which we have solved, we found some common structural characters in the LIM domain. We will discuss it in detail.

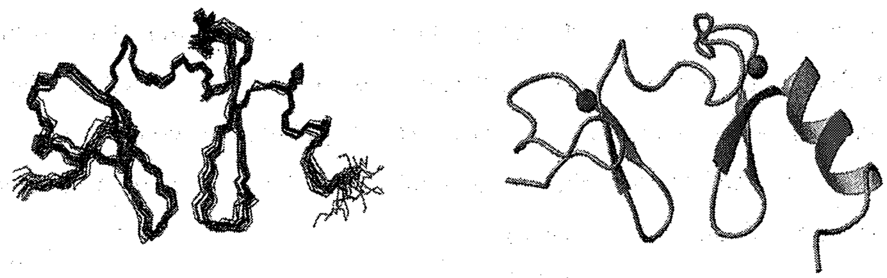

Fig. Superposition of 20 calculated structures (a) and ribbon diagram (b) of the LIM domain of CLP36 protein

NP74

Human Structure Proteomics: Solution Structure of the RGS Domain of Human Regulator of G-protein Signaling 5 (RGS 5)

○Huiping Zhang[1], Fumiaki Hayashi[1], Mikako Shirouzu[1,2], Takaho Terada[1,2], Takanori Kigawa[1], Makoto Inoue[1], Takashi Yabuki[1], Masaaki Aoki[1], Takayoshi Matsuda[1], Eiko Seki[1], Hiroshi Hirota[1], Mayumi Yoshida[1], Akiko Tanaka[1], Sumio Sugano[3], Shigeyuki Yokoyama[1,2,4]

([1]RIKEN GSC; [2]RIKEN Harima Institute; [3]The Institute of Medical Science, The University of Tokyo and [4]Graduate School of Science, The University of Tokyo)

Regulator of G-protein signaling 5 (RGS5) belongs to the small RGS protein subfamily and has been abundantly found in cardiac blood vessels. The protein is composed of 181 amino acids and contains a conserved approximately 120 amino acids domain (RGS domain), which is responsible for interaction with G-α subunits of heterotrimeric G-protein. Recently, it has been demonstrated that RGS5 plays a role in active vessel remodeling during neovascularization. A structural and functional analysis of RGS5 may be important for searching a target of antiangiogenic therapy.

We determined the solution structure of the RGS domain from human RGS5 by using multidimensional NMR spectroscopy and CYANA calculation. As a result of structural analysis, the RGS domain corresponds to an array of nine α-helices that fold into two small subdomains (Figure 1). The terminal subdomain contains the N and C-termini and is formed by α1, α2, α3, α8 and α9. The large bundle subdomain, formed by α4, α5, α6 and α 7, is a classic right-handed, antiparallel four-helix bundle. In this presentation, we will describe the structural detail of hydrophobic core and binding site, and discuss relationship between structure and function by comparing with other RGS families.

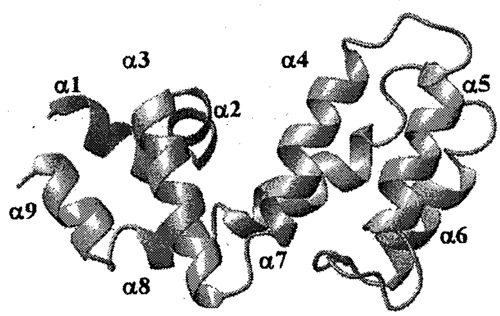

Fig. 1 Ribbon diagram of the RGS domain

NP75

Solution structure of the two CUT domains of SATB2

○Kyoko Inoue[1], Toshio Nagashima[1], Fumiaki Hayashi[1], Mikako Shirouzu[1,2], Takaho Terada[1,2], Takanori Kigawa[1], Makoto Inoue[1], Takashi Yabuki[1], Masaaki Aoki[1], Takayoshi Matsuda[1], Eiko Seki[1], Hiroshi Hirota[1], Mayumi Yoshida[1], Akiko Tanaka[1], Osamu Ohara[3,4], Shigeyuki Yokoyama[1,2,5]
([1]RIKEN Genomic Sciences Center, [2]RIKEN Harima, [3]RIKEN RCAI, [4]Kazusa DNA Research Institute, [5]Graduate School of Science, University of Tokyo)

The DNA binding protein SATB2 (Special AT-rich sequence-binding protein 2) which express in brain, kidney and pre-B cells has been identified as a gene mutated in human patient with cleft palate. It binds to the MARs (nuclear matrix attachment regions) of the endogenous immunoglobulin μ locus in pre-B cells and enhances gene expression.

SATB2 contains two CUT repeats at the N-terminal side of homeodomain. The CUT domain is a DNA-binding motif which can bind independently or in cooperation with the homeodomain. CUT domain containing proteins always accompany a homeodomain at the C-terminal side of a CUT domain or CUT repeats, and can be grouped according to the number of CUT repeats, HNF-6 has one CUT, SATB2 has two CUT repeats and Cux-2 has three. In order to characterize the CUT domain and its role in SATB2, we have undertaken a structural and functional study of the CUT domain from the KAZUSA Homo sapience cDNA library.

We determined the solution structures of the two CUT domains by using heteronuclear multidimensional spectroscopy and CYANA calculation. The solution structure of the CUT domains is basically composed of a helix bundle with four α-helices. Comparison with the structure of the CUT domain of HNF-6 (Hepatocyte nuclear Factor-6), both of our two CUT domains have an additional α-helix at the C-terminal end.

We will discuss structural detail by comparing structures and sequences among sub-families.

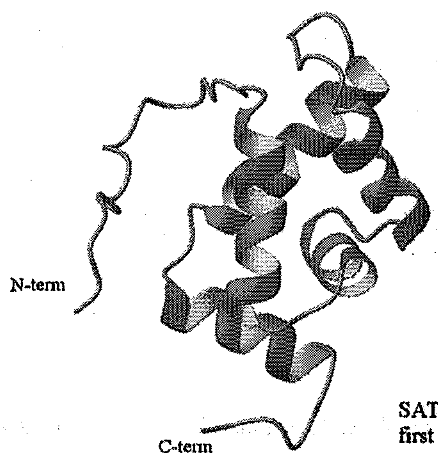

SATB2
first CUT domain

NP76

Structural and Functional analysis of MSP domains

○Hiroshi Endo[1], Fumiaki Hayashi[1], Mayumi Yoshida[1], Mikako Shirouzu[1,2], Takaho Terada[1,2], Takanori Kigawa[1], Makoto Inoue[1], Takashi Yabuki[1], Masaaki Aoki[1], Takayoshi Matsuda[1], Eiko Seki[1], Hiroshi Hirota[1], Akiko Tanaka[1], Yoshihide Hayashizaki[1], Shigeyuki Yokoyama[1,2,3]
(RIKEN GSC[1], RIKEN Harima Institute[2], Graduate School of Science, The University of Tokyo[3])

Motile Sperm Protein (MSP) was initially found in the amoeboid sperm cell of nematodes. It plays a unique but a major role in amoeboid cell locomotion by controlling the polymerization states of MSP dimer just like actin fiber in a usual cell. The progress in genome characterization reveals that higher organisms like human and mouse also have an MSP like sequence as a part of several membrane anchored proteins. MSP domain is relatively rare protein component but is ubiquitously expressed in the various kind of cells. Although apparent function of MSP domain has not been characterized, the MSP domain containing proteins tends to localize to intracellular vesicles of ER and Golgi-apparatus and to the microtubules at tight junction. This fact suggests that MSP containing protein might be related to the polar vesicle transport from ER or Golgi-apparatus to plasma membrane. In order to elucidate the structure and function of non-cytoskeletal MSP domain, we have carried out the three dimensional structural studies of two MSP domains of MSP containing 2 and VAP-A protein from RIKEN mouse cDNA library.

NMR spectral analysis was performed by using multi-dimensional heteronuclear spectroscopy and CYANA was used for structural caliculation. The global structure of the non-cytoskeletal MSP domains resemble that of the cytoskeletal type MSP protein closely but were monomer in the solution unlike the skeletal MSP protein. We will discuss the structural detail of the two MSP domains and compare them with cytoskeletal MSP protein structures.

Ribbon diagram of MSP domain of MSP containing 2

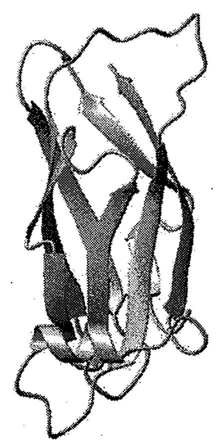

Ribbon diagram of MSP domain of VAP-33

NP77

Structural and Functional analysis of immunoglobulin like domains

○Reiko Hatta[1], Fumiaki Hayashi[1], Kayoko Nagashima[1], Chisato Kurosaki[1], Xu-rong Qin[1], Mayumi Yoshida[1], Mikako Shirouzu[1,2], Takaho Terada[1,2], Takanori Kigawa[1], Makoto Inoue[1], Takashi Yabuki[1], Masaaki Aoki[1], Takayoshi Matsuda[1], Eiko Seki[1], Hiroshi Hirota[1], Akiko Tanaka[1], Osamu Ohara[3,4], Shigeyuki Yokoyama[1,2,5]
(RIKEN GSC[1], RIKEN Harima Institute[2], RIKEN RCAI[3], 4 KAZUSA DNA Institute[4], Graduate School of Science, The University of Tokyo[5])

Immunoglobulin (Ig) and Ig-like domains form a family of the major domains found in variety of proteins related to cell adhesion, cell surface receptor and muscle protein in addition to immunoglobulin. Ig and Ig-like domains are basically classified into four types (sets): variable (V-set), constant-1(C1-set), constant-2(C2-set) and intermediate(I-set) by the sequence patterns although it sometimes hard to be classified because of the sequence diversity. The progress in structural analysis reveals the structural detail of each set of domains. Ig-like domain contains at least 7 core β-strands and forms β-sandwiched immunoglobulin fold. The difference of the four sets is basically related to the difference in the presence of the C', C'' and D β-strand but it is sometimes found that the Ig-like domains with the same β-strand topology are classified into different Ig-sets in the close inspection of the database. This kind of classification error seems to be found in all the Ig-sets.

In this study we determined four Ig-like structures by using the multi-dimensional NMR spectroscopy and CYANA structure calculation. The origin of the Ig-domains as follows, 1. obscurin, 2. Nephrin-like 2, 3. Myosin-binding protein C, 4. Myosin light chain kinase. The former two of these proteins could not be apparently classified into each Ig-set and the other two proteins have a sequence homology with I-set proteins. We will discuss the structural detail of the four Ig-like domains and compare them with typical Ig-set structures.

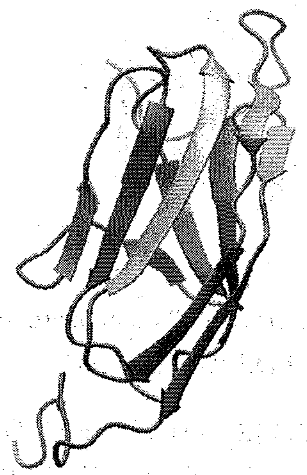

Ig-like domain (2999-3100) of obscurin

eighth Ig-like domain of myosin light chain kinase

NP78

Solution structure of nuclear move domain of nuclear distribution gene C homolog

Toshio Nagashima[1], Fumiaki Hayashi[1], Mikako Shirouzu[1,2], Takaho Terada[1,2], Takanori Kigawa[1], Makoto Inoue[1], Takashi Yabuki[1], Masaaki Aoki[1], Takayoshi Matsuda[1],Eiko Seki[1], Hiroshi Hirota[1], Mayumi Yoshida[1], Akiko Tanaka[1], Yoshihide Hayashizaki[1], and Shigeyuki Yokoyama[1,2,3]
[1]RIKEN Genomic Sciences Center, [2]RIKEN Harima, and [3]Graduate School of Science, University of Tokyo

Nuclear Distribution gene C homolog (NudC) is found not only in cytoplasm, but also small proportion in nuclear. It plays a role in neurogenesis and neuronal migration as a consequence of nuclear migration by interacting with tubulin, dynein, and Lis1 in mitosis and cytokinesis [1]. In recent years, a remarkable function that NudC overexpression led to blocking in tumor cell division was found [2]. A structural and functional analysis of NudC may be important for the development of the anticancer drug.

Excepting NLS and coiled-coil region, about 150 amino acids protein of nuclear move domain is the only domain identified in NudC. The domain is uniquely found in NudC and the family. The sequence of nuclear move domain is homologous with that of CS domain. But few structures are found in PDB. We constructed 118 amino acids protein from NudC and determined the structure by NOESY and CYANA calculation. The structural analysis resulted that its topology was beta-sandwich, and that the fold was similar in that of the superfamily of HSP20-like chaperone. In the same superfamily, CS domain, HSP20, and p23 are also involved. In this presentation, we will report a structural comparison with homologous proteins, and furthermore discuss the function of nuclear move domain based on its structure.

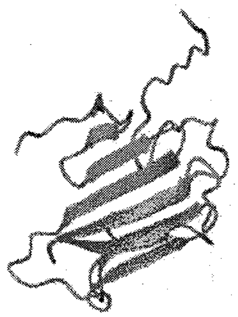

Nuclear move domain of NudC

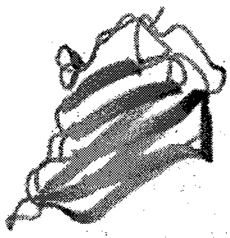

Heat shock protein 90 co-chaperone, p23
PDB ID: 1EJF [3]

[1] JP Aumais, et al, The Journal of Neuroscience, **21** (2001) [2] S-H Lin, et al, Oncogene, 1-8 (2003) [3] AJ Weaver, et al, The Journal of Biological Chemistry, **275**, 23045-23052 (2000)

NP79

KUJIRA, a package of integrated modules for systematic and interactive analysis of NMR data: Application to quick and accurate structure analysis in combination with CYANA calculations

N. Kobayashi[1], S. Koshiba[1], P. Güntert[1], S. Sugano[4], T. Kigawa[1] and S. Yokoyama[1-3].
([1]RIKEN GSC, [2]RIKEN Harima Institute, [3]Graduate School of Science, The university of Tokyo, [4]Graduate School of Frontier Sciences, The university of Tokyo)

As increasing demands of structure determination by NMR in the recent studies for structural genomics, high-throughput techniques are strongly desired. The automated NOE assignment and structure calculation program, CYANA (Güntert, 2003) for the high-throughput NMR studies has released the users from time consuming works such as manual assignments of NOE peaks. High completeness and accuracy of chemical shift assignments are nevertheless required for the structure determination with CYANA especially in the refinement stage.

We have developed a new software package, called KUJIRA, consisting of integrated modules for systematic and interactive analysis of NMR data by manual or automated assignments of main-chain and side-chain signals. NMRView (Johnson, 1994) is used in KUJIRA for displaying contour plots and controlling spectrum windows. An NMR study directed molecular viewer is also implemented in KUJIRA, which assists users to graphically recognize geometrical features of calculated structure, distance constraints and results of NOE assignments. A module in KUJIRA that is linked with the outputs of NOE assignments by CYANA calculations seamlessly controls chemical shift tables, spectrum windows and NOE assignment tables as users to find artifact or noise peaks among NOE peak table as well as miss-assignments in the chemical shift table easily. These functions allow users not only to achieve high completeness and accuracy of the chemical shift table but also to considerably save time for the structure refinement.

Güntert, P. (2003). Prog. NMR Spectrosc. 43, 105-125.
Johnson, B. A. and Blevins, R. A. (1994) J. Biomol. NMR 4, 603-614.

AP80 (PL14)

Methodological advances in a hetero-nuclear NMR-based metabolomics by stable isotope labeling of *Arabidopsis thaliana*

Yasuyo Sekiyama[1], Eisuke Chikayama[1], Takashi Hirayama[2,3,4], Kazuo Shinozaki[1,4,5], Kazuki Saito[1,3,6] and Jun Kikuchi[1,2,3]

Institution: [1]RIKEN Plant Science Center, [2]International Graduate School of Arts and Sciences, Yokohama City University., [3]CREST, JST, [4]RIKEN Genomic Sciences Center, [5]RIKEN Plant Molecular Biology Laboratory, [6]Graduate School of Pharmaceutical Sciences, Chiba University.

A combination of hetero-nuclear NMR with uniform stable isotope labeling is one of the most powerful tools for plant metabolomics [1,2]. As a preliminary investigation of this methodology, we are developing efficient methods for extraction of all the measurable metabolites from plants as well as resolving overlapped signals in the hetero-nuclear NMR spectra. By use of ^{13}C-labeled *Arabidopsis thaliana*, we presented a unique methodology for evaluation of solvent systems based on a partition coefficient based profiling of ^{1}H-^{13}C HSQC spectra [3,4]. We also reported that fluorinated solvents, such as hexafluorocacetone, are useful to enhance solubility of both hydrophobic and hydrophilic metabolites [3,4]. This result suggested that fluorinated solvents are useful for comprehensive identification of a variety of metabolites.

Furthermore, we are establishing a methodology for uniform stable isotope labeling of plants, a key technology for hetero-nuclear NMR-based metabolomics. Highly stable isotope labeling considerably increases the number of detectable signals in NMR spectra. We monitored incorporation ratio of [$^{13}C_6$]glucose into *A. thaliana* at suitable time intervals. In the ^{1}H -^{13}C HSQC spectrum of the extract of plants incubated for 21 days, 350 enriched signals were observed, suggesting that major metabolites were highly labeled by [$^{13}C_6$]glucose after 21 days. Detailed time-course of labeling and differences in ^{13}C incorporation profiles of major metabolites will be discussed in the conference.

- References -

[1] Kikuchi, J.; Shinozaki, K. and Hirayama, T. (2004) *Plant Cell Physiol.*

[2] Kikuchi, J. and Hirayama, T. (2005) *Biotech. Agri. Forestry*

[3] Sekiyama, Y.; Hirayama, T.; Shinozaki, K.; Saito, K. and Kikuchi, J. (2005) *Int. Metabol. Meeting abstract.*

[4] Chikayama, E.; Sekiyama, Y.; Shinozaki, K.; Saito, K. and Kikuchi, J. (2005) *Int. Metabol. Meeting abstract.*

NP81

SELECTIVE ME-HMBC, A NEW TECHNIQUE USEFUL FOR IMPROVING SENSITIVITY OF HMBC CROSS PEAKS OF METHINE PROTON SIGNALS ATTACHED TO A METHYL GROUP

K. Furihata, and H. Seto＊

Division of Agriculture and Agricultural Life Sciences, University of Tokyo

＊ Dept. of Applied Biology and Chemistry, Tokyo University of Agriculture

We present a new version of the HMBC technique named Selective Me-HMBC. This method enables to improve the sensitivity of HMBC cross peaks of methine proton signals attached to a methyl group. Natural products such as polyketides often contain spin systems which include a secondary methine group (-CH-CH(CH_3)-CH-). In such a spin system, methyl protons split to a doublet or a triplet with strong signal intensity. Therefore, methyl proton signals give cross peaks with stronger intensity as compared with those of methine protons in the HMBC spectra. On the other hand, a methine proton connected to a methyl group splits to a multiplet by surrounding several vicinal protons causing weak appearance of the methine proton signal. Therefore, it becomes difficult to observe cross peaks of the methine proton in the HMBC spectrum. In order to solve this problem, we have developed a new technique, Selective Me-HMBC. The point of this method is to transfer the magnetization of a methyl group to its adjacent methine proton.

This selective-Me-HMBC method consists of a combination of the 1D-COSY and HMBC methods. The 1D-COSY pulse is used for transfer of the proton magnetization from a methyl group to its adjacent methine proton.

90x(sel)- △ /2 -180x- △ /2 -90y

For a selective excitation pulse in the 1D-COSY method, selective 90 pulse (90x(sel)) can be employed. As an alternative, the SPFGSE or DPFGSE method reported recently can be used. The DPFGSE method is utilized in this experiment instead of 90x(sel) of 1D-COSY. Several methyl groups can be activated simultaneously in the selective excitation of the methyl group

Sel-Me-HMBC method was applied to model compounds, portmicin and monazomycin.

Analysis of methine protons connected to a methyl group with low sensitivity are generally difficult in the standard HMBC spectra. In the Sel-Me-HMBC spectrum, analysis becomes easy with only methine signals being observed. Effective observation of signals with low intensity is important for HMBC spectral analysis. The SEL-ME-HMBC method is a method of choice for solving this problem.

AP82

Complete Assignment and Conformation of Kadsuphilactone A, A Novel Triterpene Dilactone from *Kadsura philippinensis*

Ya-Ching Shen,*[,†] Yu-Chi Lin,[†] Chi-Fon Chang,[‡]
Tai-huang Huang,[‡] and Yuan-Bin Cheng[†]

[†] *Department of Marine Resources, National Sun Yat-Sen University, Kaohsiung, Taiwan, R.O.C.*

[‡] *Institute of Biomedical Science, Academia Sinica, Taipei, Taiwan, R.O.C.*

Kadsuphilactone A (**1**) is a novel compound isolated from *Kadsura philippinensis* Elmer (Schizandraceae). The structure of **1** was previously elucidated on the basis of extensive spectroscopic methods, including COSY, HMQC, HMBC and NOESY techniques. It possesses partial structures of rings A, B, C and D in addition to a six-membered α-methyl, α,β-unsaturated-δ-lactone. Although the structure of **1** has been confirmed by a single crystal X-ray diffraction analysis, the conformation of **1** in the liquid solution is still unknown and interesting. Due to the severe overlapping of the proton signals in rings C and D, high resolution NMR experiments were applied to investigate the stereochemistry of each proton of **1**. The results allow us to unambiguously assign the ^{1}H and ^{13}C NMR data of **1**. The high resolution COSY, NOESY and conformational studies of **1** will be presented in this symposium.

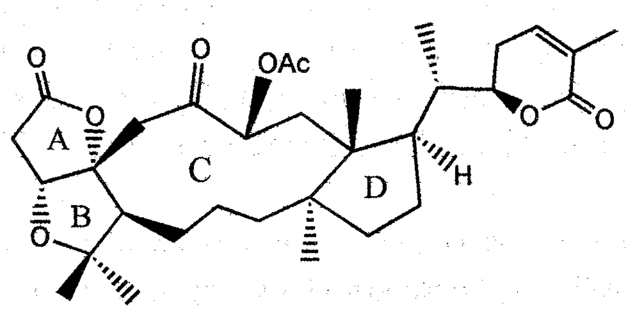

AP83

Tasumatrols P-T, Five New Taxoids from *Taxus sumatrana*

Ya-Ching Shen,†* Yun-Sheng Lin,† Shaw-Man Hsu,† Shih-Sheng Wang,†
Ching-Te Chien,‡ Yao-Haur Kuo,§ Chang-Hung Chou° and Ashraf Taha Khalil†

Department of Marine Biotechnology and Resources, National Sun Yat-Sen University, Kaohsiung 804, Taiwan, Republic of China

Division of Silviculture, Taiwan Forestry Research Institute, Taipei, Taiwan, Republic of China.

National Research Institute of Chinese Medicine, Taipei, Taiwan, Republic of China

Institute of Biology, National Sun Yat-sen University, Taiwan, Republic of China

Taxoids are highly oxygenated diterpenes mostly containing 6/8/6-membered skeleton isolated from different species of yew trees (family Taxaceae). The clinical effectiveness of paclitaxel (Taxol®) as a microtubule-stabilizing therapeutic agent for treatment of several malignancies has motivated many natural product chemists and biologists to isolate new taxoids and investigate their anti-tumor activity. A 21-carbon taxane ester was recently reported from *Taxus sumatrana* (Miq.) de Laub. (Taxaceae) growing in Taiwan. In continuous investigation, phytochemical investigation of the leaves and twigs of *Taxus sumatrana* (Taxaceae) afforded five new taxane diterpenes, tasumatrols P-T possessing 11(15→1)-*abeo*-taxane skeleton together with ten known taxanes. Tasumatrol Q is a natural 4,5-acetonide derivative while tasumatrol S had an unusual 2-hydroxy-2-phenyl-1,3-dioxolane ring. Ten known taxoids were isolated and identified as 5-decinnamoyltaxinin J, 2α,7β,13α-triacetoxy-5α,10β-dihydroxy-9-oxo-2(3→20) *abeo*taxa-4(20),11-diene, 2α,7β,13α-triacetoxy-5α,9α-dihydroxy-10-oxo-2-(3→20)*abeo*taxa-4(20),11-diene, taxumairone A, tasumatrol K, taxezopidine F, taxachitriene A, 20-deacetyltaxachitriene A, tasumatrol J, and wallifoliol. Their structures were established on the basis of extensive NMR analyses.

AP84

Structural Studies of the Stereochemical Cycloadducts of Bicyclolactone via Diels-Alder Reaction

Chanwoo Seo, Hoshik Won

Department of Applied Chemistry, Hanyang University, Ansan 425-791, Korea

Bicyclolactones obtained from the Diels-Alder cycloaddition of 3,5-dibromo-2-pyrone can undergo various palladium catalyzed cross coupling reactions to afford aryl bicyclolactones. Bromo-bicyclic diene furnished two different diastereomers endo-form (62%) and exo-form (38%) upon cycloadditions with N-Et maleimide (NEM), and their stereo chemistries were identified with NMR
In this study, the NMR signal assignments of each isomer was completely accomplished with COSY, TOCSY, NOESY and ROESY. Distance of numerous protons were obtained based on the NOE cross peak intensities of NOESY spectrum. On the basis of these distance data, distance geometry(DG) and molecular dynamic(MD) were carried out to determine the isomer structure of endo-form and exo-form.

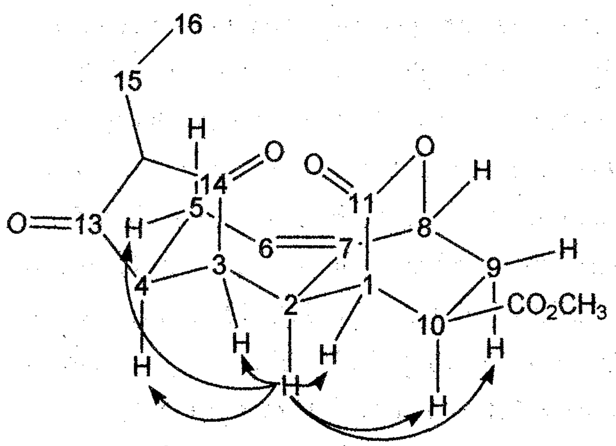

Endo-Form

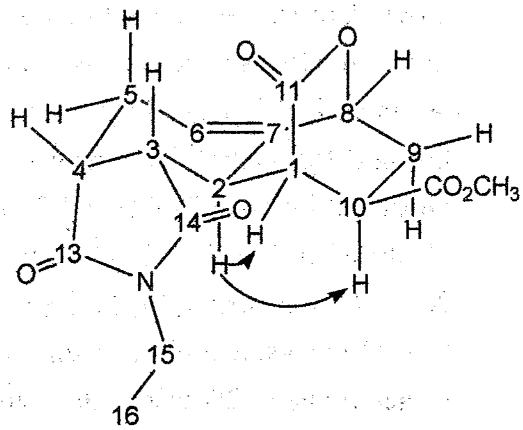

Exo-Form

AP85

Solution State Structure of gallium-binding Bleomycin-A2 by NMR

Misun Lee and Hoshik Won

Department of Applied Chemistry, Hanyang University, Ansan 425-791, Korea

Metallo-bleomycins (an anticancer drug metal complex) recognize specific tumor cell, and nocovalently bind to DNA base pair to cleave sequence. An anticancer drug metal complex, gallium-binding Bleomycin-A2 was synthesized by using microtitration in order to understand structural feature and the function of metal complexes. Complete ^{1}H,^{13}C-NMR signal assignment was accomplished by 2D NMR techniques including COSY, TOCSY, NOESY, HSQC, HMBC. Comparison of chemical shift after complexation and ROESY experiment with different mixing times provided a detail structural feature of metal binding sites. Results exhibit that nitrogens of .-aminoalanine, .-hydroxyhistidine, imidazole, and pyrimidine ring are the metal binding sites. NMR-based solution state structure determination of complex was made by 2D-NOE backcalculation and molecular dynamic computations.

AP86-1

^{129}Xe NMR of hyperpolarized xenon adsorbed on calixarenes

Young Ju Lee[(1)(2)], Ki Deok Park[(1)], Kye Chun Nam[(2)], Kikuko Hayamizu[(3)], Mineyuki Hattori[(3)]

(1) Gwangju Center, Korea Basic Science Institute(KBSI), Gwangju 500-750, Korea
(2) Department of Chemistry, Chonnam National University, Gwangju 500-750 Korea
(3) National Institute of Advanced Science and Technology (AIST), Tsukuba, Ibaraki 305-8568, Japan

^{129}Xe NMR spectroscopy has been used as an useful probe of various inorganic and organic substances such as microporous materials, polymers, liquid crystals and clathrates due to the chemical shift sensitivity to its environment and its hydrophobicity. The nuclear spin polarization of ^{129}Xe can be increased 3-5 orders of magnitude using an optical pumping, which transfers angular momentum from circularly polarized light to electronic and nuclear spins.

Calixarenes have been one of attractive subjects in host-guest chemistry field due to their easy access to synthesize and its structural variety. Nevertheless, calix[6]arenes, with pore sized acceptable xenon, are generally conformationally mobile. Therefore, we nominated capped calix[6]arene with a rigid, well-defined cavity to test binding with xenon.

We investigated the chemical shift of hyper-polarized xenon adsorbed on calixarenes at different temperatures using the optical pumping device manufactured by AIST in collaboration with Toyoko Chemical Co.

It was considered that the quadruply bridged calix[6]arene interacts with xenon gas well among these derivatives considering the notable difference of chemical shift of xenon. And we could measure the pore size of calixarene cavity by means of the xenon chemical shift depending on the pressure of xenon.

The hyper-polarized xenon NMR is expected as a promising tool on the study of adsorption on nano materials having low to moderate surface as well as high surface materials.

AP86-2

Slice selection applied to BPPLED and LED DOSY pulse sequences

Ki Deok Park, Young Ju Lee

Gwangju Center, Korea Basic Science Institute, S. Korea

High resolution DOSY (Diffusion Ordered Spectroscopy) spectroscopic methods developed in 1990's, refer to a series of 2-dimensional and 3-dimensional NMR techniques with which individual NMR spectrum from each component in a mixture of chemical compounds can be obtained.

The first application of slice selection to DOSY experiment was reported by Antalek et al..
PFG(Pulsed Field Gradient), in general, is not uniform across the gradient coil in the NMR probe and the nonuniformity of PFG is evident in the image profile of 1% doped H2O in D2O solution, which looks rather similar to the dipolar broadened powder patterns in the solid state NMR spectroscopy, with spectral edges higher than the central part of the image profile.
In fact strong and uniform gradient field can be realized only in the central region of the gradient coil.
Antalek et al. pointed out that without slice selection, aforementioned nonuniformity of PFG along the gradient coil in the probe can adversely affect the measurement of the diffusion coefficients and demonstrated the experimental results using a pulse sequence, egsteSL.

In this report, slice selection technique applied to LED and BPPLED , both of which were developed by C. S. Johnson group and are among the most widely used DOSY pulse sequences, will be shown.

AP87

NMR Studies of Oxo- and Peroxo-vanadium(V) Complexes of Malate Ligand

Sam-Soo Park, Jun-Gew Lee, Man-Ho Lee, and Jong Rack Sohn

Department of Applied Chemistry, Kyungpook National University,
Daegu 702-701, Korea

Over the past few years increasing attention has been paid to the chemistry of peroxovanadium(V) complexes. Peroxovanadium(V) complexes have been found to have antitumour and insulin mimic activities and have been studied as functional models for the halloperoxidase enzymes. In addition, a large variety of oxidation reactions can be efficiently performed by peroxovanadium(V) complexes.

Previously, we have studied vanadium(V) complexes of various ligands to understand the chemistry of vanadium by NMR spectroscopy. In view of the interest in peroxovanadium(V) complexes we have extended our research to the more complex systems involving hydrogen peroxide. In this paper we deals with oxo- and peroxo-vanadium(V) complexes that are formed when hydrogen peroxide is added to a mixture of vanadate and malic acid in aqueous solution. From the results of multinuclear nmr studies it is suggested that 2:2:1 (vanadium:malate:peroxo) complex, together with 1:2 (vanadium: malate) complex, is found mainly in the pH range 3-6.

NP88

^{2}H natural-abundance MAS-NMR under high field of 21.9 T

Takashi Mizuno[1], K. Takegoshi[2], Masataka Tansho[3] and Tadashi Shimizu[3]
([1]JEOL ltd., [2]Fac. Sci., Kyoto Univ., [3]NIMS)

In characterizing organic compounds, solid-state ^{13}C natural-abundance MAS-NMR has been widely utilized, while ^{1}H NMR has not, due to the spectral broadening by large ^{1}H-^{1}H dipole interaction. ^{2}H, a stable isotope of ^{1}H, has the low gyromagnetic ratio being 1/6.5 times of that of ^{1}H. The quadrupole coupling constant (e^2qQ/h) of ^{2}H is $\sim$ 200 kHz in case of normal organic compounds, and the ^{2}H NMR spectrum is solely governed by the heterogeneous first-order quadrupole Hamiltonian. This makes it possible to resolve ^{2}H NMR spectrum by MAS (magic-angle spinning). ^{2}H MAS-NMR would give chemically equivalent information that may be given by ^{1}H MAS-NMR, hence, ^{2}H MAS-NMR can be a useful tool to study organic molecules. However, the natural abundance ratio (0.015 %) of ^{2}H is so small that ^{2}H NMR has been done with ^{2}H-labeling.

Here, we demonstrated ^{2}H MAS-NMR under high field of 21.9 T (930 MHz). Cross-polarization for ^{1}H is applied for sensitivity enhancement. The resultant spectrum is shown in Fig. 1 with using dimedone-[2-^{2}H 100%, 3-^{2}H 10%]. The resultant chemical shift values are collected on Table 1 together with solution-state NMR data. It is notable that three peaks located at the high-field side of the labeled 2-^{2}H, which are derived from natural abundant ^{2}H spins, are observed. The chemical shift value of C-O^{2}H differs prominently from that observed in solution because of hydrogen bonding in solid-state.

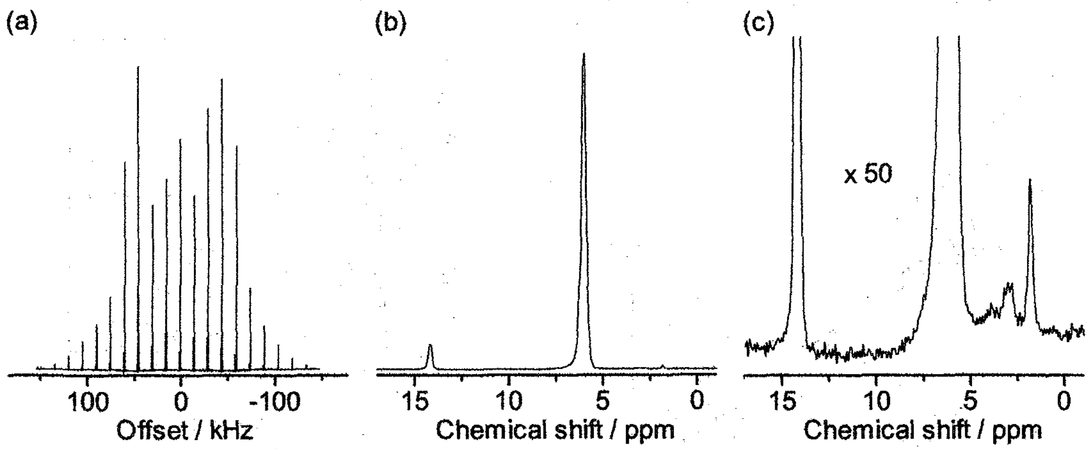

Fig. 1. (a) The whole ^{2}H CPMAS spectrum of dimedone-[2-^{2}H 100%,3-^{2}H 10%]. Contact time 20 ms and 12000 FIDs were accumulated with repetiton time of 4 s. (b) Expanded spectrum of (a) near the center peaks. (c) Expanded spectrum of (b) by 50 times in intensity.

Table 1
^{2}H Chemical shifts in solid and ^{1}H Chemical shifts in $CDCl_3$ solution of Dimedone

	CH (2)	C-OH (3)	C-H_2 (4)	C-H_2 (6)	C-H_3 (7)	C-H_3 (8)
^{2}H solid σ (ppm)	6.04	14.20	3.05	3.93	1.85	1.85
^{1}H solution σ (ppm) [1]	5.47	6.42	2.27	2.27	1.09	1.09

[1] ^{1}H solution-state chemical shift values are cited from the reference written by Takegoshi et al. *J. Magn. Reson.*, **66**, 14-31 (1986)

NP89

MQMAS with strong RF pulses using a microcoil

○Munehiro Inukai[1], Kazuyuki Takeda[1], and Masahiro Kitagawa[1]
[1]*Graduate School of Engineering Science, Osaka University, Japan*

In order to examine multiple-quantum (MQ) excitation efficiency under very strong RF irradiation in multiple-quantum magic angle spinning (MQMAS) spectroscopy of half-integer quadrupole nuclei[1, 2], a microcoil-based, tiny probe was developed as small as a coin, which is capable of attaching itself to an existing MAS probe or spinning module.

As schematically described in Fig. 1, a capillary sample tube (o.d.: 0.5 mm, i.d.: 0.3 mm) is stuck through a cap of a pencil-type 4 mm rotor (Varian). With the conventional compressed-air blowing, the capillary can be spun together with the rotor, and one end of the capillary sticking out of the rotor is inserted into the microcoil. Stable capillary spinning up to several kHz was realized, which is usable for MQMAS. Moreover, the microcoil with a diameter of 0.8 mm has brought ν_1 of up to ca. 600 kHz into practice with a 300 W power amplifier, so that such strong RF fields has now been available that one can study MQ excitation efficiency with the predicted optimal RF intensity in a straightforward single-pulse MQ excitation scheme for quadrupolar interactions of up to ca. 2 MHz.

Using this hardware, comparison of MQ excitation efficiency is made between the straightforward single-pulse method and a number of sophisticated techniques proposed thereafter such as RIACT[3, 4] and HS[5], *using their respective optimal RF intensities*.

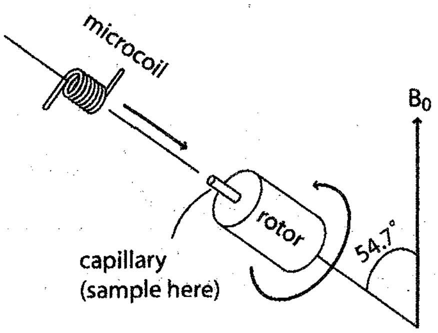

Fig. 1. Schematic description of the way employed in this work to enable microcoil MAS.

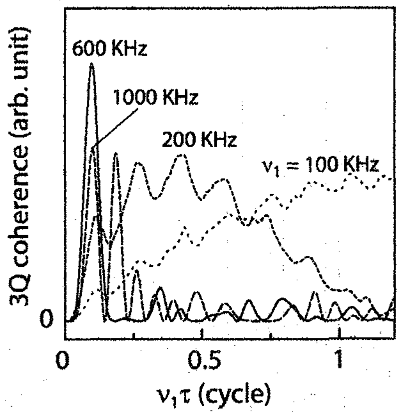

Fig. 2. Calculated excitation efficiency of triple-quantum coherence for a spin-3/2 in a powder sample for various ν_1. $e^2qQ/h = 2.0$ MHz and $\eta = 0$ were assumed. The effect of sample spinning was neglected, because the duration under interest is much shorter than a typical rotor period.

[1] L. Frydman, J.S. Harwood, J. Am. Chem. Soc. 117 (1995) 5367.
[2] A. Medek, J.S. Harwood, L. Frydman, J. Am. Chem. Soc. 117 (1995) 12779.
[3] G. Wu, D. Rovnyak, R.G. Griffin, J. Am. Chem. Soc. 118 (1996) 9326.
[4] K.H. Lim, T. Charpentier, A. Pines, J. Magn. Reson. 154 (2002) 196.
[5] R. Siegel, T.T. Nakashima, R.E. Wasylishen, Chem. Phys. Lett. 403 (2005) 353.

NP90

The Power of Super High Magnetic Field (21.8 T) Solid State NMR for Practical Inorganic Materials

Yasuhiro Tobu[1], Keiji Shimoda[1], Koji Kanehashi[1], Moriaki Hatakeyama[1], Koji Saito[1], Tadashi shimizu[2]

[1]Advanced Technology Research Laboratories, Nippon Steel Corporation
20-1 Shintomi, Futtu, Chiba 293-8511, Japan
2 Independent Administrative Institution National Institute for Materials Science
3-13 Sakura, Tsukuba, Ibaraki, 305-0003, Japan

Solid state NMR for analysis of inorganic substances must target on various nuclear, and its measurement has been very difficult, because almost targets are quadrupole and low gamma nuclei. In addition, the NMR spectra of practical inorganic materials have some problem with broadening from amorphous and mixture structure. Recently, using high magnetic field (11.7-16.4 T) improved sensitivity and resolution in NMR spectra and measuring the low frequency nuclei became possible. Furthermore, inventing the MQMAS method realized the high-resolution measurement about quadrupole nuclei [1]. However, NMR measurement for practical inorganic materials cannot still do with sufficient sensitivity and resolution, when NMR measurement for complex systems, which have very small amount concerning of the target nuclear and the nuclide exists low natural abundance, are applied. And then, much higher magnetic field (over 16.4T) is necessary to clarify the detail practical inorganic material structure from viewpoints of industrial applications.

Recently, super high magnetic field (21.8 T: ^{1}H NMR 930 MHz) became possible to use for the solid state NMR. In this research, the first observation of ^{27}Al MQMAS and the comparison to ^{27}Al NMR data for several inorganic materials within wide range magnetic fields about 7 T, 11.4 T, 16.4 T, 21.8 T, in order to clarify the effectiveness of the magnetic field improves, such as sensitivity, resolution and relaxation time.

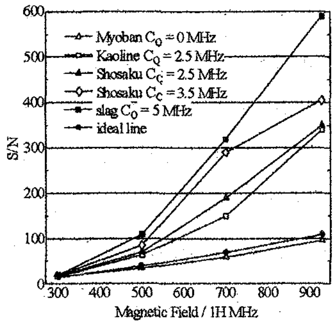

Fig. 1 Improvement of S/N

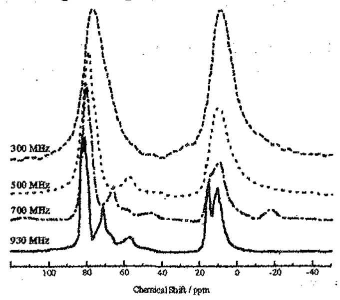

Fig.2 Improvement of resolution

As a result, the big advantage of using super high magnetic field for quadrupole nuclear was indicated below.

1. The sensitivity was very improved. Especially, large C_Q material exhibited more than five times improvement to ideal value. (see Fig.1) The sensitivity of the improvement to NMR spectra had good correlation with C_Q value.
2. The resolution was very improved (see Fig.2), because of decrease of quadrupole nuclei NMR spectral width within high Larmor frequency in the case of complex inorganic materials.
3. Magnetic field influence of the relaxation time is different according to C_Q. (detailed discussion in poster). The relaxation time for complex inorganic materials can be discussed.

All advantage of super high magnetic field is important and powerful for the analysis of practical inorganic materials to clarify the structure, and many applications will be waiting.

[1] K. Saito, K. Kanehashi, I. Komaki, Annual reports on NMR spectroscopy, 44 (2001)

AP91

Remarkable Reduction of RF Power by Duration & Amplitude Time Averaged Spin Exchange at Magic Angle in Solid-State NMR Spectroscopy.

Katsuyuki Nishimura, and Akira Naito.
Department of Applied Materials Chemistry, Division of Materials Science and Chemical Engineering, Graduate School of Engineering, Yokohama National University; 79-5 Tokiwadai, Hodogayaku, Yokohama, Kanagawa, Japan, 240-8501

We have developed cross polarization and 2D separated local field NMR techniques with low power rf field for observed nuclei as referred to TANMA-CP [1] and TANSEMA [2], respectively. In last year, a new cross polarization technique to markedly reduce rf power for both of ^{1}H and observed nuclei were developed as referred as DATANMA-CP and DATAP-CP with and without ^{1}H-homonuclear dipolar decoupling, respectively.

In this study, we extended DATANMA-CP to spin exchange type of separated local field experiment as referred as DATANSEMA. The rf power to satisfy the Hartmann-Hahn matching condition during spin exchange for observed nuclei were arbitrary reduced by alternating the direction of effective fields of ^{1}H nuclei with unequal-duration times and –amplitudes as similar as Frequency Switched Lee-Goldburg scheme. The performances of proposed techniques were compared theoretically and experimentally with previously developed PISEMA [4] and authors developed duration time averaged techniques of TANSEMA [2]. The reduction of rf fields for observed nuclei and part time of ^{1}H were shown experimentally by factor 10 and 100, respectively, at ^{13}C-NMR signals of MBBA in the liquid crystalline state without degradation of spectral quality.

The sample heating due to continuous rf irradiation of ^{1}H and observed nuclei, can be avoid effectively using DATANSEMA. This technique is especially useful for hydrated biological sample such as membrane protein and peptide associated with lipid bilayers.

Ref

1. K. Nishimura, and A. Naito, Chem. Phys. Lett. 380, (2003)569.
2. K. Nishimura, and A. Naito, Chem. Phys. Lett. 402, (2005)245.
3. K. Nishimura, and A. Naito. 43th the annual meeting of Magnetic Resonance of Japan (2004)
4. Wu, C. H., Ramamoorthy, A, and Opella, S. J. *J. Magn. Reson.* A 109 (1994) 270.

AP92 (PL3)

Novel Solid-State NMR Protein Structural Analysis by the Simulated Anneal Spectral Fitting under the Constraints of Conformation-Dependent ^{13}C Chemical Shifts

Yoh Matsuki[1,2], Hideo Akutsu[2] and Toshimichi Fujiwara[2]
[1]JST-BIRD, [2]Institute for Protein Research, Osaka University, Suita 565-0871, Japan

Usefulness of the uniformly ^{13}C-, ^{15}N-labeled samples with the multidimensional NMR techniques is now evident for protein structure analysis because a suite of NMR experiments using the ^{13}C and ^{15}N spin connectivities provide a number of structure constraints for a single sample. Recently, statistical and analytical studies on the experimental chemical shifts showed that the ^{13}C chemical shift has good correlation with the local conformation of proteins, and is a reliable source of dihedral angle information. The structure-based chemical shift can now be predicted for ^{13}C and ^{15}N in proteins with programs such as SHIFTX and PROSHIFT. We propose a novel solid-state NMR approach for structure analysis of uniformly labeled, un-oriented peptides and proteins under MAS conditions. We have combined multidimensional solid-state NMR with the prediction of the chemical shifts as a function of the 3D coordinate of a protein.

Our method fits a simulated 2D ^{13}C chemical-shift spectrum to experimental one as a function of tertiary structure of a protein. The fitting procedure is required to evaluate partly overlapped signals that are often difficult to resolve in multidimensional experiments for powdered uniformly labeled samples. The conformation space was searched by the molecular dynamics-based simulated annealing (MDSA). At each MD step, spectrum is simulated using structure-dependent chemical shifts and signal intensities calculated from the mixing efficiency. The fitting procedure provides structures under the constraints of chemical shifts and conformational energy. This method is useful for quantitative structural analysis based on chemical shifts and also for signal assignments.

The method is now being tested on uniformly ^{13}C, ^{15}N-labeled 14 residue peptide, mastoparan-X from wasp venom bound to phospholipid membrane. The spectrum fitting is performed on 2D $^{13}C_{(SQ)}$-$^{13}C_{(SQ)}$ RFDR and $^{13}C_{(DQ)}$-$^{13}C_{(SQ)}$ INADEQUATE spectra for intra-residue correlation, and 2D CA(NCO)CA spectrum for inter-residue correlations between C^{α}s of neighboring residues. Preliminary result shows that MDSA including the pseudo-energy from the experimentally observed chemical shifts and eight distance restraints can yield helical structures known for the mastoparan-X. The MDSA only with those distance restraints yielded no secondary structure. At the conference, we will also discuss the usefulness of the method for simultaneous analysis of structure and signal assignment of the peptide: the method requires no experimental signal assignments in advance.

AP93

Separation of chemical-shift anisotropy under magic-angle spinning using a new scheme of two-dimensional acquisition

M. Fukuchi and K. Takegoshi
Department of Chemistry, Graduate School of Science, Kyoto University, Kyoto 606-8502, Japan

abstract
The multiple pulse sequence proposed by Tycko et al. [1] for separation of chemical-shift anisotropy (CSA) under magic-angle spinning (MAS) is modified to realize wider f_1 spectral width without deteriorated by the glitches typical for the original sequence.

So far, several CSA recoupling techniques under MAS have been described. Here, we concern the rotor-synchronized pulse techniques. Since a fast spinning speed would increase the duty ratio of the pulse and would lead fatal distortions due to finite pulse lengths, the spectral width is limited by the spinning speed. Now, we present a new scheme of two-dimensional acquisition which widens f_1 spectral width, irrespective to the spinning speed.

We adopt the sequence proposed by Tycko et al. [1]. The sequence is composed of 4 or 6 π-pulses in one rotor period. The CSA interaction is recovered with various scaling factors depending on the timing of the pulses. The π-pulses are applied in the t_1 domain of a two-dimensional experiment, and the t_1 is incremented in units of one rotor period. Certain pulse timing, i.e. a scaling factor, is chosen to accommodate a scaled CSA powder pattern in the spectral width, that is, the spinning frequency. In our experiment, instead of incrementing t_1, we adopt a constant the t_1 but the scaling factor of CSA is incremented. This modification makes it possible to infinitely increase the t_1/f_1 spectral width. Further, the glitch peak typical for the original experiment is removed, and the other advantages of the constant-time experiment can be enjoyed.

Fig.1 shows the modified pulse sequence. n is the repetition cycle and τ_r is the rotation period. Two-dimensional acquisition is achieved with increasing the scaling factor. Suppose the m scaling factors are used, the spectral width becomes m/n times the rotor frequency. Experimental results and the details of the pulse timing will be presented in the meeting.

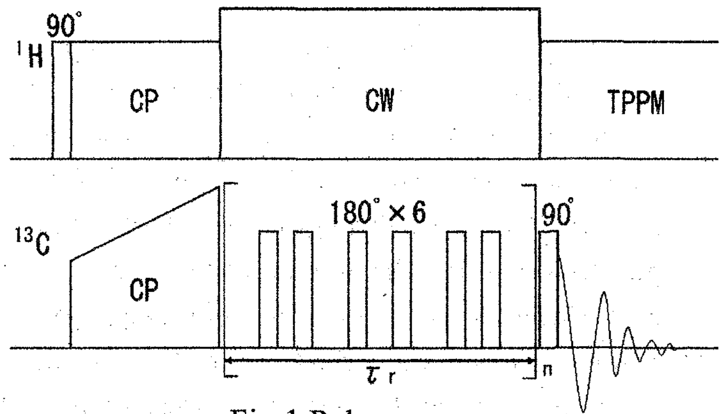

Fig.1 Pulse sequence.

Reference
[1] R. Tycko, G. Dabbagh, and P. Mirau, J. Magn. Reson. 85, 265 (1989)

AP94

One-dimensional solid-state NMR methods using selective soft pulses to detect the through-space ^{13}C-^{13}C correlation: Homonuclear cross polarization

Qing Luo, Hironori Kaji, and Fumitaka Horii
Institute for Chemical Research, Kyoto Univ., Uji, Kyoto 611-0011, Japan

Introduction. For solid organic and polymer materials, homonuclear correlations, e.g. ^{13}C-^{13}C interaction, contain important structural information. Some two-dimensional NMR methods, e.g. two-dimensional double-quantum NMR (2D DOQSY) and spin diffusion method, have been applied to reveal the homonuclear correlations. However, 2D NMR experiments are usually time-consuming and almost impossible for natural abundant samples. In this paper, we have developed a new 1D experiment, which is based on the selective soft pulses and Hartmann-Hahn magnetization transfer, to explore the homonuclear dipolar coupling. The ^{13}C-^{13}C dipolar coupling in a ^{13}C-enriched sample or natural abundant samples has been detected by this method.

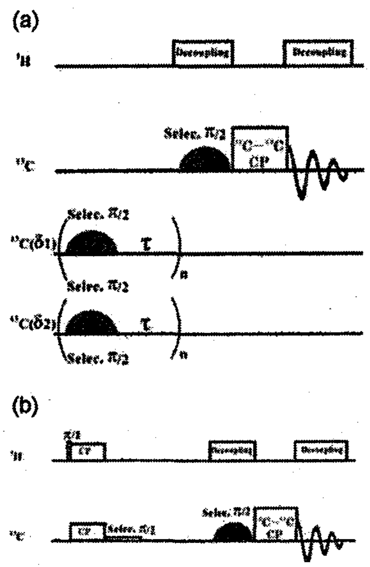

Figure 1. The pulse sequence of the selective homonuclear Hartmann-Hahn method. (a) Direct excitation, (b) ^1H-^{13}C CP excitation.

Experimental. In the ^{13}C channel, an initial selective 90° soft pulse excites the magnetization of specific carbons and it is subsequently spin-locked by the radio-frequency field. As indicated by Robyr,[1] the energy balance can be provided by the interaction with the radio-frequency. Thus, the magnetization can be transferred from the selectively excited site to its dipolar coupled sites.

The spectra were recorded on a Chemagnetics CMX-400 NMR spectrometer equipped with a 7.5 mm double channel probe. The samples are 99% ^{13}C-enriched β-alanine and natural abundant adamantane.

Results and Discussion. For the ^{13}C-enriched β-alanine, we measured the homonuclear cross polarization spectrum with different contact times. The frequency of the soft pulse was set to the resonance of the methyl groups (35.5ppm). When the contact time is in the range of 1 -16 ms, the intensity of the carbonyl peak is increased with increasing contact time. This indicates the occurrence of the ^{13}C-^{13}C CP phenomenon, proving the potential of this 1D technique to be used to explore the homonuclear dipolar coupling.

In natural abundant samples, however, the artifacts excited by the off-resonance radio-frequency become much more serious: The signal from the coupled sites is 10000 times weaker than that of 100% ^{13}C-enriched sample, whereas artifacts decrease only to 1/100. Therefore, we have developed a modified pulse sequence having the pre-saturation process by multiple shaped pulses for the artifact suppression. The spectrum obtained for the natural abundant adamantine is shown in Figure 2. The frequency of the soft pulse was set to 29.5 ppm for the CH carbons. With a contact time of 10 ms, a doublet signal can be clearly observed at 38.56 ppm for the CH_2 carbon. Since the doublet is due to the J coupling between directly bonded CH and CH_2 carbons, it is concluded that the signal is really produced through the ^{13}C- ^{13}C dipolar interaction.

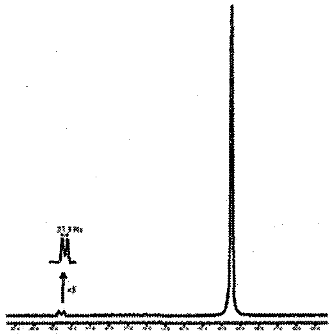

Figure 2. The spectrum obtained for natural abundant adamantine by the selective homonuclear Hartmann-Hahn method with the contact time of 10 ms.

1) P. Robyr, B. H. Meier, and R. R. Ernst, *Chem. Phys. Lett.*, **1989**, *162*, 417

AP95

A new technique for cross polarization compatible with high spinning frequencies and high magnetic fields

○ Weng Kung Peng, Kazuyuki Takeda, Masahiro Kitagawa
Graduate School of Engineering Science, Osaka University, Osaka, Japan

A new cross polarization (CP) technique, which provides efficient spin-lock and thereby efficient polarization transfer, is proposed. Instead of applying a 90-degree pulse along the y-axis followed by a locking-pulse along the x-axis, this technique utilizes adiabatic frequency sweep from far off-resonance toward on-resonance with a single phase. Throughout the sweep, each I spin packet is locked along the effective field, which is initially aligned along the z-axis and gradually tilted toward the xy-plane. Since the magnitude of the effective field is decreased gradually, Hartmann-Hahn matching profile can be broadened under high-speed magic angle spinning, similarly to ramped-amplitude [1] and frequency-modulated [2] CP schemes.

Adiabatic passage from far off-resonance to on-resonance is capable of locking each individual I spin packet even in the presence of considerable spectral distribution and/or line broadening. Thus, this technique is widely applicable for polarization transfer from spin species having large chemical shifts such as ^{19}F and experiments in high static fields. Furthermore, low RF power is sufficient for the spin lock. We call this technique Nuclear Integrated Cross Polarization (NICP). We demonstrate ^{1}H-^{13}C polarization transfer with 3 different methods (NICP, conventional CP [3,4] and frequency modulated CP [2]) in powder mixture of L-alanine and glycine. A flat matching profile with increased signal intensity is obtained for NICP as compared to the other two techniques.

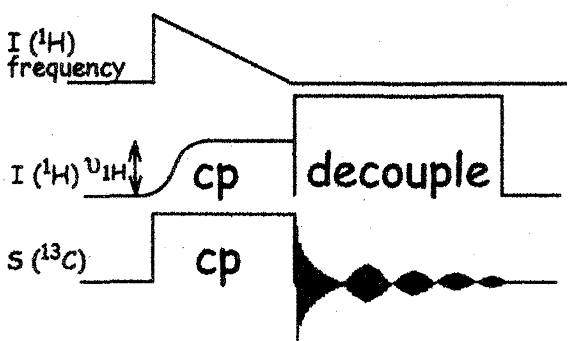

Fig 1: The pulse sequence used in the present work.

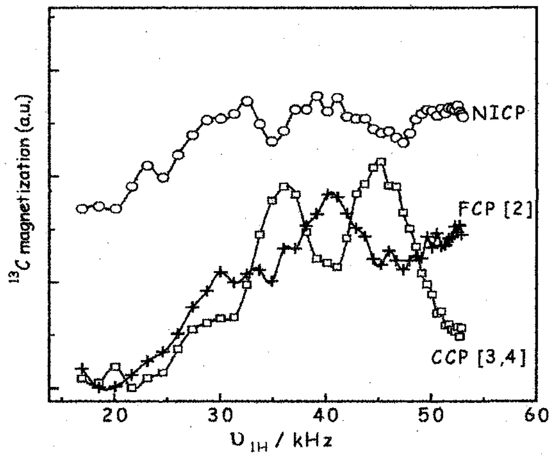

Fig 2: Hartmann-Hahn matching profiles for methyl carbon in L-alanine obtained with 3 different techniques (NICP, frequency-modulated CP [2] and conventional CP [3,4]) in a magnetic field of 12.7 T and under spinning frequency of 10 kHz.

References:

[1] G. Metz et.al., J.Magn. Reson. A 110 (1994) 219.
[2] A.C. Kolbert et.al., J.Magn. Reson. A 116 (1995) 29.
[3] S.R.Hartmann et.al., Phys. Rev. 128 (1962) 2042.
[4] A.Pines et.al., J.Chem.Phys. 59 (1973), 569.

NP96

Structural analysis of poly(γ -biphenylmethyl-L-glutamate) and poly(γ -biphenylethyl-L-glutamate) by solid state NMR

○Ayaka Minemura[1], Yuko Oonishi[1], Hiromichi Kurosu[1] and Junzi Watanabe[2]
1) School of Natural Science and Ecological Awareness, Graduate School of Humanities and Sciences, Nara Women's University, Kitauoya-Higashimachi, Nara 630-8506, Japan
2) Department of Organic and Polymeric Materials, Tokyo Institute of Technology, Ookayama, Meguro-ku, Tokyo 152-8552, Japan

【Abstract】 It is known that poly(γ -biphenylmethyl-L-glutamate)(PBPMG) shows liquid crystalline phase in a certain temperature range, but poly(γ -biphenylethyl-L-glutamate)(PBPEG) does not show liquid crystalline phase. VT ^{13}C NMR measurements and theoretical calculations ware carried out for PBPMG and PBPEG to investigate structure and mobility of the main and side chains. From the temperature dependence of chemical shifts and ^{13}C relaxation time, side chain conformation and relative mobilities are discussed.

【Experimental】 ^{13}C CP/MAS and spin-lattice relaxation time(T_1) NMR data are collected by utilizing of JNM EX-270 NMR spectrometer operating at frequency of 67.8 MHz with CP/MAS and variable temperature (VT) accessories. Spectra are obtained by an accumulation of 1000-7000 scans so as to achieve a reasonable signal-to-noise ratio.

We have considered various side chain conformations and carried out energy calculation. Three dihedral angles for PBPMG and four dihedral angles for PBPEG are varied and the each dihedral angle takes three kinds of conformation of +gauche(60 deg), trans(180 deg) and −gauche(-60 deg). The distribution of the angles and length between biphenyl group and main chain were examined.

【Results and Discussion】 The VT CP/MAS and T_1 measurements show that the mobility of the biphenyl group is restricted at room temperature and the conformational difference in methyl groups between PBPMG and PBPEG became large as the temperature is increased. By the conformational analysis using ab initio energy calculation, the distribution of the angle between biphenyl and main chain axis was found to be a quit different distribution : the angle distribution is concentrating on 50～70°, 100～120°, 130～150° in PBPMG but that is concentrating on 30～40°, 70～80°, 120～130° in PBPEG. Therefore it can be thought that these differences are one of the factors for the appearance of the liquid crystalline phase.

NP97

Higher-order Structure of Poly(ethylene-co-1,5-hexadien) as Studied by Solid State NMR and Quantum Chemistry

Yuuri Yamamoto[1], Aki Fujikawa[1], Masato Sone[2], Shigemitsu Murase[3], Naofumi Naga[4] and Hiromichi Kurosu[1]

1) School of Natural Science and Ecological Awareness, Graduate School of Humanities and Sciences, Nara Women's University, Kitauoya-Nishimachi, Nara 630-8506,Japan
2) Department of Chemical Engineering, Tokyo University of Agriculture & Technology, Koganei, Tokyo 184-8588, Japan
3) Department of Organic and Polymer Materials Chemistry, Tokyo University of Agriculture & Technology, Koganei, Tokyo 184-8588, Japan
4) Department of Applied Chemistry, Shibaura Institute of Technology, Shibaura, Minato-ku, Tokyo 108-8548, Japan

【Abstract】 Polyethylene having 1,3-distributed cyclopentane structures was prepared by copolymerization of ethylene and 1,5-hexadiene(HD) and higher-order structure was studied by solid state NMR and ^{13}C NMR shielding calculations. The amorphous structure of the polymer is drastically changed as compared with that of polyethylene even for the sample of the smallest content of HD.

【Experimental】 We have prepared poly(ethylene-co-HD) copolymer with the HD content of 1.8 ,9.7,20.3 and 50%. The ^{13}C CP/MAS NMR spectra and spin-lattice relaxation time(T_1) of the samples were measured by JNM EX-270 NMR spectrometer operating at frequency of 67.8 MHz. Spectra were obtained by an accumulation of 1000~5000 scans so as to achieve a reasonable signal-to-noise ratio.

We used the Gaussian-03 Rev.C.02 program for structural optimization and the GIAO- CHF approach with density functional theory (b3lyp) for the calculation of nuclear shields. The basis sets we have used is 6-311G(d,p).

【Results and Discussion】 The observed ^{13}C CP/MAS NMR spectra of the three copolymer samples are decomposed into three peaks. Three peaks of the CH_2 carbon are named peaks α, β, γ from downfield. The highest field peak γ (31.4 ppm) shifts lower field as compared with the amorphous polyethylene peak and the T_1 measurement shows that the mobility of the polymer became higher as the HD content is increased. This shows that even in the sample which has the smallest content of HD, the conformation of peak γ is restricted to the structure of the trans rich conformation. In order to confirm this situation, energy and shielding calculations were carried out.

NP98

Morphological Deformation and Enzymatic Degradation of Biodegradable Polyester

T. Morimura, S. Maruno, K. Kasuya, T. Yamanobe and T. Komoto
Department of Chemistry, Gunma University
1-5-1 Tenjin-cho, Kiryu, Gunma 376-8515, Japan
Phone:0277-30-1331 Fax:0277-30-1333 E-mail:yamanobe@chem.gunma-u.ac.jp

Poly(3-hydroxybutyrate) (P3HB) and poly(L-lactic acid) (PLLA) are well known as biodegradable and biocompatible thermoplastics. TEM observation revealed that the lamellar thickening took place near the surface during enzymatic degradation. In this paper, the mechanism of this lamellar thickening is investigated by using single crystal of these polyesters.

Single crystals of PLLA are grown from a 0.05% solution of p-xylene at 90℃. In Fig.1(A) is shown the TEM image of the obtained PLLA single crystals. The hexagonal crystals with 10.5nm lamellar thickness are formed. In Fig1(B) is the TEM image of PLLA after enzymatic reaction by inactive Proteinase-K. As this enzyme is inactivated, the degradation reaction does not occur. Even though the degradation does not proceed, the edge of the single crystals are deformed. This indicates the mobility of molecules near the single crystal edges is increased by the enzyme solution.

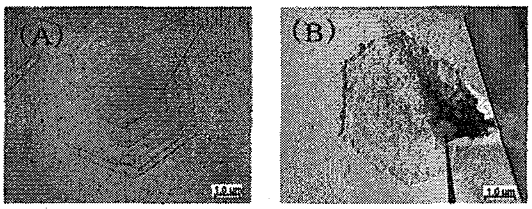

Fig.1 TEM images of PLLA crystals before (A) and after (B) enzymatic reaction

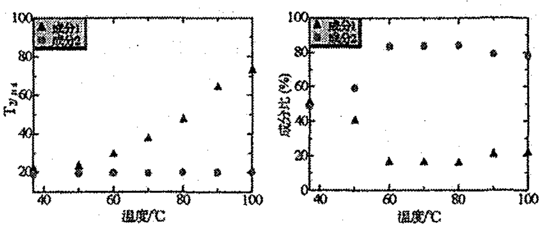
Fig.2 Temperature dependence of ^{1}H pulse NMR parameters for PLLA after enzymatic reaction of inactive Protenaise-K: T_2 (a) and fractions(b)

In Fig.2 are shown the temperature dependences of T_2 and its fraction for PLLA after enzymatic reaction by the inactive Protenaise-K. As the temperature increases above 50℃, T_2 for mobile component increases (Fig.2(A)). For the single crystals without the enzyme reaction, T_2 starts to increase at about 60℃ which is the Tg of PLLA. The fraction of the mobile and immobile components are 50% at 38℃. For the single crystals without the enzyme reaction, the fraction of immobile component is about 80%. These results indicate that the enzyme solution plasticizes and decreases the glass transition temperature. In the presentation, the plasticization by enzyme solution is discussed for PLLA and P3HB.

NP99

Crystallization Behavior and Morphology of Poly(m-xylylene adipamide)

Hiroyuki Shida, Akira Igarashi, Hiroki Uehara, Takeshi Yamanobe
and Tadashi Komoto
Department of Chemistry, Gunma University
1-5-1 Tenjin-cho, Kiryu, Gunma 376-8515, Japan
Phone:0277-30-1331 Fax:0277-30-1333 E-mail:yamanobe@chem.gunma-u.ac.jp

Poly (m-xylylene adipamide) (MXD6) is the polyamide which contains phenylene ring in the main chain. Rigid phenyl group improve the thermal and mechanical properties compared with aliphatic polyamide such as nylon6. Due to its superior physical properties, MXD6 is used for many commercial products. However, the crystallization behavior is not studied sufficiently. In this study, the crystallization of MXD6 is studied in the term of the molecular mobility and morphology by solid state NMR and TEM.

Polarized optical microscope observation indicates that the rate of crystallization is fastest at 170°C. This temperature agrees with the crystallization temperature observed by DSC. In order to investigate the change of the molecular mobility during crystallization, ^{1}H pulse NMR measurements by solid echo method are carried out. FIDs are analyzed and three components are obtained. The components with short, intermediate and long T_2 are attributed to the crystalline, intermediate and amorphous phases, respectively. In Figs.1 are shown the crystallization time dependences of the intensity ratio and T_2 for crystalline, intermediate and amorphous phases determined by ^{1}H pulse NMR (crystallization temperature:170°C). The intensity ratio of crystalline and amorphous phases rapidly increases and decreases, respectively. T_2 of amorphous phase decreases rapidly similar to the decrease in the intensity ratio. This means the mobility of MXD6 molecules in amorphous phase are restricted and the crystalline phase develops. After this stage, the intensity ratios and T_2 for crystalline phase are almost constant. This corresponds to the impingement of spherulites. Even after the impingement, the intensity ratios for intermediate and amorphous phases slightly increases and decreases, respectively. This may corresponds to the secondary crystallization. In this case, the MXD6 molecules in the amorphous phase between lamellae form fairly ordered structure and the amount of intermediate phase increases gradually. TEM observation reveals that the lamella thickness increases from 5 nm to 7 nm. This increment is very small compared with those for olefins such as PE and PP in which the sliding of molecular chain occurs during the crystallization. Therefore, the mechanism of crystallization for MXD6 is different from those for olefin polymers. The mechanism will be discussed in the presentation.

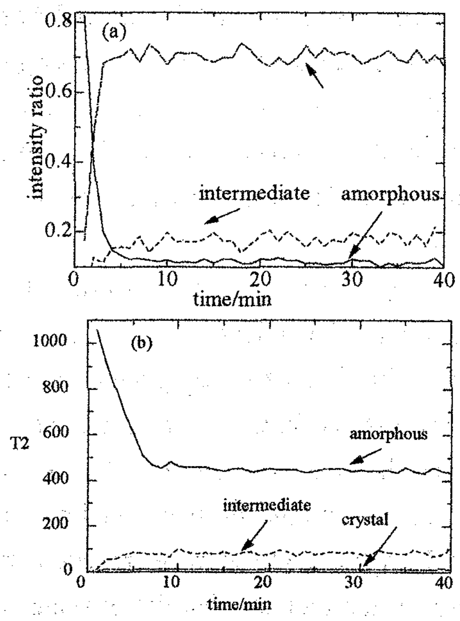

Fig.1 Time dependence of crystallinity intermediate and amorphous phases of MXD6 on crystallization time, (a)fraction (b)T_2

NP100

Dependence on Mixing Ratio of Crystallinity and Miscibility: Solid-State ^{13}C NMR study of Semicrystalline Poly (vinyl isobutyl ether) / Poly (ε-L-lysine) Blends

Yoshifumi Murata, Atsushi Asano*, Takuzo Kurotsu

Department of Applied Chemistry, National Defense Academy, Japan
Hashirimizu 1-10-20, Yokosuka, Kanagawa 239-8686, Japan
E-mail : asanoa@nda.ac.jp

Several kinds of semicrystalline polymer blends of poly(vinyl isobutyl ether) (PVIBE) and poly(ε-L-lysine) (ε-PL) were prepared by solvent-cast method from $CHCl_3$/methanol=9/1 solution. ^1H spin-lattice relaxation (T_1^H) curves were measured to study the miscibility. The crystallinity of blends was also investigated by a comparison of $T_{1\rho}^H$ (^1H-T_1 in the rotating frame) of crystalline (CR) phase and non-crystalline (NC) phase separated from the ^{13}C CPMAS NMR spectra. T_1^H curves on a semi-log plot for the NC phase of PVIBE (○) and that of ε-PL (△) in the PVIBE/ε-PL=10/1 blend (Figure 1) show no simple-straight lines, especially the initial several data points of ε-PL (△) represent a curved line. This non-linearity suggests that the insufficient ^1H spin diffusion occurs between PVIBE and ε-PL during the measuring period, and the blend is immiscible on a scale of 20-50 nm but partially miscible on a scale of 100 nm. Furthermore, the decay curves in Figure 1 were different from those obtained from the CR phases. This observation indicates that the domain size in between the CR phases is different from that estimated from the NC phases. Similar results are observed for the PVIBE/ε-PL=10/3 blend, however, such a difference in T_1^H curves were not detected in the other blends.

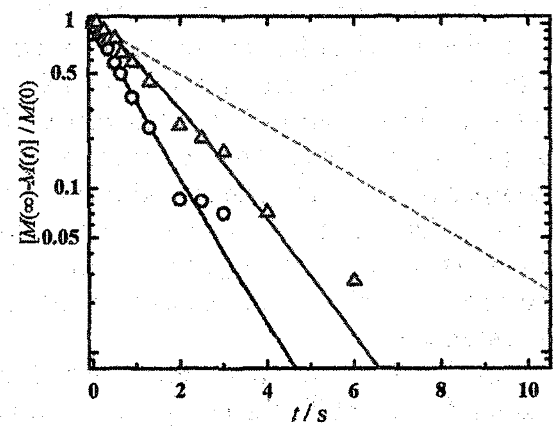

Figure 1 Observed T_1^H relaxation curves for both NC phases of PVIBE (○) and ε-PL (△) in the PVIBE/ε-PL=10/1 blend. Each solid line represents the calculated curve using the two-spin model. The broken line shows the T_1^H relaxation line of pure ε-PL: the T_1^H value is 2.8 s.

In order to study contributions of ^1H spin diffusion between PVIBE and ε-PL, the two-spin model was used to simulate the T_1^H curves. The estimated ^1H spin-diffusion rate between the NC phases for PVIBE and ε-PL is 0.57 s^{-1} and that for the CR phases is 0.25 s^{-1}. For the other blends, the estimated values are in a range of 0.1–0.2 s^{-1}, except for the CR phases in the PVIBE/ε-PL=10/3 blend: the value is 0.34 s^{-1}. These results for the miscibility are discussed with the results of crystallinity.

NP101

Crystallization Behavior of Vinylidene Chloride Copolymers

M. Mochida[1], T. Yamanobe[1], T. Komoto[1], M. Honda[2] and N. Anazawa[2]
[1]Department of Chemistry, Gunma University
1-5-1 Tenjin-cho, Kiryu, Gunma 376-8515, Japan
[2]Asahi Kasei Life&Living Corporation
1-1 Hirata-nakamachi, Suzuka-City, Mie 513-8660, Japan

Poly(vinylidene chloride) (PVDC) is a polymer with high density and high degree of crystallization. It is used as food wrapping material because of its superior gas barrier properties. However, PVDC tends to give a hydrochloride gas and crosslinks around melting point, which deteriorate the quality of the final product. In order to deterioration of PVDF, the copolymer of vinylidene chloride with other monomers such as vinyl chloride, methyl acrylate and so on, are used as a commercial products. In this study, the effects of plasticizer and comonomer on the crystallization behavior of vinylidene chloride copolymer are investigated.

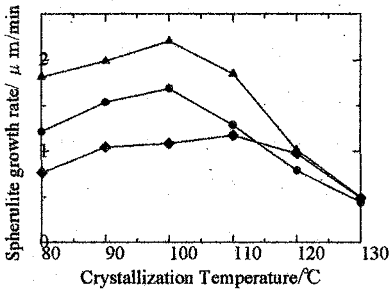

Fig.1 Crystallization temperature dependences of spherulites growth rate for sample 1(◆), sample 2(●) and sample 3(▲).

In Fig.1 is shown the temperature dependence of the spherulites growth rate for vinylidene chloride/vinyl chloride copolymers with different plasticizer. The amount of plasticizer is sample 1< sample 2 < sample 3. The effect of plasticizer appears on both the maximum growth rate temperature and the maximum growth rate. The maximum growth rate temperature decreases and the maximum growth rate increases with increasing the amount of plasticizer.

In Fig.2 is shown the crystallization time dependences of T_2 for samples 1, 2 and 3. In all samples, at initial stage of crystallization, T_2 for immobile and mobile components decreased with time rapidly and became almost constant thereafter. This behavior may correspond to the impingement of spherulites. This effect appears on T_2 of mobile component. T_2 of mobile component for sample 1 is about 200μs. Increment of plasticizer increases the T_2 of mobile component, while that of immobile component being constant. In other words, the plasticizer makes a further mobility of the mobile component. In the presentation, the results of CPMAS NMR and TEM are also discussed.

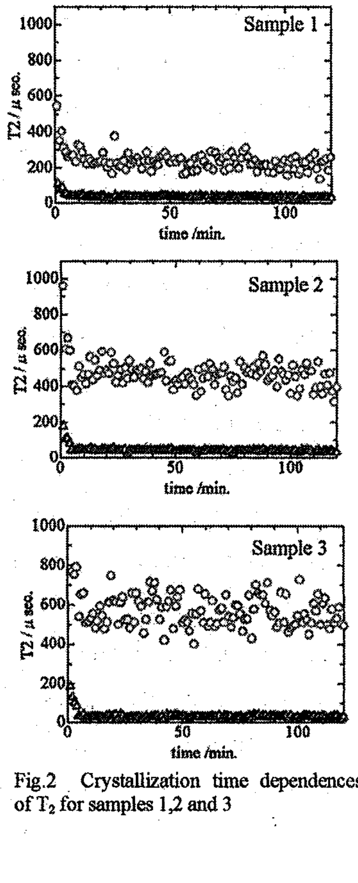

Fig.2 Crystallization time dependences of T_2 for samples 1,2 and 3

NP102

Solid State NMR Studies of Poly (alkyl propiolate) s

Kouo SUZUKI, Terumi KOHIYAMA, Yasuteru MAWATARI, Masahiro TABATA, and Toshifumi HIRAOKI
Graduate School of Engineering, Hokkaido University, Kita-ku, Sapporo 060-8628, Japan
Tel: +81-011-706-6642, Fax: +81-011-716-6175, E-mail: kouo@eng.hokudai.ac.jp

Poly (alkyl propiolate) s polymerized using [Rh (NBD) Cl] $_2$ catalyst have a cis-transoidal conformation and forms a pseudohexagonal columnar structure.[1] In this work, annealing effect of poly (n-butyl propiolate)(Pnbp) and poly (2-butyl propiolate)(P2bp) in solid was characterized by ^{13}C CP/MAS NMR spectroscopy.

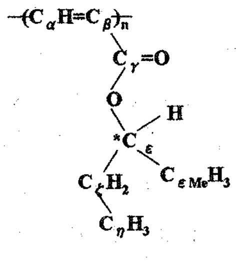

P2bp

^{13}C CP/MAS NMR spectra of P2bp with a contact time 1 ms are shown in Fig. 1, as a function of an annealing temperature. The main chain carbons of C_α and C_β are split into six peaks at least. These carbons are assigned by using a dipolar dephased spectrum; peaks at 139 and 137ppm are belonging to C_α, peaks at 132, 131, 129 and 127ppm to C_β. With increasing an annealing temperature, both of C_α and C_β resonances in the main chain became broader and a new broad signal was appeared in the low field side of C_γ resonance. Furthermore, C_ε resonance also became broader. Any change was not observed in other carbon resonances. These results indicate the isomerization of P2bp from cis-transoid to trans-transiod induced by thermal treatment, which induce to the displacement and the broadening of C_γ and C_ε resonances, respectively. The molecular weight of P2bp measured by GPC decreased as well from Mn=63000 to Mn=3200 with increasing the annealing temperature, showing the scission of the main chain. The results of Pnbp will be presented.

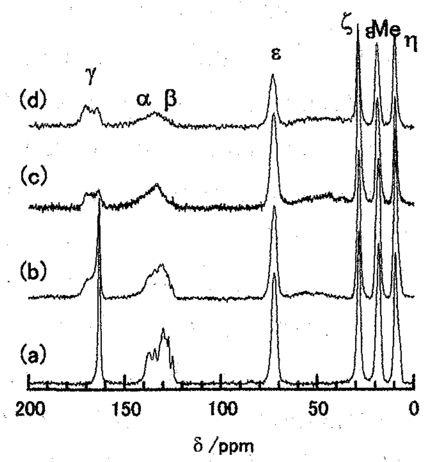

Fig.1 Annealing effect of ^{13}C CP/MAS NMR spectra of P2bp ; (a)pristine, (b)100℃, (c) 150℃, (d) 200℃.

1) M. Tabata, Y. Inaba, K. Yokota, Y. Nozaki, *J. Macromol. Sci. Pure Appl. Chem.*, A31, 465 (1994).

NP103

Conformational Transformation of Poly(β-benzyl L-aspartate) as Studied by Solid-State ^{13}C NMR

S. Kasahara, K. Takegoshi, and A. Shoji*
Department of Chemistry, Graduate School of Science, Kyoto University, Kyoto, 606-8502
**Department of Biological Science, Faculty of Engineering, Gunma University, Gunma, 376-8515*

We studied dynamics in conformational transformation of Poly(β-benzyl L-aspartate) (PBLA) by high resolution solid-state ^{13}C NMR. The transformation of the α_R-helical PBLA into ω_L-helix is known to be caused by thermal treatment of powdered samples above about 120℃. And at higher temperatures, PBLA takes β-sheet [1].

Figure 1 shows the NMR spectra of PBLA heated for various times at 150℃. The lineshape change observed for the C=O and the C_α peaks indicates that longer the heating time, more PBLA transforms into ω_L-helix and β-sheet forms. The relative peak intensities of these conformers are determined by fitting the signal to a sum of Gaussian lineshapes (Figure 2), and are collated in Table 1. The reaction rate constant of the deformation of α_R-helix is obtained to be 4.0×10^{-3} and 4.9×10^{-3} s^{-1} from C=O and C_α data, respectively.

Similar experiments at different temperatures as well as examination of the domain structures of heat-treated samples using ^1H T_1 will be discussed.

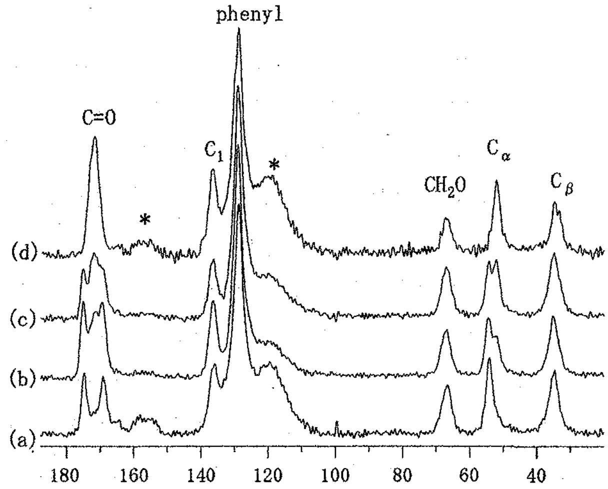

Figure 1.
^{13}C CP/MAS spectra at room temperature of (a)PBLA (no thermal treatment), heated at 150℃ for (b)1min., (c)2min. and (d) 0min. *:Unknown.

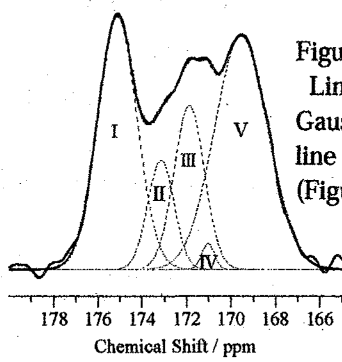

Figure 2.
Lineshape analysis using Gaussian lineshapes. Solid line is observed spectrum (Figure 1 (b)).
I, V: α_R-helix
II, III: ω_L-helix
IV: β-sheet

Table 1. Relative peak intensity (%)

	C_α carbon			C=O carbon		
min.	α_R	ω_L	β-sheet	α_R	ω_L	β-sheet
(no)	83.0	8.6	8.4	85.7	12.9	1.4
1	62.4	34.4	3.1	73.3	25.7	1.1
2	39.3	56.9	3.9	58.3	35.2	6.5
3	4.4	89.8	5.8	8.0	86.4	5.6

[1] T. Akieda, H. Miura, S. Kuroki, H. Kurosu, and I. Ando *Macromolecules*, **1992**, *25*, 5794

NP104

Transition between the glassy crystal and the plastic crystal in poly(3-alkylthiophene)

Koji Yazawa,[1] Naoki Asakawa,[1] Takakazu Yamamoto,[2] Yoshio Inoue[1]

[1]Department of Biomolecular Engineering, Tokyo Institute of Technology,

4259 Nagatsuta-cho, Midori-ku, Yokohama, Kanagawa 226-8501, JAPAN,

[2]Chemical Resources Laboratory, Tokyo Institute of Technology,

4259 Nagatsuta-cho, Midori-ku, Yokohama, Kanagawa 226-8501, JAPAN,

Introduction

Recently, regioregular type poly(3-alkylthiophene)(P3AT) has been investigated by many groups because of its high potentiality for new electronic and optoelectronic devices such as light-emitting diodes, and field-effect transistors. Up to now, almost all interest of the researchers has been the correlation between structure and function. On the other hand, molecular dynamics in solid states is also important factor determining the functions as represented by thermochromism phenomena. However, the general interpretations about their correlations have not established. In this study, we investigated the structure and the molecular dynamics of P3ATs, and proposed a general model about them.

Experiment

Poly(3-butylthiophene)(P3BT),poly(3-hexylthiophene)(P3HT), and poly(3-dodecylthio phene)(P3DDT) were synthesized by Rieke method. The powder samples were used in differential scanning calorimetry(DSC) and solid state ^{13}C NMR measurement. The casted film samples from chroloform solution were used in wide-angle X-ray diffraction,

Result and Discussion

In DSC measurements,the endothermic peak was obtained around 60°C. The FTIR spectrum which is the region of C_β-H out of plane deformation also showed the peak shift from 825cm^{-1} and 810cm^{-1} to 820cm^{-1} in the same temperature range. On the other hand, all P3ATs showed the absorption maximum of the isotropic liquid phase at 838cm^{-1}. It means that the transition around 60°C of P3BT is a kind of crystalline-crystalline transition.

In ^{13}C longitudinal relaxation time (T_1) measurements, T_1 of the C_1 carbon connecting with thiophene ring in alkyl side chains turned longer(0.3s $\rightarrow$ 0.6s) with heating from 20°C to 35°C. In this temperature range, it is known that butyl side chains are acting as liquid, indicating that is not in the slow motion region. From the result, it is assumed that the mobility of the C_1 is accelerated dramatically by twisting of thiophene ring.

We proposed a hypothesis that the transition is from the glassy crystal and the brittle crystal to the plastic crystal.

NP105

Study of Structure of Ionic Aggregates in Poly (ethylere-ran-metacrylic acid) Ionomers by Means of Nuclear Magnetic Resonance Spectrometer at High Magnetic Field 21.9T

Yusuke YAMAMOTO, Miwa MURAKAMI, Masataka TANSHO, and Tadashi SHIMIZU

High Magnetic Field Center, National Institute for Materials Science, 3-13, Sakura, Tsukuba, Ibaraki 305-0003, Japan

Introduction: Ionomer is a type of random copolymer with a small percentage of pendant acid groups, a fraction of which are neutralized by a metal cation. Ionic groups, such as a carboxylate group of ionomer are well known to form ionic aggregates that the ionomer possess unique mechanical, rheological, and thermal properties due to ionic aggregates working as physical cross linking in polymer matrices. Aims of this study are to investigate the magnetic field strength dependence of resonant signal and to clarify a local environment and structure of the metal cation in ionic aggregates using NMR spectrometer of high magnetic field.

Experimental: The ethylene-metacrylic acid copolymer (E-0.054MAA; methacrylic acid content = 5.4 mol %) was provided by Mitsui-Dupont Polychemicals, Inc. A known amount of an E-0.054MAA film was soaked into a methanol solution of NaOH for two weeks at 50 °C for two weeks and then annealed at 75 °C for 24 hours. Solid-state ^{23}Na NMR spectra were obtained on a spectrometer operating at a static magnetic field of 11.8 and 21.9 T, 132 and 246MHz for ^{23}Na nucleus, respectively. ^{23}Na chemical shift of NaCl aqueous solution, $\delta = 0$ ppm was used as an external reference. All spectra were measured at room temperature and an MAS rate of 15 kHz.

Results and Discussion: At magnetic field strength, 21.9 T, ^{23}Na MAS NMR spectra of the sample show strong narrow peak at -0.1 ppm with line width at half–height of 0.7 kHz. On the other hand, the line width at half-width is 1.3 kHz at magnetic field strength, 11.8 T. The peak is narrowed by a reduced quadrupole effect at high magnetic field. ^{23}Na MQMAS measurement at 21.9 T has been carried out to know the detail of an environment of Na ions in E-0.054MAA-Na. ^{23}Na MQMAS spectrum shows that peaks are observed having a distance from the CS axis and found to have the residual quadrupole effect by the peak of ^{23}Na ions in E-0.054MAA-Na. The real chemical shift of the main peak is determined as 2 ppm.

This work was supported by Shinkouchouseihi Program in 2004 titled "High Field Solid State NMR for Materials Research & Development" from Japan Science and Technology Agency (JST).

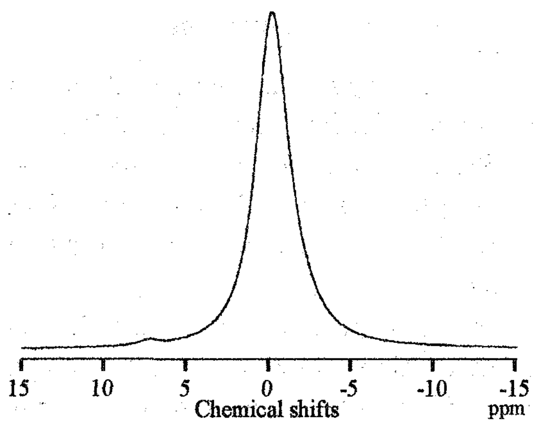

Fig.1 ^{23}Na MAS spectrum of E-0.054MAA-Na neutralized at 50 °C for two weeks, and then annealed 75 °C for 24 hours at room temperature.

NP106 (PL1)

Diffusional Behavior of Poly(β-benzyl L-aspartate) in the Rod-like and Random-Coil Forms as Studied by High Field-Gradient NMR Method

Sho Kanesaka, Shigeki Kuroki and Isao Ando
Department of Chemistry and Materials Science, Tokyo Institute of Technology

[Introduction] Recently, we have elucidated diffusional behavior of rod-like polypeptide with long *n*-alkyl side chains in the thermotropic and lyotropic liquid crystalline phases, and rod-like and random-coiled poly(diethylsiloxane)(PDES) in the isotropic and biphasic phases composed of the isotopic and the liquid crystalline regions by using pulse field-gradient spin-echo(PFGSE) ^{1}H and ^{13}C NMR methods. From these experimental results, it has been shown that the diffusion coefficients of polypeptide chains in the rod-like form the direction parallel ($D_{\parallel}$) and perpendicular ($D_{\perp}$) to the long chain axis have been determined, and then the $D_{\parallel}$ value is larger than the $D_{\perp}$ value, and that the isotropic diffusion coefficients of rod-like polypeptides decrease with an increase in the main-chain length. Then, it has been shown that the diffusion process follows the Kirkwood theory for rod-like polymers and the α-helical polypeptide is diffusing as rod-like polymer. Further, it has been shown that PDES chains in the liquid crystalline region diffuse as a rod and the diffusion coefficient is larger than that in the isotropic region which diffuses as coil. The difference in between the diffusion coefficients of the rod-like form and the random-coiled form has been explained by entanglements, but its detail has not been clarified yet.

Poly(β-benzyl L-aspartate) (PBLA) is one of the most popular synthetic-polypeptides as well as poly(β-benzyl L-glutamate) (PBLG), which has been studied for long years. It is known that PBLA takes the left-handed α-helix form in helix solvent such as chloroform and takes the random coil form in coil solvent such as trifluoroacetic acid. Structural studies on PBLA have been studied by using various spectroscopic methods including NMR. However, the diffusional behavior of PBLA in the rod-like and the random-coil forms has never been studied. From such a background, we aim to measure the diffusion coefficients (*D*) of PBLA with the rod-like form and the random-coiled form in solution as a function of PBLA concentration by using PFGSE ^{1}H NMR method and then to elucidate the diffusional behavior, and further to clarify difference in diffusion between the rod-like form and random coil.

[Results and discussion] The log-log plots of the diffusion coefficients of PBLA in the rod-like and coil-like forms have been shown against PBLA concentration in Fig. 1. From these experimental results, it is found that the diffusion coefficient of PBLA in the rod-like form is much smaller than that of PBLA in the random-coil form. This means that the radius of gyration (R_g) of PBLA in the rod-like form is much smaller compared with that in the random-coil form. Further, it is found that the diffusion of PBLA in the rod-like form has different behavior in the three PBLA concentration regions, region 1: 0.11 ~ 0.39%, region 2: 0.39 ~ 0.86% and region 3: 0.86 ~ 9.20 % and that in the random coil form has different behavior in the two PBLA concentration regions, region I: 0.20 ~ 1.03% and region II: 1.03 ~ 25.2%. From detailed analysis of the diffusional behavior, it is apparent that the diffusional behaviors of PBLA in the rod-like form and in the random coil form can be reasonably followed by Tinland theory and de Gennes theory, respectively. In region 1 and I, the polymer chains in solution collide and interact with each other. The region 2 and II assigned as the semi-dilute region from the slopes, −2.50 and −1.41, of the diffusion coefficients plotted against PBLA concentration in log-log scale. The polymer chains form partially ordered orientation in region 3, and do not form entanglements between the polymer chains efficiently with increasing PBLA concentration.

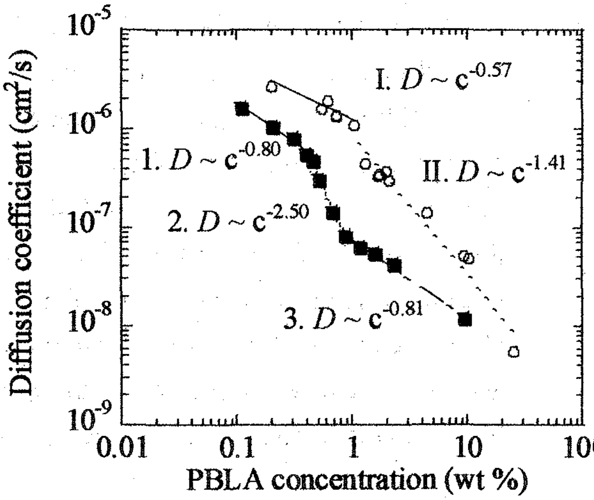

Fig. 1 log-log plots of diffusion coefficients *D* of PBLA in $CDCl_3$ solvent at f_{TFA}= 0 wt% (○) and in a mixture of $CDCl_3$ and TFA-*d* at f_{TFA} = 50 wt% (■) against the PBLA concentration at 20°C obtained from PFGSE ^{1}H NMR experiements.

AP107

Transformation of Crystal Structure of Ultra High Molecular Weight Polyethylene as Studied by Solid State NMR

T. Yamanobe, K. Hashizume, K. Kanou, H. Uehara and T. Komoto
Department of Chemistry, Gunma University
1-5-1 Tenjin-cho, Kiryu, Gunma 376-8515, Japan
Phone:0277-30-1331 Fax:0277-30-1333 E-mail:yamanobe@chem.gunma-u.ac.jp

Polyethylene has two stable crystalline structures. One is orthorhombic form in which all-trans zigzag planes are perpendicular to each other, the other is monoclinic form in which those planes are parallel to each other (Fig.1). Monoclinic form is produced from orthorhombic form by drawing and compression. On the other hand, monoclinic form transforms to orthorhombic form at high temperature. In Fig.2 is shown the solid state CPMAS NMR spectra observed at ambient temperature for drawn and compressed polyethylene which are annealed at various temperatures. Without annealing (RT in Fig.2), strong peaks for orthorhombic and monoclinic forms are observed at 32.8 and 34 ppm, respectively. Amorphous phase appears at about 31 ppm as a broad peak. The existence of intermediate phase between monoclinic and orthorhombic forms at 33.4ppm is recognized by curve fitting. At 40 and 50℃, the spectral profiles do not change so much. The amount of monoclinic form decreased with the simultaneous increment of intermediate phase and orthorhombic form above 60℃ at which the lamella thickening and increment of crystallinity take places. Therefore, the initiation of sliding motion along the main chain promotes the transformation from monoclinic form to intermediate phase or orthorhombic form. By annealing at 90℃, the monoclinic form does not disappear completely. This indicates the existence of local strained structure where the molecular motion is restricted even at 90℃. From the exchange NMR spectra, the off diagonal peak corresponding to the exchange between monoclinic form and intermediate phase or orthorhombic form is observed. The mechanism of transformation and the domain size of monoclinic form is discussed.

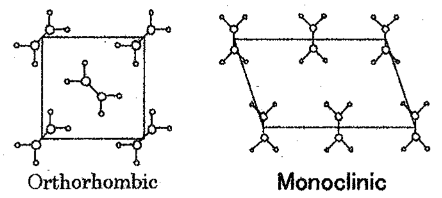

Fig.1 Crystalline Structure of orthorhombic and monoclinic form of polyethylene

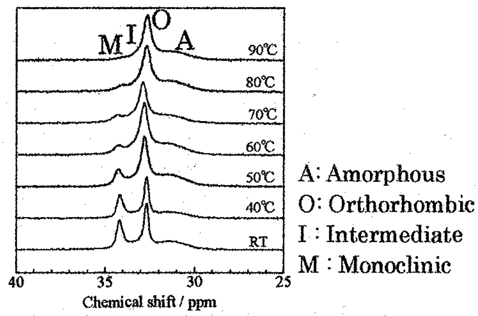

Fig.2 NMR spectra of heat-treated sample as a function of thermal treatment temperature.

AP108

Solid-State ^{13}C NMR Study on Microbial Poly(ε-L-Lysine) and its Derivatives

Shiro Maeda[1], Junnosuke Muranaka[1], Chizuru Sasaki[2] and Ko-Ki Kunimoto[2]
[1]Department of Applied Chemistry and Biotechnology, Faculty of Engineering, University of Fukui, 3-9-1 Bunkyo, Fukui 910-8507, Japan, [2]Division of Material Engineering, Graduate school of Natural Science and Technology, Kanazawa University, Kakuma-machi, Kanazawa 920-1154, Japan

Microbial poly(ε-L-Lysine) (MPL) is one of a few biodegradable homopolyamides which occur in nature and composed of L-lysine. MPL is a product of a variant of *Streptomyces alulbulus*, having amide linkage between ε-amino and α-carboxyl groups. The molecular structure and conformation of MPL and its derivatives were studied by using solid-state ^{13}C and ^{15}N NMR spectroscopy[1,2].

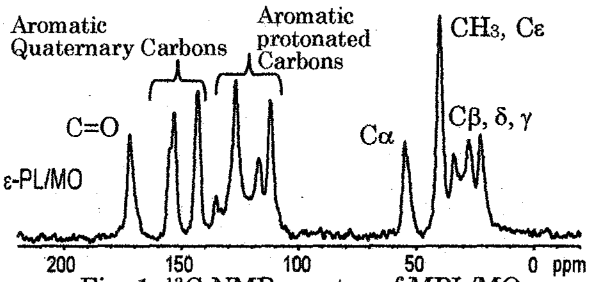

Fig. 1. ^{13}C NMR spectra of MPL/MO.

The observed CPD depolarization time constant *T*d in MPL, MPL/HCL, MPL/methyl orange (MO) and MPL/dabsyl chloride (DC) are listed in Table 1. *T*d were measured in CPD experiments by using CP/MAS pulse sequence combined with $^{13}C\rightarrow{}^{1}H$ depolarization process after $^{1}H\rightarrow{}^{13}C$ cross polarization process. *T*d was obtained from fitting a decay curve to $M(\tau)=M_0\exp(-\tau/Td)$. *T*d depends on the chemical environment of each carbon atom as shown in Table 1. Therefore, we concluded that the number of hydrogen atoms directly bonded to each carbon atom can be estimated from *T*d. The cross relaxation time constant T^{CH} and T^{CH}(TORQUE) were also measured by using standard ^{13}C CP/MAS experiment and the TORQUE sequence proposed by Tekely et al[3], respectively. T^{CH} and T^{CH}(TORQUE) were obtained from fitting a magnetization recovery curve to Eq.(1) and Eq. (2), respectively.

$$M(t)=M_0(1-\exp(-t/T^{CH})\exp(-t/T_{1\rho}(^1H)) \quad (1)$$

$$M_S(t_{CP},t_{SL})=M_S[\exp\{-(t_{SL}+t_{CP})/T_{1\rho}(I)\}-\exp\{-t_{SL}/T_{1\rho}(I)\}\exp\{-(t_{CP}/T_{CP})^{\alpha}\}]. \quad (2)$$

T^{CH} and T^{CH}(TORQUE) observed for C=O of MPL/MO are 391 μs and 531 μs, respectively. Because the value of *T*d, 422 μs is similar to these values, we think that *T*d is a time constant representing heteronuclear dipolar interactions in depolarization process.

Table 1. CPD depolarization time constant T_d/μs in MPL, MPL/HCl, MPL/MO and MPL/DC.

	Carbon types						
	C=O	Cα	Cβ	Cγ	Cδ	Cε	CH_3
MPL	680	56.7	34.9	34.9	36.6 35.6	35.6	-
MPL/HCl	539	58.5	44.5	43.6	44.5	45.9	-
MPL/MO	422	50.8	38.8	45.8	44.6	51.6	293
MPL/DC	398	48.9	46.9	47.5	50.6	50.4	381

REFERENCES 1)S. Maeda, *et al.*, *J. Mol. Struct.*, **655**, 149-155 (2003). 2)S. Maeda, *et al.*, *Polym. Bull.*, **53**, 259-267 (2005). 3)P. Tekely, *et al.*, *Solid State Nucl. Magn. Reson.*, **4**, 361-365 (1995).

AP109

Characterization of Microbial Poly(ε-L-lysine)/Poly(L-lactic acid) Blend Films by Solid-State NMR

Shiro Maeda[1], Osamu Kinoshita[1], Yasuhiro Fujiwara[1], Kensuke Sakurai[2], Chizuru Sasaki[3], and Ko-Ki Kunimoto[3]

[1]Depertment of Applied Chemistry and Biotechnology, and [2]Department of Materials Science, Faculty of Engineering, University of Fukui, Fukui 910-8507, Japan, and

[3]Division of Material Engineering, Graduate School of Natural Science and Technology, Kanazawa University, Kanazawa 920-1154, Japan

Microbial poly(ε-L-Lysine) (MPL) is a product of a variant of *Streptomyces alubulus*, having amide linkage between ε-amino and α-carboxyl group. Poly(L-lactic acid) (PLLA) is a biodegradable polyester made from natural resources such as corn starch. Figure 1 shows molecular structures of both homopolymers. The intermolecular interaction and conformation of PLLA/MPL blend film have been investigated by using solid-state ^{13}C NMR spectroscopy. PLLA and MPL were separately dissolved in chloroform and methanol, respectively. PLLA and MPL solutions were mixed with weight ratio of 1/1, 3/1, 4/1, 9/1, and 10/1. The mixed solutions were cast on a Teflon dish and dried at room temperature to make a film, then dried in vacuo.

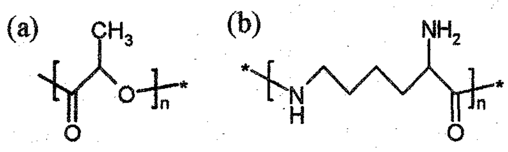

Figure 1. Molecular structure of a) PLLA and b) MPL

PLLA/MPL blend of 1/1 did not make a film. Although PLLA/MPL blend of 3/1 formed itself into a film, it was sticky and hardly drawn. PLLA/MPL blends of 4/1, 9/1, and 10/1 formed itself into white films which were easily stretched. Solid-state ^{13}C CP/MAS spectrum of PLLA/MPL blend film of 4/1 is shown in Figure 2. There appeared two carboxyl carbon peaks at 170.0 and 177.2 ppm. The former large peak was assigned to the carboxyl carbon of PLLA part and the latter small peak to that of MPL part. The chemical shift of the latter peak is almost the same as in MPL[1,2] ,where the intermolecular hydrogen bonds are made between α-NH_2 and carboxyl carbon. This may mean that miscibility is not so good in PLLA/MPL blend films. Intermolecular interaction between PLLA and MPL in the blend film is under investigation.

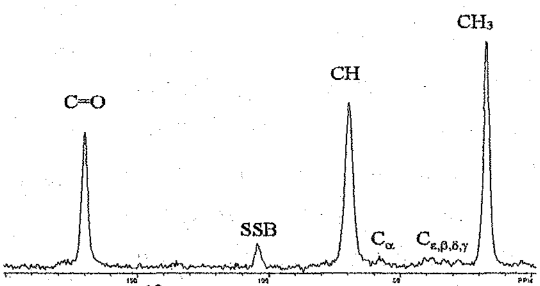

Figure 2. ^{13}C CP/MAS NMR spectrum of a blend film of PLLA/ MPL = 4/1.

REFERENCES: 1) S. Maeda, et al., *J. Mol. Struct.*, **655**, 149-155(2003). 2) S. Maeda, et al., *Polym. Bull.*, **53,** 259-267(2005)

NP110 (PL5)

Structure Analysis of Chlorosomes by ^{13}C Spin-Diffusion Solid-State NMR

Ayako Egawa[1], Kengo Akiba[1], Tadashi Mizoguchi[2], Yoshinori Kakitani[3], Yasushi Koyama[3], Toshimichi Fujiwara[1] and Hideo Akutsu[1]

[1]*Institute for Protein Research, Osaka University;* [2]*College of Science and Engineering, Ritsumeikan University;* [3]*Faculty of Science and Technology, Kwansei Gakuin University*

The photosynthetic system of green bacteria has a unique antenna complex called a chlorosome. We have studied the chlorosome mainly consists of bacteriochlorophyll (BChl) *c*. High-resolution solid-state NMR is suitable to investigate such a huge molecular complex. The ^{13}C signals of uniformly labeled BChl *c* were completely assigned by 2D RFDR and DQ dipolar correlation experiments. We have carried out 2D ^{13}C-^{13}C proton-driven spin diffusion experiments to obtain the ^{13}C-^{13}C distances. The distances were calculated from the 2D spin diffusion spectrum as a function of the mixing time τ_{mix} to distinguish between direct and indirect polarization transfer. The spin diffusion matrix **R** was obtained by minimizing the difference between the simulated and experimental signal intensities. Here, the spin diffusion process was simulated with $\mathbf{M}(\tau_{mix}) = \exp(-\mathbf{R}\tau_{mix})\mathbf{M}(0)$, in which $\mathbf{M}(\tau_{mix})$ is a peak intensity matrix at τ_{mix}. Internuclear distances were calculated from **R** by the perturbation theory for the spectral spin diffusion under magic-angle spinning, where the zero-quantum lineshape functions were estimated experimentally. About 68 intra-molecular distances obtained up to ca. 6 Å agreed with the known distances with 30% precision. This result reveals that the short-distance ^{13}C homonuclear dipolar couplings are not strong enough to truncate the long-distance ^{13}C dipolar couplings in this experiment. The structure of the BChl *c* complex was determined by simulated annealing under 63 intermolecular distance restraints. The distinction between the intra- and inter-molecular distances was confirmed by the spin diffusion experiments for a BChl *c* assembly composed of 100% ^{13}C labeled and non-labeled BChl *c* molecules with a 1:1 ratio. The determined structure indicated that BChl *c* forms an assembly consisting of strongly-overlapped dimmers as shown in Figure. This work demonstrates that the spin diffusion analysis in solid-state NMR is a powerful method to determine the structure of uniformly ^{13}C-labeled molecular assemblies.

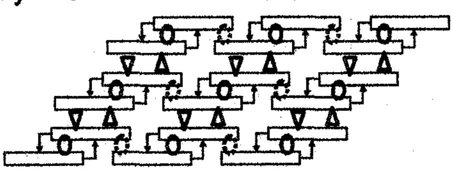

NP111

Effect of cholesterol on structure of PLC-δ1 PH domain at membrane surface studied by solid state NMR

○Akiko Hatakeyama, Takio Sugita, Masashi Okada, Hitoshi Yagisawa and Satoru Tuzi

Department of Life Science, Graduate School of Life Science, University of Hyogo, Harima Science Garden City, Kouto 3-chome, Kamigori, Hyogo, 678-1297

Phospholipase C-δ1 (PLC-δ1) is one of phosphoinositide-specific phospholipase C isozymes included in the cellular signal transduction pathways. In response to signals such as change of intracellular Ca^{2+} concentration, PLC-δ1 produces inositol(1,4,5)trisphosphate and diacylglycerol as second messengers by hydrolysis of phosphatidylinositol(4,5) bisphosphate (PIP_2) at the membrane surface. In order to understand molecular mechanisms of these functions of PLC-δ1, structural information of the protein at the membrane surface is indispensable. In the previous works, we have reported that the structure of the N-terminal PH domain of PLC-δ1 is modified at the surface of phosphatidylcholine (PC)/PIP_2 vesicle due to hydrophobic interactions with the hydrophobic layer of membrane. Here, we investigated effect of cholesterol on the structure of the PLC-δ1 PH domain at the membrane surface. Changes of dynamic structures of the [3-^{13}C]Ala-labeled PLC-δ1 PH domain and PC/PIP_2 vesicles containing different concentration of cholesterols are evaluated by solid state ^{13}C NMR and ^{1}H NMR with magic angle spinning (^{1}H MAS NMR).

While the ^{13}C DD-MAS NMR spectra of the PH domain forming complex with the vesicles containing 0-20 mol% of cholesterol reveals no conformational change caused by cholesterol, strong suppressions of the PH domain signals in the ^{13}C CP-MAS NMR spectra in the presence of cholesterol indicated increase in mobility of the domain at the membrane surface which causes decrease in cross polarization efficiency. In order to test the possibility that accumulation of negatively charged PIP_2 due to segregation induced by cholesterol causes increase in the mobility of the PH domain through electrostatic interaction, effect of cation on the CP-MAS NMR spectra were examined. In the presence of 80 mM Na^+, the CP-MAS spectrum was fundamentally identical to the spectrum in the absence of Na^+ suggesting that the electrostatic interaction between the domain and the lipid bilayer does not provide major mechanism of the increase in the mobility of the PH domain. ^{1}H MAS NMR spectra of the lipid molecules indicated that conformation of arachidonyl chain of PIP_2 is affected by cholesterol and the PH domain. This conformational change of polyunsaturated acyl-chain of PIP_2 may affect on the molecular motion of the PH domain at the membrane surface through change of the rotational and translational diffusion efficiency of the PIP_2 molecules.

NP112 (PL4)

Characterization of backbone conformations and dynamics on retinal proteins by ^{13}C solid state NMR

Izuru Kawamura[1], Naoki Kihara[1], , Satoru Tuzi[2], Yochi Ikeda[3]
Katsuyuki Nishimura[1], Hazime Saitô[2,4], Naoki Kamo[3] and Akira Naito[1]
[1]Grad. Sch. Eng., Yokohama Natl. Univ., [2]Grad. Sch. Life Sci., Univ. of Hyogo,
[3]Grad. Sch. Pharm. Sci., Hokkaido Univ., [4]Center for Quantum Life Sci., Hiroshima Univ.

Bacteriorhodopsin (bR) and *pharaonis* phoborhodopsin (*p*pR), are known as a membrane protein with proton pump activity and negative phototaxis receptor, respectively. These are retinal protein which consists of heptahelical transmembrane helix and retinal as chromophore. It is important to understand how retinal configurations activate retinal protein in molecular level. We, therefore, characterize backbone conformations and dynamics of these retinal proteins in view of retinal-protein interactions by solid-state NMR spectroscopy.

Backbone conformations of Tyrosine in bR corresponding to all-*trans* and 13-*cis* retinal configurations in the dark were investigated for Tyr-X peptide bonds of double-labeled [1-^{13}C]Tyr, [^{15}N]X-bR by REDOR (Rotational Echo DOuble Resonance) in solid-state NMR. The peak obtained from difference spectra between REDOR and Full echo experiments shows the unique signal of the Tyrosine residues except X is Ala. We successfully detected ^{13}C NMR peaks deduced from Tyr26, 64, 185 in bR at ambient temperature by REDOR. It is of interest to note that REDOR difference spectrum of [1-^{13}C]Tyr, [^{15}N]Pro-bR obviously showed two peaks at 173.4 and 177.7 ppm for Tyr185. This finding is attributed to the presence of two protein structures corresponding to the two retinal configurations in the dark; in fact Tyr185 closely lies by retinal. On the contrary, the spectra of Tyr26 and Tyr64 in bR showed one peak, respectively. REDOR spectra indicated that backbone conformations of bR were perturbed by retinal configurations in the vicinity of retinal.

*p*pR forms a complex with its cognate transducer (*p*HtrII). *p*pR-*p*HtrII interaction at the cytoplasmic surface has been regarded to be important to signal relay. In this study, local motional changes in the cytoplasmic side corresponding to the changes from [3-^{13}C] Ala *p*pR to D75N (an activated state) of the complex with *p*HtrII were investigated by ^{13}C solid-state NMR. In D75N, interhelical salt-bridge between helix C and helix G with retinal has been breakdown. The intensity of the C-terminal signals at 16.7-16.9 ppm of *p*pR decreased when *p*pR interacts with *p*HtrII (1-159) in the ^{13}C DD-MAS (Dipolar Decoupling-Magic Angle Spinning) NMR spectra. This result indicates that *p*HtrII (1-159) interacts partly with the C-terminal region of *p*pR. Because the C-terminal signals of D75N did not decrease by forming complex with *p*HtrII (1-159), it was revealed that the interaction between *p*pR and *p*HtrII (1-159) in cytoplasmic side becomes weak when *p*pR changes to an activated state.

NP113

Solid state NMR study of interaction between PLC-δ1 EF-hand domain and lipid bilayer

S. Tanaka, M. Okada, H. Yagisawa and S. Tuzi

Graduate School of Life Science, University of Hyogo, Harima Science Garden City, Kouto 3-chome, Kamigori, Hyogo 678-1297

Phospholipase C-δ1 (PLC-δ1) is one of the phosphoinositide-specific phospholipase C isomers included in the cellular signal transduction pathways, and produces second messengers, IP_3 and diacylglycerol, as products of phpsphatidylinositol (4,5) bisphosphate (PIP_2) hydrolysis in response to increase in the intracellular Ca^{2+} concentration. EF-hand domain located between the N-terminal PH-domain and the XY domain was predicted from the primary structure of PLC-δ1 as a cluster of four EF-hand motifs (EF1-EF4). Contrary to this prediction, x-ray diffraction study of PLC-δ1 proposed that part of the EF-hand domain including EF1 and EF2 takes highly disordered structure and provides flexible "tether" connecting the catalytic domain (XY domain) and the lipid binding domain (PH domain) based on the absence of this region in the electron density map.

In order to understand the structure-function relationship of the EF-hand domain of PLC-δ1 at the membrane surface, we prepared EF-hand domain fragment (aa 133-281) and investigated structure and the fragment-lipid interaction at the membrane surface by using solid state NMR. The EF-hand domain fragment was found to associate with phosphatidylcholine vesicle with significant binding affinity in the presence or absence of Ca^{2+}. The signal of [3-^{13}C]Ala labeled EF-hand domain fragment was resonated at 16.7 ppm in DD-MAS ^{13}C NMR spectra as a single peak either for the membrane binding state or solution state. Disappearance of this peak for the membrane-associated EF-hand domain in the CP-MAS ^{13}C NMR spectra due to low cross polarization efficiency indicates that the major conformation of the fragment is highly mobile random coil structure. Suppressions of the CP-MAS and DD-MAS ^{13}C NMR signals of the polar head groups and the acylchains of lipid molecules caused by the membrane association of the EF-hand fragment indicate increases in molecular motions of the lipid molecules that interfere with the frequency of ^{1}H decoupling. This suggests that the EF-hand fragment penetrates into the lipid bilayer and disturbs the structure of the hydrophobic layer of the membrane. Distribution in the gel-to-liquid crystalline phase transition temperature observed for the DMPC membrane induced by the membrane-association of the EF-hand domain is consistent with the membrane-penetrating model of the EF-hand domain described above. Absence of the influence of divalent cations (Ca^{2+}, Mg^{2+}) on the structure and dynamics of either the EF-hand domain fragment or the lipid bilayer indicates that those cations are not included in the interaction between the EF-hand domain and the membrane.

NP114

The Structural Model for the Amyloid Fibril Formed by β_2-Microglobulin Fragment Based on Solid-state NMR

○Kentaro Iwata[1], Toshimichi Fujiwara[1], Yoh Matsuki[1], Hideo Akutsu[1], Hironobu Naiki[2] and Yuji Goto[1]
[1]Inst. Protein Res., Osaka Univ., CREST/JST, [2]Fac. Med. Sci., Univ. of Fukui, CREST/JST

[Introduction]

Amyloid fibrils are highly-ordered filamentous aggregations formed by peptides and proteins with various primary sequences. Current interest in these fibrils arises from their association with many human diseases. In order to solve the basic questions about the interaction that stabilized their structure and the mechanism, it is important to characterize their common structure. However, the characterization is difficult because of intrinsically noncrystalline and insoluble nature. Solid-state NMR enables us to analyze the fibril structure at the atomic level. Here, we investigated the structure of uniformly labeled amyloid fibrils of K3 fragment, an amyloidogenic peptide from β_2-microglobulin, with solid state NMR.

[Results and Discussion]

2D solid state NMR under magic-angle spinning condition was measured with ^{13}C, ^{15}N uniformly isotope-labeled K3 amyloid fibrils. For assignment of the each peak, intra-residue spin connectivities were obtained with 2D correlation experiments for ^{13}C-^{13}C (Fig. 1) and ^{15}N-^{13}C. Sequence specific assignments were performed with ^{13}C-^{13}C and ^{15}N-^{13}C correlation experiments. The analysis of the obtained ^{13}C and ^{15}N chemical shifts by TALOS suggested that K3 fragments in the fibril form the two β-strands connected with a loop. For the further structural refinement, distance information was obtained from 2D ^{13}C-^{13}C proton-driven spin diffusion experiments at a series of mixing times. Intra- and intermolecular signals were discriminated by the same experiments using fibrils made from fully labeled and non-labeled K3 mixture. In addition, although solid-state NMR cannot detect long-range information such as β-sheet packing, atomic force microscopy (AFM) and X-ray fiber diffraction revealed that K3 amyloid fibrils contain two layers of β-sheet.

These results suggested that K3 fibril has two layers of β-sheet connected by loops and that more residues in the fibrils than those in the native β_2-microglobulin participate in the β-strand. This increment should contribute to stabilizing the fibril structure by outweighing the disadvantage of entropic effect.

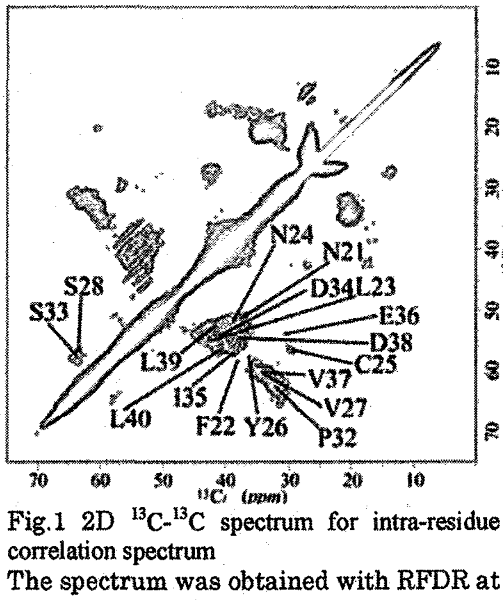

Fig.1 2D ^{13}C-^{13}C spectrum for intra-residue correlation spectrum
The spectrum was obtained with RFDR at a mixing time of 2.4 ms.

NP115

DOQSY NMR determination of the repeated biomimetic polypeptides

Yasumoto Nakazawa[1], Jacco D. van Beek[2], Beat H. Meier[2] Kousuke Ohgo[1] and Tetsuo Asakura[1]

[1]Department of Biotechnology, Tokyo University of Agriculture and Technology, Koganei, Tokyo 184-8588, Japan

[2]Laboratory for Physical Chemistry, ETH Zürich, CH-8093 Zürich, Switzerland

Tel: +81-42-388-7025, Fax: +81-42-383-7733, e-mail: yasumoto@cc.tuat.ac.jp

Model peptides based on the structure of solid proteins form a convenient tool to study complex biological systems. Isotopic labeling can be introduced more easily than in the native materials and one may focus on specific areas of interest in the proteins. In recent work we have shown that torsion-angle distributions in model peptides may be obtained using a combination of 2D spin-diffusion NMR and REDOR techniques[1-3]. Here we present an alternative approach, which allows a more detailed determination of the torsion-angle distribution, by using the double-quantum single-quantum correlation experiment (DOQSY)[4,5]. We have applied the approach to several model peptides, with sequences based on elastin[6] and silk[2,3]. A detailed analysis of the spectra taken for various model peptides will be presented.

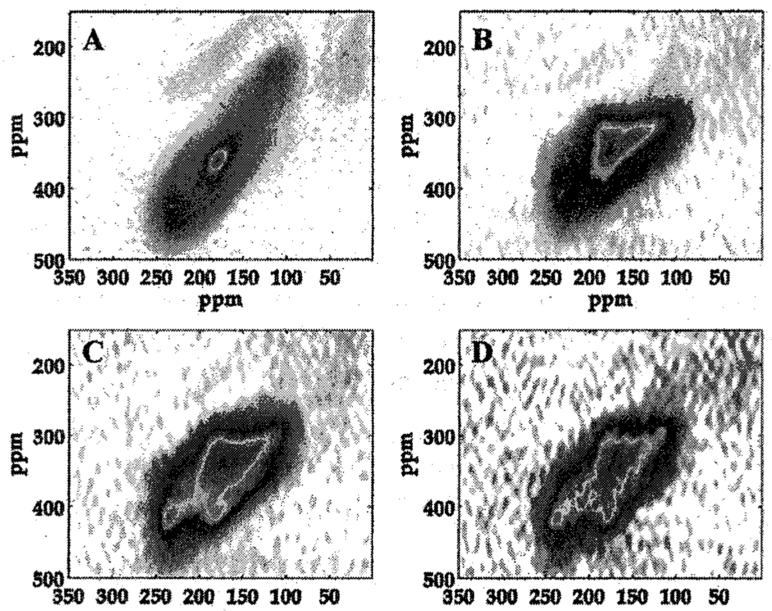

Figure 1 Experimental 2D DOQSY spectra of four model peptides, taken at room temperature. Spectra processed using the MatNMR[ref] processing package. **(A)** $(A)_5[1-^{13}C]A[1-^{13}C]A(A)_5$ (typical β-sheet) and **(B)** $(AGG)_3A[1-^{13}C]G[1-^{13}C]G(AGG)_6$ (typical 3_1-helix) **(C)** $(GPGGA)_2G[1-^{13}C]P[1-^{13}C]GGA(GPGGA)_3$ (β-turn conformation)and **(D)** $(VPGVG)_2V[1-^{13}C]P[1-^{13}C]GVG(VPGVG)_3$. (β-turn conformation)

References

[1]Ohgo, K. et al, *Macromolecules*, **2005**, 38, 6038-6047 **[2]**Ashida, J. et al, *J. Biomol. NMR*, **25**, 91-103. 2003 [3] Nakazawa, Y.; Asakura, T., *J. Am. Chem. Soc.* **2003**, 125, 7230-7237. **[4]**van Beek, J. D. et al, *Nature*, 2000, 405, 1077-1079 [5]van Beek, J. D. et al, *Proc. Natl. Acad. Sci. U S A* **2002**, 99, 10266 - 10271. [6]Debelle, L.; Tamburro, A. M. Int. *J. Biochem. Cell Biol.* **1999**, 31, 261-272.

NP116 (PL7)

Solid State NMR Analysis of Amphotericin B–Sterol Covalent Conjugates Forming a Molecular Assemblage in Membrane

Yusuke Kasai, Shigeru Matsuoka, Yuichi Umegawa, Hiroyuki Ueno, Nobuaki Matsumori, Tohru Oishi, Michio Murata

Department of Chemistry, Graduate School of Science, Osaka University, 1-16 Machikaneyama, Toyonaka, Osaka 560-0043, Japan

Amphotericin B (AmB) is a polyene macrolide antibiotic that has been used for treatment of systemic fungal infections despite its negative side effects. Its antifungal action is thought to be due to the formation of an ion-permeable channel across the lipid bilayer. The channel is presumed to be a barrel-stave type assemblage consisting of about eight pairs of AmB and membrane sterol[1)]. The selective toxicity is accounted for by its higher affinity for ergosterol in fungal membrane than cholesterol in mammalian one. However, no experimental evidence has been obtained for the direct interaction between AmB and membrane sterol.

To investigate the ion-channel structure and AmB-sterol interactions, we applied solid-state NMR for evaluating the interaction between AmB and sterol under membrane environments. First we designed and prepared AmB-sterol covalent conjugates[2)] (**1** and **2**), which should stabilize the interaction state between AmB and sterol parts, thus expectedly facilitating the distance measurements. The $^{13}C\{^{19}F\}$RDX measurements[3)] of conjugate **1** in DMPC membrane showed the significant dephasing effect at the heptaene portion. Larger dephasing was observed for 6-fluoroergosterol conjugate **1** than its cholesterol congener **2**, indicating that the ergosterol part locates closer to the heptaene part of AmB than does the cholesterol part. To our knowledge, this is the first spectroscopic evidence for the direct interaction between AmB and sterol in membrane.

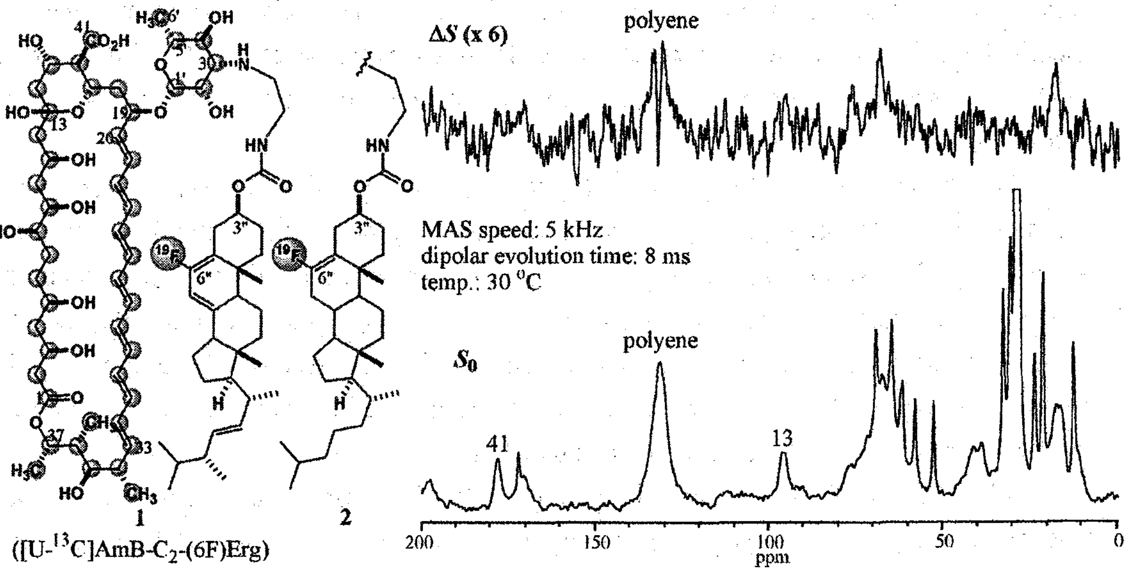

Fig 1. $^{13}C\{^{19}F\}$RDX spectra of [U-^{13}C]AmB-C$_2$-(6F)Erg **1** in DMPC (**1** : DMPC = 1 : 10, 50% wt. in 10 mM HEPES / D_2O, pH 7.0. lower: full echo spectrum S_0, upper: difference spectrum ΔS).

ref. 1) De Kruijff, K.; Demel, R. A. *Biochim. Biophys. Acta* **1974**, *339*, 57. 2) Matsumori, N. *et al. Chem. Biol.* **2004**, *11*, 673. 3) Mehta, A. K.; Schaefer, J. *J. Magn. Reson.* **2003**, *163*, 188.

NP117

Specific Interaction of Bovine Lactoferricin with Acidic Phospholipid Bilayers and Elucidation of its Antimicrobial Activity

○Masako Umeyama, Katsuyuki Nishimura, Akira Naito
Graduate School of Engineering, Yokohama National University,
79-5 Tokiwadai, Hodogaya-ku, Yokohama 240-8501 JAPAN

Bovine lactoferricin (LfcinB) is an antimicrobial peptide which consists of 25-amino acid residues with the sequence of Phe-Lys-Cys-Arg-Arg^{5}-Trp-Gln-Trp-Arg-Met^{10}-Lys-Lys-Leu-Gly-Ala^{15}-Pro-Ser-Ile-Thr-Cys^{20}-Val-Arg-Arg-Ala-Phe^{25} (LfcinB-25) forming a disulfide bond between Cys3 and Cys20. In this work, we investigated the specific interaction between LfcinB and two types of phospholipid bilayers : one is acidic phospholipid bilayers with the weight percentage of 65%DMPG, 10%CL (cardiolipin) and 25%DMPC (I) as a mimic of cell membrane of *Staphylococcus aureus*, and the other is DMPC (II) by means of solid state ^{31}P, ^{13}C and ^{1}H NMR spectroscopy.

^{31}P static NMR spectra indicated that there was specific interaction between LfcinB and acidic phospholipid bilayers, and bilayer defects were formed in the bilayer system as isotropic peaks were appeared. ^{13}C DD-MAS NMR spectra indicated that LfcinB interacted with the part of glycerol group Cα in phosphatidylglycerol of phospholipids. Gel-to-liquid crystalline phase transition temperatures (Tc) were determined by measuring the temperature variation of relative intensities of acyl chains in ^{1}H MAS NMR spectra. Tc values of DMPC, LfcinB-DMPC bilayer systems, acidic phospholipid and LfcinB-acidic phospholipid bilayer systems were 23.0℃, 24.5℃, 21.5℃ and 24.0℃, respectively. Moreover, changes of chemical shift attributed to ring current effect from Trp were observed at CH(β) peak in ^{1}H MAS NMR spectra. These results suggest that Trp resideus exsist at the interfacial region of lipid bilayers.

To characterize the bilayer defect, we measured the time course of concentration variation of K^{+} after adding LfcinB to acidic phospholipid bilayers by potassium ion selective electrode. In the experiments, potassium ion permeation across the membrane was observed. These results suggest that LfcinB interacted with acidic phospholipid bilayers at the membrane interface and caused pores in the membrane. Because these pores lead the permeability across the membrane, molecular mechanism of the antimicrobial activity could be attributed to the pore formation induced by LfcinB.

When LfcinB-25 was added to acidic phospholipid bilayers, aggregation of liposomes was observed. This result suggests that hydrophilic residues in Lfcin-B interact with the surface of acidic phospholipids. Consequently, hydrophobic regions of LfcinB-25 appear in the outside of the membrane because Trp resideus exsist at the interfacial region of lipid bilayers. These protruded residues cause further aggregation among liposomes by hydrophobic interaction.

NP118 (PL8)

Dynamic structure analysis of antibiotic peptide Alamethicin in lipid bilayers by solid-state NMR

Takashi Nagao, Daishuke Ishioka, Katsuyuki Nishimura, Akira Naito
Graduate school of Engineering, Yokohama National University,
79-5 Tokiwadai, Hodogaya-ku, Yokohama 240-8501, Japan

Alamethicin is an antibiotic peptide extracted from *Trichoderoma viride* and consisting of 20 amino acid residues (Ac-Aib-Pro-Aib-Ala-Aib-Ala-Gln-Aib-Val-Aib-Gly-Leu-Aib-Pro-Val-Aib-Aib-Glu-Gln-Phol). Alamethicin exhibits a voltage-gated ion channel activity in the lipid bilayers. Although alamethicin is a small peptide, the voltage-gated activity makes alamethicin into an extremely attractive model for a voltage dependent structural change of membrane proteins.

The barrel-stave model consisting of aggregated alamethicin helices is the most accepted model for the channel structure of alamethicin. To clarify the mechanism of the voltage-gated ion channel, it is necessary to study the structure and orientation of alamethicin in lipid bilayers.

Solid state NMR is a powerful means to analyze membrane proteins and biologically active peptides in lipid bilayers. This method is particularly useful for obtaining detailed information about orientation of peptides in lipid bilayers. In this study, [1-^{13}C]Ala6,Val9,Gly11-labeled alamethicin analogs were synthesized by Fmoc-chemistry and incorporated into DMPC (1,2-dimyristoyl-sn-glycero-3-phosphochline) bilayers for investigating the structure and orientation of alamethicin in lipid bilayers.

Dynamic structure of alamethicin in lipid bilayers was investigated by analyzing the anisotropic and isotropic chemical shifts of carbonyl carbons under the static and magic-angle spinning conditions. Isotropic shifts obtained from DD-MAS experiments showed that Ala6,Val9,Gly11 positions of alamethicin are involved in an α-helical form. We analyzed the chemical shift tensors of carbonyl carbons by considering the rotational motion of α-helix about the bilayer normal for obtaining the tilt angle γ and the phase angle ζ of the peptide plane.

These results indicate that N-terminal of alamethicin adopts an α-helical structure with the tilt angles of 9°. Furthermore, it was revealed that the side chain of Gln7 that is a hydrophilic amino acid residue in N-terminal faces toward the rotation axis. These results indicate that alamethicin helices aggregate and form the channel to allow efficient ion transportation along the pore with hydrophilic surface.

NP119

Development of phase-modulated Lee-Goldburg sequence for X-^{1}H (X=^{15}N,^{13}C) dipolar recoupling under very fast MAS

H. Ishii, M. Fukuchi, K. Takegoshi, and A. Shoji*
Department of chemistry, Graduate School of Science, KyotoUniversity
Sakyo-ku Kyoto 606-8502
***Department of Biological Science, Faculty of Engineer, Gunma University**
1-5-1 tenjin-cho Kiryu-shi Gunma 376-8515

To examine the N-H bond lengths in peptides having various secondary structures [1], we developed a phase-modulated version of the FSLG-*m2mm* sequence [2], which was proposed to recouple X-^{1}H (X=^{13}C,^{15}N) dipolar interactions under fast magic-angle spinning.The modification was necessary because some of our sepectrometers couldn't realize frequency jump. Similar to the PMLG modification of the FSLG sequence [3], we devided the 2π Lee-Goldburg pulse into 9 segments. The irradiation phases for the m=2 sequence are given by
φ_i=11.54°+(i-1)23.09° for pulses i=1-9,
φ_i=16.26°-(i-10)23.09° for pulses i=10-18,
φ_i=-φ_{i-18} for pulses i=19-36,
φ_i=φ_{i-18} for pulses i=37-54,
φ_i=φ_{i-54} for pulses i=55-72.

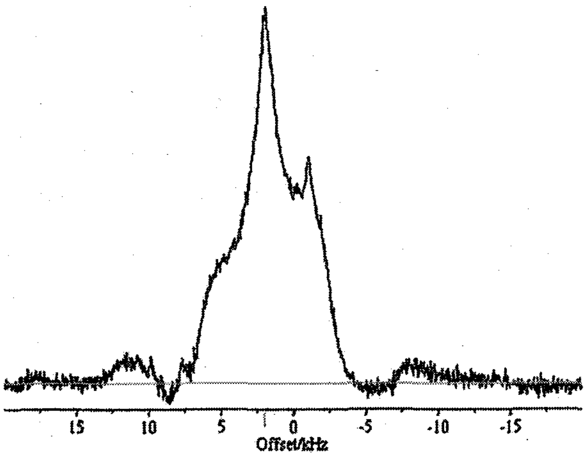

Fig.1 13C Spectrum of 2-13C Valine

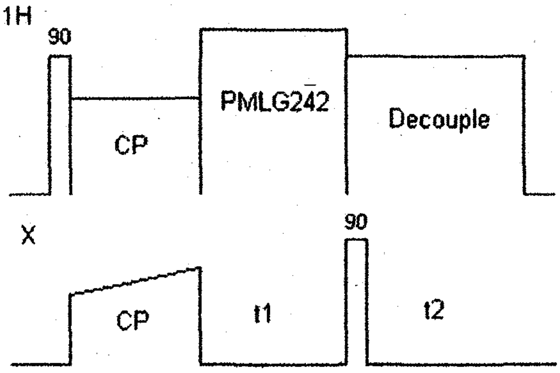

Fig.2 Pulse Sequence

Figure 1 shows the ^{13}C MAS spectrum of 2-^{13}C valine taken under PMLG-242 with the spinning speed of 10.0kHz. The strength of the ^{1}H rf field was 62.5kHz, and that of the PMLG effective field was 80.0kHz.

The observed spectrum shows rather strong signal at the higher magnetic field side, which is attributed to the other natural-abundance carbons.

Figure 2 shows the pulse sequence for 2D observation. The observed ^{1}H-^{15}N bond lengths in peptidess having various secondary structure will be discussed in the meeting.

References

[1] H.Kimura, et al. Macromolecules, 33, 6627 (2000)
[2] K.Takegoshi and T.Terao Solid State Nuclear Magnetic Resonance 13, 203 (1999)
[3] E.Vinogradov, et al. Chemical Physics Letters 314, 443 (1999)

AP120 (PL6)

Structural Analysis of Alanine Tripeptide with Anti-Parallel and Parallel β-Sheet Structures Using Solid State NMR

○Michi OKONOGI[1], Kazuo YAMAUCHI[1], Hiromichi KUROSU[2], and Tetsuo ASAKURA[1]

Department of Biotechnology, Tokyo University of Agriculture and Technology, Naka-cho 2-24-16, Koganei, Tokyo 184-8588, Japan[1]; School of Natural Science and Ecological Awareness Graduate School of Humanities and Sciences, Nara Women's University, Kitauoya-Nishimachi, Nara 630-8506, Japan[2]

Tri-L-alanine (Ala_3) can take complete anti-parallel (AP) or complete parallel (P) β-sheet structures by changing solvent treatment. Therefore Ala_3 is one of the suitable samples to study two kinds of β-sheet structures in detail.

In this study, we performed solid state NMR experiments on Ala_3 with AP or P β-sheet structures[1,2]. 2D RFDR (Radio Frequency-Driven Recoupling) experiments on [U-^{13}C]Ala_3 provided multi correlations among ^{13}C nuclei, which led to the complete assignment of ^{13}C signals (Figure). REDOR (Rotational Echo DOuble Resonance) experiments on a 1:4 mixture of ^{13}C and ^{15}N singly labeled Ala_3 provided inter-molecular ^{13}C-^{15}N distances with high accuracy (±0.1 Å). Inter-sheet inter-atomic distances were obtained from the AP structure, while intra-sheet inter-atomic distances were obtained from the P structure. In addition, the spin-lattice relaxation times of the Ala Cβ carbons are quite different between two forms (AP: av.112ms, P: av.381ms), reflecting the large difference in the intermolecular arrangement. Furthermore, theoretical calculation of ^{13}C chemical shifts are now in progress.

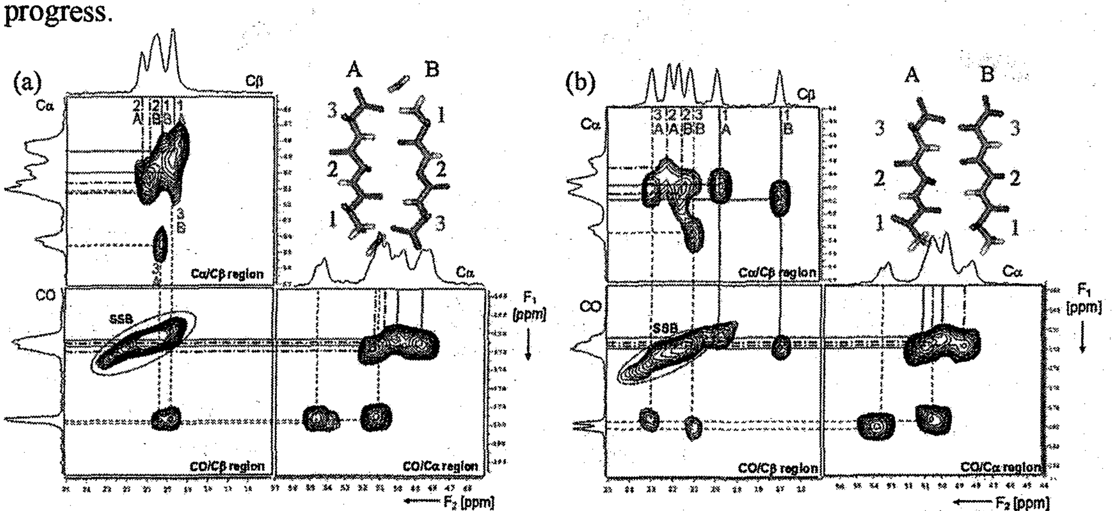

Figure 2D ^{13}C-^{13}C RFDR spectra of [U-^{13}C]Ala_3, obtained with a mixing time of 1ms. Colored lines show traces of peak assignments for each residue in crystallographically - independent molecules A and B. (a) AP structure and (b) P structure.

[References]

1) Fawcett, J. K.et al., *Acta Cryst.* **1975,** *B31*, 658. 2) Hempel, A. et al., *Biopolymers* **1991,** *31*, 187.

NP121

^{23}Na MQMAS at 21.9T (^{1}H 930MHz)

Toshihito Nakai[1], Naoyuki Fujii[1], Kenji Takasugi[1],

Hiroaki Utsumi[1], and Tadashi Shimizu[2]

1) JEOL Ltd., 1-2 Musashino 3-chome Akishima Tokyo 196-8588

2) National Institute of Materials Science, 3-13 Sakura Tsukuba 305-0003

At the ultra high field B_0 of 21.9T (^{1}H 930MHz; ^{23}Na 246 MHz), ^{23}Na MQMAS (Multiple-Quantum Magic-Angle-Spinning) spectra were first measured for Na_2HPO_4 and $Na_4P_2O_7$. For comparison, their spectra at 14.1T were observed. The ultra high field could reduce the quadrupolar frequency distribution proportional to $(e^2qQ/h)^2/B_0$, giving high spectral sensitivity. Also, it is demonstrated how strong and weak rf fields B_1 might affect to the sensitivity at 14.1T. By applying strong B_1 about 200kHz using a single resonance MQMAS probe, high sensitivity could be achieved as well as the high sensitivity at 21.9T.

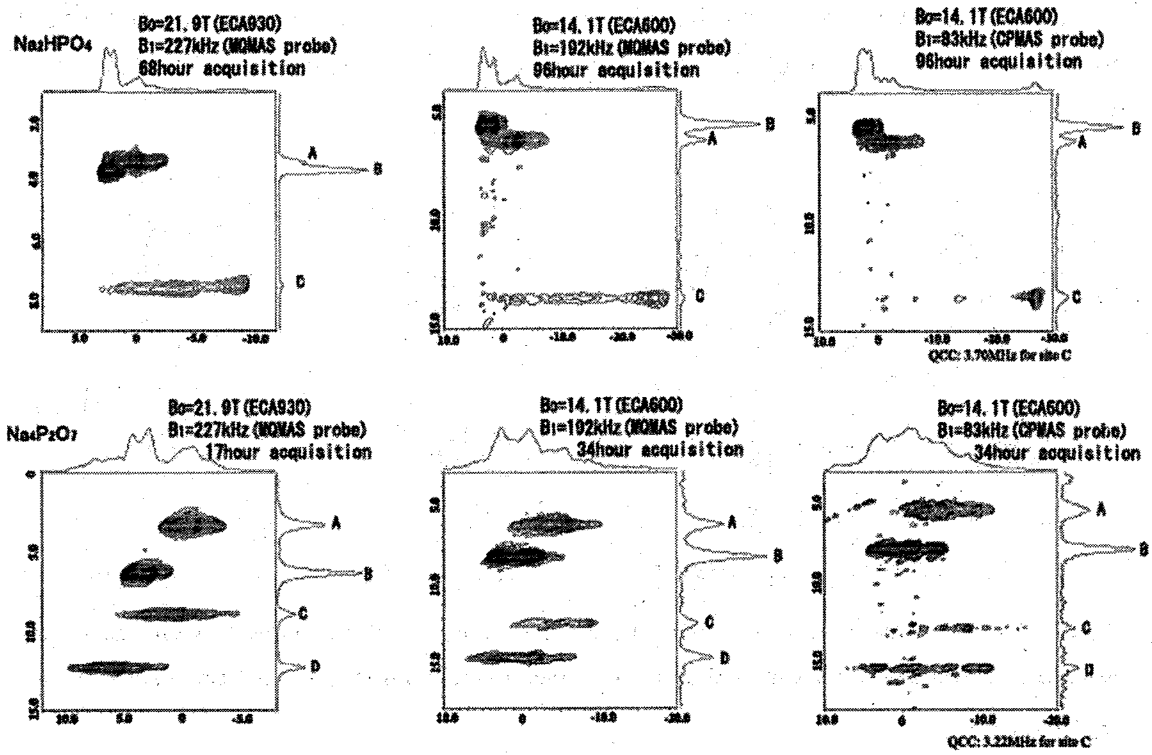

NP122

Structure of duplex oxide layer in porous alumina studied by ^{27}Al MAS and MQMAS NMR

Takahiro Iijima,[1†] Seiichi Kato,[1] Ryuichi Ikeda,[1] Shinobu Ohki,[1] Giyuu Kido,[1] Masataka Tansho[1] and Tadashi Shimizu[1]
[1]*National Institute for Materials Science, Tsukuba, Ibaraki 305-0003, Japan*
†Present address: *Department of Chemistry, Graduate School of Science, Kyoto University, Kyoto 606-8502, Japan*

In recent years, porous alumina[1-3] having uniform pores has attracted much interest in many fields. Since the size, depth and interval of the pores are highly controllable in the porous alumina materials fabricated by an anodic oxidation method, the application of them extends to accurate filters, catalyst supports, nano composites, photonic crystals, and so on. The structure of porous alumina has been proposed to be an assembly of a hexagonal column with the pore in its center by Keller and co-workers in 1953.[1] Thompson and Wood have reported that porous alumina consists of duplex oxide layers;[2] outer oxide layer existing adjacent to the pore is composed of anion-incorporated alumina, whereas inner layer existing remote from it is of pure alumina. The inhomogeneous distribution of the anion species concentrated in the intermediate part of the outer oxide has been suggested in order to account for the nonuniform refractive index observed.[3] However, the structure of alumina in each oxide layer has not been clarified yet, although such information is essential when the material having nano function is designed. This can be due to the amorphous structure of porous alumina that is reported for the material synthesized by a sol-gel method.[4]

High-resolution solid-state NMR is a powerful tool for analyzing the local structure of both crystalline and non-crystalline materials. For example, diffraction experiments are unable to provide detailed information about the local structure for the amorphous sample, while NMR remains sensitive to local bonding parameters. In particular, ^{27}Al (S = 5/2) magic-angle spinning (MAS) NMR that can distinguish the coordination environment around it has been ubiquitously used for the structural characterization of the inorganic materials. Further detailed structural information around ^{27}Al nuclei is obtainable from a two dimensional NMR method of multiple-quantum MAS (MQMAS) developed by Frydman and Harwood in 1995 for acquiring the high-resolution spectrum of half-integer quadrupole nuclei.[5] In the present work, the local structure of porous alumina fabricated by the anodic oxidation is investigated by using ^{27}Al MAS and MQMAS NMR spectra measured at 21.9 T. We will discuss the structure of both oxide layers by analyzing the obtained ^{27}Al NMR spectra.

1. F. Keller, *et al.*, *J. Electrochem. Soc.* **100**, 411 (1953).
2. G. E. Thompson and G. C. Wood, *Nature* **290**, 230 (1981).
3. J. Choi, *et al.*, *J. Appl. Phys.* **94**, 4757 (2003).
4. L. Wilcox, *et al.*, *Chem. Mater.* **15**, 51 (2003).
5. L. Frydman and J. S. Harwood, *J. Am. Chem. Soc.* **117**, 5367 (1995).
6. T. Iijima, *et al.*, *Chem. Lett.*, in press.

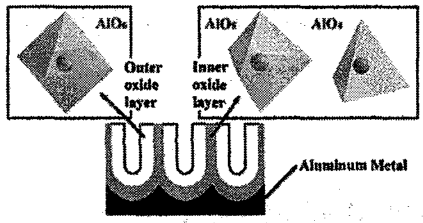

Figure: Schematic representation of porous alumina consisting of the duplex oxide layer.[6]

NP123

Research of the tautomerism for 9-hydroxyphenalenone derivatives by the solid-state exchange NMR

Hiroyuki Koyano,[a] Taisuke Manaka,[a] Daisuke Kuwahara,[a]
Tomoyuki Mochida[b]
[a] Department of Physical Chemistry, University of Electro-Communications,
[b] Department of Chemistry, Faculty of Science, Toho University

9-hydroxyphenalenone derivatives, which have intramolecular hydrogen bonds, show dielectric based on the tautomerism in the crystals. The phase transition behaviors have been researched by Mochida *et al.*[1] The origin of dielectric responses of these derivatives can be found for the polarization reversing caused by the tautomerism synchronizing with the proton transfer. Moreover, 9-hydroxyphenalenon derivatives are ideal systems to investigate the essence of the hydrogen-bonded dielectric substances, because they can be considered as the isolated hydrogen-bonded systems. One of the important factors which yield the proton tautomerism in the solid state is the presence of an intra- or an intermolecular hydrogen bond along which the proton transfer takes place. In addition, the proton transfer is highly dependent on the shape of the potential profile along the reaction coordinate. In this study, to investigate the shape of the potential curve and the height of the barrier concerning the tautomerism for 9-hydroxyphenalenone, we have examined the dynamic behavior of the proton transfer by solid-state ^{13}C NMR experiments. To begin with, we performed variable temperature CP/MAS experiments on 9-hydroxyphenalenone. In addition, the ^{13}C 1D exchange NMR experiments were performed while varying temperatures. The ^{13}C 1D exchange NMR experiments were performed using a pulse sequence with a selective excitation pulse. We calculated the rate constants $k1$ and $k2$ of the tautomerism through the exchange process plots; the equilibrium constant K was calculated from the rate constants. Moreover, the division width ($\Delta\nu$) of the carbonyl resonances at the temperature where the tautomerism is frozen was calculated from the equilibrium constant K and the division width ($\delta\nu$) at an appropriate temperature.

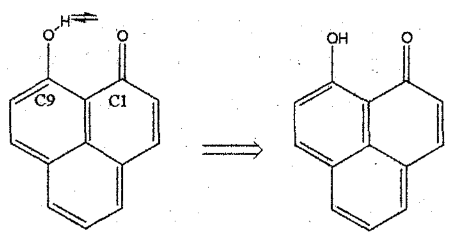

Fig.1. 9-hydroxyphenalenone and its carbonyl resonances

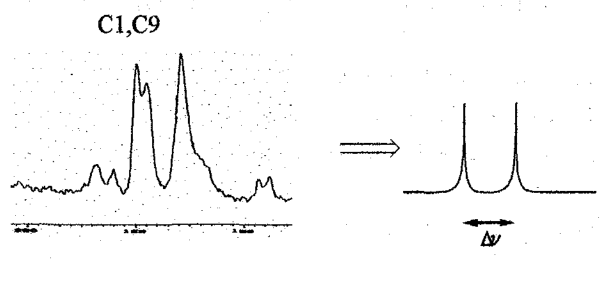

[1] T. Mochida *et al.*, J. Phys. Chem B, 107 (2003) 12315

NP124

Dynamics Analysis of a Hole-Transport Material for Organic LEDs by Solid-State ^{13}C NMR

Junya SHIMADA[1], Naoki TSUKAMOTO[1], Hironori KAJI[1,2], and Fumitaka HORII[1]

[1]Institute for Chemical Research, Kyoto University, Uji, Kyoto 611-0011, JAPAN, [2]PRESTO, JST, 4-1-8 Honcho Kawaguchi, Saitama, JAPAN

[Introduction] *N,N'*-diphenyl-*N,N'*-di(*m*-tolyl)benzidine (TPD) is a widely used hole-transport material in organic light-emitting diodes (OLEDs). In this study, dynamics analysis of amorphous TPD has been carried out by solid-state ^{13}C NMR spectroscopy. The dynamics of amorphous TPD below and around the glass transition temperature (T_g) has been investigated by one- and two-dimensional (1D and 2D) solid-state NMR by utilizing chemical shift anisotropy (CSA).

[Experimental] The TPD sample in natural abundance (NA-TPD) and phenyl-ring quaternary carbons ^{13}C-labeled TPD (^{13}CPQ-TPD) were used for 1D and 2D experiments. These samples were quenched from the melt to 0 °C to prepare amorphous samples. The DSC measurement showed that the T_g, the crystallization temperature, and the melting point were 64 °C, 152 °C and 172 °C, respectively. The solid-state NMR measurements were performed on a Chemagnetics CMX-400 Infinity spectrometer (9.4 T). Temperature range were -140 – 75 °C and 23 – 75 °C for 1D CSA and 2D CSA exchange measurements, respectively.

[Results and Discussion] From the 2D CSA exchange spectra of unlabeled amorphous TPD, π-flip motion is found to occur even below T_g. In order to investigate further details, the 1D and 2D measurements have been also performed for amourphous ^{13}CPQ-TPD. The temperature dependence of 1D CSA spectra shows that N-C bond fluctuations accompany the π-flip motion. The amplitude is 10 – 20° and the frequency is about 10^3 Hz. From the 2D CSA exchange spectra of amorphous ^{13}CPQ-TPD (see Fig.1), some specific subsecond motion is found to occur for phenyl-rings even below T_g. We are now analyzing the spectra in order to quantify the details. Above T_g, amorphous ^{13}CPQ-TPD is found to undergo the isotropic molecular motion in the order of second.

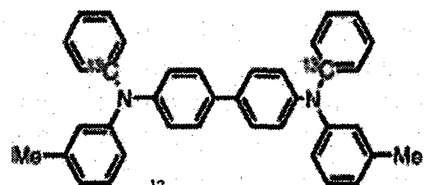

^{13}CPQ-TPD

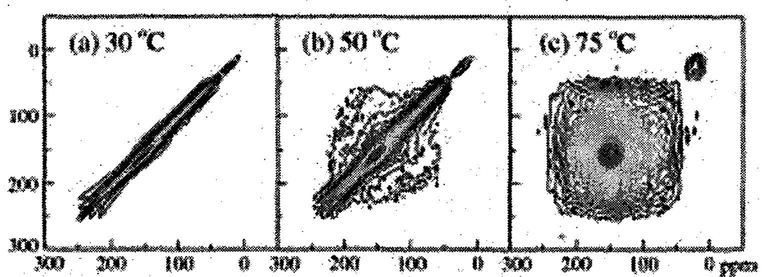

Fig.1 ^{13}C 2D CSA exchange NMR spectra of amorphous ^{13}CPQ-TPD. The mixing time is 100 ms.

AP125

Molecular dynamics in paramagnetic materials as studied by static-powder and magic-angle spinning ^{2}H NMR

Motohiro Mizuno, You Suzuki, Kazunaka Endo
Graduate School of Natural Science and Technology,
Kanazawa University, Kanazawa Kakuma-machi 920-1192, Japan

Introduction

^{2}H NMR spectroscopy is a powerful method for studying molecular dynamics and local structure in solids. However, the line broadening of a few hundred kHz for the static-powder ^{2}H NMR spectrum and the molecular motion with intermediate rate obviously lead to poor spectral resolution and low sensitivity. To remove these difficulties, the enhancements of the signal-to-noise ratio and of the sensitivity to dynamic processes due to the MAS ^{2}H NMR method have been demonstrated for the diamagnetic materials. We have developed the simulation method of the static-powder ^{2}H NMR spectrum for the paramagnetic materials. The reliable information about the molecular motion, the local structure and the paramagnetic ion can be obtained from the ^{2}H NMR spectral simulation including both the quadrupole interaction and the paramagnetic interaction. In the present study, we investigated experimentally and numerically the application of the MAS ^{2}H NMR method to the paramagnetic materials.

Experimental

The ^{2}H NMR spectra were measured by a Chemagnetics CMX-300 spectrometer at 45.826 MHz. The ^{2}H NMR MAS spectra of deuterated $[Ni(H_2O)_6][SiF_6]$ crystal were obtained using 7.5 mm rotor at 5 kHz.

Results and Discussion

The time evolution of the magnetization vector $M^+(t)$ under MAS can be written as $M^+(t) = L(t)M^+(0)$, where $L(t) = \exp\{(i\Omega(t) + W)t\}$. $\Omega(t)$ is the diagonal matrix composed by the frequencies at each deuterium site determined by the quadrupole interaction and the paramagnetic interaction. W is a kinetic matrix composed by the rate k of the deuterium jumping between each site. For the short time period Δt, by assuming time–independent $\Omega(n\Delta t)$, $L(n\Delta t) \approx \exp\{(i\Omega(n\Delta t) + W)\Delta t\}L((n-1)\Delta t)$ is obtained. $M^+(n\Delta t)$ is calculated by diagonalizing $(i\Omega(n\Delta t) + W)$. The ^{2}H NMR MAS spectrum can be obtained by Fourie transform of $M^+(n\Delta t)$. Fig. 1 shows the experimental and calculated ^{2}H NMR MAS spectra above room temperature. The asymmetric line shape of the spectrum is caused by the dipolar interaction between ^{2}H nucleus and Ni^{2+}. $[Ni(H_2O)_6]^{2+}$ in $[Ni(H_2O)_6][SiF_6]$ exhibits two types of molecular motions, a 180° flip of water molecule and a reorientation of $[Ni(H_2O)_6]^{2+}$ about its C_3-axis. The electric field gradient (EFG) at ^{2}H nucleus is already averaged by the fast 180° flip of the water molecule at 298 K. So, all simulations were performed using a constant fast jump rate $k_{H2O}=1\times10^8 s^{-1}$ for the 180° flip of the water molecule. The temperature variation of the ^{2}H NMR MAS spectrum can be explained by the reorientation of $[Ni(H_2O)_6]^{2+}$ about its C_3-axis. The quadrupole coupling parameters (e2Qq/h, η) and the rate of the reorientation of $[Ni(H_2O)_6]^{2+}$ (k_{re}) used for simulation are shown in Fig. 1. The effects of paramagnetic interaction on the ^{2}H NMR MAS spectrum will be discussed by comparing the results of the static powder ^{2}H NMR spectrum.

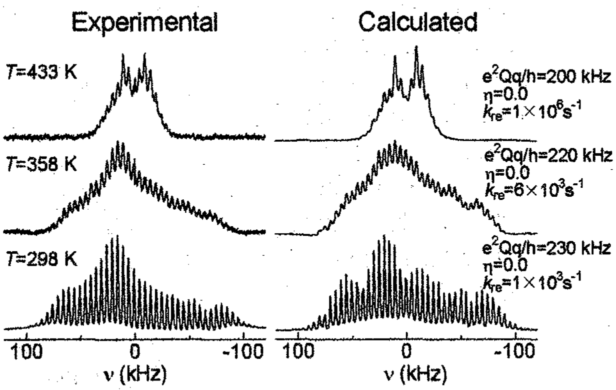

Fig.1 Experimental and calculated ^{2}H NMR MAS spectra for $[Ni(H_2O)_6][SiF_6]$.

AP126

Conformational Analysis of TPD by Two-Dimensional Solid-State Double-Quantum NMR Spectroscopy and Quantum Chemical Calculations

○Tomonori YAMADA,[1] Naoki TSUKAMOTO,[1] Hironori KAJI,[1,2] and Fumitaka HORII[1]

[1]Institute for Chemical Research, Kyoto University, Uji, Kyoto, JAPAN, [2]PRESTO, JST, 4-1-8 Honcho Kawaguchi, Saitama, JAPAN

[Introduction] *N,N'*-diphenyl-*N,N'*-di(*m*-tolyl)benzidine (TPD), which is widely known as a hole-transport material, is used as an amorphous state in organic LED. The molecular conformation is expected to change in the hole-transport process. In this study, we have analyzed the conformation of amorphous, crystalline, and dicationic TPD by two-dimensional ^{13}C double-quantum NMR spectroscopy (2D ^{13}C DOQSY) and compared the results with those of quantum chemical calculations.

[Experimental] The ^{13}C doubly labeled TPD (^{13}C2BIQ-TPD, Fig. 1) was synthesized and quenched from the melt to prepare amorphous ^{13}C2BIQ-TPD. The crystalline ^{13}C2BIQ-TPD was produced by annealing the amorphous ^{13}C2BIQ-TPD at 140°C for 10 min. ^{13}C2BIQ-TPD was doped by 3 equivalent of $SbCl_5$ and dried under vacuum to prepare dicationic ^{13}C2BIQ-TPD.

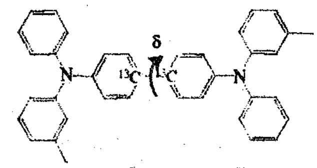

Fig. 1. ^{13}C2BIQ-TPD

2D ^{13}C DOQSY measurements were performed on a Chemagnetics CMX-400 spectrometer using the pulse sequence shown in Fig. 2.

Gaussian98 was used to optimize the geometries of neutral and dicationic TPD with density functional theory (DFT).

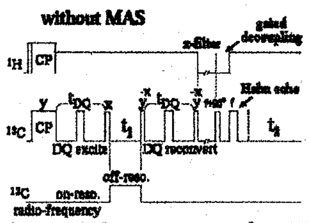

Fig. 2. Pulse sequence for 2D ^{13}C DOQSY measurements.

[Results and Discussion] Fig. 3(a) shows the experimental 2D ^{13}C DOQSY spectra for amorphous, crystalline, and dicationic ^{13}C2BIQ-TPD. From the analyses, the torsion angles, δ (see Fig. 1), are determined to be 42±1° and 2 ±1° for the crystalline and dicationic ^{13}C2BIQ-TPD, respectively. For the amorphous ^{13}C2BIQ-TPD, δ is found to be distributed and the spectrum is well reproduced by assuming the box-type distribution ranging between 30 and 50°. These results indicate that the 2D DOQSY technique is valuable for the quantitative conformational analysis of the amorphous and dicationic samples as well as the crystalline sample. The DFT-optimizations of neutral and dicationic TPD single molecules result in δ = 35° and 11°, respectively. The differences between the solid-state NMR and the DFT results are assumed to be originated from the intermolecular packing effect. We will show the results of the determination of bond lengths in TPD by two-dimensional 13C-^{13}C dipole / CSA correlation NMR.

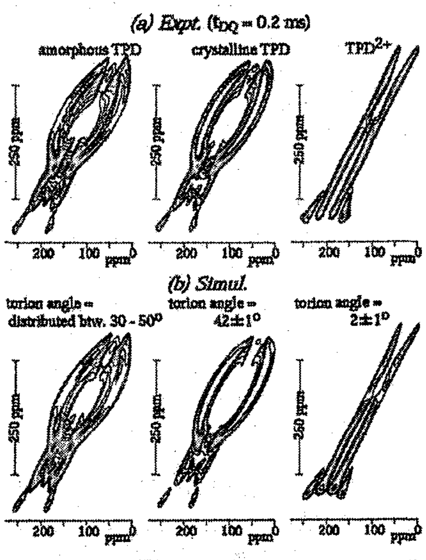

Fig.3. 2D ^{13}C DOQSY spectra of amorphous, crystalline, and dicationic ^{13}C2BIQ-TPD.

AP127

Solid State ^{7}Li NMR Study of Anode Hard-Carbons for Lithium-ion Battery Optimized to Hybrid Electric Vehicle

Kazuma Gotoh[1], Hiroyuki Ishida[1], Mariko Maeda[2], Aisaku Nagai[2], Atsushi Goto[3], Shinobu Ohki[3] and Masataka Tansho[3]
Dep. of Chemistry, Faculty of Science, Okayama Univ., 3-1-1 Tsushima-naka, Okayama 700-8530[1]
Nishiki Research Lab., Kureha Chemical Ind.,16 Nishikimachi-ochiai Iwaki, Fukushima 974-8686[2]
Tsukuba Magnet Lab., NIMS, 3-13 Sakura, Tsukuba, Ibaraki 305-0003[3]

Introduction

Hard carbon, which is one of the non-graphitizable carbons, has attracted considerable interest in recent years for an anode active material of the large size Li-ion battery. Its property of high power and durability are expected to be superior as the power source of Hybrid Electric Vehicle (HEV). The state of lithium doped in some different hard carbon samples has been investigated by wide-line ^{7}Li NMR.

Experimental

Electric capacity and crystal size factor (L_c) of three hard carbon samples prepared from petroleum pitch are given in Table. Sample (A) is Carbotron P(S)F (Kureha Chemical Industry) being in the market. (B) and (C) are improved samples for HEV having higher effective capacity and less amorphous structure than (A). Test cells using these carbons as anode active materials were made and the electrochemical evaluation was performed. Fully charged anodes were taken out from the cells and sealed into glass tubes for the NMR measurement.

Results and Discussion

All specimens showed two peaks at 5-10 ppm and 70-110 ppm ($LiCl_{aq}$: 0 ppm) at room temperature. The former is inferred the signal of lithium intercalated into graphene layers of small carbon particles mixed in the specimens[1]. The latter was split into two peaks with decreasing temperature, one overlapped to the peak of 5-10 ppm and the other shifted to 170-180 ppm which is explainable by lithium cluster in inter-graphene spaces at 180 K. This splitting is similar to the Li in non-graphitizable carbon fiver reported by Tatsumi et al.[2]. The signal of Li in graphene layers shifted to -25 ppm at 60 K, while that of the cluster disappeared below 120 K. The intensity of the cluster-lithium signal of each specimen at about 240 K was proportional to the electric capacity of Constant Voltage (CV) state observed on the electrochemical evaluation experiment.

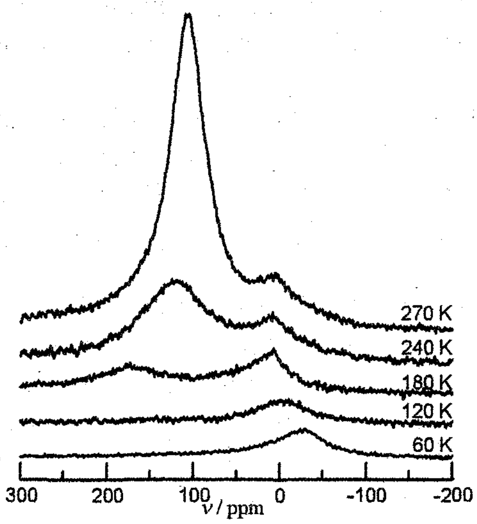

Figure Temperature dependence of ^{7}Li NMR (104.981 MHz) spectra for Li doped sample (A)

References

[1] K. Gotoh et al., Proc. of 85th Spring Meeting of CSJ (2005) 1G1-08.
[2] K. Tatsumi et al., *Chem. Commun.* (1997) 687-688.

Table Properties of hard carbon samples

sample	(A)	(B)	(C)
electric capacity(CV/whole) / $mAh \cdot g^{-1}$	160±5 / 500±10	55±5/350±10	20±10/280±15
crystal size factor (L_c) (*) / nm	1.31	1.40	1.60

(*) Calculated from XRD(002) reflection using Sherrer's equation

AP128

Effect of Chemical Exchange of Xenon in Zeolite NaY on ^{129}Xe Chemical Shift measured by High-pressure *in situ* NMR Probe

Takahiro Ueda,[ab] Hironori Omi,[b] Kuniyoshi Maezawa,[b]
Noriko Kato,[b] Keisuke Miyakubo,[b] and Taro Eguchi[ab]
[a]The Museum of Osaka University, and [b]Department of Chemistry,
Graduate School of Science, Osaka University, Toyonaka, Osaka
560-0043, Japan

Pressure-variable conventional *in situ* NMR probe developed in our laboratory is powerful tool to investigate the adsorption behavior of several gaseous species in the porous materials. Especially, xenon is one of the most interesting and useful molecular-probe to study the microstructure of void space, and we have demonstrated pressure dependence of ^{129}Xe chemical shift in some porous materials using the high-pressure *in situ* NMR probe [1,2].

However, the effect of chemical exchange of xenon between inside and outside of the micropore on the chemical shift is not negligible in this NMR probe, since xenon gas is used for the pressurizing media. For example, NaX and NaY zeolites exhibit quite different behavior in pressure dependence of ^{129}Xe chemical shift as shown in Figure 1 [1]. In NaY, the observation of a dip in the pressure dependence of δ around 6 MPa may come from the chemical exchange of xenon between inside and outside the pore, and we have interpreted by the simple two-site exchange model.

In this work, we examine experimentally the effect of chemical exchange between gaseous and adsorbed xenon in NaY on the chemical shift in the basis of the free volume around the powdered samples and the number of adsorption site in the samples. Wrapping of powder sample with paraffin paper depresses the exchange between free xenon gas and xenon in the powder sample, leading to the increase in the chemical shift of confined xenon above 1 MPa. The detailed condition that affects on the chemical exchange will be discussed.

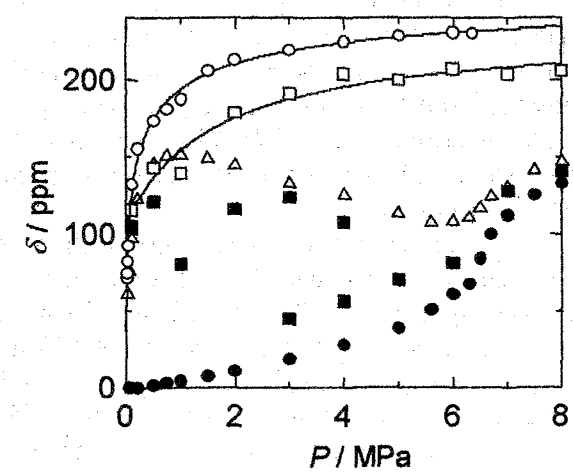

Figure 1 Pressure dependence of ^{129}Xe NMR chemical shift values of xenon confined in NaX (○), NaY (△), and NaY wrapped by paraffin paper (□, ■). The filled circle (●) shows the pressure dependence of chemical shift values of free xenon gas co-existing with the samples.

[1] N. Kato, T. Ueda, H. Omi, K. Miyakubo, and T. Eguchi, *Phys. Chem. Chem. Phys.*, **6**, 5427-5434(2004).

[2] H. Omi, B. Nagasaka, K. Miyakubo, T. Ueda, and T. Eguchi, *Phys. Chem. Chem. Phys.*, **6**, 1299-1303(2004).

AP129

Changes in sodium cation sites probed by ^{23}Na NMR and PFGNMR of adsorbed ammonia in calcined NaA

Makoto Yamaguchi
Institute of Research and Innovation
1201 Takada, Kashiwa, Chiba 2770861 Japan

Zeolites have been widely applied as adsorbents for various gas separation processes by modifying types and locations of exchangeable cations. Izumi et al. reported that NaA and partially K^+ exchanged NaA after calcination showed higher efficiency in air separation by PSA processes, possibly due to increased differences in diffusion rates.(1) In this study we examined the effect of cation exchange and calcination by probing locations of Na^+ by ^{23}Na NMR spectra. We have also done a preliminary PFGNMR measurement of diffusion of adsorbed ammonia to see how modification affected the diffusion processes.

Samples were provided by Mitsubishi Heavy Industries, Ltd. as pellets after being partially exchanged with K^+ and then calcined at 993K. For NMR measurements pellets were crushed and evacuated at 623K overnight in a glass tube and the tube was sealed off. JEOL EX270 NMR spectrometer (B_0: 6.3T) was used. For measurement of ^{23}Na (ν_0: 71.32MHz), a transient recorder (2MHz bandwidth) and a high power amplifier (1kW) were used for acquisition of signals with very short relaxation time. Free induction decay after $\pi/2$ pulse (1.2μs) was acquired with duration time of 0.5μs.

Observed spectra of untreated NaA showed a central peak due to Na^+ in 4 and 8 membered ring (MR) sites and two outer peaks due to Na^+ in 6MR sites as reported previously (2). We simulated the spectrum by the program SIMPSON (3) assuming the relative population of Na^+ in 6, 8, and 4MR sites as 8:3:1 as determined by single crystal x-ray diffraction of dried NaA (4). The simulated spectrum showed good agreement with the observed spectrum and quadrupole coupling constants (QCC) and asymmetry parameters (η) were determined as 6.0/3.8/1.4MHz and 0.05/0.13/0.73 respectively. These values are consistent with the calculated electric field gradients by the GULP program (5) after lattice energy minimization.

In the case of calcined samples, shoulder peaks of the central peak disappeared, while the outer peaks unchanged. Simulation showed that the relative population of 6, 8, and 4MR sites changed to 9:0.5:2.5, indicating that Na^+ in 8MR have moved to 4 and 6MR sites.

A preliminary measurement on diffusion of adsorbed ammonia was performed with pulsed field gradient spin echo sequences and gradient pulse width (δ) was changed under constant gradient strength. Self diffusion coefficients of ammonia were estimated to be around $10^{-10}m^2/s$, which is comparable to the diffusion coefficients of water in NaA by PFGNMR (6) and by MD simulation (7).

This paper is a part of the results from "Technology development on nitrogen isotope separation by gas phase adsorption (FY-2004)" entrusted to Institute of Research and Innovation by the Ministry of Education, Culture, Sports, Science and Technology of Japan (MEXT).

References : (1) Izumi et al., *Adsorption*, **6**, 23 (2000); **6**,205(2000);**7**,27(2001). (2) Tijink et al., *JACS*,**109**,7301 (1987). (3) M.Bak et al., *JMR*, **147**, 296 (2000). (4) Pluth et al., *JACS*, **102**, 4704 (1980). (5) J. D. Gale, *JCS Faraday Trans.* **93**,629 (1997). (6) Paoli et al., *Microporous and Mesoporous Mater.* 55, 147 (2002). (7) D. Faux, *JPC, B*103, 7803 (1999).

AP130 (PL2)

Local environments of slags: the first application of ^{43}Ca MQMAS technique

Keiji Shimoda[1], YasuhiroTobu[1], Koji Kanehashi[1], Takahiro Nemoto[2], Yuichi Shimoikeda[2], Koji Saito[1]
[1]Advanced Technology Research Laboratories, Nippon Steel Corporation, 20-1 Shintomi, Futtsu 293-8511
[2]JEOL Ltd., 3-1-2 Musashino, Akishima, Tokyo 196-8558

Inorganic materials with CaO-MgO-Al_2O_3-SiO_2 (CMAS) join, such as a slag, are of great importance for industrial applications. NMR spectroscopy is a robust tool for understanding the local environments of ions in non-crystalline materials. However, solid state ^{43}Ca NMR measurement has been difficult because ^{43}Ca has a low natural abundance (0.135%), low r.f., and a spin of $I = 7/2$ with significant second-order quadrupolar interaction. Although Dupree et al. (1997) reported natural abundance ^{43}Ca MAS spectra for some minerals, no detailed study has been reported for inorganic materials by ^{43}Ca MQMAS technique. In the present study, we present the first ^{43}Ca MQMAS spectra for ^{43}Ca-enriched model slags, and discuss the local environments of Ca^{2+} ion in the structures.

Chemical composition of model slag is for typical blast furnace slag (43.0 wt%CaO, 7.0 wt%MgO, 15.0 wt%Al_2O_3, 35.0 wt%SiO_2). We used ^{43}Ca- and ^{17}O-labeled reagents, $^{43}Ca(^{17}OH)_2$, $Mg(OH)_2$, $Al_2{}^{17}O_3$, and $Si^{17}O_2$. Two slags were prepared with different quenching rate. Rapid-quench slag was prepared by melting a mixture of reagents at 1500 °C for 30 minutes and subsequent quenching on a copper plate in air. Slow-quench slag was prepared in same manner but quenched by -20 °C/min in a furnace.

^{43}Ca NMR spectra were accumulated on a JEOL model JNM-ECA700 spectrometer (16.4 Tesla) at 47.1 MHz. Samples were spun at 18 kHz. ^{43}Ca chemical shifts were referenced to saturated $CaCl_2$ solution at 0.0 ppm. In 3QMAS, z-filter sequence was applied. Excitation and conversion pulses were optimized to 4.2 and 1.5 μs, respectively. Relaxation delays were 25 and 50 s for rapid- and slow-quench slags, respectively.

Figure 1 shows ^{43}Ca 3QMAS spectrum of the rapid-quench slag. The 2-dimentional spectrum indicates a broad distribution of Ca local environments, implying that Ca^{2+} ions are in amorphous state. The δ_{CS} and C_Q were estimated to 37.3 ppm and 3.9 MHz, respectively. Based on Dupree et al. (1997), we concluded that the rapid-quench slag has a CaO_6 species as a main component. This is the first practical information for Ca local environments in the slag structure. Moreover, the contour peak shape suggests a possibility of multi-sites. 5QMAS will expect the more detailed site separation, and is now in progress. We present a complete set of data in a poster session.

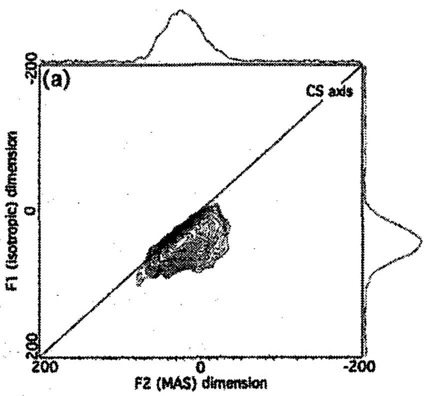

Figure 1. 3QMAS spectrum of rapid-quench slag.

**Reference*: Dupree et al. (1997) *Chem Phys Lett* 276, 339

AP131

Location, Acid Strength and Mobility of the acidic Protons in Keggin 12-$H_3PW_{12}O_{40}$: A Combined Solid-State NMR Spectroscopy and DFT Quantum Chemical Calculation Study

Jun Yang,[1] Michael J. Janik,[2] Anmin Zheng,[1] Mingjin Zhang,[2] Matthew Neurock,[2] Robert J. Davis,[2] Chaohui Ye,[1] Feng Deng[1]

[1]State Key Laboratory of Magnetic Resonance and Atomic and Molecular Physics, Wuhan Institute of Physics and Mathematics, Chinese Academy of Sciences, Wuhan 430071, P. R. China
[2]Department of Chemical Engineering, University of Virginia, Charlottesville, VA 22904-4741, USA

Solid state ^{13}C NMR experiments and quantum chemical Density Functional Theory (DFT) calculations of acetone adsorption were used to study the location of protons in anhydrous 12-tungstophosphoric acid (HPW), the mobility of the isolated and hydrated acidic protons, and the acid strength heterogeneity of the anhydrous hydroxyl groups. This study presents the first direct NMR experimental evidence that there are two types of isolated protons with different acid strength in the anhydrous Keggin HPW. Rotational Echo DOuble Resonance (REDOR) NMR experiments combined with quantum chemical DFT calculations demonstrated that acidic protons in anhydrous HPW are localized on both bridging (O_c) and terminal (O_d) atoms of the Keggin unit. The CP/MAS NMR experiments revealed that the isolated acidic protons are immobile but hydrated acidic protons are highly mobile at room temperature. The isotropic chemical shift of the adsorbed acetone suggested that the acid strength of the $H(H_2O)_n^+$ species in partially hydrated HPW is comparable to that of a zeolite, while the acidity of an isolated proton is much stronger than that of a zeolite. Isolated protons on the bridging oxygen atoms of anhydrous HPW are nearly superacidic. The present study shows the power of combining experimental evidence and quantum chemical theoretical calculations for understanding the structure and properties of complex systems.

NP132

Discrimination of enantiomers by means of NMR spectroscopy using chiral liquid crystalline solution VII - Relation with an anisotropic molecular motion –

Makiko Sugiura, Yoshinori Nakao, and Masayoshi Ito
Kobe Pharmaceutical University, Higashinada-ku, Kobe, JAPAN

Tropicamide (I), cholinergic antagonist, has been dissolved in PBLG-$CDCl_3$ chiral liquid crystalline solvent for measurement of ^{13}C NMR. Two kinds of signals corresponding two isomers (E- and Z-form) have appeared for all carbons and the additional separations of chemical shifts have been observed for several carbons. The former observation arises from the rotational barrier of the carbonyl – nitrogen bond, which is also observed in liquid solution, and the latter is the enantiomeric separation (R and S) due to the difference of chemical shift anisotropy on a chiral phase.

It is interesting to compare the measured enantiomeric chemical shift separations between these two isomers as shown bellow. For B-ring (Pyridine ring), the separations are observed on all carbons for E-form but only one carbon for Z-form, while methyl carbon of N-ethyl group show a small separation for Z-form. Generally, the larger values are observed on separations for E-form than Z-form. These differences may be attribute to their molecular stereochemistries and/or conformations.

It is possible to interpret these observations in the sense of an anisotropic molecular motion predicted from a molecular overall shape. For each isomer, assuming symmetrical-ellipsoidal molecular shape, the preferred axis of molecular tumbling motion can be defined. The molecular shape of E-form looks more "ellipticities" with longer preferred axis leading the faster tumbling motion about this axis.

From the observed values shown bellow, it is suggested that the carbons along the preferred axis show the larger enantiomeric separation and the molecule with the longer preferred axis provides the larger separations.

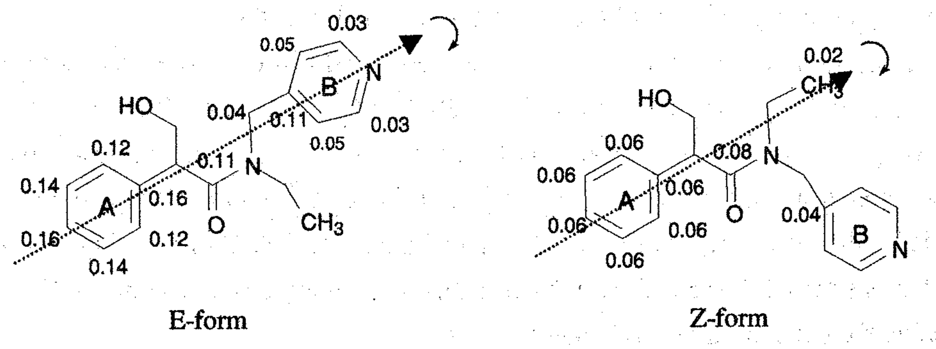

I

AP133 Diffusion of Rodlike Poly(γ-benzyl L-glutamate) in Concentrated Solution As Studied by the Field-Gradient [1]H NMR Methods

Shigeki Kuroki and Kamiguchi Kazuhiro
Department of Chemistry and Materials Science, Tokyo Institute of Technology

[Introduction] It is well known that poly(glutamate)s with long n-alkyl side chains form thermotropic liquid crystalline state by melting of the side-chain crystallites and also poly(glutamate)s such as poly(γ-benzyl L-glutamate)(PBLG), poly(γ-n-alkyl L-glutamate), etc. in solvent form the isotropic, biphasic and liquid crystalline phases which contains cholesteric and columnar liquid crystalline forms depending on the polypeptide concentration. In our previous works, we have successfully measured the diffusion coefficients of rodlike polypeptides such as α-helical poly(γ-glutamate)s having long n-alkyl side chains as a function of the α-helical chain length in the thermotropic liquid crystalline state and of α-helical poly(γ-n-octadecyl L-glutamate) and chloroform as solvent in the isotropic, biphasic and liquid crystalline phases by high field-gradient ^{1}H NMR method. Although there is no diffusion study for PBLG in liquid crystalline state, because it is difficult to observed ^{1}H spectrum of PBLG in liquid crystalline state for its very short ^{1}H T_2. In this study, we successfully elucidate the diffusional behavior of rodlike PBLG in concentrated solution as studied by the field-gradient ^{1}H NMR methods.

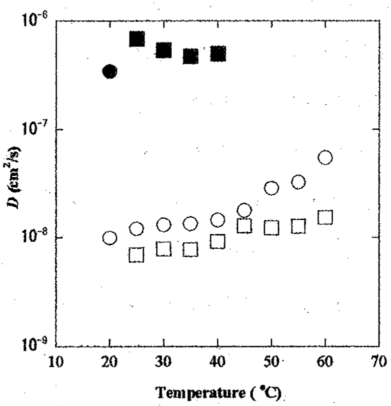

Fig.1 Plots of the diffusion coeffients (D) of PBLG169 (○;slow component, •;fast component) and PBLG 463(○;slow component, •; fast component) are shown as a function of temperature.

[Experiment] PBLG (DP (degree of polymerization) = 169 (PBLG169) and 463(PBLG463))was purchased from Sigma Chemical Co. The PBLG solution was prepared by placing PBLG and 1,4-dioxane in 10mm NMR tube. The PBLG concentrations was 25 wt %.

The self-diffusion coefficient measurements were carried out by means of a Bruker Avance 300 NMR spectrometer using pulse field gradient stimulated echo method.

[Results and Discussion] Figure 1 shows the determined diffusion coefficients of PBLG169 and PBLG463 as a function of temperature from 20 to 60 °C . For PBLG463, A single slower diffusion component (1.0 x 10^{-8} cm^2/s) exists from 45 to 60 °C which corresponds to the liquid crystal state, and faster diffusion component (about 5.0 x 10^{-7} cm^2/s) appear below 40 °C, which corresponds to the isotropic state. On the other hand, For PBLG169, a single slower diffusion component exists from 25 to 60 °C, and faster diffusion components appear at 20 °C. These results are reasonable for considering Flory's theory.

AP134

Novel fluid dynamical behavior of laser-polarized ^{129}Xe in a laminar flow

○Tatsuya Asanuma, Takashi Hiraga, and Mineyuki Hattori
National Institute of Advanced Industrial Science and Technology (AIST), Ikeda, Osaka 563-8577, Japan

Novel fluid dynamical behavior of the laser-polarized ^{129}Xe gas in a laminar flow was detected by nuclear magnetic resonance. It is shown that the density of laser-polarized ^{129}Xe spin decreases with increasing a flow rate, whose order of magnitude is different depending on inside diameters of transport capillary tubes. From a fluid dynamics point of view, the mechanism of signal loss in flow fields is clarified and the determinant parameter is discussed. The innovative aspect of this study should provide key factors for the effective delivery of ^{129}Xe gas with a higher concentration of laser-polarized ^{129}Xe.

1. Introduction

The improvement of spin exchange optical pumping recently allows the production of laser-polarized ^{129}Xe under the continuous flow [1]. The advantage of this technique is the continuous refreshment of the laser-polarized ^{129}Xe, which will be useful for *in situ* studies of materials with short spin-lattice relaxation times for ^{129}Xe. However, to establish a real-time high-resolution NMR/MRI for *in vivo* diagnosis [2], the effective delivery of laser-polarized ^{129}Xe spins to the systems of interest must be realized while maintaining the polarization. There have still been few reports of any effort to study systematically the delivery efficiency of laser-polarized noble gases using appropriate transport paths. Brunner *et al.* suggest that the nonequilibrium ^{129}Xe nuclear spin polarization can exhibit spatial variations due to spin-lattice relaxation, while it is believed to be time-independent under "laminar" flow conditions in steady state [3].

In this study, the fluid behavior of the laser-polarized ^{129}Xe using silica capillary tubes with the different inside diameter $\leq$ 0.53 mm was quantitatively investigated. The initial observation obtained with our prototype system is described.

2. Experimental

The gas flow system consists mainly of a homebuilt apparatus, similar to that shown in a previous publication [2], that provides a continuous flowing gas stream carrying the laser-polarized ^{129}Xe gas. The homebuilt probe was connected to the apparatus using a fused silica capillary tube, and then was inserted into a permanent magnet with a field $\boldsymbol{B}_0$ of 0.3±0.01 T (Fig. 1). Two silica tubes with the inside diameters of 0.25 and 0.53 mm, respectively, N025 and N053, were used as delivery paths without any pre-treatments. The interior surfaces of the tubes were not coated with any chemical reagents. The tube length L was fixed at 1 m. The natural abundance Xe gas (100%) and Rb vapor (99.99%) were mixed at 418±3 K and optically pumped at the wavelength of 794.7±1 nm, with circularly polarized light (60 W), by using two combined semiconductor lasers.

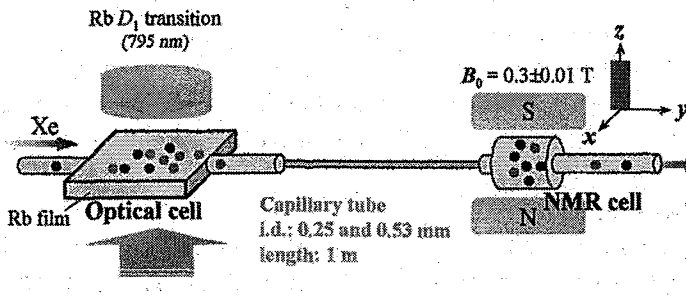

Fig. 1. A schematic of the homebuilt low-field NMR system using a capillary tube.

The signal intensity M_0 of the laser-polarized ^{129}Xe was monitored by a NMR spectrometer (Thamway Co., Ltd.) at 3.574 MHz ^{129}Xe frequency. The data were acquired in the direction of increasing an effective flow rate Q that was calculated from the difference in pressure in both ends of the tube. The maximum signal intensities M_{max} in M_0 vs Q curves were normalized by that of N053 with L of 1 m.

3. Results and Discussion

Fig. 2(a) shows the dependence of M_0 on Reynolds number Re for the laser-polarized ^{129}Xe gas. M_{max} in M_0 vs Re curves were observed at Re of 16 and 33 for N025 and N053, respectively. Re_{max} where M_{max} appeared is lower than the critical Re of 2300 where the transition from laminar to turbulent flow is expected to occur. Therefore, it is reasonable to consider that the polarization begins to decrease in the vicinity of Re_{max} due to the high Xe density where the Xe itself is the dominating source for Rb depolarization.

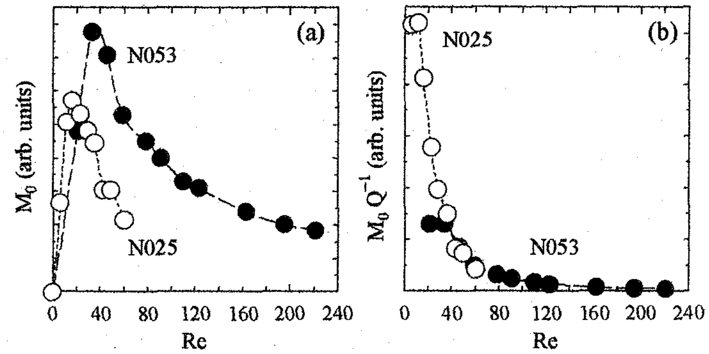

Fig. 2. (a) Reynolds number Re dependence of the signal intensity M_0 for the laser-polarized ^{129}Xe that were flowing through the different silica tubes. (b) $M_0\ Q^{-1}$ as a function of Re. The calculation of Re assumes that the Xe gas flows through a tube at 298 K. The curves are shown as eye-guidelines for the experimental data.

Fig. 2(a) also indicates that the amplitude of M_{max} for N053 is larger than that for N025. As the ^{129}Xe gas emerging from N025 reaches the equilibrium in spin density earlier than that for N053, this phenomenon is not due to the deficient uptake time. The difference of the amplitude may reflect the total amount of laser-polarized ^{129}Xe delivered into the NMR cell ($M_0 \propto d \times Q$). The influence of a sudden contraction or expansion in both ends of the tube is also pointed out, because the depolarization can be promoted by the flow fluctuation.

Another feature in Fig. 2(a) is that M_0 vs Re curve for N053 is asymmetric on both sides of the maximum. This result can be explained that the incline in the high Re region depends on the balance between the decrease of the ^{129}Xe spin density d and the increase of the effective flow rate Q.

In Fig. 2(b), $M_0\ Q^{-1}$ is shown as a function of Re, which gives the essential information on the number of laser-polarized ^{129}Xe spin per mole in the Xe atmosphere. Although $M_0\ Q^{-1}$ for N053 decreased monotonically with increasing Re over 33, the drastic decrease over Re of 11 was observed for N025. $M_{max}\ Q^{-1}$ for N025 was *ca.* 3 times larger than that for N053. This fact indicates that the spin density d of laser-polarized ^{129}Xe is higher for N025 than N053 if Re is below 33, in spite of the similar chemical nature of the tube wall. According to our analysis, it means that the effect of the restricted motion near the tube boundaries on the signal loss could be microscopically detected as the variation of macroscopic magnetization M_0. In fact, Song *et al.* showed that image distortions due to diffusion in MRI were present only at the sample boundaries [4]. The xenon's high sensitivity to its local magnetic environment is successfully applied to probe the local properties of a fluid bound layer.

References

[1] E. Brunner, *Magn. Reson. Chem.*, **37**, S14 (1999).

[2] M. Hattori *et al.*, *International Congress Series*, **1265**, 144 (2004).

[3] E. Brunner *et al.*, *J. Magn. Reson.*, **138**, 155 (1999).

[4] Y. -Q. Song *et al.*, *J. Chem. Phys.*, **108**. 6233 (1998).

AP135

TR-dependent Steady-State iDQC *in vivo* MRI of Mice Brains

Dennis W. Hwang, Chao-Hsiung Hsu, Chieh-Wei Chang,
Wen-Yih I. Tseng, and Lian-Pin Hwang
Department of Chemistry, National Taiwan University,
No.1, Sec. 4, Roosevelt Road, Taipei, Taiwan 106

Intermolecular double quantum coherence (iDQC) MRI images of the brain normally encounter the problem of a low signal-to-noise ratio (SNR). Additionally, the contrast in iDQC images is similar to that obtained by the conventional MRI, such as. T_1- and T_2-weighted spin-echo MRI. Hence, iDQC MRI has not much benefit for clinical applications. In the present work iDQC MRI of a mouse brain was performed with a CRAZED-type sequence (FIG.1) with short repetition time (TR) which provided significant advantages including a short acquisition time and novel contrasts.

FIG. 1

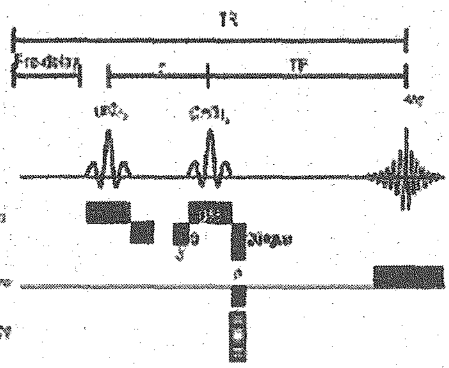

FIG. 2

The resulting images allowed the intricate structures of the mouse brain to be visualized in detail. The complex anatomy of this region shows multiple layers of the hippocampus such as 1.Corpus callosum, 2.-4. Hippocampus, and 5.Internal capsule in FIG.2.

As the signal in the iDQC MRI contains contributions from both single and double quantum coherence, the dependence of the contributions on both TR and filtering gradient pulse direction were investigated.

NP136

Imaging of a recovery process in a rat spinal cord injury model using manganese enhanced MRI

Akihiko Fujikawa[1], Yuko Kawai[3], Ichio Aoki[4], Takayuki Yamaji[2], Hiroyuki Takamatsu[1], Sousuke Miyoshi[1], Shintaro Nishimura[1], Masahiro Umeda[4], Toshihiro Higuchi[3] and Chuzo Tanaka[3]
[1]Advanced Technology Platform Research Laboratory, [2]Applied Pharmacology II Research Laboratory, Astellas Pharma Inc., Ibaraki, Japan; and [3]Department of Neurosurgery, [4]Dwpartment of Medical Informatics, Meiji University of Oriental Medicine, Kyoto, Japan

[INTRODUCTION] Magnetic resonance imaging (MRI) is an important technique for understanding anatomy and function under normal and pathological conditions in vivo, and it has been widely used in the diagnosis of spinal cord injury (SCI) in recent years. It has been shown that manganese can serve as MRI contrast agent for neuronal activity in the cerebrum in the rat (1). Here we describe a functional recovery process of SCI and the use of manganese enhanced MRI (MEMRI) for imaging of the spinal cord contusion in the rat. This study may be important information for neurotrophic drug development for neurodegenerative diseases as it provides a means to observe the recovery process of the spinal cord and could potentially correlate imaging with pathology in the injured rat.

[METHODS] Six-week old male SD rats (Shimizu Experimental Animals, Japan) were used. Animals were anesthetized by an intraperitoneal injection of pentobarbital (50mg/kg), and the thoracic spinal cord injury was produced by dropping a 10g weight from 5cm height on exposed cord. $MnCl_2$ was infused intravenously at least 24 hours prior to MEMRI scanning. The MRI acquisitions were performed on 4.7-T horizontal MRI (Biospec, Bruker BioSpin, GmbH) using a self-made 25mm surface coil fitted the back of rat body. Motor function assessment in rat SCI model was carried out according to Tarlov/Klinger test. Image reconstruction and analysis were performed using ParaVision (Bruker BioSpin) and MRVision (MRVision Co.,). Statistical significance was determined using SYSTAT (Systat software Inc.).

[RESULTS] We observed their hindlimbs as motor function score and MRI evaluations were scaned once a week over 4 weeks from contusion injury in the rats. The damage area was detected as a high signal domain for each T2-weighted measurements. On the other hand, the signal intensity of the MEMRI showed a clearly demarcated low-signal area at the center of the spinal cord in the injured area, and enhanced locus were detected in the intact spine to the contrary. In this study, we have shown a correlation between the image analysis results that were obtained from MRI and neurological symptom.

[REFERENCES] (1) Aoki, I et al. Neuroimage 2004 Jul; 22 (3): 1046-59

AP137

Brain Tissue Segmentation on the 3D MDEFT Image Obtained at 4.7T

N. Takaya[1], H. Watanabe[1], M. Yamaguchi[1,2], F. Mitsumori[1]
[1]National Institute for Environmental Studies
[2]University of Tsukuba

We demonstrated that MDEFT method gave high tissue contrast between grey matter (GM) and white matter (WM) in the human brain at 4.7T by optimizing the parameter. High contrast to noise ratio at high field is beneficial to classify the tissue type in the brain image. However, non-uniform image intensity at high field due to increased B_1 inhomogeniety causes a great difficulty in the automated tissue segmentation. Therefore, the correcting process of the inhomogeneous signal intensity in the image comes to be essential at high field. In the present work we compared two kinds of intensity correction techniques on the 3D MDEFT image obtained at 4.7T. These intensity correction techniques are based on algorithms using Bayesian framework provided in SPM99 software, and Legendre polynomials in Brain Voyager (Rainer Goebel, Brain Innovation B.V.).

3D MDEFT images of the brain were obtained on a 4.7T/92.5cm system (Varian, PaloAlto). The image data were transferred to a UNIX workstation or a Windows computer for further processing. Tissue segmentation was performed in the standard SPM99 software, which gave three probability images (GM, WM, and CSF). Segmented probability images were evaluated by visual inspection.

We compared the segmented results on the intensity corrected images by 2~8th order Legendre polynomials and that by Bayesian framework. Figure 1 shows two results by Bayesian framework (upper column) and by 6th order polynomials (lower column). Basal ganglia and sub-cortical WM were better represented in the lower column. The 6th order correction, however, enhanced peripheral region, causing erroneous classification of non-brain tissue (scalp and born marrow) to CSF or GM. Thus, we removed residual non-brain tissue from the sum of probability images of GM, WM, and CSF after the intensity correction by using Brain Extraction Tool (BET) in FSL software. Effect of BET process was almost negligible on WM and GM segments, but CSF segment was approximately 10 to 20% reduced. The intracranial volume, i.e. the sum of GM, WM, and CSF, obtained in the corrected image was similar to the previously reported value. We concluded that the intensity correction using 6th order polynomials accompanied with a BET process was best suited to the segmentation of MDEFT images obtained at 4.7T.

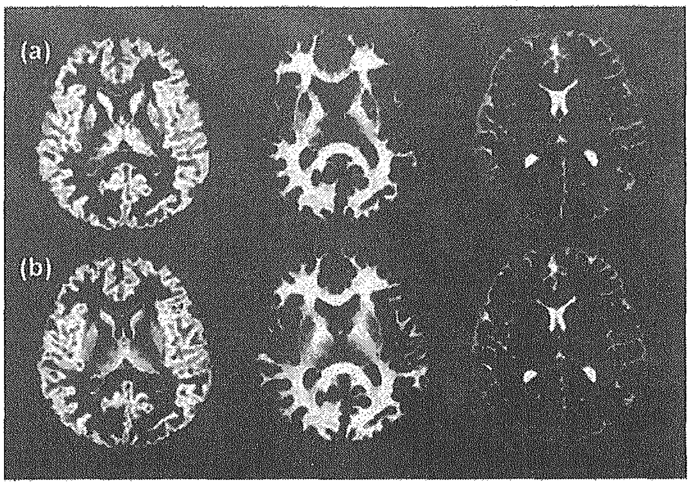

Fig.1. (a) Probability images of GM, WM, and CSF (left to right) segmented by SPM99 from the intensity corrected image by Bayesian framework and (b) those from the image corrected by 6th order polynomials (plus BET).

AP138

Anisotropic diffusion of water in plant stem

Nobuaki Ishida
National Food Research Institute

Diffusion coefficient of cell-associated water is widely used for studying and characterizing biological tissues because it is closely related to biological event of cells and structure of the compartments in which water is enclosed. In this study, we studied diffusion phenomena of water in plant stem and anisotropic character of diffusion depends on tissues is observed.

Materials and Methods

Plant: A stem of *Aucuba japonica* Thunb. was cut and inserted in the water vessel till the measurement.

MRI measurement: Bruker DRX300WB and MRI accessories were used for MRI measurements. Plant sample which were inserted in the water vessel to supply water was set in the detector of 15mm in diameter. Pulse-gradient spin-echo and pulse-gradient stimulated-echo sequence were used for the measurement of diffusion weighted images.

Results and Discussion

MR image (A) and calculated parameter images (B-F) were shown in Figure. In the vascular tissue, T1 was short comparing to pith and surrounding cortex tissue, but T2 was long on the contrary. This was thought to be the characteristic feature in vascular system of plant, the reason of which is not known so far. Because water flow in vascular tissue perpendicular to the image slice could not be observed by flow encoding phase shift, water flow is thought to be suppressed under dark condition in probe. Diffusion coefficient was calculated using diffusion weighted images at diffusion time of 20ms for three different axes. Fig. D-F were diffusion coefficient images along with z (slice), x and y axes, respectively. Anisotropic diffusion was observed. The value by z-gradient (perpendicular to the image slice) was two times larger than that of x and y axis (image plane) in vascular tissue, that is, diffusion coefficient is larger along with the axis of vascular system. Compartment size of cells was estimated by the measurement of restricted diffusion of water on images using diffusion time from 20ms to 400ms. Vascular cells are aligned along stem body with long shape. The compartment size of vascular tissue was estimated more than 100 micro meters along with z-axis and less than half of it along x-axis.

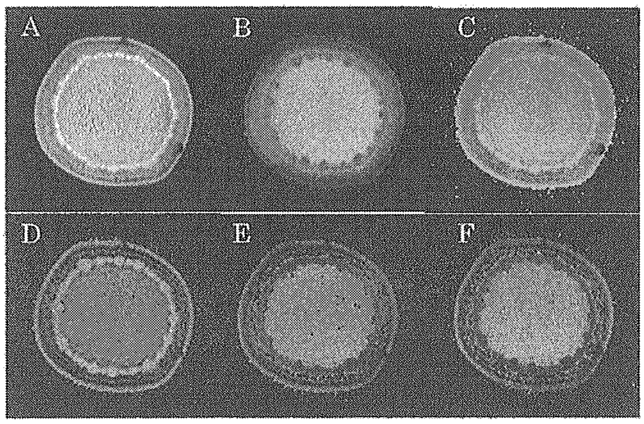

MR image and parameter images of plant stem
A: MR image, B: T1-image, C: T2-image
D-F: diffusion-coefficient images
(D: z-grad., E: x-grad., F: y-grad.)

AP139

Analysis of Hyperpolarized ^{129}Xe Washout Curve by Simultaneous Measurment in Mouse Lungs and Brain.

Takashi Masutani*, Michiko Narazaki, Akari Kaneko, Akiko Nakabou, Tsuyoshi Ueyama, Tetsuya Wakayama, Atsuomi Kimura, and Hideaki Fujiwara

Division of Medical Physics and Engineering, Graduate School of Medicine, Osaka University, Osaka, Japan

The purpose of this work is to establish the method of analysis of the ^{129}Xe washout curve in mouse brain with the aid of simultaneous measurement of washout curve in lungs in the same mouse. As a result of such analysis, enhancement of reliability is expected in deducing parameters related to the brain function, such as relaxation time or cerebral blood flow.

[Results and Discussion] By switching the position of a mouse in a short time FOV was converted from lungs to brain and *vice versa,* giving good reproducibility in the resulting data. Thus, the simultaneous measurement was realized in the washout curve measurement. In analyzing the washout curve in lungs and brain, the lungs washout slope was determined first, and then the brain washout curve was analyzed using the resulting slope in lungs after subtracting the effect of pulse angle in the lungs measurement. The commercial software ORIGIN was used in the calculation. As the result we have obtained the ^{129}Xe T_1 value of 13.8(sec) in mouse brain. Here we quoted a reference value for the blood perfusion rate (F_i) in brain tissue. The T_1 value obtained in the present study is close to the T_1 value reported with human brain(14sec).

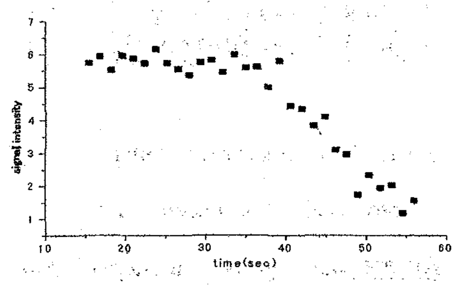

Fig.1. mouse brain washout curve

AP140

Compartment Model Analysis of the Dynamics Observed in Hyperpolarized ^{129}Xe NMR Spectroscopy in Mouse

Akari Kaneko,* Michiko Narazaki, Atsuomi Kimura and Hideaki Fujiwara
Division of Medical Physics and Engineering, Graduate School of Medicine, Osaka University, Osaka, Japan

Time-dependent spectra measured on mice inhaling or exhaling hyperpolarized ^{129}Xe gas enable us to predict the physiological parameter of lungs (and even brain) for a diagnostic use. Over the past decade several tens of articles have discussed the compartment model in order to explain and analyze the dynamics observed in hyperpolarized ^{129}Xe NMR spectroscopy.[1)]

It is well known that ^{129}Xe exhibits a wide spread of chemical shift depending on the state of surroundings. We have already reported that the exchange between the two sites (gas phase and the dissolved phase) was observed *in vivo* and the exchange rate was determined by means of the two-dimensional exchange spectroscopy (2D-EXSY).[2)] So far little attention has been given to this exchanging phenomenon in the model mentioned above. To take account of this effect, we present a compartment model (Fig.1) improved the conventional model composed of two-compartment (lungs and tissues).

The differential equation, which describes the time-dependent concentration in each compartment, was solved by analytical method. The spectral data obtained from mouse chest (Fig.2) were analyzed on the basis of the model proposed here. A feasible method for the derivation of physiological and NMR parameters is discussed.

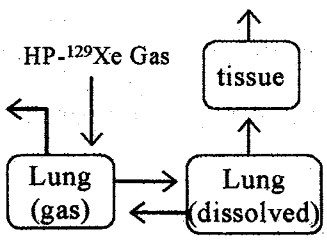

Fig.1. The compartment model proposed in the present study.

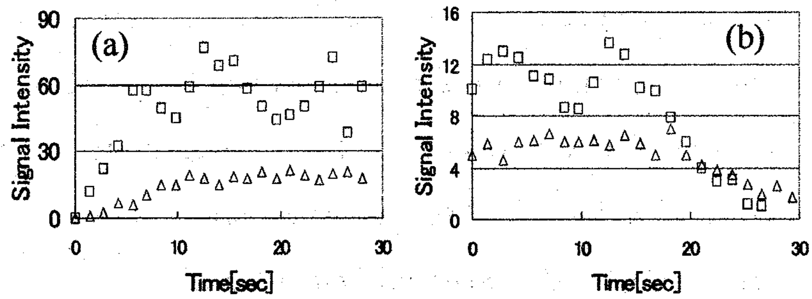

Fig.2. Time-dependent ^{129}Xe spectra of dissolved(△) and gas(□)from mouse chest. [(a): uptake, (b): washout]

References [1] A. Kimura *et al.*, *Magnetic Resonance in Medical Science*, **3** (2005) 199-205.
[2] H. Fujiwara *et al.*, *International Congress Series*, **1265** (2004) 124–130.

NP141

NMR-based Metabolomics

Newly Developed Software for Integrated NMR-spectroscopic and Multivariate Analysis "Alice2 for Metabolome"

Kazunori Arifuku[1], Itiro Ando[2], Masako Fujiwara [1]
[1] JEOL DATUM LTD, [2] Environmental Research Center LTD

For the analysis of mixture samples by NMR spectroscopy, large numbers of spectral processing are required. Each ^{1}H NMR spectrum is bucket-integrated and the datasets are submitted to chemometric solutions. We have developed integrated software "Alice2 for Metabolome"(JEOL). The essential modules of Principal Component Analysis (PCA) and Soft Independent Modeling of Class Analogy (SIMCA) are implemented in the software. It allowed for an easy and rapid analysis on classified results and corresponding spectra through a single graphical interface.

SIMCA approach generates the modelling power responsible for characterizing each model and the discrimination power responsible for classification between the two models via variables. The variables with higher values of discrimination power can be selected out of the overall variables are used to PCA and SIMCA for better classification of all the samples.

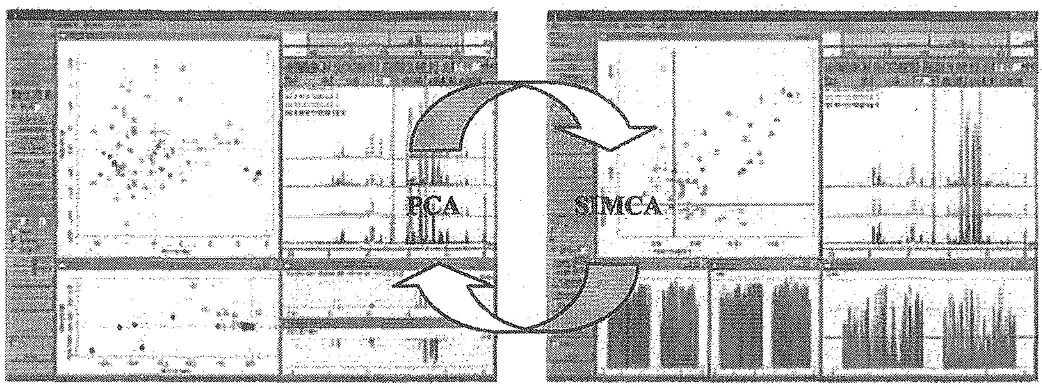

By our new software, chemometric pattern recognition methods successfully extracted inherent information of samples. The combination of PCA and SIMCA methods identified the novel biomarker variables contributing to the classification. For chemometric analysis, "Alice2 for Metabolome" software provides high through put processing of spectral data. This integrated approach will give a powerful tool for wide range of mixture analysis such as food, beverage, polymer or bio-fluid samples, and for metabolic responses to patho-physical stimuli as well.

NP142

Automatic RF Power Determination by MUSASHI

Katsuo Asakura, Tomomitsu Kurimoto, and Nobuaki Nemoto
JEOL Ltd., 3-1-2 Musashino, Akishima, Tokyo 196-8558

We report here a new approach to determine the RF power level corresponding to fixed 90° pulse length using MUSASHI (MUltilpe Spectra Analyzing System with Hyper Intelligence)[1] that is a program designed to obtain 90° pulse length from a nutation experiment using non-linear least square curve fitting method. In general, because larger numbers of pulses are used in triple-resonance experiments, the accumulation of the inaccuracy of pulse lengths finally causes large amount of signal loss, even if the degree of the inaccuracy of each pulse length would be small. Therefore, it is of utmost importance for optimum results to determine accurate 90° pulse lengths and to use them in actual measurements. There are two different ways to determine 90° pulses; one is the way to detect the suitable pulse length at the particular RF (radio frequency wave) power level, and the other is the way to detect the suitable power level at the particular pulse length. As we already reported,[1] the way to detect the pulse length is easy for MUSASHI. However, on the other hand, the way to determine the RF power level for the fixed pulse width was not so straightforward for MUSASHI, because RF power level is usually controlled with an attenuator, this attenuator level is a ratio value defined by dB (decibel) and as RF power in dB increasing linearly, the signal intensities does not draw a beautiful dumped sinusoid so far. We notice that we can avoid this by setting the variable attenuator values as correspond to regular interval flip angle so that signal intensity draws sine curve. The attenuator value and flip angle are relates as described in Eq. 1, where ϕ is flip angle in degree; ATN_{90} and ATN_{ϕ} are attenuation levels corresponding to 90° flip and ϕ degree flip, respectively;

$$ATN_{\phi} = ATN_{90} - 20\log\left(\frac{\phi}{90°}\right) \quad \cdots \ (1)$$

When NMR signals are acquired varying the attenuator values corresponding flip angles following Eq.1 from 0° to 450° based on the calculated approximate 90° pulse power level, the signal intensity draws the sine curve. The sine curve obtained thus is sent to the program and used to determine the actual 90° pulse power level as to fit the model function below,

$$I_x = A\sin\left(\frac{\pi}{2}\times 10^{\left(\frac{B-x}{20}\right)} + C\right) + D \quad \cdots \ (2)$$

where Ix is signal intensity, x is attenuator value, A, B, C and D are parameters to be determined by MUSASHI. This technique is extremely effective to determine 90° pulse power level in the shaped pulse of which it must be the specified pulse length to secure a specific excitation bandwidth.

[1]Kurimoto et al., *Chem. Lett.,* **34**, 540-541 (2005); Asakura et al., *Chem. Lett.,* **34**, 670-671 (2005).

AP143

Non-equispaced Fourier Transforms for Multidimensional Filter Diagonalization Method Evolution Matrices

Kenji Takasugi[1] and Sseziwa Mukasa[2]

[1]JEOL Ltd., 3-1-2 Musashino, Akishima, Tokyo 196-8558, Japan. [2]JEOL USA, Inc., 11 Dearborn Road, Peabody, MA 01960, United States

The core of the Filter Diagonalization Method (FDM) requires the solution of a generalized eigenvalue problem involving two evolution matrices. The elements of the evolution matrices are a function of basis function $\vec{\varphi}$ representing frequencies in the space to be reconstructed. Specifically for a pair of basis functions $\vec{\varphi}_j$ and $\vec{\varphi}_{j'}$

$$U_{jj'} = \sum_{\sigma=0}^{2^{D_n}-1} \sum_{l=\vec{\sigma}'\vec{M}+1}^{(\vec{\sigma}''+1)} \prod_{k=0}^{D_n-1} \left(\frac{e^{i\sigma_k\left(\tau_{n_k}\left(\vec{M}_{n_k}+1\right)\left(\vec{\varphi}_{j_{n_k}}-\vec{\varphi}_{j'_{n_k}}\right)+\pi\right)}}{1-e^{i\tau_{n_k}\left(\vec{\varphi}_{j_{n_k}}-\vec{\varphi}_{j'_{n_k}}\right)}} \times e^{il_{n_k}}\vec{\varphi}_{j_{n_k}} + \frac{e^{i\sigma_k\left(\tau_{n_k}\left(\vec{M}_{n_k}+1\right)\left(\vec{\varphi}_{j'_{n_k}}-\vec{\varphi}_{j_{n_k}}\right)+\pi\right)}}{1-e^{i\tau_{n_k}\left(\vec{\varphi}_{j'_{n_k}}-\vec{\varphi}_{j_{n_k}}\right)}} \times e^{il_{n_k}}\vec{\varphi}_{j'_{n_k}} \right) \times \prod_{k=0}^{D_m-1}\left(\vec{M}_{m_k} - \left|\vec{M}_{m_k} - \vec{l}_{m_k}\right| + 1\right) e^{i l_{m_k}\vec{\varphi}_{m_k}} \times c_{\vec{l}+\vec{p}}$$

where; n is the ordered set of dimensions in which $\vec{\varphi}_{j_i} \neq \vec{\varphi}'_{j_i}$ and m is the ordered set of dimensions for which $\vec{\varphi}_{j_i} = \vec{\varphi}'_{j_i}$, D_n is the length of n, D_m is the length of m, $\vec{\sigma}'$ is the vector of the same dimensionality as the data c formed from the binary representation of σ with zeroes inserted for positions that are in m, $\vec{\sigma}''$ is $\vec{\sigma}'$ with ones inserted at the positions that are elements of m, σ_k is the value of the digit in the n_k^{th} place of the binary representation of σ, $\vec{\tau}$ is the vector of sampling rates in each dimension and $\vec{M}$ is the vector $\left(\vec{N}-2\right)/2$ where $\vec{N}$ is the size of the data in each dimension.

Expanding the product over and making appropriate substitutions the elements of the evolution matrix can be expressed as

$$U_{jj'} = \sum_{k=0}^{D_n-1}\sum_{k'=0}^{D_n-1}\sum_{\sigma=0}^{2^{D_n}-1}\sum_{l=\vec{\sigma}'\vec{M}+1}^{\left(\vec{\sigma}''+1\right)\vec{M}} a_{n_k} \times b_{n_k} \times \prod_{q=0}^{D_m-1} d_{m_q} e^{i\vec{l}\vec{\varphi}_{j_{m_q}}\vec{\varphi}_{j_{n_k}}\vec{\varphi}_{j'_{n_{k'}}}} c_{\vec{l}+\vec{p}}$$

which is equivalent to D dimensional Fourier sums evaluated at frequency

$$\omega = \vec{\varphi}_{j_{m_q}}\vec{\varphi}_{j_{n_k}}\vec{\varphi}_{j'_{n_{k'}}}\left(q=0..D_m-1, k, k'=0..D_n-1\right)$$

For all $PU_{jj'}$ with equivalent n and m, the sums can be evaluated in $O\left(\prod_{i=0}^{D-1}\alpha\vec{M}_i\log\alpha\vec{M}_i+\rho^D P\right)$ time where α and ρ are parameters, typically 2 and 6 respectively using non-equispaced fast Fourier transform (NFFT), as opposed to $O\left(P\prod_{i=0}^{D-1}\vec{M}_i\right)$ by evaluating the sum at each $U_{jj'}$.

Finally matrices interpolation by NFFT reduces the time for processing with FDM dramatically.

AP144

NMR-based Metabolomics

Chemometric Method for Mixture Analysis Using ^{1}H-NMR Spectra; Classification of Teas in the World

Masako Fujiwara[1], Itiro Ando[2], Kazunori Arifuku[1],
[1]JEOL DATUM LTD, [2]Envioronmental Research Center LTD

For NMR-based Metabolomic analysis, there has never been established a standard and integrated method of spectral processing and chemometirc procedure well-suited to each bio-mixture samples. It might be one of the reasons why NMR-based metabolomics has never been spread among bio-NMR researchers. Regarding this, we have developed a software for easy analysis of mixture; "Alice2 for Metabolome"(JEOL). An inspection experiment of the software functionality was carried out by using tea samples. ^{1}H NMR spectra of about 200 kinds of green, oolong, black and other tea infusions were measured using JEOL ECA-500 spectrometer. PCA (Principal Component Analysis) can provide survey of whole system diagonositcs, and then each category of tea was made as a pre-defined model for comparison in SIMCA (Soft Independent Modelling for Class Analogy). Advantage of SIMCA is that is able to generate the marker variables contributing to discriminate between two models, and then the variables with higher discrimination power can be selected for submitting to PCA for better classification. In this way unexpected synchronous markers are easily overlooked. This procedure provides the standard multivariate chemometric method for analysis of multi-factorial complex mixtures.

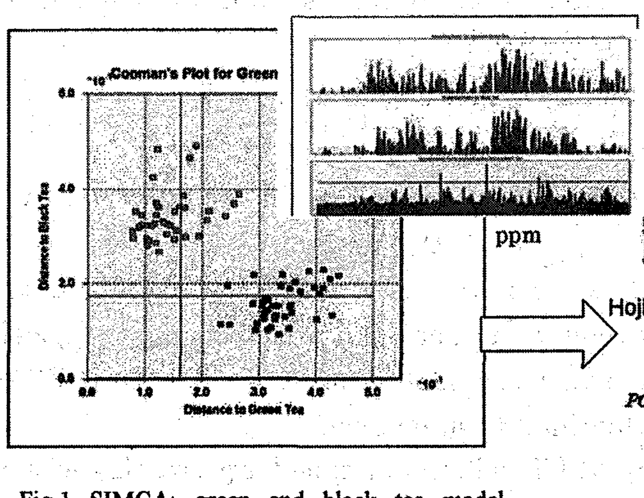

Fig.1 SIMCA: green and black tea model, modeling and discrimination power (up-right) via variables

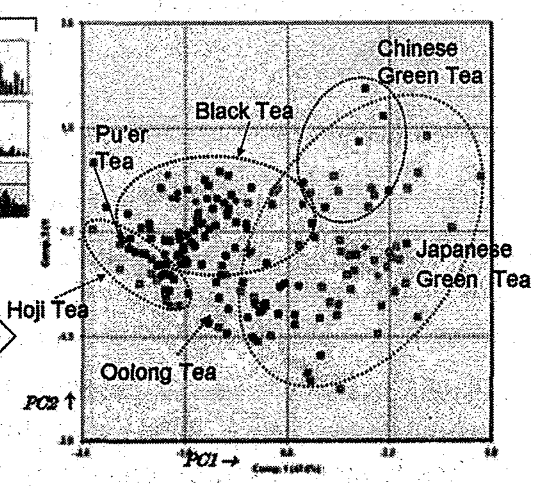

Fig.2 PCA score plot of 175 kinds of tea by selected variables through SIMCA

AP145

Orientational restraints in Cyana

Kimmo Pääkkönen[1], Peter Güntert[1]

1) RIKEN Genomic Sciences Center, 1-7-22, Suehiro, Tsurumi, Yokohama 230-0045, Japan

Residual dipolar coupling (RDC) and pseudo contact shift restraints have been implemented to Cyana (Güntert 2003). They provide orientational and distance information that is complementary to the traditional short distance NOE information (Prestegard et al. 2004).

The RDCs in Cyana can be used similarly to other restraints. For using RDCs, only measured dipolar coupling values with error limits are needed as input, and several different dipole types and orientations are supported. Scaling of the dipoles and estimation of rhombic and axial components of the alignment tensor are done automatically. It is also possible to give the rhombic and axial components manually. Two different methods, direct refinement of dipole values and orientation independent restraints, were implemented. RDCs and pseudo contact shifts can be used both in normal structure calculations and in the automated NOESY assignment.

Pseudo contact shifts arise from interaction with paramagnetic metal ions that are attached to the protein (Bertini et al. 2001) . Due to increased relaxation rates, the signals closest to the metal ion cannot be observed. However, signals a bit further from the metal ion are measurable and they experience chemical shift changes, which are related to both distance from the metal ion and the alignment tensor of the metal ion. This long range information is complementary to the short distance NOE information.

References

Bertini, I., Luchinat, C., and Piccioli, M. 2001. Paramagnetic probes in metalloproteins. *Methods Enzymol* **339:** 314-340.

Güntert, P. 2003. Automated NMR protein structure calculation. *Prog Nucl Mag Res Sp* **43:** 105-125.

Prestegard, J.H., Bougault, C.M., and Kishore, A.I. 2004. Residual dipolar couplings in structure determination of biomolecules. *Chem Rev* **104:** 3519-3540.

AP146

Homodimeric structure determination without manually assigned inter-monomer constraints in the CYANA program

Yi-Jan Lin, Peter Güntert

Tatsuo Miyazawa Memorial Program, RIKEN Genomic Sciences Center, 1-7-22, Suehiro, Tsurumi, Yokohama 230-0045, Japan

The NMR technique for protein structure determination in solution has been applied increasingly to investigate symmetric oligomers, especially symmetric dimers. Homodimeric proteins show a special difficulty for the structure determination. The corresponding nuclei in both monomers have equivalent magnetic environments and therefore their chemical shifts are degenerate. Only one set of signals from one monomer is observed in the spectra. Due to the degeneration of chemical shifts in the symmetric dimers, spectral overlap is reduced and only one monomer has to be assigned compared to monomeric proteins with similar molecular weight, whereas the NOE assignment and structure calculation become more complicated and difficult. Although several automated approaches for combined automatic NOESY assignment and structure calculation have been developed [1-3], a limiting factor for the application of these automated NOE assignment procedures to symmetric dimers is the difficulty to distinguish inter-molecular from intra-molecular NOEs or from NOEs consisting of both intra- and inter-molecular signals. At present, the availability of information about the interface of homodimers using experimental methods such as asymmetric labeling and X-filtered experiments or the knowledge of homologous structures still play an important role for the structure determination of symmetric dimers. Hence, NMR structure determination for homodimeric proteins will be speeded up if the structure could be determined without previously assigned inter-monomer restraints and without a priori assumptions on the tertiary and quaternary structure. In this poster we will present the development in homodimeric structure determination without manually assigned inter-molecular constraints using the CYANA [4] program for automated NOE assignment and structure calculation.

References

1. Herrmann, T., Güntert, P. and Wüthrich, K. (2002) *J. Mol. Biol.* **319**, 209-227

2. Nilges, M., Macias, M. J., O'Donoghue, S. I., and Oschkinat, H. (1997) *J. Mol. Biol.* **269**, 408-422

3. Nilges, M., (1993), *Proteins* **17**, 297

4. Güntert, P. Prog. NMR Spectrosc. 43, 105-125

AP147

Metabolic characterization of small intestinal tissue in rats following hemorrhagic shock using multivariate statistical batch processing of ^{1}H NMR spectra of PCA extracts of the tissue.

Keiko Hirakawa[1], Kaoru Koike[2], Kazunori Arifuku[3], Kyoko Uekusa[1], Youkichi Ohno[1 and 4], Kengo Onodera[5], Junichi Aiboshi[5] and Yasuhiro Yamamoto[6]
[1]NMR Laboratory and Department of Legal Medicine, Nippon Medical School
[4]Field of Social Medicine, Legal Medicine, Nippon Medical School Graduate School of Medicine
[5]Department of Critical Care Medicine, Nippon Medical School
[6]Field of Surgery, Emergency and Critical Care Medicine, Nippon Medical School, Graduate School of Medicine
[1,4,5 and 6] 1-1-5, Sendagi, Bunkyo-ku, Tokyo 113-8602 JAPAN
[2]Field of Surgery, Emergency and Critical Care Medicine, Tohoku University Graduate School of Medicine
1-1 Seiryo-machi, Aoba-ku, Sendai, Miyagi 980-8574 JAPAN
[3]Joint Technology Division, JEOL DATUM LTD.
1156 Nakagami-cho, Akishima Tokyo 196-0022 JAPAN

Multivariate statistical batch processing analysis of ^{1}H NMR spectra of acid soluble extract of small intestine rats was employed to establish time dependent metabolic variations of the tissue in resuscitated with shed blood following hemorrhagic shock(HS) by withdrawing blood. All the data of spectral processing and multivariate analysis (PCA and SIMCA) were performed within Alice2 for metabolme ® . We were successful to visualizing the metabolic profiles of the tissue in each time point.

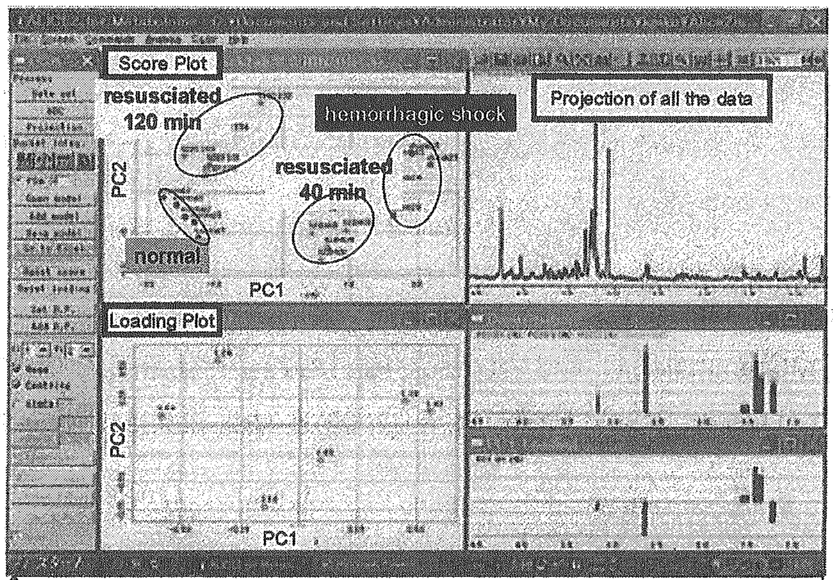

PCA results of the data analyzed by Alice2 for metabolome

AP148

Towards structure determinations of complex and membrane proteins using the Stereo-Array Isotope Labeling (SAIL) method and the CYANA program

○Teppei Ikeya[1,2], Tsutomu Terauchi[2,3], Peter Güntert[4] and Masatsune Kainosho[2,3]

1) Japan Biological Information Consortium (JBiC)
2) Graduate School of Science, Tokyo Metropolitan University
3) CREST, Japan Science and Technology Agency (JST)
4) RIKEN Genomic Sciences Center

Our recently developed SAIL (Stereo-Array Isotope Labeling) method provides a complete stereo- and regiospecific pattern of stable isotopes, which provides much sharper resonance lines and reduced signal overlap. SAIL makes it possible to rapidly and precisely determine 3D structures of proteins with higher molecular weight. One of our major goals is to determine the structures of larger than 50 KDa complex and membrane proteins using NMR. Future improved SAIL technologies will presumably include new SAIL amino acids and new automated assignment and structure calculation methods optimal for SAIL proteins. To facilitate the design of new SAIL amino acids for more effective structure determinations, we performed model structure calculations for proteins with simulated SAIL patterns and evaluated the relationship between the reduction of the proton density and the accuracy of the structures. Additionally, we discuss the effect of lower proton densities on the network-anchoring in the automated NOE assignment algorithm of CYANA and strategies for its optimization for the SAIL method.

References:

Güntert, P., Mumenthaler, C. and Wüthrich, K. (1997) J. Mol. Biol. 273, 283-298
Herrmann, T., Güntert, P. and Wüthrich, K. (2002) J. Mol. Biol. 319, 209-227

AP149

Toward highly efficient molecular identification algorithm in a hetero-nuclear NMR-based metabomics

Eisuke Chikayama[1], Yasuyo Sekiyama[1], Takashi Hirayama[2,3,4,5], Kazuki Saito[1,3,6], Kazuo Shinozaki[1,4,5] and Jun Kikuchi[1,2,3]

[1]*RIKEN Plant Science Center,* [2]*Int. Grad. Sch. Arts Sci., Yokohama City Univ.,* [3]*CREST, JST,* [4]*RIKEN Genomic Sciences Center,* [5]*RIKEN Plant Mol. Biol. Lab.,* [6]*Grad. Sch. Pharm. Sci., Chiba Univ.*

A metabomics, analysis of all measurable metabolites in an organic cell, is becoming one of the most enthusiastic research areas in the post genomics and proteomics era. Although MS-based metabomics methods are widely used due to their high sensitivity, their molecular identification efficiency is relatively low. Even the advanced laboratory, it is approximately 20 %, therefore major strategy in the MS-based metabomics research is classification of un-identified metabolite data using statistical analysis. On the other hand, NMR-based metabomics approaches have emerged with the advantage of their high reproducibility, non-invasive measurements, and ability of molecular structure determination. Development of the methods for efficient molecular identification in metabolite mixture state are important issues in the field of the NMR-based metabomics. Therefore, we are establishing the methods for highly efficient molecular identification from nD-NMR spectra on the following two principles: (1) generally, the chemical shifts of metabolites in a mixture state are almost identical values of isolated compounds those observed at same pH/temperature/ion strength, (2) the ambiguity of the cross peak assignments can be overcome by using several nD-NMR methods. We are investigating these principles by comparing large numbers of the chemical shifts of major metabolites observed in the mixture states, and of in-house standardized database measured in the isolated states. In order to analyze the NMR spectra, we have also developed a specialized Java application program that can identify large numbers of metabolites by searching the standardized chemical shift database. The practical aspects in application of the Java program will be discussed in the conference.

AP150

New approach for assessment of protein structure from NMR spectra using reduced relaxation matrix

Masashi Yokochi, Yoshihiro Kobashigawa and Fuyuhiko Inagaki

Department of Structural Biology, Graduate School of Pharmaceutical Sciences, Hokkaido University,
N-12, W-6, Kita-ku, Sapporo, 060-0812, Japan

To assess accuracy of NMR protein structures from NMR data and to improve precision of protein structures using NMR data are everlasting problems in solution NMR spectroscopy. We can only improve precision of protein structures taking account of statistical similarity as goodness-to-fit to true structure. Although, there is no way to figure out the true structure beyond confidence limit which should be estimated from actual NMR dataset, ultimately NMR spectra. As a result, we are always at the tradeoff point between precision and implicit accuracy without knowing the true answer. Our interest is to define confidence limit of accuracy of NMR protein structures and to improve precision confidentially relying on actual NMR spectra and to maximally avoid subjection or hypothesis in the protein structure calculation.

New approach was developed improving conventional complete relaxation matrix method. It reduces matrix size significantly by careful approximation analysis of differential longitudinal relaxation equations, which makes reduced relaxation matrix per a proton spin (small size 50*50 at most, real asymmetric) in comparison with the complete relaxation matrix per a molecule (huge size over 1000*1000 sparse real symmetric matrix). It de-convolutes trace line of interested region of 3D NOESY-HSQC spectra in real time on today's usual computer. This method does not require NOESY peak information at all, but chemical shift table and ensemble of protein structures so that it can avoid potential problem, which accompanies subjection such as intentional manipulation of NOESY peak information. Direct spectral de-convolution using the reduced relaxation matrix (DSD-rRM) method can be applied to several protein structure determination and refinement processes.

Implementation of DSD-rRM method is provided as a part of our 'Olivia' system, which is free of charge software and available at the following website. (hppt://fermi.pharm.hokudai.ac.jp/olivia/)

AP151

Combination of Isomer Generation and NMR Simulation for Structure Elucidation - Examples of Artemisinin and Uncarine E

Nguyen Tien Tai [a], Ho Tu Bao [b], Dam Hieu Chi [b]

[a] Institute of Chemistry, Vietnamese Academy of Science and Technology; 18 HoangQuocViet road, Hanoi, VIETNAM.
[b] Japan Advanced Institute of Science and Technology; 1-1 Asahidai, Tatsunokuchi, Ishikawa, 923-1292 JAPAN.

Key words: NMR, isomer generation, simulation.

The computer-aided structure elucidation, based on MS and NMR data, is demonstrated on (applied for) identification of two natural compounds, denoted as I and II. The identification procedure consists of four steps:

The first, general chemical formulas are defined based on the experimental MS and NMR data. They are $C_{15}H_{22}O_5$ and $C_{21}H_{24}N_2O_4$, respectively for the cases of I and II compounds.

The second, all possible structures are generated by isomer generation program. As the number of the computer generated structures is very large, some restrictions, obtained from 1D NMR data, are applied for reducing the number of generated isomers.

The third, all generated isomers are graphically simulated and predicted, generating 13C NMR spectra.

The forth, all simulated 13C NMR spectra are compared with the experimental ones. Some techniques of data mining are applied on the matching process.

By this four steps approach, all experimental 13C NMR spectra of I and II compounds are assigned. They are identified as Artemisinin and Uncarine E, respectively. The first is well-known as material for anti malaria drug and the second is used in traditional fold medicines.

The Artemisinin and Uncarine samples are extracted from Vietnam plants. MS and NMR data are measured on HP-5989B Engine and AVANCE500 spectrometers, respectively.

NP152

Development of low temperature (< 4K) NMR cryostat probe (cryo-probe)

Y. Mogami, A. Ikeda, T. Momose, and K. Takegoshi
Department of Chemistry, Graduate School of Science, Kyoto University,
Kyoto 606-8502, Japan

We developed a cryo-probe for NMR measurement below liquid He temperature (Fig. 1). The cryostat was made of non-magnetic material; copper, brass, SUS304, and SUS316L etc.

The sample is immersed in liquid He transferred by the stainless steel tube from the He vessel placed at the top of the probe (outside of the magnet). The temperature of the sample is controlled by He pressure of the sample chamber.

Figure 2 illustrates the resonance circuit placed at the bottom of the probe. The liquid He temperature and room temperature is separated by the double vacuum layers. To make heat conduction small, the line is separated by ceramic condensers.

The circuit was tuned for 300MHz. Figure. 3 shows the ^{1}H spectrum of γ-picoline measured at 4K. The rf strength of 50kHz was achieved by ^{1}H output power of 56W. Experimental results will be shown in the meeting.

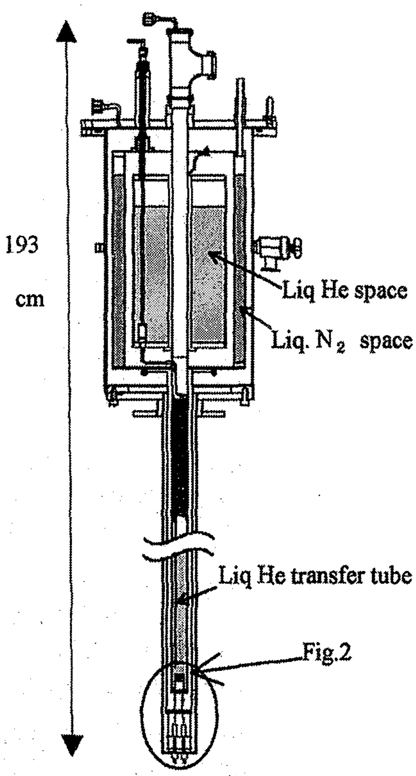

Fig.1

Drawing of cryo-probe

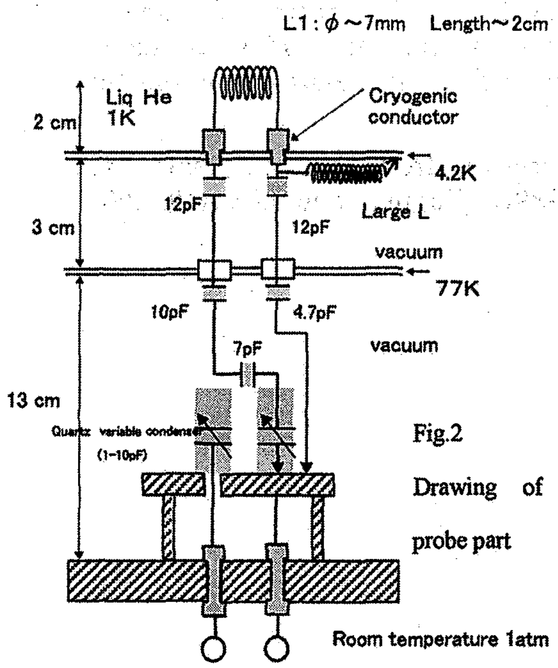

Fig.2

Drawing of probe part

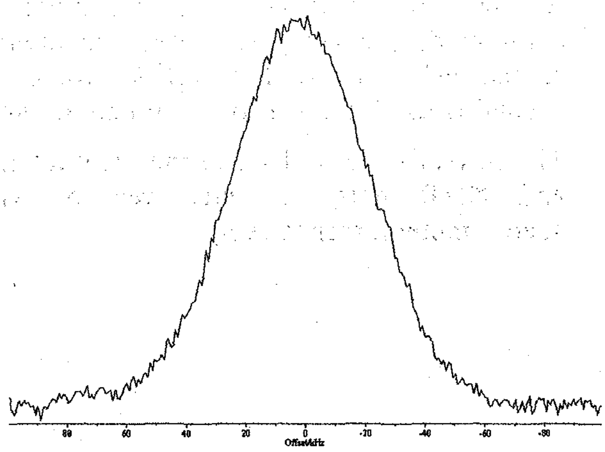

Fig.3

^{1} H spectrum of γ-picoline at 4K observed by solid-echo method

AP153

A cooling system for long time solid-state MAS experiments with sensitivity enhancement at liquid nitrogen temperature

Hiroki Takahashi[1], Fumihiko Yonezawa[2], Hideo Akutsu[1] and Toshimichi Fujiwara[1]

[1]*Institute for Protein Research, Osaka University, 3-2 Yamadaoka, Suita, Osaka 565-0871, Japan*
[2]*AIRTECH CO., LTD. 3-28-18 Shinyoshidahigashi, Kohoku-ku, Yokohama, Kanagawa 223-0058, Japan*

Solid-state NMR spectroscopy is one of the powerful methods for the structural analysis of supramolecular systems. X-ray or solution-state NMR experiments are not applicable to such systems–e.g., membrane proteins. During the decades, a variety of methods were proposed for the structural study such as resonance assignments, distance measurements, dihedral angle determination, etc. In all cases, however, the applicability of these techniques to such systems is limited due to the low sensitivity and the low resolution of the signals in the solids. The latter problem is overcome by multi-dimensional (3D or 4D) NMR experiments that require the high sensitivity. The purpose of this work is to develop the system that can be used for the increase of the sensitivity. Cooling the samples to the very low temperature is a way to acquire the high sensitivity. The magnetization is inversely proportional to the absolute temperature of the sample according to Curie's law. Furthermore, the thermal noise is reduced in proportion to the square root of the temperature. We will show the system that creates the liquid nitrogen temperature at the rotor in MAS probes. The low temperature is achievable with flowing of bubbled nitrogen gas. However, that operation consumes liquid nitrogen massively for long time experiments. The system operated in this study creates nitrogen gas with the nitrogen separators. The amount of liquid nitrogen consumption is reduced by 4.3 times in this system. Nitrogen gas with purity of 99 % is generated from the compressed air through series of five nitrogen separators. The nitrogen gas is cooled to around 190 K in the chiller and then chilled through the heat exchanger with liquid nitrogen at 77 K. As the result, the temperature at the samples is 110 K. Theoretically, the signal to noise ratio at 110 K is 4.5 times lager than that at room temperature. Actually, the preliminary experiments suggest that the sensitivity at 220 K is 1.5 times higher than that at 340 K in accordance with Curie's law. Development of bearing and drive gas for MAS is currently under progress. The large sensitivity enhancement is expected by combining this system and the ^{1}H detection technique which we presented at the 43rd NMR conference for deuterated samples under very fast MAS and high magnetic fields.

AP154

System for storing hyperpolarized 129Xe gas during production in a 4.7T magnetic field

Atsushi Wakai[1,2], Kazuhiro Nakamura[1,2], Jeff Kershaw[1,2], David Wright[1,2], Iwao Kanno[1]
[1]Akita Research Institute of Brain and Blood Vessels, Akita, Japan,
[2]Akita Industry Promotion Foundation, Akita, Japan

MR techniques using hyperpolarized ^{129}Xe have the potential to provide quantitative measurements of cerebral blood blow and oxygenation in human brain tissue. Large volumes (>0.5L) of highly polarized ^{129}Xe (>20%) will be essential for these measurements. A promising method to produce the required gas is to optically pump a helium diluted mixture of Rb vapor and ^{129}Xe gas at high pressure and then reconcentrate the ^{129}Xe by freezing. However, this method suffers from polarization loss by a fast relaxation process in temperatures close to the ^{129}Xe melting point and in low fields (0.01∼0.1T). In an attempt to suppress this relaxation, we constructed a system that can be placed in the field of a 4.7T MRI. A ^{129}Xe storage cell was placed in the magnet bore and connected to the diluted gas supply line, a liquid nitrogen (LN_2) line and a vacuum line. The LN_2 line allowed LN_2 to circulate around the central Cu tube and freeze the ^{129}Xe out of the gas mixture. The vacuum line had two roles; first to evacuate the thermal shield, and secondly to allow the introduction of a warm fluid into the shield space to quickly thaw the ^{129}Xe ice. Before and after freezing, the ^{129}Xe gas flowed into a sample cell placed inside a birdcage coil tuned to the ^{129}Xe resonance and also sitting in the magnet. The sustained polarization ratio (= polarization after thawing/polarization before freezing) was estimated from the NMR signals. The ratio was found to be 0.6-0.7, and the relaxation time of ^{129}Xe ice at around 77K was 1.2-1.6 hours. These results indicate that the current system is not efficient enough to provide sufficient polarized ^{129}Xe gas for human use. Improvements are needed. (Acknowledgement: Akita Prefecture Collaboration of Regional Entities for the Advancement of Technological Excellence, Japan Science and Technology Agency.)

AP155

^{75}As, $^{113,115}In$ and ^{123}Sb NMR studies of indirect nuclear spin-spin coupling in InX (X = As, Sb)

Takahiro Iijima,[1†] Kenjiro Hashi,[1] Atsushi Goto,[1] Tadashi Shimizu[1] and Shinobu Ohki[2]
[1]*National Institute for Materials Science, Tsukuba, Ibaraki 305-0003, Japan*
[2]*CREST, Japan Science and Technology Agency, Kawaguchi, Saitama 332-0012, Japan*
[†]Present address: *Department of Chemistry, Graduate School of Science, Kyoto University, Kyoto 606-8502, Japan*

The discovery of factoring algorithm by Shor[1] that enables us to factorize large integer numbers drastically faster than do by usual methods has motivated many researchers to develop quantum computers (QCs). Several systems such as Josephson junction, ion trap and NMR have been proposed so far as physical systems to implement the quantum computing. Among them, NMR having an excellent property in the decoherence time is a promising candidate for the practically used QC. Indeed, a 7-qubits QC has been realized by liquid-state NMR using five ^{19}F and two ^{13}C nuclei in a molecule as qubits.[2] Moving into solid state equipping a periodicity is, however, desirable in terms of the scalability of the qubit. Recently, semiconductors are suggested to be a device material of the solid-state NMR QC.[3,4] It is efficient to use the semiconductor for the NMR QC, because we can utilize highly advanced processing techniques and an optically pumping method for initializing the qubit. Some NMR QCs performed on the semiconductor use an indirect nuclear spin-spin interaction for a quantum gate of the controlled-NOT operation. It is important for finding the material suitable for the solid-state NMR QC to estimate accurately the indirect spin coupling in several semiconductors and to obtain information about correlation with the electron structure, but has not been completely clarified yet.

Although the studies of the indirect nuclear spin coupling in the semiconductors open up in 1950s,[5] many of them have focused on III-V semiconductor of InP. Since the InX (X = P, As, Sb) semiconductors adopt zinc-blende crystal-structure with the lattice parameter that differs a little each other and thus have similar band structure, we can expect to acquire the correlation of the electron structure and the indirect spin coupling by measuring their J values correctly.

In the present work, we measure the single-, double- and triple-resonance NMR of ^{75}As, $^{113,115}In$ and ^{123}Sb with or without CP and MAS for the InX (X = As, Sb) semiconductors in order to obtain accurately the coupling constant J for the indirect nuclear spin-spin interaction between neighboring spins of $^{113,115}In$ and X. The reduced coupling constant is calculated for discussing the correlation between the indirect spin-spin coupling and the electron structure of the InX (X = P, As, Sb) semiconductors.

1. P. W. Shor, *Proc. of the 35th Annual IEEE Symposium on Foundation of Computer Sicence*, 1994.
2. L. M. K. Vandersypen, *et al.*, *Nature* **414**, 883 (2001).
3. B. E. Kane, *Nature* **393**, 133 (1998).
4. T. Shimizu, *et al.*, *Superlattice. Microst.* **32**, 313 (2002).
5. R. G. Shulman, *et al.*, *Phys. Rev.* **100**, 692 (1955).

AP156

Establishment of annotation processing system for BMRB database at PDBj

Eiichi Nakatani[1,2], Yoh Matsuki[1,2], Haruki Nakamura[2], Hideo Akutsu[2]
[1]*Japan Science and Technology Agency - BIRD,*
[2]*Institute for Protein Research, Osaka University*

BMRB is a database of NMR data for proteins and nucleic acids, which is maintained by BioMagResBank (UW-Madison, WI, USA; PI, John L. Markley). New BMRB data format (NMR-STAR Version 3.0) have been developed by BioMagResBank, and the data deposition interface and softwares for annotation processing have just been renewed.

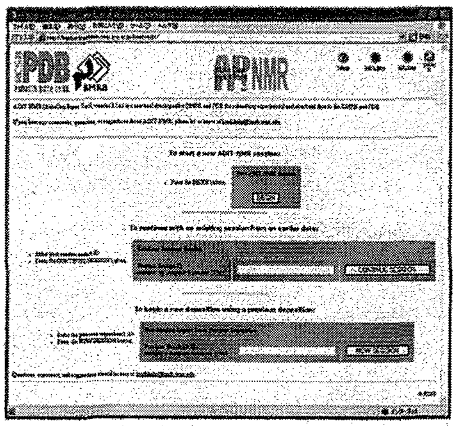

In December 2004, a local deposition site with ADIT-NMR as a BMRB WWW deposition interface was established at Institute for Protein Research (IPR), Osaka University as an activity of PDBj (Protein Data Bank japan ; http://www.pdbj.org), and we began to accept NMR data from researchers as well. Furthermore, we have started the annotation processing of deposited entries via the ADIT-NMR in August 2005.

Fig.1 The top page of ADIT-NMR

The annotation processing at PDBj is performed according to the procedure same as that at BioMagResBank. The BMRB softwares are used for validating and checking data format, verifying chemical shift assignment, tracking for entries of PDBj, and so on. All entries are transmitted to BioMagResBank after annotation processing at PDBj. These entries are added to BMRB database web servers, and are released to public from BMRB and PDBj.

In the poster session, we show how we validate and annotate deposited entry.

- Checking functions
- Verifying of chemical shift assignment
- Entry tracking system
- The sympathize system of data editing version
- Others

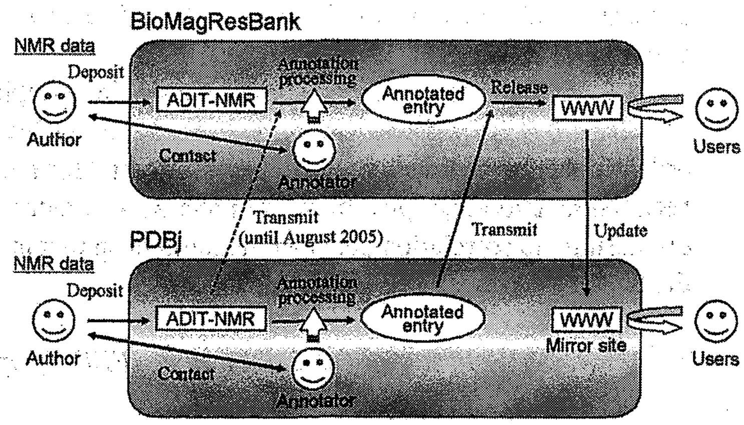

Fig.2 The flow of entries between PDBj and BioMagResBank

Deposit your NMR data to PDBj BMRB site.
(URL: http://bmrbadit.protein.osaka-u.ac.jp/bmrb-adit/)

Author Index

Author index

O

P

Keyword Index

Keyword index

D

Attendee List

Name	Affiliation/Address	Tel/Fax/E-mail
A		
Takamasa Abe 阿部　孝政	理化学研究所 ゲノム科学総合研究センター 230-0045 神奈川県鶴見区末広町１－７－２２ 西研究棟W１０３	045-503-9212 045-503-9210 tabe@gsc.riken.jp
Hideo Akutsu 阿久津　秀雄	大阪大学蛋白質研究所 565-0871 吹田市山田丘３－２	06-6879-8597 06-6879-8599 akutsu@protein.osaka-u.ac.jp
Isao Ando 安藤　勲	東京工業大学名誉教授 247-0052 神奈川県鎌倉市今泉２－１９－３	0467-47-0366 0467-47-0366 Solidnmr@aol.com iando@polymer.titech.ac.jp
Takahiro Araki 荒木　貴宏	(株)三菱化学科学技術研究センター 横浜分析センター 227-8502 神奈川県横浜市青葉区鴨志田町 1000	045-963-3131 045-963-4261 araki.takahiro@mg.m-kagaku.cp.jp
Naoki Asakawa 浅川　直紀	東京工業大学大学院生命理工学研究科 226-8501 横浜市緑区長津田町 4259 B-55	045-924-5796 045-925-5827 nasakawa@bio.titech.ac.jp
Tetsuo Asakura 朝倉　哲郎	東京農工大学 184-8588 小金井市中町２－２４－１６	042-383-7733 042-383-7733 mutsugi@cc.tuat.ac.jp
Atsushi Asano 浅野　敦志	防衛大学校 239-8686 横須賀市走水１－１０－２０	046-841-3810 046-844-5901 asanoa@nda.ac.jp
Fumio Asanoma 浅野間　文夫	奈良先端科学技術大学院大学 物質創成科学研究科 630-0101 生駒市高山町８９１６－５	090-9626-1953 — asanoma@ms.naist.jp
Tatuya Asanuma 浅沼　達哉	独立行政法人産業技術総合研究所 光技術研究部門 563-8577 大阪府池田市緑丘 1-8-31	072-751-4263 072-751-9637 t-asanuma@aist.go.jp
Jun Ashida 芦田　淳	バリアンテクノロジーズジャパンリミテッド 108-0023 港区芝浦４－１６－３６	03-5232-1238 — jun.ashida@varianinc.com
D		
Makoto Demura 出村　誠	北海道大学大学院理学研究科 060-0810 札幌市北区北 10 条西 8 丁目	011-706-2771 011-706-2771 demura@sci.hokudai.ac.jp
Takeo Domoto 堂本　竹雄	ブルカー・バイオスピン株式会社 マーケティング部 305-0051 茨城県つくば市二の宮 3-21-5	029-852-1234 029-858-0322 takeo.domoto@bruker-biospin.jp
E		
Taro Eguchi 江口　太郎	大阪大学総合学術博物館 560-0043 豊中市待兼山町１－１６	06-6850-6710 06-6850-6720 eguchi@museum.osaka-u.ac.jp

Name	Affiliation/Address	Tel/Fax/E-mail
Buichiro Ena 江奈　武一郎	住化分析センター 300-3294 茨城県つくば市北原６番 住友化学株式会社 筑波	029-864-4182 029-864-4746 ena@scas.co.jp
Hiroshi Endo 遠藤　弘	理化学研究所 ゲノム科学総合研究センター 230-0045 横浜市鶴見区 末広町 1丁目 7－22 C116	045-503-9642 — endo@gsc.riken.jp
F		
Akihiko Fujikawa 藤川　昭彦	アステラス製薬株式会社 925-0613 羽咋市飯山町ヲ32	0767-26-3311 0767-26-3314 fujikawa@mprcf.or.jp
Yuko Fujimoto 藤本　侑子	福井大学工学部生物応用化学科 910-8507 福井市文京３－９－１	0776-27-8635 0776-27-8747 1370570@icpc00.icpc.fukui-u.ac.jp
Hideaki Fujiwara 藤原　英明	大阪大学大学院医学系研究科保健学専攻医用物理工学講座 565-0871 吹田市山田丘 1-7	06-6879-2573 06-6879-2573 fujiwara@sahs.med.osaka-u.ac.jp
Toshimichi Fujiwara 藤原　敏道	大阪大学蛋白質研究所 565-0871 大阪府吹田市山田丘 3-2	06-6879-8598 06-6879-8599 tfjwr@protein.osaka-u.ac.jp
Yasuhiro Fujiwara 藤原　康博	福井大学工学部生物応用化学科 910-8507 福井市文京３－９－１	0776-27-8635 0776-27-8747 1370589@icpc00.icpc.fukui-u.ac.jp
Jun Fukazawa 深澤　隼	京都大学大学院理学研究科化学専攻分子構造化学 606-8502 京都市左京区北白川追分町	075-753-4012 075-753-4000 fukazawa@kuchem.kyoto-u.ac.jp
Hiroyuki Fukui 福井　洋之	北見工業大学工学部化学システム工学科 090-8507 北海道北見市公園町165	0157-26-9402 0157-24-7719 fukui@gaea.chem.kitami-it.ac.jp
Eri Fukushi 福士　江里	北海道大学大学院農学研究科 060-8589 札幌市北区北９西９	011-706-4134 — feria@cen.agr.hokudai.ac.jp
Junko Fukutomi 福富　淳子	大阪大学大学院医学系研究科保健学専攻医用物理工学講座 565-0871 吹田市山田丘 1-7	06-6879-2577 06-6879-2577 sf3j-fktm@asahi-net.or.jp
Kazuo Furihata 降旗　一夫	東京大学大学院農学生命科学研究科、応用生命化学専攻 113-8657 東京都文京区弥生 1-1-1	03-5841-5460 03-5841-8485 furihata@iam.u-tokyo.ac.jp
Kyoko Furuita 古板　恭子	奈良先端科学技術大学院大学 630-0192 奈良県生駒市高山町8916-5 学生宿舎1-501	090-4566-1169 — k-furuit@bs.naist.jp
Hirosuke Furuta 古田　浩祐	杏林製薬(株)創薬研究所 329-0114 下都賀郡野木町野木2399－1	0280-56-2201 0280-57-1293 hirosuke.furuta@mb.kyorin-pharm.co.jp

Name	Affiliation/Address	Tel/Fax/E-mail
G		
Kazuma Gotoh 後藤　和馬	岡山大学理学部 700-8530 岡山市津島中 3-1-1	086-251-7776 — kgotoh@cc.okayama-u.ac.jp
H		
Toshiyuki Hamada 濱田　季之	理化学研究所・ゲノム科学総合研究センター 230-0045 神奈川県横浜市鶴見区末広町 1-7-22 理化学研究所横浜研究所 W103	045-503-9212 045-503-9210 thamada@gsc.riken.jp
Hajime Hamajima 浜島　斉	三和化学研究所 分析センター 511-0406 三重県いなべ市北勢町塩崎363	0594-72-6221 0594-82-0072 h_hamajima@mb4.skk-net.com
Eiji Hara 原　英二	富山化学工業株式会社 930-8508 富山市下奥井2－4－1	076-431-8218 — EIJI_HARA@toyama-chemical.co.jp
Jun Hasegawa 長谷川　淳	第一製薬株式会社 134-8630 江戸川区北葛西 1-16-13	03-3680-0151 03-5696-4266 haseg7li@daiichipharm.co.jp
Akiko Hatakeyama 畠山　明子	兵庫県立大学大学院 生命理学研究科 678-1297 兵庫県赤穂郡上郡町光都 3-2-1	0791-58-0182 0791-58-0182 rj04z030@stkt.u-hyogo.ac.jp
Minoru Hatanaka 畑中　稔	独立行政法人理化学研究所 230-0045 横浜市鶴見区末広町 1-7-22	045-503-9229 045-503-9228 minoruh@gsc.riken.go.jp
Reiko Hatta 八田　玲子	RIKEN GSC 230-0045 横浜市鶴見区末広町 1-7-22 理化学研究所ゲノム科学総合研究センター	045-503-9267 045-503-9641 rei8@gsc.riken.jp
Mineyuki Hattori 服部　峰之	(独)産業技術総合研究所 305-8568 茨城県つくば市梅園1－1－1 中央第2	029-861-5537 029-861-5540 mhattori@m.aist.go.jp
Fumiaki Hayashi 林　文晶	理化学研究所 ゲノム科学総合研究センター 230-0045 横浜市鶴見区末広町 1 丁目 7-22	045-503-9462 — fhayashi@gsc.riken.jp
Kokoro Hayashi 林　こころ	奈良先端科学技術大学院大学 バイオサイエンス研究科 630-0101 生駒市高山町8916－5	0743-72-5577 — ko-haya@bs.naist.jp
Sigenobu Hayashi 林　繁信	産業技術総合研究所 計測フロンティア研究部門 ナノ移動解析研究グループ 305-8565 茨城県つくば市東1－1－1 中央第5	029-861-4515 029-861-4515 hayashi.s@aist.go.jp
Fahu He	RIKEN, GSC 230-0045 1-7-22 Suehiro-cho, Tsurumi-ku, Yokohama	045-503-9461 045-503-9460 hefahu@gsc.riken.go.jp

Name	Affiliation/Address	Tel/Fax/E-mail
Hikaru Hemmi 逸見　光	独立行政法人食品総合研究所 305-8642 つくば市観音台2－1－12	029-838-8033 — hemmi@nfri.affrc.go.jp
Tetsu Hinomoto 日元　徹	日本電子株式会社 196-8558 昭島市武蔵野3－1－2	042-542-2136 042-546-8068 hinomoto@jeol.co.jp
Yuuki Hirai 平井　佑紀	JSR株式会社 物性分析室 510-8552 三重県四日市市川尻町100 A28A	0593-45-8059 0593-45-8107 Yuuki_Hirai@jsr.co.jp
Keiko Hirakawa 平川　慶子	日本医科大学 NMR 研究施設 法医学教室 113-8602 東京都文京区千駄木1－1－5	03-3822-2131 03-5814-5680 hirakawa@nms.ac.jp
Yuuka Hirao 平尾　優佳	横浜市立大学大学院 230-0045 横浜市鶴見区末広町1－7－29	045-508-7218 045-508-7362 yuuka@tsurumi.yokohama-cu.ac.jp
Tosifumi Hiraoki 平沖　敏文	北海道大学大学院工学研究科応用物理学専攻 060-8628 北海道札幌市北区北 13 西8	011-706-6640 011-716-6175 hiraoki@eng.hokudai.ac.jp
Kiyomi Hirata 平田　清美	株式会社巴商会 144-8505 東京都大田区南蒲田1－1－25	03-3734-1124 03-3739-1070 k-hirata@tomoeshokai.co.jp
Hiroshi Hirota 廣田　洋	理化学研究所 ゲノム科学総合研究センター 230-0045 横浜市鶴見区末広町1－7－22	045-503-9211 045-503-9210 hirota@gsc.riken.jp
Toshihiro Hodai 蓬台　俊宏	大阪大学理学研究科村田研究室 560-0043 豊中市待兼山町 1-16	06-6850-5789 — toshi@ch.wani.osaka-u.ac.jp
Fumitake Horii 堀井　文敬	京都大学化学研究所 611-0011 宇治市五ケ庄	0774-38-3150 0774-38-3148 horii@scl.kyoto-u.ac.jp
Noriko Horiike 堀池　則子	旭化成株式会社 基盤技術研究所 416-8501 静岡県富士市鮫島2－1	0545-62-3161 0545-62-3159 horiike.nb@om.asahi-kasei.co.jp
Hiromitsu Hoshika 星加　博光	奈良先端科学技術大学院大学 573-0047 大阪府枚方市山之上1－21－1	072-846-8609 072-846-8609 hi-hoshi@bs.naist.jp
Kazuo Hosoda 細田　和男	群馬大学工学部生物化学工学科 376-8515 桐生市天神町1－5－1	0277-30-1439 — pen@jig.ce.gunma-u.ac.jp
I		
Shunsuke Igarashi 五十嵐　俊介	東京大学薬学部薬学系研究科 生命物理化学教室 113-0032 東京都文京区本郷 7-3-1	03-5841-4812 03-5841-4818 igarashi@nmrlab.f.u-tokyo.ac.jp

Name	Affiliation/Address	Tel/Fax/E-mail
Akiko Iihara 飯原　亜希子	ゾイジーン(株)蛋白合成事業部　蛋白合成Aグループ 227-8502 横浜市青葉区鴨志田町1000番地 三菱化学科学技術研究センター内	045-963-3916 045-963-3926 6308790@cc.m-kagaku.co.jp
Takahiro Iijima 飯島　隆広	京都大学大学院理学研究科化学専攻分子構造化学研究室 606-8502 京都市左京区北白川追分町	075-753-4012 075-753-4000 iijima@kuchem.kyoto-u.ac.jp
Hiroshi Ikeda 池田　博	東京工業大学 226-8501 横浜市緑区長津田町4259－B44 生命理工学研究科生物プロセス専攻	045-924-5755 045-924-5780 hikeda@bio.titech.ac.jp
Takahisa Ikegami 池上　貴久	大阪大学蛋白質研究所 565-0871 大阪府吹田市山田丘3－2	06-6879-8598 06-6879-8599 tiik@protein.osaka-u.ac.jp
Teppei Ikeya 池谷　鉄兵	首都大学東京 230-0045 横浜市鶴見区末広町 1-7-22, C519	045-503-9464 045-503-9343 tikeya@bi.a.u-tokyo.ac.jp
Misako Imachi 井町　美佐子	ブルカー・バイオスピン株式会社　アプリケーション部 305-0051 茨城県つくば市二の宮 3-21-5	029-852-1235 029-858-0322 misako.imachi@bruker-biospin.jp
Kyoko Inoue 井上　匡子	理研　横浜研究所　GSC －	045-503-9462 045-503-9641 kyokoino@gsc.riken.jp
Munehiro Inukai 犬飼　宗弘	大阪大学基礎工学研究科 560-8531 大阪府豊中市待兼山町 1-3　D-423	06-6850-6323 06-6850-6321 inukai@qc.ee.es.osaka-u.ac.jp
Yasutaka Inukai 犬飼　康天	住友化学株式会社　有機合成研究所 554-8558 大阪市此花区春日出中3－1－98	06-6466-5171 06-6466-5459 inukaiy@sc.sumitomo-chem.co.jp
Nobuaki Ishida 石田　信昭	独立行政法人食品総合研究所 305-8642 つくば市観音台2－1－12	029-838-8057 029-838-7996 nobu@affrc.go.jp
Hiroki Ishii 石井　裕規	京都大学大学院理学研究科化学専攻 606-8502 京都市左京区北白川追分町	075-753-4012 075-753-4000 hiroki@kuchem.kyoto-u.ac.jp
Takeshi Ishii 石井　毅	群馬大学工学部生物機能第二 376-8515 桐生市天神町1－5－1	090-7171-1665 － ishii@jig.ce.gunma-u.ac.jp
Michiko Ishizu 石津　美智子	横浜市立大学大学院　国際総合科学研究科 生体超分子科学専攻　生体超分子機能科学研究室 230-0045 横浜市鶴見区末広町1－7－9	045-508-7218 045-508-7362 m-ishizu@tsurumi.yokohama-cu.ac.jp
Yoshiko Itezono 射手園　佳子	中外製薬鎌倉研究所 247-8530 鎌倉市梶原 200	0467-47-2209 0467-45-6815 itezonoysk@chugai-pharm.co.jp

Name	Affiliation/Address	Tel/Fax/E-mail
Takuhiro Ito 伊藤　拓宏	東京大学大学院理学系研究科 113-0033 東京都文京区本郷7－3－1	03-5841-4395 03-5841-8057 t_ito@biochem.s.u-tokyo.ac.jp
Yoko Ito 伊藤　陽子	横浜市立大学大学院総合理学研究科 230-0045 神奈川県横浜市鶴見区末広町 1-7-29	045-508-7236 045-508-7368 ito-yoko@gsc.riken.jp
Yukikko Iwase 岩瀬　由紀子	福岡大学薬学部中央機器室 814-0180 福岡市城南区七隈8－19－1	092-871-6631 092-863-0389 wase@fukuoka-u.ac.jp
Takashi Iwashita 岩下　孝	(財)サントリー生物有機科学研究所 618-8503 三島郡島本町若山台1－1	075-962-6044 075-962-2115 iwashita@sunbor.or.jp
Kentaro Iwata 岩田　健太郎	大阪大学蛋白質研究所構造形成研究室 565-0871 吹田市山田丘3－2	06-6879-8615 06-6879-8616 kentaro@protein.osaka-u.ac.jp
Shinichi Iwaya 岩屋　信一	日本システム企画株式会社 151-0073 渋谷区笹塚2－21－12	03-3377-1106 03-3377-2214 shigen@jspkk.co.jp
Hiroshi Kadohara 門原　寛	ブルカー・バイオスピン株式会社 マーケティング部 532-0004 大阪府大阪市淀川区西宮原 1-8-29	06-6394-8989 06-6394-9559 hiroshi.kadohara@bruker-biospin.jp
Masatsune Kainosho 甲斐荘　正恒	東京都立大学大学院理学科 192-0397 東京都八王子市南大沢 1-1	0426-77-2544 0426-77-2544 kainosho@nmr.chem.metro-u.ac.jp
Hironori Kaji 梶　弘典	京都大学 化学研究所 分子材料化学研究領域 611-0011 宇治市五ヶ庄	0774-38-3149 0774-38-3148 kaji@scl.kyoto-u.ac.jp
Shingo Kakita 垣田　信吾	協和発酵工業株式会社 194-8533 町田市旭町3－6－6	042-725-2555 042-726-8330 skakita@kyowa.co.jp
Yuji Kamatari 鎌足　雄司	岐阜大学 501-1194 岐阜市柳戸 1－1	058-230-6145 058-230-6144 kamatari@cc.gifu-u.ac.jp
Atsushi Kameda 亀田　篤司	大阪大学蛋白質研究所 蛋白質構造形成研究室 565-0871 吹田市山田丘3－2	06-6879-8615 06-6879-8616 atkame@protein.osaka-u.ac.jp
Tunenori Kameda 亀田　恒徳	農業生物資源研究所 305-8634 つくば市大わし1－2	029－838-6213 029-838-6159 kamedat@affrc.go.jp
Miya Kamihira 上平　美弥	静岡県立大学食品栄養科学部 422-8526 静岡県静岡市駿河区谷田56－1	054-264-5525 054-264-5551 kamihira@smail.u-shizuoka-ken.ac.jp

Name	Affiliation/Address	Tel/Fax/E-mail
Masakatsu Kamiya 神谷　昌克	北海道大学大学院理学研究科生物科学専攻 060-0810 北海道札幌市北区北10条西8丁目	011-706-2985 011-706-2111 mkamiya@sci.hokudai.ac.jp
Sho Kanasaka 金坂　将	住友化学 300-3294 つくば市北原６番	0298-64-4182 — kanesakas@sc.sumitomo-chem.co.jp
Akari Kaneko 金子　暁里	大阪大学医学部保健学科 医用物理工学講座医用物理化学研究室 565-0871 大阪府吹田市山田丘１－７	06-6879-2577 06-6879-2577 kaneko@sahs.med.osaka-u.ac.jp
Yusuke Kasai 葛西　祐介	大阪大学大学院理学研究科 560-0043 大阪府豊中市待兼山町１－１６	06-6850-5790 — kasai@ch.wani.osaka-u.ac.jp
Masato Katahira 片平　正人	横浜市立大学　大学院国際総合科学研究科 生体超分子科学専攻 230-0045 横浜市鶴見区末広町１－７－29	045-508-7213 045-508-7361 katahira@tsurumi.yokohama-cu.ac.jp
Ritsuko Katahira 片平　律子	協和発酵工業(株)バイオフロンティア研究所 194-8533 町田市旭町 3-6-6	042-725-2555 — rkatahira@kyowa.co.jp
Taeko Kataoka 片岡　妙子	独立行政法人　産業技術総合研究所 生物情報解析研究センター　つくば分子認識解析チーム 305-8566 茨城県つくば市東 1-1-1 中央第６	029-861-6126 029-861-6135 aeo-kataoka@aist.go.jp
Yukiko Doi-Katayama 片山　由貴子	理化学研究所　ゲノム科学総合研究センター タンパク質構造・機能研究グループ 230-0045 神奈川県横浜市鶴見区末広町１丁目７－２２	045-503-9214 045-503-9210 yukikodk@gsc.riken.jp
Koichi Kato 加藤　晃一	名古屋市立大学大学院薬学研究科 467-8603 名古屋市瑞穂区田辺通３－１	052-836-3447 052-836-3447 kkato@phar.nagoya-cu.ac.jp
Yuko Kato 加藤　祐子	東和大学　工学部 815-8510 福岡市　南区　筑紫丘　１－１－１	092-541-1512 092-552-2707 yukato@tohwa-u.ac.jp
Ikumi Kawahara 河原　郁美	奈良先端科学技術大学院大学　バイオサイエンス研究科 生体高分子構造学講座 630-0101 奈良県生駒市高山町８９１６－５	0743-72-5577 0743-72-5579 i-kawaha@bs.naist.jp
Izuru Kawamura 川村　出	横浜国立大学大学院工学府　内藤研究室 240-8501 横浜市保土ヶ谷区常盤台 79-5 横浜国立大学 大学院工学研究棟 303	045-339-4231 045-339-4251 d04sa202@ynu.ac.jp
Keiichi Kawano 河野　敬一	北海道大学大学院理学研究科 060-0810 札幌市北区北 10 条西 8 丁目	011-706-2770 011-706-2770 kawano@sci.hokudai.ac.jp
Makiko Kawano 河野　牧子	㈱科学技術研究所　研究第一部　NMR/MS 測定グループ 140-0001 東京都品川区北品川３－１０－２	03-3474-6629 03-3474-6650 manakada@sankyo.co.jp

Name	Affiliation/Address	Tel/Fax/E-mail
Takanori Kigawa 木川　隆則	理化学研究所 230-0045 横浜市鶴見区末広町 1-7-22	045-503-9203 045-503-9643 kigawa@jota.gsc.riken.jp
Sunnmi Kim 金　善美	(株)三菱化学科学技術研究センター 227-8502 神奈川県横浜市青葉台鴨志田 1000	045-963-3131 045-963-4261 kim.sunmi@ms.m-kagaku.co.jp
Paakkonen Kimmo キモ　パーッコネン	理化学研究所ゲノム科学総合研究センター 230-0045 横浜市鶴見区末広町 1-7-22, C519	045-503-9465 045-503-9343 kimmo@gsc.riken.go.jp
Atuomi Kimura 木村　敦臣	大阪大学大学院保健学専攻 565-0871 大阪府吹田市山田丘 1-7	06-6879-2577 06-6879-2577 kimura@sahs.med.osaka-u.ac.jp
Osamu Kinoshita 木下　理	福井大学工学部生物応用化学科 910-8507 福井市文京３－９－１	0776-27-8635 0776-27-8747 osamu@acbio.fukui-u.ac.jp
Ryo Kitahara 北原　亮	理化学研究所播磨研究所 679-5148 佐用郡三日月町光都１－１－１	0791-58-2838 0791-58-2835 kitahara@spring8.or.jp
Mamoru Kitsukawa 橘川　守	昭和電工㈱ 分析物性センター 267-0056 千葉市緑区大野台 1-1-1	043-226-5223 043-226-5222 Mamoru_Kitsukawa@sdk.co.jp
Kirokazu Kobayashi 小林　広和	大阪大学総合学術博物館 560-0043 豊中市待兼山町 1-16	06-6850-5769 06-6850-5785 hirawk@ch.wani.osaka-u.ac.jp
Kuniko Kobayashi 小林　邦子	三菱化学生命科学研究所 194-8511 町田市南大谷 11 号	042-724-6289 042-724-6296 kuniko@libra.ls.m-kagaku.co.jp
Toshitatsu Kobayashi 小林　俊達	奈良先端科学技術大学院大学 630-0192 生駒市高山町８９１６－５	0743-72-5577 0743-72-5579 t-kobaya@bs.naist.jp
Toshiyuki Kohno 河野　俊之	三菱化学生命科学研究所 194-8511 町田市南大谷１１号	042-724-6285 042-724-6296 tkohno@libra.ls.m-kagaku.co.jp
Chojiro Kojima 児嶋　長次郎	奈良先端科学技術大学院大学バイオサイエンス研究科 630-0192 生駒市高山町 8916-5	0743-72-5571 — kojima@bs.naist.jp
Ryohei Komatsu 小松　領平	福井大学大学院工学研究科生物応用化学専攻 910-8507 福井市文京３－９－１	0776-27-8635 0776-27-8747 ryohei@acbio.fukui-u.ac.jp
Hiroyuki Koshino 越野　広雪	独立行政法人理化学研究所 351-0198 和光市広沢 2-1	048-467-9361 048-462-4627 koshino@riken.jp

Name	Affiliation/Address	Tel/Fax/E-mail
Hiroyuki Kouno 甲野　裕之	ブルカー・バイオスピン株式会社　アプリケーション部 305-0051　茨城県つくば市二の宮 3-21-5	029-852-1235 029-858-0322 Hiroyuki.kono@bruker-biospin.jp
Takahide Kouno 河野　隆英	富山医科薬科大学薬学部構造生物学研究室 930-0194　富山市杉谷 2630	076-434-7574 076-434-5061 pd029003@st.toyama-mpu.ac.jp
Hiroyuki Koyano 古家野　宏行	電気通信大学 182-8585　調布市調布ヶ丘 1−5−1 東 6−110	0424-43-5730 — koyano@cia.uec.ac.jp
Yasuhiro Kumaki 熊木　康裕	北海道大学大学院 060-0810　札幌市北区北 10 条西 8 丁目	011-706-3572 011-706-3572 kumaki@sci.hokudai.ac.jp
Hideto Kuribayashi 栗林　秀人	バリアン　テクノロジーズ　ジャパン　リミテッド 108-0023　東京都港区芝浦 4-16-36 住友芝浦ビル 8F	03-5232-1238 03-5232-1264 hideto.kuribayashi@varianinc.com
Junichi Kurita 栗田　順一	バリアンテクノロジーズジャパンリミテッド 134-0084　東京都港区芝浦4−16−36　住友芝浦ビル	03-5232-1238 03-5232-1264 junichi.kurita@varianinc.com
Yukio Kuroda 黒田　幸夫	ブルカー・バイオスピン株式会社　技術サービス部 305-0051　茨城県つくば市二の宮 3-21-5	029-852-1236 029-858-0322 yukio.kuroda@bruke.jp
Shigeki Kuroki 黒木　重樹	東京工業大学大学院理工学研究科物質科学専攻 152-8552　東京都目黒区大岡山2−12−1−S1−20	03-5734-2880 03-5734-2889 skuroki@polymer.titech.ac.jp
Hiromichi Kurosu 黒子　弘道	奈良女子大学 630-8506　奈良市北魚屋西町	0742-20-3461 0742-20-3461 kurosu@cc.nara-wu.ac.jp
Katsuhiko Kushida 串田　克彦	バリアンテクノロジーズジャパンリミテッド 134-0084　東京都港区芝浦4−16−36　住友芝浦ビル	03-5232-1238 03-5232-1264 katsuhiko.kushida@varianinc.com
Hideki Kusunoki 楠　英樹	三菱化学生命科学研究所 194-8511　町田市南大谷11	042-724-6289 — kusunoki@libra.ls.m-kagaku.co.jp
Daisuke Kuwahara 桑原　大介	機器分析センター 182-0026　東京都調布市調布ヶ丘 1-5-1	0424-43-5730 0424-43-5501 kuwahara@cia.uec.ac.jp
L		
Hua Li Hua Li (李　華)	理化学研究所ゲノム科学総合研究センター 230-0045　横浜市鶴見区末広町1丁目7−22	045-503-9317 045-503-9643 lihua@gsc.riken.go.jp
M		

Name	Affiliation/Address	Tel/Fax/E-mail
Shiro maeda 前田　史郎	福井大学工学部生物応用化学科 910-8507 福井市文京3－9－1	0776-27-8635 0776-27-8747 maeda@acbio.fukui-u.ac.jp
Michal Malon マロニュ　ミハル	理化学研究所 351-0198 埼玉県和光市平沢 2-1	048-467-9361 048-462-4627 malon@riken.jp
Waelchli Markus マーカス　ベルヘリ	ブルカー・バイオスピン株式会社 アプリケーション部 305-0051 茨城県つくば市二の宮 3-21-5	029-852-1235 029-858-0322 markus.waelchli@bruker-biospin.jp
Kyosuke Maruyoshi 丸吉　京介	大阪大学大学院理学研究科 560-0043 大阪府豊中市待兼山町1－16	06-6850-5790 06-6850-5774 maru@ch.wani.osaka-u.ac.jp
Hidefumi Masumoto	University of Tsukuba —	+81-29-853-5421 — masumoto@ctlab.bk.tsukuba.ac.jp
Takashi Masutani 枡谷　隆史	大阪大学医学部保健学科 医用物理工学講座医用物理化学研究室 565-0871 大阪府吹田市山田丘1－7	06-6879-2577 06-6879-2577 mr0043mt@yahoo.co.jp
Yoh Matsuki 松木　陽	大阪大学たんぱく質研究所 565-0871 吹田市山田丘 3-2	06-6879-8598 06-6879-8599 yoh@protein.osaka-u.ac.jp
Koushi Matubara 松原　康史	三菱化学科学技術研究センター 横浜分析センター 有機分析グループ 227-8502 横浜市青葉区鴨志田町 1000	045-963-3166 045-963-4261 3709437@cc.m-kagaku.co.jp
Nobuaki Matumori 松森　信明	大阪大学大学院理学研究科化学専攻 560-0043 大阪府豊中市待兼山町 1-1	06-6850-5569 06-6850-5569 matsmori@chem.sci.osaka-u.ac.jp
Shunsuke Meshitsuka 飯塚　舜介	鳥取大学大学院医学系研究科 683-8503 米子市西町86	0859-34-8286 0859-34-8068 mesh@grape.med.tottori-u.ac.jp
Ayaka Minemura 峯村　綾香	奈良女子大学生活環境学部 630-8268 奈良県奈良市大豆山町3メゾン K's4－D	090-7949-7492 — mineaya@crux.ocn.ne.jp
Katsuhiko Minoura 箕浦　克彦	大阪薬科大学 569-1094 高槻市奈佐原4の20の1	072-690-1039 072-690-1039 minoura@gly.oups.ac.jp
Masaki Mishima 三島　正規	奈良先端科学技術大学院大学バイオサイエンス研究科 630-0192 奈良県生駒市高山町 8916-5	0743-72-5576 0743-72-5579 misima@bs.naist.jp
Fumiyuki Mitsumori 三森　文行	国立環境研究所 環境ホルモン・ダイオキシン研究プロジェクト 305-8506 つくば市小野川16－2	029-850-2862 029-850-2880 mitumori@nies.go.jp

Name	Affiliation/Address	Tel/Fax/E-mail
Youhei Miyanoiri 宮ノ入　洋平	横浜市立大学大学院国際総合科学研究科 生体超分子科学専攻計測科学講座 230-0045 横浜市鶴見区末広町１－７－２９	045-508-7215 045-508-7361 y-miyanoiri@tsurumi.yokohama-cu.ac.jp
Hirotsugu Miyashiro 宮代　博継	富山大学 930-0194 富山市杉谷２６３０	076-434-7632 076-434-4656 miyahiro@ms.toyama-mpu.ac.jp
Chiyoko Mizukuchi 水口　千代子	インフォコム株式会社 バイオサイエンス部 サイエンスグループ 101-0062 東京都千代田区神田駿河台 3-11 三井住友海上駿河台別館	03-3518-3860 03-3518-3960 c.mizukuchi@infocom.co.jp
Hideaki Mizuno	Brain Science Institute, RIKEN 351-0198 2-1 Hirosawa, Wako city, Saitama	+81-48-462-1111 +81-48-467-5924 hmizuno@brain.riken.jp
Kazuko Mizuno 水野　和子	福井大学工学部 910-8507 福井市文京 3-9-1	0776-27-8759 0776-27-8759 mizuno@acbio2.acbio.fukui-u.ac.jp
Takashi Mizuno 水野　敬	日本電子株式会社　分析機器本部 196-8558 昭島市武蔵野３－１－２	042-542-2236 042-546-8068 tmizuno@jeol.co.jp
Masahiro Mochida 望田　昌弘	群馬大学工学部材料工学科 376-8515 群馬県桐生市天神町１－５－１	0277-30-1331 0277-30-1333 yamanobe@chem.gunma-u.ac.jp
Yuki Mogami 最上　裕貴	京都大学大学院理学研究科化学専攻 606-8502 京都市左京区北白川追分町	075-753-4012 075-753-4000 ymogami@kuchem.kyoto-u.ac.jp
Tomohito Morikawa 森川　友仁	三菱化学生命科学研究所 194-8511 町田市南大谷１１号	042-724-6289 — tmorik@libra.ls.m-kagaku.co.jp
Daisuke Morimura 森村　太亮	群馬大学工学部材料工学科 376-8515 群馬県桐生市天神町１－５－１	0277-30-1331 0277-30-1333 yamanobe@chem.gunma-u.ac.jp
Shin Morita 森田　慎	横浜私立大学大学院総合理学研究科 202-0011 西東京市泉町５－１６－１９－５０２	0424-24-4829 0424-24-4829 moritashinn@tsurumi.yokohama-cu.ac.jp
Miwa Murakami 村上　美和	物質・材料研究機構 305-0003 つくば市桜３－１３	029-863-5466 — MURAKAMI.Miwa@nims.go.jp
Junnosuke Muranaka 村中　淳之介	福井大学工学部生物応用化学科 910-8507 福井市文京３－９－１	0776-27-8635 0776-27-8747 muranaka@acbio.fukui-u.ac.jp
Yoshifumi Murata 村田　義文	防衛大学校 239-8686 横須賀市走水１－１０－２０	046-841-3810 — g43025@nda.ac.jp

Name	Affiliation/Address	Tel/Fax/E-mail
N		
Satoshi Nagao 長尾　聡	筑波大学大学院数理物質科学研究科 305-8571　つくば市天王台1－1－1　理科系修士棟 D402	029-853-7365 — s_nagao@dmb.chem.tsukuba.ac.jp
Takashi Nagao 永尾　隆	横浜国立大学大学院工学研究院 240-8501　横浜市保土ヶ谷区常磐台 79-5	045-339-4231 045-339-4251 takashi_a_nagao@jsr.co.jp
Kaz Nagashima 永嶋　一臣	東京磁気共鳴 160-0015　東京都新宿区大京町 31 番地 VIP 新宿御苑 605	03-3357-1380 — knaga@tmagres.com
Toshio Nagashima 長島　敏雄	RIKEN GSC タンパク質構造・機能研究グループ 230-0045　横浜市鶴見区末広町 1-7-22	042-503-9462 045-503-9641 toshion@gsc.riken.go.jp
Akira Naito 内藤　晶	Yokohama National University, Graduate School of Engineering 240-8501　79-5 Tokiwadai, Hodogaya-ku, Yokohama, Japan	+81-45-339-4232 +81-45-339-4251 naito@ynu.ac.jp
Toshihito Nakai 中井　利仁	日本電子株式会社 AID 応用研究グループ 196-8588　東京都昭島市武蔵野3－1－2	042-542-2241 042-546-8068 tnakai@jeol.co.jp
Takashi Nakamura 仲村　高志	独立行政法人理化学研究所 351-0198　埼玉県和光市広沢 2-1	048-467-9362 048-462-4627 takashi.nakamura@riken.jp
Yoshiyuki Nakamura 中村　義之	東京工業大学資源化学研究所 226-8503　横浜市緑区長津田町4259－R1-33	045-924-5110 045-924-5109 ynakamur@res.titech.ac.jp
Manabu Nakano 中野　学	北大院理 060-0810　札幌市北区北 10 条西 8 丁目 北海道大学理学研究科 2 号館 7 階	011-706-2985 — nakano@sci.hokudai.ac.jp
Michiko Nakano 中野　路子	自然科学研究機構　分子科学研究所 444-8787　愛知県岡崎市明大寺町字東山 5-1	0564-59-5524 0564-59-5523 michiko@ims.ac.jp
Tadashi Nemoto 根本　直	独立行政法人　産業技術総合研究所 305-8566　つくば市東1-1	029-861-6126 029-861-6135 tadashi.nemoto@aist.go.jp
Yuki Nishigaya 西ヶ谷　有輝	奈良先端科学技術大学院大学 630-0101　奈良県生駒市高山町 8916-5	0743-72-5572 — yu-nishi@bs.naist.jp
Katsuyuki Nishimura 西村　勝之	横浜国立大学　大学院工学研究院 240-8501　神奈川県横浜市保土ヶ谷区常盤台 79 番 5 号	045-339-4224 045-339-4224 nishimur@ynu.ac.jp
Yusaku Nishina 仁科　勇作	(株)日曹分析センター 250-0216　小田原市高田 345	0465-42-8201 0465-42-3586 y.nishina@nippon-soda.co.jp

Name	Affiliation/Address	Tel/Fax/E-mail
Yusuke Nishiyama 西山　裕介	理化学研究所 230-0045　神奈川県横浜市鶴見区末広町1	045-503-9229 045-503-9228 nishi@gsc.riken.go.jp
Yasuo Noda 野田　康夫	関西学院大学　理工学部 669-1337　三田市学園2丁目1番地	079-565-8511 079-565-9077 yasuonoda@kwansei.ac.jp
Ayumi Nojiri 野尻　鮎美	福井大学工学部生物応用化学科 910-8507　福井市文京3－9－1	0776-27-8635 0776-27-8747 1370506@icpc00.icpc.fukui-u.ac.jp
Makoto Nomura 野村　誠	奈良先端科学技術大学院大学バイオサイエンス研究科 630-0192　生駒市高山町8916番地5奈良先端大バイオD5F	0743-72-5572 0743-72-5579 m-nomura@bs.naist.jp
Mitsuru Nomura 野村　充	木原記念横浜生命科学振興財団 230-0045　横浜市鶴見区末広町 1-7-29	045-508-7247 045-508-7362 m-nomura@tsurumi.yokohama-cu.ac.jp
O		
Takashi Ogino 荻野　孝史	国立精神・神経センター神経研究所 187-8502　東京都小平市小川東町4－1－1	042-341-2712 042-341-7521 ogino@ncnp.go.jp
Ryutaro Ohashi 大橋　竜太郎	京都大学大学院理学研究科化学専攻 606-8502　京都市左京区北白川追分町	075-753-4012 075-753-4000 ryu@kuchem.kyoto-u.ac.jp
Wakana Ohashi 大橋　若奈	理研GSC 230-0045　横浜市鶴見区末広町1－7－22	045-503-9212 045-503-9210 wohashi@gsc.riken.jp
Masanobu Ohta 太田　将信	医薬化学研究所 532-8505　田辺製薬株式会社	06-6300-2588 06-6300-2586 ohta-m@tanabe.co.jp
Atushi Okada 岡田　敦司	大正製薬株式会社　医薬研究所リード探索研究室 331-9530　さいたま市北区吉野町 1-403	048-669-3061 048-652-7254 a.okada@po.rd.taisho.co.jp
Hajime Okamoto 岡本　大	電気通信大学 182-8585　調布市調布ヶ丘1－5－1東6号館109室	0424-43-5730 — okamoto@x-ray.cia.uec.ac.jp
Michi Okonogi 小此木　美智	東京農工大学　工学部　朝倉研究室 184-8588　東京都小金井市中町 2-24-16	042-388-7025 042-383-7733 y5641105@gc.tuat.ac.jp
Yasushi Ohno 大野　靖	日本たばこ産業(株)医薬総合研究所 569-1125　大阪府高槻市紫町1－1	072-681-9700 072-681-9725 yasushi.ono@ims.jti.co.jp
Takeshi Ota	NTT Basic Research Laboratories *243-0198　3-1, Morinosato Wakamiya, Atsugi-shi, Kanagawa*	+81-46-240-3127 +81-46-240-4727 ota@will.brl.ntt.co.jp

Name	Affiliation/Address	Tel/Fax/E-mail
S.Otomo(Z.-Y.Wang) 大友　征宇	茨城大学　理学部 310-8512　水戸市文京 2-1-1	029-228-8352 029-228-8352 otomo@mx.ibaraki.ac.jp
P		
Guentert Peter ペーター　ギュンタート	理化学研究所ゲノム科学総合研究センター 230-0045　横浜市鶴見区末広町 1-7-22, C519	045-503-9345 045-503-9343 guentert@gsc.riken.go.jp
Q		
Xu-rong Qin 秦　旭栄	理化学研究所 232-0045　横浜市鶴見区末広町1－7－22	045-503-9462 045-503-9641 qin@gsc.riken.jp
S		
Shin Saito 齊藤　伸	北海道大学大学院理学研究科 060-0810　札幌市北区北 10 条西 8 丁目	011-706-3806 011-706-3806 shinshin@sci.hokudai.ac.jp
Hajime Saitou 斉藤　肇	広島大学量子生命科学研究センター 739-8526　東広島市鏡山1丁目	078-856-2876 078-856-2876 hsaito@siren.ocn.ne.jp
Kouji Saitou 斎藤　公児	新日本製鐵(株)先端技術研究所 293-8511　富津市新富20－1	0439-80-2270 0439-80-2746 saito@re.nsc.co.jp
Taiichi Sakamoto 坂本　泰一	千葉工業大学 275-0016　千葉県習志野市津田沼2－17－1	047-478-0317 — tsakamoto@sky.it-chiba.ac.jp
Tiseko Sakuma 佐久間　千勢子	東京薬科大学　中央分析センター 192-0392　東京都八王子市堀之内1432－1	0426-76-4041 0426-76-5894 sakumac@ps.toyaku.ac.jp
Aiko Sakurai 櫻井　愛子	㈱三菱化学科学技術研究センター　横浜分析センター 227-8502　横浜市青葉区鴨志田町1000	045-963-3166 045-963-4261 sakurai.aiko@mp.m-kagaku.co.jp
Hiroaki Sasakawa 笹川　拡明	分子科学研究所 444-8787　岡崎市明大寺東山 5-1	0564-59-5503 0564-59-5503 sasakawa@ims.ac.jp
Emi Sato 佐藤　恵美	福井大学　工学部　生物応用化学科 910-8507　福井市文京3－9－1	0776-27-8635 0776-27-8747 1370364@icpc00.icpc.fukui-u.ac.jp
Hajime Sato 佐藤　一	ブルカー・バイオスピン株式会社　アプリケーション部 305-0051　茨城県つくば市二の宮 3-21-5	029-852-1235 029-858-0322 hajime.sato@bruker-biospin.jp
Hiroko Sato 佐藤　寛子	国立情報学研究所 101-8430　東京都千代田区一ツ橋 2-1-2	03-4212-2501 03-3556-1916 cheminfo@nii.ac.jp

Name	Affiliation/Address	Tel/Fax/E-mail
Mitsuhiro Sekiguchi 関口　光広	アステラス製薬創薬推進研究所分析第 2 研究室 305-8585 茨城県つくば市御幸が丘 21	029-863-7012 029-852-9585 mitsuhiro.sekiguchi@jp.astellas.com
Yoshiaki Seo 瀬尾　芳輝	獨協医科大学 生理学(生体制御) 321-0293 都賀郡壬生町大字北小林 880	0282-87-2125 0282-86-7835 yseo@dokkyomed.ac.jp
Hiroyuki Shida 志田　裕幸	群馬大学工学部材料工学科 376-8515 群馬県桐生市天神町１－５－１	0277-30-1331 0277-30-1333 yamanobe@chem.gunma-u.ac.jp
Ichio Shimada 嶋田　一夫	東京大学大学院薬学系研究科 113-0033 文京区本郷 7-3-1	03-5841-4810 03-03815-6540 shimada@iw-nmr.f.u-tokyo.ac.jp
Hideaki Shimojo 下條　秀朗	横浜市立大学大学院総合理学研究科 230-0045 横浜市鶴見区末広町１－７－２９	045-508-7218 — shimojo@tsurumi.yokohama-cu.ac.jp
Mai Shinagawa 品川　麻衣	味の素株式会社 210-8681 川崎市川崎区鈴木町１－１	044-244-7145 044-210-5872 mai_shinagawa@ajinomoto.com
Heisaburo Shindo 神藤　平三郎	東京薬科大学 192-0392 八王子市堀之内1432－1	0426-76-4537 0426-76-4537 shindo@ps.toyaku.ac.jp
Masahiro Sirakawa 白川　昌宏	京都大学大学院工学研究科 615-8510 京都市西京区京都大学桂	075-383-2535 075-383-2541 shirakawa@moleng.kyoto-u.ac.jp
Tetsuya Suetake 末武　徹也	理化学研究所ゲノム科学総合研究センター 230-0045 横浜市鶴見区末広町１－７－２２	045-503-9462 045-503-9641 suetake@gsc.riken.jp
Makiko Sugiura 杉浦　眞喜子	神戸薬科大学中央分析室 658-8558 神戸市東灘区本山北町 4 - 19 - 1	078-441-7591 078-441-7591 makiko-s@kobepharma-u.ac.jp
Manrao Suraj	スペクトラガス インク 210-0025 川崎市川崎区下並木 6-1-407	044-222-2148 044-245-4530 surajmanra@aol.com
Hideo Suzuki 鈴木　英男	スペクトラガス インク 210-0025 川崎市川崎区下並木 6-1-407	044-222-2148 044-245-4530 suzukitrd@yahoo.co.jp
Hiroaki Suzuki 鈴木　宏昭	茨城大学 理学部 310-8512 水戸市文京 2-2-1	029-228-8352 029-228-8352 hirosuzu@mx.ibaraki.ac.jp
Kouichi Suzuki 鈴木　浩一	産業技術総合研究所 計測フロンティア研究部門 ナノ移動解析研究グループ 305-8565 茨城県つくば市東 1-1-1	029-861-4506 029-861-4506 suzuki-koh@aist.go.jp

Name	Affiliation/Address	Tel/Fax/E-mail
Kouo Suzuki 鈴木　晃生	北海道大学大学院工学研究科 応用物理学専攻ソフトマター工学研究室 060-8628　札幌市北区北 13 条西 8 丁目	011-706-6642 — kouo@eng.hokudai.ac.jp
You Suzuki 鈴木　陽	金沢大学大学院 920-0923　金沢市桜町15－34ドエル風見鶏202	070-5477-1120 — yoh-suzu@wriron1.s.kanazawa-u.ac.jp
T		
Hiroki Takahashi 高橋　大樹	大阪大学蛋白質研究所 565-0871　大阪府吹田市山田丘3－2	06-6879-8598 06-6879-8599 daiki@protein.osaka-u.ac.jp
Masato Takahashi 高橋　雅人	理化学研究所 230-0045　横浜市鶴見区末広町1－7－22　C110	045-503-91115154 — masatot@gsc.riken.go.jp
Seizo Takahashi 高橋　征三	日本女子大学理学部物質生物科学科 112-8681　文京区目白台2－8－1	03-5981-3670 03-5981-3656 t_seizo@fc.jwu.ac.jp
Hiroyuki Takashima 高島　浩幸	ノバルティスファーマ筑波研究所 300-2611　つくば市大久保8ノバルティスファーマ筑波研究所	029-865-2285 029-865-2385 hiroyuki.takashima@novartis.com
Nobuhiro Takaya 高屋　展宏	国立環境研究所 305-8506　茨城県つくば市小野川16－2	029-850-2862 — takaya.nobuhiro@nies.go.jp
Toshio Takayama 高山　俊夫	神奈川大学工学部応用化学科 221-8686　横浜市神奈川区六角橋 3-27-1	045-481-5661 045-413-9770 takayt01@kanagawa-u.ac.jp
Kazuyuki Takeda 武田　和行	大阪大学　大学院基礎工学研究科 560-8531　豊中市待兼山町1－3　D421	06-6850-6321 06-6850-6321 takeda@qc.ee.es.osaka-u.ac.jp
Kiyonori Takegoshi 竹腰　清乃理	京都大学大学院理学研究科化学 606-8502　京都市左京区北白川追分町	075-753-4015 — takeyan@kuchem.kyoto-u.ac.jp
Takeshi Takizawa 滝沢　剛	三共株式会社　創薬基盤研究所　研究第一グループ 140-8710　品川区広町1－2－58	03-3492-3131 — takizawa@sankyo.co.jp
Tomomi Tamura 田村　友美	ブルカー・バイオスピン株式会社　マーケティング部 532-0004　大阪府大阪市淀川区西宮原 1-8-29	06-6394-8989 06-6394-9559 tomomi.tamura@bruker-biospin.jp
Hiroki Tanaka 田中　宏樹	大阪大学蛋白質研究所 565-0871　吹田市山田丘 3-2	06-6879-8598 06-6879-8599 htnk@protein.osaka-u.ac.jp
Rikou Tanaka 田中　利好	三菱化学生命科学研究所蛋白質立体構造研究グループ 194-8511　東京都町田市南大谷11号	042-724-6284 042-724-6296 rikou@libra.ls.m-kagaku.co.jp

Name	Affiliation/Address	Tel/Fax/E-mail
Ryo Tanaka 田中　亮	研究開発室 211-8502　神奈川県川崎市中原区中丸子 1280	044-435-5866 044-435-6678 tanaka-ryo@toyoko-jp.com
Satoko Tanaka 田中　聡子	兵庫県立大院　生命理 678-1297　赤穂郡上郡町光都３－２－１	0791-58-0182 — rj04w022@stkt.u-hyogo.ac.jp
Takeshi Tanaka 田中　剛史	三菱化学生命科学研究所 194-8511　町田市南大谷 11 号	042-724-6289 042-724-6296 takeshi@libra.ls.m-kagaku.co.jp
Yoshitsugu Tanaka 田中　彬嗣	九州大学 812-8582　福岡市東区馬出３－１－１	092-642-6551 092-642-6551 y.tanaka@adm.phar.kyushu-u.ac.jp
Michikazu Tanio 谷生　道一	三菱化学生命科学研究所 194-8511　町田市南大谷１１号	042-724-6293 042-724-6296 tanio@libra.ls.m-kagaku.co.jp
Masataka Tansho 丹所　正孝	（独）物質・材料研究機構強磁場研究センター 305-0003　つくば市桜３－１３	029-863-5489 029-863-5571 TANSHO.Masataka@nims.go.jp
Shin-ichi Tate 楯　真一	生物分子工学研究所 565-0874　大阪府吹田市古江台６－２－３	06-6872-8218 06-6872-8210 tate@beri.or.jp
Takehiko Terao 寺尾武彦	京都大学大学院理学研究科化学専攻 606—8502 京都市左京区北白川追分町	075-753-4011 075-753-4000 terao@beige.plala.or.jp
Naoya Tochio 栃尾　尚哉	理化学研究所ゲノム科学総合研究センター 230-0045　神奈川県横浜市鶴見区末広町 1-7-22	045-503-9317 045-503-9643 tochio@gsc.riken.jp
Hiroshi Toda 戸田　洋志	大日本住友製薬(株)薬物動態研究所 564-0053　大阪府吹田市江の木町 33-94	06-6337-5888 06-6338-7656 hiroshi-toda@ds-pharma.co.jp
Akihiro Tsutsumi 堤　耀廣	北海道大学 069-0834　江別市文京台東町３０－１１	011-386-4168 011-386-4168 a-tsutsumi@mub.biglobe.ne.jp
Satoru Tuzi 辻　暁	兵庫県立大学大学院生命理学研究科 678-1297　兵庫県赤穂郡上郡町光都 3-2-1	0791-58-0180 — tuzi@sci.u-hyogo.ac.jp
U		
Osamu Ubukata 生方　修	三共株式会社　創薬基盤研究所 140-8710　品川区広町１－２－５８	03-3492-3131 03-5436-8578 oubuka@sankyo.co.jp
Takahiro Ueda 上田　貴洋	大阪大学総合学術博物館 560-0043　大阪府豊中市待兼山町１－１６	06-6850-5769 06-6850-5785 ueda@museum.osaka-u.ac.jp

Name	Affiliation/Address	Tel/Fax/E-mail
Takumi Ueda 上田　卓見	東京大学大学院薬学系研究科 113-0033 文京区本郷 7-3-1	03-5841-4814 03-5841-4818 ueda@nmrlab.f.u-tokyo.ac.jp
Sadao Ueki 植木　定雄	ブルカー・バイオスピン株式会社 マーケティング部 305-0051 茨城県つくば市二の宮 3-21-5	029-852-1234 029-858-0322 sadao.ueki@bruker.jp
Kyoko Uekusa 植草　協子	日本医科大学 法医学教室 NMR 研究施設 113-8602 東京都文京区千駄木 1-1-5	03-3822-2131 03-5814-5680 uekusa@nms.ac.jp
Teruyuki Uematsu 上松　照幸	株式会社巴商会 144-8505 東京都大田区南蒲田 1－1－25	03-3734-1124 03-3739-1070 uematsu@tomoeshokai.co.jp
Yuichi Umekawa 梅川　雄一	大阪大学大学院理学研究科化学専攻生体分子化学研究室 560-0043 大阪府豊中市待兼山町 1-16 大阪大学理学部棟 C121	06-6850-5569 06-6850-5569 yume@ch.wani.osaka-u.ac.jp
Yoshitaka Umetsu 梅津　喜崇	北海道大学大学院理学研究科 060-0810 札幌市北区北 10 条西 8 丁目	011-706-2985 — umetsu@sci.hokudai.ac.jp
Masako Umeyama 梅山　万左子	横浜国立大学大学院工学府 240-8501 神奈川県横浜市保土ケ谷区常盤台79－5	045-339-4231 045-339-4251 d05sa201@ynu.ac.jp
Hiroaki Utsumi 内海　博明	日本電子株式会社 AIDARG1T 196-8558 昭島市武蔵野 3-1-2	042-542-2241 042-546-8068 utumi@jeol.co.jp
W		
Takeshi Wada 和田　武	ブルカー・バイオスピン株式会社 マーケティング部 305-0051 茨城県つくば市二の宮 3-21-5	029-852-1234 029-858-0322 takeshi.wada@bruker-biospin.jp
Hisanori Wakamatsu 若松　永憲	獨協医科大学生理学(生体制御)教室 321-0293 栃木県下都賀郡壬生町北小林880	0282-87-2125 — h-waka@dokkyomed.ac.jp
Kaori Wakamatsu 若松　馨	群馬大学工学部 376-8515 桐生市天神町1－5－1	0277-30-1439 0277-30-1439 wakamats@bce.gunma-u.ac.jp
Hidehiro Watanabe 渡邊　英宏	独立行政法人国立環境研究所 305-8506 茨城県つくば市小野川 16-2	029-850-2138 029-850-2880 hidewata@nies.go.jp
Hiroyuki Watanabe 渡辺　裕之	バリアンテクノロジーズジャパンリミテッド 134-0084 東京都港区芝浦4－16－36 住友芝浦ビル	03-5232-1238 03-5232-1264 hiroyuki.watanabe@varianinc.com
X		

Name	Affiliation/Address	Tel/Fax/E-mail
Xianyu Xue 薛　献宇	岡山大学地球物質科学研究センター 682-0193　東伯郡三朝町山田 827	0858-43-3824 0858-43-3450 xianyu@misasa.okayama-u.ac.jp
Y		
Hiromasa Yagi 八木　宏昌	大阪大学蛋白質研究所 565-0871　大阪府吹田市山田丘 3-2	06-6879-8598 06-6879-8599 hyagi@protein.osaka-u.ac.jp
Tomonori Yamada 山田　知典	京都大学化学研究所 611-0011　京都府宇治市五ケ庄	0774-38-3152 0774-38-3148 t-yamada@t01.mbox.media.kyoto-u.ac.jp
Nahoko Yamaji 山路　奈保子	(財)サントリー生物有機科学研究所 618-8503　三島郡島本町若山台 1-1-1	075-962-6142 — yamaji@sunbor.or.jp
Akihiko Yamamoto 山本　明彦	ブルカー・バイオスピン株式会社　技術サービス部 305-0051　茨城県つくば市二の宮 3-21-5	029-852-1236 029-858-0322 akihiko.yamamoto@bruker-biospin.jp
Hiroko Yamamoto 山本　寛子	大阪大学 669-1544　兵庫県武庫が丘 7-6-2-504	080-3058-6334 — mahiro165@hotmail.com
Yasuhiko Yamamoto 山本　泰彦	筑波大学大学院数理物質科学研究科 305-8571　茨城県つくば市天王台 1-1-1	029-853-6521 029-853-6521 yamamoto@chem.tsukuba.ac.jp
Yusuke Yamamoto 山本　裕輔	物質・材料研究機構 305-0003　つくば市桜3丁目13	029-863-5484 029-863-5571 YAMAMOTO.Yusuke@nims.go.jp
Yuuri Yamamoto 山本　優理	奈良女子大学 630-8262　奈良市北袋町17－2 若草女子学生ハイツ203号室	090-8231-0651 — yuuri-in-nara@s9.dion.ne.jp
Takeshi Yamanobe 山延　健	群馬大学工学部 376-8515　桐生市天神町 1-5-1	0277-30-1331 0277-30-1333 yamanobe@chem.gunma-u.ac.jp
Kazuo Yamauchi 山内　一夫	東京農工大学大学院　共生技術科学研究部 184-8588　小金井市中町 2-24-16	042-388-7025 042-388-7733 kyamauch@cc.tuat.ac.jp
Hidehito Yashima 八島　秀仁	ブルカー・バイオスピン株式会社　マーケティング部 305-0051　茨城県つくば市二の宮 3-21-5	029-852-1234 029-858-0322 hidehito.yashima@bruker-biospin.jp
Takako Yokoi 横井　貴子	アステラス製薬株式会社創薬推進研究所分析第二研究室 305-8585　茨城県つくば市御幸が丘 21	029-863-6487 029-852-9585 takako.yokoi@jp.astellas.com
Mayumi Yoshida 好田　真由美	理化学研究所　ゲノム科学総合研究センター 230-0045　横浜市鶴見区末広町1－7－22　C116	045-503-9642 045-503-9641 myoshida@gsc.riken.jp

Name	Affiliation/Address	Tel/Fax/E-mail
Uekusa Yoshinori 植草　義徳	静岡県立大学大学院生活健康科学研究科 食品栄養科学専攻食品機能学研究室 422-8526 静岡市駿河区谷田 52-1	054-264-5525 — p5107@mail.f.u-shizuoka-ken.ac.jp
Z		
Huiping Zhang 張　恵平	理研横浜研究所タンパク質構造研究チーム 230-0045 横浜市鶴見区鶴見中央２－１０－２－７０２	045-503-9462 045-503-9641 huiping@gsc.riken.jp

name	Affiliation/address	Tel/Fax/E-mail
B		
J.J. Babon	The Walter and Eliza Hall Institute of Medical Research 1G Royal Parade, Parkville	- - -
C		
Jerry Chan	National Taiwan University, Department of Chemistry No. 1, Sec. 4, Roosevelt Road, Taipei, 106, Taiwan	+886-2-33662994 - chanjcc@ntu.edu.tw
Chi-Fon Chang	Genomics Research Center, Academia Sinica 128 Academia Road, Section 2, Nankang, Taipei, 115, Taiwan	+886-2-2789-9157 +886-2-2788-7641 chifon@gate.sinica.edu.tw
Chung-ke Chang	Academia Sinica, Institute of Biomedical Sciences 128, Sec. 2, Academia Road, Nankang, Taipei, 115, Taiwan	+886-2-27899039 +886-2-27887641 chungke@ibms.sinica.edu.tw
Chinpan Chen	Institute of Biomedical Sciences, Academia Sinica Academia Sinica, Taipei, 115, Taiwan	+886-226523035 +886-227887641 bmchinp@ibms.sinica.edu.tw
Jyawei Cheng	Institute of Biotechnology and Department of Life Science, National Tsing Hua University Hsinchu, 300, Taiwan.	+886-3-5742763 +886-3-5738243 jwcheng@life.nthu.edu.tw
Hae-Kap Cheong	Korea Basic Science Institute, Magnetic Resonance Team Eoeun-dong 52, Yuseong-gu, Daejeon, 305-333, Republic of Korea	+82-42-865-3417 +82-42-865-3649 haekap@kbsi.re.kr
Seung-Wook Chi	Korea Research Institute of Bioscience and Biotechnology P.O. Box 115, Yusong, Daejon, 305-600, Korea	+82-42-865-3417 +82-42-865-3649 swchi@kribb.re.kr
K.-H. Chin	Institute of Biochemistry, National Chung-Hsing University Taichung, 40227, Taiwan	- - -
Ko-Hsin Chin	National Chung-Hsing University, Institute of Biochemistry Taichung, 40227, Taiwan, R.O.C.	+886-4-22840468 - shchou@nchu.edu.tw
Sung Jae Cho	KAIST, Dep. of Chemistry 373-1, Guseong-dong, Yuseong-gu, Daejon. 305-701, Korea	+82-42-869-2868 +82-42-869-8120 vesicle@dreamwiz.com
Byong-Seok Choi	KAIST, Department of Chemistry 373-1, Guseong-dong, Yuseong-gu, Daejon. 305-701, Korea	+82-42-869-2828 +82-42-869-2810 byongseok.choi@kaist.ac.kr
Shan-Ho Chou	National Chung-Hsing University, Institute of Biochemistry 250, Kuo-Kwang Rd. Taichung, 40227, Taiwan	+886-4-2285-3486 - shchou@nchu.edu.tw
Woei-Jer Chuang	National Cheng Kung University, Department of Biochemistry 1 University Rd, 701, Taiwan	+8866-23535355515 +8866-2741694 wjcnmr@mail.ncku.edu.tw

name	Affiliation/address	Tel/Fax/E-mail
D		
Feng Deng	Wuhan Institute of Physics and Mathematics, Chinese Academy of Sciences Wuhan 430071, China	+86-27-87198820 +86-27-87199291 dengf@wipm.ac.cn
Peter Duxson	University of Melbourne, Department of Chemical and Biomolecular Engineering Monash Rd. University of Melbourne, Parkville, 3010, Australia	+613-83448755 +613-8344 4153 pduxson@pgrad.unimelb.edu.au
F		
Lucio Frydman	Weizmann Institute Weizmann Institute, 76100 Rehovot, Israel	+972-8-9344903 +972-8-9344321 Lucio.Frydman@weizmann.ac.il
H		
Kee Sung Han	Daegu Center, Korea Basic Science Institute 1370 Sankyuckdong, Bukgu, Daegu 702-701, Republic of Korea	+82-53-950-7914 +82-53-959-3405 hanks@kbsi.re.kr
Kyou-Hoon Han	Korea Research Institute of Bioscience and Biotechnology P.O. Box 115 Yusong, Daejon, 305-600, Korea	+82-42-860-4250 +82-42-860-4259 khhan600@kribb.re.kr
Woong Han	Yonsei University, Department of Biochemistry 134 Shinchon-Dong, Seodaemun-Gu, Seoul, 120-749, Korea	+82-2-2123-2706 +82-2-361-9897 hanwoong@spin.yonsei.ac.kr
Eunmi Hong	Yonsei University, Department of Biochemistry Seoul, 120-749, Korea	+82-2-2123-2706 +82-2-363-2706 turtulee@spin.yonsei.ac.kr
Chun-Hua Hsu	Institute of Biological Chemistry, Academia Sinica 128 Sec. 2, Academia Rd, Nankang, Taipei, 115 Taiwan, R.O.C	+886-2-27855696 +886-2-27889759 chhsu@gate.sinica.edu.tw
Shang-Te D. Hsu	Department of Chemistry University of Cambridge Lensfield Road, Cambridge CB2 1EW, United Kingdom	+44 1223 336366 +44 1223 336362 stdh2@cam.ac.uk
Shing-Jong Huang	Institute of Atomic and Molecular Sciences, Academia Sinica P.O. Box 23-166, Taipei, 106,Taiwan	+886-223668288 +886-223620200 jongjen@gate.sinica.edu.tw
Tai-huang Huang	Academia Sinica, Institute of Biomedical Sciences 128 Academy Road, Nankang, Taipei, 11529, Taiwan, R.O.C.	+886-2-2652-3036 +886-2-2788-7641 bmthh@gate.sinica.edu.tw
Eunha Hwang	Korea Basic Science Institute 52 Yeoeun-dong, Yusung-gu, Daejeon, 305-333, Republic of Korea	+82-42-865-3648 +82-42-865-3649 hwang0131@kbsi.re.kr
Lian-Pin Hwang	National Taiwan University, Department of Chemistry No.1, Sec. 4, Roosevelt Road, Taipei, 106, Taiwan	+886-2-33665927 +886-2-33663294 lphwang@ntu.edu.tw

name	Affiliation/address	Tel/Fax/E-mail
I		
Mitsu Ikura	Division of Signaling Biology, Ontario Cancer Institute and Department of Medical Biophysics, University of Toronto 610 University Ave., Toronto, Ontario, M5G 2M9,Canada	- - -
J		
Malene R. Jensen	University of Copenhagen UDneivpetr. soitef Ctspheamrkeistnr y5 DK-2100 Copenhagen Ø, Denmark	+45-35320302 +45-35320322 led@kiku.dk
Changwen Jin	Beijing NMR Center, Peking University No 5 Yi-He-Yuan Road, Zhong_Guan_Cun, Hai-Dian, 100871, Beijing	+86-10-62756004 +86-10-62753790 changwen@pku.edu.cn
Hyun-Seob Jung	Department of biochemistry, Yonsei university Seoul, 120-749, Republic of Korea	+82-02-80203114 - junghs@spin.yonsei.ac.kr -
Jinwon Jung	Yonsei University, Department of Biochemistry 134 Shinchon-Dong Seodaemoon-Gu Seoul, 120-749, Korea	+82-2-2123-2706 - solwind@spin.yonsei.ac.kr
Jin-Won Jung	Yonsei University 134 Shinchon-Dong Seodaemoon-Gu, Seoul, 120-749, Korea	+82-2-2123-2706 +82-2-362-9897 solwind@spin.yonsei.ac.kr
Young-Sang Jung	Yonsei University, Department of Biochemistry 403 GwaHakGwan Biochemistry Depart. Yonsei Univ. Seoul, 120-749, South Korea	+82-2-2123-2706 - young@spin.yonsei.ac.kr
K		
Byoung Soo Kim	POSTECH, Department of chemistry Chem. Building Room 118, POSTECH, San 31, HyoJadong, Namgu, Pohang City, Kyungbuk, 790-784, Korea	+82-054-279-2778 - fowardj@postech.ac.kr
Byoungkook Kim	KAIST, Department of Chemistry 373-1, Guseong-dong, Yuseong-Gu, Daejon, Korea	+82-42-869-2868 +82-42-869-8120 bkkim@nmr.kaist.ac.kr
Eun-Hee Kim	Korea Basic Science Institute 52 Yeoeun-dong Yusung-gu Daejeon, 305-333, Republic of Korea	+82-42-865-3438 +82-42-865-3649 keh@kbsi.re.kr
hyunjung kim	Department of Physical Pharmacy, Seoul National University College of Pharmacy, Seoul National University, Shinlim-dong, Kwanak-gu, Seoul, 151-742, South Korea	+82-2-880-7868 - lbj@nmr.snu.ac.kr
Seong-Ok Kim	KAIST, Dept. of Chem. 373-1 Kusung-Dong, Yusung-Gu, Taejon, 305-701, Korea	+82-42-869-2868 +82-42-869-8120 sokim@kaist.ac.kr
Tae-Sik Kim	Department of applied chemistry, Hanyang Univ. 2-405, 1271 Sa-1-dong, Sangrok-gu, Ansan, Gyunggi-do, 426-791, South Korea	+82-31-400-4224 - kts7941@hanmail.net
Won Je Kim	Seoul National University college og Pharmacy Room No. 21-417, Department of Physical Pharmacy, College of Pharmacy, Seoul National University, 151-742, Korea	+82-2-880-7868 - wjwillwin@hotmail.com

name	Affiliation/address	Tel/Fax/E-mail
Yong-Chul Kim	Yonsei University, Department of Biochemistry ShinChon dong, Seoul, 120-749, Korea	+82-02-2123-2706 - yckim@spin.yonsei.ac.kr
Hyun-Suk Ko	Konkuk University, Department of Biotechnology 322 Danwol-Dong, Chungju, Chungbuk, 380-701, Korea	+82-43-840-3925 ysetin@naver.com
Junsang Ko	KAIST, Department of Chemistry 373-1 Kusung-Dong, Yusung-Gu, Taejon, 305-701, Korea	+82-42-869-2868 +82-42-869-8120 s_jsko@kaist.ac.kr
Sunggeon Ko	yonsei university 403, kwahakwon , Yonsei Univ, seodaemoongu seoul, 120-749, Korea	+82-221232706 +82-23629897 tyrosine@spin.yonsei.ac.kr
Bon-Kyung Koo	Yonsei University, Department of Biochemistry Seoul , 120-749, Korea	+82-2-2123-2706 +82-2-363-2706 bongbong@spin.yonsei.ac.kr
Werner Kremer	Institut für Biophysik und Physikalische Biochemie, Universität Regensburg Universitätsstr. 31, 93040 Regensburg, Germany	- - -
Zhihe Kuang	The University of Adelaide and The Walter and Eliza Hall Institute of Medical Research 1G Royal Parade, Parkville, VIC, 3050, Australia	+613-93452452 +613-93470852 kuang@wehi.edu.au
Ēriks Kupče	Varian Ltd. 28 Manor Rd., Walton-on-Thames, UK	+44-7767615224 +44-1865203878 eriks.kupce@varianinc.com
L		
Yen-Ting Lai	Taiwan, National Tsing-Hua University Room 308, Life Science Building II, Tsing-Hua University, HsinChu City, 30001, Taiwan	+886-915982292 - g924225@oz.nthu.edu.tw
Jens J. Led	University of Copenhagen UDneivpetr. soitef Ctspheamrkeistnr y5 DK-2100 Copenhagen Ø, Denmark	+45-35320302 +45-35320322 led@kiku.dk
Bong Jin Lee	College of Pharmacy, seoul National University San 56-1, Shillim-Dong, Kwanak-Gu, Seoul, 151-742, Korea	+82-2-880-7869 +82-2-872-3632 lbj@nmr.snu.ac.kr
Changjun Lee	Department of applied chemistry, Hanyang Univ. 2-405, 1271 Sa-1-dong, Sangrok-gu, Ansan, Gyunggi-do, 426-791, South Korea	+82-31-400-4224 - lchj3@nate.com
Chul-Jin Lee	Yonsei University, Department of Biochemistry 134 Sinchon-dong, Seodaemun-Gu , 120-749, South Korea	+82-2-2123-2706 - cjlee@spin.yonsei.ac.kr
Hyeong Ju Lee	Department of Chemistry, POSTECH NMR Lab. Dept. of Chem. POSTECH Hyoja-dong Pohang, 790-784, Korea	+82-54-279-2778 +82-54-279-3399 posnmrhj@postech.ac.kr

name	Affiliation/address	Tel/Fax/E-mail
Kyuhong Lee	Korea Basic Science Institute 52 Yeoeun-Dong, Yuseong-Ku, Daejeon 305-333, Korea	+82-42-865-3644 +82-42-865-3649 khlee@kbsi.re.kr
Man-Ho Lee	Kyungpook National University, Department of Applied Chemistry 1370 Sankyuk-dong, Buk-gu, Daegu, Romania, 702-701, Korea	+82-53-950-5584 +82-53-950-6594 mhlee@knu.ac.kr
Misun Lee	Department of Applied Chemistry, Hanyang University 2-405, 1271 Sa-1-dong, Sangrok-gu, Ansan, Gyunggi-do, 426-791, South Korea	+82-31-400-4224 - nuwana7@hanmail.net
SangGap Lee	Department of Physics, Korea Advanced Institute of Science and Technology 373-1 Guseong-dong, Yuseong-gu, Daejeon 305-701, Korea	+82-42-869-2573 +82-42-869-2510 leesg@kaist.ac.kr
Wei-Tin Lee	Academia Sinica 128 Sec. 2, Academia Rd, Nankang, Taipei, 115, Taiwan	+82-42-869-2573 +82-42-869-2510 leesg@kaist.ac.kr
Weontae Lee	Department of Biochemistry and Biomolecular NMR Labortory, Yonsei University Seoul 120-749, Korea	- - -
Young Ju Lee	Gwangju Center, Korea Basic Science Institute, Department of Chemistry, Chonnam National University Yongbong 300 Gwangju , 500-757, S. Korea	+82-62-530-0513 +82-62-530-0519 yjlee@kbsi.re.kr
Jun Li	NMR Laboratory, Shanghai Institute of Materia Medica, Shanghai Institutes for Biological Sciences, Chinese Academy of Sciences 555 Zu Chong Zhi Road, Zhangjiang Hi-tech park Shanghai,201203 China	+86-21-50806036 +86-21-50806036 dhLin@mail.shcnc.ac.cn
Donghai Lin	NMR Laboratory, Shanghai Institute of Materia Medica, Shanghai Institutes for Biological Sciences, Chinese Academy of Sciences 555 Zu Chong Zhi Road, Zhangjiang Hi-Tech Park, Pudong, Shanghai	+86-21-50806036 +86-21-50806036 dhlin@mail.shcnc.ac.cn
Ku Feng Lin	Tsing Hua University, Department of Life Science 101, Section 2 Kuang Fu Road, Hsinchu, 30013, Taiwan	+886-35715131 +886-35715934 g894271@life.nthu.edu.tw
Yong Yuk Lin	DSO National Laboratories 20 Science Park Drive, 118230, Singapore	+65-6871 2904 +65-6873 0742 yyuklin@dso.org.sg
Maili Liu	Wuhan Institute of Physics and Mathematics Wuhan 430071, PR China	+82-27-87197305 +82-27-87199291 ml.liu@wipm.ac.cn
Yang Liu	National University of Singapore, Department of Biological Sciences Science Drive 4, S3 level 2 FGL lab1, 119260, Singapore	+65-68741687 +65-68722013 g0203575@nus.edu.sg
Yu Nan Liu	Tsing hua university, department of life science 101, Section 2 Kuang Fu Road, Hsinchu, 30013, Taiwan	+886-35715131 +886-35715943 veal@tcts.seed.net.tw

name	Affiliation/address	Tel/Fax/E-mail
Yuan-Chao Lou	Academia Sinica, Institute of Biomedical Sciences 128, Sec.2, Academia Road, Nankang, Taipei 115, Taiwan	+886-227899162 - yclou@ibms.sinica.edu.tw
Ping-Chiang Lyu	National TsingHua University, Institute of Bioinformatics and Structural Biology 101 Kuang -Fu Rd. sec. II, Hsinchu, 30043, Taiwan	+886-3-5742762 +886-3-5715934 pclyu@life.nthu.edu.tw
M		
Suhyun Ma	Yonsei University, Department of biochemistry college of science, Yonsei University, Seoul, 120-749, Korea	+82-2-2123-2706 +82-2-363-2706 suhyunma@spin.yonsei.ac.kr
Joel Peter Mackay	University of Sydney School of MMB, University of Sydney, Sydney, NSW, 2006, Australia	+61-2-93513906 +61-2-93514726 j.mackay@mmb.usyd.edu.au
Haydyn D. T. Mertens	Bio21 Molecular Science and Biotechnology Institute, The University of Melbourne Victoria, 3010, Australia	+61-3-83442273 +61-3-93481421 hmertens@unimelb.edu.au
Yu Keung Mok	National University of Singapore, Department of Biological Sciences 14 Science Drive 4, 117543, Singapore	+65-68742967 +65-67792486 dbsmokh@nus.edu.sg
Hye Seon Moon	Postech, Department of chemistry San 31 Hyojadong, Namgu, Pohang, Kyungbuk 790-784, Korea	+82-54-279-2778 - sunny310@postech.ac.kr
N		
Kate Nairn	CSIRO Manufacturing and Infrastructure Technology Private Bag 33, Clayton South, Victoria, 3169, Australia	+61-395452667 +61-395441128 kate.nairn@csiro.au
Raymond S. Norton	Walter and Eliza Hall Institute of Medical Research 1G Royal Parade Parkville, 3050, Australia	+61-3-9345-2306 +61-3-9345-2686 ray.norton@wehi.edu.au
O		
Kiyoshi Ozawa	Australian National University Canberra ACT 0200, Australia	+61-2-612-54181 +61-2-612-50750 ozawa@rsc.anu.edu.au
P		
Chin-Ju Park	KAIST 373-1 Guseong-dong, Yuseong-gu, Daejon, 305701, Korea	+82-42-869-2868 +82-42-869-2810 cjp@kaist.ac.kr
Heeyong Park	Yonsei University, Department of Biochemistry College of Science, Yonsei University, Seoul, 120-749, Korea	+82-2-2123-2706 +82-2-363-2706 heeyong@spin.yonsei.ac.kr
Jiyoung Park	KAIST. Dept. of Chemistry 373-1, Guseong-dong, Yuseong-gu, Daejon, 305-701, Korea	+82-42-869-2868 +82-42-869-8120 jiyoung01@kaist.ac.kr

name	Affiliation/address	Tel/Fax/E-mail
Weng Kung Peng	Osaka University Graduate School Of Engineering Science, Osaka University, Toyonaka, Osaka, 560-8531, Japan	+81-6-6850-6323 +81-6-6850-6321 peng@qc.ee.es.osaka-u.ac.jp
A. Pines	University of California Berkeley Berkeley, CA 94720, USA	
R		
Simone Rochfort	Environmental Health and Chemistry, PIRVic, Department of Primary Industries 621 Sneydes Rd, Werribee, Australia 3030, Australia	+61-3-9742-9704 +61-3-9742-9704 simone.rochfort@dpi.vic.gov.au
S		
A. Samoson	National Institute of Chemical Physics and Biophysics Akadeemia Tee 23, Tallinn 12618 ESTONIA	+372-639-8310 - ago@kbfi.ee
Jacob Schaefer	Department of Chemistry, Washington University One Brookings Drive, St. Louis, MO, 63130, U. S. A.	314-935-6844 314-935-4481 jschaefer@wustl.edu
Chanwoo Seo	Department of applied chemistry, Hanyang Univ. 2-405, 1271 Sa-1-dong, Sangrok-gu, Ansan, Gyunggi-do, 426-791, South Korea	+82-31-400-4224 - scw1997@naver.com
Frances Separovic	University of Melbourne, School of Chemistry Melbourne VIC, 3010, Australia	+61-3-8344-6464 +61-3-9347-5180 fs@unimelb.edu.au
Ya-Ching Shen	Institute of Marine Resources National Sun Yat-sen University 70 Lien-Hai Rd., Kaohsiung, 80424, Taiwan	+88-6-7-5252000 * 5058 +88-6-7-5255020 ycshen@mail.nsysu.edu.tw
Yunyu Shi	Hefei National Laboratory for Physical Sciences at Microscale and School of Life Sciences, University of Science and Technology of China Hefei, 230026, China	+86-551-3607464 +86-551-3601443 yyshi@ustc.edu.cn
Jae Sun Shin	KAIST, Department of chemistry 373-1 Kusung-Dong, Yusung-Gu, Taejon, 305-701, Korea	+82-42-869-2860 +82-42-869-8120 whoa@kaist.ac.kr
Joon Shin	Department of Biochemistry, Yonsei University 134, Shinchon-Dong,Seodaemun-Gu,Seoul, 120-749, Korea	+82-2-2123-2706 +82-2-361-9897 hsun@hkucc.hku.hk
Hyunsoo So	Sogang University, Department of Chemistry Sinsu-dong, Mapo-ku, Seoul, 121-742, Korea	+82-2-705-8442 +82-2-701-0967 hyunso@sogang.ac.kr
Na young Sohn	Department of Physical Pharmacy,College of Pharmacy, Seoul National University Shinlim-dong, Kwanak-gu, Seoul, 151-742, South Korea	+82-2-880-7868 - lbj@nmr.snu.ac.kr
Shih-Che Sue	Institute of Biomedical Sciences, Academica Sinica Nankang, Taipei, 115, Tawain	+88-6-227899039 +88-6-227887641 sc_sue@ibms.sinica.edu.tw

name	Affiliation/address	Tel/Fax/E-mail
Hongzhe Sun	Department of Chemistry, The University of Hong Kong Chong Yuet Ming Chemistry Building, The University of Hong Kong, Pokfulam Road,Hong Kong	+852-28598974 +852-28571586 hsun@hkucc.hku.hk
T		
Nguyen Tien Tai	Institute of Chemistry, Vietnamese Academy of Science and Technology 18 Hoang Quoc Viet, Nghiado, Hanoi, Vietnam	+84-4-7564406 +84-4-8361283 nttai@ich.ncst.ac.vn
Sook Lan Tan	DSO National Laboratories 20 Science Park Drive, 118230, Singapore	+65-6871 2841 +65-6873 0742 tsooklan@dso.org.sg
Mark Ming-Daw Tsai	Genomics Research Center, Academia Sinica 128,Academia Road, Sec.2, Nankang Dist.,Taipei, 115, Taiwan	+886-2-27899930 - lhchen@gate.sinica.edu.tw
W		
Markus Wälchli	Bruker–BioSpin Japan 21-5-3 Ninomiya Tsukuba-shi Ibaraki 305-0051	+81-29 – 852 – 1234 +81-29 – 858 – 0322 markus.waelchli@bruker-biospin.jp
Hui Wang	The University of Hong Kong, Department of Chemistry Room309, Chong Yuet Ming Chemistry Building, The University of Hong Kong, Pokfulam Road, 666666, Hong Kong	+852-61962168 +852-28571586 whui@hkusua.hku.hk
Iren Wang	National Taiwan University, Institute of Biochemical Sciences Institute of Biological Chemistry, Academia Sinica 128 Academia Road, Section 2, Nankang,Taipei, 115, Taiwan	+886-227899162 +886-227887641 iwang@gate.sinica.edu.tw
Wenning Wanga	Department of Chemistry, Fudan University Shanghai 200433, China	- - -
Anthony Watts	Biochemistry Department, Oxford University Oxford, OX1 3QU, UK.	+44 (0)1865 275268 +44 (0)1865 275234 awatts@bioch.ox.ac.uk
Hoshik Won	Department of applied chemistry, Hanyang Univ. 2-405, 1271 Sa-1-dong, Sangrok-gu, Ansan, Gyunggi-do, 426-791, South Korea	+82-31-400-4224 - won@guanine.hanyang.ac.kr
Hyung-Sik Won	Konkuk University, Department of Biotechnology 322 Danwol-Dong, Chungju, Chungbuk, 380-701, Korea	+82-43-840-3589 +82-43-852-3616 wonhs@kku.ac.kr
Shih Hsiung Wu	Institute of Biological Chemistry, Academia Sinica 128, Sec II Academic Road, Nankang Taipei, 115, Taiwan	+886-2-27855696 +886-2-26539142 shwu@gate.sinica.edu.tw
Wen-Jin Wu	Institute of Biomedical Sciences, Academia Sinica B2-NMR Institute of Biomedicla Sciences, Academia Sinica, Taipei 11529, Taiwan	+886-2-2789-9157 - winston@ibms.sinica.edu.tw
Y		

name	Affiliation/address	Tel/Fax/E-mail
Daiwen Yang	National University of Singapore 14 Science Drive 4, Singapore 117543	+65-6874-1014 +65-6779-2486 dbsydw@nus.edu.sg
Jun Yang	Wuhan Institute of Physics and Mathematics, Chinese Academy of Sciences Wuhan 430071, P. R. China	- - -
Z		
Mingjie Zhang	Department of Biochemistry, Molecular Neuroscience Center, Hong Kong University of Science and Technology Clear Water Bay, Kowloon, Hong Kong, P. R. China	- - -